



NASA-TM-81308 19810025595

1980

Ames Research Center Publications: A Continuing Bibliography

ulation of the Tilt Rotor Concept: The XV-15's Role. Future Requirements and Roles of Computers in Aerody
puting Viscous Flows. A Simple Method for Estimating Minimum Autorotative Descent Rate of Single Rotor
and Dynamic Stability Analysis of the Space Shuttle Vehicle-Orbiter. Comparison of Measured and Calculate
mpulsive Noise. Effect of High Lift Flap Systems on the Conceptual Design of a 1985 Short-Haul Commerc
on Multicyclic Control by Swashplate Oscillation. Low-Speed Aerodynamic Characteris
Model at High Angles of Attack and Sideslip. Generalization of Huffman Coding to Mi
w. Optimum Horizontal Guidance Techniques for Aircraft. Quasi-Optimal Control of a M
ce and Control for Investigating Aircraft Noise-Impact Reduction. Trajectory Module
Aircraft Synthesis Program ACSYNT. A Flight Investigation of the Stability, Control, and
Augmented Jet Flap STOL Airplane. G-Seat System Step Input and Sinusoidal Response Charac
Cost/Performance Measurement System on a Research Aircraft Project. Application of Special-Pur
Aircraft Real-Time Simulation. Wing Analysis Using a Transonic Potential Flow Computational
Hardware Analysis. Phenomenological Aspects of Quasi-Stationary Controlled and Uncontro
low Separations. A Method for the Analysis of the Benefits and Costs for Aeronautical Res
CTOL Aircraft Research. Closed-Form Equations for the Lift, Drag, and Pitching-Moment C

ing Schemes. High Angle of Incidence I
Maneuverable Transonic Aircraft.
from Four Helicopter Rotor
Analysis. Multi-Calculation
the Three Stage Comp
Ratio Propulsion
a Harrier V/STOL
Intersection Problem
Model Volume 2:
Rotor in a Wind Tun
of Advanced Turbopro
Applied to a Helicopter in t
Automatic and Manual Flight Direct

XV-15 Tilt Rotor Aircraft in Helicopter Mode. Application of Advanced Technologies to Small Short-
Large Scale Swivel Nozzle Thrust Deflector. High Angle Canard Missile Test in the Ames 11-Fc
Study of Commuter Airplane Design Optimization. Application of Second-Order Turbulent Mode
Radiated Aerodynamic Sound. Infrastructure Dynamics: A Selected Bibliography. The Effect of Tip
Helicopter Noise Due to Blade/Vortex Interaction. A Study of Test Section Configuration for Shock Tul
airfoils. A Mach Line Panel Method for Computing the Linearized Supersonic Flow Over Planar Wing
on of Short Haul Air Transportation in the Southeastern United States. Development and Flight Tests
Navigation During Terminal Area and Landing Operations. Prop-Fan Data Support Study. Study to Det
onal and Performance Criteria for STOL Aircraft Operating in Low Visibility Conditions. Executive Summ
of an Intra-Regional Air Service in the Bay Area and a Technology Assessment of Transm
hology Assessment of Transportation System Investments. Requirements for Regiona
on of a Flight Program to Determine Neighborhood Reactions to Small Transport Air
ing Response at Subsonic and Transonic Speeds. Phase 1: F-111A Flight Data Analysis
approach, Results and Conclusions. An Investigation of Wing Buffeting Response at Su
Phase 2: F-111A Flight Data Analysis. Volume 2: Plotted Power Spectra. An Investigation of Wing Buffeting Flow
sonic and Transonic Speeds. Phase 2: F-111A Flight Data Analysis. Volume 3: Tabulated Power Spectra. Wings v
und through a Sheared Flow. Pioneer Venus Spacecraft Charging Model. Abstracts for the Planetary Geology Exper
on Aeolian Processes. Effects of Mass Addition on Blunt-Body Boundary-Layer Transition and Heat Transfer. Semi-
enna Performance Study. Part 2: Broadband Antenna Techniques Survey. Cable Strumming Suppression. Status of S
pects of Using Numerical Methods to Study Complex Flows at High Reynolds Numbers. Magnetometer Correcting
Mechanism for Pioneer Venus. The Role of Time-History Effects in the Aerodynamics of Aircraft Finite
Future Computer Requirements for Computational Aerodynamics. Computational Aerodynamics and Heat Transfer. Exec
ity. Three-Dimensional Computational Aerodynamics in the 1980's. Numerical Aerodynamics in the 1980's. NASA
Study, Executive Summary. Preliminary Study for a Numerical Aerodynamic Simulation Facility. NASA
es. Fluid Interaction with Spinning Toroidal Tanks. Theoretical Contamination of Cryogenic Preloa
ivity and Toxicity Studies of Candidate Aircraft Passenger Seat Materials. Calculated Rate the Iter
+ O Yields Cl + O₂ Between 220 and 1000 Deg K. On the Period of the Coherent Structure in Sulfur.
ndary Layers at Large Reynolds Numbers. Simple Torsion Test for Shear Moduli Determination of Orthotropic Composites. Future
amic Stall of an Oscillating Airfoil. A Review of NASA-Sponsored Technology Assessment Projects. Lagrangian Bimolecular R
omputation of Inviscid Compressible Flows. Engineering Tests of the C-141 Telescope. Calculation of Supersonic Viscous Proper
ynamic Characteristics of an 0.075-Scale F-15 Airplane Model at High Angles of Attack and Sideslip. Response at Subsonic and T

1980

Ames Research Center Publications: A Continuing Bibliography



National Aeronautics and
Space Administration

Ames Research Center
Moffett Field, California 94035

FOREWORD

Ames Research Center Publications: A Continuing Bibliography lists Ames-sponsored literature indexed during 1980 in *Scientific and Technical Aerospace Reports* (STAR), *Limited Scientific and Technical Aerospace Reports* (LSTAR), *International Aerospace Abstracts* (IAA), and *Computer Program Abstracts* (CPA) and is divided into two sections. Section I contains citations and abstracts of published works listed by directorate and by type of publication (NASA formal report, NASA technical memorandum, NASA contractor report, journal article, meeting paper, book or chapter of a book, patents, and computer programs); Section II is comprised of subject, author, contract number, and report number indexes.

Copies of publications cited in this bibliography may be ordered from the following sources:

Category	Source
NASA Report Literature:	
Formal Reports	National Technical Information Service (NTIS)
Technical Memorandums	5285 Port Royal Road
Contractor Reports	Springfield, VA 22161
	NASA Scientific and Technical Information Facility (STIF)
	P.O. Box 8757
	Baltimore/Washington International Airport
	MD 21240
Journal Articles, Books, Conference/Meeting Papers	Consult citation for source of availability
Computer Programs	Computer Software Management and Information Center (COSMIC)
	112 Barrow Hall
	University of Georgia
	Athens, GA 30601
Patents:	
Patent Application Specifications	National Technical Information Service (NTIS)
Printed Copies of Patents	Commissioner of Patents and Trademarks
	U.S. Patent and Trademark Office
	Washington, DC 20231

The Library Branch Staff will advise Ames requestors whether form ARC 80 "Library Resource Request" or ARC 81 "Published Material Request" should be used to order copies of published works from either the Ames Technical Library, 202-3, extension 5157, or the Life Sciences Library, 239-13, extension 5387.

Because *Ames Research Center Publications: A Continuing Bibliography* is based upon the indexing services of STAR, LSTAR, IAA, and CPA, some published work may not be included. If this is the case, send two copies of the published work to Betty Sherwood, 202-3, and the citation will appear in the next annual bibliography.

Betty Sherwood, Compiler

TABLE OF CONTENTS

	Page
SECTION I – PUBLICATIONS (By Organization)	
OFFICE OF THE DIRECTOR (D)	1
ADMINISTRATION (A)	3
AERONAUTICS AND FLIGHT SYSTEMS (F)	4
ASTRONAUTICS (S)	34
LIFE SCIENCES (L)	82
RESEARCH SUPPORT (R)	98
ARMY RESEARCH AND TECHNOLOGY LABORATORIES (AVRADCOM) (X)	100
AEROMECHANICS LABORATORY (Y)	101
AIR FORCE HUMAN RESOURCES LABORATORY TECHNOLOGY OFFICE (H)	103
COMPUTER PROGRAMS	105
SECTION II – INDEXES	
PUBLICLY AVAILABLE PUBLICATIONS	107
RESTRICTED DOCUMENTS	244
COMPUTER PROGRAMS	253

SECTION I
PUBLICATIONS

OFFICE OF THE DIRECTOR

NASA FORMAL REPORTS

N80-15033* National Aeronautics and Space Administration.
Ames Research Center, Moffett Field, Calif.

CLASSICAL AERODYNAMIC THEORY

R. T. Jones, comp. Dec. 1979 308 p refs
(NASA-RP-1050; A-7556) Avail: NTIS HC A14/MF A01 CSDL
O1A

A collection of papers on modern theoretical aerodynamics is presented. Included are theories of incompressible potential flow and research on the aerodynamic forces on wing and wing sections of aircraft and on airship hulls. For individual titles, see N80-15034 through N80-15047.

NASA TECHNICAL MEMORANDA

N80-16035* National Aeronautics and Space Administration.
Ames Research Center, Moffett Field, Calif.

WING FLAPPING WITH MINIMUM ENERGY

R. T. Jones Jan. 1980 18 p refs
(NASA-TM-81174; A-8076) Avail: NTIS HC A02/MF A01
CSDL O1A

For slow flapping motions it is found that the minimum energy loss occurs when the vortex wake moves as a rigid surface that rotates about the wing root - a condition analogous to that determined for a slow-turning propeller. The optimum circulation distribution determined by this condition differs from the elliptic distribution, showing a greater concentration of lift toward the tips. It appears that very high propulsive efficiencies are obtained by flapping. Author

NASA CONTRACTOR REPORTS

N80-15865* SRI International Corp., Menlo Park, Calif.
DOCUMENTATION OF THE ANALYSIS OF THE BENEFITS AND COSTS OF AERONAUTICAL RESEARCH AND TECHNOLOGY MODELS, VOLUME 1 Final Report
J. C. Bobick, R. L. Braun, and R. E. Denny Jul. 1979 203 p
(Contract NAS2-10026; SRI Proj. 7759)
(NASA-CR-152278) Avail: NTIS HC A10/MF A01 CSDL
12B

The analysis of the benefits and costs of aeronautical research and technology (ABC-ART) models are documented. These models were developed by NASA for use in analyzing the economic feasibility of applying advanced aeronautical technology to future civil aircraft. The methodology is composed of three major modules: fleet accounting module, airframe manufacturing module, and air carrier module. The fleet accounting module is used to estimate the number of new aircraft required as a function of time to meet demand. This estimation is based primarily upon the expected retirement age of existing aircraft and the expected change in revenue passenger miles demanded. Fuel consumption estimates are also generated by this module. The airframe manufacturer module is used to analyze the feasibility of the manufacturing the new aircraft demanded. The module includes logic for production scheduling and estimating manufacturing costs. For a series of aircraft selling prices, a cash flow analysis is performed and a rate of return on investment is calculated. The air carrier module provides a tool for analyzing the financial

feasibility of an airline purchasing and operating the new aircraft. This module includes a methodology for computing the air carrier direct and indirect operating costs, performing a cash flow analysis, and estimating the internal rate of return on investment for a set of aircraft purchase prices. R.C.T.

CONFERENCE PAPERS

A80-10765 * The development and use of large-motion simulator systems in aeronautical research and development. J. C. Dusterberry (NASA, Ames Research Center, Moffett Field, Calif.) and M. D. White (G. E. Cooper Associates, Saratoga, Calif.). In: 50 years of flight simulation; Proceedings of the Conference, London, England, April 23-25, 1979. Session 2. (A80-10758 01-09) London, Royal Aeronautical Society, 1979, p. 1-16. 23 refs.

The paper examines the evolution of manned aircraft simulators with large-motion systems and provides a brief description of important design details along with physical descriptions of a number of systems. Attention is given to the use of large translational motions in providing the simulator pilot with a close approximation of the cues of aircraft flight; examples are cited comparing pilot reactions to simulators with and without motion. How these simulators have been used in programs that effectively influenced aircraft design and operating problems is discussed. B.J.

A80-24268 * Singular perturbations and the sounding rocket problem. M. D. Ardema (NASA, Ames Research Center, Moffett Field, Calif.). In: Joint Automatic Control Conference, Denver, Colo., June 17-21, 1979, Proceedings. (A80-24226 08-63) New York, American Institute of Chemical Engineers, 1979, p. 901-907. 9 refs. *

In this paper, Goddard's problem of maximizing the final altitude of a sounding rocket (a singular problem of optimal control) is analyzed using singular perturbation methods. The problem is first cast in singular perturbation form and then solved to zero order by adding boundary-layer corrections to the reduced solution. For a quadratic drag law, a closed-form solution is obtained, although consideration of a numerical example indicates that this solution is not useful for practical sounding rockets. However, use of state variable transformations allows a very accurate numerical approximation to be constructed. It is concluded that application of singular perturbation methods to the well-known sounding rocket problem indicates that these methods may have utility in dealing with singular problems of optimal control. (Author)

A80-31009 * # Some observations on supersonic wing design. R. T. Jones (NASA, Ames Research Center, Moffett Field, Calif.). In: The evolution of aircraft wing design; Proceedings of the Symposium, Dayton, Ohio, March 18, 19, 1980. (A80-31001 12-05) New York, American Institute of Aeronautics and Astronautics, Inc., 1980, p. 91-94. 10 refs. (AIAA 80-3040)

The paper presents a brief review on the development of supersonic wing design. Attention is given to linearized aerodynamic theory, emphasizing equations for drag and ratios of slopes and Mach lines. Diagrams that depict conditions for minimum drag as well as the effects of fore-and-aft dimension of wings and Mach numbers on areas of lateral entrainment are presented.

C.F.W.

D

ADMINISTRATION

NASA TECHNICAL MEMORANDA

N80-18985*# National Aeronautics and Space Administration.
Ames Research Center, Moffett Field, Calif.

**AMES RESEARCH CENTER PUBLICATIONS: A CONTINU-
ING BIBLIOGRAPHY, 1978**

Feb. 1980 139 p

(NASA-TM-81175; A-8079) Avail: NTIS HC A07 CSCL 05B

This bibliography lists formal NASA publications, journal articles, books, chapters of books, patents and contractor reports issued by Ames Research Center which were indexed by Scientific and Technical Aerospace Abstracts, Limited Scientific and Technical Aerospace Abstracts, and International Aerospace Abstracts in 1978. Citations are arranged by directorate, type of publication and NASA accession numbers. Subject, personal author, corporate source, contract number, and report/accession number indexes are provided.

Author

A

AERONAUTICS AND FLIGHT SYSTEMS

NASA FORMAL REPORTS

N80-10107*# National Aeronautics and Space Administration. Ames Research Center, Moffett Field, Calif.

WORKSHOP ON THRUST AUGMENTING EJECTORS

A. E. Lopez, ed., D. G. Koenig, ed., D. S. Green, ed. (Naval Air Development Center, Warminster, Penn.), and K. S. Nagaraja, ed. (Air Force Flight Dynamics Lab) Sep. 1979 509 p Conf. held at Moffett Field, Calif., 28-29 Jun. 1978; Sponsored by NADC and AFFDL (NASA-CP-2093; A-7887) Avail: NTIS HC A22/MF A01 CSCL 01A

The state of the art of ejector technology is assessed and the desired direction of future studies in all aspects of ejector thrust augmenting systems is delineated. For individual titles, see N80-10108 through N80-10133.

N80-11068*# National Aeronautics and Space Administration. Ames Research Center, Moffett Field, Calif.

WIND-TUNNEL/FLIGHT CORRELATION STUDY OF AERO-DYNAMIC CHARACTERISTICS OF A LARGE FLEXIBLE SUPERSONIC CRUISE AIRPLANE CXB-70-1). 1: WIND-TUNNEL TESTS OF A 0.03-SCALE MODEL AT MACH NUMBERS FROM 0.6 TO 2.53

James Daugherty, C. Nov. 1979 222 p refs (NASA-TP-1514; A-7712) Avail: NTIS HC A10/MF A01 CSCL 01C

The longitudinal and lateral forces and moments for a 0.03 scale deformed rigid, static force model of the XB-70-1 airplane were determined. Control effectiveness was determined for the elevon in pitch and roll, for the canard, and for the rudders. Component effects of the canard, deflected with tips, variable position canopy, bypass doors, and bleed dump fairing were measured. The effects of small variations in inlet mass flow ratio and small amounts of asymmetric deflection of the wing tips were assessed.

A.W.H.

N80-11869*# National Aeronautics and Space Administration. Ames Research Center, Moffett Field, Calif.

A CLOSED-FORM SOLUTION FOR NOISE CONTOURS

Elwood C. Stewart and Thomas M. Carson Nov. 1979 40 p refs (NASA-TP-1432; A-7660) Avail: NTIS HC A03/MF A01 CSCL 20A

An analytical approach for generating noise contours that overcome the difficulties of existing programs is described. This approach is valid for arbitrarily complex paths and reveals the importance of various factors that influence contour shape and size. The calculations are simple enough to be implemented on a small, hand-held programmable calculator, and a program for the HP-67 calculator is illustrated. The method is fast, simple, and gives the area, the contour, and its extremities for arbitrary flight paths for both takeoffs and landings.

R.C.T.

N80-15069*# National Aeronautics and Space Administration. Ames Research Center, Moffett Field, Calif.

THE EFFECTS OF MOTION AND g-SEAT CUES ON PILOT SIMULATOR PERFORMANCE OF THREE PILOTING TASKS

Thomas W. Showalter and Benton L. Parris Jan. 1980 45 p refs (NASA-TP-1601; A-7875) Avail: NTIS HC A03/MF A01 CSCL 01C

Data are presented that show the effects of motion system cues, g-seat cues, and pilot experience on pilot performance during takeoffs with engine failures, during in-flight precision turns, and during landings with wind shear. Eight groups of USAF pilots flew a simulated KC-135 using four different cueing systems. The basic cueing system was a fixed-base type (no-motion cueing) with visual cueing. The other three systems were produced by the presence of either a motion system or a g-seat, or both. Extensive statistical analysis of the data was performed and representative performance means were examined. These data show that the addition of motion system cueing results in significant improvement in pilot performance for all three tasks; however, the use of g-seat cueing, either alone or in conjunction with the motion system, provides little if any performance improvement for these tasks and for this aircraft type.

Author

N80-15129*# National Aeronautics and Space Administration. Ames Research Center, Moffett Field, Calif.

EVALUATION OF APPROXIMATE METHODS FOR THE PREDICTION OF NOISE SHIELDING BY AIRFRAME COMPONENTS

Warren F. Ahtye and Geraldine McCulley (Informatics, Inc., Palo Alto, Calif.) Washington Jan. 1980 105 p refs (NASA-TP-1004; A-6961) Avail: NTIS HC A06/MF A01 CSCL 21E

An evaluation of some approximate methods for the prediction of shielding of monochromatic sound and broadband noise by aircraft components is reported. Anechoic-chamber measurements of the shielding of a point source by various simple geometric shapes were made and the measured values compared with those calculated by the superposition of asymptotic closed-form solutions for the shielding by a semi-infinite plane barrier. The shields used in the measurements consisted of rectangular plates, a circular cylinder, and a rectangular plate attached to the cylinder to simulate a wing-body combination. The normalized frequency, defined as a product of the acoustic wave number and either the plate width or cylinder diameter, ranged from 4.6 to 114. Microphone traverses in front of the rectangular plates and cylinders generally showed a series of diffraction bands that matched those predicted by the approximate methods, except for differences in the magnitudes of the attenuation minima which can be attributed to experimental inaccuracies. The shielding of wing-body combinations was predicted by modifications of the approximations used for rectangular and cylindrical shielding. Although the approximations failed to predict diffraction patterns in certain regions, they did predict the average level of wing-body shielding with an average deviation of less than 3 dB. M.M.M.

N80-15138*# National Aeronautics and Space Administration.
Ames Research Center, Moffett Field, Calif.
**EFFECTS OF PRIMARY ROTOR PARAMETERS ON FLAP-
PING DYNAMICS**

Robert T. N. Chen Jan. 1980 63 p refs
(NASA-TP-1431; A-7777) Avail: NTIS HC A04/MF A01 CSCL
01A

The effects of flapping dynamics of four main rotor design features that influence the agility, stability, and operational safety of helicopters are studied. The parameters include flapping hinge offset, flapping hinge restraint, pitch-flap coupling, and blade lock number. First, the flapping equations of motion are derived that explicitly contain the design parameters. The dynamic equations are then developed for the tip-path plane, and the influence of individual and combined variations in the design parameters determined. The steady state flapping response is examined with respect to control input and aircraft angular rate which leads to a feedforward control law for control decoupling through cross feed, and a feedback control law to decouple the steady state flapping response. The condition for achieving perfect decoupling of the flapping response due to aircraft pitch and roll rates without using feedback control is also found for the hover case. It is indicated that the frequency of the regressing flapping mode of the rotor system can become low enough to require consideration in the assessment of handling characteristics.

J.M.S.

N80-17081*# National Aeronautics and Space Administration.
Ames Research Center, Moffett Field, Calif.
**FLIGHT TESTS OF THE TOTAL AUTOMATIC FLIGHT
CONTROL SYSTEM (TAF COS) CONCEPT ON A DHC-6 TWIN
OTTER AIRCRAFT**

William R. Wehrend, Jr. and George Meyer Feb. 1980 73 p
refs
(NASA-TP-1513; A-7901) Avail: NTIS HC A04/MF A01 CSCL
01C

Flight control systems capable of handling the complex operational requirements of the STOL and VTOL aircraft designs as well as designs using active control concepts are considered. Emphasis is placed on the total automatic flight control system (TAF COS) (TAF COS). Flight test results which verified the performance of the system concept are presented.

J.M.S.

N80-17984*# National Aeronautics and Space Administration.
Ames Research Center, Moffett Field, Calif.
**AN EXPERIMENTAL INVESTIGATION OF TWO LARGE
ANNULAR DIFFUSERS WITH SWIRLING AND DISTORTED
INFLOW**

William T. Eckert, James P. Johnston (Stanford Univ., Calif.),
Tad D. Simons (Stanford Univ., Calif.), Kenneth W. Mort, and V.
Robert Page Feb. 1980 106 p refs
(NASA-TP-1628; AVRADCOM-TR-79-40; A-7436) Avail: NTIS
HC A06/MF A01 CSCL 01A

Two annular diffusers downstream of a nacelle-mounted fan were tested for aerodynamic performance, measured in terms of two static pressure recovery parameters (one near the diffuser exit plane and one about three diameters downstream in the settling duct) in the presence of several inflow conditions. The two diffusers each had an inlet diameter of 1.84 m, an area ratio of 2.3, and an equivalent cone angle of 11.5, but were distinguished by centerbodies of different lengths. The dependence of diffuser performance on various combinations of swirling, radially distorted, and/or azimuthally distorted inflow was examined. Swirling flow and distortions in the axial velocity profile in the annulus upstream of the diffuser inlet were caused by the intrinsic flow patterns downstream of a fan in a duct and by artificial intensification of the distortions. Azimuthal distortions or defects were generated by the addition of four artificial devices (screens and fences). Pressure recovery data indicated beneficial effects of both radial distortion (for a limited range of distortion levels) and inflow swirl. Small amounts of azimuthal distortion created by the artificial devices produced only small effects on diffuser performance. A large artificial distortion device was required to produce enough azimuthal flow distortion to significantly degrade the diffuser static pressure recovery. Author

N80-19022*# National Aeronautics and Space Administration.
Ames Research Center, Moffett Field, Calif.
**ANALYSIS OF FUEL-CONSERVATIVE CURVED DECELER-
ATING APPROACH TRAJECTORIES FOR POWERED-LIFT
AND CTOL JET AIRCRAFT**

Frank Neuman Apr. 1980 38 p refs
(NASA-TP-1650; A-7988) Avail: NTIS HC A03/MF A01 CSCL
02A

A method for determining fuel conservative terminal approaches that include changes in altitude, speed, and heading are described. Three different guidance system concepts for STOL aircraft were evaluated in flight: (1) a fixed trajectory system; (2) a system that included a fixed path and a real time synthesized capture flight path; and (3) a trajectory synthesizing system. Simulation results for the augmentor wing jet STOL research aircraft and for the Boeing 727 aircraft are discussed. The results indicate that for minimum fuel consumption, two guidance deceleration segments are required.

A.W.H.

N80-19126*# National Aeronautics and Space Administration.
Ames Research Center, Moffett Field, Calif.
**APPLICATION OF THE CONCEPT OF DYNAMIC TRIM
CONTROL TO AUTOMATIC LANDING OF CARRIER
AIRCRAFT**

G. Allan Smith and George Meyer Apr. 1980 87 p refs
(NASA-TP-1512; A-7801) Avail: NTIS HC A05/MF A01 CSCL
01C

The results of a simulation study of an alternative design concept for an automatic landing control system are presented. The alternative design concept for an automatic landing control system is described. The design concept is the total aircraft flight control system (TAF COS). TAF COS is an open loop, feed forward system that commands the proper instantaneous thrust angle of attack, and roll angle to achieve the forces required to follow the desired trajectory. These dynamic trim conditions are determined by an inversion of the aircraft nonlinear force characteristics. The concept was applied to an A-7E aircraft approaching an aircraft carrier. The implementation details with an airborne digital computer are discussed. The automatic carrier landing situation is described. The simulation results are presented for a carrier approach with atmospheric disturbances, an approach with no disturbances, and for tailwind and headwind gusts.

A.W.H.

N80-25318*# National Aeronautics and Space Administration.
Ames Research Center, Moffett Field, Calif.
**LARGE-SCALE WIND-TUNNEL TESTS OF INVERTING
FLAPS ON A STOL UTILITY AIRCRAFT MODEL**

Terrell W. Feistel and Joseph P. Morelli Jun. 1980 56 p refs
(NASA-TP-1696; AVRADCOM-TM-80-A-1; A-7061) Avail:
NTIS HC A04/MF A01 CSCL 01C

A unique inverting flap system was investigated on a large scale deflected slipstream model in the Ames 40 by 80 foot wind tunnel. The subject tests utilized 33% chord double-slotted flaps on a low aspect ratio wing that was fully immersed in the propeller slipstream. Evaluation of the flap effectiveness is aided by comparisons with the results of tests of other flap systems on the same twin propeller, twin tail boom STOL utility aircraft mode. No extreme or abrupt force or moment increments were encountered when the flaps were deflected through a wide range, corresponding to the complete retraction/extension spectrum. The lift and descent capability of the inverting flaps compared very favorably with that of the other flap systems that have been tested on this model, including some with much greater mechanical complexity. As expected, the flaps caused large nose down, pitching moment increments at the high lift settings; however, the trimmed characteristics are still competitive with those obtained from the more complicated flap systems. It is believed that these flaps may have promising potential application to the design of relatively simple STOL utility aircraft with improved performance capabilities. In addition, they may merit consideration as retrofits to existing aircraft with less effective flap systems.

J.M.S.

N80-25588*# National Aeronautics and Space Administration. Ames Research Center, Moffett Field, Calif.
PROCEEDINGS OF THE AERO-OPTICS SYMPOSIUM ON ELECTROMAGNETIC WAVE PROPAGATION FROM AIRCRAFT

Apr. 1980 666 p refs Symp. held at Moffett Field, Calif., 14-15 Aug. 1979 Sponsored in part by AFWL (NASA-CP-2121; A-8090) Avail: NTIS HC A99/MF A01 CSCL 20D

Wind-tunnel and flight experiments concerning natural and induced turbulence around an airplane and the effects on propagation characteristics of an emitter mounted in the airplane are described. Some of the papers are concerned with phase distortion of the propagating radiation, and others deal with mechanical jitter of the optical elements when exposed to open-cavity turbulence. The results include both aerodynamic and optical measurements and a consideration of the relationship between the two. Primary emphasis is on the dynamic disturbances, but theoretical and experimental evaluations of steady-state distortions are also presented. For individual titles, see N80-25589 through N80-25612.

N80-28329*# National Aeronautics and Space Administration. Ames Research Center, Moffett Field, Calif.

ALGORITHM FOR FIXED-RANGE OPTIMAL TRAJECTORIES

Homer Q. Lee and Heinz Erzberger Jul. 1980 86 p refs (NASA-TP-1565; A-8003) Avail: NTIS HC A05/MF A01 CSCL 17G

An algorithm for synthesizing optimal aircraft trajectories for specified range was developed and implemented in a computer program written in FORTRAN IV. The algorithm, its computer implementation, and a set of example optimum trajectories for the Boeing 727-100 aircraft are described. The algorithm optimizes trajectories with respect to a cost function that is the weighted sum of fuel cost and time cost. The optimum trajectory consists at most of a three segments: climb, cruise, and descent. The climb and descent profiles are generated by integrating a simplified set of kinematic and dynamic equations wherein the total energy of the aircraft is the independent or time like variable. At each energy level the optimum airspeeds and thrust settings are obtained as the values that minimize the variational Hamiltonian. Although the emphasis is on an off-line, open-loop computation, eventually the most important application will be in an on-board flight management system. E.D.K.

NASA TECHNICAL MEMORANDA

N80-10516*# National Aeronautics and Space Administration. Ames Research Center, Moffett Field, Calif.

COUPLED ROTOR AND FUSELAGE EQUATIONS OF MOTION

William Warmbrodt Oct. 1979 82 p refs (NASA-TM-81153) Avail: NTIS HC A05/MF A01 CSCL 20K

The governing equations of motion of a helicopter rotor coupled to a rigid body fuselage are derived. A consistent formulation is used to derive nonlinear periodic coefficient equations of motion which are used to study coupled rotor/fuselage dynamics in forward flight. Rotor/fuselage coupling is documented and the importance of an ordering scheme in deriving nonlinear equations of motion is reviewed. The nature of the final equations and the use of multiblade coordinates are discussed. A.W.H.

N80-11033*# National Aeronautics and Space Administration. Ames Research Center, Moffett Field, Calif.

AERODYNAMIC INTERACTIONS FROM REACTION

CONTROLS FOR LATERAL CONTROL OF THE M2-F2 LIFTING-BODY ENTRY CONFIGURATION AT TRANSONIC AND SUPERSONIC AND SUPERSONIC MACH NUMBERS

Rodney O. Bailey and Jack J. Brownson Washington Nov. 1979 125 p refs (NASA-TM-78534; A-7624) Avail: NTIS HC A06/MF A01 CSCL 01A

Tests were conducted in the Ames 6 by 6 foot wind tunnel to determine the interaction of reaction jets for roll control on the M2-F2 lifting-body entry vehicle. Moment interactions are presented for a Mach number range of 0.6 to 1.7, a Reynolds number range of 1.2×10^6 to the 6th power to 1.6×10^6 to the 6th power (based on model reference length), an angle-of-attack range of -9 deg to 20 deg, and an angle-of-sideslip range of -6 deg to 6 deg at an angle of attack of 6 deg. The reaction jets produce roll control with small adverse yawing moment, which can be offset by horizontal thrust component of canted jets. A.R.H.

N80-12100*# National Aeronautics and Space Administration. Ames Research Center, Moffett Field, Calif.

V/STOL FLIGHT SIMULATION

Nov. 1979 52 p refs (NASA-TM-81156; A-8012) Avail: NTIS HC A04/MF A01 CSCL 01C

The requirements for a new research aircraft to provide in-flight V/STOL simulation were reviewed. The required capabilities were based on known limitations of ground based simulation and past/current experience with V/STOL inflight simulation. Results indicate that V/STOL inflight simulation capability is needed to aid in the design and development of high performance V/STOL aircraft. Although a new research V/STOL aircraft is preferred, an interim solution can be provided by use of the X-22A, the CH-47B, or the 4AV-8B aircraft modified for control/display flight research. R.C.T.

N80-12991*# National Aeronautics and Space Administration. Ames Research Center, Moffett Field, Calif.

IN DEPTH REVIEW OF THE 1979 AIAA LIGHTER-THAN-AIR SYSTEMS TECHNOLOGY CONFERENCE

Mark D. Ardema Nov. 1979 20 p Conf. held at Palo Alto, Calif., 11-13 Jul. 1979 (NASA-TM-81158) Avail: NASA. Ames Res. Center, Moffett Field, Calif. 94035 CSCL 02A

The lighter than air (LTA) systems technology conference is reviewed. Highlights of the conference were: (1) the interest shown in patrol and surveillance airships, particularly for coastal patrol missions; (2) the session devoted to overviews of foreign activity; and (3) heavy lift and long range transport aircraft design considerations. A.W.H.

N80-13003*# National Aeronautics and Space Administration. Ames Research Center, Moffett Field, Calif.

FORCE AND MOMENT DATA FROM A WIND-TUNNEL TEST OF A TILT-NACELLE V/STOL PROPULSION SYSTEM WITH AN ATTITUDE CONTROL VANE

Mark D. Betzina Nov. 1979 108 p refs (NASA-TM-81157; A-8013) Avail: NTIS HC A06/MF A01 CSCL 01A

A large scale, tilt nacelle V/STOL propulsion system, with an attitude control vane assembly mounted in the exhaust, was tested. The effectiveness of the control vane as well as the aerodynamic characteristics of the entire propulsion system were determined. The results, in the form of tabulated coefficients, for both the vane forces and moments and the total forces and moments produced by the propulsion system are presented. A.W.H.

N80-13041*# National Aeronautics and Space Administration. Ames Research Center, Moffett Field, Calif.

FLIGHT TEST OF NAVIGATION AND GUIDANCE SENSOR ERRORS MEASURED ON STOL APPROACHES

David N. Warner and F. J. Moran Dec. 1979 42 p
(NASA-TM-81154; A-8008) Avail: NASA. Ames Res. Center, Moffett Field, Calif. 20546 CSCL 01D

Navigation and guidance sensor error characteristics were measured during STOL approach-flight investigations. Data from some of the state sensors of a digital avionics system were compared to corresponding outputs from an inertial navigation system. These sensors include the vertical gyro, compass, and accelerometers. Barometric altimeter data were compared to altitude measured by a tracking radar. Data were recorded with the Augmentor Wing Jet STOL Research Aircraft parked and in flight.

Author

N80-14049*# National Aeronautics and Space Administration. Ames Research Center, Moffett Field, Calif.

EFFECT OF TIP PLANFORM ON BLADE LOADING CHARACTERISTICS FOR A TWO-BLADED ROTOR IN HOVER

John D. Ballard, Kenneth L. Orloff, and Alan B. Luebs (Gates Lear Corp., Wichita, Kan.) Nov. 1979 89 p refs
(NASA-TM-78615; A-7939) Avail: NTIS HC A05/MF A01 CSCL 01A

A laser velocimeter was used to study the flow surrounding a 2.13 m diam. two-bladed, teetering model-scale helicopter rotor operating in the hover condition. The rotor system employed interchangeable blade tips over the outer 25% radius. A conventional rectangular planform and an experimental ogee tip shape were studied. The radial distribution of the blade circulation was obtained by measuring the velocity tangent to a closed rectangular contour around the airfoil section at a number of radial locations. A relationship between local circulation and bound vorticity was invoked to obtain the radial variations in the sectional lifting properties of the blade. The tip vortex-induced velocity was also measured immediately behind the generating blade and immediately before the encounter with the following blade. The mutual influence between blade loading, shed vorticity, and the structure of the encountered vortex are quantified by the results presented and are discussed comparatively for the rectangular and ogee planforms. The experimental loading for the rectangular tip is also compared with predictions of existing rotor analysis.

Author

N80-14108* National Aeronautics and Space Administration. Ames Research Center, Moffett Field, Calif.

QUIET SHORT-HAUL RESEARCH AIRCRAFT FAMILIARIZATION DOCUMENT

Robert C. McCracken Nov. 1979 96 p
(NASA-TM-81149; A-7975) Avail: NASA. Ames Res. Center, Moffett Field, Calif. 94035 CSCL 01C

The design features and general characteristics of the NASA Quiet Short-Haul Research Aircraft are described. Aerodynamic characteristics and performance are discussed based on predictions and early flight-test data. Principle airplane systems, including the airborne data-acquisition system, are also described. The aircraft was designed and built to fulfill the need for a national research facility to explore the use of upper surface-blowing propulsive-lift technology in providing short takeoff and landing capability, and perform advanced experiments in various technical disciplines such as aerodynamics, propulsion, stability and control, handling qualities, avionics and flight-control systems, trailing-vortex phenomena, acoustics, structure and loads, operating systems, human factors, and airworthiness/certification criteria. An unusually austere approach using experimental shop practices resulted in a low cost and high research capability.

Author

N80-14138*# National Aeronautics and Space Administration. Ames Research Center, Moffett Field, Calif.

PILOT CONTROL THROUGH THE TAFCOS AUTOMATIC FLIGHT CONTROL SYSTEM

William R. Wehrend, Jr. Dec. 1979 42 p refs
(NASA-TM-81152; A-7996) Avail: NTIS HC A03/MF A01 CSCL 01C

The set of flight control logic used in a recently completed flight test program to evaluate the total automatic flight control system (TAFCOS) with the controller operating in a fully automatic mode, was used to perform an unmanned simulation on an IBM 380 computer in which the TAFCOS concept was extended to provide a multilevel pilot interface. A pilot TAFCOS interface for direct pilot control by use of a velocity-control-wheel-steering mode was defined as well as a means for calling up conventional autopilot modes. It is concluded that the TAFCOS structure is easily adaptable to the addition of a pilot control through a stick-wheel-throttle control similar to conventional airplane controls. Conventional autopilot modes, such as airspeed-hold, altitude-hold, heading-hold, and flight path angle-hold, can also be included.

A.R.H.

N80-15067*# National Aeronautics and Space Administration. Ames Research Center, Moffett Field, Calif.

NASA/ARMY XV-15 TILT ROTOR RESEARCH AIRCRAFT WIND-TUNNEL TEST PROGRAM PLAN

James A. Weiberg and Martin D. Maisel (AVRADCOM Res. and Technol. Labs.) Mar. 1979 73 p refs
(NASA-TM-78562; A-7740; AVRADCOM-TR-79-7(AM)) Avail: NASA. Ames Research Center, Moffett Field, Calif. 94035 CSCL 01C

To ensure that the XV-15 tilt rotor research aircraft will meet the requirements of the program plan and the contract model specification and statement of work, one of the two aircraft will be tested in the Ames 40 x 80 foot wind tunnel to provide an initial assessment of the aerodynamic characteristics, structural loads, and rotor/pylon/wing dynamics in a simulated flight environment for correlation with estimated values. The tests will also serve to verify the functional operation of the aircraft systems and on-board instrumentation in a flight environment. The management structure, operational plan, support requirements and responsibilities, safety provisions and reporting requirements for conduct of the wind tunnel tests are defined and related to other phases of the program.

A.R.H.

N80-16024*# National Aeronautics and Space Administration. Ames Research Center, Moffett Field, Calif.

NASA QUIET SHORT-HAUL RESEARCH AIRCRAFT EXPERIMENTERS' HANDBOOK

Robert C. McCracken Jan. 1980 29 p
(NASA-TM-81162; A-8053) Avail: NASA. Ames Research Center, Moffett Field, Calif. 94035 CSCL 02A

A summary of guidelines and particulars concerning the use of the NASA-Ames Research Center Quiet Short-Haul Research Aircraft for applicable flight experiments is presented. Procedures for submitting experiment proposals are included along with guidelines for experimenter packages, an outline of experiment selection processes, a brief aircraft description, and additional information regarding support at Ames.

J.M.S.

N80-16036*# National Aeronautics and Space Administration. Ames Research Center, Moffett Field, Calif.

A COMPARISON OF CALCULATED AND EXPERIMENTAL

LIFT AND PRESSURE DISTRIBUTIONS FOR SEVERAL HELICOPTER ROTOR SECTIONS

John Conlon Jan. 1980 33 p refs
(NASA-TM-81160; A-8029) Avail: NTIS HC A03/MF A01
CSCL 01A

The use of computational techniques in predicting lift coefficients and pressure distributions of two dimensional airfoil sections was studied. The computer code FLO6/IBL was used to solve the compressible, two dimensional flow about four different airfoil sections. The lift coefficients of the airfoils were calculated at various angles of attack at subsonic Mach numbers and compared with experimental data. A.W.H.

N80-16300*# National Aeronautics and Space Administration. Ames Research Center, Moffett Field, Calif.

TURBULENCE MEASUREMENTS IN THE BOUNDARY LAYER OF A LOW-SPEED WIND TUNNEL USING LASER VELOCIMETRY

Edward T. Schairer Feb. 1980 25 p refs
(NASA-TM-81165; A-8058) Avail: NTIS HC A02/MF A01
CSCL 20D

Laser velocimeter measurements in an incompressible, turbulent boundary layer along the wall of a low-speed wind tunnel are presented. The laser data are compared with existing hot-wire anemometer measurements of a flat plate, incompressible, turbulent, boundary layer with zero pressure gradient. An argument is presented to explain why previous laser velocimeter measurements in zero pressure gradient, turbulent boundary layers have shown an unexpected decrease in turbulent shear stresses near the wall. M.M.M.

N80-17717*# National Aeronautics and Space Administration. Ames Research Center, Moffett Field, Calif.

AN ASSESSMENT OF FUTURE COMPUTER SYSTEM NEEDS FOR LARGE-SCALE COMPUTATION

Peter Lykos and John White Feb. 1980 57 p Prepared in cooperation with Illinois Inst. of Tech., Chicago
(NASA-TM-78613; A-7929) Avail: NTIS HC A04/MF A01
CSCL 09B

Data ranging from specific computer capability requirements to opinions about the desirability of a national computer facility are summarized. It is concluded that considerable attention should be given to improving the user-machine interface. Otherwise, increased computer power may not improve the overall effectiveness of the machine user. Significant improvement in throughput requires highly concurrent systems plus the willingness of the user community to develop problem solutions for that kind of architecture. An unanticipated result was the expression of need for an on-going cross-disciplinary users group/forum in order to share experiences and to more effectively communicate needs to the manufacturers. K.L.

N80-18047*# National Aeronautics and Space Administration. Ames Research Center, Moffett Field, Calif.

V/STOLAND AVIONICS SYSTEM FLIGHT-TEST DATA ON A UH-1H HELICOPTER

Fredric A. Baker, Dean N. Jaynes, Lloyd D. Corliss, Sam Liden (Sperry Rand Corp., Phoenix, Ariz.), Robert B. Merrick, and Daniel C. Dugan Feb. 1980 68 p refs
(NASA-TM-78591; A-7831) Avail: NTIS HC A04/MF A01
CSCL 01C

The flight-acceptance test results obtained during the acceptance tests of the V/STOLAND (versatile simplex digital avionics system) digital avionics system on a Bell UH-1H helicopter in 1977 at Ames Research Center are presented. The system provides navigation, guidance, control, and display functions for NASA terminal area VTOL research programs and for the Army handling qualities research programs at Ames Research Center.

The acceptance test verified system performance and contractual acceptability. The V/STOLAND hardware navigation, guidance, and control laws resident in the digital computers are described. Typical flight-test data are shown and discussed as documentation of the system performance at acceptance from the contractor. M.M.M.

N80-19025*# National Aeronautics and Space Administration. Ames Research Center, Moffett Field, Calif.

WORKSHOP ON AIRCRAFT SURFACE REPRESENTATION FOR AERODYNAMIC COMPUTATION

T. J. Gregory, ed. and John Ashbaugh, ed. Feb. 1980 560 p Workshop held at Ames Research Center, Moffett Field, Calif., 1-2 Mar. 1978
(NASA-TM-81170; A-8075) Avail: NTIS HC A24/MF A01
CSCL 02A

Papers and discussions on surface representation and its integration with aerodynamics, computers, graphics, wind tunnel model fabrication, and flow field grid generation are presented. Surface definition is emphasized. R.E.S.

N80-19127*# National Aeronautics and Space Administration. Ames Research Center, Moffett Field, Calif.

FLIGHT EVALUATION OF CONFIGURATION MANAGEMENT SYSTEM CONCEPTS DURING TRANSITION TO THE LANDING APPROACH FOR A POWERED-LIFT STOL AIRCRAFT

James A. Franklin and Robert C. Innis Mar. 1980 32 p refs
(NASA-TM-81146; A-7957) Avail: NTIS HC A03/MF A01
CSCL 01C

Flight experiments were conducted to evaluate two control concepts for configuration management during the transition to landing approach for a powered-lift STOL aircraft. NASA Ames' augmentor wing research aircraft was used in the program. Transitions from nominal level-flight configurations at terminal area pattern speeds were conducted along straight and curved descending flightpaths. Stabilization and command augmentation for attitude and airspeed control were used in conjunction with a three-cue flight director that presented commands for pitch, roll, and throttle controls. A prototype microwave system provided landing guidance. Results of these flight experiments indicate that these configuration management concepts permit the successful performance of transitions and approaches along curved paths by powered-lift STOL aircraft. Flight director guidance was essential to accomplish the task. Author

N80-21286*# National Aeronautics and Space Administration. Ames Research Center, Moffett Field, Calif.

THREE-DIMENSIONAL INTERACTIONS AND VORTICAL FLOWS WITH EMPHASIS ON HIGH SPEEDS

David J. Peake and Murray Tobak Mar. 1980 225 p refs
(NASA-TM-81169; A-6035) Avail: NTIS HC A10/MF A01
CSCL 01A

Diverse kinds of three-dimensional regions of separation in laminar and turbulent boundary layers are discussed that exist on lifting aerodynamic configurations immersed in flows from subsonic to hypersonic speeds. In all cases of three dimensional flow separation, the assumption of continuous vector fields of skin-friction lines and external-flow streamlines, coupled with simple topology laws, provides a flow grammar whose elemental constituents are the singular points: nodes, foci, and saddles. Adopting these notions enables one to create sequences of plausible flow structures, to deduce mean flow characteristics, expose flow mechanisms, and to aid theory and experiment where lack of resolution in numerical calculations or wind tunnel observation causes imprecision in diagnosing the three dimensional flow features. R.E.S.

N80-21287*# National Aeronautics and Space Administration. Ames Research Center, Moffett Field, Calif.

AN EXPERIMENTAL EVALUATION OF A HELICOPTER ROTOR SECTION DESIGNED BY NUMERICAL OPTIMIZATION

R. M. Hicks and W. J. McCroskey (Army Aviation Res. and Development Command, St. Louis, Mo.) Mar. 1980 131 p refs

(NASA-TM-78622; AVRADCOM-TR-79-44; A-7956) Avail: NTIS HC A07/MF A01 CSCL 01C

The wind tunnel performance of a 10-percent thick helicopter rotor section design by numerical optimization is presented. The model was tested at Mach number from 0.2 to 0.84 with Reynolds number ranging from 1,900,000 at Mach 0.2 to 4,000,000 at Mach numbers above 0.5. The airfoil section exhibited maximum lift coefficients greater than 1.3 at Mach numbers below 0.45 and a drag divergence Mach number of 0.82 for lift coefficients near 0. A moderate 'drag creep' is observed at low lift coefficients for Mach numbers greater than 0.6. M.G.

N80-22297*# National Aeronautics and Space Administration. Ames Research Center, Moffett Field, Calif.

A NEW ALGORITHM FOR HORIZONTAL CAPTURE TRAJECTORIES

John D. McLean Mar. 1980 21 p refs

(NASA-TM-81186; A-8111) Avail: NTIS HC A02/MF A01 CSCL 17G

An algorithm which transfers an aircraft from an initial position and heading to a final position and heading was developed for onboard synthesis of horizontal flight paths. The algorithm finds all solutions possible, and selects the one with minimum path length. Degenerate conditions in which one or more of the basic segments is missing are handled without difficulty. The solution to this problem is derived, and a FORTRAN listing of the algorithm is provided. E.D.K.

N80-23249* National Aeronautics and Space Administration. Ames Research Center, Moffett Field, Calif.

CONCEPTUAL STUDIES OF A LONG-RANGE TRANSPORT WITH AN UPPER SURFACE BLOWING PROPULSIVE LIFT SYSTEM

John A. Cochran May 1980 24 p

(NASA-TM-81196; A-8169) Avail: NASA. Ames Res. Center, Moffett Field, Calif. 94035 CSCL 01C

The application of propulsive lift technology to the long range, heavy lift transport mission was studied. The level of propulsive lift technology studied was that which is represented by the Quiet Short-Haul Research Aircraft (QSRA). This technology uses the upper surface blowing technique (USB) to develop high lift coefficients. Results indicate that field lengths of less than 3000 ft are feasible at landing gross weights and that even at maximum takeoff gross weight, a reduction in field length is available as compared to a conventional aircraft. Further study of the concept is recommended. J.M.S.

N80-23295* National Aeronautics and Space Administration. Ames Research Center, Moffett Field, Calif.

OPERATIONS MANUAL: VERTICAL MOTION SIMULATOR (VMS) S.08

A. David Jones May 1980 70 p

(NASA-TM-81180; A-8095) Avail: Issuing Activity CSCL 14B

The Ames Research Center Vertical Motion Simulator (VMS) is described in terms useful to the researcher who intends to use it. A description of the VMS and its performance are presented together with the administrative policies governing its operation. The management controls over its use are detailed, including data requirements, user responsibilities, and scheduling procedures. This information is given in a form that should facilitate communication with the NASA operations group during initial simulator use. J.M.S.

N80-23317*# National Aeronautics and Space Administration. Ames Research Center, Moffett Field, Calif.

STATIC CALIBRATION OF A TWO-DIMENSIONAL WEDGE NOZZLE WITH THRUST VECTORING AND SPANWISE BLOWING

Michael J. Harris (Naval Ship Research and Development Center, Bethesda, Md.) and Michael D. Falarski Apr. 1980 38 p refs (NASA-TM-81161; A-8043) Avail: NTIS HC A03/MF A01 CSCL 21E

The results of a static calibration of the two dimensional wedge nozzles on a STOL configuration of a large-scale fighter model are reported. These nozzles internally turn the efflux produced by two turbojets down 25 degrees and exhaust it over the deflected trailing edge of the wing. This arrangement provides direct thrust lift, enhances wing lift by producing supercirculation, and provides thrust vectoring by varying the deflection of the wing's trailing edge. The thrust is vectored from 10 deg to 38 deg. This system was calibrated with spanwise blowing for augmentation of the leading-edge vortex. When 16% of the turbojet efflux is blown spanwise, the thrust recovered is 92% of the thrust produced when the total efflux is exhausted longitudinally. E.D.K.

N80-24262*# National Aeronautics and Space Administration. Ames Research Center, Moffett Field, Calif.

COMPARISON OF CALCULATED AND MEASURED MODEL ROTOR LOADING AND WAKE GEOMETRY

Wayne Johnson Apr. 1980 34 p refs Prepared in cooperation with Army Research and Technology Labs., Moffett Field, Calif. (NASA-TM-81189; AVRADCOM-TR-80-A-4; A-8149) Avail: NTIS HC A03/MF A01 CSCL 01A

The calculated blade bound circulation and wake geometry are compared with measured results for a model helicopter rotor in hover and forward flight. Hover results are presented for rectangular tip and ogee tip planform blades. The correlation is quite good when the measured wake geometry characteristics are used in the analysis. Available prescribed wake geometry models are found to give fair predictions of the loading, but they do not produce a reasonable prediction of the induced power. Forward flight results are presented for twisted and untwisted blades. Fair correlation between measurements and calculations is found for the bound circulation distribution on the advancing side. The tip vortex geometry in the vicinity of the advancing blade in forward flight was predicted well by the free wake calculation used, although the wake geometry did not have a significant influence on the calculated loading and performance for the cases considered. Author

N80-24293*# National Aeronautics and Space Administration. Ames Research Center, Moffett Field, Calif.

A CANDIDATE V/STOL RESEARCH AIRCRAFT DESIGN CONCEPT USING AN S-3A AIRCRAFT AND 2 PEGASUS 11 ENGINES

Bedford A. Lampkin May 1980 24 p refs

(NASA-TM-81204; A-8197) Avail: NTIS HC A02/MF A01 CSCL 01C

A candidate V/STOL research aircraft concept which uses an S-3A airframe and two Pegasus 11 engines was studied to identify a feasible V/STOL national flight facility that could be obtained at the lowest possible cost for the demonstration of V/STOL technology, inflight simulation, and flight research. The rationale for choosing the configuration, a description of the configuration, and the capability of a fully developed aircraft are discussed. R.E.S.

N80-24294*# National Aeronautics and Space Administration. Ames Research Center, Moffett Field, Calif.

WIND-TUNNEL TESTS OF THE XV-15 TILT ROTOR AIRCRAFT

James A. Weiberg and Martin D. Maisel Apr. 1980 133 p refs Prepared in cooperation with Army Research and Technology Labs., Moffett field, Calif.
(NASA-TM-81177; AVRADCOM-TR-80-A-3; A-8089) Avail: NTIS HC A07/MF A01 CSCL 01C

The XV-15 aircraft was tested in the Ames 40 by 80 Foot Wind Tunnel for preliminary evaluation of aerodynamic and aeroelastic characteristics prior to flight. The tests were undertaken to investigate the aircraft performance, stability, control and structural loads for flight modes from helicopter through transition and airplane mode up to the tunnel capability of 170 knots. Results from these tests are presented. Author

N80-25306*# National Aeronautics and Space Administration. Ames Research Center, Moffett Field, Calif.
EQUATIONS FOR DETERMINING AIRCRAFT MOTIONS FOR ACCIDENT DATA

Ralph E. Bach, Jr. and Rodney C. Wingrove Jun. 1980 24 p refs
(NASA-TM-78609; A-7913) Avail: NTIS HC A02/MF A01 CSCL 01C

Procedures for determining a comprehensive accident scenario from a limited data set are reported. The analysis techniques accept and process data from either an Air Traffic Control radar tracking system or a foil flight data recorder. Local meteorological information at the time of the accident and aircraft performance data are also utilized. Equations for the desired aircraft motions and forces are given in terms of elements of the measurement set and certain of their time derivatives. The principal assumption made is that aircraft side force and side-slip angle are negligible. An estimation procedure is outlined for use with each data source. For the foil case, a discussion of exploiting measurement redundancy is given. Since either formulation requires estimates of measurement time derivatives, an algorithm for least squares smoothing is provided. E.D.K.

N80-27287*# National Aeronautics and Space Administration. Ames Research Center, Moffett Field, Calif.

EXPERIMENTAL STUDIES OF SCALE EFFECTS ON OSCILLATING AIRFOILS AT TRANSONIC SPEEDS

Sanford S. Davis Jul. 1980 16 p refs
(NASA-TM-81216; A-8259) Avail: NTIS HC A02/MF A01 CSCL 01A

Experimental data are presented on the effect of Reynolds number on unsteady pressures induced by the pitching motion of an oscillating airfoil. Scale effects are discussed with reference to a conventional airfoil (NACA 64A010) and a supercritical airfoil (NLR 7301) at mean-flow conditions that support both weak and strong shock waves. During the experiment the Reynolds number was varied from 3,000,000 to 12,000,000 at a Mach number and incidence necessary to induce the required flow. Both fundamental frequency and complete time history data are presented over the range of reduced frequencies that is important in aeroelastic applications. The experimental data show that viscous effects are important in the case of the supercritical airfoil at all flow conditions and in the case of the conventional airfoil under strong shock-wave conditions. Some frequency-dependent viscous effects were also observed. Author

N80-28296*# National Aeronautics and Space Administration. Ames Research Center, Moffett Field, Calif.

A COMPREHENSIVE ANALYTICAL MODEL OF ROTORCRAFT AERODYNAMICS AND DYNAMICS. PART 1: ANALYSIS DEVELOPMENT

Wayne Johnson Jun. 1980 442 p refs Prepared in cooperation with Army Aviation Research and Development Command, Moffett Field, Calif. 2 Vol.
(NASA-TM-81182; AVRADCOM-TR-80-A-5-Pt-1; A-8100) Avail: NTIS HC A19/MF A01 CSCL 01B

Structural, inertia, and aerodynamic models were combined to form a comprehensive model of rotor aerodynamics and dynamics that is applicable to a wide range of problems and a wide class of vehicles. A digital computer program is used to calculate rotor performance, loads, and noise; helicopter vibration and gust response; flight dynamics and handling qualities; and system aeroelastic stability. The analysis is intended for use in the design, testing, and evaluation of rotors and rotorcraft, and to be a basis for further development of rotary wing theories.

A.R.H.

N80-28297*# National Aeronautics and Space Administration. Ames Research Center, Moffett Field, Calif.

A COMPREHENSIVE ANALYTICAL MODEL OF ROTORCRAFT AERODYNAMICS AND DYNAMICS. PART 2: USER'S MANUAL

Wayne Johnson Jul. 1980 97 p Prepared in cooperation with Army Aviation Research and Development Command, Moffett Field, Calif. 2 Vol.

(NASA-TM-81183; AVRADCOM-TR-80-A-6-Pt-2; A-8101) Avail: NTIS HC A05/MF A01 CSCL 01B

The use of a computer program for a comprehensive analytical model of rotorcraft aerodynamics and dynamics is described. The program calculates the loads and motion of helicopter rotors and airframe. First the trim solution is obtained, then the flutter, flight dynamics, and/or transient behavior can be calculated. Either a new job can be initiated or further calculations can be performed for an old job. E.D.K.

N80-28298*# National Aeronautics and Space Administration. Ames Research Center, Moffett Field, Calif.

A COMPREHENSIVE ANALYTICAL MODEL OF ROTORCRAFT AERODYNAMICS AND DYNAMICS. PART 3: PROGRAM MANUAL

Wayne Johnson Jun. 1980 155 p Prepared in cooperation with Army Aviation Research and Development Command, St. Louis, Mo.

(NASA-TM-81184; AVRADCOM-TR-80-A-7; A-8102) Avail: NTIS HC A08/MF A01 CSCL 01B

The computer program for a comprehensive analytical model of rotorcraft aerodynamics and dynamics is described. This analysis is designed to calculate rotor performance, loads, and noise; the helicopter vibration and gust response; the flight dynamics and handling qualities; and the system aeroelastic stability. The analysis is a combination of structural, inertial, and aerodynamic models that is applicable to a wide range of problems and a wide class of vehicles. The analysis is intended for use in the design, testing, and evaluation of rotors and rotorcraft and to be a basis for further development of rotary wing theories.

Author

N80-28305*# Oklahoma State Univ., Stillwater. School of Mechanical and Aerospace Engineering.

STUDY OF BOUNDARY-LAYER TRANSITION USING TRANSONIC-CONE PRESTON TUBE DATA Semiannual Progress Report, Jan. - Jun. 1980

T. D. Reed and P. M. Moretti Jun. 1980 99 p refs
(Contract NsG-2396)
(NASA-TM-81103) Avail: NTIS HC A05/MF A01 CSCL 01A

The laminar boundary layer on a 10 degree cone in a transonic wind tunnel was studied. The inviscid flow and boundary layer development were simulated by computer programs. The effects of pitch and yaw angles on the boundary layer were examined. Preston-tube data, taken on the boundary-layer-transition cone in the NASA Ames 11 ft transonic wind tunnel, were used to develop a correlation which relates the measurements to theoretical values of laminar skin friction. The recommended correlation is based on a compressible form of the classical law-of-the-wall. The computer codes successfully simulate the laminar boundary layer for near-zero pitch and yaw angles.

However, in cases of significant pitch and/or yaw angles, the flow is three dimensional and the boundary layer computer code used here cannot provide a satisfactory model. The skin-friction correlation is thought to be valid for body geometries other than cones. A.R.H.

N80-28338* National Aeronautics and Space Administration. Ames Research Center, Moffett Field, Calif.

A PILOTED SIMULATOR ANALYSIS OF THE CARRIER LANDING CAPABILITY OF THE QUIET SHORT-HAUL RESEARCH AIRCRAFT

Dennis W. Riddle Jul. 1980 41 p refs
(NASA-TM-78508; A-7528) Avail: NASA. Ames Res. Center, Moffett Field, Calif. 94035 CSCL 01C

A moving-base carrier landing simulation was conducted to evaluate the carrier landing capability of the Quiet Short-Haul Research Aircraft. Statistical results show that for an optimized approach configuration utilizing direct lift control, landings to a full stop can be safely executed (without use of arresting gear) with 40% of the landing deck remaining and without exceeding 50% of the design touchdown sink rate. Even under adverse sea state and wind conditions, the maximum allowable touchdown sink rate and minimum touchdown pitch attitude limits were never exceeded. Using the optimized approach configuration, successful go-arounds can be executed at any time during the approach, even when into the landing flare maneuver. L.F.M.

N80-28340* National Aeronautics and Space Administration. Ames Research Center, Moffett Field, Calif.

PARAMETRIC STUDY OF MODERN AIRSHIP PRODUCTIVITY

Mark D. Ardema and Kenneth Flaig Jul. 1980 52 p refs
(NASA-TM-81151; A-7993) Avail: NTIS HC A04/MF A01 CSCL 01C

A method for estimating the specific productivity of both hybrid and fully buoyant airships is developed. Various methods of estimating structural weight of deltoid hybrids are discussed and a derived weight estimating relationship is presented. Specific productivity is used as a figure of merit in a parametric study of fully buoyant ellipsoidal and deltoid hybrid semi-buoyant vehicles. The sensitivity of results as a function of assumptions is also determined. No airship configurations were found to have superior specific productivity to transport airplanes. L.F.M.

N80-28341* National Aeronautics and Space Administration. Ames Research Center, Moffett Field, Calif.

A PILOT'S ASSESSMENT OF HELICOPTER HANDLING-QUALITY FACTORS COMMON TO BOTH AGILITY AND INSTRUMENT FLYING TASKS

Ronald M. Gerdes Jul. 1980 20 p refs
(NASA-TM-81217; A-8263) Avail: NTIS HC A02/MF A01 CSCL 01C

A series of simulation and flight investigations were undertaken to evaluate helicopter flying qualities and the effects of control system augmentation for nap-of-the-Earth (NOE) agility and instrument flying tasks. Handling quality factors common to both tasks were identified. Precise attitude control was determined to be a key requirement for successful accomplishment of both tasks. Factors that degraded attitude controllability were improper levels of control sensitivity and damping, and rotor system cross coupling due to helicopter angular rate and collective pitch input. Application of rate command, attitude command, and control input decouple augmentation schemes enhanced attitude control and significantly improved handling qualities for both tasks. The NOE agility and instrument flying handling quality considerations, pilot rating philosophy, and supplemental flight evaluations are also discussed. L.F.M.

N80-28371* National Aeronautics and Space Administration. Ames Research Center, Moffett Field, Calif.

A MATHEMATICAL REPRESENTATION OF AN ADVANCED HELICOPTER FOR PILOTED SIMULATOR INVESTIGATIONS OF CONTROL SYSTEM AND DISPLAY VARIATIONS

Edwin W. Aiken Jul. 1980 51 p refs
(NASA-TM-81203; AVRADCOM-TM-80-A-02; A-8194) Avail: NTIS HC A04/MF A01 CSCL 01C

A mathematical model of an advanced helicopter is described. The model is suitable for use in control/display research involving piloted simulation. The general design approach for the six degree of freedom equations of motion is to use the full set of nonlinear gravitational and inertial terms of the equations and to express the aerodynamic forces and moments as the reference values and first order terms of a Taylor series expansion about a reference trajectory defined as a function of longitudinal airspeed. Provisions for several different specific and generic flight control systems are included in the model. The logic required to drive various flight control and weapon delivery symbols on a pilot's electronic display is also provided. Finally, the model includes a simplified representation of low altitude wind and turbulence effects. This model was used in a piloted simulator investigation of the effects of control system and display variations for an attack helicopter mission. L.F.M.

N80-28373* National Aeronautics and Space Administration. Ames Research Center, Moffett Field, Calif. Flight Research Lab.

A SUMMARY OF JOINT US-CANADIAN AUGMENTOR WING POWERED-LIFT STOL RESEARCH PROGRAMS AT THE AMES RESEARCH CENTER, NASA, 1975-1980

W. S. Hindson (National Research Council of Canada, Ottawa) and G. Hardy Jul. 1980 64 p refs Presented at Canadian Aeron. Inst. Meeting, Ottawa, 25-26 Mar. 1980
(NASA-TM-81215; LTR-FR-75) Avail: NTIS HC A04/MF A01 CSCL 01C

Several different flight research programs carried out by NASA and the Canadian Government using the Augmentor Wing Jet STOL Research Aircraft to investigate the design, operational, and systems requirements for powered-lift STOL aircraft are summarized. Some of these programs considered handling qualities and certification criteria for this class of aircraft, and addressed pilot control techniques, control system design, and improved cockpit displays for the powered-lift STOL approach configuration. Other programs involved exploiting the potential of STOL aircraft for constrained terminal-area approaches within the context of present or future air traffic control environments. Both manual and automatic flight control investigations are discussed, and an extensive bibliography of the flight programs is included. Author

N80-29255* National Aeronautics and Space Administration. Ames Research Center, Moffett Field, Calif.

ANALYSIS OF TRANSONIC SWEPT WINGS USING ASYMPTOTIC AND OTHER NUMERICAL METHODS

H. K. Cheng, S. Y. Meng, R. Chow (Grumman Aerospace Corp., Bethpage, N.Y.), and R. Smith May 1980 31 p refs Presented at the 18th AIAA Aerospace Sci. Meeting, Pasadena, Calif., 14-16 Jan. 1980 Prepared in cooperation with Univ. of Southern California, Los Angeles
(Contract N00014-75-C-0520; NR Proj. 061-192)
(NASA-TM-80762; AD-A085587; USCAE-138) Avail: NTIS HC A03/MF A01 CSCL 20/4

Asymptotic theories for high-aspect-ratio wings in transonic flow developed recently show that the three dimensional (3-D) mixed-flow calculations may be reduced to solving a set of 2-D problems at each span station. For wings with surfaces generated from a single airfoil shape, local similitude exists in the 3-D flow structure, permitting the problems to be solved once for all span stations. This paper reviews this theoretical development. The essential elements in the theory will be identified. Their relationship to the lifting-line theory and related classical methods are discussed. Examples of similarity solutions are

demonstrated for high subcritical and slightly super-critical component flows; comparisons with relaxation solutions to a full potential equation are made. The study also examines the adequacy of the existing full-potential computer code. Outstanding problems remaining for subsequent development are discussed. GRA

N80-29295* National Aeronautics and Space Administration. Ames Research Center, Moffett Field, Calif.

A HEAD-UP DISPLAY FORMAT FOR APPLICATION TO TRANSPORT AIRCRAFT APPROACH AND LANDING

Richard S. Bray Jul. 1980 42 p
(NASA-TM-81199; A-8180) Avail: NTIS HC A03/MF A01 CSCL 01D

A head up display (HUD) format used in simulator studies of the application of HUD to the landing of civil transport aircraft is described in detail. The display features an indication of the aircraft's instantaneous flightpath that constitutes the primary controlled element. Discrete ILS error and altitude signals are scaled and positioned to provide precise guidance modes when tracked with the flightpath symbol. Consideration is given to both the availability and nonavailability of inertial velocity information in the aircraft. Author

N80-31386* National Aeronautics and Space Administration. Ames Research Center, Moffett Field, Calif.

COMPARISON OF CALCULATED AND MEASURED BLADE LOADS ON A FULL-SCALE TILTING PROPROTOR IN A WIND TUNNEL

Wayne Johnson Sep. 1980 22 p Prepared in cooperation with Army Aviation Research and Development Command, St. Louis, Mo.

(NASA-TM-81228; USAVRADCOM-TR-80-A-8) Avail: NTIS HC A02/MF A01 CSCL 01C

The loads measured in a wind tunnel on a full-scale tilting propotor are compared with calculated results. The data consists primarily of oscillatory beamwise bending moments at 35% radial station, oscillatory spindle chord bending moments, and oscillatory pitch link loads. The measured and calculated results as a function of thrust are compared over a range of nacelle angles from 0 to 75 deg, and a range of speeds from 80 to 185 knots.T.M.

N80-31407* National Aeronautics and Space Administration. Ames Research Center, Moffett Field, Calif.

EFFECTS OF ROTOR PARAMETER VARIATIONS ON HANDLING QUALITIES OF UNAUGMENTED HELICOPTERS IN SIMULATED TERRAIN FLIGHT

Peter D. Talbot, Daniel D. Dugan, Robert T. N. Chen, and Ronald M. Gerdes Aug. 1980 88 p refs
(NASA-TM-81190; A-8158) Avail: NTIS HC A05/MF A01 CSCL 01C

A coordinated analysis and ground simulator experiment was performed to investigate the effects on single rotor helicopter handling qualities of systematic variations in the main rotor hinge restraint, hub hinge offset, pitch-flap coupling, and blade lock number. Teetering rotor, articulated rotor, and hingeless rotor helicopters were evaluated by research pilots in special low level flying tasks involving obstacle avoidance at 60 to 100 knots airspeed. The results of the experiment are in the form of pilot ratings, pilot commentary, and some objective performance measures. Criteria for damping and sensitivity are reexamined when combined with the additional factors of cross coupling due to pitch and roll rates, pitch coupling with collective pitch, and longitudinal static stability. Ratings obtained with and without motion are compared. Acceptable flying qualities were obtained within each rotor type by suitable adjustment of the hub parameters, however, pure teetering rotors were found to lack control power for the tasks. A limit for the coupling parameter $L_{sub q/L_{sub p}}$ of 0.35 is suggested. Author

N80-33345* National Aeronautics and Space Administration. Ames Research Center, Moffett Field, Calif.

EXPERIMENTAL UNSTEADY AERODYNAMICS OF CONVENTIONAL AND SUPERCRITICAL AIRFOILS

Sanford S. Davis and Gerald Malcolm, N. Aug. 1980 100 p refs Document includes a microfiche supplement
(NASA-TM-81221; A-8294) Avail: NTIS HC A04/MF A01 CSCL 01A

Experimental data on the unsteady aerodynamics of oscillating airfoils in transonic flow are presented. Two 0.5 m-chord airfoil models - an NACA 64A010 and an NLR 7301 - were tested in the NASA-Ames 11 by 11 foot Transonic Wind Tunnel at Mach numbers to 0.85, at chord Reynolds numbers to 12 million and at mean angles of attack to 4 deg. The airfoils were subjected to both pitching and plunging motions at reduced frequencies to 0.3 (physical frequencies to 53 Hz). The new hardware and the extensive use of computer-experiment integration developed for this test are described. The geometrical configuration of the model and the test arrangement are described in detail. Mean and first harmonic data are presented in both tabular and graphical form to aid in comparisons with other data and with numerical computations. T.M.

N80-33349* National Aeronautics and Space Administration. Ames Research Center, Moffett Field, Calif.

COMPARISON OF CALCULATED AND MEASURED HELICOPTER ROTOR LATERAL FLAPPING ANGLES

Wayne Johnson Jul. 1980 27 p refs Prepared in cooperation with Army Aviation Research and Development Command, St. Louis, Mo.

(NASA-TM-81213; AVRADCOM-TR-80-A-11; A-8239) Avail: NTIS HC A03/MF A01 CSCL 01A

Calculated and measured values of helicopter rotor flapping angles in forward flight are compared for a model rotor in a wind tunnel and an autogiro in gliding flight. The lateral flapping angles can be accurately predicted when a calculation of the nonuniform wake-induced velocity is used. At low advance ratios, it is also necessary to use a free wake geometry calculation. For the cases considered, the tip vortices in the rotor wake remain very close to the tip-path plane, so the calculated values of the flapping motion are sensitive to the fine details of the wake structure, specifically the viscous core radius of the tip vortices. Author

N80-33777* National Aeronautics and Space Administration. Ames Research Center, Moffett Field, Calif.

STABILITY OF NONUNIFORM ROTOR BLADES IN HOVER USING A MIXED FORMULATION

Wendell B. Stephens (Army Research and Technology Labs., Moffett Field, Calif.), Dewwy H. Hodges (Army Research and Technology Labs., Moffett Field, Calif.), John H. Avila (Technology Development of California, Santa Clara), and Ru-Mei Kung (Technology Development of California, Santa Clara) Aug. 1980 23 p refs Presented at the 6th European Rotorcraft and Powered Lift Aircraft Forum, Bristol, England, 16-19 Sep. 1980
(NASA-TM-81226; A-8314; AVRADCOM-TR-80-A-10; Paper-13) Avail: NTIS HC A02/MF A01 CSCL 01C

A mixed formulation for calculating static equilibrium and stability eigenvalues of nonuniform rotor blades in hover is presented. The static equilibrium equations are nonlinear and are solved by an accurate and efficient collocation method. The linearized perturbation equations are solved by a one step, second order integration scheme. The numerical results correlate very well with published results from a nearly identical stability analysis based on a displacement formulation. Slight differences in the results are traced to terms in the equations that relate moments to derivatives of rotations. With the present ordering scheme, in which terms of the order of squares of rotations are neglected with respect to unity, it is not possible to achieve completely equivalent models based on mixed and displacement formulations. The one step methods reveal that a second order Taylor expansion is necessary to achieve good convergence for nonuniform rotating

blades. Numerical results for a hypothetical nonuniform blade, including the nonlinear static equilibrium solution, were obtained with no more effort or computer time than that required for a uniform blade. Author

X80-10130*# National Aeronautics and Space Administration. Ames Research Center, Moffett Field, Calif.
TEST RESULTS FROM A JET-EFFECTS V/STOL FIGHTER MODEL WITH VECTORING NON-AXISYMMETRIC NOZZLES Final Report
 D. B. Smeltzer and A. D. Levin Jun. 1980 792 p refs
 (NASA-TM-81210; A-8224) Unclassified report

NOTICE: Available to U.S. Government Agencies and NASA Contractors.

A 1/8-scale jet effects model of a twin-engined V/STOL fighter was tested in the 11 foot transonic wind tunnel at Ames Research Center. The effect of various nozzle configurations on the model forces, moments and surface pressures was measured. Various exhaust nozzle configurations representing both vectored and nonvectored thrust were investigated. Lift, drag, pitching moment were obtained for the entire metric portion of the model (the vertical tails were not metric) and for one exhaust nozzle. Approximately 200 surface static pressures were also measured. Nozzles with two-dimensional geometries representing flight at cruise, combat, and dash were tested with vectored and nonvectored thrust. A reference circular nozzle and an elliptical nozzle were also tested with nonvectored thrust. The test matrix included Mach numbers from 0.4 to 1.4; angles of attack from 0 deg to 12 deg; nozzle pressure ratios from 1 to 10; and nozzle deflections from 0 deg to 20 deg. The Reynolds number was held constant at 8,200,000 per meter for all testing. Author

NASA CONTRACTOR REPORTS

N80-10137*# Michigan Univ., Ann Arbor. Dept. of Aerospace Engineering.
MATH MODELING AND COMPUTER MECHANIZATION FOR REAL TIME SIMULATION OF ROTARY-WING AIRCRAFT Final Report, 1 Jun. 1977 - 31 Mar. 1979
 Robert M. Howe Mar. 1979 21 p refs
 (Grant NSG-2245)
 (NASA-CR-162400) Avail: NTIS HC A02/MF A01 CSCL 01A

Mathematical modeling and computer mechanization for real time simulation of rotary wing aircraft is discussed. Error analysis in the digital simulation of dynamic systems, such as rotary wing aircraft is described. The method for digital simulation of nonlinearities with discontinuities, such as exist in typical flight control systems and rotor blade hinges, is discussed. A.W.H.

N80-10148*# Northwestern Univ., Evanston, Ill. Transportation Center.
FACTORS AFFECTING THE RETIREMENT OF COMMERCIAL TRANSPORT JET AIRCRAFT
 Frank A. Spencer Aug. 1979 296 p refs
 (Grant NSG-2149)
 (NASA-CR-152308) Avail: NTIS HC A13/MF A01 CSCL 01C

The historical background of the technology and economics of aircraft replacement and retirement in the prejet era is reviewed in order to determine whether useful insights can be obtained applicable to the jet era. Significant differences between the two periods are noted. New factors are identified and examined. Topics discussed include concern over current policies regarding deregulation, regulatory reform, and retroactive noise regulations; financing and compliance legislation; aging; economic environment

and inflation; technological progress; fuel efficiency and cost; and a financial perspective of replacement decisions. A.R.H.

N80-11097*# Systems Technology, Inc., Mountain View, Calif.
A COMPILATION AND ANALYSIS OF HELICOPTER HANDLING QUALITIES DATA. VOLUME 1: DATA COMPILATION Report, Sep. 1976 - Feb. 1978
 Robert K. Heffley, Wayne F. Jewell, John M. Lehman, and Richard A. VanWinkle Aug. 1979 387 p refs
 (Contract NAS2-9344)
 (NASA-CR-3144; TR-1087-1) Avail: NTIS HC A17/MF A01 CSCL 01C

A collection of basic descriptive data, stability derivatives and transfer functions for six degrees of freedom, quasi-static model is introduced. The data are arranged in a common, compact format for each of the five helicopters represented. The vehicles studied include the BO-105, AH-1h, and the CH53D. R.C.T.

N80-12059*# General Dynamics/Convair, San Diego, Calif. Convair Div.
WIND TUNNEL INVESTIGATION OF AN OBLIQUE WING TRANSPORT MODEL AT MACH NUMBERS BETWEEN 0.6 AND 1.4
 R. L. Black, J. K. Beamish, and W. K. Alexander Jul. 1975 334 p refs
 (Contract NAS2-8127)
 (NASA-CR-137697; HST-TR-344-0) Avail: NTIS HC A15/MF A01 CSCL 01A

Models of three practical oblique-wing transport configurations were tested in the NASA Ames 11 foot wind tunnel. The three configurations used a common forward fuselage, wing, and support system but employed different aft fuselage sections simulating alternate propulsion system installations. These included an integrated propulsion system, pylon-mounted nacelles, and clean (no propulsion system) configuration. The tests were conducted over a Mach number range from 0.6 to 1.4 and at sweep angles from 0 to 60 degrees. The nominal unit Reynolds number was 1.83 million per meter and the angle of attack range was -3 to +6 degrees. The models were mounted in the tunnel by means of a lower blade support system. The interference effects of this lower blade and the flow inclination were determined by using an image blade system and testing the configuration in both the upright and inverted positions. M.M.M.

N80-12776*# American Mathematical Society, Providence, R.I.
SYSTEM THEORY AS APPLIED DIFFERENTIAL GEOMETRY

Robert Hermann Nov. 1979 67 p refs
 (Grant NSG-2252)
 (NASA-CR-3209) Avail: NTIS HC A04/MF A01 CSCL 09B

The invariants of input-output systems under the action of the feedback group was examined. The approach used the theory of Lie groups and concepts of modern differential geometry, and illustrated how the latter provides a basis for the discussion of the analytic structure of systems. Finite dimensional linear systems in a single independent variable are considered. Lessons of more general situations (e.g., distributed parameter and multidimensional systems) which are increasingly encountered as technology advances are presented. R.C.T.

N80-12782*# Notre Dame Univ., Ind. Dept. of Electrical Engineering.
MODULAR THEORY OF INVERSE SYSTEMS Final Report, 1 Jun. - 31 Dec. 1979

Dec. 1979 57 p refs Submitted for publication
(Grant NSG-2388)
(NASA-CR-162491) Avail: NTIS HC A04/MF A01 CSCL 12A

The relationship between multivariable zeros and inverse systems was explored. A definition of zero module is given in such a way that it is basis independent. The existence of essential right and left inverses were established. The way in which the abstract zero module captured previous definitions of multivariable zeros is explained and examples are presented. R.C.T.

N80-12996* Princeton Univ., N. J. Flight Research Lab.
AN EXPLORATORY INVESTIGATION OF THE STOL LANDING MANEUVER Final Report
Patrick H. Whyte Washington NASA Dec. 1979 74 p refs
(Contract NAS2-7350)
(NASA-CR-3191; AMS-1231-T) Avail: NTI
HC A04/MF A01 CSCL 01A

The parameters influencing the STOL landing are identified and their effect on the ease and quality of the flare maneuver is discussed. Data from actual landings, supported by pilot commentary and pilot opinion rating, are analyzed. Hypotheses concerning the prediction of STOL handling qualities in the flare are proposed, and suggestions for future research are presented. A.W.H.

N80-14048* TRW Defense and Space Systems Group, Redondo Beach, Calif.
A THREE DIMENSIONAL VORTEX WAKE MODEL FOR MISSILE AT HIGH ANGLES ON ATTACK Final Report
J. Steven Sheffield and F. D. Deffenbaugh Jan. 1980 59 p refs
(Contract NAS2-9579)
(NASA-CR-3208; TRW-30584-6003-RU-00) Avail: NTIS
HC A04/MF A01 CSCL 01A

A three dimensional model for the steady flow past missile and aircraft nose shaped bodies is presented based on augmenting a potential solution with a wake composed of vortex filaments. The vortex positions are determined by the requirement that they, in some sense, align with the flow. The aerodynamic loads on the body are compared with experimental values and used to evaluate the model. The vortex positions compare well with flow visualization results for slender bodies at high angles of attack. The approximations in the wake near the body cause peaks in the force distributions more severe than in the measured values. For given vortex strengths and body attachment points multiple steady vortex positions were not found. Author

N80-15869* Stanford Univ., Calif. Dept. of Aeronautics and Astronautics.
CHARACTERIZATION OF ACOUSTIC DISTURBANCES IN LINEARLY SHEARED FLOWS
S. P. Koutsoyannis Jul. 1978 40 p refs
(Grants NSG-2215; NSG-2233; NSG-2007)
(NASA-CR-162577; SU-JIAA-TR-12) Avail: NTIS
HC A03/MF A01 CSCL 20A

The equation describing the plane wave propagation, the stability, or the rectangular duct mode characteristics in a compressible inviscid linearly sheared parallel, but otherwise homogeneous flow, is shown to be reducible to Whittaker's equation. The resulting solutions, which are real, viewed as functions of two variables, depend on a parameter and an argument, the values of which have precise physical meanings depending on the problem. The exact solutions in terms of Whittaker functions are used to obtain a number of known results of plane wave propagation and stability in linearly sheared flows as limiting cases in which the speed of sound goes to infinity (incompressible limit) or the shear layer thickness, or wave number,

goes to zero (vortex sheet limit). The usefulness of the exact solutions is then discussed in connection with the problems of plane wave propagation and the stability of a finite thickness layer with a linear velocity profile. Author

N80-15871* Stanford Univ., Calif. Dept. of Aeronautics and Astronautics.
AN EXPERIMENTAL STUDY OF THE STRUCTURE AND ACOUSTIC FIELD OF A JET IN A CROSS STREAM
Ivan Camelier and K. Karamcheti Jan. 1976 134 p refs
(Grants NGL-05-020-526; NSG-2007)
(NASA-CR-162464; SU-JIAA-TR-2) Avail: NTIS
HC A07/MF A01 CSCL 20A

The plane of symmetry of a high speed circular jet was surveyed to measure the mean and turbulent velocity fields by using constant temperature hot wire anemometry. The intensity of the noise radiated from the jet was determined in the tunnel test section by utilizing the cross-correlation at a particular time delay between the signals of two microphones suitably located along a given direction. Experimental results indicate that the turbulent intensity inside the crossflow jet increases by a factor of $(1 + 1/2)$ as compared to the turbulent intensity of the same jet under free conditions, with r indicating the ratio of the jet velocity by the cross stream velocity. The peak observed in the turbulence spectra obtained inside the potential core of the jet has a frequency that increases by the same factor with respect to the corresponding frequency measured in the case of the free jet. The noise radiated by the jet becomes more intense as the crossflow velocity increases. The measured acoustic intensity of the crossflow jet is higher than the value which would be expected from the increase of the turbulent intensity only. A.R.H.

N80-15872* Stanford Univ., Calif. Joint Inst. for Aeronautics and Acoustics.
ON THE OUTPUT OF ACOUSTICAL SOURCES
H. Levine May 1979 35 p refs
(Grant NSG-2215)
(NASA-CR-162576; SU-JIAA-TR-16) Avail: NTIS
HC A03/MF A01 CSCL 20A
Contents: (1) a theoretical basis for local power calculation; (2) source radiation in the presence of a half-plane; (3) radiation from a line source near an edge at which a Kutta condition holds; (4) radiation by a point source above a plane independence boundary; and (5) power output of a point source in a uniform flow. A.R.H.

N80-15873* Stanford Univ., Calif. Dept. of Aeronautics and Astronautics.
ACOUSTIC RESONANCES AND SOUND SCATTERING BY A SHEAR LAYER
S. P. Koutsoyannis, K. Karamcheti, and D. C. Galant (NASA, Ames Research Center, Moffett Field, Calif.) Sep. 1979 46 p refs
(Grants NSG-2233; NSG-2308)
(NASA-CR-162575; SU-JIAA-TR-20) Avail: NTIS
HC A03/MF A01 CSCL 20A

The energy reflection coefficient is evaluated numerically for plane waves incident on a plane shear layer having a linear velocity profile. The shear layer is found to exhibit no resonances and no Brewster angles. The behavior of the reflection coefficient depends crucially on the parameter τ , a nondimensional measure of the disturbance Strouhal number with respect to the disturbance Mach number in the mean flow direction. For moderate values of τ , the amplified reflection regime degenerates into the total reflection one, whereas in the ordinary reflection regime the variation of the reflection coefficient with τ depends on whether or not the corresponding vortex sheet has a Brewster

angle. The results indicate that caution should be exercised in uncritically modeling a finite thickness shear layer by a corresponding vortex sheet. K.L.

N80-16030*# McDonnell Aircraft Co., St. Louis, Mo.
INVESTIGATION OF GROUND EFFECTS ON LARGE AND SMALL SCALE MODELS OF A THREE FAN V/STOL AIRCRAFT CONFIGURATION

E. P. Schuster, T. D. Carter, and D. W. Esker Jul. 1979 149 p refs

(Contract NAS2-9690)

(NASA-CR-152240; MDC-A5702) Avail: NASA, Ames Research Center, Moffett Field, Calif. Attn: Hervey Quigley CSCL 01A

Induced lift of a subsonic, three fan, lift/cruise, V/STOL aircraft configuration was investigated using scale models of a multimission aircraft whose design incorporates a nose mounted lift fan and two lift/cruise units located over the wing. Configuration effects were assessed for lift improvement devices, lift/cruise nozzle rails, nozzle perimeter plates, and alternate nose fan exit hubs. Tests were conducted at four model heights ($H/D = 0.95, 1.53, 3.06$ and 6.45 , where D is the average nozzle exit diameter equal to 0.997 m.) Results are presented and discussed. A.R.H.

N80-16031*# Vought Corp., Dallas, Tex.
APPLICATION OF NUMERICAL OPTIMIZATION TO THE DESIGN OF WINGS WITH SPECIFIED PRESSURE DISTRIBUTIONS Final Report

H. P. Haney and R. R. Johnson Feb. 1980 108 p

(Contract NAS2-9653)

(NASA-CR-3238) Avail: NTIS HC A06/MF A01 CSCL 01A

A practical procedure for the optimum design of transonic wings is demonstrated. The procedure uses an optimization program based on the method of feasible directions coupled with an aerodynamic analysis program which solves the three-dimensional potential equation for subsonic through transonic flow. Two new wings for the A-7 aircraft were designed by using the optimization procedure to achieve specified surface pressure distributions. The new wings, along with the existing A-7 wing, were tested in the Ames 11 ft transonic wind tunnel. The experimental data show that all of the performance goals were met. However, comparisons of the wind tunnel results with the theoretical predictions indicate some differences at conditions for which strong shock waves occur.

Author

N80-16837*# California Inst. of Tech., Pasadena.
SECOND SOUND SHOCK WAVES AND CRITICAL VELOCITIES IN LIQUID HELIUM 2 Ph.D. Thesis

Timothy Neal Turner 1979 231 p refs

(Grant NsG-7508)

(NASA-CR-162687) Avail: NTIS HC A11/MF A01 CSCL 20A

Large amplitude second-sound shock waves were generated and the experimental results compared to the theory of nonlinear second-sound. The structure and thickness of second-sound shock fronts are calculated and compared to experimental data. Theoretically it is shown that at $T = 1.88$ K, where the nonlinear wave steepening vanishes, the thickness of a very weak shock must diverge. In a region near this temperature, a finite-amplitude shock pulse evolves into an unusual double-shock configuration consisting of a front steepened, temperature raising shock followed by a temperature lowering shock. Double-shocks are experimentally verified. It is experimentally shown that very large second-sound shock waves initiate a breakdown in the superfluidity of helium 2, which is dramatically displayed as a limit to the maximum attainable shock strength. The value of the maximum shock-induced relative velocity represents a significant lower bound to the intrinsic critical velocity of helium 2. M.G.

N80-17722* Systems Technology, Inc., Mountain View, Calif.
THE ANALYSIS OF DELAYS IN SIMULATOR DIGITAL COMPUTING SYSTEMS. VOLUME 1: FORMULATION OF AN ANALYSIS APPROACH USING A CENTRAL EXAMPLE SIMULATOR MODEL Final Report

Robert K. Heffley, Wayne F. Jewell, Richard F. Whitbeck, and Ted M. Schulman Feb. 1980 101 p refs

(Contract NAS2-10106)

(NASA-CR-152340; STI-TR-1140-1-Vol-1) Avail: NASA Ames Res. Center, Moffett Field, Calif. 94035 CSCL 09B

The effects of spurious delays in real time digital computing systems are examined. Various sources of spurious delays are defined and analyzed using an extant simulator system as an example. A specific analysis procedure is set forth and four cases are viewed in terms of their time and frequency domain characteristics. Numerical solutions are obtained for three single rate one- and two-computer examples, and the analysis problem is formulated for a two-rate, two-computer example. K.L.

N80-18029*# Boeing Vertol Co., Philadelphia, Pa.
SYNTHESIS OF ROTOR TEST DATA FOR REAL-TIME SIMULATION

M. A. McVeigh Mar. 1979 232 p refs

(Contract NAS2-9015)

(NASA-CR-152311; D210-11505-1)

Avail: NTIS

HC A11/MF A01 CSCL 01C

A mathematical model of a hingeless tilting rotor is presented. The model was obtained by a systematic curve fit procedure applied to an extensive set of model scale wind tunnel data. The math model equations were used in a real time flight simulation model of a hingeless tilt rotor XV-15 to assess changes in flying qualities compared to those obtained using a previous rotor model. Extensive plots of the rotor derivatives are given. Discussions of attempts to apply multivariable linear regression techniques to the data and the use of an analytical rotor representation are included. Author

N80-18030*# Boeing Vertol Co., Philadelphia, Pa.
A HINGELESS ROTOR XV-15 DESIGN INTEGRATION FEASIBILITY STUDY. VOLUME 1: ENGINEERING DESIGN STUDIES Final Report

J. P. Magee and H. R. Alexander Mar. 1978 473 p

(Contract NAS2-9015)

(NASA-CR-152310; D210-11360-1-Vol-1)

Avail: NTIS

HC A20/MF A01 CSCL 01C

A design integration feasibility study was carried out to investigate what modifications to the basic XV-15 were necessary to accomplish a flight demonstration of the XV-15 with a Boeing hingeless rotor. Also investigated were additional modifications which would exploit the full capability provided by the combination of the new rotor and the existing T53 engine. An evaluation of the aircraft is presented and the data indicate improved air vehicle performance, acceptable aeroelastic margins, lower noise levels and improved flying qualities compared with the XV-15 aircraft. Inspection of the rotor system data provided shows an essentially unlimited life rotor for the flight spectrum anticipated for the XV-15. R.E.S.

N80-18722* Systems Technology, Inc., Mountain View, Calif.
THE ANALYSIS OF DELAYS IN SIMULATOR DIGITAL COMPUTING SYSTEMS. VOLUME 2: FORMULATION OF DISCRETE STATE TRANSITION MATRICES, AN ALTERNATIVE PROCEDURE FOR MULTIRATE DIGITAL COMPUTATIONS Final Report

Warren F. Clement and Wayne F. Jewell Feb. 1980 44 p refs

(Contract NAS2-10106)

(NASA-CR-152341; STI-TR-1140-1-Vol-2) Avail: NASA, Ames Res. Center, Moffett Field, Calif. 94035 CSCL 09B

F

The effects of spurious delays in real time digital computing systems are examined for the two-computer, multirate problem. A transition matrix which combines the computational algorithms and multirate effects is formulated. Some examples are provided which demonstrate the analysis approach and suggest applications. K.L.

N80-19055*# Analytical Mechanics Associates, Inc., Mountain View, Calif.

NAVIGATION SYSTEMS FOR APPROACH AND LANDING OF VTOL AIRCRAFT

Stanley F. Schmidt and Richard L. Mohr Oct. 1979 63 p refs

(Contract NAS2-9430)

(NASA-CR-152335; AMA-79-15)

Avail: NTIS

HC A04/MF A01 CSCL 17G

The formulation and implementation of navigation systems used for research investigations in the V/STOLAND avionics system are described. The navigation systems prove position and velocity in a cartesian reference frame aligned with the runway. They use filtering techniques to combine the raw position data from nav aids (e.g., TACAN, MLS) with data from onboard inertial sensors. The filtering techniques which use both complementary and Kalman filters, are described. The software for the navigation systems is also described. R.E.S.

N80-19454*# Florida Univ., Gainesville. Dept. of Engineering Sciences.

VORTICITY ASSOCIATED WITH MULTIPLE JETS IN A CROSSFLOW

Susan Braden 25 Apr. 1980 39 p refs Presented at the AIAA Southeastern Regional Student Conf., Atlanta, 24-25 Apr. 1980

(Grant NsG-2288)

(NASA-CR-162855) Avail: NTIS HC A03/MF A01 CSCL 20D

Vortex patterns from multiple subsonic jets exiting perpendicularly through a flat plate into a subsonic crossflow were investigated. Tandem and transverse jet configurations were examined using a paddle wheel sensor to indicate the presence and relative magnitude of streamwise vorticity in the flow. Results are presented in the form of contour plots of rotational speed of the paddle wheel as measured in planes downstream from the jets and perpendicular to the crossflow. Well developed diffuse contrarotating vortices were observed for the configurations studied. The location and strength of these vortices depended on the multiple jet configuration and the distance downstream from the jets. K.L.

N80-21891*# Systems Applications, Inc., San Rafael, Calif. **INTRODUCTORY STUDY OF THE CHEMICAL BEHAVIOR OF JET EMISSIONS IN PHOTOCHEMICAL SMOG Final Report**

Gary Z. Whitten and Henry Hogo May 1976 115 p refs Sponsored in part by FAA, Washington, D. C.

(Contract NAS2-8821)

(NASA-CR-152345; EF76-04R)

Avail: NTIS

HC A06/MF A01 CSCL 13B

Jet aircraft emissions data from the literature were used as initial conditions for a series of computer simulations of photochemical smog formation in static air. The chemical kinetics mechanism used in these simulations was an updated version which contains certain parameters designed to account for hydrocarbon reactivity. These parameters were varied to simulate the reaction rate constants and average carbon numbers associated with the jet emissions. The roles of surface effects, variable light sources, NO/NO₂ ratio, continuous emissions, and untested mechanistic parameters were also assessed. The results of

these calculations indicate that the present jet emissions are capable of producing oxidant by themselves. The hydrocarbon/nitrous oxides ratio of present jet aircraft emissions is much higher than that of automobiles. These two ratios appear to bracket the hydrocarbon/nitrous oxides ratio that maximizes ozone production. Hence an enhanced effect is seen in the simulation when jet exhaust emissions are mixed with automobile emissions. A.R.H.

N80-22305*# Science Applications, Inc., Los Angeles, Calif. Economic Analysis Div.

PARAMETRIC STUDY OF HELICOPTER AIRCRAFT SYSTEMS COSTS AND WEIGHTS

Michael N. Beltramo Jan. 1980 179 p refs

(Contract NAS2-8703)

(NASA-CR-152315) Avail: NTIS HC A09/MF A01 CSCL 01C

Weight estimating relationships (WERs) and recurring production cost estimating relationships (CERs) were developed for helicopters at the system level. The WERs estimate system level weight based on performance or design characteristics which are available during concept formulation or the preliminary design phase. The CER (or CERs in some cases) for each system utilize weight (either actual or estimated using the appropriate WER) and production quantity as the key parameters. R.E.S.

N80-22357*# Massachusetts Inst. of Tech., Cambridge. Aeroelastic and Structures Research Lab.

THE DESIGN, TESTING AND EVALUATION OF THE MIT INDIVIDUAL-BLADE-CONTROL SYSTEM AS APPLIED TO GUST ALLEVIATION FOR HELICOPTERS Final Report

Robert Miller McKillip, Jr. Feb. 1980 92 p refs

(Grant NsG-2266)

(NASA-CR-152352; ASRL-TR-196-1)

Avail: NTIS

HC A05/MF A01 CSCL 01C

A type of active control for helicopters was designed and tested on a four foot diameter model rotor. A single blade was individually controlled in pitch in the rotating frame over a wide range of frequencies by electromechanical means. By utilizing a tip mounted accelerometer as a sensor in the feedback path, significant reductions in blade flapping response to gust were achieved at the gust excitation frequency as well as at super and subharmonics of rotor speed. E.D.K.

N80-23099*# General Electric Co., Cincinnati, Ohio.

ANALYTICAL STUDY OF THE EFFECTS OF WIND TUNNEL TURBULENCE ON TURBOFAN ROTOR NOISE Final Report

P. R. Giebe and E. J. Kerschen Dec. 1979 126 p

(Contract NAS2-10002)

(NASA-CR-152359) Avail: NTIS HC A06/MF A01 CSCL 20A

The influence of tunnel turbulence on turbofan rotor noise was carried out to evaluate the effectiveness of the NASA Ames 40 by 80 foot tunnel in simulating flight levels of fan noise. A previously developed theory for predicting rotor/turbulence interaction noise was refined and extended to include first-order effects of inlet turbulence anisotropy. This theory was then verified by carrying out extensive data/theory comparisons. The resulting model computer program was then employed to carry out a parametric study of the effects of fan size, blade number, and operating line on rotor/turbulence noise for outdoor test stand. NASA Ames wind tunnel, and flight inlet turbulence conditions. A major result of this study is that although wind tunnel rotor/turbulence noise levels are not as low as flight levels they are substantially lower than the outdoor test stand levels and do not mask other sources of fan noise. A.R.H.

N80-23328*# Systems Technology, Inc., Hawthorne, Calif.
PRACTICAL OPTIMAL FLIGHT CONTROL SYSTEM DESIGN FOR HELICOPTER AIRCRAFT. VOLUME 1: TECHNICAL REPORT

L. G. Hofmann, Susan A. Riedel, and Duane McRuer May 1980 273 p refs
(Contract NAS2-9946)
(NASA-CR-3275; TR-1127-1-I) Avail: NTIS
HC A12/MF A01 CSCL 01C

A method by which modern and classical theory techniques may be integrated in a synergistic fashion and used in the design of practical flight control systems is presented. A general procedure is developed, and several illustrative examples are included. Emphasis is placed not only on the synthesis of the design, but on the assessment of the results as well. R.C.T.

N80-24264*# California Polytechnic State Univ., San Luis Obispo. Dept. of Aeronautical Engineering.
EFFECTS OF FREE-STREAM TURBULENCE ON DIFFUSER PERFORMANCE

Jon A. Hoffmann Jun. 1980 51 p refs
(Grant NSG-2391)
(NASA-CR-163194) Avail: NTIS HC A04/MF A01 CSCL 01A

An experimental evaluation of the effects of free stream turbulence on the performance of a subsonic two dimensional diffuser was made. The diffuser's static pressure recovery coefficient was increased 11.4 and 21.1 percent at total. Divergence angles of 12 and 20 degrees respectively were obtained when the value of the inlet integral free stream scale of turbulence in the flow direction was at least 7.5 times larger than the inlet boundary layer displacement thickness, and when the inlet total free stream turbulence intensity was at least 3.5 percent. It is hypothesized that a larger scale of turbulence transmits the free stream energy to the wall more effectively and when coupled with large turbulence intensities, acts to decrease the distortion and delay separation within the diffuser. J.M.S.

N80-24268*# Boeing Commercial Airplane Co., Seattle, Wash.
A GENERAL PANEL METHOD FOR THE ANALYSIS AND DESIGN OF ARBITRARY CONFIGURATIONS IN INCOMPRESSIBLE FLOWS Final Report

Forrester T. Johnson Washington NASA May 1980 200 p refs
(Contract NAS2-7729)
(NASA-CR-3079; D6-43808) Avail: NTIS HC A09/MF A01 CSCL 01A

A method for solving the linear integral equations of incompressible potential flow in three dimensions is presented. Both analysis (Neumann) and design (Dirichlet) boundary conditions are treated in a unified approach to the general flow problem. The method is an influence coefficient scheme which employs source and doublet panels as boundary surfaces. Curved panels possessing singularity strengths, which vary as polynomials are used, and all influence coefficients are derived in closed form. These and other features combine to produce an efficient scheme which is not only versatile but eminently suited to the practical realities of a user-oriented environment. A wide variety of numerical results demonstrating the method is presented. Author

N80-24269*# Beam Engineering, Inc., Sunnyvale, Calif.
SIMPLE TURBULENCE MODELS AND THEIR APPLICATION TO BOUNDARY LAYER SEPARATION Final Report

Alan J. Wadcock Washington NASA May 1980 71 p refs
(Contract NAS2-10093)
(NASA-CR-3283) Avail: NTIS HC A04/MF A01 CSCL 01A

Measurements in the boundary layer and wake of a stalled airfoil are presented in two coordinate systems, one aligned with

the airfoil chord, the other being conventional boundary layer coordinates. The NACA 4412 airfoil is studied at a single angle of attack corresponding to maximum lift, the Reynolds number based on chord being 1.5×10^6 to the 6th power. Turbulent boundary layer separation occurred at the 85 percent chord position. The two-dimensionality of the flow was documented and the momentum integral equation studied to illustrate the importance of turbulence contributions as separation is approached. The assumptions of simple eddy-viscosity and mixing-length turbulence models are checked directly against experiment. Curvature effects are found to be important as separation is approached. Author

N80-26270*# Boeing Commercial Airplane Co., Seattle, Wash.
AN ADVANCED PANEL METHOD FOR ANALYSIS OF ARBITRARY CONFIGURATIONS IN UNSTEADY SUBSONIC FLOW Contractor Report, Mar. 1976 - Feb. 1980

Arthur R. Dusto and Michael A. Epton Feb. 1980 198 p refs
(Contract NAS2-7729)
(NASA-CR-152323; D6-48846) Avail: NTIS
HC A09/MF A01 CSCL 01A

An advanced method is presented for solving the linear integral equations for subsonic unsteady flow in three dimensions. The method is applicable to flows about arbitrary, nonplanar boundary surfaces undergoing small amplitude harmonic oscillations about their steady mean locations. The problem is formulated with a wake model wherein unsteady vorticity can be convected by the steady mean component of flow. The geometric location of the unsteady source and doublet distributions can be located on the actual surfaces of thick bodies in their steady mean locations. The method is an outgrowth of a recently developed steady flow panel method and employs the linear source and quadratic doublet splines of that method. Author

N80-28303*# De Havilland Aircraft Co. Ltd., Downsview (Ontario).

PHASE 1 WIND TUNNEL TESTS OF THE J-97 POWERED, EXTERNAL AUGMENTOR V/STOL MODEL

D. B. Garland Jul. 1980 101 p refs
(Contract NASw-2797)
(NASA-CR-152255; DHC-DND-79-4) Avail: NTIS
HC A06/MF A01 CSCL 01A

Test results are presented for a large scale, external augmentor V/STOL model in a 40 ft by 80 ft wind tunnel. The model was powered by a GE J97 engine and featured longitudinal ejectors alongside and external to the fuselage together with an augmentor flap on the low aspect ratio, double-delta wing. A static thrust augmentation ratio of 1.60 was measured for the fuselage augmentor at a nozzle pressure ratio of 3.0 and a nozzle exhaust gas temperature of 700 C. At forward speed the model showed a strong positive lift interference due to the augmentor flap, and a marked absence of negative lift interference due to the fuselage augmentor jet system. The nose-up moment of the fuselage augmentor inlet flow was approximately cancelled by a 60 deg deflection of the augmentor flap. An assessment of the thrust and drag components to allow the prediction of transition performance of aircraft designs based on the present conceptual model was made. Lateral tests showed strong but well ordered effects of power. L.F.M.

N80-28369*# United Technologies Research Center, East Hartford, Conn.

ANALYTICAL DESIGN AND EVALUATION OF AN ACTIVE CONTROL SYSTEM FOR HELICOPTER VIBRATION REDUCTION AND GUST RESPONSE ALLEVIATION

R. B. Taylor, P. E. Zwicke, P. Gold, and W. Miao Jul. 1980 165 p refs Prepared in cooperation with Sikorsky Aircraft, Stratford, Conn.

(Contract NAS2-10121)

(NASA-CR-152377) Avail: NTIS HC A08/MF A01 CSCL 01C

An analytical study was conducted to define the basic configuration of an active control system for helicopter vibration and gust response alleviation. The study culminated in a control system design which has two separate systems: narrow band loop for vibration reduction and wider band loop for gust response alleviation. The narrow band vibration loop utilizes the standard swashplate control configuration to input controller for the vibration loop is based on adaptive optimal control theory and is designed to adapt to any flight condition including maneuvers and transients. The prime characteristics of the vibration control system is its real time capability. The gust alleviation control system studied consists of optimal sampled data feedback gains together with an optimal one-step-ahead prediction. The prediction permits the estimation of the gust disturbance which can then be used to minimize the gust effects on the helicopter. E.D.K.

N80-31408* Princeton Univ., N. J. Dept. of Mechanical and Aerospace Engineering.

A SIMULATOR STUDY OF CONTROL AND DISPLAY AUGMENTATIONS FOR HELICOPTERS Final Report

J. C. Adamson, Gerardus J. Born, and Theodore A. Dukes Jan. 1980 104 p refs

(Contract NAS2-9437)

(NASA-CR-163451; AD-A087201; MAE-1428) Avail: NTIS HC A06/MF A01 CSCL 01/4

A fixed-based simulator study of a decelerating approach to hover on instruments was performed with five different control augmentation systems ranging from damping feedbacks to attitude command with heading-hold. On a CRT display the environment was simulated by the view of landing pad and the horizon. Superimposed on this image was all flight information needed, together with special symbology for self-contained landing aid based on airborne measurements only; there were a total of four display augmentation levels. Among other findings, the statistically significant differences in data obtained with six test pilots suggest that a relatively inexpensive addition to the display (i.e., quickening of an error rate vector with short term attitude information) makes up for the difference between rate command and attitude command control systems. A quantitative objective measure of improvements was found to suggest the major findings of the report. GRA

N80-31760* Stanford Univ., Calif. Joint Inst. for Aeronautics and Acoustics.

AN EXPERIMENTAL STUDY OF MULTIPLE JET MIXING

D. Krothapalli, D. Baganoff, and K. Karamcheti Jun. 1979 162 p refs

(Grants NSG-2007; NSG-2233)

(NASA-CR-163537; SU-JIAA-TR-23) Avail: NTIS HC A08/MF A01 CSCL 20D

Measurements of an incompressible jet issuing from an array of rectangular lobes, equally spaced with their small dimensions in a line, both as a free jet, and as a confined jet, are carried out in three parts: (1) on a single rectangular free jet, (2) on the same jet in a multiple free jet configuration, and (3) on the same jet in a multiple jet configuration with confining surfaces (two parallel plates are symmetrically placed perpendicular to the long dimension of each lobe covering the entire flow field under consideration). In the case of a single rectangular free jet, the flow field of the jet is characterized by the presence of three distinct regions in the axial mean velocity decay and are referred to as: potential core region, two dimensional type region, and axisymmetric type region. In the case of a multiple free jet, the flow field for downstream distance X greater than $60D$ (D = width of a lobe) resembles that of a jet exiting from a two dimensional nozzle with its short dimension being the long dimension of the lobe. S.F.

N80-32337* Boeing Commercial Airplane Co., Seattle, Wash. **LARGE SCALE WIND TUNNEL INVESTIGATION FOR FUTURE MODIFICATIONS TO THE QUIET SHORT-HAUL RESEARCH AIRCRAFT**

Donald N. Hultman Sep. 1980 35 p refs

(Contract NAS2-9196)

(NASA-CR-152349) Avail: NTIS HC A03/MF A01 CSCL 01A

Results of wind tunnel investigation performed to eliminate the leading edge blowing system on the baseline quiet short haul research aircraft are presented. This was accomplished by repositioning the leading edge flaps to a slotted position. Gap, overlap, and deflection angle variations were investigated. A configuration was established that satisfies QSRA performance and safety requirements. A.R.H.

N80-32338* Lear Siegler, Inc., Santa Monica, Calif. Astronics Div.

A COMPARISON OF FLIGHT AND SIMULATION DATA FOR THREE AUTOMATIC LANDING SYSTEM CONTROL LAWS FOR THE AUGMENTOR WING JET STOL RESEARCH AIRPLANE

B. Feinreich and G. Gevaert [1980] 18 p refs

(Contract NAS2-10324)

(NASA-CR-152365) Avail: NTIS HC A02/MF A01 CSCL 01A

Automatic flare and decrab control laws for conventional takeoff and landing aircraft were adapted to the unique requirements of the powered lift short takeoff and landing airplane. Three longitudinal autoland control laws were developed. Direct lift and direct drag control were used in the longitudinal axis. A fast time simulation was used for the control law synthesis, with emphasis on stochastic performance prediction and evaluation. Good correlation with flight test results was obtained. S.F.

N80-32339* Nielsen Engineering and Research, Inc., Mountain View, Calif.

A CORRELATION METHOD TO PREDICT THE SURFACE PRESSURE DISTRIBUTION OF AN INFINITE PLATE OR A BODY OF REVOLUTION FROM WHICH A JET IS ISSUING Final Report, 1 Dec. 1978 - 1 May 1980

Stanley C. Perkins, Jr. and Michael R. Mendenhall Jan. 1980 200 p refs

(Contract NAS2-10125)

(NASA-CR-152345; NEAR-TR-211)

Avail: NTIS HC A09/MF A01 CSCL 01A

A correlation method to predict pressures induced on an infinite plate by a jet exhausting normal to the plate into a subsonic free stream was extended to jets exhausting at angles to the plate and to jets exhausting normal to the surface of a body of revolution. The complete method consisted of an analytical method which models the blockage and entrainment properties of the jet and an empirical correlation which accounts for viscous effects. For the flat plate case, the method was applicable to jet velocity ratios up to ten, jet inclination angles up to 45 deg from the normal, and radial distances up to five diameters from the jet. For the body of revolution case, the method was applicable to a body at zero degrees angle of attack, jet velocity ratios 1.96 and 3.43, circumferential angles around the body up to 25 deg from the jet, axial distances up to seven diameters from the jet, and jet-to-body diameter ratios less than 0.1. R.C.T.

N80-32353* Lockheed-California Co., Burbank.

APPLICATION OF ADVANCED TECHNOLOGIES TO SMALL, SHORT-HAUL TRANSPORT AIRCRAFT Final Report, Jun. 1979 - Jun. 1980

T. G. Coussens and R. H. Tullis Jun. 1980 203 p refs
(Contract NAS2-10264)
(NASA-CR-152363; LR-29450) Avail: NTIS
HC A10/MF A01 CSCL 01C

The performance and economic benefits available by incorporation of advanced technologies into the small, short haul air transport were assessed. Low cost structure and advanced composite material, advanced turboprop engines and new propellers, advanced high lift systems and active controls; and alternate aircraft configurations with aft mounted engines were investigated. Improvements in fuel consumed and aircraft economics (acquisition cost and direct operating cost) are available by incorporating selected advanced technologies into the small, short haul aircraft. T.M.

N80-32777* Systems Control, Inc., Palo Alto, Calif. Aeronautical and Marine Systems Div.

DYNAMIC MODAL ESTIMATION USING INSTRUMENTAL VARIABLES

H. Salzwedel Jul. 1980 66 p refs.
(Contract NAS2-10339)
(NASA-CR-152396; TR-6419-01) Avail: NTIS
HC A04/MF A01 CSCL 20K

A method to determine the modes of dynamical systems is described. The inputs and outputs of a system are Fourier transformed and averaged to reduce the error level. An instrumental variable method that estimates modal parameters from multiple correlations between responses of single input, multiple output systems is applied to estimate aircraft, spacecraft, and off-shore platform modal parameters. E.D.K.

N80-32815* California Univ., Berkeley. Space Sciences Lab.

IRRIGATED LANDS ASSESSMENT FOR WATER MANAGEMENT APPLICATIONS PILOT TEST (APT) Final Report

Robert N. Colwell, John E. Estes, and Larry Tinney, Principal Investigators 31 Jan. 1980 156 p refs Original contains imagery. Original photography may be purchased from the EROS Data Center, Sioux Falls, S.D. 57198 ERTS
(Grant NSG-2207)

(E80-10324; NASA-CR-163404; SSL-Ser-21-Issue-5) Avail: NTIS HC A08/MF A01 CSCL 08H

There are no author-identified significant results in this report.

N80-33177* Stanford Univ., Calif. Joint Inst. for Aeronautics and Acoustics.

MODAL CONTENT OF NOISE GENERATED BY A COAXIAL JET IN A PIPE

E. J. Kerschen and J. P. Johnston May 1978 271 p refs
(Grants NSG-2007; NSF GK-37294; NSF ENG-76-00819)
(NASA-CR-163575; SU-JIAA-TR-11) Avail: NTIS
HC A12/MF A01 CSCL 20A

Noise generated by air flow through a coaxial obstruction in a long, straight pipe was investigated with concentration on the modal characteristics of the noise field inside the pipe and downstream of the restriction. Two measurement techniques were developed for separation of the noise into the acoustic duct modes. The instantaneous mode separation technique uses four microphones, equally spaced in the circumferential direction, at the same axial location. The time-averaged mode separation technique uses three microphones mounted at the same axial location. A matrix operation on time-averaged data produces the modal pressure levels. This technique requires the restrictive assumption that the acoustic modes are uncorrelated with each other. The measured modal pressure spectra were converted to modal power spectra and integrated over the frequency range

200-6000 Hz. The acoustic efficiency levels (acoustic power normalized by jet kinetic energy flow), when plotted vs. jet Mach number, showed a strong dependence on the ratio of restriction diameter to pipe diameter. The acoustic energy flow analyses based on the thermodynamic energy equation and on the results of Mohring both resulted in orthogonality properties for the eigenfunctions of the radial mode shape equation. These orthogonality relationships involve the eigenvalues and derivatives of the radial mode shape functions. F.O.S.

N80-33351* Sikorsky Aircraft, Stratford, Conn.
ANALYSIS AND CORRELATION OF TEST DATA FROM AN ADVANCED TECHNOLOGY ROTOR SYSTEM Final Report, Mar. 1979 - Jun. 1980

D. Jepson, R. Moffitt, and J. Bissell Hilzinger Jul. 1980 169 p refs

(Contract NAS2-10211)
(NASA-CR-152366; SER-510034) Avail: NTIS
HC A08/MF A01 CSCL 01A

The performance and blade vibratory loads characteristics for an advanced rotor system as predicted by analysis and as measured in a 1/5 scale model wind tunnel test, a full scale model wind tunnel test and flight test were compared. The 1/5 scale model rotor predicted conservative full scale rotor performance as expected due to Reynolds number effects. Although blade vibratory moment trends with advance ratio were predicted by the 1/5 scale model, the absolute values of the blade vibratory moments were underpredicted. The full scale model predicted forward flight performance within + or - 5%. Blade vibratory loads, however, were underpredicted. The result of rotor inflow distortions imparted by the flow over the fuselage. The coupled normal modes (Y201) elastic rotor blade analysis incorporating variable inflow was able to predict most of the trends of the test data at the higher advance ratios, but was unable to predict the absolute magnitude of the blade 1/2 peak to peak moments at all cruise speed and rotor lift conditions. A.R.H.

N80-33381* Human Resources Research Organization, Alexandria, Va.

CIVIL HELICOPTER WIRE STRIKE ASSESSMENT STUDY, VOLUME 1: FINDINGS AND RECOMMENDATIONS Final Report

Clyde H. Tuomela and Mark F. Brennan Oct. 1980 66 p refs
(Contract NAS2-10505)

(NASA-CR-152389; HumRRO-FR-MTD(CA)-80-13) Avail: NTIS HC A04/MF A01 CSCL 01C

Approximately 208 civil helicopter wire strike accidents for a ten year period 1970 to 1979 are analyzed. It is found that 83% of the wire strikes occurred during bright clear weather. Analysis of the accidents is organized under pilot, environment, and machine factors. Methods to reduce the wire strike accident rate are discussed, including detection/warning devices, identification of wire locations prior to flight, wire cutting devices, and implementation of training programs. The benefits to be gained by implementing accident avoidance methods are estimated to be fully justified by reduction in injury and death and reduction of aircraft damage and loss. J.M.S.

N80-33396* General Dynamics/Convair, San Diego, Calif.
APPLICATION OF ADVANCED TECHNOLOGIES TO SMALL, SHORT-HAUL AIR TRANSPORTS Final Report

Cliff Adcock, Carl Coverston, and Bill Knapton Sep. 1980 212 p

(Contract NAS2-10267)
(NASA-CR-152364) Avail: NTIS HC A10/MF A01 CSCL 01C

A study was conducted of the application of advanced technologies to small, short-haul transport aircraft. A three abreast, 30 passenger design for flights of approximately 100 nautical

miles was evaluated. Higher wing loading, active flight control, and a gust alleviation system results in improved ride quality. Substantial savings in fuel and direct operating cost are forecast. An aircraft of this configuration also has significant benefits in forms of reliability and operability which should enable it to sell a total of 450 units through 1990, of which 80% are for airline use. L.F.M.

N80-33397*# General Dynamics Corp., Groton, Conn.
STUDY FOR CONCEPTUAL DESIGN OF VEO, VTOL EXHAUST NOZZLE
 W. C. Bittrick Jul. 1980 91 p
 (Contract NAS2-10127)
 (NASA-CR-152388) Avail: NTIS HC A05/MF A01 CSCL 01C

Design requirements for a VEO Wing V/STOL exhaust nozzle with a two dimensional shape and having the capability for upper surface blowing, spanwise blowing, and 90 deg turning of the exhaust flow for VTOL were established. A preliminary design of the nozzle that identified the actuation scheme, key dimensions, the flowpath, and the recommended materials were prepared. The airplane characteristics resulting from integrating the study nozzle were established. T.M.

N80-33398*# Bolt, Beranek, and Newman, Inc., Cambridge, Mass.
PILOT/VEHICLE MODEL ANALYSIS OF VISUAL AND MOTION CUE REQUIREMENTS IN FLIGHT SIMULATION
Final Report
 Sheldon Baron, Roy Lancraft, and Greg Zacharias Washington
 NASA Oct. 1980 165 p refs
 (Contract NAS2-10145)
 (NASA-CR-3312; Rept-4300) Avail: NTIS HC A08/MF A01 CSCL 05E

The optimal control model (OCM) of the human operator is used to predict the effect of simulator characteristics on pilot performance and workload. The piloting task studied is helicopter hover. Among the simulator characteristics considered were (computer generated) visual display resolution, field of view and time delay. Author

N80-33401*# Boeing Vertol Co., Philadelphia, Pa.
VASCOMP 2. THE V/STOL AIRCRAFT SIZING AND PERFORMANCE COMPUTER PROGRAM. VOLUME 6: USER'S MANUAL, REVISION 3 Final Report, Oct. 1979 - Jul. 1980
 Allen H. Schoen, Harold Rosenstein, Kaydon Stanzione, and John S. Wisniewski May 1980 627 p refs Revision
 (Contracts NAS2-6107; N62269-79-C-0706)
 (NASA-CR-163639; AD-A088833; D8-0375-Vol-6-Rev-3)
 Avail: NTIS HC A99/MF A01 CSCL 09/2

This report describes the use of the V/STOL Aircraft Sizing and Performance Computer Program (VASCOMP II). The program is useful in performing aircraft parametric studies in a quick and cost efficient manner. Problem formulation and data development were performed by the Boeing Vertol Company and reflects the present preliminary design technology. The computer program, written in FORTRAN IV, has a broad range of input parameters, to enable investigation of a wide variety of aircraft. User oriented features of the program include minimized input requirements, diagnostic capabilities, and various options for program flexibility. GRA

N80-33718*# National Aeronautics and Space Administration. Ames Research Center, Moffett Field, Calif.
A RAPID IMPLICIT-EXPLICIT SOLUTION TO THE TWO-DIMENSIONAL TIME DEPENDENT INCOMPRESSIBLE

NAVIER-STOKES EQUATIONS Final Report

Joseph E. Davis Oct. 1980 24 p refs
 (NASA Order A-50807-B)
 (NASA-CR-3330) Avail: NTIS HC A02/MF A01 CSCL 20D
 A second-order time-accurate and spatially factored algorithm was used in a finite difference scheme for the numerical solution of the time-dependent, incompressible, two dimensional Navier-Stokes equations in conservation-law form using vorticity and stream function variables. The systems of equations are solved at each time step by an iterative technique. Numerical results were obtained for a circular cylinder at a Reynolds number of 15, and an NACA 0012 airfoil at zero angle of attack at Reynolds numbers of 10 to the third and 10 to the fourth powers. The results are in agreement with another numerical technique, and the computing time required to obtain the steady state solution at the Reynolds number of 10 to the 4th power was 49.7 sec on CDC 7600 computer using a 65 x 84 computational grid. A.R.H.

X80-10005*# Boeing Commercial Airplane Co., Seattle, Wash.
QUIET SHORT-HAUL RESEARCH AIRCRAFT PREDICTED FLIGHT CHARACTERISTICS
 Clarence C. Flora, Robin Middleton, and Donald K. Schafer Oct. 1979 168 p refs
 (Contract NAS2-9081)
 (NASA-CR-152203) Unclassified report

NOTICE: Available to U.S. Government Agencies and NASA Contractors.

The aircraft design, including systems and flight controls, is described along with its typical performance characteristics. Flying qualities for the normal airplane and characteristics after significant failures are covered. The aircraft is predicted to have satisfactory flying qualities for aircraft normal states and acceptable, safe flying qualities for failure states. K.L.

X80-10006*# Boeing Co., Seattle, Wash.
QSRA PHASE 2 FLIGHT SIMULATION MATHEMATICAL MODEL Final Report
 Donald K. Schafer, Clarence C. Flora, Laura E. Nicol, Arley C. Marley, Robin Middleton, and James H. Vincent Sep. 1979 393 p refs
 (Contract NAS2-9081)
 (NASA-CR-152197) Unclassified report

NOTICE: Available to U.S. Government Agencies and Their Contractors.

The mathematical model which was developed for the quiet short-haul research aircraft (QSRA), was changed from a multi-faceted model to a final format that reflects the delivered airplane configurations. The highlights and limitations of each module of the QSRA simulation mathematical model are presented. R.E.S.

X80-10106*# Boeing Commercial Airplane Co., Seattle, Wash. BCAC Preliminary Design Dept.
THE DEVELOPMENT OF A QUIET SHORT-HAUL RESEARCH AIRCRAFT Final Report
 May 1980 196 p refs
 (Contract NAS2-9081)
 (NASA-CR-152298) Unclassified report

NOTICE: Available to U.S. Government Agencies and Their Contractors.

The design and certification criteria for practical quiet propulsive lift short haul aircraft are discussed. Takeoff and landing and other near terminal operations associated with the propulsive lift mode of flight are emphasized. R.C.T.

JOURNAL ARTICLES

A80-17717 * **Formulation of coupled rotor/fuselage equations of motion.** W. Warmbrodt (NASA, Ames Research Center, Moffett Field, Calif.) and P. Friedmann (California, University, Los Angeles, Calif.). *Vertica*, vol. 3, no. 3-4, 1979, p. 245-271. 19 refs. Grant No. NSG-1578.

The governing equations of motion of a helicopter rotor coupled to a rigid body fuselage are derived. A consistent formulation is used to derive nonlinear periodic coefficient equations of motion which can be used to study coupled rotor/fuselage dynamics in forward flight. The methodology of rotor/fuselage coupling is clearly described and the importance of an ordering scheme in deriving consistent nonlinear equations of motion is reviewed. The final equations which are presented in partial differential form can be used to model coupled rotor/fuselage aeroelastic response or stability problems. (Author)

A80-18538 # **Constrained optimum trajectories with specified range.** H. Erzberger and H. Lee (NASA, Ames Research Center, Moffett Field, Calif.). *Journal of Guidance and Control*, vol. 3, Jan.-Feb. 1980, p. 78-85. 7 refs.

The characteristics of optimum fixed-range trajectories whose structure is constrained to climb, steady cruise, and descent segments are derived by application of optimal control theory. The performance function consists of the sum of fuel and time costs, referred to as direct operating costs (DOC). The state variable is range-to-go and the independent variable is energy. In this formulation a cruise segment always occurs at the optimum cruise energy for sufficiently large range. At short ranges (500 n. mi. and less) a cruise segment may also occur below the optimum cruise energy. The existence of such a cruise segment depends primarily on the fuel flow vs thrust characteristics and on thrust constraints. If thrust is a free control variable along with airspeed, it is shown that such cruise segments will not generally occur. If thrust is constrained to some maximum value in climb and to some minimum in descent, such cruise segments generally will occur. The performance difference between free thrust and constrained thrust trajectories has been determined in computer calculations for an example transport aircraft. (Author)

A80-19117 * **Saturn's magnetic field and magnetosphere.** E. J. Smith (California Institute of Technology, Jet Propulsion Laboratory, Pasadena, Calif.), L. Davis, Jr. (California Institute of Technology, Pasadena, Calif.), D. E. Jones (Brigham Young University, Provo, Utah), P. J. Coleman, Jr. (California, University, Los Angeles, Calif.), D. S. Colburn, P. Dyal (NASA, Ames Research Center, Moffett Field, Calif.), and C. P. Sonett (Arizona, University, Tucson, Ariz.). *Science*, vol. 207, Jan. 25, 1980, p. 407-410. 14 refs. Contract No. NAS7-100.

Results of Pioneer Saturn vector helium magnetometer measurements of the magnetic field and magnetosphere of Saturn are reported. The detection of a bow shock at 23.7 Saturn radii and the magnetosphere crossing at 17.4 Saturn radii suggest an equatorial surface field of 0.3 gauss, which is similar to that of the earth, and the polarity of the field is observed to be similar to that of Jupiter and opposite to the earth's. An increase of magnetic field strength with decreasing radius indicates the dipole nature of the magnetic field, which modified by the compression of the magnetosphere by the solar wind and the presence of a ring current in the middle magnetosphere. Inversions of the field measurements to obtain equivalent dipole source vectors reveal that the tilt angle between the magnetic dipole and the rotation axis is less than 1 deg, and spherical harmonic analysis of the data indicates that the magnetic field is more uniform than those of the earth and Jupiter, consistent with a small Saturn core. An apparent hydromagnetic wake associated with Titan was also observed. A.L.W.

A80-20828 * # **Acoustic characteristics of two hybrid inlets at forward speed.** M. D. Falarski (NASA, Ames Research Center, Moffett Field, Calif.) and M. T. Moore (General Electric Co., Cincinnati, Ohio). (*American Institute of Aeronautics and Astronautics, Aeroacoustics Conference, 5th, Seattle, Wash., Mar. 12-14, 1979, Paper 79-0678.*) *Journal of Aircraft*, vol. 17, Feb. 1980, p. 106-111. 8 refs.

A wind tunnel investigation of the acoustic and aerodynamic characteristics of two hybrid inlets installed on a JT15D-1 turbofan engine was performed. The hybrid inlets combined moderate throat Mach number and wall acoustic treatment to suppress the fan inlet noise. Acoustic and aerodynamic data were recorded over a range of flight and engine operating conditions. In a simulated flight environment, the hybrid inlets provided significant levels of suppression at both design and off-design throat Mach numbers with good aerodynamic performance. A comparison of inlet noise at quasi-static and forward-speed conditions in the wind tunnel showed a reduction in the fan tones, demonstrating the flight cleanup effect. High angles of attack produced slight increases in fan noise at the high acoustic directivity angles. (Author)

A80-21224 * # **Toward new small transports for commuter airlines.** D. J. Giulianetti and L. J. Williams (NASA, Ames Research Center, Moffett Field, Calif.). *Astronautics and Aeronautics*, vol. 18, Feb. 1980, p. 16-25. 7 refs.

The article discusses the results of a survey of commuter airline operators and large and small airframe manufacturers conducted by the Small Transport Aircraft Technology Office of the NASA Ames Research Center. Attention is given to economic concerns of the operator and manufacturer, as well as social concerns of the passenger, community, and system. Discussion also covers research and technology opportunities for improving commuter aircraft, and provides a background of information on the commuter and short-haul local-service air carriers, regulations pertaining to their aircraft, and operations, overall airline interfaces, and facility requirements. M.E.P.

A80-21225 * # **Small Transport Aircraft Technology.** T. L. Galloway (NASA, Ames Research Center, Moffett Field, Calif.). *Astronautics and Aeronautics*, vol. 18, Feb. 1980, p. 26-35.

The article surveys the results of the NASA-instituted Small Transport Aircraft Technology (STAT) research effort aimed at generating advanced technologies for application to new small, short haul transports having significantly better performance, efficiency, and environmental compatibility. Discussion covers fuselage designs and bonded aluminum-honeycomb wing construction which reduces the number of parts and fasteners, and gives a smoother outer contour. Topics discussed include: advanced aluminum alloys, composite primary structures, propellers, engine components, icing protection, avionics, flight controls, aerodynamics, and gust load alleviation. M.E.P.

A80-27384 * **The Quiet Short-Haul Research Aircraft /OSRA/.** J. L. Martin (NASA, Ames Research Center, Moffett Field, Calif.). (*Society of Experimental Test Pilots, Symposium, 23rd, Beverly Hills, Calif., Sept. 26-29, 1979.*) *Society of Experimental Test Pilots, Technical Review*, vol. 14, no. 4, 1979, p. 77-93. 10 refs.

The Quiet Short-Haul Research Aircraft (OSRA), designed to expand the technology base of the upper-surface blowing propulsive-lift principle in order to establish criteria for the U.S. aircraft industry and for advanced STOL aircraft, is considered. The aircraft, which includes a three-axis, single channel, limited authority series type stability augmentation system, and a high-speed data system is described. Also discussed are STOL and acoustic performance, and handling qualities, particularly thrust effects. The OSRA has demon-

strated its ability, even with the critical engine inoperative, to approach at 66 knots (wing loading of 83 lb/sq ft) and on a 9 degree glidepath; to maneuver in a 700-ft radius turn, and to land in an FAA field length of 1450 ft (over a 35-ft obstacle). J.P.B.

A80-28019 * # Implicit model following and parameter identification of unstable aircraft. J. V. Lebacqz (NASA, Ames Research Center, Moffett Field, Calif.; Calspan Advanced Technology Center, Buffalo, N.Y.) and K. S. Govindaraj (Calspan Advanced Technology Center, Buffalo, N.Y.). *Journal of Guidance and Control*, vol. 3, Mar.-Apr. 1980, p. 119-123. 11 refs.

A transformation in the s-plane is described which has utility in implicit model-following optimal control design application and in estimation or parameter identification problems. The objective of the transformation is, for the control problem, to achieve an unstable closed-loop system, and, for the estimation problem, to alleviate algorithm convergence problems that may arise in identifying unstable systems. For the control problem, the transformation is a shift along the real (σ) axis of the plant and model poles and zeros. This transformation is shown to be equivalent to a modified performance index but offers the advantage of compatibility with existing optimal control solution algorithms. For the estimation problem, the data are multiplied by an exponential function and the assumed measurement and process noise covariances are appropriately modified. Examples of both control and estimation applications are presented. (Author)

A80-28418 * # Strouhal number influence on flight effects on jet noise radiated from convecting quadrupoles. R. Dash (NASA, Ames Research Center, Moffett Field; Stanford University, Stanford, Calif.). *AIAA Journal*, vol. 18, Mar. 1980, p. 337-339.

The paper reports a complementary extension of previous work to include the high-frequency features reflected in the discussion of the higher Strouhal number influence on flight effects. It is found that, in addition to the usual features of flight effects on noise from ordinary flows, the high Strouhal number flows exhibit some more interesting features which are uniquely characteristic to them. The additional features are as follows: (1) Flight effects are more favorable to hot jets than to cold jets; (2) the higher the Strouhal number of the jet flow, the lesser the forward arc amplification due to flight; (3) as the Strouhal number increases, the peak amplification angle in the forward quadrant and the peak suppression angle in the aft quadrant move toward 90 deg and get closer, thus reducing the amplification exposure to a constricted angular region; (4) the silence zone is disturbed and displaced from its normal position parallel to the jet flow to give rise to multiple crossings of flight curves with the static line; and (5) the occurrence of multiple crossings is a strange phenomenon solely characteristic of high Strouhal number with high subcritical jet flows in flight. S.D.

A80-33123 * The promise of multicyclic control. J. L. McCloud, III (NASA, Ames Research Center, Moffett Field, Calif.). *Vertica*, vol. 4, no. 1, 1980, p. 29-41. 17 refs.

The rough ride a helicopter endures is known to be self-generated. This roughness results in fatiguing blade loads and vibration which can be eliminated or greatly reduced by multicyclic control. Rotor performance may also be improved. Several types of rotors which have employed multicyclic control are reviewed and compared. Their differences are highlighted and their potential advantages and disadvantages are discussed. The flow field these rotors must operate in is discussed, and it is shown that simultaneous elimination of vibration and oscillatory blade loads is not an inherent solution to the roughness problem. The use of rotor blades and energy absorbers is proposed. Input-output relations are considered

and a gain control for ROMULAN, a multicyclic controlling computer program, is introduced. Implications of the introduction of multicyclic systems into helicopters are also discussed. (Author)

A80-38049 * Examination of group-velocity criterion for breakdown of vortex flow in a divergent duct. C.-Y. Tsai (NASA, Ames Research Center, Moffett Field, Calif.) and S. E. Widnall (MIT, Cambridge, Mass.). *Physics of Fluids*, vol. 23, May 1980, p. 864-870. 15 refs.

A group-velocity criterion for vortex breakdown implied by wave trapping theory is applied to vortex flows in a slightly divergent duct that exhibits breakdown. The group velocities for both symmetric ($n = 0$) and nonsymmetric ($n = \text{plus or } -1$) modes of wave propagation are calculated for the experimental data. It is found that the flow ahead of the breakdown region is always supercritical and stable to these modes of disturbances. However, the flow field behind the breakdown region may be either supercritical or subcritical to the modes $n = 0$ and $n = 1$, and always supercritical to mode $n = -1$. The flow field behind this breakdown region is unstable to the asymmetric mode disturbance ($n = 1$) for a finite range of wavenumbers. The calculated frequencies of the unstable disturbances are in good agreement with the frequencies obtained from the experimental measurements. (Author)

CONFERENCE PAPERS

N80-10109* # National Aeronautics and Space Administration. Ames Research Center, Moffett Field, Calif.

NASA OVERVIEW

David G. Koenig *In its Workshop on Thrust Augmenting Ejectors* Sep. 1979 p 23-40 refs (For primary document see N80-10107 01-02)

Avail: NTIS HC A22/MF A01 CSCL 01A

The history of NASA efforts at Ames Research Center in researching the performance and application of thrusting augmentors is reviewed. Current objectives include: (1) parametric description of thrust augmentor application to STOL and V/STOL; (2) the use of theoretical and empirical data; (3) aircraft-augmentor integration; and (4) key design considerations for STOL transport and V/STOL fighter aircraft. Test facilities are described and ejector development and performance are assessed. A.R.H.

N80-15164* # National Aeronautics and Space Administration. Ames Research Center, Moffett Field, Calif.

CONTROL OF FOREBODY THREE-DIMENSIONAL FLOW SEPARATIONS

David J. Peake and F. Kevin Owen (Owen Intern., Inc., Palo Alto, Calif.) *In AGARD Aerodyn. Characteristics of Controls* Sep. 1979 49 p refs (For primary document see N80-15149 06-08)

Avail: NTIS HC A22/MF A01 CSCL 01C

The development of the turbulent symmetric and asymmetric vortex flow about the lee side of a 5 deg semiangle conical forebody at high relative incidence was investigated. The cone was immersed in a Mach 0.6 airstream at a Reynolds number of 13.5×10^6 to the 6th power based on the 1.4 m axial length of the cone. Small amounts of air injected normally or tangentially to the cone surface, but on one side of the leeward meridian and beneath the vortex farthest from the wall, were effective in biasing the asymmetry. With this reorientation of the forebody vortices, the amplitude of the side force could be reduced to the point where its direction was reversed. This phenomenon was obtained either by changing the blowing rate at constant incidence or by changing incidence at constant blowing rate. Normal injection appeared more effective than tangential injection. The contrarotating vortices in the penetrating jet flow were of

opposite hand to the rotational directions of the forebody vortices. A distinctively organized and stable flow structure emerged with the jet vortices positioned above the forebody vortices. K.L.

N80-21246*# National Aeronautics and Space Administration. Ames Research Center, Moffett Field, Calif.

AN ACCEPTABLE ROLE FOR COMPUTERS IN THE AIRCRAFT DESIGN PROCESS c60

Thomas J. Gregory and Leonard Roberts *In AGARD The Use of Computers as a Design Tool* Jan. 1980 7 p refs (For primary document see N80-21243 12-01)

Avail: NTIS HC A19/MF A01 CSCL 09B

Some of the reasons why the computerization trend is not wholly accepted are explored for two typical cases: computer use in the technical specialties and computer use in aircraft synthesis. The factors that limit acceptance are traced in part, to the large resources needed to understand the details of computer programs, the inability to include measured data as input to many of the theoretical programs, and the presentation of final results without supporting intermediate answers. Other factors are due solely to technical issues such as limited detail in aircraft synthesis and major simplifying assumptions in the technical specialties. These factors and others can be influenced by the technical specialist and aircraft designer. Some of these factors may become less significant as the computerization process evolves, but some issues, such as understanding large integrated systems, may remain issues in the future. Suggestions for improved acceptance include publishing computer programs so that they may be reviewed, edited, and read. Other mechanisms include extensive modularization of programs and ways to include measured information as part of the input to theoretical approaches. J.M.S.

N80-25590*# National Aeronautics and Space Administration. Ames Research Center, Moffett Field, Calif.

OVERVIEW OF 6- X 6-FOOT WIND TUNNEL AERO-OPTICS TESTS

Donald A. Buell *In its Proc. of the Aero-Optics Symp. on Electromagnetic Wave Propagation from Aircraft* Apr. 1980 p 35-90 refs (For primary document see N80-25588 16-34)

Avail: NTIS HC A99/MF A01 CSCL 20D

The splitter-plate arrangement used in tests in the 6 x 6 foot wind tunnel and how it was configured to study boundary layers, both heated and unheated, shear layers over a cavity, separated flows behind spoilers, accelerated flows around a turret, and a turret wake are described. The flows are characterized by examples of the steady-state pressure and of velocity profiles through the various types of flow layers. R.E.S.

N80-25594*# National Aeronautics and Space Administration. Ames Research Center, Moffett Field, Calif.

UNSTEADY DENSITY AND VELOCITY MEASUREMENTS IN THE 6 FOOT X 6 FOOT WIND TUNNEL

William C. Rose (Rose Eng. and Res., Inc.) and Dennis A. Johnson *In its Proc. of the Aero-Optics Symp. on Electromagnetic Wave Propagation from Aircraft* Apr. 1980 p 153-181 refs (For primary document see N80-25588 16-34)

Avail: NTIS HC A99/MF A01 CSCL 20D

The methods used and the results obtained in four aero-optic tests are summarized. It is concluded that the rather large values of density fluctuation appear to be the result of much higher Mach number than freestream and the violent turbulence in the flow as it separates from the turret. A representative comparison of fairing on-fairing off rms density fluctuation indicates essentially no effect at $M = 0.62$ and a small effect at $M = 0.95$. These data indicate that some slight improvement in optical quality can be expected with the addition of a fairing, although at M

$= 0.62$ its effect would be nil. Fairings are very useful in controlling pressure loads on turrets, but will not have first order effects on optical quality. Scale sizes increase dramatically with increasing azimuth angle for a representative condition. Since both scale sizes and fluctuation levels increase (total turbulence path length also increases) with azimuth angle, substantial optical degradation might be expected. For shorter wave lengths, large degradations occur. R.E.S.

N80-25600*# National Aeronautics and Space Administration. Ames Research Center, Moffett Field, Calif.

OPTIMIZED LASER TURRETS FOR MINIMUM PHASE DISTORTION

G. N. Vanderplaats, Allen E. Fuhs (Naval Postgraduate School), and Gregory A. Blaisdell (Calif. Inst. of Tech., Pasadena) *In its Proc. of the Aero-Optics Symp. on Electromagnetic Wave Propagation from Aircraft* Apr. 1980 p 339-362 refs Sponsored by AFWL (For primary document see N80-25588 16-34)

Avail: NTIS HC A99/MF A01 CSCL 20D

An analysis and computer program which optimizes laser turret geometry to obtain minimum phase distortion is described. Phase distortion due to compressible, inviscid flow over small perturbation laser turrets in subsonic or supersonic flow is calculated. The turret shape is determined by a two dimensional Fourier series; in a similar manner, the flow properties are given by a Fourier series. Phase distortion is calculated for propagation at several combinations of elevation and azimuth angles. A sum is formed from the set of values, and this sum becomes the objective function for an optimization computer program. The shape of the turret is varied to provide minimum phase distortion. M.G.

N80-27347*# National Aeronautics and Space Administration. Ames Research Center, Moffett Field, Calif.

EFFECTIVENESS OF ADVANCED FUEL-CONSERVATIVE PROCEDURES IN THE TRANSITIONAL ATC ENVIRONMENT

L. Tobias and Paul J. Obrien (National Aviation Facilities Experimental Center, Atlantic City, N.J.) *In AGARD Air Traffic Management: Civil/Mil. Systems and Technol.* Feb. 1980 14 p refs (For primary document see N80-27324 18-04)

Avail: NTIS HC A13/MF A01 CSCL 17G

The real time simulation (involving both the pilot and the air traffic controller) of fuel conservative approaches, profile descents, and four dimensional area navigation to assess the effectiveness of the procedures is discussed. Generally, results indicate some difficulties with the procedures tested in a mixed traffic environment and point to the need for computer assistance for effective implementation of candidate procedures. M.G.

A80-19303 * # Large scale model tests of a new technology V/STOL concept. D. C. Whitley (De Havilland Aircraft Co., Ltd., Downsview, Ontario, Canada) and D. G. Koenig (NASA, Ames Research Center, Large Scale Aerodynamics Branch, Moffett Field, Calif.). *American Institute of Aeronautics and Astronautics, Aerospace Sciences Meeting, 18th, Pasadena, Calif., Jan. 14-16, 1980, Paper 80-0233*. 9 p.

An ejector design concept for V/STOL aircraft, featuring a double-delta configuration with two large chordwise ejector slots adjacent to the fuselage side and a tailplane or canard for longitudinal control is examined. Large scale model tests of the concept have shown that ejector systems are capable of significant thrust augmentation at realistic supply pressures and temperatures, so that power plant size and weight can be reduced accordingly. A thrust augmentation of at least 1.75 can be achieved for the isolated ejector, not making allowance for duct and nozzle losses. Substantial reductions in velocity, temperature and noise of the lifting jet are

assured due to mixing within the ejector - this lessens the severity of ground erosion and the thrust loss associated with reingestion. Consideration is also given to the effect of ground proximity, longitudinal aerodynamic characteristics, transition performance, and lateral stability. V.L.

A80-20637 * Application of parametric weight and cost estimating relationships to future transport aircraft. M. N. Beltramo, M. A. Morris (Science Applications, Inc., Los Angeles, Calif.), and J. L. Anderson (NASA, Ames Research Center, Moffett Field, Calif.). *Society of Allied Weight Engineers, Annual Conference, 38th, New York, N.Y., May 7-9, 1979, Paper 1292.* 23 p.

A model comprised of system level weight and cost estimating relationships for transport aircraft is presented. In order to determine the production cost of future aircraft its weight is first estimated based on performance parameters, and then the cost is estimated as a function of weight. For initial evaluation CERs were applied to actual system weights of six aircraft (3 military and 3 commercial) with mean empty weights ranging from 30,000 to 300,000 lb. The resulting cost estimates were compared with actual costs. The average absolute error was only 4.3%. Then the model was applied to five aircraft still in the design phase (Boeing 757, 767 and 777, and BAC HS146-100 and HS146-200). While the estimates for the 757 and 767 are within 2 to 3 percent of their assumed break-even costs, it is recognized that these are very sensitive to the validity of the estimated weights, inflation factor, the amount assumed for non-recurring costs, etc., and it is suggested that the model may be used in conjunction with other information such as RDT&E cost estimates and market forecasts. The model will help NASA evaluate new technologies and production costs of future aircraft. L.M.

A80-22729 * # Noise generation by a lifting wing/flap combination at Reynolds numbers to 2.8×10 to the 6th. J. M. Kendall (California Institute of Technology, Jet Propulsion Laboratory, Molecular Physics and Chemistry Section, Pasadena, Calif.) and W. F. Ahtye (NASA, Ames Research Center, Moffett Field, Calif.). *American Institute of Aeronautics and Astronautics, Aerospace Sciences Meeting, 18th, Pasadena, Calif., Jan. 14-16, 1980, Paper 80-0035.* 12 p. 12 refs. NASA-supported research.

Measurements relating to the noise source location and intensity within various frequency bands were made for an 0.75 m-chord wing/flap model installed in the Ames 7 x 10-foot wind tunnel. A directional microphone system, located outside the open-wall tunnel was scanned in a two-dimensional array of aiming points about the positive-pressure side of the model to determine the principal locations of noise production, and the intensity of each of these. It was found for the case of the flaps being differentially deflected (0 deg, 35 deg) at the half-span station that noise production was concentrated in the immediate region of the resultant surface discontinuity. For equal deflection of the halves (0 deg, 0 deg or 35 deg, 35 deg), noise was produced uniformly along the length of the gap between the wing and the flap. Simulated flap-mounting brackets generated considerable noise in certain cases, but reduced the noise in others. Trailing edge noise did not appear to be important in comparison with other sources. (Author)

A80-22751 * # Transonic swept-wing analysis using asymptotic and other numerical methods. H. K. Cheng, S. Y. Meng (Southern California, University, Los Angeles, Calif.), R. Chow (Grumman Aerospace Corp., Bethpage, N.Y.), and R. C. Smith (NASA, Ames Research Center, Moffett Field, Calif.). *American Institute of Aeronautics and Astronautics, Aerospace Sciences Meeting, 18th, Pasadena, Calif., Jan. 14-16, 1980, Paper 80-0342.* 24 p. 62 refs. Contract No. N00014-75-C-0520; Grant No. NCA2-OR730-601.

The paper presents asymptotic methods for high-aspect-ratio wings in transonic flow developed for straight unyawed wings and for oblique wings. They show that the three-dimensional mixed-flow calculations may be reduced to solving a set of two-dimensional problems at each span station; the development of this theory and the related computational studies are reviewed. Differences between the piloted (oblique) wing, the swept-back wing, and the swept-forward-wing in the induced upwash are discussed; examples of similarity solutions are demonstrated for high subcritical and slightly supercritical component flows, and comparisons made with relaxation solutions of a full potential equation. The examples include oblique and symmetric swept wings, and the adequacy of the existing full-potential computer code is examined. A.T.

A80-23955 * # Control of forebody vortex orientation to alleviate side forces. D. J. Peake, D. A. Johnson (NASA, Ames Research Center, Moffett Field, Calif.), and F. K. Owen. *American Institute of Aeronautics and Astronautics, Aerospace Sciences Meeting, 18th, Pasadena, Calif., Jan. 14-16, 1980, Paper 80-0183.* 32 p. 28 refs. USAF-supported research; Contracts no. NAS2-9663; No. NAS2-10352.

The paper deals with the salient phenomena of three-dimensional symmetric and asymmetric separated flows about typical forebodies at high angles of attack. Particular consideration is given to pressure, forces, and laser vapor screen measurements carried out on a 5-deg semiangle cone in a Mach 0.6 flow under turbulent conditions and supportive tests using a 16-deg semiangle tangent ogive. V.T.

A80-26628 * Automated design using numerical optimization. G. N. Vanderplaats (NASA, Ames Research Center, Moffett Field, Calif.). *Society of Automotive Engineers, Aerospace Meeting, Los Angeles, Calif., Dec. 3-6, 1979, Paper 791061.* 12 p. 56 refs.

Numerical optimization concepts are described with limited technical detail. The purpose is to provide the nonspecialist with sufficient information to judge the applicability of these methods to his particular design problem. The concepts are first described in physical terms to give a basic understanding of the iterative procedure employed by these methods. Next, the typical engineering task is presented and converted to a form amenable to solution by numerical optimization. Basic algorithms for solving this problem are identified. Numerous applications are referenced, emphasizing the structural design discipline. The state of the art allows for the routine solution of nonlinear design problems of approximately 20 independent variables subject to 100 or more constraints. In many applications, much larger design problems may be solved. Selected references are provided which describe the methods and applications in more detail. (Author)

A80-26957 * # Measurements of control stability characteristics of a wind-tunnel model using a transfer function method. I. Chopra (NASA, Ames Research Center, Moffett Field; NASA/Stanford, Joint Institute for Aeronautics and Acoustics, Stanford, Calif.) and J. D. Ballard (NASA, Ames Research Center, Moffett Field, Calif.). In: *Aerodynamic Testing Conference, 11th, Colorado Springs, Colo., March 18-20, 1980, Technical Papers.* (A80-26929 10-09) New York, American Institute of Aeronautics and Astronautics, Inc., 1980, p. 256-261. (AIAA 80-0457)

Recent state-of-the-art techniques in rotor systems include the use of active feedback to augment the dynamic control characteristics of an aircraft system. A recent test of a stoppable rotor with blade circulation blowing was conducted in the Ames Research Center's 40- by 80-ft wind tunnel. A major part of the test schedule was dedicated to the acquisition of data to determine the stability of

a closed-loop hub-moment feedback control system. Therefore, the open-loop control response was measured at several flight conditions to ascertain the stability of the system prior to the final closed-loop feedback control test. Measurements were made during both the stopped and rotating rotor modes, and open-loop Bode plots were obtained for the control loops associated with the moments about the longitudinal and lateral axis. (Author)

A80-26967 * # High-resolution LDA measurements of Reynolds stress in boundary layers and wakes. K. L. Orloff and L. E. Olson (NASA, Ames Research Center, Moffett Field, Calif.). In: Aerodynamic Testing Conference, 11th, Colorado Springs, Colo., March 18-20, 1980, Technical Papers. (A80-26929 10-09) New York, American Institute of Aeronautics and Astronautics, Inc., 1980, p. 363-374. 11 refs. (AIAA 80-0436)

The turbulent character of the boundary layer and wake associated with an airfoil has been studied at a Reynolds number of 1,000,000 and a Mach number of 0.1. To accomplish these measurements, a unique laser Doppler anemometer (LDA) has been developed that is capable of sensing two velocity components from a remote distance of 2.13 m. Using special simultaneity logic and counter-type signal processors, the geometrical features of the LDA have been exploited to provide variable spatial resolution as low as 0.2 mm. By combining the LDA with an on-line computerized data acquisition and display system, it has been possible to measure mean velocity and Reynolds stress tensor distribution at several locations along the upper surface of a 0.9-m-chord, flapped airfoil installed in the Ames 7- by 10-Foot Wind Tunnel. (Author)

A80-27241 * Aircraft motion analysis using limited flight and radar data. R. C. Wingrove, R. E. Bach, Jr. (NASA, Ames Research Center, Aircraft Guidance and Navigation Branch, Moffett Field, Calif.), and E. K. Parks (Arizona, University, Tucson, Ariz.). In: Society of Flight Test Engineers, Annual Symposium, 10th, Las Vegas, Nev., September 4-6, 1979, Proceedings. (A80-27226 10-05) Lancaster, Calif., Society of Flight Test Engineers, 1979. 18 p. 11 refs.

The development and application of methods for reconstructing, from a limited set of recorded data, a comprehensive scenario of aircraft motions before and during an accident are described. The accuracy of these analytical methods is investigated using data recorded onboard the Ames CV-990 research aircraft. In these experiments, the expanded set of data, derived from either foil or ATC records, is compared with corresponding values measured by the research instrumentation system onboard the aircraft. The results indicate that many of the derived quantities are in good agreement with the corresponding onboard measurements. A recent application of this procedure using actual accident records is presented and potential applications are briefly reviewed. (Author)

A80-29494 * # Diagnosis of separated flow regions on wind-tunnel models using an infrared camera. A. Bandettini and D. J. Peake (NASA, Ames Research Center, Moffett Field, Calif.). In: ICIASF '79; International Congress on Instrumentation in Aerospace Simulation Facilities, 8th, Monterey, Calif., September 24-26, 1979, Record. (A80-29476 11-35) New York, Institute of Electrical and Electronics Engineers, Inc., 1979, p. 171-185. 8 refs.

A novel technique utilizing an infrared-sensitive imaging camera has been used to determine the location of three-dimensional (3-D) separated flow regions on an inclined 5 deg semiangle fiberglass cone. The results illustrate that there is a change in the contrast of the infrared (IR) signature on the cone surface corresponding with the location where the skin-friction lines merge toward lines of 3-D separation. This technique should offer a convenient means for locating separated flow regions on wind-tunnel models while obtaining simultaneous force, skin-friction, and pressure data. (Author)

A80-29501 * # Computer/experiment integration for unsteady aerodynamic research. S. S. Davis (NASA, Ames Research Center, Moffett Field, Calif.). In: ICIASF '79; International Congress on Instrumentation in Aerospace Simulation Facilities, 8th, Monterey, Calif., September 24-26, 1979, Record. (A80-29476 11-35) New York, Institute of Electrical and Electronics Engineers, Inc., 1979, p. 237-250. 9 refs.

The use of a minicomputer for the acquisition and analysis of unsteady aerodynamic data is described. Some of the novel features of the system include: on-line digitization, a signal-averaging algorithm, Fourier decomposition, graphical display, and on-line theoretical computations to compare with the ongoing experiment. The system's capabilities are described using some data from a recently completed oscillating airfoil experiment. (Author)

A80-32448 * # Total aircraft flight-control system - Balanced open- and closed-loop control with dynamic trim maps. G. A. Smith and G. Meyer (NASA, Ames Research Center, Moffett Field, Calif.). In: Challenge of the '80s; Proceedings of the Third Digital Avionics Systems Conference, Fort Worth, Tex., November 6-8, 1979. (A80-32417 12-06) New York, Institute of Electrical and Electronics Engineers, Inc., 1979, p. 215-223. 5 refs.

The availability of the airborne digital computer has made possible a Total Aircraft Flight Control System (TAF COS) that uses virtually the complete nonlinear propulsive and aerodynamic data for the aircraft to construct dynamic trim maps that represent an inversion of the aircraft model. The trim maps, in series with the aircraft, provide essentially a linear feed-forward path. Basically, open-loop trajectory control is employed with only a small perturbation feedback signal required to compensate for inaccuracy in the aircraft model and for external disturbances. Simulation results for application to an automatic carrier-landing system are presented. Flight-test results for a STOL aircraft operating automatically over a major portion of its flight regime are presented. The concept promises a more rapid and straightforward design from aerodynamic principles, particularly for highly nonlinear configurations, and requires substantially less digital computer capacity than conventional automatic flight-control system designs. (Author)

A80-34997 * # Multicyclic control for helicopters - Research in progress at Ames Research Center. J. L. McCloud, III (NASA, Ames Research Center, Moffett Field, Calif.). In: Structures, Structural Dynamics, and Materials Conference, 21st, Seattle, Wash., May 12-14, 1980, Technical Papers. Part 1. (A80-34993 14-39) New York, American Institute of Aeronautics and Astronautics, Inc., 1980, p. 77-81. 19 refs. (AIAA 80-0671; AHS Paper 80-70)

The term multicyclic control describes a blade pitch control technique used by helicopter designers to alleviate vibration in rotorcraft. Because rotor-induced vibrations are periodic, a multicyclic system, synchronized to the main rotor's azimuth position, is suitable. Many types of rotors - ranging from the jet-flap and circulation-control rotors to the conventional full-blade feathering rotors - have utilized multicyclic control. Multicyclic control systems may be designed to reduce blade-bending stresses, to reduce rotor-induced vibration, and to improve rotor performance. Rotor types are reviewed, primarily to highlight their differences. The increased use of composites in blade construction is seen to indicate that vibration alleviation will be the prime focus of multicyclic control. Adaptive feedback control systems, which also incorporate gust alleviation, are considered to be the ultimate application of multicyclic control. (Author)

A80-34998 * # Multicyclic control of a helicopter rotor considering the influence of vibration, loads, and control motion. T. J. Brown and J. L. McCloud, III (NASA, Ames Research Center,

F

Moffett Field, Calif.). In: Structures, Structural Dynamics, and Materials Conference, 21st, Seattle, Wash., May 12-14, 1980, Technical Papers, Part 1. (A80-34993 14-39) New York, American Institute of Aeronautics and Astronautics, Inc., 1980, p. 82-100. 7 refs. (AIAA 80-0673; AHS Paper 80-72)

Weighted multiple linear regression is used to establish a transfer function matrix relationship between higher harmonic control inputs and transducer vibration outputs for a controllable twist rotor. Data used in the regression were taken from the test of a KAMAN controllable twist rotor conducted in the Ames Research Center's 40-by 80-Foot Wind Tunnel in June 1977. Optimal controls to minimize fixed system vibrational levels are calculated using linear quadratic regulatory theory with a control deflection penalty included in the performance criteria. Control sensitivity to changes in control travel, forward speed, and lift and propulsive forces is examined. It is found that the linear transfer matrix is a strong function of forward speed and a weak function of lift and propulsive force. An open-loop strategy is proposed for systems with limited control travel. (Author)

A80-35038 * # Unsteady aerodynamics of conventional and supercritical airfoils. S. S. Davis and G. N. Malcolm (NASA, Ames Research Center, Moffett Field, Calif.). In: Structures, Structural Dynamics, and Materials Conference, 21st, Seattle, Wash., May 12-14, 1980, Technical Papers, Part 1. (A80-34993 14-39) New York, American Institute of Aeronautics and Astronautics, Inc., 1980, p. 417-433. 20 refs. (AIAA 80-0734)

The unsteady aerodynamics of a conventional and a supercritical airfoil are compared by examining measured chordwise unsteady pressure time-histories from four selected flow conditions. Although an oscillating supercritical airfoil excites more harmonics, the strength of the airfoil's shock wave is the more important parameter governing the complexity of the unsteady flow. Whether they are conventional or supercritical, airfoils that support weak shock waves induce unsteady loads that are qualitatively predictable with classical theories; flows with strong shock waves are sensitive to details of the shock-wave and boundary-layer interaction and cannot be adequately predicted. (Author)

A80-36002 * # Upper surface blowing noise of the NASA-Ames quiet short-haul research aircraft. A. J. Bohn (Boeing Commercial Airplane Co., Seattle, Wash.) and M. D. Shovlin (NASA, Ames Research Center, Moffett Field, Calif.). *American Institute of Aeronautics and Astronautics, Aeroacoustics Conference, 6th, Hartford, Conn., June 4-6, 1980, Paper 80-1064.* 8 p. 7 refs.

An experimental study of the propulsive-lift noise of the NASA-Ames quiet short-haul research aircraft (QSRA) is described. Comparisons are made of measured QSRA flyover noise and model propulsive-lift noise data available in references. Developmental tests of trailing-edge treatments were conducted using sawtooth-shaped and porous USB flap trailing-edge extensions. Small scale parametric tests were conducted to determine noise reduction/design relationships. Full-scale static tests were conducted with the QSRA preparatory to the selection of edge treatment designs for flight testing. QSRA flight and published model propulsive-lift noise data have similar characteristics. Noise reductions of 2 to 3 dB were achieved over a wide range of frequency and directivity angles in static tests of the QSRA. These noise reductions are expected to be achieved or surpassed in flight tests planned by NASA in 1980. (Author)

A80-38085 * Test section configuration for aerodynamic testing in shock tubes. W. J. Cook (Iowa State University of Science and Technology, Ames, Iowa), L. L. Presley, and G. T. Chapman

(NASA, Ames Research Center, Moffett Field, Calif.). In: Shock tubes and waves; Proceedings of the Twelfth International Symposium, Jerusalem, Israel, July 16-19, 1979. (A80-38078 15-34) Jerusalem, Magnes Press, 1980, p. 127-136. 7 refs. Grant No. NSG-2152.

This paper presents results of a study of the test section configuration required to minimize or alleviate interference effects on model flow produced by the presence of test section walls in the aerodynamic testing of two dimensional transonic airfoils in a shock tube. Tests at a nominal Mach number of 0.85 and a chord Reynolds number of 2,000,000 were carried out by means of schlieren photography and pressure measurements for several symmetric airfoil profiles using shock tube test sections with unmodified straight walls, contoured walls, and slotted walls with adjacent chambers. Results were compared with corresponding results from conventional wind tunnel tests of the airfoils. Results for the straight wall tests show major airfoil flow distortions. Results from contoured wall tests and those performed using a slotted wall test section developed in this study exhibit essential agreement with wind tunnel results. The collective results show that test sections for aerodynamic testing can be designed for shock tubes that will alleviate wall interference effects. (Author)

A80-38641 * # A measurement of forward-flight effects on the noise from a JT15D-1 turbofan engine in the NASA-Ames 40-by 80-Foot Wind Tunnel. W. F. Ahtye (NASA, Ames Research Center, Moffett Field, Calif.). *American Institute of Aeronautics and Astronautics, Aeroacoustics Conference, 6th, Hartford, Conn., June 4-6, 1980, Paper 80-1026.* 18 p. 8 refs.

A Pratt and Whitney JT15D-1 turbofan engine was tested in two facilities at Ames Research Center: the outdoor Static Test Facility and the 40-by 80-Foot Wind Tunnel. The primary purposes of the test were to determine the effects of forward velocity on the turbofan spectra in the forward quadrant for the cruise inlet and to compare these wind-tunnel spectra with outdoor spectra to determine the possibility of simulating forward-velocity effects from purely outdoor measurements. The wind-tunnel data show a reduction in the blade-passage frequency tones of the order of 10 dB with increasing forward velocity at subsonic fan-tip speeds. No forward-velocity variation was observed at supersonic tip speeds. Comparison of in-duct spectra for the cruise inlet at forward velocity, with spectra from outdoor tests with a distortion-control inlet shows excellent agreement for the in-duct data when allowance is made for different in-duct volumes. This is also reflected in good agreement for the far-field spectra at small forward angles. The comparisons of wind-tunnel and outdoor data also indicate that at least for the JT15D-1, it may be possible to approximate the shape of the far-field spectra at large directivity angles from an outdoor measurement with the cruise inlet, providing an effective inflow control device is used. (Author)

A80-38905 * # Potential benefits for propfan technology on derivatives of future short- to medium-range transport aircraft. I. M. Goldsmith (Douglas Aircraft Co., Long Beach, Calif.) and J. V. Bowles (NASA, Ames Research Center, V/STOL Systems Technology Branch, Moffett Field, Calif.). *AIAA, SAE, and ASME, Joint Propulsion Conference, 16th, Hartford, Conn., June 30-July 2, 1980, AIAA Paper 80-1090.* 10 p.

It is noted that several NASA-sponsored studies have identified a substantial potential fuel savings for high subsonic speed aircraft utilizing the propfan concept compared to the equivalent technology turbofan aircraft. Attention is given to a feasibility study for propfan-powered short- to medium-haul commercial transport aircraft conducted to evaluate potential fuel savings and identify critical technology requirements using the latest propfan performance data. An analysis is made of the design and performance characteristics of a wing-mounted and two-aft-mounted derivative propfan aircraft configurations, based on a DC-9 Super 80 airframe, which are compared to the baseline turbofan design. Finally, recommendations for further research efforts are also made. M.E.P.

A80-38984 * # Study of cooling air inlet and exit geometries for horizontally opposed piston aircraft engines. J. Katz, V. R. Corsiglia, and P. R. Barlow (NASA, Ames Research Center, Moffett Field, Calif.). *AIAA, SAE, and ASME, Joint Propulsion Conference, 16th, Hartford, Conn., June 30-July 2, 1980, AIAA Paper 80-1242*. 8 p. 10 refs.

A semispan wing and nacelle of a typical general aviation twin-engine aircraft was tested to evaluate the cooling capability and drag of several nacelle shapes; the nacelle shapes included cooling air inlet and exit variations. The tests were conducted in the Ames Research Center's 40- by 80-Foot Wind Tunnel. It was found that the cooling air inlet geometry of opposed piston engine installations has a major effect on inlet pressure recovery, but only a minor effect on drag. Exit location showed a large effect on drag, especially for those locations on the sides of the nacelle where the suction characteristics were based on interaction with the wing surface pressures. (Author)

A80-43286 * # A vortex-lattice method for the calculation of the nonsteady separated flow over delta wings. D. Levin and J. Katz (NASA, Ames Research Center, Moffett Field, Calif.). *American Institute of Aeronautics and Astronautics, Aircraft Systems Meeting, Anaheim, Calif., Aug. 4-6, 1980, Paper 80-1803*. 8 p. 20 refs.

An analysis is made of the wake structure and the forces on a delta wing as it undergoes nonsteady motion, wherein the flow separates at the leading edge. Comparisons of these predictions with existing experimental and theoretical data for the nonsteady linear and nonlinear motions indicate good agreement. It was found that the time-dependent, wake-shedding numerical procedure applied here for the wake rollup and the lift force calculation resulted in considerable saving of computer time over methods using the iterative wake rollup procedure. Calculated results for various motions of the delta wing, including the plunging motion, are presented for both the separated and the attached flow cases. (Author)

A80-43315 * # Effect of propeller slipstream on the drag and performance of the engine cooling system for a general aviation twin-engine aircraft. J. Katz, V. R. Corsiglia, and P. R. Barlow (NASA, Ames Research Center, Moffett Field, Calif.). *American Institute of Aeronautics and Astronautics, Aircraft Systems Meeting, Anaheim, Calif., Aug. 4-6, 1980, Paper 80-1872*. 8 p. 7 refs.

The pressure recovery of incoming cooling air and the drag associated with engine cooling of a typical general aviation twin-engine aircraft was investigated experimentally. The semispan model was mounted vertically in the 40- by 80-Foot Wind Tunnel at Ames Research Center. The propeller was driven by an electric motor to provide thrust with low vibration levels for the cold-flow configuration. It was found that the propeller slipstream reduces the frontal air spillage around the blunt nacelle shape. Consequently, this slipstream effect promotes flow reattachment at the rear section of the engine nacelle and improves inlet pressure recovery. These effects are most pronounced at high angles of attack, that is, climb condition. For the cruise condition those improvements were more moderate. (Author)

A80-44142 * # Calculations of transonic flow about an airfoil in a wind tunnel. L. S. King and D. A. Johnson (NASA, Ames Research Center, Moffett Field, Calif.). *American Institute of Aeronautics and Astronautics, Fluid and Plasma Dynamics Conference, 13th, Snowmass, Colo., July 14-16, 1980, Paper 80-1366*. 12 p. 28 refs.

A combined experimental and numerical study was performed to include wind-tunnel wall interference effects in calculations for

airfoil flows at transonic speeds. Pressure-survey-tube and laser-Doppler velocimeter measurements were made in the flow field about an airfoil in the 2- by 2-Foot Transonic Wind Tunnel at Ames Research Center. The results were then used as boundary data in a Navier-Stokes code modified by incorporating a pressure condition on the upper and lower computational boundaries. Comparison of calculated results and experimental data obtained from the surface of the airfoil indicates that the pressure-boundary condition is particularly effective in moving the shock to a position near that observed experimentally when the flow remains attached. For flows with large separation, shock position and viscous-layer properties are not well predicted, principally because of the inadequacies of the algebraic turbulence models employed with the method. (Author)

A80-44154 * # A comprehensive comparison between experiment and prediction for a transonic turbulent separated flow. D. A. Johnson, C. C. Horstman (NASA, Ames Research Center, Moffett Field, Calif.), and W. D. Bachalo (Spectron Development Laboratories, Inc., Costa Mesa, Calif.). *American Institute of Aeronautics and Astronautics, Fluid and Plasma Dynamics Conference, 13th, Snowmass, Colo., July 14-16, 1980, Paper 80-1407*. 19 p. 19 refs.

Attempts to predict surface pressure distributions on lifting surfaces have been relatively unsuccessful in the transonic regime when the shock wave is of sufficient strength to produce an extensive region of turbulent separated flow. For these conditions, the viscous flow behavior must be accurately described even to obtain reasonable predictions of surface pressure. The present paper addresses this problem. Detailed comparisons between prediction and experiment are made for a transonic, turbulent boundary-layer separation (freestream Mach number = 0.875) for which the turbulent flow properties (including the turbulent Reynolds stress) had been measured by the laser velocimeter technique from upstream of the separated region through reattachment. The flow was generated on an axisymmetric 'bump' model designed to simulate the flow on an airfoil at transonic conditions. The numerical methods used in the comparisons include the solution of the time-dependent, mass-averaged Navier-Stokes equations, and the solution of the compressible boundary-layer equations by the inverse method. Solutions were obtained for the well established Cebeci-Smith algebraic turbulence model and the more recently developed Wilcox-Rubesin two-equation turbulence model. (Author)

A80-44155 * # Separated skin-friction measurements - Source of error: An assessment and elimination. F. K. Owen and D. A. Johnson (NASA, Ames Research Center, Moffett Field, Calif.). *American Institute of Aeronautics and Astronautics, Fluid and Plasma Dynamics Conference, 13th, Snowmass, Colo., July 14-16, 1980, Paper 80-1409*. 10 p. 19 refs. Contract No. NAS2-10352.

Potential sources of error in the use of heated surface gages for separated-skin-friction measurement are studied. Emphasis is placed on the interpretation of local skin-friction measurements in two- and three-dimensional separated turbulent-shear flows before they are used to test the validity of current and proposed computer codes. V.T.

A80-45556 * # A new approach to active control of rotorcraft vibration. N. K. Gupta (Integrated Systems, Inc., Stanford, Calif.), R. W. Du Val (NASA, Ames Research Center, Moffett Field, Calif.), and J. Fuller (Systems Control, Inc., Palo Alto, Calif.). In: *Guidance and Control Conference, Danvers, Mass., August 11-13, 1980, Collection of Technical Papers. (A80-45514 19-17)* New York, American Institute of Aeronautics and Astronautics, Inc., 1980, p. 347-358. 13 refs. (AIAA 80-1778)

A state-variable feedback approach is utilized for active control of rotorcraft vibration. Fuselage accelerations are passed through undamped second-order filters with resonant frequencies at N/rev. The resulting outputs contain predominantly the N/rev vibration components, phase shifted by 180 deg, and are used to drive the blade pitch to cancel this component of fuselage vibration. The linear-quadratic-gaussian (LQG) method is used to design a feedback control system utilizing these filtered accelerations. The design is based on a nine-degree-of-freedom linear model of the Rotor System Research Aircraft (RSRA) in hover and is evaluated on a nonlinear blade-element simulation of the RSRA for this flight condition. The system is shown to essentially eliminate vibrations at N/rev in all axes. The required blade-pitch amplitude is within the capability of conventional actuators at the N/rev frequency. (Author)

A80-45856 * # Pressure measurements on an ogive-cylinder at high angles of attack with laminar, transitional, or turbulent separation. P. J. Lamont (NASA, Ames Research Center, Moffett Field, Calif.). In: Atmospheric Flight Mechanics Conference, Danvers, Mass., August 11-13, 1980, Collection of Technical Papers. (A80-45855 20-01) New York, American Institute of Aeronautics and Astronautics, Inc., 1980, p. 1-10. 7 refs. (AIAA 80-1556)

This paper reports results from pressure tests on an ogive-cylinder in the low-turbulence 12-foot pressure wind tunnel. The results consist of pressure distributions over a wide range of Reynolds numbers and angles of attack. The tests encompassed a complete coverage of different roll orientations shown to be essential in order to fully define all the possible flow conditions. When the various roll-angle results are combined, it is possible to interpret the effects of changing angle of attack or Reynolds number. Two basic mechanisms for producing asymmetric flow are identified. One mechanism operates in both the laminar and the fully turbulent separation regimes; this mechanism is the one qualitatively described by the impulsive flow analogy. The other mechanism occurs only in the transitional separation regime. This asymmetric flow has the same form as that in the two-dimensional crossflow on a circular cylinder in the transitional flow regime. Finally, these results make it possible to draw up critical Reynolds number boundaries between the laminar, transitional, and fully turbulent separation regimes throughout the angle-of-attack range from 20 to 90 deg. (Author)

A80-45879 * # Mathematical modeling of the aerodynamics of high-angle-of-attack maneuvers. L. B. Schiff, M. Tobak, and G. N. Malcolm (NASA, Ames Research Center, Moffett Field, Calif.). In: Atmospheric Flight Mechanics Conference, Danvers, Mass., August 11-13, 1980, Collection of Technical Papers. (A80-45855 20-01) New York, American Institute of Aeronautics and Astronautics, Inc., 1980, p. 222-235. 48 refs. (AIAA 80-1583)

This paper is a review of the current state of aerodynamic mathematical modeling for aircraft motions at high angles of attack. The mathematical model serves to define a set of characteristic motions from whose known aerodynamic responses the aerodynamic response to an arbitrary high angle-of-attack flight maneuver can be predicted. Means are explored of obtaining stability parameter information in terms of the characteristic motions, whether by wind-tunnel experiments, computational methods, or by parameter-identification methods applied to flight-test data. A rationale is presented for selecting and verifying the aerodynamic mathematical model at the lowest necessary level of complexity. Experimental results describing the wing-rock phenomenon are shown to be accommodated within the most recent mathematical model by admitting the existence of aerodynamic hysteresis in the steady-state variation of the rolling moment with roll angle. Interpretation of the experimental results in terms of bifurcation theory reveals the general conditions under which aerodynamic hysteresis must exist. (Author)

A80-45882 * # Computations of the Magnus effect for slender bodies in supersonic flow. W. B. Sturek (U.S. Army, Ballistics Research Laboratory, Aberdeen Proving Ground, Md.) and L. B. Schiff (NASA, Ames Research Center, Moffett Field, Calif.). In: Atmospheric Flight Mechanics Conference, Danvers, Mass., August 11-13, 1980, Collection of Technical Papers. (A80-45855 20-01) New York, American Institute of Aeronautics and Astronautics, Inc., 1980, p. 260-270. 13 refs. (AIAA 80-1586)

A recently reported Parabolized Navier-Stokes code has been employed to compute the supersonic flow field about spinning cone, ogive-cylinder, and boattailed bodies of revolution at moderate incidence. The computations were performed for flow conditions where extensive measurements for wall pressure, boundary layer velocity profiles and Magnus force had been obtained. Comparisons between the computational results and experiment indicate excellent agreement for angles of attack up to six degrees. The comparisons for Magnus effects show that the code accurately predicts the effects of body shape and Mach number for the selected models for Mach numbers in the range of 2-4. (Author)

A80-45894 * # A variational technique for smoothing flight-test and accident data. R. E. Bach, Jr. (NASA, Ames Research Center, Moffett Field, Calif.). In: Atmospheric Flight Mechanics Conference, Danvers, Mass., August 11-13, 1980, Collection of Technical Papers. (A80-45855 20-01) New York, American Institute of Aeronautics and Astronautics, Inc., 1980, p. 383-391. 16 refs. (AIAA 80-1601)

The problem of determining aircraft motions along a trajectory is solved using a variational algorithm that generates unmeasured states and forcing functions, and estimates instrument bias and scale-factor errors. The problem is formulated as a nonlinear fixed-interval smoothing problem, and is solved as a sequence of linear two-point boundary value problems, using a sweep method. The algorithm has been implemented for use in flight-test and accident analysis. Aircraft motions are assumed to be governed by a six-degree-of-freedom kinematic model; forcing functions consist of body accelerations and winds, and the measurement model includes aerodynamic and radar data. Examples of the determination of aircraft motions from typical flight-test and accident data are presented. (Author)

A80-45907 * # Model development for automatic guidance of a VTOL aircraft to a small aviation ship. T. Goka, J. A. Sorensen, S. F. Schmidt (Analytical Mechanics Associates, Inc., Mountain View, Calif.), and C. H. Paulk, Jr. (NASA, Ames Research Center, Moffett Field, Calif.). In: Atmospheric Flight Mechanics Conference, Danvers, Mass., August 11-13, 1980, Collection of Technical Papers. (A80-45855 20-01) New York, American Institute of Aeronautics and Astronautics, Inc., 1980, p. 497-505. 10 refs. Contract No. NAS2-10288. (AIAA 80-1617)

This paper describes a detailed mathematical model which has been assembled to study automatic approach and landing guidance concepts to bring a VTOL aircraft onto a small aviation ship. The model is used to formulate system simulations which in turn are used to evaluate different guidance concepts. Ship motion (Sea State 5), wind-over-deck turbulence, MLS-based navigation, implicit model following flight control, lift fan V/STOL aircraft, ship and aircraft instrumentation errors, various steering laws, and appropriate environmental and human factor constraints are included in the model. Results are given to demonstrate use of the model and simulation to evaluate performance of the flight system and to choose appropriate guidance techniques for further cockpit simulator study. (Author)

A80-45912 * # A pilot modeling technique for handling-qualities research. R. A. Hess (NASA, Ames Research Center,

Moffett Field, Calif.). In: Atmospheric Flight Mechanics Conference, Danvers, Mass., August 11-13, 1980, Collection of Technical Papers. (A80-45855 20-01) New York, American Institute of Aeronautics and Astronautics, Inc., 1980, p. 536-549. 31 refs. (AIAA 80-1624)

A brief survey of the more dominant analysis techniques used in closed-loop handling-qualities research is presented. These techniques are shown to rely on so-called classical and modern analytical models of the human pilot which have their foundation in the analysis and design principles of feedback control. The optimal control model of the human pilot is discussed in some detail and a novel approach to the a priori selection of pertinent model parameters is discussed. Frequency domain and tracking performance data from 10 pilot-in-the-loop simulation experiments involving 3 different tasks are used to demonstrate the parameter selection technique. Finally, the utility of this modeling approach in handling-qualities research is discussed. (Author)

A80-45916 * # Flying-qualities criteria for wings-level-turn maneuvering during an air-to-ground weapon delivery task. R. I. Sammonds (NASA, Ames Research Center, Moffett Field, Calif.) and J. W. Bunnell, Jr. (USAF, Wright Aeronautical Laboratories, Wright-Patterson AFB, Ohio). In: Atmospheric Flight Mechanics Conference, Danvers, Mass., August 11-13, 1980, Collection of Technical Papers. (A80-45855 20-01) New York, American Institute of Aeronautics and Astronautics, Inc., 1980, p. 583-595. (AIAA 80-1628)

A moving-base simulator experiment conducted at Ames Research Center demonstrated that a wings-level-turn control mode improved flying qualities for air-to-ground weapons delivery compared with those of a conventional aircraft. Evaluations of criteria for dynamic response for this system have shown that pilot ratings correlate well on the basis of equivalent time constant of the initial response. Ranges of this time constant, as well as digital-system transport delays and lateral-acceleration control authorities that encompassed Level I through Level III handling qualities, were determined. (Author)

A80-49703 * The future of short-haul transport aircraft. L. J. Williams (NASA, Ames Research Center, Moffett Field, Calif.). *Society of Automotive Engineers, International Air Transportation Meeting, Cincinnati, Ohio, May 20-22, 1980, Paper 800755*. 35 p. 12 refs.

Owing to recent economic and regulatory changes and escalating fuel costs, major airlines have begun to shift their short-haul service to longer, more profitable routes, leaving short-haul operations to rapidly growing commuter airlines. The short-haul routes are currently serviced by small turboprop-powered aircraft. The results of some recent design studies aimed at replacing the turboprops with specialized propeller- and rotor-driven aircraft are discussed. Some potential future designs are illustrated and discussed. V.P.

A80-49832 * Aircraft simulation data management - A prototype system. D. F. Crane (NASA, Ames Research Center, Moffett Field, Calif.), P. Thomas, J. R. Maurer, and D. E. Tweten (Computer Sciences Corp., Mountain View, Calif.). In: Summer Computer Simulation Conference, Newport Beach, Calif., July 24-26, 1978, Proceedings. (A80-49826 22-66) Montvale, N.J., AFIPS Press, 1978, p. 367-371.

Piloted flight simulations are used throughout the aircraft development process to evaluate design concepts, handling qualities and operational procedures. Simulation project managers are often inundated with data but without a convenient and efficient way to make the correlations and analyses necessary to evaluate system performance. A computer-based Simulation Management System (SIMS) is under development. SIMS will permit simulation project

engineers to quickly acquire, access, display, edit, analyze, and document the information necessary to more efficiently manage the research program. SIMS features interactive, associative access to simulation data. This paper describes SIMDEM, a prototype system designed to demonstrate these concepts and procedures in order to obtain feedback from simulator users to guide system design. (Author)

AMES FUNDED RESEARCH JOURNAL ARTICLES

A80-18545 * A real-time electronic imaging system for solar X-ray observations from sounding rockets. J. M. Davis, J. W. Ting, and M. Gerassimenko (American Science and Engineering, Inc., Cambridge, Mass.). *Space Science Instrumentation*, vol. 5, Dec. 1979, p. 51-71. 20 refs. Contract No. NAS2-8683.

A real-time imaging system for displaying the solar coronal soft X-ray emission, focussed by a grazing incidence telescope, is described. The design parameters of the system, which is to be used primarily as part of a real-time control system for a sounding rocket experiment, are identified. Their achievement with a system consisting of a microchannel plate, for the conversion of X-rays into visible light, and a slow-scan vidicon, for recording and transmission of the integrated images, is described in detail. The system has a quantum efficiency better than 8 deg above 8 A, a dynamic range of 1000 coupled with a sensitivity to single photoelectrons, and provides a spatial resolution of 15 arc seconds over a field of view of 40 x 40 square arc minutes. The incident radiation is filtered to eliminate wavelengths longer than 100 A. Each image contains 3.93 x 10 to the 5th bits of information and is transmitted to the ground where it is processed by a mini-computer and displayed in real-time on a standard TV monitor. (Author)

A80-21906 * Integral equations for flows in wind tunnels. J. A. Fromme and M. A. Golberg (Nevada, University, Las Vegas, Nev.). *Journal of Integral Equations*, vol. 1, Sept. 1979, p. 249-273. 47 refs. Grant No. NSG-2140.

This paper surveys recent work on the use of integral equations for the calculation of wind tunnel interference. Due to the large number of possible physical situations, the discussion is limited to two-dimensional subsonic and transonic flows. In the subsonic case, the governing boundary value problems are shown to reduce to a class of Cauchy singular equations generalizing the classical airfoil equation. The theory and numerical solution are developed in some detail. For transonic flows nonlinear singular equations result, and a brief discussion of the work of Kraft and Kraft and Lo on their numerical solution is given. Some typical numerical results are presented and directions for future research are indicated. (Author)

A80-30566 * # Analysis of two-dimensional incompressible flows by a subsurface panel method. J. Moran (Minnesota, University, Minneapolis, Minn.), K. Cole, and D. Wahl. *AIAA Journal*, vol. 18, May 1980, p. 526-533. 6 refs. Grant No. NSG-2316; Contract No. N00014-76-0182.

A new approach to panel methods is explored for two-dimensional steady incompressible flows. The method uses linear distributions of sources and vortices on straight-line panels, but satisfies boundary conditions on the actual body surface, at nodes that are also end points of the panels. The result is continuity in body-surface velocity distribution, without recourse to numerical quadrature for the velocity influence coefficients. The method is unusually sensitive to the distribution of the nodes. For example, it almost always fails to give acceptable results when the nodes are

distributed randomly. However, the continuity of the velocity distribution makes possible a unique node redistribution scheme, which may be iterated to give accurate results reliably. (Author)

A80-31804 * Characterization of acoustic disturbances in linearly sheared flows. S. P. Koutsoyannis (Stanford University, Stanford, Calif.). *Journal of Sound and Vibration*, vol. 68, Jan. 22, 1980, p. 187-202. 19 refs. Grants No. NSG-2007; No. NSG-2215.

Inviscid fluctuations in a compressible linearly sheared, but otherwise homogeneous, parallel two-dimensional flow are considered. The equation describing the plane wave propagation (PWP), the stability, or the rectangular duct mode characteristics in such a flow is shown to be reducible to Whittaker's equation. The exact solutions are applied to problems of PWP and stability in linearly sheared flows as limiting cases in which the speed of sound goes to infinity (incompressible limit) or the shear layer thickness, or wave number, goes to zero (vortex sheet limit). With respect to the PWP it is shown that the shear layer possesses no resonances and no Brewster angles, while with regard to the problem of the stability of a finite thickness shear layer with a linear velocity profile, it is shown that the thin layer is unstable to long wavelength disturbances for all Mach numbers. J.P.B.

A80-31805 * A note of sound radiation from distributed sources. H. Levine (Stanford University, Stanford, Calif.). *Journal of Sound and Vibration*, vol. 68, Jan. 22, 1980, p. 203-207. Grant No. NSG-2007.

The power output from a normally vibrating strip radiator is expressed in alternative general forms, one of these being chosen to refine and correct some particular estimates given by Heckl for different numerical ratios of strip width to wave length. An exact and explicit calculation is effected for sinusoidal velocity profiles when the strip width equals an integer number of half wave lengths. (Author)

A80-32676 * A scaling theory for linear systems. R. W. Brockett (Harvard University, Cambridge, Mass.) and P. S. Krishnaprasad (Case Western Reserve University, Cleveland, Ohio). *IEEE Transactions on Automatic Control*, vol. AC-25, Apr. 1980, p. 197-207. 22 refs. Contract No. N00014-75-C-0648; Grants No. DAAG29-75-C-0139; No. NSG-2265.

A theory of scaling for rational (transfer) functions in terms of transformation groups is developed. Two different four-parameter scaling groups which play natural roles in studying linear systems are identified and the effect of scaling on Fisher information and related statistical measures in system identification are studied. The scalings considered include change of time scale, feedback, exponential scaling, magnitude scaling, etc. The scaling action of the groups studied is tied to the geometry of transfer functions in a rather strong way as becomes apparent in the examination of the invariants of scaling. As a result, the scaling process also provides new insight into the parameterization question for rational functions. (Author)

A80-36401 * # Unified aerodynamic-acoustic theory for a thin rectangular wing encountering a gust. R. Martinez and S. E. Widnall (MIT, Cambridge, Mass.). *AIAA Journal*, vol. 18, June 1980, p. 636-645. 17 refs. Grant No. NSG-2142.

A linear aerodynamic-acoustic theory is developed for the prediction of the surface pressure distribution and three-dimensional acoustic far-field for a flat plate rectangular wing encountering a stationary short-wavelength oblique gust. It is suggested that for an infinite-span wing, leading- and trailing-edge responses to a short-wavelength gust are essentially independent. This idea is used to solve for the two-dimensional pressure field due to the passage of an infinite-span wing through an oblique gust. By allowing the field point to come down to the wing's surface, one finds an expression for the surface pressure distribution which agrees with that given in the two-dimensional aerodynamic theories of Amiet and Adamczyk. Spanwise Fourier superposition of two-dimensional solutions to the infinite-span wing problem is used to approximate the three-dimensional acoustic field due to the interaction of a stationary oblique gust with a flat-plate rectangular wing traveling at a subsonic speed. (Author)

A80-37806 * Output of acoustical sources. H. Levine (Stanford University, Stanford, Calif.). *Acoustical Society of America, Journal*, vol. 67, June 1980, p. 1935-1946. 5 refs. Grant No. NSG-2215.

Acoustic radiation from a source, here viewed as an immobile point singularity with periodic strength and a given multipolar nature, is affected by the presence of nearby structural elements (e.g., rigid or impedance surfaces) as well as that of a background flow in the medium. An alternative to the conventional manner of calculating the net source output by integrating the energy flux over a distant control surface is described; this involves a direct evaluation of the secondary wavefunction at the position of the primary source and obviates the need for a (prospectively difficult) flux integration. Various full and half-planar surface configurations with an adjacent source are analyzed in detail, and the explicit results obtained, in particular, for the power factor of a dipole brings out a substantial rise in its output as the source nears the sharp edge of a half-plane. (Author)

A80-38034 * # Aerodynamic coefficients in generalized unsteady thin airfoil theory. M. H. Williams (Princeton University, Princeton, N.J.). *AIAA Journal*, vol. 18, July 1980, p. 850-852. Grant No. NSG-2194.

Two cases are considered: (1) rigid body motion of an airfoil-flap combination consisting of vertical translation of given amplitude, rotation of given amplitude about a specified axis, and rotation of given amplitude of the control surface alone about its hinge; the upwash for this problem is defined mathematically; and (2) sinusoidal gust of given amplitude and wave number, for which the upwash is defined mathematically. Simple universal formulas are presented for the most important aerodynamic coefficients in unsteady thin airfoil theory. The lift and moment induced by a generalized gust are evaluated explicitly in terms of the gust wavelength. Similarly, in the control surface problem, the lift, moment, and hinge moments are given as explicit algebraic functions of hinge location. These results can be used together with any of the standard numerical inversion routines for the elementary loads (pitch and heave). S.D.

A80-42758 * The inversion of singular integral equations by expansion in Jacobi polynomials. M. H. Williams (Princeton University, Princeton, N.J.). *Institute of Mathematics and Its Applications, Journal*, vol. 25, June 1980, p. 413-426. 6 refs. Grant No. NSG-2194.

A80-43129 * # Reformulation of Possio's kernel with application to unsteady wind tunnel interference. J. A. Fromme (Martin Marietta Aerospace, Denver, Colo.) and M. A. Golberg (Nevada, University, Las Vegas, Nev.). (AIAA, ASME, ASCE, and AHS, Structures, Structural Dynamics and Materials Conference, 20th, St. Louis, Mo., Apr. 4-6, 1979.) *AIAA Journal*, vol. 18, Aug. 1980, p. 951-957. 9 refs. Grant No. NsG-2140.

An efficient method for computing the Possio kernel has remained elusive up to the present time. In this paper the Possio is reformulated so that it can be computed accurately using existing high precision numerical quadrature techniques. Convergence to the correct values is demonstrated and optimization of the integration procedures is discussed. Since more general kernels such as those associated with unsteady flows in ventilated wind tunnels are analytic perturbations of the Possio free air kernel, a more accurate evaluation of their collocation matrices results with an exponential improvement in convergence. An application to predicting frequency response of an airfoil-trailing edge control system in a wind tunnel compared with that in free air is given showing strong interference effects. (Author)

A80-45488 * A note on sound radiation into a uniformly flowing medium. H. Levine (Stanford University, Stanford, Calif.). *Journal of Sound and Vibration*, vol. 71, July 8, 1980, p. 1-8. Grant No. NsG-2007.

The influence of a uniform cross flow on the power output from an idealized mechanical source, namely a vibrating strip set in a coplanar rigid wall, is studied within the framework of linear acoustic theory, and the time-average power output is characterized by appropriate expansions (of exact integral representations), for both small and large wave length/strip width ratios, in the subsonic flow regime. Since boundary layers are ignored, the model source envisaged furnishes only a limited accounting of fluid-acoustical coupling effects. (Author)

A80-47048 * Asymptotic behavior of the efficiencies in Mie scattering. C. Acquista, J. A. Cooney, J. Wimp (Drexel University, Philadelphia, Pa.), and A. Cohen (Drexel University, Philadelphia, Pa.; Jerusalem, Hebrew University, Jerusalem, Israel). *Optical Society of America, Journal*, vol. 70, Aug. 1980, p. 1023-1025. 5 refs. Army-NSF-supported research; Grants No. NsG-6019; No. NsG-2357.

Consideration is given to the asymptotic behavior of the Mie scattering and extinction efficiencies for large absorbing spheres as sphere size approaches infinity. It is shown that the method used by Chylek (1975) for evaluating the infinite sums over the Mie partial wave coefficients representing these efficiencies and proving that the extinction efficiency approaches 2 is invalid, despite the correctness of the result, and that the limiting expression for the scattering efficiency obtained by this method is also incorrect. An analytical expression is then derived from geometrical optics considerations for the scattering efficiency limit which is valid when the imaginary component of the refractive index is much less than 1. A.L.W.

A80-52645 * # Effect of tip vortex structure on helicopter noise due to blade-vortex interaction. S. E. Widnall and T. L. Wolf (MIT, Cambridge, Mass.). *Journal of Aircraft*, vol. 17, Oct. 1980, p. 705-711. 14 refs. Grant No. NsG-2142.

A potential cause of helicopter impulsive noise, commonly called blade slap, is the unsteady lift fluctuation on a rotor blade due to interaction with the vortex trailed from another blade. The relationship between vortex structure and the intensity of the acoustic signal is investigated. Unsteady lift on the blades due to blade-vortex interaction is calculated using linear unsteady aero-

dynamic theory, and expressions are derived for the directivity, frequency spectrum, and transient signal of the radiated noise. The inviscid rollup model of Betz is used to calculate the velocity profile in the trailing vortex from the spanwise distribution of blade tip loading. A few cases of tip loading are investigated, and numerical results are presented for the unsteady lift and acoustic signal due to blade-vortex interaction. The intensity of the acoustic signal is shown to be quite sensitive to changes in tip vortex structures. (Author)

AMES FUNDED RESEARCH CONFERENCE PAPERS

N80-25591*# Raman Aeronautics Research and Engineering, Inc., Palo Alto, Calif.

PRESSURE AND TEMPERATURE FIELDS ASSOCIATED WITH AERO-OPTICS TESTS

K. R. Raman In NASA. Ames Res. Center Proc. of the Aero-Optics Symp. on Electromagnetic Wave Propagation from Aircraft Apr. 1980 p 91-121 ref (For primary document see N80-25588 16-34)

(Contract NAS2-9920)

Avail: NTIS HC A99/MF A01 CSCL 20D

The experimental investigation carried out in a 6 x 6 ft wind tunnel on four model configurations in the aero-optics series of tests are described. The data obtained on the random pressures (static and total pressures) and total temperatures are presented. In addition, the data for static pressure fluctuations on the Coelostat turret model are presented. The measurements indicate that the random pressures and temperature are negligible compared to their own mean (or steady state) values for the four models considered, thus allowing considerable simplification in the calculations to obtain the statistical properties of the density field. In the case of the Coelostat model tests these simplifications cannot be assumed a priori and require further investigation.

R.E.S

F

A80-14810 * Feedback invariants for nonlinear systems. R. W. Brockett (Harvard University, Cambridge, Mass.). In: A link between science and applications of automatic control; Proceedings of the Seventh Triennial World Congress, Helsinki, Finland, June 12-16, 1978. Volume 2, (A80-14794 03-63) Oxford and New York, Pergamon Press, 1979, p. 1115-1120. 10 refs. Contract No. N00014-75-C-0648; Grants No. DAAG29-76-0139; No. NsG-2265.

The effect of nonlinear feedback on nonlinear systems is discussed for problems where the controls are entered linearly. The invariance of certain quantities under feedback are established, and it is shown that these quantities contain enough information to determine if the system can be linearized using feedback and change of coordinates. Attention is given to scalar input systems emphasizing a new F-invariant property. C.F.W.

A80-14833 * Optimal washout for control of a moving base simulator. M. Kurosaki (Stanford University, Stanford, Calif.). In: A link between science and applications of automatic control; Proceedings of the Seventh Triennial World Congress, Helsinki, Finland, June 12-16, 1978. Volume 2, (A80-14794 03-63) Oxford and New York, Pergamon Press, 1979, p. 1311-1318. 10 refs. Grant No. NsG-2178.

A general form of an optimal washout filter is derived using state-space linear optimal control theory, and this is applied to the design of washout filters of various types of moving base motion simulators, including the NASA's vertical motion simulator. Attention is given to the linear elements of a washout filter. One of the nonlinearities considered is braking which may be required near the end of the simulator excursion to prevent a crash. Although the

general form of the optimal washout filter is applicable to time-variant system, the applications analyzed in the study are restricted to time-invariant cases. V.T.

A80-17480 * **Quest for ultrahigh resolution in X-ray optics.** J. M. Davis, A. S. Krieger, J. K. Silk, and R. C. Chase (American Science and Engineering, Inc., Cambridge, Mass.). In: Space optics: Imaging X-ray optics workshop; Proceedings of the Seminar, Huntsville, Ala., May 22-24, 1979. (A80-17469 05-89) Bellingham, Wash., Society of Photo-Optical Instrumentation Engineers, 1979, p. 96-108; Discussion, p. 108. 7 refs. Contracts No. NAS5-9041; No. NASw-2347; No. NAS2-7424; No. NAS2-8683; No. NAS5-25496; No. NAS8-27758.

A program of solar X-ray astronomy using grazing incidence optics has culminated in X-ray images of the corona having one arc second spatial resolution. These images have demonstrated that, in general, X-ray optics can be fabricated to their specifications and can provide the level of resolution for which they are designed. Several aspects of these programs relating to the performance of X-ray optics in regard to resolution, including the point response function, the variation of resolution with off-axis position and the recognition that nearly all solar X-ray images have been film limited, are discussed. By extending the experience gained on this and other programs it is clearly possible to design and fabricate X-ray optics with sub arc sec resolution. The performance required to meet the scientific objectives for the remainder of the century are discussed in relation to AXIO, an Advanced X-Ray Imaging Observatory for solar observations which is proposed for flight on the Space Shuttle. Several configurations of AXIO are described, each of which would be a major step in the quest for ultrahigh-resolution observations.

(Author)

A80-20873 * **On the Routh approximation technique and least squares errors.** M. F. Aburdene and R.-N. P. Singh (MIT, Cambridge, Mass.). In: Modeling and simulation. Volume 10 - Proceedings of the Tenth Annual Pittsburgh Conference, Pittsburgh, Pa., April 25-27, 1979. Part 2. (A80-20862 06-66) Pittsburgh, Pa., Instrument Society of America, 1979, p. 485-488. Grant No. NGL-22-009-124.

A new method for calculating the coefficients of the numerator polynomial of the direct Routh approximation method (DRAM) using the least square error criterion is formulated. The necessary conditions have been obtained in terms of algebraic equations. The method is useful for low frequency as well as high frequency reduced-order models.

(Author)

A80-22733 * # **Propeller slipstream/wing interaction in the transonic regime.** M. H. Rizk (Flow Research Co., Kent, Wash.). *American Institute of Aeronautics and Astronautics, Aerospace Sciences Meeting, 18th, Pasadena, Calif., Jan. 14-16, 1980, Paper 80-0125.* 9 p. 11 refs. Contract No. NAS2-9913.

An inviscid model for the interaction between a thin wing and a nearly uniform propeller slipstream is presented. The model allows the perturbation velocities due to the interaction to be potential although the undisturbed slipstream velocity is rotational. A finite difference scheme is used to solve the governing equation. Numerical examples indicate that the slipstream has a strong effect on the aerodynamic properties of the wing section within the slipstream and lesser effects elsewhere. The slipstream swirling motion strongly affects the wing load distribution, however, its effect on the wing's total lift and wave drag is small. The axial velocity increment in the slipstream has a small effect on the wing lift, however, it causes a large increase in wave drag.

(Author)

A80-23937 * # **Experimental investigation of the asymmetric body vortex wake.** W. L. Oberkampf, T. P. Shivananda (Texas, University, Austin, Tex.), and F. K. Owen. *American Institute of Aeronautics and Astronautics, Aerospace Sciences Meeting, 18th, Pasadena, Calif., Jan. 14-16, 1980, Paper 80-0174.* 11 p. 8 refs. Contracts No. F08635-77-C-0049; No. NAS2-9663.

An experimental investigation of the asymmetric body vortex wake of a circular cylinder in high subsonic flow is presented. Laser velocimeter, force and moment, and surface hot wire measurements were obtained for a freestream Mach number of 0.6 and Reynolds number (based on body diameter) of 0.62×10^6 to the 6th. Two component laser velocimeter measurements were made at three body cross-flow planes, $x/d = 4, 8$, and 12 , and angles of attack of $25, 35$, and 45 deg. Laser vapor screen photographs were also obtained at these body stations and angles of attack. Surface hot wire measurements were used to determine if any vortex switching occurred at various angles of attack of the body. The laser velocimeter measurements are related to the vapor screen photographs and side force measurements. These results show that more than one asymmetric body vortex wake configuration can exist for the same angle of attack and body roll angle.

(Author)

A80-32427 * **A comparison of computer architectures for the NASA demonstration advanced avionics system.** C. L. Seacord, D. G. Bailey, and J. C. Larson (Honeywell, Inc., Avionics Div., Minneapolis, Minn.). In: Challenge of the '80s; Proceedings of the Third Digital Avionics Systems Conference, Fort Worth, Tex., November 6-8, 1979. (A80-32417 12-06) New York, Institute of Electrical and Electronics Engineers, Inc., 1979, p. 51-57. Contract No. NAS2-10021.

The paper compares computer architectures for the NASA demonstration advanced avionics system. Two computer architectures are described with an unusual approach to fault tolerance: a single spare processor can correct for faults in any of the distributed processors by taking on the role of a failed module. It was shown the system must be used from a functional point of view to properly apply redundancy and achieve fault tolerance and ultra reliability. Data are presented on complexity and mission failure probability which show that the revised version offers equivalent mission reliability at lower cost as measured by hardware and software complexity.

A.T.

A80-35977 * # **Fan noise caused by the ingestion of anisotropic turbulence - A model based on axisymmetric turbulence theory.** E. J. Kerschen (GE Corporate Research and Development Center, Schenectady, N.Y.) and P. R. Gliebe (General Electric Co., Aircraft Engine Business Group, Evendale, Ohio). *American Institute of Aeronautics and Astronautics, Aeroacoustics Conference, 6th, Hartford, Conn., June 4-6, 1980, Paper 80-1021.* 13 p. 23 refs. Contract No. NAS2-10002.

An analytical model of fan noise caused by inflow turbulence, a generalization of earlier work by Mani, is presented. Axisymmetric turbulence theory is used to develop a statistical representation of the inflow turbulence valid for a wide range of turbulence properties. Both the dipole source due to rotor blade unsteady forces and the quadrupole source resulting from the interaction of the turbulence with the rotor potential field are considered. The effects of variations in turbulence properties and fan operating conditions are evaluated. For turbulence axial integral length scales much larger than the blade spacing, the spectrum is shown to consist of sharp peaks at the blade passing frequency and its harmonics, with negligible broadband content. The analysis can then be simplified considerably and the total sound power contained within each spectrum peak becomes independent of axial length scale, while the width of the peak is inversely proportional to this parameter. Large axial length scales are characteristic of static fan test facilities, where the transverse contraction of the inlet flow produces highly anisotropic turbulence. In this situation, the rotor/turbulence interaction noise is mainly caused by the transverse component of turbulent velocity.

(Author)

A80-35978 * # Analytical study of the effects of wind tunnel turbulence on turbofan rotor noise. P. R. Gliebe (General Electric Co., Aircraft Engine Group, Cincinnati, Ohio). *American Institute of Aeronautics and Astronautics, Aeroacoustics Conference, 6th, Hartford, Conn., June 4-6, 1980, Paper 80-1022*. 13 p. 16 refs. Contract No. NAS2-10002.

An analytical study of the effects of wind tunnel turbulence on turbofan rotor noise was carried out to evaluate the effectiveness of the NASA Ames 40 by 80-foot wind tunnel in simulating flight levels of fan noise. A previously developed theory for predicting rotor/turbulence interaction noise, refined and extended to include first-order effects of inlet turbulence anisotropy, was employed to carry out a parametric study of the effects of fan size, blade number, and operating line for outdoor test stand, NASA Ames wind tunnel, and flight inlet turbulence conditions. A major result of this study is that although wind tunnel rotor/turbulence noise levels are not as low as flight levels, they are substantially lower than the outdoor test stand levels and do not mask other sources of fan noise. (Author)

A80-35994 * # Distortion-rotor interaction noise produced by a drooped inlet. E. B. Smith, M. T. Moore, and P. R. Gliebe (General Electric Co., Aircraft Engine Group, Cincinnati, Ohio). *American Institute of Aeronautics and Astronautics, Aeroacoustics Conference, 6th, Hartford, Conn., June 4-6, 1980, Paper 80-1050*. 10 p. 8 refs. Contract No. NAS2-8675.

The 'drooped' inlet used on most wing mounted engines produces a wall static pressure distortion at the fan face of about plus or minus 2%. The interaction of the fan rotor with this fixed distortion pattern produces blade passing frequency and harmonic tone levels in flight which contribute to forward radiated engine noise spectra. Data from a wind tunnel test, using both a drooped inlet and an inlet with no droop, show large changes in forward radiated noise levels over a limited fan speed range. An analytical model of this fan noise mechanism is developed and is used to account for the major features of the measured results. (Author)

A80-45735 * # Top inlet system feasibility for transonic-supersonic fighter aircraft applications. T. L. Williams and B. L. Hunt (Northrop Corp., Hawthorne, Calif.). *American Institute of Aeronautics and Astronautics, Aircraft Systems Meeting, Anaheim, Calif., Aug. 4-6, 1980, Paper 80-1809*. 15 p. 5 refs. Contract No. NAS2-10584.

Top inlet flow field and inlet performance data are presented which provide preliminary insight into the feasibility of upper-fuselage mounted inlet systems for transonic-supersonic fighter aircraft. Presented data span the Mach 0.2 to 2.0 envelope and enable evaluation of the influence of key aircraft configuration variables - inlet location, wing position, wing leading-edge extension (LEX) planform area, and variable incidence canards - on top inlet performance. The viability of this concept relative to more conventional inlet/airframe integrations is assessed via comparative evaluation of top and conventional inlet flow field parameters at transonic and supersonic speeds. It is shown that the action of the wing LEX vortex system produces a significant improvement in top inlet performance. Currently available transonic-supersonic data indicate that top inlet systems pose a viable configuration option for fighter aircraft requiring moderate angle of attack capability. However, recently acquired data indicate that increased angle of attack capability may be obtained by increasing wing leading-edge sweep angle. (Author)

A80-46693 * # VTOL in-ground effect flows for closely spaced jets. M. J. Siclari, W. G. Hill, Jr., R. C. Jenkins, and D. Migdal (Grumman Aerospace Corp., Bethpage, N.Y.). *American Institute of*

Aeronautics and Astronautics, Aircraft Systems Meeting, Anaheim, Calif., Aug. 4-6, 1980, Paper 80-1880. 16 p. 10 refs. Contract No. NAS2-10097.

The interaction of two vertically impinging incompressible jets is studied through the invention of physical flow models that approximate the behavior of colliding wall jets as the incident jets are brought closer together. The mechanism for upwash formation is studied and momentum models for the upwash sheet are postulated. An approximate method for computing the ground isobar pattern of jet and upwash deflection zones is presented and compared with test data. A method for computing the upwash impingement force in the absence of secondary induced flow effects is also presented and reasonably good agreement is achieved with experimental data for cylindrical fuselage shapes of circular and rectangular cross section. (Author)

PATENTS

N80-32392* National Aeronautics and Space Administration. Ames Research Center, Moffett Field, Calif.

AIRCRAFT ENGINE NOZZLE Patent

Norman E. Sorensen and Eldon A. Latham, inventors (to NASA) Issued 29 Jul. 1980 7 p Filed 23 Mar. 1979 Supersedes N79-23971 (17 - 15, p 1934)

(NASA-Case-ARC-10977-1; US-Patent-4,214,703;

US-Patent-Appl-SN-023436; US-Patent-Class-239-127.3;

US-Patent-Class-60-264; US-Patent-Class-239-265.33) Avail: US Patent and Trademark Office CSCL 21E

A variable area exit nozzle arrangement for an aircraft engine was a substantially reduced length and weight which comprises a number of longitudinally movable radial vanes and a number of fixed radial vanes. The movable radial vanes are alternately disposed with respect to the fixed radial vanes. A means is provided for displacing the movable vanes along the longitudinal axis of the engine relative to the fixed radial vanes which extend across the main exhaust flow of the engine.

Official Gazette of the U.S. Patent and Trademark Office.

F

ASTRONAUTICS

NASA FORMAL REPORTS

N80-15726*# National Aeronautics and Space Administration. Ames Research Center, Moffett Field, Calif.

STRATOSPHERIC AEROSOL MODIFICATION BY SUPERSONIC TRANSPORT OPERATIONS WITH CLIMATE IMPLICATIONS

O. B. Toon, R. P. Turco (R and D Assoc., Marina Del Rey, Calif.), J. B. Pollack, R. C. Whitten, I. G. Poppoff, and P. Hamill (Systems and Applied Sciences Corp., Hampton, Va.) Jan. 1980 20 p refs (NASA-RP-1058; A-7938) Avail: NTIS HC A02/MF A01 CSCL 04B

The potential effects on stratospheric aerosols of supersonic transport emissions of sulfur dioxide gas and submicron size soot granules are estimated. An interactive particle-gas model of the stratospheric aerosol is used to compute particle changes due to exhaust emissions, and an accurate radiation transport model is used to compute the attendant surface temperature changes. It is shown that a fleet of several hundred supersonic aircraft, operating daily at 20 km, could produce about a 20% increase in the concentration of large particles in the stratosphere. Aerosol increases of this magnitude would reduce the global surface temperature by less than 0.01 K. Author

N80-20527*# National Aeronautics and Space Administration. Ames Research Center, Moffett Field, Calif.

PROGRESS IN TURBULENCE MODELING FOR COMPLEX FLOW FIELDS INCLUDING EFFECTS OF COMPRESSIBILITY

David C. Wilcox (DCW Industries, Inc., Studio City, Calif.) and Morris W. Rubesin Washington Apr. 1980 73 p refs (NASA-TP-1517; A-7916) Avail: NTIS HC A04/MF A01 CSCL 20D

Two second-order-closure turbulence models were devised that are suitable for predicting properties of complex turbulent flow fields in both incompressible and compressible fluids. One model is of the 'two-equation' variety in which closure is accomplished by introducing an eddy viscosity which depends on both a turbulent mixing energy and a dissipation rate per unit energy, that is, a specific dissipation rate. The other model is a 'Reynolds stress equation' (RSE) formulation in which all components of the Reynolds stress tensor and turbulent heat-flux vector are computed directly and are scaled by the specific dissipation rate. Computations based on these models are compared with measurements for the following flow fields: (a) low speed, high Reynolds number channel flows with plane strain or uniform shear; (b) equilibrium turbulent boundary layers with and without pressure gradients or effects of compressibility; and (c) flow over a convex surface with and without a pressure gradient. A.R.H.

N80-18997*# National Aeronautics and Space Administration. Ames Research Center, Moffett Field, Calif.

AN ASSESSMENT OF GROUND-BASED TECHNIQUES FOR DETECTING OTHER PLANETARY SYSTEMS. VOLUME 1: AN OVERVIEW

David C. Black, ed. and William E. Brunk, ed. (NASA, Washington, D.C.) Feb. 1980 48 p refs Workshop held at Cambridge, Mass., Nov. 1979 (NASA-CP-2124; A-8002) Avail: NTIS HC A03/MF A01 CSCL 03A

The feasibility and limitations of ground-based techniques for detecting other planetary systems are discussed as well as the level of accuracy at which these limitations would occur and the extent to which they can be overcome by new technology and instrumentation. Workshop conclusions and recommendations are summarized and a proposed high priority program is considered. A.R.H.

N80-20003*# National Aeronautics and Space Administration. Ames Research Center, Moffett Field, Calif.

CONFERENCE OF REMOTE SENSING EDUCATORS (CORSE-78)

Washington Mar. 1978 664 p refs Conf. held at Stanford, Calif., 26-30 Jun. 1978

(NASA-CP-2102; A-7755) Avail: NTIS HC A99/MF A01 CSCL 05I

Ways of improving the teaching of remote sensing students at colleges and universities are discussed. Formal papers and workshops on various Earth resources disciplines, image interpretation, and data processing concepts are presented. An inventory of existing remote sensing and related subject courses being given in western regional universities is included. For individual titles, see N80-20004 through N80-20017.

N80-23912*# National Aeronautics and Space Administration. Ames Research Center, Moffett Field, Calif.

VOLCANIC FEATURES OF HAWAII. A BASIS FOR COMPARISON WITH MARS

M. H. Carr (U.S. Geological Survey, Menlo Park, Calif.) and R. Greeley Washington 1980 216 p refs Original contains color illustrations

(NASA-SP-403; LC-80-600024) Avail: NTIS MF A01; SOD HC \$14.00 CSCL 08K

Despite the difference in size Martian and Hawaiian volcanoes have numerous characteristics in common. Specific features such as lava channels, collapsed lava tubes, levees and flow fronts, all very common in Hawaii, are also abundant on the flanks of some of the Martian volcanoes. Striking differences also exist, such as the apparent lack of radial rift zones on some Martian volcanoes and the paucity of cinder and spatter cones. Some of the best photographs of Martian and Hawaiian volcanic features are presented. Descriptive legends are provided for each picture. An overview of the geological processes and structures depicted is included. A.R.H.

N80-25224*# National Aeronautics and Space Administration. Ames Research Center, Moffett Field, Calif.

AN ASSESSMENT OF GROUND-BASED TECHNIQUES FOR DETECTING OTHER PLANETARY SYSTEMS. VOLUME 2: POSITION PAPERS

David C. Black and William E. Brunk Mar. 1980 253 p refs Prepared in cooperation with NASA, Washington, D.C. (NASA-CP-2124; A-8114) Avail: NTIS HC A12/MF A01 CSCL 03A

The capabilities of several astronomical interferometer system concepts are assessed and the effects of the Earth's atmosphere on astrometric precision are examined in detail. Included is an examination of the use of small aperture interferometry to detect planets in binary star systems. It is estimated that, for differential astrometric observation, an amplitude interferometer having two separate telescopes should permit observations of stars as faint as 14th magnitude and a positional accuracy of 0.00005 arc-sec. Instrumental, atmospheric, and photon noise errors that apply to interferometric observation are examined. It is suggested that the effects of atmospheric turbulence may be eliminated with the use of two color refractometer systems. Several sites for future telescopes dedicated to the search for planetary systems are identified.

M.G.

N80-27260* National Aeronautics and Space Administration. Ames Research Center, Moffett Field, Calif.

PROJECT ORION: A DESIGN STUDY OF A SYSTEM FOR DETECTING EXTRASOLAR PLANETS

David C. Black, ed. 1980 214 p refs Original contains color illustrations (NASA-SP-436; LC-80-11728) Avail: NTIS MF A01; SOD HC \$5.50 CSCL 03B

A design concept for a ground based astrometric telescope that could significantly increase the potential accuracy of astrometric observations is considered. The state of current techniques and instrumentation is examined in the context of detecting extrasolar planets. Emphasis is placed on the direct detection of extrasolar planets at either visual or infrared wavelengths. The design concept of the imaging stellar interferometer (ISI), developed under Project Orion, is described. The Orion ISI employs the state-of-the-art technology and is theoretically capable of attaining 0.00010 arc sec/yr accuracy in relative astrometric observations.

J.M.S.

NASA TECHNICAL MEMORANDA

N80-10239* National Aeronautics and Space Administration. Ames Research Center, Moffett Field, Calif.

PIONEER SATURN ENCOUNTER

Sep. 1979 29 p Original contains color illustrations (NASA-TM-80807) Avail: NTIS HC A03/MF A01 CSCL 22A

The Pioneer Saturn Spacecraft, which began its journey as Pioneer 11, provided the first close view of the rings of Saturn as well as its system of moons. Its payload of 11 operating instruments obtained or confirmed data about the mass, temperature, composition, radiation belts, and atmosphere of the planet and its larger satellite, Titan. It made photometric and polarization measurements of Iapetus, Rhea, Dione, and Tethys, as well as discovered additional rings. Scientific highlights of the mission are summarized. Color imagery provided by the photopolarimeter is included along with illustrations of the planet's magnetic field and radiation belts.

A.R.H.

N80-11676* National Aeronautics and Space Administration. Ames Research Center, Moffett Field, Calif.

EFFICIENCY OF AEROSOL COLLECTION ON WIRES EXPOSED IN THE STRATOSPHERE

Homer Y. Lem (LFE Environmental Analysis Labs. Div.) and Neil H. Farlow Oct. 1979 29 p refs (NASA-TM-81147; A-7958) Avail: NTIS HC A03/MF A01 CSCL 04A

The theory of inertial impaction is briefly presented. Strato-

spheric aerosol research experiments were performed duplicating Wong et al. experiments. The use of the curve of inertial parameters vs particle collection efficiency, derived from Wong et al., was found to be justified. The results show that stratospheric aerosol particles of all sizes are collectible by wire impaction technique. Curves and tables are presented and used to correct particle counts for collection efficiencies less than 100% R.E.S.

N80-12720* National Aeronautics and Space Administration. Ames Research Center, Moffett Field, Calif.

ANALYSIS OF COASTAL UPWELLING AND THE PRODUCTION OF A BIOMASS

John T. Howe Nov. 1979 28 p refs (NASA-TM-78614; A-7931) Avail: NTIS HC A03/MF A01 CSCL 08A

The coastal upwelling index derived from weather data is input to a set of coupled differential equations that describe the production of a biomass. The curl of the wind stress vector is discussed in the context of the physical extent of the upwelling structure. An analogy between temperature and biomass concentration in the upwelled coastal water is derived and the relationship is quantified. The use of remote satellite or airborne sensing to obtain biomass rate production coefficients is considered.

K.L.

N80-13265* National Aeronautics and Space Administration. Ames Research Center, Moffett Field, Calif.

FIRE-RESISTANT MATERIALS FOR AIRCRAFT PASSENGER SEAT CONSTRUCTION

L. L. Fewell, G. C. Tesoro (MIT, Boston), A. Moussa (MIT, Boston), and D. A. Kourtides Nov. 1979 20 p refs (NASA-TM-78617; A-7946) Avail: NTIS HC A02/MF A01 CSCL 11G

The thermal response characteristics of fabric and fabric-foam assemblies are described. The various aspects of the ignition behavior of contemporary aircraft passenger seat upholstery fabric materials relative to fabric materials made from thermally stable polymers are evaluated. The role of the polymeric foam backing on the thermal response of the fabric-foam assembly is also ascertained. The optimum utilization of improved fire-resistant fabric and foam materials in the construction of aircraft passenger seats is suggested.

M.M.M.

N80-13333* National Aeronautics and Space Administration. Ames Research Center, Moffett Field, Calif.

OPERATIONAL PROCEDURES FOR GROUND STATION OPERATION: ATS-3 HAWAII-AMES SATELLITE LINK EXPERIMENT

Kenji Nishioka and Emanuel H. Gross Dec. 1979 31 p (NASA-TM-81155; A-8011) Avail: NASA. Ames Research Center, Moffett Field, Calif. 94035 CSCL 17B

Hardware description and operational procedures for the ATS-3 Hawaii-Ames satellite computer link are presented in basic step-by-step instructions. Transmit and receive channels and frequencies are given. Details such as switch settings for activating the station to the sequence of turning switches on are provided. Methods and procedures for troubleshooting common problems encountered with communication stations are also provided.

R.E.S.

N80-14941* National Aeronautics and Space Administration. Ames Research Center, Moffett Field, Calif.

AN EXTENDED SOFT-CUBE MODEL FOR THE THERMAL ACCOMMODATION OF GAS ATOMS ON SOLID SURFACES

John R. Burke and D. J. Hollenbach Jan. 1980 61 p refs
Prepared in cooperation with San Francisco State Univ.
(NASA-TM-81163; A-8047) Avail: NTIS HC A04/MF A01
CSCL 20K

A numerical soft cube model was developed for calculating thermal accommodation coefficients α and trapping fractions $f_{sub t}$ for the interaction of gases incident upon solid surfaces. A semiempirical correction factor c which allows the calculation of α and $f_{sub t}$ when the collision times are long compared to the surface oscillator period were introduced. The processes of trapping, evaporation, and detailed balancing were discussed. The numerical method was designed to treat economically and with moderate (+ or - 20 percent) accuracy the dependence of α and $f_{sub t}$ on finite and different surface and gas temperatures for a large number of gas/surface combinations. Comparison was made with experiments of rare gases on tungsten and on alkalis, as well as one astrophysical case of H₂ on graphite. The dependence of α on the soft cube dimensionless parameters is presented graphically. R.C.T.

N80-15854*# National Aeronautics and Space Administration.
Ames Research Center, Moffett Field, Calif.

**STUDIES IN ASTRONOMICAL TIME SERIES ANALYSIS:
MODELING RANDOM PROCESSES IN THE TIME DO-
MAIN**

Jeffrey D. Scargle Dec. 1979 215 p refs
(NASA-TM-81148; A-7959) Avail: NTIS HC A10/MF A01
CSCL 12A.

Random process models phased in the time domain are used to analyze astrophysical time series data produced by random processes. A moving average (MA) model represents the data as a sequence of pulses occurring randomly in time, with random amplitudes. An autoregressive (AR) model represents the correlations in the process in terms of a linear function of past values. The best AR model is determined from sampled data and transformed to an MA for interpretation. The randomness of the pulse amplitudes is maximized by a FORTRAN algorithm which is relatively stable numerically. Results of test cases are given to study the effects of adding noise and of different distributions for the pulse amplitudes. A preliminary analysis of the optical light curve of the quasar 3C 273 is given. K.L.

N80-18105*# National Aeronautics and Space Administration.
Ames Research Center, Moffett Field, Calif.

**A SMALL-SCALE TEST FOR FIBER RELEASE FROM
CARBON COMPOSITES**

W. J. Gilwee, Jr. and R. H. Fish Feb. 1980 9 p refs Presented
at Conf. on Advanced Composites, Special Topics, El Segundo,
Calif., 4-6 Dec. 1979
(NASA-TM-81179; A-7962) Avail: NTIS HC A02/MF A01
CSCL 11D

A test method was developed to determine relative fiber loss from pyrolyzed composites with different resins and fiber construction. Eleven composites consisting of woven and unwoven carbon fiber reinforcement and different resins were subjected to the burn and impact test device. The composites made with unidirectional tape had higher fiber loss than those with woven fabric. Also, the fiber loss was inversely proportional to the char yield of the resin. K.L.

N80-18869*# National Aeronautics and Space Administration.
Ames Research Center, Moffett Field, Calif.

**CONTROL SYSTEM DESIGNS FOR THE SHUTTLE IN-
FRARED TELESCOPE FACILITY**

J. David Rowell (Stanford Univ., Calif.), Eric K. Parsons (Stanford Univ., Calif.), and Kenneth R. Lorell Feb. 1980 40 p refs
(NASA-TM-81159; A-8018) Avail: NTIS HC A03/MF A01
CSCL 12B

The Shuttle Infrared Telescope Facility (SIRTF) image motion compensation system is described in detail and performance is analyzed with respect to system noise inputs, environmental disturbances, and error sources such as bending and feedforward scale factor. It is concluded that the SIRTF accuracy and stability requirements can be met with this design. K.L.

N80-23250*# National Aeronautics and Space Administration.
Ames Research Center, Moffett Field, Calif.

**LEEWARD FLOW OVER DELTA WINGS AT SUPERSONIC
SPEEDS**

Joachim G. Szodrach Apr. 1980 49 p refs
(NASA-TM-81187; A-8117) Avail: NTIS HC A03/MF A01
CSCL 01A

A survey was made of the parameters affecting the development of the leeward symmetric separated flow over slender delta wings immersed in a supersonic stream. The parameters included Mach number, Reynolds number, angle of attack, leading-edge sweep angle, and body cross-sectional shape, such that subsonic and supersonic leading-edge flows are encountered. It was seen that the boundaries between the various flow regimes existing about the leeward surface may conveniently be represented on a diagram with the components of angle of attack and Mach number normal to the leading edge as governing parameters. R.E.S.

N80-24914*# National Aeronautics and Space Administration.
Ames Research Center, Moffett Field, Calif.

**COMPARISON OF THE NIMBUS-4 BUV OZONE DATA WITH
THE AMES TWO-DIMENSIONAL MODEL**

W. J. Borucki and I. J. Eberstein May 1980 46 p refs
Prepared in cooperation with NASA. Goddard Space Flight
Center
(NASA-TM-81207; A-8139) Avail: NTIS HC A03/MF A01
CSCL 04A

A comparison is made of the first two years of Nimbus 4 backscattered ultraviolet (BUV) ozone measurements with the predictions of the Ames two dimensional model. The ozone observations used consist of the mixing ratio on the 1, 2, 5, and 10 mb pressure surfaces. The data are zone and time averaged to obtain seasonal means for 1970 and 1971 and are found to show strong and repeatable meridional and seasonal dependencies. The model used for comparison with the observations extends from 80 N to 80 S latitude and from altitudes of 0 to 60 km with 5 deg horizontal grid spacing and 2.5 km vertical grid spacing. Chemical reaction and photolysis rates are diurnally averaged and the photodissociation rates are corrected for the effects of scattering. The large altitude, latitude, and seasonal changes in the ozone data agree with the model predictions. Model predictions of the sensitivity of the comparisons to changes in the assumed mixing ratios of water vapor, odd nitrogen, and odd chlorine, as well as to changes in the ambient temperature and transport parameters are also shown. E.D.K.

N80-26266*# National Aeronautics and Space Administration.
Ames Research Center, Moffett Field, Calif.

**A COMPUTER PROGRAM TO GENERATE TWO-
DIMENSIONAL GRIDS ABOUT AIRFOILS AND OTHER
SHAPES BY THE USE OF POISSON'S EQUATION**

Reese L. Sorenson May 1980 62 p refs
(NASA-TM-81198; A-8178) Avail: NTIS HC A04/MF A01
CSCL 01A

A method for generating two dimensional finite difference grids about airfoils and other shapes by the use of the Poisson differential equation is developed. The inhomogeneous terms are automatically chosen such that two important effects are imposed on the grid at both the inner and outer boundaries. The first effect is control of the spacing between mesh points along mesh

lines intersecting the boundaries. The second effect is control of the angles with which mesh lines intersect the boundaries. A FORTRAN computer program has been written to use this method. A description of the program, a discussion of the control parameters, and a set of sample cases are included. E.D.K.

N80-27418* National Aeronautics and Space Administration. Ames Research Center, Moffett Field, Calif.

SHAPE CHANGE OF GALILEO PROBE MODELS IN FREE-FLIGHT TESTS

Chul Park and Charles F. Derose Jun. 1980 41 p refs (NASA-TM-81209; A-8223) Avail: NTIS HC A03/MF A01 CSCL 22B

Scale models of the Galileo Probe made of polycarbonate, AXF5Q graphite, carbon-carbon composite, and carbon-phenolic were flown in a free flight range in an ambient gas of air, krypton, or xenon. Mach numbers varied between 14 and 24, Reynolds numbers between 300,000 and 1,000,000, stagnation pressures between 31 and 200 atm, and stagnation point heat transfer rates between 10 and 1,000 kW/sq cm. Shadowgraphs indicate gouging ablation of the aft portion of the frustum; the gouging was moderate in air and severe in the noble gases. The graphite models break in the same region. An explanation of the phenomena is offered in terms of the strong compression and shear caused by the reattachment of a turbulent separated flow. Conditions are calculated for similar tests appropriate for Von Karman Facility of the Arnold Engineering Development Center in which a larger model can be flown in argon. Author

N80-29622* National Aeronautics and Space Administration. Ames Research Center, Moffett Field, Calif.

TURBULENT STRUCTURES IN WALL-BOUNDED SHEAR FLOWS OBSERVED VIA THREE-DIMENSIONAL NUMERICAL SIMULATORS

A. Leonard Jul. 1980 30 p refs Presented at Turbulence Conf.: The Role of Coherent Structures in Modeling of Turbulence and Mixing, Madrid, 25-27 Jun. 1980 (NASA-TM-81219; A8280) Avail: NTIS HC A03/MF A01 CSCL 20D

Three recent simulations of tubulent shear flow bounded by a wall using the Illiac computer are reported. These are: (1) vibrating-ribbon experiments; (2) study of the evolution of a spot-like disturbance in a laminar boundary layer; and (3) investigation of turbulent channel flow. A number of persistent flow structures were observed, including streamwise and vertical vorticity distributions near the wall, low-speed and high-speed streaks, and local regions of intense vertical velocity. The role of these structures in, for example, the growth or maintenance of turbulence is discussed. The problem of representing the large range of turbulent scales in a computer simulation is also discussed. R.K.G.

N80-31473* National Aeronautics and Space Administration. Ames Research Center, Moffett Field, Calif.

CHEMICAL RESEARCH PROJECTS OFFICE: AN OVERVIEW AND BIBLIOGRAPHY, 1975-1980

D. A. Kourtides, A. H. Heimbuch, and J. A. Parker Aug. 1980 36 p (NASA-TM-81227; A-8317) Avail: NTIS HC A03/MF A01 CSCL 07D

The activities of the Chemical Research Projects Office at Ames Research Center, Moffett Field, California are reported. The office conducts basic and applied research in the fields of polymer chemistry, computational chemistry, polymer physics, and physical and organic chemistry. It works to identify the chemical research and technology required for solutions to problems of national urgency, synchronous with the aeronautic and space effort. It conducts interdisciplinary research on chemical problems,

mainly in areas of macromolecular science and fire research. The office also acts as liaison with the engineering community and assures that relevant technology is made available to other NASA centers, agencies, and industry. Recent accomplishments are listed in this report. Activities of the three research groups, Polymer Research, Aircraft Operating and Safety, and Engineering Testing, are summarized. A complete bibliography which lists all Chemical Research Projects Office publications, contracts, grants, patents, and presentations from 1975 to 1980 is included.

L.F.M.

N80-31775* National Aeronautics and Space Administration. Ames Research Center, Moffett Field, Calif.

DATA ACQUISITION TECHNIQUES FOR EXPLOITING THE UNIQUENESS OF THE TIME-OF-FLIGHT MASS SPECTROMETER: APPLICATION TO SAMPLING PULSED GAS SYSTEMS

Kenneth A. Lincoln Aug. 1980 15 p refs Presented at the Dyn. Mass Spectrometry Symp., Canterbury, England, 7-10 July 1980 (NASA-TM-81224; A-8308) Avail: NTIS HC A02/MF A01 CSCL 14B

Mass spectra are produced in most mass spectrometers by sweeping some parameter within the instrument as the sampled gases flow into the ion source. It is evident that any fluctuation in the gas during the sweep (mass scan) of the instrument causes the output spectrum to be skewed in its mass peak intensities. The time of flight mass spectrometer (TOFMS) with its fast, repetitive mode of operation produces spectra without skewing or varying instrument parameters and because all ion species are ejected from the ion source simultaneously, the spectra are inherently not skewed despite rapidly changing gas pressure or composition in the source. Methods of exploiting this feature by utilizing fast digital data acquisition systems, such as transient recorders and signal averagers which are commercially available are described. Applications of this technique are presented including TOFMS sampling of vapors produced by both pulsed and continuous laser heating of materials. E.D.K.

S

N80-32435* National Aeronautics and Space Administration. Ames Research Center, Moffett Field, Calif.

RADIANT PANEL TESTS ON AN EPOXY/CARBON FIBER COMPOSITE

R. Ballard, D. E. Cagliostro, M. Gross, Ming Ta Hsu, and W. Winslow Mar. 1980 41 p refs Prepared in cooperation with San Jose State Univ., California (NASA-TM-81185; A-8110) Avail: Issuing Activity CSCL 07B

The toxicity of epoxy/carbon fiber composites in fire environments is addressed. A radiant panel test chamber was developed to study the effects of pyrolysis of polymeric materials. The thermal response of the sample and the composition of gas and aerosol produced are determined. Toxicological effects of the gas and aerosol in the chamber are determined by studying changes in cardiac action, respiration, blood enzymes, and delayed escape responses in test animals. Data are presented for pyrolysis of an epoxy/carbon fiber composite at 2.5 W/sq cm. Nonflame and flame modes produced different gas and aerosol compositions and had different toxic effects. Nonflame modes produced large quantities of organic aerosols and carbon monoxide. These were not lethal but could hinder escape and may pose a long term toxic effect. The flame condition produced hydrogen cyanide in addition to other toxic products. M.G.

N80-32700* National Aeronautics and Space Administration. Ames Research Center, Moffett Field, Calif.

TWO-PHOTON EXCITATION OF NITRIC OXIDE FLUORESCENCE AS A TEMPERATURE INDICATOR IN UNSTEADY GAS-DYNAMIC PROCESSES

R. L. McKenzie and K. P. Gross (Polyatomics Research, Inc., Mountain View, Calif.) Sep. 1980 56 p refs Submitted for publication
(NASA-TM-81220; A-8284) Avail: NTIS HC A04/MF A01 CSCL 14B

A laser induced fluorescence technique, suitable for measuring fluctuating temperatures in cold turbulent flows containing very low concentrations of nitric oxide is described. Temperatures below 300 K may be resolved with signal to noise ratios greater than 50 to 1 using high peak power, tunable dye lasers. The method relies on the two photon excitation of selected ro-vibronic transitions. The analysis includes the effects of fluorescence quenching and shows the technique to be effective at all densities below ambient. Signal to noise ratio estimates are based on a preliminary measurement of the two photon absorptivity for a selected rotational transition in the NO gamma (0,0) band. S.F.

N80-32822* National Aeronautics and Space Administration. Ames Research Center, Moffett Field, Calif.

INFRARED-TEMPERATURE VARIABILITY IN A LARGE AGRICULTURAL FIELD

John P. Millard, Robert C. Goettelman (LFE Corp., Richmond, Calif.), and Mary L. LeRoy, Principal Investigators Aug. 1980 26 p refs Submitted for publication Original contains imagery. Original photography may be purchased from the EROS Data Center, Sioux Falls, S.D. 57198 ERTS (E80-10331; NASA-TM-81222; A-8283) Avail: NTIS HC A03/MF A01 CSCL 02C

The combined effect of water carved gullies, varying soil color, moisture state of the soil and crop, nonuniform phenology, and bare spots was measured for commercially grown barley planted on varying terrain. For all but the most rugged terrain, over 80% of the area within 4, 16, 65, and 259 ha cells was at temperatures within 3 C of the mean cell temperature. The result of using relatively small, 4 ha instantaneous field of views for remote sensing applications is that either the worst or the best of conditions is often observed. There appears to be no great advantage in utilizing a small instantaneous field of view instead of a large one for remote sensing of crop canopy temperatures. The two alternatives for design purposes are then either a very high spatial resolution, of the order of a meter or so, where the field is very accurately temperature mapped, or a low resolution, where the actual size seems to make little difference.

N80-33493* National Aeronautics and Space Administration. Ames Research Center, Moffett Field, Calif.

INFLUENCE OF QUALITY CONTROL VARIABLES ON FAILURE OF GRAPHITE/EPOXY UNDER EXTREME MOISTURE CONDITIONS

Linda L. Clements (Advanced Research and Applications Corp., Sunnyvale, Calif.) and Pauline R. Lee Oct. 1980 24 p refs (NASA-TM-81246; A-8382) Avail: NTIS HC A02/MF A01 CSCL 11D

Tension tests on graphite/epoxy composites were performed to determine the influence of various quality control variables on failure strength as a function of moisture and moderate temperatures. The extremely high and low moisture contents investigated were found to have less effect upon properties than did temperature or the quality control variables of specimen flaws and prepreg batch to batch variations. In particular, specimen flaws were found to drastically reduce the predicted strength of the composite, whereas specimens from different batches of prepreg displayed differences in strength as a function of temperature and extreme moisture exposure. The findings illustrate the need for careful specimen preparation, studies of flaw sensitivity, and careful quality control in any study of composite materials. Author

NASA CONTRACTOR REPORTS

N80-11470* Beech Aircraft Corp., Boulder, Colo.

PRSA HYDROGEN TANK THERMAL ACOUSTIC OSCILLATION STUDY Final Report

D. H. Riemer Sep. 1979 76 p refs

(Contract NAS2-10229)

(NASA-CR-152319; BAC-ER-14887)

Avail: NTIS

HC A05/MF A01 CSCL 13G

The power reactant storage assembly (PRSA) hydrogen tank test data were reviewed. Two hundred and nineteen data points illustrating the effect of flow rate, temperature ratio and configuration were identified. The test data were reduced to produce the thermal acoustic oscillation parameters. Frequency and amplitude were determined for model correlation. A comparison of PRSA hydrogen tank test data with the analytical models indicated satisfactory agreement for the supply and poor agreement for the full line. R.C.T.

N80-13170* Lockheed Missiles and Space Co., Palo Alto, Calif.

HYGROTHERMAL DAMAGE MECHANISMS IN GRAPHITE-EPOXY COMPOSITES

Frank W. Crossman, R. Ernest Mauri, and W. John Warren Dec. 1979 156 p refs

(Contract NAS2-9563)

(NASA-CR-3189; LMSC-D626480)

Avail: NTIS

HC A08/MF A01 CSCL 11D

T300/5209 and T300/5208 graphite epoxy laminates were studied experimentally and analytically in order to: (1) determine the coupling between applied stress, internal residual stress, and moisture sorption kinetics; (2) examine the microscopic damage mechanisms due to hygrothermal cycling; (3) evaluate the effect of absorbed moisture and hygrothermal cycling on inplane shear response; (4) determine the permanent loss of interfacial bond strength after moisture absorption and drying; and (5) evaluate the three dimensional stress state in laminates under a combination of hygroscopic, thermal, and mechanical loads. Specimens were conditioned to equilibrium moisture content under steady exposure to 55% or 95% RH at 70 C or 93 C. Some specimens were tested subsequent to moisture conditioning and 100 cycles between -54 C and either 70 C or 93 C. K.L.

N80-14184* Acurex Corp., Mountain View, Calif.

GALILEO PROBE THERMAL PROTECTION: ENTRY HEATING ENVIRONMENTS AND SPALLATION EXPERIMENTS DESIGN Final Report

A. Balakrishnan, W. Nicolet, S. Sandhu, and J. Dodson Nov. 1979 133 p refs

(Contract NAS2-9909; Acurex Proj. 7396)

(NASA-CR-152334; FR-79-21/AS)

Avail: NTIS

HC A07/MF A01 CSCL 22B

A valid procedure was developed for predicting wall heating and ablation rates about the probe forebody. Entropy layer effects on convective heating rate were analyzed and the computed results are given. A feasibility study to perform an experiment, the selection of a candidate test facility, and the definition of a test matrix are described. The material selection, fabrication, and evaluation of the metal containing carbon-carbon composites for use on the Galileo probe are summarized. The effect of various Jovian atmospheric models on entry heating environment is considered as well as the effect of the nonspherical shape of the planet on entry trajectory. A.R.H.

N80-16166*# Idaho Univ., Moscow. Dept. of Chemical Engineering.

PERFLUOROETHER TRIAZINE ELASTOMERS Final Report, 1 Mar. 1979 - 29 Feb. 1980

Roger A. Korus 1980 25 p refs

(Grant NSG-2367)

(NASA-CR-162748) Avail: NTIS HC A02/MF A01 CSCL 06C

In order to obtain high performance elastomers with the high thermal stability and chemical inertness of perfluoroalkylene triazine and a low glass transition temperature, perfluoroether triazine elastomers were synthesized. The procedure for elastomer synthesis is described as well as general experimental methods. Results are presented and discussed. The screening of catalysts for the dehydration of perfluoroether diamide is also considered.

A.R.H.

N80-19448*# DCW Industries, Studio City, Calif.
RECENT IMPROVEMENTS TO THE SPINNING BODY VERSION OF THE EDDYBL COMPUTER PROGRAM Interim Report

David C. Wilcox Nov. 1979 32 p refs

(Contract NAS2-10343)

(NASA-CR-152347; DCW-R-24-01)

Avail: NTIS

HC A03/MF A01 CSCL 20D

A conventional mixing length model specialized for thick boundary layers and a general model for pressure-strain correlation terms were added to the spinning version of EDDYBL. The models are discussed and modifications to the code input and output are presented.

K.L.

N80-21926*# Beam Engineering, Inc., Sunnyvale, Calif.
HIGH RESOLUTION VERTICAL PROFILES OF WIND, TEMPERATURE AND HUMIDITY OBTAINED BY COMPUTER PROCESSING AND DIGITAL FILTERING OF RADIOSONDE AND RADAR TRACKING DATA FROM THE ITCZ EXPERIMENT OF 1977

Edwin F. Danielson, R. Stephen Hipskind (Oregon State Univ.), and Steven E. Gaines (San Jose State Univ., Calif.) Apr. 1980 117 p refs

(Contract NAS2-10023)

(NASA-CR-3269) Avail: NTIS HC A06/MF A01 CSCL 04B

Results are presented from computer processing and digital filtering of radiosonde and radar tracking data obtained during the ITCZ experiment when coordinated measurements were taken daily over a 16 day period across the Panama Canal Zone. The temperature relative humidity and wind velocity profiles are discussed.

A.W.H.

N80-22484*# Ultrasystems, Inc., Irvine, Calif.
STUDY OF CROSSLINKING AND DEGRADATION MECHANISMS IN SEALANT POLYMER CANDIDATES Final Report

K. L. Paciorek, J. Kaufman, T. I. Ito, J. H. Nakahara, and R. H. Kratzer Mar. 1980 63 p refs

(Contract NAS2-9779)

(NASA-CR-152346; SN-3003-F) Avail: NASA. Ames Res. Center

Practical cross-linking and/or chain extension processes for perfluoroalkylether based sealants were studied. The two linking groups investigated were 1, 2, 4-oxadiazoles and s-triazines. The synthesis of difunctional, fully characterized, prepolymers and the evaluation of the curing reactions utilizing these materials are discussed.

E.D.K.

N80-22635*# B & K Engineering, Inc., Towson, Md.
LONG TERM TESTS OF THE HEPP LIQUID TRAP DIODE HEAT PIPE PROTOTYPE Final Report

Apr. 1980 11 p refs

(Contract NAS2-10203)

(NASA-CR-152358; BKO67-1004)

Avail: NTIS

HC A02/MF A01 CSCL 20D

The test results which were obtained with the HEPP liquid trap diode heat pipe prototype after it had been in storage for almost 27 months are presented. Transport data were obtained over the range of 150 to 220 K and reverse mode shutdown was measured with nominal operation at 180 K.

J.M.S.

N80-24369*# Virginia Polytechnic Inst. and State Univ., Blacksburg. Dept. of Engineering Science and Mechanics.
THE VISCOELASTIC BEHAVIOR OF A COMPOSITE IN A THERMAL ENVIRONMENT

D. H. Morris, H. F. Brinson, W. I. Griffith, and Y. T. Yeow (Allied Chemical Corp., Morristown, N. J.) Dec. 1979 28 p refs

(Grant NSG-2038)

(NASA-CR-163187; VPI-E-79-40)

Avail: NTIS

HC A03/MF A01 CSCL 11D

A proposed method for the accelerated predictions of modulus and life times for time dependent polymer matrix composite laminates is presented. The method, based on the time temperature superposition principle and lamination theory, is described in detail. Unidirectional reciprocal of compliance master curves and the shift functions needed are presented and discussed. Master curves for arbitrarily oriented unidirectional laminates are predicted and compared with experimental results obtained from master curves generated from 15 minute tests and with 25 hour tests. Good agreement is shown. Predicted 30 deg and 60 deg unidirectional strength master curves are presented and compared to results of creep rupture tests. Reasonable agreement is demonstrated. In addition, creep rupture results for a (90 deg + or - 60 deg/90 deg) sub 2s laminate are presented.

Author

N80-24370*# Virginia Polytechnic Inst. and State Univ., Blacksburg. Dept. of Engineering Science and Mechanics.
THE ACCELERATED CHARACTERIZATION OF VISCOELASTIC COMPOSITE MATERIALS Ph.D. Thesis

W. I. Griffith, D. H. Morris, and H. F. Brinson Apr. 1980 167 p refs

(Grant NSG-2038)

(NASA-CR-163188; VPI-E-80-15)

Avail: NTIS

HC A08/MF A01 CSCL 11D

Necessary fundamentals relative to composite materials and viscoelasticity are reviewed. The accelerated characterization techniques of time temperature superposition and time temperature stress superposition are described. An experimental procedure for applying the latter to composites is given along with results obtained on a particular T300/934 graphite/epoxy. The accelerated characterization predictions are found in good agreement with actual long term tests. A postcuring phenomenon is discussed that necessitates thermal conditioning of the specimen prior to testing. A closely related phenomenon of physical aging is described as well as the effect of each on the glass transition temperature and strength. Creep rupture results are provided for a variety of geometries and temperatures for T300/934 graphite/epoxy. The results are found to compare reasonably with a modified kinetic rate theory.

A.R.H.

N80-25586*# Drexel Univ., Philadelphia, Pa. Dept. of Physics and Atmospheric Science.

FEASIBILITY STUDIES FOR LIGHT SCATTERING EXPERIMENTS TO DETERMINE THE VELOCITY RELAXATION OF SMALL PARTICLES IN A FLUID Final Report, Jan. 1979 - May 1980

Charles Acquista and Lorenzo M. Narducci May 1980 18 p refs

(Grant NsG-2357)

(NASA-CR-163214) Avail: NTIS HC A02/MF A01 CSCL 20D

An approach for measuring the non-Markoffian component in the relaxation mechanism of a Brownian particle is proposed which combines desirable features of both the shock wave experiment and conventional light scattering experiments. It is suggested that the radiation pressure generated by a C.W. laser be used to guide an individual spherical particle to terminal velocity. At an appropriate time, the beam intensity is suddenly lowered to a value at which the radiation pressure is negligible, and the ensuing velocity relaxation is measured directly. A.R.H.

N80-26364*# Martin Marietta Corp., Denver, Colo.

COMET NUCLEUS IMPACT PROBE FEASIBILITY STUDY Final Report

Angelo J. Castro 15 Apr. 1980 69 p refs

(NASA Order A-71116-B)

(NASA-CR-152375; MCR-80-1002) Avail: NTIS

HC A04/MF A01 CSCL 22A

A top level listing of the comet nucleus impact probe (CNIP) feasibility experiments requirements are presented. A conceptual configuration which shows that the feasibility of engineering the experiment is possible and describes the candidate hardware is discussed. The design studies required in order to design the operating experiment are outlined. An overview of a program plan used to estimate a rough order of magnitude cost for the CNIP experiment is given. E.D.K.

N80-28330*# Analytical Mechanics Associates, Inc., Mountain View, Calif.

ANALYTICAL METHODOLOGY FOR DETERMINATION OF HELICOPTER IFR PRECISION APPROACH REQUIREMENTS

Anil V. Phatak Jul. 1980 124 p refs

(Contract NAS2-10291)

(NASA-CR-152367) Avail: NTIS HC A06/MF A01 CSCL 17G

A systematic analytical approach to the determination of helicopter IFR precision approach requirements is formulated. The approach is based upon the hypothesis that pilot acceptance level or opinion rating of a given system is inversely related to the degree of pilot involvement in the control task. A nonlinear simulation of the helicopter approach to landing task incorporating appropriate models for UH-1H aircraft, the environmental disturbances and the human pilot was developed as a tool for evaluating the pilot acceptance hypothesis. The simulated pilot model is generic in nature and includes analytical representation of the human information acquisition, processing, and control strategies. Simulation analyses in the flight director mode indicate that the pilot model used is reasonable. Results of the simulation are used to identify candidate pilot workload metrics and to test the well known performance-work-load relationship. A pilot acceptance analytical methodology is formulated as a basis for further investigation, development and validation. Author

N80-29815*# California Univ., Santa Barbara.

USE OF COLLATERAL INFORMATION TO IMPROVE LANDSAT CLASSIFICATION ACCURACIES Semiannual Progress Report, Oct. 1979 - Mar. 1980

Alan H. Strahler and John E. Estes, Principal Investigators Mar. 1980 75 p refs Original contains imagery. Original photography may be purchased from the EROS Data Center, Sioux Falls, S.D. 57198 ERTS

(Grant NsG-2377)

(E80-10268; NASA-CR-163340)

Avail: NTIS

HC A04/MF A01 CSCL 08B

There are no author-identified significant results in this report.

N80-32417*# Martin Marietta Corp., Denver, Colo.

TITAN PROBE TECHNOLOGY ASSESSMENT AND TECHNOLOGY DEVELOPMENT PLAN STUDY Final Report

Angelo J. Castro Jul. 1980 191 p refs

(Contract NAS2-10380)

(NASA-CR-152381; TPT-MA-02-3)

Avail: NTIS

HC A09/MF A01 CSCL 22B

The need for technology advances to accomplish the Titan probe mission was determined by defining mission conditions and requirements and evaluating the technology impact on the baseline probe configuration. Mission characteristics found to be technology drivers include (1) ten years dormant life in space vacuum; (2) unknown surface conditions, various sample materials, and a surface temperature; and (3) mission constraints of the Saturn Orbiter Dual Probe mission regarding weight allocation. The following areas were identified for further development: surface sample acquisition system; battery powered system; nonmetallic materials; magnetic bubble memory devices, and the landing system. Preentry science, reliability, and weight reduction and redundancy must also be considered. A.R.H.

N80-33334*# Cornell Univ., Ithaca, N. Y. Center for Radiophysics and Space Research.

ONE MILLIMETER CONTINUUM OBSERVATIONS OF EXTRAGALACTIC THERMAL SOURCES

Thomas Leonard Roellig [1980] 168 p refs

(Grant NsG-2347)

(NASA-CR-163590; CRSR-753)

Avail: NTIS

HC A08/MF A01 CSCL 03B

The results of 1 mm observations of extragalactic thermal sources are reported. The methods of making 1 mm observations are described. The instrumentation used to make the observation is described. T.M.

N80-33319*# Lockheed Missiles and Space Co., Sunnyvale, Calif. Electro-Optics Lab.

LARGE DEPLOYABLE REFLECTOR (LDR) Final Report

W. H. Aiff Jul. 1980 124 p refs

(Contract NAS2-10427)

(NASA-CR-152402; LMSC-D766449)

Avail: NTIS

HC A06/MF A01 CSCL 03A

The feasibility and costs were determined for a 1 m to 30 m diameter ambient temperature, infrared to submillimeter orbiting astronomical telescope which is to be shuttle-deployed, free-flying, and have a 10 year orbital life. Baseline concepts, constraints on delivery and deployment, and the sunshield required are examined. Reflector concepts, the optical configuration, alignment and pointing, and materials are also discussed. Technology studies show that a 10 m to 30 m diameter system which is background and diffraction limited at 30 micron m is feasible within the stated time frame. A 10 m system is feasible with current mirror technology, while a 30 m system requires technology still in development. A.R.H.

X80-10009*# Scientific Service, Inc., Redwood City, Calif.
FIRE TESTING OF NASA SAMPLES, PHASE 1
C. Wilton, G. Kamburoff, and J. Boyes Feb. 1979 161 p
(Contract NAS2-9945)
(NASA-CR-152339)

Unclassified report

NOTICE: Available to U.S. Government Agencies and Their Contractors.

The results of the burning and impact testing of graphite epoxy test samples to determine the quantity and distribution of graphite fibers that might be released from aircraft crash/fire situations are reported. The design, construction, and calibration of the impact/fire test facility is described along with the tests conducted including sample preparation, test procedure, data collection, and test results. The test parameters, photographs, and data for each of the tests are presented. J.M.S.

X80-10025*# Science Applications, Inc., La Jolla, Calif.
ANALYTICAL PREDICTION OF ATMOSPHERIC PLUMES AND ASSOCIATED PARTICLES DISPERSAL GENERATED BY LARGE OPEN FIRES
Oct. 1978 92 p refs
(Contract NAS2-10039)
(NASA-CR-152337; SAI-78-009-WH)

Unclassified report

NOTICE: Available to U.S. Government Agencies and Their Contractors.

The transport and dispersion of carbon fibers and clumps of fibers in a pool fire and in the atmospheric plume created by the fire are considered. The issue of characterizing the downwind dispersion of fiber materials caused by various postulated fires under a variety of atmospheric conditions is addressed. The key outputs of the models developed are characterizations of the particulate-laden pool fire and subsequent particle dispersion in the atmosphere, leading to a quantification of the fiber concentration as a function of distance from the fire and the accumulative areal surface density. These results can then allow the extent of the potential hazard and the conditions under which it may occur to be determined. A.R.H.

X80-10026*# Science Applications, Inc., Canoga Park, Calif.
Combustion Dynamics and Propulsion Technology Div.
PRELIMINARY REPORT: IMPROVEMENT OF A MATHEMATICAL MODEL OF A LARGE OPEN FIRE
P. T. Harsha, W. N. Bragg, and R. B. Edelman Sep. 1979 49 p refs
(Contract NAS2-10327)
(NASA-CR-152338; SAI-79-014-CP/R)

Unclassified report

NOTICE: Available to U.S. Government Agencies and Their Contractors.

A mathematical model was developed to provide the necessary detailed prediction of the characteristics of large liquid fuel fires. It includes a characterization of the transport and consumption of carbon fibers in the fire, coupled to a solution of the mass, momentum, and energy transport equations for the gas phase, and a model for the gas phase chemistry involved in hydrocarbon fuel combustion. M.M.M.

X80-10057*# SRI International Corp., Menlo Park, Calif.
LIDAR DETERMINATION OF THE COMPOSITION OF ATMOSPHERIC AEROSOLS Final Report
M. L. Wright Feb. 1980 52 p refs
(Contract NAS2-10126; SRI Proj. 8127)
(NASA-CR-152355)

Unclassified report

NOTICE: Available to U.S. Government Agencies and Their Contractors.

The feasibility of making remote measurements of the chemical composition of atmospheric aerosols by means of the differential scatter (DISC) lidar technique was investigated. This technique uses characteristic differences in the infrared backscatter spectra of aerosols to identify their chemical composition. It is concluded that the DISC system can, under some conditions, measure the chemical composition of atmospheric aerosols. E.D.K.

JOURNAL ARTICLES

A80-10366 * Silt-clay aggregates on Mars. R. Greeley (NASA, Ames Research Center, Space Sciences Div., Moffett Field, Calif.; Arizona State University, Tempe, Ariz.). *Journal of Geophysical Research*, vol. 84, Oct. 10, 1979, p. 6248-6254. 34 refs. Grants No. NSG-2284; No. NSG-2286.

Viking observations suggest abundant silt and clay particles on Mars. It is proposed that some of these particles agglomerate to form sand size aggregates that are redeposited as sandlike features such as drifts and dunes. Although the binding for the aggregates could include salt cementation or other mechanisms, electrostatic bonding is considered to be a primary force holding the aggregates together. Various laboratory experiments conducted since the 19th century, and as reported here for simulated Martian conditions, show that both the magnitude and sign of electrical charges on windblown particles are functions of particle velocity, shape and composition, atmospheric pressure, atmospheric composition and other factors. Electrical charges have been measured for saltating particles in the wind tunnel and in the field, on the surfaces of sand dunes, and within dust clouds on earth. Similar, and perhaps even greater, charges are proposed to occur on Mars, which could form aggregates of silt and clay size particles. (Author)

A80-10685 * Gas dynamics in barred spirals - Gaseous density waves and galactic shocks. W. W. Roberts, Jr., G. D. van Albada (Virginia, University, Charlottesville, Va.), and J. M. Huntley (NASA, Ames Research Center, Moffett Field, Calif.). *Astrophysical Journal, Part 1*, vol. 233, Oct. 1, 1979, p. 67-84. 43 refs. NSF Grant No. AST-72-05124-A04.

Steady-state gasdynamical studies, previously limited to tightly wound normal spiral galaxies, are extended to models of barred spirals with a 5% to 10% perturbing potential. The models show that a strong wave manifestation is an important constituent of the bar structure in many barred spirals and that a density-wave shock wave can form a bar structure as pronounced as the narrow bars often evident in optical photographs of barred spirals. The dark narrow dust lanes often observed along the leading edges of bar structures are identified as tracers of shocks, and it is found that strong shocks along a bar structure during even a small part of a galaxy's lifetime might easily deplete a large enough proportion of the gas to cause a lack of gas in the inner annuli encompassing the bar by the time of the present epoch. It is emphasized that even moderate-amplitude barlike perturbations in the disk can drive large noncircular gas motions, typically 50 to 150 km/s. F.G.M.

A80-12828 * # Some observations regarding the statistical determination of stress rupture regression lines. P. P. Pizzo (NASA, Ames Research Center, Materials Science and Applications Office, Moffett Field; General Electric Co., San Jose, Calif.). *ASME, Transactions, Journal of Pressure Vessel Technology*, vol. 101, Nov. 1979, p. 286-291. 9 refs.

Observations concerning the statistical evaluation of creep data are presented. Methods currently employed in the determination of stress rupture regression lines can result in conflicting and necessarily invalid results. Anomalous behavior is principally associated with the selection of the dependent variable. However, it is the least squares method of curve fitting which introduces regression bias. Methods to improve the validity of least squares regressions are suggested.

(Author)

A80-13143 * **Infrared methane spectra between 1120 per cm and 1800 per cm - A new atlas.** R. D. Blatherwick, A. Goldman (Denver, University, Denver, Colo.), B. L. Lutz (Lowell Observatory, Flagstaff, Ariz.; New York, State University, Stony Brook, N.Y.), P. M. Silvaggio, and R. W. Boese (NASA, Ames Research Center, Space Sciences Div., Moffett Field, Calif.). *Applied Optics*, vol. 18, Nov. 15, 1979, p. 3798-3804. 9 refs. NSF-NASA-NOAA-supported research.

A new atlas of CH₄ lines in the 1120-1800-per cm region has been generated, based on laboratory spectra taken with a Nicolet interferometer at 0.06-per cm resolution with 635-cm path length at pressures of 0.98 torr, 4.86 torr, and 19.97 torr. A compilation of line positions and line intensities includes 1339 CH₄ lines, several hundred of which have not been previously observed. (Author)

A80-14058 * **The dynamics and stability of radiatively driven gas clouds. I - Plane-parallel slabs.** M. R. Haas (NASA, Ames Research Center, Space Science Div., Moffett Field, Calif.). *Astrophysical Journal, Part 1*, vol. 233, no. 3, Nov. 1, 1979, p. 816-830. 47 refs.

A combination of numerical and analytical techniques has been used to investigate the dynamics and stability of optically thin plane-parallel radiatively driven slabs of gas confined by the thermal gas pressure of a high-temperature low-density medium. Scaling laws allow the individual model 'clouds' to be characterized by a single free parameter, χ , a normalized column density which measures the strength of the acceleration due to radiation pressure relative to that due to thermal gas pressure. It is found that these clouds are stable and coherently accelerated only when χ is small. In this regime a simple slab model is constructed which accurately reproduces the more complex gasdynamic results. The low- χ clouds are marginally able to reach the high velocities seen in the atmospheres of quasi-stellar objects, but only if their motion is subsonic with respect to the external confining medium. This implies either that the medium is extremely hot and tenuous or that it is moving outward with the clouds. (Author)

A80-14293 * **On the 'thickness' of Saturn's rings caused by satellite and solar perturbations and by planetary precession.** J. A. Burns, J. N. Cuzzi, R. H. Durisen (NASA, Ames Research Center, Moffett Field, Calif.), and P. Hamill (NASA, Ames Research Center, Moffett Field, Calif.; NASA, Langley Research Center, Hampton, Va.). *Astronomical Journal*, vol. 84, Nov. 1979, p. 1783-1801. 36 refs. Grants No. NCA2-OR175-701; No. NCA2-OR175-801; No. NCA2-OR050-802.

In the present paper, long-period and secular variations of the longitude of ascending node are derived for a particle orbiting an oblate precessing planet subjected to perturbation by an exterior satellite moving along a low-inclination orbit. It is shown that precession of Saturn under the solar torque, which causes the Laplace plane to be noninertial, is also effective in producing a forced inclination. The height above the Laplace plane associated with this variation is several meters for a particle located in the middle of the ring. V.P.

A80-15201 * **Flash-fire propensity and heat-release rate studies of improved fire resistant materials.** L. L. Fewell (NASA, Ames Research Center, Moffett Field, Calif.). *Journal of Fire and Flammability*, vol. 10, Oct. 1979, p. 274-295. 11 refs.

Twenty-six improved fire resistant materials were tested for flash-fire propensity and heat-release rate properties. The tests were conducted to obtain a descriptive index based on the production of ignitable gases during the thermal degradation process and on the response of the materials under a specific fire load. (Author)

A80-15488 * **Are solar spectral variations a drive for climatic change.** J. R. Pollack, W. J. Borucki, and W. B. Toon (NASA, Ames Research Center, Space Sciences Div., Moffett Field, Calif.). *Nature*, vol. 282, Dec. 6, 1979, p. 600-603. 34 refs.

The effects of UV variations on atmospheric ozone content and climate for time scales encompassing the 27-day solar rotation period, the sunspot period, twice the solar magnetic, and also longer time periods are examined. The studies of the relationship between solar UV variations, atmospheric ozone content and atmospheric temperatures were conducted by estimating the impact of such variations on tropospheric temperature. The total luminosity constant is then held and the dependence of the ozone variations on the forcing period is calculated. It is concluded that solar UV variations on time scales of weeks to months occasionally perturb total ozone and stratospheric temperatures by noticeable amounts but result in only minor changes in the troposphere. C.F.W.

A80-15655 * # **A new atlas of infrared methane spectra between 1120 per cm and 1800 per cm.** R. D. Blatherwick, A. Goldman (Denver, University, Denver, Colo.), B. L. Lutz (Lowell Observatory, Flagstaff, Ariz.; New York, State University, Stony Brook, N.Y.), P. M. Silvaggio, and R. W. Boese (NASA, Ames Research Center, Space Sciences Div., Moffett Field, Calif.). Research supported by NSF, NASA, and NOAA. Denver, Colo., University of Denver, 1979. 83 p. 10 refs.

An atlas of 1339 methane absorption lines in the range 1120 to 1800 reciprocal centimeters, including the $\nu(4)$ and $\nu(2)$ bands, is presented. Laboratory spectra were obtained by a Nicolet Fourier transform Michelson interferometer with a resolution of approximately 0.06 reciprocal cm and a path length of 6.35 m of 0.98, 4.86 and 19.97 torr. Observed spectra are also compared with spectral intensities calculated line-by-line on the basis of tabulated intensities of the observed spectral lines. A.L.W.

A80-16167 * **Isothermal-desorption-rate measurements in the vicinity of the Curie temperature for H₂ chemisorbed on nickel films.** M. R. Shanabarger (NASA, Ames Research Center, Moffett Field; California, University, Santa Barbara, Calif.). *Physical Review Letters*, vol. 43, Dec. 24, 1979, p. 1964-1967. 9 refs. Grants No. NSG-222; No. AF-AFOSR-71-2007.

Measurements of the isothermal desorption rate of H₂ chemisorbed onto polycrystalline nickel films made for temperatures spanning the Curie temperature of the nickel film are presented. Desorption kinetics were followed by measuring the decay of the change in resistance of the nickel film brought about by hydrogen chemisorption after gas-phase H₂ had been rapidly evacuated. The desorption rate is found to undergo an anomalous decrease in the vicinity of the Curie temperature, accompanied by an increase in the desorption activation energy and the equilibrium constant for the chemisorbed hydrogen. The results are interpreted in terms of anomalous variations in rate constants for the formation of the precursor molecular adsorbed state and the chemisorbed atomic state due to the phase transition in the nickel. The changes in rate

constants are also considered to be in qualitative agreement with theoretical predictions based on a spin coupling between the adatom and the magnetic substrate. A.L.W.

A80-16407 * Airborne stellar spectrophotometry from 1.2 to 5.5 microns - Absolute calibration and spectra of stars earlier than M3. D. W. Strecker, E. F. Erickson, and F. C. Witteborn (NASA, Ames Research Center, Moffett Field, Calif.). *Astrophysical Journal Supplement Series*, vol. 41, Nov. 1979, p. 501-512. 28 refs.

Airborne infrared spectrophotometry (1.2-5.5 microns, 1.5% resolution) is presented for 13 stars which have been extensively used as infrared calibration objects: alpha Lyr, alpha CMA, alpha UMi, beta Dra, and mu Her; the K giants beta Gem, alpha UMa, alpha Boo, gamma-1 And, and alpha Tau; and the M giants beta And, beta Peg, and alpha Cet. These spectra, obtained using NASA's Kuiper Airborne Observatory and Lear Jet Observatory, are virtually free of the interfering effects of terrestrial absorptions. Absolute calibration of the spectrophotometry was based on the theoretical model of alpha Lyr by Schild, Peterson, and Oke (1971), which fits photometric measurements at shorter wavelengths. The resulting flux densities are compared with previous ground-based photometry.

(Author)

A80-16410 * Molecule formation and infrared emission in fast interstellar shocks. I - Physical processes. D. Hollenbach (NASA, Ames Research Center, Astrophysical Experiments Branch, Moffett Field; California, University, Berkeley, Calif.) and C. F. McKee (California, University, Berkeley, Calif.). *Astrophysical Journal Supplement Series*, vol. 41, Nov. 1979, p. 555-592. 112 refs. NSF Grants No. AST-75-02181; No. AST-77-23069.

The paper analyzes the structure of fast shocks incident upon interstellar gas of ambient density from 10 to the 7th per cu cm, while focusing on the problems of formation and destruction of molecules and infrared emission in the cooling, neutral post shock gas. It is noted that such fast shocks initially dissociate almost all preexisting molecules. Discussion covers the physical processes which determine the post shock structure between 10 to the 4 and 10 to the 2 K. It is shown that the chemistry of important molecular coolants H₂, CO, OH, and H₂O, as well as HD and CH, is reduced to a relatively small set of gas phase and grain surface reactions. Also, the chemistry follows the slow conversion of atomic hydrogen into H₂, which primarily occurs on grain surfaces. The dependence of this H₂ formation rate on grain and gas temperatures is examined and the survival of grains behind fast shocks is discussed. Post shock heating and cooling rates are calculated and an appropriate, analytic, universal cooling function is developed for molecules other than hydrogen which includes opacities from both the dust and the lines.

M.E.P.

A80-17111 * SCF and CI calculations of the dipole moment function of ozone. L. A. Curtiss (Argonne National Laboratory, Argonne, Ill.), S. R. Langhoff (NASA, Ames Research Center, Moffett Field, Calif.), and G. D. Carney (Virginia Polytechnic Institute and State University, Blacksburg, Va.). *Journal of Chemical Physics*, vol. 71, Dec. 15, 1979, p. 5016-5021. 29 refs.

The constant and linear terms in a Taylor series expansion of the dipole moment function of the ground state of ozone are calculated with Cartesian Gaussian basis sets ranging in quality from minimal to double zeta plus polarization. Results are presented at both the self-consistent field and configuration-interaction levels. Although the algebraic signs of the linear dipole moment derivatives are all established to be positive, the absolute magnitudes of these quantities, as well as the infrared intensities calculated from them, vary considerably with the level of theory. (Author)

A80-18948 * Nitrogen fertiliser and stratospheric ozone - Latitudinal effects. R. C. Whitten, W. J. Borucki (NASA, Ames Research Center, Moffett Field, Calif.), L. A. Capone, C. A. Riegel (San Jose State University, San Jose, Calif.), and R. P. Turco (R & D Associates, Marina del Rey, Calif.). *Nature*, vol. 283, Jan. 10, 1980, p. 191, 192. 11 refs.

Substantial increases in atmospheric N₂O resulting from the increased use of nitrogen fertilizers might cause large (to 10%) decreases in the stratospheric ozone content. Such ozone decreases would be caused by catalytic reaction cycles involving odd-nitrogen that is formed by N₂O decomposition in the upper stratosphere. Turco et al. (1978), using a background chlorine level of 2 ppbv, have shown that if the measured values of specified reactions are used a 50% increase in N₂O would lead to a 2.7% increase in the stratospheric column density, although the ozone content above 30 km would be reduced by more than 5%; they also estimated (unpublished data) that the change in the ozone column density caused by doubling the N₂O abundance would be very close to zero (within about 0.1%). The present paper extends these calculations of N₂O/ozone effects to two dimensions, thereby identifying the latitude dependence expected for such ozone perturbations. The effects of changes in stratospheric chlorine levels on predicted ozone changes are also discussed. B.J.

A80-19114 * Pioneer Saturn. J. W. Dyer (NASA, Ames Research Center, Moffett Field, Calif.). *Science*, vol. 207, Jan. 25, 1980, p. 400, 401.

The Pioneer Saturn spacecraft, designated Pioneer 11 until its encounter with Jupiter, is presented, and its trajectory is reported. The 550-pound spin-stabilized spacecraft carries 12 scientific instruments, 11 of which were operational during its encounters with Jupiter and Saturn. After the successful completion of the Pioneer 10 Jupiter fly-by, for which Pioneer 11 was intended as a back-up, the Pioneer 11 spacecraft was committed to a Saturn-bound trajectory, and was sent on a spiral trajectory around Jupiter to approach Saturn. After mid-course maneuvers, the spacecraft arrived at Saturn on September 1, 1979, where it penetrated the ring plane outside of the visible rings, descending from above the ecliptic plane late in the morning quadrant, and making measurements of the planetary magnetosphere and its interaction with the solar wind, infrared radiation and gravitational and atmospheric effects on the radio signal. Pioneer Saturn departed from Saturn slightly above the ring plane, crossing the orbit of Titan 25 hr after Saturn flyby, and became the second spacecraft to escape the solar system. A.L.W.

A80-19116 * Preliminary results on the plasma environment of Saturn from the Pioneer 11 plasma analyzer experiment. J. H. Wolfe, J. D. Mihalov, H. R. Collard, D. D. McKibbin (NASA, Ames Research Center, Space Science Div., Moffett Field, Calif.), L. A. Frank (Iowa, University, Iowa City, Iowa), and D. S. Intriligator (Southern California, University, Los Angeles, Calif.). *Science*, vol. 207, Jan. 25, 1980, p. 403-407. 10 refs.

The Ames Research Center Pioneer 11 plasma analyzer experiment provided measurements of the solar wind interaction with Saturn and the character of the plasma environment within Saturn's magnetosphere. It is shown that Saturn has a detached bow shock wave and magnetopause quite similar to those at earth and Jupiter. The scale size of the interaction region for Saturn is roughly one-third that at Jupiter, but Saturn's magnetosphere is equally responsive to changes in the solar wind dynamic pressure. Saturn's outer magnetosphere is inflated, as evidenced by the observation of large fluxes of corotating plasma. It is postulated that Saturn's magnetosphere may undergo a large expansion when the solar wind pressure is greatly diminished by the presence of Jupiter's extended magnetospheric tail when the two planets are approximately aligned along the same solar radial vector. (Author)

A80-19391 * **Core cooling by subsolidus mantle convection.** G. Schubert (California, University, Los Angeles, Calif.), P. Cassen, and R. E. Young (NASA, Ames Research Center, Moffett Field, Calif.). (*Topical Conference on Origins of Planetary Magnetism, Houston, Tex., Nov. 8-11, 1978.*) *Physics of the Earth and Planetary Interiors*, vol. 20, Nov. 1979, p. 194-208. 26 refs. NSF Grant No. EAR-77-15198; Grant No. NGR-05-007-317.

Although vigorous mantle convection early in the thermal history of the earth is shown to be capable of removing several times the latent heat content of the core, a thermal evolution model of the earth in which the core does not solidify can be constructed. The large amount of energy removed from the model earth's core by mantle convection is supplied by the internal energy of the core which is assumed to cool from an initial high temperature given by the silicate melting temperature at the core-mantle boundary. For the smaller terrestrial planets, the iron and silicate melting temperatures at the core-mantle boundaries are more comparable than for the earth; the models incorporate temperature-dependent mantle viscosity and radiogenic heat sources in the mantle. The earth models are constrained by the present surface heat flux and mantle viscosity and internal heat sources produce only about 55% of the earth model's present surface heat flow. (Author)

A80-19397 * **Theories for the origin of lunar magnetism.** W. D. Daily (Eyring Research Institute, Provo, Utah) and P. Dyal (NASA, Ames Research Center, Moffett Field, Calif.). (*Topical Conference on Origins of Planetary Magnetism, Houston, Tex., Nov. 8-11, 1978.*) *Physics of the Earth and Planetary Interiors*, vol. 20, Nov. 1979, p. 255-270. 91 refs. Grant No. NSG-2082.

This paper reviews the major theories which have been proposed to explain the remanent magnetism found in the lunar crust. A total of nine different mechanisms for lunar magnetism are discussed and evaluated in light of the theoretical and experimental constraints pertinent to lunar magnetism. It is concluded that none of these theories in their present state of development satisfy all the known constraints. However, the theories which agree best with the present understanding of the moon are meteorite impact magnetization, thermoelectric dynamo field generation, and an early solar wind field. (Author)

A80-19741 * **OCS, stratospheric aerosols and climate.** R. P. Turco (R & D Associates, Marina del Rey, Calif.), R. C. Whitten, O. B. Toon, J. B. Pollack (NASA, Ames Research Center, Moffett Field, Calif.), and P. Hamill (Systems and Applied Sciences Corp., Hampton, Va.). *Nature*, vol. 283, Jan. 17, 1980, p. 283-286. 37 refs. Contract No. NAS2-9881.

The carbonyl sulfide budget in the atmosphere is examined, and the effects of stratospheric sulfate aerosol particles, formed in part from atmospheric carbonyl sulfate, on global climate are considered. From tropospheric measurements of carbon disulfide and the rate constant for the conversion of carbon disulfide to carbonyl sulfide, it is estimated that five Tg of carbonyl sulfide/year could be generated from carbon disulfide in the atmosphere. Direct sources of OCS include the refining and combustion of fossil fuels (1 Tg/year), natural and agricultural fires (0.2 to 0.3 Tg/year), and soils (0.5 Tg/year), yielding a total influx of from 1 to 10 Tg/year, up to 50% of which may be anthropogenic. Considerations of carbonyl sulfide sinks and concentrations indicate an atmospheric lifetime of one year, with OCS the major atmospheric sulfur compound. It is estimated that a ten-fold increase in atmospheric carbonyl sulfide would cause an optical depth perturbation comparable to that of a modest volcanic eruption, leading to an average global surface temperature decrease of 0.1 K, in addition to a possible greenhouse effect. A.L.W.

A80-20126 * # **Space applications of superconductivity.** D. B. Sullivan (National Bureau of Standards, Electromagnetic Technology Div., Boulder Colo.) and J. W. Vorreiter (NASA, Ames Research Center, Moffett Field, Calif.). *Cryogenics*, vol. 19, Nov. 1979, p. 627-631. 5 refs. NASA Order A-437018.

Some potential applications of superconductivity in space are summarized, e.g., the use of high field magnets for cosmic ray analysis or energy storage and generation, space applications of digital superconducting devices, such as the Josephson switch and, in the future, a superconducting computer. Other superconducting instrumentation which could be used in space includes: low frequency superconducting sensors, microwave and infrared detectors, instruments for gravitational studies, and high-Q cavities for use as stabilizing elements in clocks and oscillators. V.L.

A80-20275 * **Photoexcitation and ionization in molecular oxygen - Theoretical studies of electronic transitions in the discrete and continuous spectral intervals.** A. Gerwer, C. Asaro, B. V. McKoy (California Institute of Technology, Pasadena, Calif.), and P. W. Langhoff (NASA, Ames Research Center, Computational Chemistry Group, Moffett Field; Stanford University, Stanford, Calif.; Indiana University, Bloomington, Ind.). *Journal of Chemical Physics*, vol. 72, Jan. 1, 1980, p. 713-727. 60 refs. Research supported by the Petroleum Research Fund, National Research Council, and NSF.

A80-20593 * **Automatic mesh-point clustering near a boundary in grid generation with elliptic partial differential equations.** J. L. Steger and R. L. Sorenson (NASA, Ames Research Center, Moffett Field, Calif.). *Journal of Computational Physics*, vol. 33, Dec. 1979, p. 405-410. 12 refs.

Elliptic partial differential equations are used to generate a smooth grid that permits a one-to-one mapping in such a way that mesh lines of the same family do not cross. Problems that arise due to lack of clustering at crucial points or intersections of mesh lines at highly acute angles, are examined and various forcing or source terms are used (to correct the problems) that are either compatible with the maximum principle or are so locally controlled that mesh lines do not intersect. Attention is given to various schematics of unclustered grids and grid detail about (highly cambered) airfoils. C.F.W.

A80-20662 * **Red and nebulous objects in dark clouds - A survey.** M. Cohen (NASA, Ames Research Center, Moffett Field, Calif.). *Astronomical Journal*, vol. 85, Jan. 1980, p. 29-35. 22 refs. NSF Grants No. AST-77-13511; No. AST-77-19896.

A search on the NGS-PO Sky Survey photographs has revealed 150 interesting nebulous and/or red objects, mostly lying in dark clouds and not previously catalogued. Spectral classifications are presented for 55 objects. These indicate a small number of new members of the class of Herbig-Haro objects, a significant number of new T Tauri stars, and a few emission-line hot stars. It is argued that hot, high-mass stars form preferentially in the dense cores of dark clouds. The possible symbiosis of high and low mass stars is considered. A new morphology class is defined for cometary nebulae, in which a star lies on the periphery of a nebulous ring. (Author)

A80-21448 * **Oxygen index tests of thermosetting resins.** W. J. Gilwee, Jr., J. A. Parker, and D. A. Kourtidis (NASA, Ames Research Center, Chemical Research Projects Office, Moffett Field, Calif.). *Journal of Fire and Flammability*, vol. 11, Jan. 1980, p. 22-31. 8 refs.

The flammability characteristics of nine thermosetting resins under evaluation for use in aircraft interiors are described. These resins were evaluated using the Oxygen Index (ASTM 2863) testing procedure. The test specimens consisted of both neat resin and glass reinforced resin. When testing glass-reinforced samples it was observed that Oxygen Index values varied inversely with resin content. Oxygen values were also obtained on specimens exposed to temperatures up to 300 C. All specimens experienced a decline in Oxygen Index when tested at an elevated temperature. (Author)

A80-21559 * **Temperature dependence of intensities of the 8-12 micron bands of CFC13.** R. Nanes (California State University, Fullerton, Calif.), P. M. Silvaggio, and R. W. Boese (NASA, Ames Research Center, Moffett Field, Calif.). *Journal of Quantitative Spectroscopy and Radiative Transfer*, vol. 23, Feb. 1980, p. 211-220. 19 refs. Grant No. NCA2-OR253-701.

The absolute intensities of the 8-12 micron bands from Freon 11 (CFC13) were measured at temperatures of 294 and 216 K. Intensities of the bands centered at 798, 847, 934, and 1082 per cm are all observed to depend on temperature. The temperature dependence for the 847 and 1082 per cm fundamental regions is attributed to underlying hot bands; for the $\nu_2 + \nu_5$ combination band (934 per cm), the observed temperature dependence is in close agreement with theoretical prediction. The implication of these results on atmospheric IR remote-sensing is briefly discussed.

(Author)

A80-21560 * **Band model calculations for CFC13 in the 8-12 micron region.** P. M. Silvaggio, R. W. Boese (NASA, Ames Research Center, Moffett Field, Calif.), and R. Nanes (California State University, Fullerton, Calif.). *Journal of Quantitative Spectroscopy and Radiative Transfer*, vol. 23, Feb. 1980, p. 221-227. 11 refs. Grant No. NCA2-OR253-701.

A Goody random band model with a Voigt line profile is used to calculate the band absorption of CFC13 at various pressures at room and stratospheric (216 K) temperatures. Absorption coefficients and line spacings are computed.

(Author)

A80-21757 * **The surface and atmosphere of Pluto.** D. P. Cruikshank and P. M. Silvaggio (NASA, Ames Research Center, Moffett Field, Calif.). *Icarus*, vol. 41, Jan. 1980, p. 96-102. 14 refs. Grants No. NGR-33-010-082; No. NGL-12-001-057.

A new spectrum of Pluto in the region 1.4 to 1.9 microns provides confirmation of the presence of solid methane on the planet's surface. Considerations of the vapor pressure of methane gas above the solid indicate the presence of a tenuous atmosphere of this gas, the surface partial pressure of which is variable from perihelion to aphelion. The implication of a high surface albedo, the newly derived mass of Pluto, and inferences as to the range of plausible bulk mean densities indicate that the radius of Pluto should lie in the range 1200 to 1800 km.

(Author)

A80-21758 * **Saturn's rings - 3-mm observations and derived properties.** E. E. Epstein (Aerospace Corp., Los Angeles, Calif.), M. A. Janssen (California Institute of Technology, Jet Propulsion Laboratory, Pasadena, Calif.), J. N. Cuzzi (NASA, Ames Research Center, Moffett Field, Calif.), W. G. Fogarty (Wisconsin, University, Milwaukee, Wis.), and J. Mottmann (California State University, San Luis Obispo, Calif.). *Icarus*, vol. 41, Jan. 1980, p. 103-118. 40 refs. Contract No. NAS7-100.

Three-millimeter Saturn observations, obtained from 1965 through 1977 and with Jupiter as a reference, have been used to

derive a ring brightness temperature of 18 ± 8 K. The brightness temperature of the disk of Saturn is 156 ± 9 K. Part of the ring brightness (approximately 6 K) may be accounted for as disk emission which is scattered from the rings; the remainder (12 ± 8 K) is attributed to ring particle thermal emission. Because this thermal component brightness temperature is so much less than the particle physical temperature, limits are placed on the mean size and composition of the ring particles. In particular, as found by others, the particles cannot be rocky, but must be either metallic or composed of extremely low-loss dielectric material such as water ice. If the particles are pure water ice, for example, then a simple slab model and a multiple-scattering model both give upper limits to the particle sizes of approximately 1 m, a value three times smaller than previously available. The multiple-scattering model gives a particle single-scattering albedo at 3 mm of 0.83 ± 0.13 .

(Author)

A80-21759 * **Titan aerosols - Optical properties and vertical distribution.** K. Rages and J. B. Pollack (NASA, Ames Research Center, Space Science Div., Moffett Field, Calif.). *Icarus*, vol. 41, Jan. 1980, p. 119-130. 27 refs. NASA-supported research.

An analysis of Titan's solar phase variation as a function of wavelength together with the continuum geometric albedo makes it possible to set limits on the real part of the refractive index and on the average particle size of the aerosol component of Titan's atmosphere of between about 1.5 and 2.0 and between 0.20 microns and about 0.35 microns, respectively. If the real part of the refractive index is known the average particle size can be determined to within a few percent, and varies inversely with the real part of the refractive index. Using this information in a two-layer model of a methane-aerosol atmosphere and comparing the result with Titan's visible and near-infrared methane spectrum leads to the conclusion that the top layer of Titan's atmosphere contains 0.01 km atm of methane and 2.5 extinction optical depths of aerosol, while the data are consistent with a bottom layer containing 2.2 km atm of methane and about 7.5 aerosol optical depths for a real part of the refractive index equal to 1.7 and an average particle size of 0.25 microns.

(Author)

A80-21991 * # **Singlet oxygenation of 1,2-poly(1,4-hexadiene)s.** M. A. Golub (NASA, Ames Research Center, Moffett Field, Calif.), M. L. Rosenberg (NASA, Ames Research Center, Moffett Field; San Jose State University, San Jose, Calif.), and R. V. Gemmer (American Cyanamid Co., Stamford, Conn.). *Journal of Polymer Science, Part A - Polymer Chemistry*, vol. 17, 1979, p. 3751-3757. 13 refs.

The microstructural changes that occur in cis and trans forms of 1,2-poly(1,4-hexadiene) during methylene blue-photosensitized oxidation were examined by infrared and (C-13)-NMR spectroscopy. The singlet oxygenation of these polymers yielded the expected allylic hydroperoxides accompanied by double bond shifts to new vinyl and trans-vinylene double bonds. The photosensitized oxidation exhibited zero-order kinetics; the relative rates for the cis- and trans-1,2-poly(1,4-hexadiene)s were approximately 3.8:1.0. (Author)

A80-21992 * # **Synthesis of perfluoroalkylether oxadiazole elastomers.** R. W. Rosser (NASA, Ames Research Center, Moffett Field, Calif.), R. A. Korus, I. M. Shalhoub, and H. Kwong (San Jose State University, San Jose, Calif.). *Journal of Polymer Science, Part B - Polymer Letters*, vol. 17, 1979, p. 635-640. 7 refs.

A method for the simultaneous chain extension and crosslinking of perfluoroalkylethers which yields a thermally stable perfluoroalkylether oxadiazole elastomer crosslinked by trifunctional perfluoroalkylether-1,3,5-triazine is reported. In the preparation, hydroxylamine crystals prepared from hydroxylamine hydrochloride to which sodium butoxide had been added is mixed with perfluoro-

alkylether dinitrile to obtain the monomer, as the nitrile is converted to amidoxime. Monomers are heated at 140 to 200 C to form poly(perfluoroalkylether oxadiazole) with a 1,2,4-oxadiazole structure by a step-growth polymerization reaction. Simultaneous chain extension and crosslinking are observed to occur when the purified monomer is heated directly and when the remaining nitrile in the monomer is allowed to react with excess ammonia to form the corresponding amidine, which is then heated. Weight loss studies show the thermal stability of the perfluoroalkylether elastomer to be generally better than fluorosilicone or polyester elastomers, especially in air, indicating its potential usefulness for high-performance elastomeric applications. A.L.W.

A80-22191 * **The infrared spectrum of the carbon star Y Canum Venaticorum between 1.2 and 30 microns.** J. H. Goebel, J. D. Bregman, D. Goorvitch (NASA, Ames Research Center, Moffett Field, Calif.), D. W. Strecker (Ball Corp., Ball Aerospace Systems Div., Boulder, Colo.), R. C. Puetter, R. W. Russell, S. P. Willner (California, University, San Diego, Calif.), B. T. Soifer (California Institute of Technology, Pasadena, Calif.), W. J. Forrest, and J. R. Houck (Cornell University, Ithaca, N.Y.). *Astrophysical Journal, Part 1*, vol. 235, Jan. 1, 1980, p. 104-113. 46 refs. NSF Grants No. AST-76-82890; No. AST-77-20516; Grants No. NGR-05-005-055; No. NGR-33-010-081.

The paper deals with spectrophotometric observations covering the essentially complete wavelength interval between 1.2 and 30.0 microns. The observations confirm the identification of the C3 band at 5.2 microns. They show that if SiC2 is present, the SiC1 absorption band at 5.7 microns would be obscured by C3 at a 1% spectral resolution. Silicon carbide emission at 11.5 microns exists simultaneously with C3 absorption at 5.2 microns, requiring a contribution of both species to the violet opacity of Y CVn. V.P.

A80-22194 * **Comparison of predicted and observed spectral energy distribution of K and M stars. I - Alpha Bootis.** G. C. Augason, B. J. Taylor, D. W. Strecker, E. F. Erickson, and F. C. Witteborn (NASA, Ames Research Center, Moffett Field, Calif.). *Astrophysical Journal, Part 1*, vol. 235, Jan. 1, 1980, p. 138-145. 44 refs.

The K2 IIIp star Alpha Bootis has been observed from the ground at 0.536 to 1.070 microns, and from an airplane at 1.21 to 3.90 microns. In the present paper, an absolute flux curve, constructed from these observations with an overall precision greater than + or - 2% in F-lambda, is compared with previous photometry and spectrometry. V.P.

A80-22948 * **Meteoroid ablation spheres from deep-sea sediments.** M. B. Blanchard (NASA, Johnson Space Center, Houston, Tex.), D. E. Brownlee (California Institute of Technology, Pasadena, Calif.), T. E. Bunch (NASA, Ames Research Center, Moffett Field, Calif.), P. W. Hodge (Washington, University, Seattle, Wash.), and F. T. Kyte (San Jose State University, San Jose, Calif.). *Earth and Planetary Science Letters*, vol. 46, no. 2, Jan. 1980, p. 178-190. 34 refs. Contract No. NAS2-9325; Grant No. NSG-2278.

The paper deals with an examination of spheres that are magnetically extracted from mid-Pacific abyssal clays that are up to half a million years old. The spheres are divided into three groups using their dominant mineralogy - namely, iron, glassy, and silicate. Most spheres were formed from particles that completely melted as they separated from their parent meteoroids during the ablation process. It is concluded that the mineralogy and composition of the deep-sea spheres are identical in many respects to the meteorite fusion crusts, laboratory-created ablation debris, and the ablated interplanetary dust particles in the stratospheric collection. C.F.W.

A80-22978 * **In search of other planetary systems.** D. C. Black (NASA, Ames Research Center, Space Sciences Div., Moffett Field, Calif.). *Space Science Reviews*, vol. 25, Jan. 1980, p. 35-81. 41 refs.

Numerous recent developments have led to an increasing awareness of and interest in the detection of other planetary systems. A brief review of the modern history of this subject is presented with emphasis on the status of data concerning Barnard's star. A discussion is given of plausible observable effects of other planetary systems with numerical examples to indicate the nature of the detection problem. Possible types of information (in addition to discovery) that observations of these effects might yield (e.g., planetary mass and temperature) are outlined. Also discussed are various candidate detection techniques (e.g., astrometric observations) which might be employed to conduct a search, the current state-of-the-art of these techniques in terms of measurement accuracy, and the capability of existing or planned facilities (e.g., space telescope) to perform a search. Finally, consideration is given to possible search strategies and the scope of a comprehensive search program. (Author)

A80-23322 * **The properties of clusters in the gas phase. IV - Complexes of H2O and HNOx clustering on NOx/-.** N. Lee, A. W. Castleman, Jr. (Cooperative Institute for Research in Environmental Sciences, Boulder, Colo.), and R. G. Keese (NASA, Ames Research Center, Space Sciences Div., Moffett Field, Calif.; Cooperative Institute for Research in Environmental Sciences, Boulder, Colo.). *Journal of Chemical Physics*, vol. 72, Jan. 15, 1980, p. 1089-1094. 30 refs. Contract No. EP-78-S-02-4776; Grant No. DAAG29-76-G-0276.

Thermodynamic quantities for the gas-phase clustering equilibria of NO2(-) and NO3(-) were determined with high-pressure mass spectrometry. A comparison of values of the free energy of hydration derived from the data shows good agreement with formerly reported values at 296 K. New data for larger NO2(-) and NO3(-) hydrates as well as NO2(-)(HNO2)n were obtained in this study. To aid in understanding the bonding and stability of the hydrates of nitrite and nitrate ions, CNDO/2 calculations were performed, and the results are discussed. A correlation between the aqueous-phase total hydration enthalpy of a single ion and its gas-phase hydration enthalpy was obtained. Atmospheric implications of the data are also briefly discussed. (Author)

A80-23324 * **Photoexcitation and ionization in molecular fluorine - Stieltjes-Tchebycheff calculations in the static-exchange approximation.** A. E. Orel, T. N. Rescigno (California, University, Lawrence Livermore Laboratory, Livermore, Calif.), B. V. McKoy (California Institute of Technology, Pasadena, Calif.), and P. W. Langhoff (NASA, Ames Research Center, Computational Chemistry Group, Moffett Field; Stanford University, Stanford, Calif.; Indiana University, Bloomington, Ind.). *Journal of Chemical Physics*, vol. 72, Jan. 15, 1980, p. 1265-1275. 51 refs. Research supported by the Petroleum Research Fund, National Research Council, and NSF; Contract No. W-7405-eng-48.

A80-23420 * **Galaxy collisions - A preliminary study.** R. H. Miller (Chicago, University, Chicago, Ill.) and B. F. Smith (NASA, Ames Research Center, Theoretical and Planetary Studies Branch, Moffett Field, Calif.). *Astrophysical Journal, Part 1*, vol. 235, Jan. 15, 1980, p. 421-436. 33 refs. NSF Grant No. AST-76-14289; Contract No. NCA2-OR-108-902.

Collisions of spherical galaxies were studied in a series of numerical experiments to see what happens when galaxies collide. Each experiment starts with two model galaxies, each consisting of

50,000 stars, moving toward each other along a specified orbit. The series of experiments provides a systematic sampling of the parameter space spanned by the initial orbital energy and the initial angular momentum. Deeply penetrating collisions are emphasized. The collisions reported here scale to relative velocities as great as 500 km/s, well into the range for collisions within clusters of galaxies. It is found that: (1) the galaxies contract momentarily to about half their original sizes shortly after close passage; and (2) the initial galaxies blend into a single dynamical system while they are near each other. (Author)

A80-25365 * **High-frequency continuum observations of young stars.** M. Cohen (NASA, Ames Research Center, Moffett Field, Calif.; California, University, Berkeley, Calif.). *Royal Astronomical Society, Monthly Notices*, vol. 190, Mar. 1980, p. 865-872, 22 refs. NSF Grants No. AST-75-13511; No. AST-77-19896.

31-GHz and/or 90-GHz radio continuum observations have been made towards 48 young stars. Only three signals are definitely detected and are shown to represent late O or early B stars. None of the 'continuum T Tauri stars' were detected, suggesting that these are unlikely to be hot stars. Some early B stars should have been detectable if they have normal Stromgren zones. Their undetectability may well signify that circumstellar dust modifies the ionization of surrounding gas. (Author)

A80-25660 * **Integrated band intensities of gaseous N₂O/5.** R. W. Lovejoy (Lehigh University, Bethlehem, Pa.), C. Chackerian, Jr., and R. W. Boese (NASA, Ames Research Center, Moffett Field, Calif.). *Applied Optics*, vol. 19, Mar. 1, 1980, p. 744-748. 16 refs. Grant No. NCA2-OR380-801.

Values for mid-IR integrated band intensities of gaseous N₂O₅ were determined at room temperature. The absorptions studied were at 1720, 1246, 743, and 557/cm. The integrated intensities were 2204, 581, 685, and 699/atm cm, respectively. Implications of these results for the stratospheric detection of N(2)O(5) are discussed. (Author)

A80-26088 * **Stratospheric aerosol modification by supersonic transport and space shuttle operations - Climate implications.** R. P. Turco (R & D Associates, Marina del Rey, Calif.), O. B. Toon, J. B. Pollack, R. C. Whitten, I. G. Poppoff (NASA, Ames Research Center, Moffett Field, Calif.), and P. Hamill (Systems and Applied Sciences Corp., Hampton, Va.). *Journal of Applied Meteorology*, vol. 19, Jan. 1980, p. 78-89. 31 refs.

The potential effects on stratospheric aerosols of supersonic transport emissions of sulfur dioxide gas and submicron soot granules, and space shuttle rocket emissions of aluminum oxide particulates are estimated. An interactive particle-gas model of the stratospheric aerosol layer is used to calculate changes due to exhaust emissions, and an accurate radiation transport model is employed to compute the effect of aerosol changes on the earth's average surface temperature. It is concluded that the release of large numbers of small particles (soot or aluminum oxide) into the stratosphere should not lead to a corresponding significant increase in the concentration of large, optically active aerosols, but that the increase in large particles is severely limited by the total mass of sulfate available to make large particles in situ, and by the rapid loss of small seed particles via coagulation. We find that a fleet of several hundred advanced supersonic aircraft operating daily at 20 km, or the launch of one space shuttle rocket per week, could produce roughly a 20% increase in the large-particle concentration of the stratosphere. We find, in addition, that aerosol increases of this magnitude would reduce the global surface temperature by less than 0.01 K. (Author)

A80-26101 * **On the three-dimensional shapes of elliptical galaxies.** R. H. Miller (Chicago, University, Chicago, Ill.) and B. F. Smith (NASA, Ames Research Center, Theoretical and Planetary Studies Branch, Moffett Field, Calif.). *Astrophysical Journal, Part 1*, vol. 235, Feb. 1, 1980, p. 793-802. 44 refs. Grant No. NCA2-OR108-801.

The paper considers the hypothesis that elliptical galaxies are oblate axisymmetric objects flattened by rotation. It was found that (1) rotation does not flatten axisymmetric elliptical galaxies appreciably and elliptical galaxy models can rotate rapidly and yet show little flattening, (2) several systems remained axisymmetric when the quantity t used as a measure of rotation was greater than 0.14, and (3) models with similar shapes can have quite different internal dynamics. A.T.

A80-26107 * **Fragmentation of rotating protostellar clouds.** J. E. Tohline (NASA, Ames Research Center, Space Science Div., Moffett Field; Lick Observatory, Santa Cruz, Calif.). *Astrophysical Journal, Part 1*, vol. 235, Feb. 1, 1980, p. 866-881. 30 refs. Grant No. NCA2-OR660-703.

With a three-dimensional hydrodynamic computer code, the behavior of rotating, isothermal gas clouds as they collapse from Jeans unstable configurations is examined in order to determine whether they are susceptible to fragmentation during the initial dynamic collapse phase of evolution. It is found that a gas cloud will not fragment unless (1) it begins collapsing from a radius much smaller than the Jeans radius (i.e., the cloud initially encloses many Jeans masses) and (2) irregularities in the cloud's initial structure (specifically, density inhomogeneities) enclose more than one Jeans mass of material. Instead of fragmenting, most of the models collapse to a ring configuration. The rings appear to be less susceptible to fragmentation from arbitrary perturbations in their structure than has previously been indicated in other work. Because the models, which include the effects of gas pressure, do not readily fragment during a phase of dynamic collapse, it is suggested that gas clouds in the galactic disk undergo fragmentation only during quasi-equilibrium phases of their evolution. (Author)

A80-26358 * **Plains and channels in the Lunae Planum-Chryse Planitia region of Mars.** E. Theilig (Arizona State University, Tempe, Ariz.) and R. Greeley (NASA, Ames Research Center, Space Science Div., Moffett Field, Calif.; Arizona State University, Tempe, Ariz.). *Journal of Geophysical Research*, vol. 84, Dec. 30, 1979, p. 7994-8010. 35 refs. Contract No. NAS1-15178.

The Lunae Planum-Chryse Planitia region provides the opportunity to study a sequence of channeling events and to determine their temporal and genetic relationships to plains units in the northern hemisphere of Mars. Two sets of small channels and four major channel systems can be divided into four periods of channeling by superposition and contact relationships to the plains. All of the channels are considered to have formed by water erosion. The first two channeling events occurred early in the history of this area and formed small, narrow channels within the old rugged terrain. These channel events were separated by deposition of a mantle unit. The small channels probably formed by runoff of surface water or by a sapping process. These channels preceded the emplacement of vast volcanic plains in both Lunae Planum and Chryse Planitia. Channels postdating the plains are Vedra, Maumee, Bahram, and Maja valles; the first three of these deposited a sedimentary unit on the western slope of Chryse Planitia that was eroded by Maja Vallis. These large-scale channels were probably formed predominantly by catastrophic floods and may represent two periods of water release from Juventae Chasma. The origin of Bahram Vallis remains uncertain. (Author)

A80-26370 * **Mars - The north polar sand sea and related wind patterns.** H. Tsoar (Arizona State University, Tempe, Ariz.;

Negev, University, Beersheba, Israel), R. Greeley (NASA, Ames Research Center, Space Sciences Div., Moffett Field, Calif.; Arizona State University, Tempe, Ariz.), and A. R. Peterfreund (Arizona State University, Tempe, Ariz.). *Journal of Geophysical Research*, vol. 84, Dec. 30, 1979, p. 8167-8180. 54 refs. Grant No. NSG-7415.

Viking Orbiter 2 images of the north polar region reveal an enormous sand sea (erg) covering an area of greater than 500,000 sq km around the perennial ice cap. All dunes are either transverse or barchan. The various dune morphologies and modifications of primary dune types reflect a wind regime having more than one wind direction. In the summer, two major wind directions prevail: (1) off-pole winds that become easterly due to coriolis forces and (2) on-pole winds that become westerly. During the winter and/or spring, only the on-pole winds exist. Strong winds greater than 75 m/s are required for sand accumulation to form the thick transverse dunes. The strongest winds in the north polar region are thought to exist during summer over the transverse dune field between 110 deg and 220 deg W; this area is a relatively warm belt (temperature greater than 230 K) between two ice zones (temperature less than 220 K). The lack of well-developed longitudinal dunes implies that the dune field is young. The relationship of the present dune field to the perennial ice indicates that the dunes began to form after the formation of the present ice cap. (Author)

A80-26992 * **Ring formation in rotating protostellar clouds.** J. E. Tohline (NASA, Ames Research Center, Moffett Field; Lick Observatory, Santa Cruz, Calif.). *Astrophysical Journal, Part 1*, vol. 236, Feb. 15, 1980, p. 160-171. 27 refs. Grant No. NCA2-OR660-703.

The formation of a ring during the dynamic collapse of a rotating gas cloud is shown to be an understandable physical phenomenon. By analytically integrating the equation of motion for particles in the equatorial plane of a rotating cloud which collapses in a gravitational potential well defined by a $(1 - r\text{-squared})$ mass density distribution the mechanism which initiates the growth of the toroidal structure is demonstrated. An analysis of the ring formation process indicates that the ring should develop in rotating, self-gravitating gas clouds which collapse from a wide range of axisymmetric initial conditions; the degree of central condensation and the initial distribution of angular momentum in a cloud should affect only the position and size of the developing ring. Ring formation, being a dynamic process in collapsing gas clouds, cannot be explained in terms of the classical ring instability that arises in rapidly rotating, equilibrium spheroids. Conditions in a cloud which should inhibit ring formation are also discussed. (Author)

A80-26996 * **Collapsing cloud models for Bok globules.** K. R. Villere and D. C. Black (NASA, Ames Research Center, Space Science Div., Moffett Field, Calif.). *Astrophysical Journal, Part 1*, vol. 236, Feb. 15, 1980, p. 192-200. 15 refs.

The dynamic collapse of rotating gas clouds is calculated for a wide range of initial conditions. Properties of cloud models are compared with observed radio and optical properties of Bok globules, to test the hypothesis that globules undergo collapse and to determine parameters which are not easily observed. Five of the six globules studied are consistent with collapse models. It is inferred that these objects have masses of about 100 solar masses and ages smaller than their free-fall times. Inferred initial densities are much larger than minimum densities for gravitational collapse, suggesting that collapse is initiated by strong external compression or that globules are fragments of larger condensed clouds. Values inferred for the $(C-13)/O/H_2$ ratio are smaller than previous estimates and depend strongly on cloud density. (Author)

A80-27125 * **Absolute intensities and pressure broadening coefficients measured at different temperatures for the 201/II-000 band of C-12/O2-16 at 4978/cm.** F. P. J. Valero, R. W. Boese (NASA, Ames Research Center, Moffett Field, Calif.), and C. B. Suarez. *Journal of Quantitative Spectroscopy and Radiative Transfer*, vol. 23, Mar. 1980, p. 337-341. 6 refs.

A80-27391 * **Threshold windspeeds for sand on Mars - Wind tunnel simulations.** R. Greeley (Arizona State University, Tempe, Ariz.), R. Leach (NASA, Ames Research Center, Moffett Field; Santa Clara, University, Santa Clara, Calif.), B. White (California, University, Davis, Calif.), J. Iversen (Iowa State University of Science and Technology, Ames, Iowa), and J. Pollack (NASA, Ames Research Center, Space Sciences Div., Moffett Field, Calif.). *Geophysical Research Letters*, vol. 7, Feb. 1980, p. 121-124. 24 refs. NASA-suppported research.

Wind friction threshold speeds for particle movement were determined in a wind tunnel operating at martian surface pressure with a 95 percent CO₂ and 5 percent air atmosphere. The relationship between friction speed and free-stream velocity is extended to the critical case for Mars of momentum thickness Reynolds numbers between 425 and 2000. It is determined that the dynamic pressure required to initiate saltation is nearly constant for pressures between 1 bar and 4 mb for atmospheres of both air and CO₂. (Author)

A80-27415 * **Computational aerodynamics on large computers.** W. F. Ballhaus and F. R. Bailey (NASA, Ames Research Center, Moffett Field, Calif.). (*Symposium on Computers in Aerodynamics, Farmingdale, N.Y., June 4, 5, 1979.*) *Computers and Fluids*, vol. 8, Mar. 1980, p. 133-144. 22 refs.

Three examples of advances in computational aerodynamics; (1) three-dimensional inviscid transonic analysis, (2) design calculations for wings, and (3) the computation of viscous-induced aileron buzz, are reviewed. Attention is given to wing surface pressures, design optimization, computer memory, speed and advanced solution methods on parallel computer architecture. It is determined that many implicit approximate-factorization schemes, that have been developed for Navier-Stokes equations, can be coded to run efficiently on microprocessors. C.F.W.

A80-28027 * # **Unified treatment of lifting atmospheric entry.** P. R. Nachtsheim (NASA, Ames Research Center, Thermo- and Gas-Dynamics Div., Moffett Field, Calif.) and L. L. Lehman (Stanford University, Stanford, Calif.). *Journal of Spacecraft and Rockets*, vol. 17, Mar.-Apr. 1980, p. 119-122.

This paper presents a unified treatment of the effect of lift on peak acceleration during atmospheric entry. Earlier studies were restricted to different regimes because of approximations invoked to solve the same transcendental equation. This paper shows the connection between the earlier studies by employing a general expression for the peak acceleration and obtains solutions to the transcendental equation without invoking the earlier approximations. Results are presented and compared with earlier studies where appropriate. (Author)

A80-28080 * **On the comparative evolution of Ganymede and Callisto.** P. Cassen, R. T. Reynolds (NASA, Ames Research Center, Theoretical and Planetary Studies Branch, Moffett Field,

Calif.), and S. J. Peale (California, University, Santa Barbara, Calif.). *Icarus*, vol. 41, Feb. 1980, p. 232-239. 18 refs. Grants No. NGR-05-010-062; No. NCA2-OR680-805.

The paper examines the differences in the apparent ages of the surfaces of Ganymede and Callisto revealed by Voyager images. The differences could be due to the persistence of tectonic activity on Ganymede beyond the time of early, heavy bombardment. The slightly greater radioactive content expected in Ganymede could prolong such activity by 0.5 million years beyond the cessation of endogenic surface activity on Callisto. It is concluded that if the different ages of the surfaces of Ganymede and Callisto are due to differences in internal evolution, the slightly higher radioactive content of Ganymede is the most likely cause; tidal dissipation could not have been important for Ganymede for more than 10 to the 8th power years, and it was never important for Callisto. A.T.

A80-28086 * **Calculations of the evolution of the giant planets.** P. Bodenheimer (NASA, Ames Research Center, Space Sciences Div., Moffett Field; Lick Observatory, Santa Cruz, Calif.), A. S. Grossman (NASA, Ames Research Center, Space Sciences Div., Moffett Field, Calif.; Iowa State University of Science and Technology, Ames, Iowa), W. M. DeCampi (California Institute of Technology, Pasadena, Calif.), G. Marcy (Lick Observatory, Santa Cruz, Calif.), and J. B. Pollack (NASA, Ames Research Center, Space Sciences Div., Moffett Field, Calif.). *Icarus*, vol. 41, Feb. 1980, p. 293-308. 31 refs. NSF Grants No. AST-76-17590; No. AST-76-80801.

Evolutionary calculations are presented for spherically symmetric protoplanetary configurations with a homogeneous solar composition and with masses of 1000, 1500, 28,500 and 42,000 solar masses. Recent improvements in equation-of-state and opacity calculations are incorporated. Sequences start as subcondensations in the solar nebula with densities of 10 to the -10th to 10 to the -11th g/cu cm, evolve through a hydrostatic phase lasting 100 thousand to 10 million years, undergo dynamic collapse due to dissociation of molecular hydrogen, and regain hydrostatic equilibrium with densities of about 1 g/cu cm. The nature of the objects at the onset of the final phase of cooling and contraction is discussed and compared with previous calculations. (Author)

A80-29086 * **Photosensitized oxidation of unsaturated polymers.** M. A. Golub (NASA, Ames Research Center, Moffett Field, Calif.). *Pure and Applied Chemistry*, vol. 52, 1980, p. 305-323. 45 refs.

A review of the photosensitized oxidation of singlet oxygenation of unsaturated hydrocarbon polymers and of their model compounds is presented. The cis and trans forms of 1,4-polyisoprene, 1,4-polybutadiene and 1,2-poly(1,4-hexadiene) are studied, and their microstructural changes which occur on reaction with (IO₂) in solution were investigated by infrared, (H-1) and (C-13) NMR spectroscopy. The polymers yielded allylic hydroperoxides with shifted double bonds according to the 'ene' mechanism of simple olefins. It was shown that single oxygenation of unsaturated polymers is similar to their low molecular weight analogs, and that the differences are due to secondary processes affecting the (IO₂)-reacted polymers. A.T.

A80-29321 * **16-30 micron spectroscopy of Titan.** J. F. McCarthy, J. R. Houck, W. J. Forrest (Cornell University, Ithaca, N.Y.), and J. B. Pollack (NASA, Ames Research Center, Moffett Field, Calif.). *Astrophysical Journal, Part 1*, vol. 236, Mar. 1, 1980, p. 701-705. 14 refs. Grant No. NGR-33-010-081.

Titan has been observed from 16 to 30 micron with a resolution of 1 micron. Earlier broad-band data are consistent with the new measurements, which show that the disk integrated flux is nearly constant over the observed range of wavelengths. Limits on the CH₄,

H₂, and N₂ column densities and pressures at the bottom of the upper layer are derived. These indicate that if the atmosphere gas is CH₄, an H₂-CH₄ mix, or N₂, the inversion layer must be at pressures less than 30 millibars. (Author)

A80-29762 * **Stratospheric ozone decrease due to chlorofluoromethane photolysis - Predictions of latitude dependence.** W. J. Borucki, R. C. Whitten, H. T. Woodward (NASA, Ames Research Center, Space Sciences Div., Moffett Field, Calif.), L. A. Capone, C. A. Riegel, and S. Gaines (San Jose State University, San Jose, Calif.). *Journal of the Atmospheric Sciences*, vol. 37, Mar. 1980, p. 686-697. 56 refs.

A two-dimensional model is used to predict the 1990 reduction in ozone due to the chlorine compounds formed by chlorofluoromethane (CFM) photolysis when the CFM release rate is held constant at the 1975 value. The predicted globally averaged ozone reduction of 3.5% is similar to that predicted by one-dimensional models that did not include chlorine nitrate chemistry, and used lower values for the reactions rates of NO + HO₂ yielding NO₂ + OH and O₃ + HO₂ yielding OH + 2O₂. When the 5.7 ppbv increase in chlorine compounds predicted by one-dimensional models to occur under steady-state conditions is simulated by the two-dimensional model, a 26% decrease in atmospheric ozone is predicted. The latitude dependence of the ozone reduction is discussed in terms of the relevant photochemical reaction and transport. The chemical reactions that most strongly influence the meridional dependence of the ozone depletion are identified as those associated with the reactions of chlorine monoxide and atomic oxygen, the recombination of ozone and atomic oxygen, and the photodissociation of molecular oxygen. (Author)

A80-29959 * **An investigation of previously derived Hyades, Coma, and M67 reddennings.** B. J. Taylor (NASA, Ames Research Center, Moffett Field; San Jose State University, San Jose, Calif.). *Astronomical Journal*, vol. 85, Mar. 1980, p. 242-248. 45 refs.

New Hyades polarimetry and field star photometry were obtained to check the Hyades reddening, which was found to be nonzero in a previous study (Taylor, 1978). The new Hyades polarimetry implies essentially zero reddening. Four photometric techniques which are assumed to be insensitive to blanketing are used to compare the Hyades to nearby field stars and are found to yield essentially zero reddening. A simultaneous solution for the Hyades, Coma, and M67 reddennings is made, and the results are E(B-V) = 3 plus or minus 2(sigma) mmag, -1 plus or minus 3(sigma) mmag, and 46 plus or minus 6(sigma) mmag, respectively. B.J.

A80-30458 * **Relativistic scattered wave calculations on UF6.** D. A. Case (California, University, Davis, Calif.) and C. Y. Yang (NASA, Ames Research Center, Moffett Field; Surface Analytic Research, Inc., Los Altos, Calif.). *Journal of Chemical Physics*, vol. 72, Mar. 15, 1980, p. 3443-3448. 37 refs. Research supported by the Petroleum Research Fund and NSF; Contracts No. W-7405-eng-48; No. NAS2-10187.

Self-consistent Dirac-Slater multiple scattering calculations are presented for UF₆. The results are compared critically to other relativistic calculations, showing that the results of all molecular orbital calculations are in qualitative agreement, as measured by energy levels, population analyses, and spin-orbit splittings. A detailed comparison is made to the relativistic X alpha(RX alpha) method of Wood and Boring, which also uses multiple scattering theory, but incorporates relativistic effects in a more approximate fashion. For the most part, the RX alpha results are in agreement with the present results. (Author)

S

A80-30829 * # Pioneer Venus spacecraft design and operation. G. J. Nothwang (NASA, Ames Research Center, Moffett Field, Calif.). *IEEE Transactions on Geoscience and Remote Sensing*, vol. GE-18, Jan. 1980, p. 5-10.

The Pioneer Venus Orbiter and Multiprobe spacecraft design and operation enabled both remote and in-situ measurements of the Venusian environment from the outermost fringes of the atmosphere all the way to the surface. Both spacecraft were spin-stabilized and solar-cell powered from launch to Venus. Since orbit insertion, the Orbiter has been transmitting measurements from a highly elliptical 24-h orbit with periapsis altitudes down to about 150 km. Data rates up to 2048 bits/s have been utilized through a despun high-gain antenna transmitting at S-band frequency. Spacecraft attitudes, orbit periods, and periapsis altitudes are being maintained as required with a hydrazine propulsion system. The Multiprobe spacecraft (Bus with all four Probes attached) performed the necessary Probe checkouts and deployed the Probes to achieve the desired Probe and Bus targeting. Silver-zinc batteries provided the necessary power on each of the four Probes from separation from the Bus through the entry/descent sequence. Data rates of 256 and 128 bits/s on the Large Probe were maintained with 40-W radiated power, and 64 and 16 bits/s on the Small Probes were maintained with 10-W radiated power, through omni antennas directly to Earth-based stations. Each Probe's entry/descent sequence was controlled with a hardwired entry sequence programmer to achieve the desired scientific and spacecraft operations. (Author)

A80-30830 * Pioneer Venus occultation radio science data generation. A. L. Berman (California Institute of Technology, Jet Propulsion Laboratory, Pasadena, Calif.) and R. Ramos (NASA, Ames Research Center, Moffett Field, Calif.). *IEEE Transactions on Geoscience and Remote Sensing*, vol. GE-18, Jan. 1980, p. 11-14. Contract No. NAS7-100.

The paper deals with the Pioneer Venus Orbiter (signal) occultation experiment. During Pioneer Venus Orbiter radio science operations, an open-loop receiver baseband frequency output bandwidth was substantially reduced. This was made possible by programming an open-loop receiver first local oscillator with the predicted Doppler frequency profile so as to maintain the baseband signal within a narrow receiver output bandwidth. V.T.

A80-30831 * Pioneer Venus Multiprobe entry telemetry recovery. R. B. Miller (California Institute of Technology, Jet Propulsion Laboratory, Pasadena, Calif.) and R. Ramos (NASA, Ames Research Center, Moffett Field, Calif.). *IEEE Transactions on Geoscience and Remote Sensing*, vol. GE-18, Jan. 1980, p. 15-19. Contract No. NAS7-100.

The Entry Phase of the Pioneer Venus Multiprobe Mission involved data transmission over only a two-hour span. The criticality of recovery of those two hours of data, coupled with the fact that there were no radio signals from the Probes until their arrival at Venus, dictated unique telemetry recovery approaches on the ground. The result was double redundancy, use of spectrum analyzers to aid in rapid acquisition of the signals, and development of a technique for recovery of telemetry data without the use of real-time coherent detection which is normally employed by all other NASA planetary missions. (Author)

A80-30832 * Pioneer Venus Unified Abstract Data Library and Quick Look Data Delivery System. J. A. Ferandin, C. L. Weeks (NASA, Ames Research Center, Moffett Field, Calif.), and R. D. Pak (Bendix Field Engineering Corp., Sunnyvale, Calif.). *IEEE Transactions on Geoscience and Remote Sensing*, vol. GE-18, Jan. 1980, p. 19-27.

Development of the Pioneer Venus (PV) Unified Abstract Data System (UADS) and Quick Look Data System (QLDS) was prompted by the need to provide PV investigators rapid and easy access to PV mission data. The UADS is intended to maximize the scientific benefits of the mission by facilitating the exchange of reduced scientific data. QLDS provides a method by which sampled daily mission data is rapidly transmitted to principal investigators providing them a quick look at that orbit's data. (Author)

A80-30833 * Pioneer Venus Orbiter Radar Mapper - Design and operation. G. H. Pettengill (MIT, Cambridge, Mass.), D. F. Horwood (Hughes Aircraft Co., El Segundo, Calif.), and C. H. Keller (NASA, Ames Research Center, Moffett Field, Calif.). *IEEE Transactions on Geoscience and Remote Sensing*, vol. GE-18, Jan. 1980, p. 28-32.

The Radar Mapper Experiment, carried aboard the Pioneer Venus Orbiter spacecraft, is designed to obtain a near-global picture of the topography, meter-scale surface slopes and reflectivity of Venus. Constraints imposed by the choice of orbit limit radar coverage to a latitude band lying between 74 deg N and 61 deg S completely around the planet. In addition to the altimetry objectives, the experiment seeks an image of the radar scattering properties of the surface at oblique incidence. Sensitivity limits the imaged region to a band around the planet lying between 45 deg N and 10 deg S. Altimetric error is less than 200 m; altimetric surface 'footprint' size varies from about 10 km in diameter at a spacecraft altitude of 200 km, to 50 km at a maximum altitude of 4700 km. Imaging varies from 20 to 40 km, depending on spacecraft altitude. (Author)

A80-30836 * The 'Pioneer Venus Orbiter plasma analyzer experiment. D. S. Intriligator (Southern California, University, Los Angeles, Calif.), J. H. Wolfe, and J. D. Mihalov (NASA, Ames Research Center, Space Sciences Div., Moffett Field, Calif.). *IEEE Transactions on Geoscience and Remote Sensing*, vol. GE-18, Jan. 1980, p. 39-43. 5 refs. Contract No. NAS2-9478.

The plasma analyzer experiment on the Pioneer Venus Orbiter was designed to determine the basic characteristics of the plasma environment of Venus and the nature of the solar wind interaction at Venus. The plasma analyzer experiment is an electrostatic energy-per-unit charge (E/Q) spectrometer which measures ions and electrons. There is a curved plate electrostatic analyzer system with multiple collectors. The experiment obtains the three dimensional plasma distribution function. Some of the scientific objectives of the instrument are briefly discussed, the general characteristics of the experiment are summarized, and some of the analyses based on the data are presented. (Author)

A80-30847 * The infrared radiometer on the sounder probe of the Pioneer Venus mission. R. W. Boese, R. J. Twarowski (NASA, Ames Research Center, Moffett Field, Calif.), J. Gilland, R. E. Hassig (Ball Corp., Ball Aerospace Systems Div., Boulder, Colo.), and F. G. Brown (Santa Barbara Research Center, Goleta, Calif.). *IEEE Transactions on Geoscience and Remote Sensing*, vol. GE-18, Jan. 1980, p. 97-100.

The functional aspects of the Large Probe Infrared Radiometer Instrument are presented taking into account the experiment's objective to measure the net thermal flux as the Venus Probe descended into the planet's atmosphere, as well as to detect water vapor, cloud layers and their infrared opacity. The optical elements, including the detectors are described and a brief review of the instrument's calibration is given. C.F.W.

A80-30849 * **Atmosphere structure instruments on the four Pioneer Venus entry probes.** A. Seiff, J. E. Lepetich (NASA, Ames Research Center, Moffett Field, Calif.), and D. W. Juergens (Ball Corp., Ball Aerospace Systems Div., Gardena, Calif.). *IEEE Transactions on Geoscience and Remote Sensing*, vol. GE-18, Jan. 1980, p. 105-111. 7 refs.

Measurements of temperature, pressure, and deceleration during descent, and of deceleration during high speed entry of the four Pioneer Venus entry probes were used to define the structure, and differences in structure of the atmosphere of Venus at the four widely separated entry sites. This paper describes the sensors and steps taken to realize highly accurate measurements in the design and selection of the sensors and analog electronics. (Author)

A80-30852 * **Data acquisition for measuring the wind on Venus from Pioneer Venus.** J. R. Smith (California Institute of Technology, Jet Propulsion Laboratory, Pasadena, Calif.) and R. Ramos (NASA, Ames Research Center, Moffett Field, Calif.). *IEEE Transactions on Geoscience and Remote Sensing*, vol. GE-18, Jan. 1980, p. 126-130. Contracts No. NAS7-100; No. NAS2-9476.

The Pioneer Venus Differential Long Baseline Interferometry experiment was designed to measure the motion in three dimensions of the Pioneer probes during their fall to the surface of Venus, using a combination of Doppler and long baseline ratio interferometric methods. The altitude profiles of wind speed and direction that may be deduced from these data are expected to contribute significantly to the understanding of the dynamics of the Venus atmosphere. The design of the experiment and the equipment and software techniques that were developed specially for this experiment are described. (Author)

A80-32416 * **Na + Xe collisions in the presence of two nonresonant lasers.** P. L. De Vries, C. H. Chang, T. F. George (Rochester, University, Rochester, N.Y.), B. Laskowski, and J. R. Stallcop (NASA, Ames Research Center, Moffett Field, Calif.). *Chemical Physics Letters*, vol. 69, Feb. 1, 1980, p. 417, 418. 5 refs. NSF Grant No. CHE-77-27826; Contracts No. F49620-78-C-0005; No. W-7405-eng-48; Grant No. NSG-2198.

Na+Xe collisions in the presence of two distinct laser fields (rhodamine 110 and Nd:glass) are investigated with reference to the response to nonresonant radiation of alkali metals collisionally perturbed by a buffer gas. It is found that the excited Na-asterisk (4s)+Xe state is produced with a measurable cross section due to two-photon absorption with field intensities as low as 10 MW/sq cm. V.L.

A80-32825 * **Synthesis of perfluoroalkylether triazine elastomers.** R. W. Rosser (NASA, Ames Research Center, Moffett Field, Calif.) and R. A. Korus (San Jose State University, San Jose, Calif.). *Journal of Polymer Science, Part B - Polymer Letters*, vol. 18, 1980, p. 135-139. 7 refs.

A method of perfluoroalkylether triazine elastomer synthesis is described. To form an elastomer, the resultant polymer is heated in a closed oven at slightly reduced pressures for 1-day periods at 100, 130 and 150 C. A high-molecular-weight perfluoroalkylether triazine elastomer is produced that exhibits thermal and oxidative stability. This material is potentially useful in applications such as high-temperature seals, 'O' rings, and wire enamels. S.D.

A80-32826 * **Transient solution for megajoule energy release in a lumped-parameter series RLC circuit.** G. Barnes (California State University, Sacramento, Calif.) and R. E. Dannenberg (NASA, Ames Research Center, Moffett Field, Calif.). *Journal of Applied Physics*, vol. 51, Jan. 1980, p. 750-753.

A method is developed for optimizing the energy release from a megajoule capacitive discharge in a series RLC circuit with an RL load. Both the resistance and inductance of the load are represented by effective values that characterize their behavior during the discharge. Using Kirchhoff's laws, equations utilizing the load impedance and the external circuit impedance are derived for determining the instantaneous load voltage and energy characteristics. A program (ERES) computes and displays the load characteristics and the circuit current. Use of the ERES program allows a designer to perturbate values of the circuit elements in order to produce the desired time distribution for the load energy input.

(Author)

A80-33844 * **The role of cesium suboxides in low-work-function surface layers studied by X-ray photoelectron spectroscopy - Ag-O-Cs.** S.-J. Yang (Stanford University, Stanford, Calif.) and C. W. Bates, Jr. (NASA, Ames Research Center; Stanford Joint Institute for Surface and Microstructure Research, Moffett Field; Stanford University, Stanford, Calif.). *Applied Physics Letters*, vol. 36, Apr. 15, 1980, p. 675-677. 22 refs. NSF Grants No. DMR-77-24222-A1; No. ECS-79-09453.

The oxidation of cesium on silver substrates has been studied using photoyield measurements and X-ray photoelectron spectroscopy. The occurrence of two O1s peaks in the core-level spectrum at 527.5 and 531.5-eV binding energy for cesium and oxygen exposures giving the optimum photoyield proves that two oxides of cesium exist in high-photoyield surfaces, and not Cs2O alone as previously thought. From the shape and position of the cesium peaks and the Auger parameter, the assignment of the O1s peaks at 527.5- and 531.5-eV binding energies to oxygen in Cs2O and Cs11O3, respectively, can be made. Hence the total cesium-oxygen layer is a mixed phase consisting of Cs2O + Cs11O3, approximately 20-40 A thick. (Author)

A80-34223 * **Release-rate calorimetry of multilayered materials for aircraft seats.** L. L. Fewell, J. A. Parker (NASA, Ames Research Center, Moffett Field, Calif.), F. Duskin, H. Speith, and E. Trabold (Douglas Aircraft Co., Long Beach, Calif.). *SAMPE Quarterly*, vol. 11, Apr. 1980, p. 8-13.

Multilayered samples of contemporary and improved fire-resistant aircraft seat materials were evaluated for their rates of heat release and smoke generation. Top layers with glass-fiber block cushion were evaluated to determine which materials, based on their minimum contributions to the total heat release of the multilayered assembly, may be added or deleted. The smoke and heat release rates of multilayered seat materials were then measured at heat fluxes of 1.5 and 3.5 W/cm2. Abrasion tests were conducted on the decorative fabric covering and slip sheet to ascertain service life and compatibility of layers. (Author)

A80-34435 * **The stratospheric sulfate aerosol layer - Processes, models, observations, and simulations.** R. C. Whitten, O. B. Toon (NASA, Ames Research Center, Space Science Div., Moffett Field, Calif.), and R. P. Turco (R&D Associates, Marina del Rey, Calif.). *Pure and Applied Geophysics*, vol. 118, no. 1-2, 1980, p. 86-127. 98 refs.

After briefly reviewing the observational data on the stratospheric sulfate aerosol layer, the chemical and physical processes that are likely to fix the properties of the layer are discussed. We present appropriate continuity equations for aerosol particles, and show how to solve the equations on a digital computer. Simulations of the unperturbed aerosol layer by various published models are discussed and the sensitivity of layer characteristics to variations in several aerosol model parameters is studied. We discuss model applications to anthropogenic pollution problems and demonstrate that moderate levels of aerospace activity (supersonic transport and Space Shuttle operations) will probably have only a negligible effect on global climate. Finally, we evaluate the possible climatic effect of a ten-fold increase in the atmospheric abundance of carbonyl sulfide. (Author)

A80-34652 * Types of leeside flow over delta wings (Zur Systematik der Leeseiten-Strömung bei Deltaflügeln). J. Szodrach (NASA, Ames Research Center, Moffett Field, Calif.; Berlin, Technische Universität, Berlin, West Germany). *Zeitschrift für Flugwissenschaften und Weltraumforschung*, vol. 4, Mar.-Apr. 1980, p. 72-81. 19 refs. In German.

It is noted that so far most systematic investigations on the lee side flow over delta wings at supersonic speeds are concerned with flat upper surfaces. On the basis of these results, the paper makes an attempt to characterize the different types of flow over a wing with a delta-shaped upper surface by varying a number of parameters. It is concluded that the work should be considered a first step toward systematizing the flow over delta-shaped lee sides as well. M.E.P.

A80-34980 * On the numerical solution of time-dependent viscous incompressible fluid flows involving solid boundaries. P. Moin and J. Kim (NASA, Ames Research Center, Moffett Field, Calif.). *Journal of Computational Physics*, vol. 35, May 1980, p. 381-392. 17 refs.

An inherent numerical problem associated with the fully explicit pseudospectral numerical simulation of the incompressible Navier-Stokes equation for viscous flows with no-slip walls is described. A semi-implicit scheme which circumvents this numerical difficulty is presented. In this algorithm the equation of continuity rather than the Poisson equation for pressure is solved directly. Pseudospectral formulation of the channel flow problem using Fourier series and Chebyshev polynomials expansions is given for this scheme. An example demonstrating the applicability of the method is given.

(Author)

A80-35115 * Monoceros R2 - Far-infrared observations of a very young cluster. H. A. Thornson, Jr., P. M. Harvey (Steward Observatory, Tucson, Ariz.), I. Gatley, K. Sellgren (California Institute of Technology, Pasadena, Calif.), and M. W. Werner (NASA, Ames Research Center, Moffett Field; California Institute of Technology; Hale Observatories, Pasadena, Calif.). *Astrophysical Journal, Part 1*, vol. 237, Apr. 1, 1980, p. 66-71. 25 refs. Grants No. NGR-03-002-390; No. NGR-05-002-281; No. NGL-05-002-207.

The young infrared cluster in Mon R2 has been observed at wavelengths from 30 microns to 1 mm and at angular resolutions from 16 arcsec to 1 arcmin. The brightest sources - RS 1 and IRS 3 - have luminosities equivalent to those of early B-type stars. It is not possible to estimate reliably the evolutionary stage of IRS 3, but IRS 1 appears to be powered by a star close to B0 V. The star probably dominates the energetics of the cluster. The gas density estimated from the infrared and radio molecular data is much larger than that of the associated, extended H II region. This appears consistent with the idea that the ionized zone is expanding out from the back of the molecular cloud.

(Author)

A80-35151 * The settling of helium and the ages of globular clusters. P. D. Noerdlinger (NASA, Ames Research Center, Moffett Field, Calif.; Michigan State University, East Lansing, Mich.) and R. J. Arigo (Michigan State University, East Lansing, Mich.; Brown University, Providence, R.I.). *Astrophysical Journal, Part 2 - Letters to the Editor*, vol. 237, Apr. 1, 1980, p. L15, L16. 10 refs.

Model low-mass globular-cluster stars were evolved with their helium allowed to diffuse under the influence of gravity, thermal diffusion, and concentration gradient. The evolution tended to speed up. Also, the turnoff point moved toward lower luminosity and slightly lower surface temperature. If the luminosity at turnoff is used as the sole criterion for determining the age of a globular cluster, the inferred ages of such clusters are reduced by about 22% from starting values in the vicinity of 15 billion years. (Author)

A80-35330 * Performance properties of graphite reinforced composites with advanced resin matrices. D. A. Kourtides (NASA, Ames Research Center, Moffett Field, Calif.). *Plastics Design and Processing*, Jan. 1980, p. 2-12. 11 refs.

The contribution of the resin matrix to the performance of the composite is studied with particular emphasis on the flammability, and thermal and mechanical properties. Of the several thermoset and thermoplastic matrices examined, the lowest fire-resistant properties of the composite have been observed with epoxy matrices. Bismaleimide A composites exhibit high fire-resistant properties, low moisture absorption, and good mechanical properties at 23 C. Bismaleimide B and phenolic retain their mechanical properties at elevated temperatures but have lower mechanical properties than the epoxy composites at ambient temperatures. Phenolic-novolac, polyethersulfone, and polyphenylsulfone composites exhibit high oxygen index and low smoke evolution. V.L.

A80-36040 * # Scattering by nonspherical particles of size comparable to wavelength - A new semi-empirical theory and its application to tropospheric aerosols. J. B. Pollack and J. N. Cuzzi (NASA, Ames Research Center, Space Sciences Div., Moffett Field, Calif.). *Journal of the Atmospheric Sciences*, vol. 37, Apr. 1980, p. 868-881. 30 refs.

A semiempirical theory is developed which is based on simple physical principles and comparisons with laboratory measurements. The ultimate utility of this approach rests on its ability to successfully reproduce the observed single-scattering phase function for a wide variety of particle shapes, sizes and refractive indices. This approximate theory is developed for evaluating the interaction of randomly oriented, nonspherical particles with the total intensity component of electromagnetic radiation. Mie theory is used when the particle size parameter x (ratio of particle circumference to wavelength) is less than some upper bound $x_{sub 0}$ (about 5). For x greater than $x_{sub 0}$, the interaction is divided into three components: diffraction, external reflection and transmission. The application of the theory is illustrated by considering the influence of the shape of tropospheric aerosols on their contribution to the earth's global albedo. S.D.

A80-36244 * Permittivity and attenuation of wet snow between 4 and 12 GHz. W. I. Linlor (NASA, Ames Research Center, Moffett Field, Calif.). *Journal of Applied Physics*, vol. 51, May 1980, p. 2811-2816.

The permittivity and attenuation of prepared samples of wet snow are measured and curves presented showing the dependence of these quantities of snow wetness and frequency. Equations are given that express the experimentally determined relation between attenuation per unit length and volume-percent wetness at any frequency between 4 and 12 GHz. Additional equations are given for the calculation of permittivity from the snow density, attenuation per unit length, and frequency. Water retention characteristics of snow are described. Some applications of the techniques, such as runoff forecasting from mountain snowpacks, are proposed. (Author)

A80-36305 * Atmospheric aerosols and climate. O. B. Toon and J. B. Pollack (NASA, Ames Research Center, Space Sciences Div., Moffett Field, Calif.). *American Scientist*, vol. 68, May-June 1980, p. 268-278. 50 refs.

The impact of terrestrial aerosols on the earth's climate and solar and infrared radiation budget are considered. Attention is given to the optical properties of aerosols, that is, optical depth, the single scattering albedo, and the asymmetry parameter, and to the relation between the optical depth and surface temperature for tropospheric and stratospheric aerosols. Also considered are experimental projects

to determine the single scattering albedo, as well as the optical properties of natural aerosols such as sea salt, soil, and sulfates, and their variability. In addition, the impact of volcanic activity and the question of whether aerosols cause climatic warming or cooling are discussed, and the available observational evidence linking aerosols and climate is reviewed. J.P.B.

A80-36651 * Whole planet cooling and the radiogenic heat source contents of the earth and moon. G. Schubert, D. Stevenson (California, University, Los Angeles, Calif.), and P. Cassen (NASA, Ames Research Center, Moffett Field, Calif.). *Journal of Geophysical Research*, vol. 85, May 10, 1980, p. 2531-2538. 38 refs. NSF Grant No. EAR-77-15198; Grant No. NGR-05-007-317.

Thermal evolution models based on subsolidus whole mantle convection which indicate that the surface heat flows of the earth and the moon do not necessarily provide good measures of the total amounts of radioactives in these bodies have been constructed. These models assume an initially hot state, but with a wide variety of choices for the parameters characterizing the rheology and convective vigor. All models are constrained to be consistent with present-day surface heat fluxes, and many of the terrestrial models are consistent with the mantle viscosities indicated by postglacial rebound. In the lunar models, heat generation is typically only 70-80% of the surface heat flow, even with allowance for the strong near-surface enhancement of radioactives. Despite the simplicity of these models, the persistence of a significant difference between heat generation and heat output indicates that this difference is real and should be incorporated in geochemical modeling of planets. A.T.

A80-36750 * Pioneer Venus sounder and small probes Nephelometer instrument. B. Ragent, T. Wong (NASA, Ames Research Center, Moffett Field, Calif.), J. E. Blamont (CNRS, Service d'Aéronomie, Verrières-le-Buisson, Essonne, France), A. J. Eskovitz, L. N. Harnett, and A. Pallai (TRW Defense and Space Systems Group, Redondo Beach, Calif.). *IEEE Transactions on Geoscience and Remote Sensing*, vol. GE-18, Jan. 1980, p. 111-117. Contract No. NAS2-8805.

The Nephelometer instrument flown on all four of the probes of the Pioneer Venus mission is described. The instruments functioned well, returning data on the backscattering properties of the Venusian clouds and ambient solar radiation in several wavelength intervals as a function of altitude at four widely separated planetary locations. The design considerations, instrument construction, calibration and performance are discussed. (Author)

A80-37179 * Changes induced on the surfaces of small Pd clusters by the thermal desorption of CO. D. L. Doering, H. Poppa, and J. T. Dickinson (NASA, Ames Research Center; Stanford Joint Institute for Surface and Microstructure Research, Moffett Field, Calif.). (*American Vacuum Society, National Symposium, 26th, New York, N.Y., Oct. 1-5, 1979.*) *Journal of Vacuum Science and Technology*, vol. 17, Jan.-Feb. 1980, p. 198-200. 9 refs. Grant No. NCA2-OR-840-801.

The stability and adsorption/desorption properties of supported Pd crystallites less than 5 nm in size were studied by Auger electron spectroscopy and repeated flash thermal desorption of CO. The Pd particles were grown epitaxially on heat-treated, UHV-cleaved mica at a substrate temperature of 300 C and a Pd impingement flux of 10 to the 13th atoms/sq cm s. Auger analysis allowed in situ measurement of relative particle dispersion and contamination, while FTD monitored the CO desorption properties. The results show that significant changes in the adsorption properties can be detected. Changes in the Pd Auger signal and the desorption spectrum during the first few thermal cycles are due to particle coalescence and facetting and the rate of this change is dependent on the temperature and duration of the desorption. Significant reductions in the

amplitude of the desorptions peak occur during successive CO desorptions which are attributed to increases of surface carbon, induced by the desorption of CO. The contamination process could be reversed by heat treatment in oxygen or hydrogen. (Author)

A80-37180 * Direct /TEM/ observation of the catalytic oxidation of amorphous carbon by Pd particles. R. D. Moorhead, H. Poppa, and K. Heinemann (NASA, Ames Research Center; Stanford Joint Institute for Surface and Microstructure Research, Moffett Field, Calif.). (*American Vacuum Society, National Symposium, 26th, New York, N.Y., Oct. 1-5, 1979.*) *Journal of Vacuum Science and Technology*, vol. 17, Jan.-Feb. 1980, p. 248-250. 7 refs.

The catalytic oxidation of amorphous carbon substrates by Pd particles is observed by in situ transmission electron microscopy. Various modes of selective attack of the carbon substrate in the immediate neighborhood of Pd particles are observed, which can be correlated with different degrees of particle mobility. Using amorphous substrates we have been able to demonstrate that the particle-substrate interaction is influenced by the structure of the particle. This has not previously been noted. (Author)

A80-37193 * Comparison of the early stages of condensation of Cu and Ag on Mo(100) with Cu and Ag on W(100). F. Soria (NASA, Ames Research Center; Stanford Joint Institute for Surface and Microstructure Research, Moffett Field, Calif.; Consejo Superior de Investigaciones Científicas, Instituto di Física de Materiales, Madrid, Spain) and H. Poppa (NASA, Ames Research Center; Stanford Joint Institute for Surface and Microstructure Research, Moffett Field, Calif.). (*American Vacuum Society, National Symposium, 26th, New York, N.Y., Oct. 1-5, 1979.*) *Journal of Vacuum Science and Technology*, vol. 17, Jan.-Feb. 1980, p. 449-452. 13 refs.

The adsorption and condensation of Cu and Ag, up to several monolayers in thickness, onto Mo(100) has been observed at pressures below 2 times 10 to the -10th torr in a study that used combined LEED, Auger, TDS (Thermal Desorption Spectroscopy), and work function measurements in a single experimental setup. The results show that Cu behaves similarly on Mo(100) and W(100) substrates, while some differences are found for Ag adsorption. (Author)

A80-37598 * Origin and evolution of planetary atmospheres. J. B. Pollack (NASA, Ames Research Center, Space Sciences Div., Moffett Field, Calif.) and Y. L. Yung (California Institute of Technology, Pasadena, Calif.). In: Annual review of earth and planetary sciences. Volume 8. (A80-37593 15-42) Palo Alto, Calif., Annual Reviews, Inc., 1980, p. 425-487. 53 refs.

The current understanding of the origin and evolution of the atmospheres of solar system objects is reviewed. Physical processes that control this evolution are described in an attempt to develop a set of general principles that can help guide studies of specific objects. Particular emphasis is placed on the planetary and satellite atmospheres of the inner solar system objects; current hypotheses on the origin and evolution of these objects are critically considered. B.J.

A80-38432 * Fragmentation in a rotating protostar - A comparison of two three-dimensional computer codes. A. P. Boss (California, University, Santa Barbara, Calif.) and P. Bodenheimer (NASA, Ames Research Center, Space Science Div., Moffett Field; Lick Observatory, Santa Cruz, Calif.). *Astrophysical Journal, Part 1*, vol. 234, Nov. 15, 1979, p. 289-295. 12 refs. NSF Grant No. AST-76-17590; Grants No. NCA2-OR-660-703; No. NCA2-OR-

680-805; No. NGR-05-010-062.

The collapse of an isothermal protostellar cloud with pressure, gravity, and rotation included is followed with two independent computer codes. For the initial condition, a nonaxisymmetric perturbation of mode $m = 2$ and 50% amplitude is introduced into a cloud of 1 solar mass with a mean density of 1.44×10 to the -17 g/cm and a uniform angular velocity of 1.6×10 to the -12 rad/sec. The collapse is followed through an increase in density of over four orders of magnitude to the point where a binary protostar forms. The agreement between the results of the two calculations is good. (Author)

A80-39375 * Protostellar formation in rotating interstellar clouds. III - Nonaxisymmetric collapse. A. P. Boss (NASA, Ames Research Center, Space Sciences Div., Moffett Field; California, University, Santa Barbara, Calif.). *Astrophysical Journal, Part 1*, vol. 237, May 1, 1980, p. 866-876. 15 refs. Grants No. NGR-05-010-062; No. NCA2-OR-680-805.

The paper discusses a full three spatial-dimension gravitational hydrodynamic code used to follow the collapse of isothermal rotating clouds subjected to various nonaxially symmetric perturbations (NAP). An initially axially symmetric cloud collapsed to form a ring which then fragmented into a binary protostellar system; a low thermal energy cloud with a large bar-shaped NAP collapsed and fragmented into a binary, and higher thermal energy clouds damp out such NAPs while higher rotational energy clouds produce binaries with wider separations. The three-dimensional calculations indicate that isothermal interstellar clouds may fragment into protostellar objects while still in the isothermal regime. Interstellar clouds and their fragments may pass through collapse phases with fragmentation and reduction of spin angular momentum terminating in the formation of pre-main-sequence stars with the observed pre-main-sequence rotation rates. A.T.

A80-40138 * Radiatively driven winds for different power law spectra. M. Beltrametti (NASA, Ames Research Center, Moffett Field, Calif.; Heidelberg, Universität, Heidelberg, West Germany). *Astronomy and Astrophysics*, vol. 86, no. 1-2, June 1980, p. 169-180. 12 refs.

The analytic solutions for radiatively driven winds are given for the case in which the winds are driven by absorption of line and continuum radiation. The wind solutions are analytically estimated for different parameters of the central source and for different power law spectra. For flat spectra, three sonic points can exist; it is shown, however, that only one of these sonic points is physically realistic. Parameters of the central source are given which generate winds of further interest for explaining the narrow and broad absorption lines in quasars. For the quasar model presented here, winds which could give rise to the narrow absorption lines are generated by central sources with parameters which are not realistic for quasars. A.T.

A80-40642 * Excitation mechanisms for the unidentified infrared emission features. E. Dwek, K. Sellgren, B. T. Soifer (California Institute of Technology, Pasadena, Calif.), and M. W. Werner (NASA, Ames Research Center, Moffett Field; California Institute of Technology, Pasadena, Calif.). *Astrophysical Journal, Part 1*, vol. 238, May 15, 1980, p. 140-147. 41 refs. NSF Grants No. PHY-76-83685; No. AST-77-20516; Grant No. NGR-05-002-281.

Infrared and radio observations of various objects are analyzed to put observational constraints on the mechanism which gives rise to the unidentified emission features at 3.3, 3.4, 6.2, 7.7, 8.6, and 11.3 microns. The results show that gas-grain collisions or fluorescence is not likely to be the excitation mechanism responsible for the observed features. Thermal emission by dust is reanalyzed and it is

concluded that this mechanism can explain the emission features. A simple model in which the emission features arise in a population of small, hot, interstellar grains is constructed. These grains are very efficient radiators, and the emitting materials only need be a minor grain constituent to provide the power that is emitted in the features. The model offers, therefore, a simple explanation for the absence of these features in absorption. (Author)

A80-40907 * # Experimental investigation of a three dimensional turbulent boundary layer with a non disappearing pressure gradient (Experimentelle Untersuchung einer dreidimensionalen, turbulenten Grenzschicht mit nicht verschwindenden Druckgradienten). U. Müller (NASA, Ames Research Center, Moffett Field, Calif.). *Rheinisch-Westfälische Technische Hochschule, Aerodynamisches Institut, Abhandlungen*, no. 24, 1980, p. 36-43. 12 refs. In German.

The results of measuring profiles of temporally determined velocities and Reynolds tension, wall shear stresses and pressure distribution in a three dimensional, turbulent boundary layer with pressure gradients in both tangential directions are reported. For determining the velocities X wire probes were used whose cooling was gauged according to magnitude and direction of the flow and was described with an effective cooling speed. In the evaluation consideration is given to the directional sensitivity of the hot wire. The ratio of the turbulence viscosities is calculated for both tangential directions and is found to be approximately N equals 1.2. Further, the profiles of the mixing path lengths for the flow direction are found to vary only slightly with increasing X-coordinates, while the boundary layer thickness increases substantially. The relationships of turbulent shear stress to turbulent, kinetic fluctuation energy is approximately constant over a large part of the boundary layer. M.E.P.

A80-40926 * Thermal expansion and swelling of cured epoxy resin used in graphite/epoxy composite materials. M. J. Adamson (NASA, Ames Research Center, Materials Science and Applications Office, Moffett Field, Calif.). *Journal of Materials Science*, vol. 15, July 1980, p. 1736-1745. 32 refs.

The paper presents results of experiments in which the thermal expansion and swelling behavior of an epoxy resin system and two graphite/epoxy composite systems exposed to water were measured. It was found that the cured epoxy resin swells by an amount slightly less than the volume of the absorbed water and that the swelling efficiency of the water varies with the moisture content of the polymer. Additionally, the thermal expansion of cured epoxy resin that is saturated with water is observed to be more than twice that of dry resin. Results also indicate that cured resin that is saturated with 7.1% water at 95 C will rapidly increase in moisture content to 8.5% when placed in 1 C water. The mechanism for this phenomenon, termed reverse thermal effect, is described in terms of a slightly modified free-volume theory in conjunction with the theory of polar molecule interaction. Nearly identical behavior was observed in two graphite/epoxy composite systems, thus establishing that this behavior may be common to all cured epoxy resins. (Author)

A80-41175 * Ground-state rotational constants of /C-13/H3D. C. Chackerian, Jr. (NASA, Ames Research Center, Moffett Field, Calif.) and G. Guelachvili (Paris XI, Université, Orsay, Essonne, France). *Journal of Molecular Spectroscopy*, vol. 80, 1980, p. 244-248. 12 refs.

Rotational constants for the vibrational ground state of (C-13)H3D, which has been detected in the atmospheres of Jupiter and Saturn, are reported. High-resolution spectra of monodeutero-methane were obtained in the region 1800 to 2500 kayzers by a vacuum Fourier interferometer, and the values of the rotational

constants B0, D0J, D0JK, H0JJJ, H0JJK and H0JJK were calculated by an analysis of ground-state combination differences in the nu 2(A1) band. The calculated frequency and intensity of this transition are found to be in agreement with the observed values. A.L.W.

A80-41323 * **Recommended conventions for defining transition moments and intensity factors in diatomic molecular spectra.** E. E. Whiting (NASA, Ames Research Center, Moffett Field, Calif.), A. Schadee (Sterrewacht Sonnenborgh, Utrecht, Netherlands), J. B. Tatum (Victoria, University, Victoria, British Columbia, Canada), J. T. Hougen (National Bureau of Standards, Washington, D.C.), and R. W. Nicholls (York University, Downsview, Ontario, Canada). *Journal of Molecular Spectroscopy*, vol. 80, 1980, p. 249-256. 5 refs.

A80-42659 * **Meteorological and air pollution modeling for an urban airport.** P. R. Swan (NASA, Ames Research Center, Moffett Field, Calif.) and I. Y. Lee (San Jose State University, San Jose, Calif.). *Journal of Applied Meteorology*, vol. 19, May 1980, p. 534-544. 7 refs.

Results are presented of numerical experiments modeling meteorology, multiple pollutant sources, and nonlinear photochemical reactions for the case of an airport in a large urban area with complex terrain. A planetary boundary-layer model which predicts the mixing depth and generates wind, moisture, and temperature fields was used; it utilizes only surface and synoptic boundary conditions as input data. A version of the Hecht-Seinfeld-Dodge chemical kinetics model is integrated with a new, rapid numerical technique; both the San Francisco Bay Area Air Quality Management District source inventory and the San Jose Airport aircraft inventory are utilized. The air quality model results are presented in contour plots; the combined results illustrate that the highly nonlinear interactions which are present require that the chemistry and meteorology be considered simultaneously to make a valid assessment of the effects of individual sources on regional air quality. A.T.

A80-42744 * **Smoke and dust particles of meteoric origin in the mesosphere and stratosphere.** D. M. Hunten (Arizona, University, Tucson, Ariz.), R. P. Turco (R&D Associates, Marina del Rey, Calif.), and O. B. Toon (NASA, Ames Research Center, Space Sciences Div., Moffett Field, Calif.). *Journal of the Atmospheric Sciences*, vol. 37, June 1980, p. 1342-1357. 63 refs. Grant No. NSG-7558.

A height profile of ablated mass from meteors is calculated, assuming an incoming mass of 10 to the -16th g/sq cm/s (44 metric tons per day) and the velocity distribution of Southworth and Sekanina, which has a mean of 14.5 km/s. The profile peaks at 84 km. The fluxes of micrometeorites and residual meteoroids are also calculated. The coagulation of the evaporated silicates into 'smoke' particles is then followed by means of a model adapted from a previous study of the stratospheric sulfate layer. Numerous sensitivity tests are made. Features of the results are a sharp cutoff of the particle distribution above 90 km, and a surface area close to 10 to the -9th sq cm/cu cm all the way from 30 to 85 km. Some confirmation is obtained from balloon studies of condensation nuclei, although the various measurements differ greatly. The optical scattering and extinction are shown to be undetectable. Several potential applications are suggested: nucleation of sulfate particles and noctilucent clouds, scavenging of metallic ions and atoms, and perhaps other aeronautical effects. The latter are limited to processes that can be influenced by a collision time of the order of a day.

(Author)

A80-42902 * **Cryogenic systems for spacecraft.** J. W. Vorreiter (NASA, Ames Research Center, Moffett Field, Calif.). *Contemporary Physics*, vol. 21, May-June 1980, p. 201-217. 28 refs.

It is noted that the use of cryogenic components on spacecraft, already quite common, will likely increase in the future. Attention is given to a number of applications including earth observation, atmospheric measurements, infrared astronomy and magnetic field measurements. These applications are discussed with regard to their cryogenic requirements. Further, four cryogenic instruments provided by the United States to be launched on spacecraft in the near future are described. Finally, other missions being planned that will use cryogenic instrumentation are also considered. M.E.P.

A80-43135 * # **Asymptotic features of shock-wave boundary-layer interaction.** M. Y. Hussaini, B. S. Baldwin, and R. W. MacCormack (NASA, Ames Research Center, Moffett Field, Calif.). *AIAA Journal*, vol. 18, Aug. 1980, p. 1014-1016. 9 refs. Contracts No. NAS1-14101; No. NAS1-14472.

A semi-implicit method is applied to solve the Navier-Stokes equations numerically and to evaluate the features of the free-interaction phenomenon that occurs when a shock wave impinges on a Blasius boundary layer. Comparisons are made with predictions of the triple-deck theory and experiment. Results include pressure and skin-friction distribution in the free-interaction region for various values of Reynolds number. V.T.

A80-43638 * # **Measurements of NO, O3, and temperature at 19.8 km during the total solar eclipse of 26 February 1979.** W. L. Starr, R. A. Craig, M. Loewenstein, and M. E. McGhan (NASA, Ames Research Center, Moffett Field, Calif.). *Geophysical Research Letters*, vol. 7, July 1980, p. 553-555. 6 refs.

Local measurements of stratospheric NO and O3 mixing ratios and air temperature were made during the total solar eclipse of 26 February 1979. The instrumentation was carried aboard a U-2 aircraft flown at an altitude of 19.8 km in the region near 47 deg N, 112 deg W. Eclipse maximum occurred approximately in the middle of the 2-3/4-hr measurement period. The NO mixing ratio was reduced at least a factor of 25 at the maximum of the eclipse. The decrease and recovery of NO during the passage of the Moon's shadow over the measurement region follows approximately the predictions of two independent models. No change was observed in either the O3 mixing ratio or the air temperature that could be attributed to the eclipse. (Author)

A80-44959 * **Self-gravitating gas flow in barred spiral galaxies.** J. M. Huntley (NASA, Ames Research Center, Theoretical and Planetary Studies Branch, Moffett Field, Calif.; IBM Thomas J. Watson Research Center, Yorktown Heights, N.Y.). *Astrophysical Journal, Part 1*, vol. 238, June 1, 1980, p. 524-538. 42 refs.

A series of two-dimensional numerical experiments is performed in order to test the response of an isothermal, self-gravitating gas disk to a uniformly rotating, barlike gravitational potential. The barlike potential is an equilibrium stellar model from the n-body calculations of Miller and Smith (1979). In the bar-dominated, central regions of the disk, a gas bar whose phase depends primarily on the location of principal resonances in the disk is formed. This response can be understood in terms of orbit-crowding effects. In the gas-dominated outer regions of the disk, two-armed trailing spiral waves are formed. The local pitch angle of these waves increases with increasing fractional gas mass. These self-gravitating gas waves are not self-sustaining. They are driven from the ends of equilibrium stellar bars,

S

and their phase does not depend on the location of resonances in the disk. The relevance of these self-gravitating waves to observations and models of barred spiral galaxies is discussed. It is concluded that these waves and their associated ringlike structures may be consistent with the morphological distribution of gas features in barred spiral galaxies. (Author)

A80-44965 * **The spectrum of IRC + 10216 from 2.0 to 8.5 microns.** F. C. Witteborn, D. W. Strecker, E. F. Erickson, S. M. Smith, J. H. Goebel, and B. J. Taylor (NASA, Ames Research Center, Moffett Field, Calif.). *Astrophysical Journal, Part 1*, vol. 238, June 1, 1980, p. 577-584. 29 refs.

Low-resolution spectra of IRC + 10216 have been obtained from 2 to 8.5 microns from NASA's Kuiper Airborne Observatory at an altitude of 12.5 km (41,000 feet). Observations were made during 1976 January and 1977 February. In both sets of data, the spectral flux reaches its maximum between 6.0 and 6.6 microns and the previously reported 3.1-micron feature is observed; no obvious new absorption features have been found. The new data together with other spectral data and measurements of the spatial extent of IRC + 10216 impose conditions that must be met by models of the continuum. Several simple models for 2-8.5 micron radiation are examined. The new continuum data impose a constraint on the size of the grains in the cooler, optically thin part of the object. Earlier photometry has been combined with the present data to yield an improved value of the average period: 644 + or - 17 days. It appears that the variability is irregular and that the minima have been deeper in recent years than they were in 1965-1969. (Author)

A80-44967 * **Far-infrared spectra of W51-IRS 2 and W49 NW.** E. F. Erickson and A. T. Tokunaga (NASA, Ames Research Center, Moffett Field, Calif.). *Astrophysical Journal, Part 1*, vol. 238, June 1, 1980, p. 596-600. 42 refs.

Measurements of the far-infrared spectra of the powerful H II regions W51-IRS 2 and W49 NW from 65 to 345 per cm with about 9 per cm resolution were obtained by using an airborne Michelson interferometer. The most remarkable feature of the far-infrared spectra of the two regions is the smoothness of the continuum; no evidence is found in the spectra for features of H₂O ice at 45 and 62 microns. The spectrum of W51 is well fitted by a 70 K blackbody with a diameter of 14 arc sec, but the spectrum of W49 NW is narrower than a blackbody. The implications of the apparently high peak optical depths of these sources are discussed. J.P.B.

A80-44993 * **An optical emission-line phase of the extreme carbon star IRC +30219.** M. Cohen (NASA, Ames Research Center, Moffett Field, Calif.). *Astrophysical Journal, Part 2 - Letters to the Editor*, vol. 238, June 1, 1980, p. L81-L85. 8 refs. Research supported by the National Research Council; NSF Grant No. AST-77-19896.

Optical spectroscopic monitoring of the extreme carbon star IRC +30219 has revealed striking changes between 1977 and 1980. The stellar photosphere was barely visible in early 1979. There was an emission line spectrum consisting of H, forbidden O I, forbidden O II, forbidden N I, forbidden N II, forbidden S II, and He I. It is likely that these lines arose in a shocked region where recent stellar mass loss encountered the extensive circumstellar envelope. By late 1979, this emission-line spectrum had vanished, and the photosphere had reappeared. The weakening of the photospheric features in early 1979 was caused by increased attenuation of starlight and overlying thermal emission, both due to recently condensed hot dust grains. (Author)

A80-45333 * **An ab initio calculation of the zero-field splitting parameters of the 3A-double prime state of formaldehyde.** E. R. Davidson, J. C. Ellenbogen (Washington, University, Seattle, Wash.), and S. R. Langhoff (NASA, Ames Research Center, Moffett Field, Calif.). *Journal of Chemical Physics*, vol. 73, July 15, 1980, p. 865-869. 11 refs. NIH-supported research.

The spin dipole-dipole and spin-orbit contributions to the zero-field splitting of the 3A-double prime state of formaldehyde have been evaluated at the excited state experimental geometry. Ab initio CI wave functions were generated from a Dunning double zeta plus polarization bases set using 3A-double prime rhf orbitals. Twelve states of each symmetry were used to evaluate the second-order spin-orbit effect. The resulting values of D and E were 0.19 and 0.03 kayser with the principal magnetic axes rotated 36 deg from the CO bond. The values of alpha and beta relative to the inertial axes were calculated to be 0.03 and 0.01 kayser compared to the experimental values of 0.05 plus or minus 0.01 and 0.02 plus or minus 0.02 kayser. (Author)

A80-45359 * **Equivalent-cone calculation of nitric oxide production rate during Space Shuttle re-entry.** C. Park and J. V. Rakich (NASA, Ames Research Center, Moffett Field, Calif.). *Atmospheric Environment*, vol. 14, no. 8, 1980, p. 971, 972.

The amount of nitric oxide likely to be produced in the shock layer around a Space Shuttle orbiter vehicle during its reentry is calculated at one point on the trajectory. An equivalent-cone is defined as one that produces the same amount of nitric oxide as the orbiter. The amounts of nitric oxide produced by the cone are calculated at points along the trajectory to determine their total and altitudinal distribution. The results show that about 14 tonne nitric oxide is produced at each entry, the peak occurring at 68 km altitude. (Author)

A80-45812 * **The effect of dense cores on the structure and evolution of Jupiter and Saturn.** A. S. Grossman (NASA, Ames Research Center, Space Sciences Div., Moffett Field, Calif.; Erwin W. Fick Observatory, Ames, Iowa), J. B. Pollack, R. T. Reynolds, A. L. Summers (NASA, Ames Research Center, Space Sciences Div., Moffett Field, Calif.), and H. C. Graboske, Jr. (California, University, Livermore, Calif.). *Icarus*, vol. 42, June 1980, p. 358-379. 50 refs. Grant No. NCA2-OR-340-902.

The evolutionary and static models of Jupiter and Saturn were calculated with homogeneous solar composition mantles and dense cores of material consisting of solar abundances of SiO₂, MgO, Fe, and Ni. Evolutionary sequences for Jupiter were calculated with cores of mass ranging from 2 to 8% of the Jovian mass; the Saturn sequences ranged from cores of mass of 16 to 22% of total mass. Two envelope mixtures representative of the solar abundances were used: they contained mass fraction of 0.74 and 0.77 of hydrogen, respectively, and 0.24 and 0.21 mass fractions of helium. For Jupiter, the observations of the temperature at 1 bar pressure, of radius and of internal luminosity were best fit by evolutionary models with a core mass of about 6.5% and chemical composition of 0.77 mass fraction of hydrogen and 0.21 mass fraction of helium. The cooling time calculated for Saturn was 2.6 x 10 to the 9th yr, almost a factor of 2 less than the percentage of the solar system. A.T.

A80-48762 * **Computational study of alkali-metal-noble gas collisions in the presence of nonresonant lasers - Na + Xe + h/2pi/omega sub 1 + h/2pi/omega sub 2 system.** P. L. DeVries, C. Chang, T. F. George (Rochester, University, Rochester, N.Y.), B. Laskowski, and J. R. Stallcop (NASA, Ames Research Center, Moffett Field, Calif.). *Physical Review A - General Physics, 3rd Series*, vol. 22, Aug. 1980, p. 545-550. 7 refs. Research supported by

the Alfred P. Sloan Foundation and Henry Dreyfus Foundation; NSF Grant No. CHE-77-27826; Grant No. NSG-2198; Contracts No. F49620-78-C-0005; No. W-7405-eng-48.

The collision of Na with Xe in the presence of both the rhodamine-110 dye laser and the Nd-glass laser is investigated within a quantum-mechanical close-coupled formalism, utilizing *ab initio* potential curves and transition dipole matrix elements. Both one- and two-photon processes are investigated; the Na + Xe system is not asymptotically resonant with the radiation fields, so that these processes can only occur in the molecular collision region. The one-photon processes are found to have measurable cross sections at relatively low intensities; even the two-photon process has a significant section for field intensities as low as 10 MW/sq cm.

(Author)

A80-49341 * Numerical calculations of the collapse of nonrotating, magnetic gas clouds. E. H. Scott (San Francisco State University, San Francisco, Calif.) and D. C. Black (NASA, Ames Research Center, Theoretical and Planetary Studies Branch, Moffett Field, Calif.). *Astrophysical Journal, Part 1*, vol. 239, July 1, 1980, p. 166-172. 16 refs. Grant No. NCA2-OR-660-703.

Results of the first self-consistent numerical calculations of the dynamic collapse of a magnetized protostellar gas cloud are presented. Symmetry about an axis parallel to the initial magnetic field direction has been assumed, so that the calculations could be performed on a two-dimensional grid. Also, the cloud was taken to be nonrotating and isothermal, and the magnetic field was assumed to remain frozen in to the gas. As starting models for the calculations, gas spheres with uniform density and magnetic field were used. The time evolution of the clouds has been calculated for roughly two initial free-fall times, at which point the central density has increased by a factor of approximately 10,000 to 1,000,000. Several such calculations have been performed for different values of the cloud's initial thermal, magnetic, and gravitational energies. In virtually all cases it is found that, once a flattened core forms in the cloud, the central magnetic field strength, B , varies with gas density, ρ , according to $(d \log B / d \log \rho) = 1/2$. This behavior is independent of the initial energy ratios mentioned above. It is also found that the magnetic field is able to prevent completely the collapse of part of the outer envelope of the cloud. (Author)

A80-49383 * Effect of three-body interactions on the structure of small clusters. T. Halicioglu (NASA, Ames Research Center, Moffett Field; Polyatomics Research, Inc., Mountain View, Calif.) and P. J. White (NASA, Ames Research Center, Moffett Field, Calif.). *Journal of Vacuum Science and Technology*, vol. 17, Sept.-Oct. 1980, p. 1213-1215. 23 refs. Contract No. NAS2-1069.

Minimum energy configurations of microclusters (up to six atoms) have been calculated using two- and three-body interactions. Structural changes were parametrically analyzed as a function of the intensity of three-body forces. The results are qualitative in nature; they indicate, however, that three-body interactions play an important role in the equilibrium structure of microclusters. The effect of the intensity of the three-body interactions on the structure of small clusters is not manifested in a continuous manner. Rather, changes in the energetically most stable structure occur abruptly. The results are in qualitative agreement with experimental observations as well as other calculations. (Author)

A80-50144 * Properties of clusters in the gas phase. V. Complexes of neutral molecules onto negative ions. R. G. Keesee (NASA, Ames Research Center, Space Sciences Div., Moffett Field, Calif.; Cooperative Institute for Research in Environmental Sciences,

Boulder, Colo.), N. Lee, and A. W. Castleman, Jr. (Cooperative Institute for Research in Environmental Sciences, Boulder, Colo.). *Journal of Chemical Physics*, vol. 73, Sept. 1, 1980, p. 2195-2202. 37 refs. NSF Grant No. ATM-79-13801; Contract No. EP-78-S-002-4776; Grants No. NSG-2248; No. DAAG29-79-C-0133.

Ion-molecules association reactions of the form $A(-)(B)n + B = A(-)(B)n$ were studied over a range of temperatures in the gas phase using high pressure mass spectrometry. Enthalpy and entropy changes were determined for the stepwise clustering reactions of (1) sulfur dioxide onto $Cl(-)$, $I(-)$, and $NO_2(-)$ with n ranging from one to three or four, and onto $SO_2(-)$ and $SO_3(-)$ with n equal to one; and (2) carbon dioxide onto $Cl(-)$, $I(-)$, $NO_2(-)$, $CO_3(-)$, and $SO_3(-)$ with n equal to one. From these data and earlier hydration results, the order of the magnitude of the enthalpy changes on the association of the first neutral for a series of negative ions was found to parallel the gas-phase basicity of those anions. (Author)

A80-50149 * Theoretical treatment of the spin-orbit coupling in the rare gas oxides NeO, ArO, KrO, and XeO. S. R. Langhoff (NASA, Ames Research Center, Moffett Field, Calif.). *Journal of Chemical Physics*, vol. 73, Sept. 1, 1980, p. 2379-2386. 27 refs.

Off-diagonal spin-orbit matrix elements are calculated as a function of internuclear distance for the rare gas oxides NeO, ArO, KrO, and XeO using the full microscopic spin-orbit Hamiltonian, including all one- and two-electron integrals, and POL-CI wave functions comparable to those of Dunning and Hay (1977). A good agreement was found when comparing these results in detail with the calculations of Cohen, Wadt and Hay (1979) that utilize an effective one-electron one-center spin-orbit operator. For the rare gas oxide molecules, it is suggested that the numerical results are a more sensitive test of the wave functions (particularly to the extent of charge transfer) than the exact evaluation of all terms in the full spin-orbit operator. A.C.W.

A80-51050 * Alternating direction implicit methods for parabolic equations with a mixed derivative. R. M. Beam and R. F. Warming (NASA, Ames Research Center, Computational Fluid Dynamics Branch, Moffett Field, Calif.). *SIAM Journal on Scientific and Statistical Computing*, vol. 1, Mar. 1980, p. 131-159. 21 refs.

Alternating direction implicit (ADI) schemes for two-dimensional parabolic equations with a mixed derivative are constructed by using the class of all $A(0)$ -stable linear two-step methods in conjunction with the method of approximate factorization. The mixed derivative is treated with an explicit two-step method which is compatible with an implicit $A(0)$ -stable method. The parameter space for which the resulting ADI schemes are second-order accurate and unconditionally stable is determined. Some numerical examples are given. (Author)

A80-51378 * Curves of growth for van der Waals broadened spectral lines. C. Park (NASA, Ames Research Center, Moffett Field, Calif.). *Journal of Quantitative Spectroscopy and Radiative Transfer*, vol. 24, Oct. 1980, p. 289-292. 6 refs.

Curves of growth are evaluated for a spectral line broadened by the van der Waals interactions during collisions. The growth of the equivalent widths of such lines is shown to be dependent on the product of the perturber density and the $6/10$ power of the van der Waals potential coefficient. When the parameter is small, the widths grow as the $1/2$ power of the optical depth as they do for the Voigt profile; but when the parameter is large, they grow as $2/3$ power and, hence, faster than the Voigt profile. An approximate analytical expression for the computed growth characteristics is given. (Author)

S

A80-51965 * Vibration-rotation line shifts for 1 sigma g + H2/V,J/-1S/O/ He computed via close coupling - Temperature dependence. G. E. Hahne and C. Chackerian, Jr. (NASA, Ames Research Center, Moffett Field, Calif.). *Journal of Chemical Physics*, vol. 73, Oct. 1, 1980, p. 3223-3231. 47 refs.

The density shifting of vibration-rotation transitions of H2 perturbed by He was computed (as a function of temperature) with no adjustable parameters. The calculation was carried out using the framework of the impact theory of Baranger with S-matrix elements obtained via close coupling calculations which incorporated the ab initio H2-H2 system potential of Tsapline et al.(1977). Vibrational and rotational inelasticity were neglected in the calculations; nevertheless good agreement with experimental data was obtained, up to moderate temperatures, for the density shift. A much poorer comparison was obtained for the density broadening. (Author)

A80-52399 * Discovery of optical molecular emission from the bipolar nebula surrounding HD 44179. G. D. Schmidt (Lick Observatory, Santa Cruz, Calif.), M. Cohen (NASA, Ames Research Center, Moffett Field, Calif.), and B. Margon. *Astrophysical Journal, Part 2 - Letters to the Editor*, vol. 239, Aug. 1, 1980, p. L133-L138. 21 refs. NSF Grants No. AST-78-19753; No. AST-77-27745.

Spectrophotometry and spectropolarimetry with HD 44179 are presented. These measurements reveal that the very broad bump evident in previous low-resolution spectra possesses a large amount of structure, including groups of narrow emission lines and several diffuse features. A reduction in polarization, but constant position angle, through the bump indicates that this emission originates within the nebula itself and merely dilutes the polarized scattered starlight. A few very weak atomic emission lines are detected, but the overall feature, which strongly resembles the emission spectra of some molecules, remains unidentified. Constraints on the excitation mechanism are discussed. (Author)

A80-53235 * Tidal dissipation, orbital evolution, and the nature of Saturn's inner satellites. S. J. Peale (Joint Institute for Laboratory Astrophysics, Boulder, Colo.; California, University, Santa Barbara, Calif.), P. Cassen, and R. T. Reynolds (NASA, Ames Research Center, Moffett Field, Calif.). *Icarus*, vol. 43, July 1980, p. 65-72. 35 refs. Grants No. NGR-05-010-062; No. NCA2-OR-680-85.

Estimates of tidal damping times of the orbital eccentricities of Saturn's inner satellites place constraints on some satellite rigidities and dissipation functions Q. These constraints favor rock-like rather than ice-like properties for Mimas and probably Dione. Photometric and other observational data are consistent with relatively higher densities for these two satellites, but require lower densities for Tethys, Enceladus, and Rhea. This leads to a nonmonotonic density distribution for Saturn's inner satellites, apparently determined by different mass fractions of rocky materials. In spite of the consequences of tidal dissipation for the orbital eccentricity decay and implications for satellite compositions, tidal heating is not an important contributor to the thermal history of any Saturnian satellite. (Author)

CONFERENCE PAPERS

N80-20010*# National Aeronautics and Space Administration. Ames Research Center, Moffett Field, Calif.

NASA'S WESTERN REGIONAL APPLICATIONS TRAINING ACTIVITY

Charles E. Poulton *In its Conf. of Remote Sensing Educators (CORSE-78) Mar. 1980 p 181-196* (For primary document see N80-20003 10-99)

Avail: NTIS HC A99/MF A01 CSCL 05I

Direct involvement of educational institutions in the transfer of remote sensing technology must be increased so that the training component of the Western Regional Applications Program can be expanded within the various states. The implications of essential goals in remote sensing education and training are considered in relation to the functions of the NASA University Affairs program. A.R.H.

N80-20016*# National Aeronautics and Space Administration. Ames Research Center, Moffett Field, Calif.

DATA REDUCTION BY COMPUTER PROCESSING

Dale R. Lumb *In its Conf. of Remote Sensing Educators (CORSE-78) Mar. 1980 p 391-452* refs (For primary document see N80-20003 10-99)

Avail: NTIS HC A99/MF A01 CSCL 09B

The automated analysis of remote sensing data, specifically digital processing of LANDSAT or other image data in numerical form was considered in a technical workshop which covered the teaching of digital image processing, including both theoretical and applied subjects and laboratory experience, and also reviewed NASA developed image processing software, and hardware/software systems employed at NASA-Ames Research Center in support of the Western Regional Applications Program (WRAP). A course titled Image Processing Lab, one of two courses required for a graduate minor in remote sensing at Arizona is examined as well as the rationale, content, and hardware/software support for this course. A.R.H.

N80-21257*# National Aeronautics and Space Administration. Ames Research Center, Moffett Field, Calif.

USE OF ADVANCED COMPUTERS FOR AERODYNAMIC FLOW SIMULATION

F. R. Bailey and W. F. Ballhaus *In AGARD The Use of Computers as a Design Tool Jan. 1980 12 p* refs Prepared in cooperation with Army Research and Technology Labs., Moffett Field, Calif. (For primary document see N80-21243 12-01)

Avail: NTIS HC A19/MF A01 CSCL 01A

The current and projected use of advanced computers for large-scale aerodynamic flow simulation applied to engineering design and research is discussed. The design use of mature codes run on conventional, serial computers is compared with the fluid research use of new codes run on parallel and vector computers. The role of flow simulations in design is illustrated by the application of a three dimensional, inviscid, transonic code to the Sabreliner 60 wing redesign. Research computations that include a more complete description of the fluid physics by use of Reynolds averaged Navier-Stokes and large-eddy simulation formulations are also presented. Results of studies for a numerical aerodynamic simulation facility are used to project the feasibility of design applications employing these more advanced three dimensional viscous flow simulations. M.G.

N80-26347*# Jet Propulsion Lab., California Inst. of Tech., Pasadena.

PIONEER VENUS MULTIPROBE ENTRY TELEMTRY RECOVERY

R. B. Miller and R. Ramos (NASA, Ames Res. Center) *In its The Telecommun. and Data Acquisition Rept. 15 Jun. 1980 p 43-49* refs (For primary document see N80-26341 17-12)

Avail: NTIS HC A09/MF A01 CSCL 09F

N80-26361*# Jet Propulsion Lab., California Inst. of Tech., Pasadena.

DATA ACQUISITION FOR MEASURING THE WIND ON VENUS FROM PIONEER VENUS

c91

J. R. Smith and R. Ramos (NASA, Ames Res. Center) *In its The Telecommun. and Data Acquisition Rept.* 15 Jun. 1980 p 140-149 refs (For primary document see N80-26341 17-12) Avail: NTIS HC A09/MF A01 CSCL 03B

The data acquisition and processing techniques used in the Pioneer Venus differential long baseline interferometry experiment are described. The experiment was designed to measure the motion in three dimensions of the Pioneer probes during their fall to the surface of Venus, using a combination of Doppler and long baseline ratio interferometric methods. The design of the experiment and the equipment and software techniques that were developed specially for this experiment are also described. M.G.

N80-27658*# National Aeronautics and Space Administration. Ames Research Center, Moffett Field, Calif.

DEVELOPMENTS IN THE COMPUTATION OF TURBULENT BOUNDARY LAYERS

Morris W. Rubesin *In AGARD Turbulent Boundary Layers* Jan. 1980 23 p refs (For primary document see N80-27647 18-34) Avail: NTIS HC A17/MF A01 CSCL 20D

Two methods of turbulence computation are discussed in terms of their basic similarities. It is shown that the two methods are interrelated and that each can gain from advances in the other. The degree of success of a pair of increasingly complex Reynolds stress models to broaden their range of applicability is examined through comparison with experimental data for a variety of flow conditions. An example of a large eddy simulation is presented, compared with experimental results, and used to evaluate the models for pressure rate of strain correlation and dissipation in the Reynolds averaged equations. R.C.T.

N80-27659*# National Aeronautics and Space Administration. Ames Research Center, Moffett Field, Calif.

A NAVIER-STOKES FAST SOLVER FOR TURBULENCE MODELING APPLICATIONS

J. D. Murphy and M. W. Rubesin *In AGARD Turbulence Boundary Layers* Jan. 1980 16 p refs (For primary document see N80-27647 18-34)

Avail: NTIS HC A17/MF A01

A computer code for the evaluation and/or optimization of the predicative potential of second order turbulent closure models in simple two dimensional flow configurations is discussed. A procedure for the numerical solution of the steady constant property Navier-Stokes equations are described together with algebraic, one dimensional and two dimensional equations of turbulence closure models. Four turbulence models are compared with several sets of experimental data. The effects of initial conditions and boundary conditions are also described. The effects of purely numerical parameters, such as mesh size, boundary locations, and convergence criteria are presented. R.C.T.

N80-27661*# National Aeronautics and Space Administration. Ames Research Center, Moffett Field, Calif.

LARGE EDDY SIMULATION OF TURBULENT CHANNEL FLOW: ILLIAC 5 CALCULATION

John Kim and Parviz Moin *In AGARD Turbulent Boundary Layers* Jan. 1980 18 p refs (For primary document see N80-27647 18-34)

Avail: NTIS HC A17/MF A01 CSCL 20D

The capabilities of large eddy simulation in the prediction and analyses of wall-bounded turbulent shear flows are demonstrated. The dynamical equations for large scale field motions are derived. The computational grid network is described and its relation to the observed physical length scales in the flow are discussed. Some aspects of the mechanics and structure of the flow are examined both in the vicinity of the wall and in regions away from the wall. An attempt is made to correlate numerical results with laboratory observations. Other significant observations and conclusions are presented. R.C.T.

N80-33379*# National Aeronautics and Space Administration. Ames Research Center, Moffett Field, Calif.

NUMERICAL SOLUTION TECHNIQUES FOR UNSTEADY TRANSONIC AERODYNAMICS PROBLEMS

William F. Ballhaus and John O. Bridgeman *In AGARD Spec. Course on Unsteady Aerodyn.* Jun. 1980 24 p refs (For primary document see N80-33363 24-02)

Avail: NTIS HC A11/MF A01 CSCL 01A

Basic concepts of finite difference solution techniques for unsteady transonic flows are presented. The hierarchy of mathematical formulations that approximate the Navier-Stokes equations are reviewed. The basic concepts involved in constructing numerical algorithms to solve these formulations are given. Semi-implicit and implicit schemes are constructed and analyzed. The discussion focuses primarily on techniques for solving the low frequency transonic small disturbance equation. This is the simplest formulation that contains the essence of inviscid unsteady transonic flow physics. The low frequency formulation is emphasized here because codes based on this theory can be run in minutes of processor time on currently available computers. Furthermore, numerical techniques involved in solving this simple formulation also apply to the more complicated formulations. Extensions to these formulations are briefly described. An indication of the present capability for solving unsteady transonic flows is provided. Important areas of future research for the advancement of computational unsteady transonic aerodynamics are described. E.D.K.

A80-12603 * The 60-MW Shuttle interaction heating facility. W. Winovich and W. C. A. Carlson (NASA, Ames Research Center, Moffett Field, Calif.). *In: International Instrumentation Symposium, 25th, Anaheim, Calif., May 7-10, 1979, Proceedings. Part 1.* (A80-12601 02-35) Pittsburgh, Pa., Instrument Society of America, 1979, p. 59-75, 20 refs.

An arc-heated wind-tunnel system described in the present paper will simulate aerodynamic heating in large-scale tests of the thermal protection system of the Shuttle Orbiter Vehicle during entry. The system provides for large-scale subsystem tests in high-enthalpy streams with boundary layer flows at high Reynolds numbers and for large test-body sizes in stagnation flows. The discussion covers the design concept of the arc-jet systems, the extensive hardware developments of the arc heater to provide reliable operation, and verification and performance measurements of the system's operating envelopes. V.P.

A80-14987 * An explicit algorithm for a fluid approach to nonlinear optics propagation using splitting and rezoning techniques. F. P. Mattar, J. Teichmann (Montréal, Université, Montréal, Canada), L. R. Bissonnette (Defence Research Establishment Valcartier, Courcellette, Quebec, Canada), and R. W. McCormack (NASA, Ames Research Center, Moffett Field, Calif.). *In: Gas-flow and chemical lasers; Proceedings of the Second International Symposium, Rhode-Saint-Genèse, Belgium, September 1978.* (A80-14954 03-36) Washington, D.C., Hemisphere Publishing Corp., 1979, p. 437-448, 18 refs. Research supported by the Mobil Oil Corp.

The paper presents a three-dimensional analysis of the nonlinear light matter interaction in a hydrodynamic context. It is reported that the resulting equations are a generalization of the Navier-Stokes equations subjected to an internal potential which depends solely upon the fluid density. In addition, three numerical approaches are presented to solve the governing equations using an extension of McCormack predict-corrector scheme. These are a uniform grid, a dynamic rezoned grid, and a splitting technique. It is concluded that the use of adaptive mapping and splitting techniques with McCormack two-level predictor-corrector scheme results in an efficient and reliable code whose storage requirements are modest compared with other second order methods of equal accuracy.

M.E.P.

A80-15518 * A temperature dependent fatigue failure criterion for graphite/epoxy laminates. A. Rotem and H. G. Nelson (NASA, Ames Research Center, Moffett Field, Calif.). In: New developments and applications in composites; Proceedings of the Symposium, St. Louis, Mo., October 16, 17, 1978. (A80-15501 04-24) Warrendale, Pa., Metallurgical Society of AIME, 1979, p. 283-298. 8 refs.

A fatigue failure criterion applicable to composite materials is developed and applied to predict the fatigue behavior of graphite/epoxy laminates with particular emphasis on the influence of temperature. Tensile stress-strain curves and tension-tension fatigue curves for various unidirectional, angle-ply and symmetrically balanced laminates were developed at test temperatures of 25 C, 74 C and 114 C. In general for most laminates a reduction in both static strength and fatigue strength is observed with increasing temperature. This reduction appeared more severe in fatigue loading than in static tensile loading and most severe where the shear stress in the lamina is the dominant failure mode. Through an analytical formulation of shifting functions for the influences of temperature, all fatigue data are shown to be capable of being reduced to a single reference curve at some temperature. Additionally, examples are given which demonstrate the capability of the fatigue failure criterion to predict failure of complex symmetrically balanced laminates from relevant parameters obtained from the observed behavior of unidirectional and angle-ply laminates. (Author)

A80-17435 * Design alternatives for the Shuttle Infrared Telescope Facility. F. C. Witteborn, L. S. Young, and J. H. Miller (NASA, Ames Research Center, Moffett Field, Calif.). In: Space optics; Proceedings of the Seminar, Huntsville, Ala., May 22-24, 1979. (A80-17432 05-89) Bellingham, Wash., Society of Photo-Optical Instrumentation Engineers, 1979, p. 24-30. 18 refs.

The paper discusses the Shuttle Infrared Telescope Facility (SIRTF), a versatile astronomical telescope that can accommodate photometric, spectroscopic, and polarimetric measurements. It is expected to be 100 to 1000 times more sensitive than any existing infrared telescope; detailed designs of cooled IR telescopes were made for the Infrared Astronomical Satellite and the Small Helium Cooled Infrared Telescope for Spacelab 2. Rocket tests verified the capability of using superfluid helium as a cryogen in zero gravity. Constraints on funds for Shuttle payloads require an evolutionary approach to the development of the full potential of SIRTF, necessitating consideration of design alternatives involving the optical configuration, the cryogen, the mechanical structure, and size of SIRTF. A.T.

A80-18235 * # Experimental and computational study of transonic flow about swept wings. A. Bertelrud, M. Y. Bergmann, and T. J. Coakley (NASA, Ames Research Center, Moffett Field, Calif.). *American Institute of Aeronautics and Astronautics, Aerospace Sciences Meeting, 18th, Pasadena, Calif., Jan. 14-16, 1980, Paper 80-0005.* 17 p. 12 refs.

An experimental investigation of NACA 0010 and 10% circular arc wing models, swept at 45 deg, spanning a channel, and at zero angle of attack is described. Measurements include chordwise and spanwise surface pressure distributions and oil-flow patterns for a range of transonic Mach numbers and Reynolds numbers. Calculations using a new three-dimensional Navier-Stokes code and a two-equation turbulence model are included for the circular-arc wing flow. Reasonable agreement between measurements and computations is obtained. (Author)

A80-18384 * # An entry and landing probe for Titan. J. P. Murphy, J. N. Cuzzi (NASA, Ames Research Center, Moffett Field, Calif.), A. J. Butts, and P. C. Carroll (Martin Marietta Aerospace, Denver, Colo.). *American Institute of Aeronautics and Astronautics, Aerospace Sciences Meeting, 18th, Pasadena, Calif., Jan. 14-16, 1980, Paper 80-0117.* 11 p.

Results of a recent study of entry and landing probes for the exploration of Titan are presented. The probes considered were based on a wide range of exploration mission possibilities. They included: an atmospheric science probe; an intermediate, atmospheric and limited surface science probe; and a larger atmospheric and expanded surface science probe. Because of lower gravity on Titan and its atmosphere characteristics, the entry environment is less severe than that of Mars. However, the large uncertainties in the current definition of the atmosphere and uncertainties in Titan's surface characteristics have required trade-offs of various combinations of entry and descent shapes and hard lander configurations. Results show that all probe classes are feasible without major developments. (Author)

A80-19271 * # Supersonic flow over three-dimensional ablated nosetips using an unsteady implicit numerical procedure. P. Kutler (Flow Simulations, Inc., Sunnyvale, Calif.), J. A. Pedelty (Flow Simulations, Inc., Sunnyvale, Calif.; Iowa State University of Science and Technology, Ames, Iowa), and T. H. Pulliam (NASA, Ames Research Center, Moffett Field; Flow Simulations, Inc., Sunnyvale, Calif.). *American Institute of Aeronautics and Astronautics, Aerospace Sciences Meeting, Pasadena, Calif., Jan. 14-16, 1980, Paper 80-0063.* 12 p. 28 refs.

The three-dimensional supersonic flow over passive, that is, nonablating, indented nosetips of reentry vehicles is determined using an unsteady implicit numerical algorithm which solves either the inviscid Euler equations or the 'thin-layer' Navier-Stokes equations. A nonorthogonal independent variable transformation is used to map the distorted physical domain, containing multiple zones of embedded subsonic flow and separated flow regions into a rectangular computational volume at whose boundaries the required permeable or impermeable boundary conditions are simulated. Use of the implicit algorithm results in faster convergence to the steady state because of a larger allowable time step over conventional explicit schemes. The numerical results obtained compare favorably with existing numerical solutions and experimental data for simple spheres which validates the program. Results are also presented for analytically defined indented bodies for both laminar and turbulent flow conditions that demonstrate the program's capability for computing such flows. (Author)

A80-19273 * # Numerical simulation of steady supersonic flow over an ogive-cylinder-boattail body. L. B. Schiff (NASA, Ames Research Center, Moffett Field, Calif.) and W. B. Sturek (U.S. Army, Ballistics Research Laboratory, Aberdeen Proving Ground, Md.). *American Institute of Aeronautics and Astronautics, Aerospace Sciences Meeting, 18th, Pasadena, Calif., Jan. 14-16, 1980, Paper 80-0066.* 12 p. 14 refs.

A recently reported parabolized Navier-Stokes code has been employed to compute the supersonic flow field surrounding an ogive-cylinder-boattail body at incidence. The computations were performed for flow conditions where an extensive series of experimental surface pressure and turbulent boundary-layer profile measurements had been obtained. Comparison between the computational results and experimental measurements for angles of attack up to 6 deg show excellent agreement. At angles greater than 6 deg discrepancies are observed which are tentatively attributed to three-dimensional turbulence modeling errors. (Author)

A80-19274 * # **A diagonal form of an implicit approximate-factorization algorithm with application to a two dimensional inlet.** D. S. Chaussee (Flow Simulations, Inc., Sunnyvale, Calif.) and T. H. Pulliam (NASA, Ames Research Center, Moffett Field, Calif.). *American Institute of Aeronautics and Astronautics, Aerospace Sciences Meeting, 18th, Pasadena, Calif., Jan. 14-16, 1980, Paper 80-0067.* 9 p. 17 refs.

A modification of an implicit approximate-factorization finite-difference algorithm applied to the two dimensional Euler and Navier-Stokes equations in general curvilinear coordinates is presented for supersonic free stream flow about and through inlets. The modification transforms the coupled system of equations into an uncoupled diagonal form which requires less computation work. For steady-state applications the resulting diagonal algorithm retains the stability and accuracy characteristics of the original algorithm. Solutions are given for inviscid and laminar flow about a two dimensional wedge inlet configuration. Comparisons are made between computed results and exact theory. (Author)

A80-22727 * # **An experimental and numerical investigation of a three-dimensional shock wave separated turbulent boundary layer.** M. I. Kussoy, J. R. Viegas, and C. C. Horstman (NASA, Ames Research Center, Moffett Field, Calif.). *American Institute of Aeronautics and Astronautics, Aerospace Sciences Meeting, 18th, Pasadena, Calif., Jan. 14-16, 1980, Paper 80-0002.* 21 p. 32 refs.

A detailed investigation of a flow in which a three-dimensional shock wave separates a two-dimensional turbulent boundary layer is presented. The resulting flow field is highly three-dimensional with a significant portion of flow separation on the surface at the 0 deg azimuthal coordinate (windward) plane as well as a large zone of secondary surface flow off this plane. Mean and fluctuating experimental measurements were obtained throughout the entire flow field. These measurements included mean pressures, flow angles and shear on the surface, as well as yaw angles, static pressures, turbulent shear stresses and turbulent kinetic energies on selected planes throughout the flow field. In addition, numerical predictions of this flow, obtained by solving the Navier-Stokes equations with an algebraic eddy viscosity turbulence model, are presented. These computations can reasonably predict both the surface and flow-field quantities, despite the extremely complicated nature of the experimental flow. (Author)

A80-22731 * # **Forebody and base region real-gas flow in severe planetary entry by a factored implicit numerical method. I - Computational fluid dynamics.** C. K. Lombard (Pacific Engineering Design Analysis Co., Palo Alto, Calif.), W. C. Davy, and M. J. Green (NASA, Ames Research Center, Thermal Protection Branch, Moffett Field, Calif.). *American Institute of Aeronautics and Astronautics, Aerospace Sciences Meeting, 18th, Pasadena, Calif., Jan. 14-16, 1980, Paper 80-0065.* 13 p. 22 refs. Contract No. NAS2-10144.

A new code for the simulation of full (forebody and base region) flowfields about bluff bodies in the hypersonic regime of severe planetary entry is described. The present 'maximally conservative, maximally differenced' formulation of the unsteady compressible Navier-Stokes equations for 2-D axisymmetric 3-D flow is contrasted for stability with previous formulations of Viviani, Kutler, et al, and Thomas and Lombard. Discrete metric relations peculiar to the axisymmetric finite volume formulation are presented along with a general discussion of their relations to and consequences of failure to close computational cells. A computational mesh of curvilinear coordinate topology singular in the flow regime is presented that permits aligned capturing of the major physical features of the complex flowfield. (Author)

A80-23691 * **Electrical conductivity anomalies associated with circular lunar maria.** P. Dyal (NASA, Ames Research Center, Moffett Field, Calif.) and W. D. Daily (Eyring Research Institute,

Provo, Utah). In: *Lunar and Planetary Science Conference, 10th, Houston, Tex., March 19-23, 1979, Proceedings. Volume 3.* (A80-23677 08-91) New York, Pergamon Press, Inc., 1979, p. 2291-2297. 8 refs. Grant No. NSG-2082.

A strong anisotropy is observed in magnetic field fluctuations measured by the Lunokhod 2 magnetometer located on the eastern edge of Mare Serenitatis. This anisotropy can be explained by a regional anomaly in the subsurface electrical conductivity distribution associated with the mare similar to the proposed conductivity anomaly associated with Mare Imbrium. The Serenitatis magnetic field anisotropy is compared to the field fluctuation measured by the Apollo 16 magnetometer 1100 km to the south, and this comparison indicates that the subsurface conductivity distribution can be modeled by a nonconducting layer in the lunar lithosphere which is 150 km thick beneath the highlands and 300 km thick beneath Serenitatis. The decrease in electrical conductivity of the upper mantle beneath the mare may result from lower temperatures due to transport of thermal energy and radioactive heat sources to the surface during mare flooding. This proposed anomaly, along with that proposed for Mare Imbrium, strengthens the possibility of regional anomalies in electrical conductivity associated with all circular lunar maria. (Author)

A80-23716 * **Monte Carlo simulation of lunar megaregolith and implications.** H. R. Aggarwal (Santa Clara, University, Santa Clara, Calif.) and V. R. Oberbeck (NASA, Ames Research Center, Moffett Field, Calif.). In: *Lunar and Planetary Science Conference, 10th, Houston, Tex., March 19-23, 1979, Proceedings. Volume 3.* (A80-23677 08-91) New York, Pergamon Press, Inc., 1979, p. 2689-2705. 30 refs.

A realistic Monte Carlo model closely simulating the evolution of the lunar megaregolith over a large area of 67 million sq. km of the front surface of the moon is presented. Craters larger than 100 km in diameter observed over the entire surface of the moon and those less than 100 km lying in the referenced area are included in the simulation. A total of 21,664 craters are processed. The model predicts the average thickness of the megaregolith to be about 1.9-2.0 km. Curves for the variation of the regolith thickness across the simulated area are given and show that about 50% of the area is covered with regolith less than 1 km thick. The model produces crater structures similar to the ones observed in the lunar highlands, it partially supports the layering theory for crater structures that the variations in strength and density of target materials may be responsible for the observed differences in the morphologies of lunar craters, and rules out the possibility that all craters when formed are bowl-shaped with a fixed depth/diameter ratio characteristic of small craters. (Author)

A80-23727 * **Endogenic craters on basaltic lava flows - Size frequency distributions.** R. Greeley (NASA, Ames Research Center, Space Science Div., Moffett Field, Calif.; Arizona State University, Tempe, Ariz.) and D. E. Gault (Murphys Center for Planetology, Murphys, Calif.). In: *Lunar and Planetary Science Conference, 10th, Houston, Tex., March 19-23, 1979, Proceedings. Volume 3.* (A80-23677 08-91) New York, Pergamon Press, Inc., 1979, p. 2919-2933. 28 refs. Grant No. NSG-7415.

Circular crater forms, termed collapse depressions, which occur on many basalt flows on the earth have also been detected on the moon and Mars and possibly on Mercury and Io. The admixture of collapse craters with impact craters would affect age determinations of planetary surface units based on impact crater statistics by making them appear anomalously old. In the work described in the present paper, the techniques conventionally used in planetary crater counting were applied to the determination of the size range and size frequency distribution of collapse craters on lava flows in Idaho, California, and New Mexico. Collapse depressions range in size from 3 to 80 m in diameter; their cumulative size distributions are similar to those of small impact craters on the moon. V.P.

A80-23935 * # Implicit computations of unsteady transonic flow governed by the full-potential equation in conservation form. P. M. Goorjian (NASA, Ames Research Center, Moffett Field, Calif.). *American Institute of Aeronautics and Astronautics, Aerospace Sciences Meeting, 18th, Pasadena, Calif., Jan. 14-16, 1980, Paper 80-0150*. 19 p. 29 refs.

An alternating-direction implicit algorithm is presented for solving the conservative, full-potential equation for unsteady, transonic flow. A new development is the time-linearization of the density function. This linearization reduces the solution process from one of solving a system of two equations at each mesh point to one of solving a single equation. Two sample cases are computed. First, a one-dimensional traveling shock wave is computed and compared with the analytic solution. Second, a two-dimensional case is computed of a flow field that results from a thickening and subsequently thinning airfoil. The resulting flow field, which includes a traveling shock wave, is compared to the flow field obtained from the low-frequency, small-disturbance, transonic equation. (Author)

A80-23957 * # Numerical experiments in boundary-layer stability. A. Wray and M. Y. Hussaini (NASA, Ames Research Center, Moffett Field, Calif.). *American Institute of Aeronautics and Astronautics, Aerospace Sciences Meeting, 18th, Pasadena, Calif., Jan. 14-16, 1980, Paper 80-0275*. 10 p.

Numerical solution of the three-dimensional incompressible Navier-Stokes equations is used to study the instability of a flat-plate boundary layer in a manner analogous to the vibrating-ribbon experiments. Flow-field structures are observed which are very similar to those found in the vibrating-ribbon experiment to which computational initial conditions have been matched. Streamwise periodicity is assumed in the simulation so that the evolution occurs in time, but the events which constitute the instability are so similar to the spatially occurring ones of the laboratory that it seems clear the physical processes involved are the same. A spectral and finite difference numerical algorithm is employed in the simulation. (Author)

A80-24586 * Aqueous activity on asteroids - Evidence from carbonaceous meteorites. J. F. Kerridge (California, University, Los Angeles, Calif.) and T. E. Bunch (NASA, Ames Research Center, Moffett Field, Calif.). In: *Asteroids*. (A80-24551 08-91) Tucson, Ariz., University of Arizona Press, 1979, p. 745-764. 54 refs. NASA-supported research.

Carbonaceous chondrites of groups CI and CM were formed by impact brecciation and aqueous alteration of earlier generations of mineral phases within the surface regions of two or more parent bodies. Those parent bodies were probably asteroids, rather than comets, although a problem still exists in delivering such material safely to earth. Aqueous activity may have been widespread on asteroids. (Author)

A80-24590 * Primordial heating of asteroidal parent bodies. C. P. Sonett (Arizona, University, Tucson, Ariz.) and R. T. Reynolds (NASA, Ames Research Center, Moffett Field, Calif.). In: *Asteroids*. (A80-24551 08-91) Tucson, Ariz., University of Arizona Press, 1979, p. 822-848. 97 refs. NASA-supported research.

Most meteorites show evidence of thermal processing either because of metamorphic changes or as a result of melting and differentiation. Proposed mechanisms for supplying this energy generally rely upon short-lived radioisotopes or electrical induction, though accretion is sometimes mentioned, and more exotic models have been discussed. Interest in isotopic heating has been heightened by the discovery of Al-26 in Allende inclusions and also by the proposal that a lunar core and dynamo resulted from the radioactive decay of superheavy elements during the early solar system.

Electrical induction as a heat source can be scaled to a broad range of solar system conditions, but corroborative evidence for these conditions is inconclusive. The accretion mechanism is probably not viable for the asteroidal and meteorite parent bodies, because the high kinetic energy requirement is inconsistent with the formation of the objects and their regoliths in the presence of a weak gravitational field. (Author)

A80-26881 * A small-scale test for fiber release from carbon composites. W. J. Gilwee, Jr. and R. H. Fish (NASA, Ames Research Center, Moffett Field, Calif.). In: *Advanced composites - Special topics; Proceedings of the Conference, El Segundo, Calif., December 4-6, 1979*. (A80-26878 09-24) El Segundo, Calif., Technology Conferences, 1979, p. 45-54.

A burn/impact test apparatus is used to determine the amount of fiber release from carbon fiber composites after burn and impact. The calculation of the theoretical char binder content of the composite is made based on the temperature of the test specimen and the char yield of the resin as determined by thermogravimetric analysis. The test results indicate that carbon fiber release depends on the type of reinforcement used. There was more fiber release with the quasi-isotropic composite made with unidirectional tape than with the woven fabric reinforcement. The amount of fiber release in the impact chamber after burning is coincident with the calculated char binder. V.L.

A80-27407 * On the construction and application of implicit factored schemes for conservation laws. R. F. Warming and R. M. Beam (NASA, Ames Research Center, Computational Fluid Dynamics Branch, Moffett Field, Calif.). In: *Computational fluid dynamics*. (A80-27402 10-34) Providence, R.I., American Mathematical Society, 1978, p. 85-129. 37 refs.

Efficient, noniterative, implicit finite difference algorithms are systematically developed for nonlinear conservation laws including purely hyperbolic systems and mixed hyperbolic-parabolic systems. Utilization of a rational fraction or Padé time differencing formulas, yields a direct and natural derivation of an implicit scheme in a delta form. Attention is given to advantages of the delta formation and to various properties of one- and two-dimensional algorithms. C.F.W.

A80-27408 * An efficient explicit-implicit-characteristic method for solving the compressible Navier-Stokes equations. R. W. McCormack (NASA, Ames Research Center, Computational Fluid Dynamics Branch, Moffett Field, Calif.). In: *Computational fluid dynamics*. (A80-27402 10-34) Providence, R.I., American Mathematical Society, 1978, p. 130-155. 22 refs.

Explicit, implicit, and characteristic finite-difference methods are applied to solve model equations representative of the compressible Navier-Stokes equations. An approach is then formulated for solving the Navier-Stokes equation at high Reynolds numbers. The approach has drastically reduced the computation time required to obtain viscous flow solutions. Computational results for shock wave separated flows are presented. (Author)

A80-27736 * # Investigation of a reattaching turbulent shear layer - Flow over a backward-facing step. J. Kim (NASA, Ames Research Center, Moffett Field; Stanford University, Stanford, Calif.), S. J. Kline, and J. P. Johnston (Stanford University, Stanford, Calif.). In: *Flow in primary, non-rotating passages in turbomachines; Proceedings of the Winter Annual Meeting, New York, N.Y., December 2-7, 1979*. (A80-27732 10-02) New York, American

Society of Mechanical Engineers, 1979, p. 41-48, 19 refs.

The paper studies incompressible flow over a backward-facing step in order to investigate the flow characteristics in the separated shear layer, the reattachment zone, and the redeveloping boundary layer after reattachment. It is shown that turbulent intensities and shear stress reach maxima in the reattachment zone, followed by rapid decay near the surface after reattachment. In addition, it is found that downstream of reattachment, the flow returns very slowly to the structure of an ordinary turbulent boundary layer.

M.E.P.

A80-27965 * # Effects of moisture on apparent flexure strength and on torsion and flexure fatigue properties of graphite-epoxy composites. H. T. Sumison and M. J. Adamson (NASA, Ames Research Center, Moffett Field, Calif.). In: Methods for predicting material life in fatigue; Proceedings of the Winter Annual Meeting, New York, N.Y., December 2-7, 1979. (A80-27951 10-39) New York, American Society of Mechanical Engineers, 1979, p. 265-274, 14 refs.

The effects of moisture and temperature on unidirectional and multi-ply laminates of T300/934 and AS/3501 graphite-epoxy systems were investigated. Properties studied were static flexure strength and flexure and torsion fatigue strengths at room temperature and at 74 C. Specimens with increased moisture content showed a reduced static flexure strength; water as the test environment had only a negligible influence. In flexure fatigue and torsion fatigue, the water environment caused somewhat reduced fatigue strengths at room temperature and significantly greater degradation in 74 C water. The failure mode in all cases was interlaminar delamination.

(Author)

A80-29479 * # A technique for evaluating the Jovian entry-probe heat-shield material with a gasdynamic laser. R. R. Dickey and J. H. Lundell (NASA, Ames Research Center, Moffett Field, Calif.). In: ICIASF '79; International Congress on Instrumentation in Aerospace Simulation Facilities, 8th, Monterey, Calif., September 24-26, 1979, Record. (A80-29476 11-35) New York, Institute of Electrical and Electronics Engineers, Inc., 1979, p. 26-32.

The paper presents a technique for evaluating the Jovian entry-probe heat-shield material with a gasdynamic laser. This entry probe of Project Galileo will incorporate a forebody heat shield of carbon phenolic ablative; at the expected peak radiant intensity of 42 kW/sq cm this material can be evaluated by a CO₂ gasdynamic laser. The typically quasigaussian spatial distribution of the laser output beam is converted to a spatially uniform beam by a new optical integrator; the ablation results can be related to the imposed intensity and then to the flight situation with a uniform beam. The tests show that the carbon phenolic tends to spall under intense radiation, and this process is quantified by a particle capture technique.

A.T.

A80-29506 * Application of laser velocimetry to an unsteady transonic flow. H. L. Seegmiller, J. G. Marvin, D. R. Harrison, and G. Kojima (NASA, Ames Research Center, Moffett Field, Calif.). In: ICIASF '79; International Congress on Instrumentation in Aerospace Simulation Facilities, 8th, Monterey, Calif., September 24-26, 1979, Record. (A80-29476 11-35) New York, Institute of Electrical and Electronics Engineers, Inc., 1979, p. 284-293, 9 refs.

Measurements of mean velocity, turbulent kinetic energy, and turbulent shear stress have been obtained in an unsteady but periodic flow. Polystyrene spheres, 0.35-0.55 microns in diameter, were injected into the tunnel settling chamber to seed the flow for a laser velocimeter. Synchronized counters together with an encoding interface and digital-to-analog converters were used to record the data on an analog tape recorder. Profiles of velocity and turbulence quantities are presented for several times during the periodic flow.

(Author)

A80-31848 * The role of magnetic fields in the collapse of protostellar gas clouds. E. H. Scott and D. C. Black (NASA, Ames Research Center, Theoretical and Planetary Studies Branch, Moffett Field, Calif.). In: Giant molecular clouds in the Galaxy; Proceedings of the Third Gregynog Astrophysics Workshop, Cardiff, Wales, August 1977. (A80-31827 12-90) Oxford and New York, Pergamon Press, 1980, p. 303-311, 12 refs.

The paper presents the results of a numerical calculation of the collapse of an idealized protostellar gas cloud including the effects of a 'frozen-in' magnetic field. The 'traditional' picture of magnetic effects on gas clouds and recent observational and theoretical work on the subject are summarized. Attention is given to the method of calculation and the results are interpreted. It is found that the central magnetic field in the collapsing cloud model follows a ρ to the 1/2 power relation, and the discussion implies that this is a general result which should hold true for some range of initial conditions around those chosen. In addition, it is found that the outer envelope of the cloud will be held up by tension in the field lines.

M.E.P.

A80-34050 * Scattering by non-spherical particles of size comparable to a wavelength - A new semi-empirical theory. J. B. Pollack and J. N. Cuzzi (NASA, Ames Research Center, Space Sciences Div., Moffett Field, Calif.). In: Light scattering by irregularly shaped particles. New York, Plenum Publishing Corp., 1980, p. 113-125, 17 refs.

An approximate method is proposed for evaluating the interaction of randomly oriented, nonspherical particles with the total intensity component of electromagnetic radiation. When the particle size parameter, x , the ratio of particle circumference to wavelength, is less than some upper bound $x(o)$ (about 5), Mie theory is used. For x greater than $x(o)$, the interaction is divided into three components: diffraction, external reflection, and transmission. Physical optics theory is used to obtain the first of these components; geometrical optics theory is applied to the second; and a simple parameterization is employed for the third. The predictions of this theory are found to be in very good agreement with laboratory measurements for a wide variety of particle shapes, sizes, and refractive indexes. Limitations of the theory are also noted.

(Author)

A80-34788 * Advanced thermoset resins for fire-resistant composites. D. A. Kourtidis and J. A. Parker (NASA, Ames Research Center, Moffett Field, Calif.). In: New horizons - Materials and processes for the eighties; Proceedings of the Eleventh National Conference, Boston, Mass., November 13-15, 1979. (A80-34751 14-23) Azusa, Calif., Society for the Advancement of Material and Process Engineering, 1979, p. 551-563, 8 refs.

The thermal and flammability properties of some thermoset polymers and composites are described. The processing and evaluation of composites fabricated from currently used resins and advanced fire-resistant resins are also described. Laboratory test methodology used to qualify candidate composite materials includes thermochemical characterization of the polymeric compounds and evaluation of the glass reinforced composites for flammability and smoke evolution. The use of these test methods will be discussed in comparing advanced laminating resins and composites consisting of modified epoxies, phenolics and bismaleimide, with conventional baseline materials consisting of epoxy.

(Author)

A80-34790 * Ambient curing fire resistant foams. C. L. Hamermesh, P. A. Hogenson, C. Y. Tung (Rockwell International Corp., Los Angeles, Calif.), P. M. Sawko, and S. R. Riccitiello (NASA, Ames Research Center, Moffett Field, Calif.). In: New horizons - Materials and processes for the eighties; Proceedings of the Eleventh National Conference, Boston, Mass., November 13-15,

1979. (A80-34751 14-23) Azusa, Calif., Society for the Advancement of Material and Process Engineering, 1979, p. 574-581. 5 refs. Research supported by the Rockwell International Corp.; Contract No. NAS2-9469.

The feasibility of development of an ambient curing foam is described. The thermal stability and flame spread index of the foams were found to be comparable to those of the high-temperature cured polyimide foams by Monsanto two-foot tunnel test and NASA T-3 Fire test. Adaptation of the material to spray in place applications is described. (Author)

A80-34904 * Solution of Boltzmann equation for highly nonequilibrium diatomic gases rotational translational energy relaxation. K. K. Yoshikawa (NASA, Ames Research Center, Moffett Field, Calif.). In: Rarefied gas dynamics; Proceedings of the Eleventh International Symposium, Cannes, France, July 3-8, 1978. Volume 1. (A80-34876 14-77) Paris, Commissariat à l'Energie Atomique, 1979, p. 389-406. 14 refs. Research supported by the University of Tokyo.

The direct simulation Monte Carlo method is applied to solve the Boltzmann equation for collisions between internally excited diatomic gases in highly nonequilibrium states. The semiclassical transition probability is incorporated in the simulation for energy exchange between rotational and translational energy. The results provide details on the fundamental mechanisms of gas kinetics where analytical methods are impractical. The validity of the local Maxwellian assumption and relaxation time, rotational-translational energy transition, and a velocity analysis of the inelastic collision are discussed in detail. (Author)

A80-35051 * # Graphite composites with advanced resin matrices. D. A. Kourtidis (NASA, Ames Research Center, Moffett Field, Calif.). In: Structures, Structural Dynamics, and Materials Conference, 21st, Seattle, Wash., May 12-14, 1980, Technical Papers. Part 2. (A80-34993 14-39) New York, American Institute of Aeronautics and Astronautics, Inc., 1980, p. 544-554. 11 refs. (AIAA 80-0758)

The effect of processing variables on the flammability and mechanical properties for state-of-the-art and advanced resin matrices for graphite composites were studied. Resin matrices which were evaluated included state-of-the-art epoxy, phenolic-novolac, phenolic-xylok, two types of bismaleimides, benzyl, polyether-sulfone, and poly(p-phenylene sulfone). Comparable flammability and thermochemical data on graphite-reinforced laminates prepared with these resin matrices are presented, and the relationship of some of these properties to the anaerobic char yield of the resins is described. (Author)

A80-35052 * # Release-rate calorimetry of multilayered materials for aircraft seats. L. L. Fewell, J. A. Parker (NASA, Ames Research Center, Moffett Field, Calif.), F. Duskin, H. Spieth, and E. Trabold (Douglas Aircraft, Co., Long Beach, Calif.). In: Structures, Structural Dynamics, and Materials Conference, 21st, Seattle, Wash., May 12-14, 1980, Technical Papers. Part 2. (A80-34993 14-39) New York, American Institute of Aeronautics and Astronautics, Inc., 1980, p. 555-564. (AIAA 80-0759)

Multilayered samples of contemporary and improved fire-resistant aircraft seat materials (foam cushion, decorative fabric, slip sheet, fire-blocking layer, and cushion-reinforcement layer) were evaluated for their rates of heat release and smoke generation. Top layers (decorative fabric, slip sheet, fire blocking, and cushion reinforcement) with glass-fiber block cushion were evaluated to determine which materials, based on their minimum contributions to the total heat release of the multilayered assembly, may be added or

deleted. Top layers exhibiting desirable burning profiles were combined with foam cushion materials. The smoke and heat-release rate of multilayered seat materials were then measured at heat fluxes of 1.5 and 3.5 W/sq cm. Choices of contact and silicon adhesives for bonding multilayered assemblies were based on flammability, burn and smoke generation, animal toxicity tests, and thermal gravimetric analysis. (Author)

A80-37427 * Internal image motion compensation system for the Shuttle Infrared Telescope Facility. K. R. Lorell (NASA, Ames Research Center, Space Projects Div., Moffett Field, Calif.), E. K. Parsons, and J. D. Powell (Stanford University, Stanford, Calif.). In: Automatic control in space; Proceedings of the Eighth Symposium, Oxford, England, July 2-6, 1979. (A80-37426 15-12) Oxford, Pergamon Press, Ltd., 1980, p. 1-7. 9 refs.

The Shuttle Infrared Telescope Facility (SIRTF) is being designed as a 1-m, cryogenically cooled telescope capable of a thirty-fold improvement over currently available infrared instruments. The SIRTF, mounted in the Orbiter bay on the Instrument Pointing System (IPS), requires that the image at the focal plane be stabilized to better than 0.1 arcsec with an absolute accuracy of 1 arcsec in order to attain this goal. Current estimates of IPS performance for both stability and accuracy indicate that additional stabilization will be necessary to meet the SIRTF requirements. An Image Motion Compensation (IMC) system, utilizing a Charge Coupled Device (CCD) star tracker located at the focal plane and a steerable mirror in the SIRTF optical path, has been designed to work in conjunction with the IPS. (Author)

A80-38114 * Shock tube studies of radiative base heating of Jovian probe. H. Shirai and C. Park (NASA, Ames Research Center, Entry Technology Branch, Moffett Field, Calif.). In: Shock tubes and waves; Proceedings of the Twelfth International Symposium, Jerusalem, Israel, July 16-19, 1979. (A80-38078 15-34) Jerusalem, Magnes Press, 1980, p. 419-428. 7 refs.

A 6.4-cm-diameter scale model of the Jovian entry vehicle is tested in an electric-arc-driven shock tube and a 5-cm-diameter sphere model is tested in a combustion-driven shock tube and in an electric-arc-driven shock tunnel. The radiative heat-transfer rate and pressure on the front and the base regions are measured in the absence of ablation with sensors imbedded in the models in a stream consisting of 10% hydrogen in a bath of either neon or argon. The measured radiative heat-transfer rates and pressures range to about 22 kW/sq cm and 12 atm, respectively, at the front stagnation point. The ratio of the radiative heat-transfer rate at the base stagnation point to that at the front stagnation point is found to be about 1/4 for the sphere at Mach 1.8, about 1/30 for the sphere at Mach 4.8, and about 1/6 for the scale model at Mach 1.7. The present experimental results agree well with the theoretical predictions of Park, thus indicating that Park's theory is valid. (Author)

A80-38131 * 'GAIM' - Gas-addition, impedance-matched arc driver. R. E. Dannenberg (NASA, Ames Research Center, Moffett Field, Calif.). In: Shock tubes and waves; Proceedings of the Twelfth International Symposium, Jerusalem, Israel, July 16-19, 1979. (A80-38078 15-34) Jerusalem, Magnes Press, 1980, p. 599-606. 7 refs.

A conceptual view for a GAIM energy/driver system to maximize shock-tube performance through efficient interfacing of the energy source with the gas dynamics of the arc driver is presented. Electrical and arc-chamber requirements are evaluated utilizing two new computer codes. One code calculates the shock wave generated for a selected time rate and magnitude of arc-energy input; the other computes the values of external circuit elements

required to produce the selected energy input, with the driver represented as the load element of the electrical discharge circuit. Results indicate that the energy-storage capability and the driver arrangement needed to produce the highest shock Mach number can be achieved by means of driver gas addition and by impedance matching (GAIM). Design criteria are presented for arc energy requirements necessary to produce given shock-wave speeds. Shock velocities as high as the 70 km/sec required for simulating Jovian entry now seem possible in shock-tube operation. Practical implementation of a GAIM system is discussed. (Author)

A80-39715 * **Conditional replenishment using motion prediction.** D. N. Hein and H. W. Jones, Jr. (NASA, Ames Research Center, Moffett Field, Calif.). In: Applications of digital image processing III; Proceedings of the Seminar, San Diego, Calif., August 27-29, 1979. (A80-39704 16-35) Bellingham, Wash., Society of Photo-Optical Instrumentation Engineers, 1979, p. 268-277. 13 refs. Contract No. NAS2-9703; Grant No. NCA2-OR-363-702.

Conditional replenishment is an interframe video compression method that uses correlation in time to reduce video transmission rates. This method works by detecting and sending only the changing portions of the image and by having the receiver use the video data from the previous frame for the non-changing portion. The amount of compression that can be achieved through this technique depends to a large extent on the rate of change within the image, and can vary from 10 to 1 to less than 2 to 1. An additional 3 to 1 reduction in rate is obtained by the intraframe coding of data blocks using a 2-dimensional variable rate Hadamard transform coder. A further additional 2 to 1 rate reduction is achieved by using motion prediction. Motion prediction works by measuring the relative displacements of a subpicture from one frame to the next. The subpicture can then be transmitted by sending only the value of the 2-dimensional displacement. Computer simulations have demonstrated that data rates of 2 to 4 Mega-bits/second can be achieved while still retaining good fidelity in the image. (Author)

A80-41305 * **Issues arising from the demonstration of Landsat-based technologies to inventories and mapping of the forest resources of the Pacific Northwest states.** D. L. Peterson and D. H. Card (NASA, Ames Research Center, Moffett Field, Calif.). In: Remote sensing of earth resources. Volume 7 - Annual Remote Sensing of Earth Resources Conference, 7th, Tullahoma, Tenn., March 27-29, 1978, Technical Papers. (A80-41301 17-43) Tullahoma, Tenn., University of Tennessee, 1980, p. 65-99. 13 refs.

A80-41563 * # **On the combination of kinematics with flow visualization to compute total circulation - Application to vortex rings in a tube.** J. G. Brasseur (NASA, Ames Research Center, Moffett Field, Calif.) and I.-D. Chang (Stanford University, Stanford, Calif.). *American Institute of Aeronautics and Astronautics, Fluid and Plasma Dynamics Conference, 13th, Snowmass, Colo., July 14-16, 1980, Paper 80-1330.* 12 p. 9 refs. Research supported by Stanford University; NSF Grant No. ENG-74-22615.

To date the computation of the total circulation, or strength of a vortex has required detailed measurements of the velocity field within the vortex. In this paper a method is described in which the kinematics of the vortical flow field is exploited to calculate the strength of a vortex from relatively simple flow visualization measurements. There are several advantages in the technique, the most important being the newly acquired ability to calculate the transient changes in strength of a single vortex as it evolves. The method is applied to the study of vortex rings, although the development can be carried over directly to study vortex pairs, and it is expected that it can be generalized to other flows which contain regions of concentrated vorticity. The accuracy of the method as

applied to vortex rings, assessed in part by comparing with the laser Doppler velocimeter (LDV) measurements of Sullivan et al., is shown to be excellent. (Author)

A80-41569 * # **Tests of subgrid-scale models in strained turbulence.** O. J. McMillan (Nielsen Engineering and Research, Inc., Mountain View, Calif.), J. H. Ferziger (Stanford University, Stanford, Calif.), and R. S. Rogallo (NASA, Ames Research Center, Moffett Field, Calif.). *American Institute of Aeronautics and Astronautics, Fluid and Plasma Dynamics Conference, 13th, Snowmass, Colo., July 14-16, 1980, Paper 80-1339.* 11 p. 19 refs. Navy-sponsored research.

Strained and sheared turbulence is computed by direct simulation and it is shown that the results are in good qualitative agreement with experiments. It is found that after large amounts of strain have been applied to turbulence, the energy flow to the small scales is reduced and, in some cases, reversed. Eddy viscosity models are shown to be very poor in strained turbulence and, when they are used, the mean strain should not be included in them. Finally, new models proposed by Bardina et al. have been tested and found to offer considerable promise for the future. (Author)

A80-41587 * # **Skin friction measurements by a new non-intrusive double-laser-beam oil viscosity balance technique.** D. J. Monson (NASA, Ames Research Center, Physical Sciences Branch, Moffett Field, Calif.) and H. Higuchi (Dynamics Technology, Inc., Torrance, Calif.). *American Institute of Aeronautics and Astronautics, Fluid and Plasma Dynamics Conference, 13th, Snowmass, Colo., July 14-16, 1980, Paper 80-1373.* 10 p. 9 refs.

A portable dual-laser-beam interferometer that nonintrusively measures skin friction by monitoring the thickness change of an oil film subject to shear stress is described. The method is an advance over past versions in that the troublesome and error-introducing need to measure the distance to the oil leading edge and the starting time for the oil flow has been eliminated. The validity of the method was verified by measuring oil viscosity in the laboratory, and then using those results to measure skin friction beneath the turbulent boundary layer in a low-speed wind tunnel. The dual-laser-beam skin friction measurements are compared with Preston tube measurements, with mean velocity profile data in a 'law-of-the-wall' coordinate system, and with computations based on turbulent boundary-layer theory. Excellent agreement is found in all cases. This validation and the aforementioned improvements appear to make the present form of the instrument usable to measure skin friction reliably and nonintrusively in a wide range of flow situations in which previous methods are not practical. (Author)

A80-41597 * # **Nonreflecting far-field boundary conditions for unsteady transonic flow computation.** D. Kwak (NASA, Ames Research Center, Applied Computational Aerodynamics Branch, Moffett Field, Calif.). *American Institute of Aeronautics and Astronautics, Fluid and Plasma Dynamics Conference, 13th, Snowmass, Colo., July 14-16, 1980, Paper 80-1393.* 10 p. 12 refs.

The approximate nonreflecting far-field boundary condition, as proposed by Engquist and Majda, is implemented in the computer code LTRAN2. This code solves the implicit finite-difference representation of the small disturbance equations for unsteady transonic flows about airfoils. The nonreflecting boundary condition and the description of the algorithm for implementing these conditions in LTRAN2 are discussed. Various cases are computed and compared with results from the older, more conventional procedures. One concludes that the nonreflecting far-field boundary approximation allows the far-field boundary to be located closer to the airfoil; this permits a decrease in the computer time required to obtain the solution through the use of fewer mesh points. (Author)

A80-41608 * # Computation of supersonic turbulent flows over an inclined ogive-cylinder-flare. C. M. Hung (NASA, Ames Research Center, Computational Fluid Dynamics Branch, Moffett Field, Calif.) and D. S. Chaussee (Flow Simulations, Inc., Sunnyvale, Calif.). *American Institute of Aeronautics and Astronautics, Fluid and Plasma Dynamics Conference, 13th, Snowmass, Colo., July 14-16, 1980, Paper 80-1410.* 13 p. 14 refs.

A supersonic turbulent flow over an ogive-cylinder-flare has been solved numerically. Initially, the parabolized Navier-Stokes equations are solved for the ogive cylinder back to a location upstream of the shock-wave and boundary-layer interaction. Then, the time-dependent Navier-Stokes equations with a thin-layer approximation are solved for the remaining cylinder-flare portion. Results for a Mach number of 2.9 and a unit Reynolds number of 11.42×10 to the 6th/m are obtained for angles of attack $\alpha = 0, 4$, and 8 deg. Good agreement has been found between computed and experimental results of the surface pressure on the ogive-cylinder portion, and for the interaction region at $\alpha = 0$ and 4 deg. The role of circumferential communication in a three-dimensional shock-wave and boundary-layer interaction flow field is discussed. (Author)

A80-43200 * # Galileo probe forebody entry thermal protection - Aerothermal environments and heat shielding requirements. W. E. Nicolet (Thermal Sciences, Inc., Sunnyvale, Calif.), W. C. Davy (NASA, Ames Research Center, Moffett Field, Calif.), and J. F. Wilson (Informatics, Inc., Palo Alto, Calif.). *American Society of Mechanical Engineers, Intersociety Environmental Systems Conference, San Diego, Calif., July 14-17, 1980, Paper 80-ENAS-24.* 10 p. 17 refs. Members, \$1.50; nonmembers, \$3.00.

Solutions are presented for the aerothermal heating environments and the material thermal response for the forebody heatshield on the candidate 242 kg Galileo probe entering the modeled nominal and cold-dense Jovian atmospheres. In the flowfield analysis, a finite difference procedure was employed to obtain benchmark predictions of pressure, radiation and convective heating rates (both laminar and turbulent) and the corresponding wall blowing obtained under the steady state approximation. The fluxes over the probe flank were found to be in a range where spallation is an important mass loss mechanism. The predicted heating rates were also used as boundary conditions for the charring materials ablation which was used to predict thermochemical based surface recession, mass loss and bondline temperatures. The contingency factor of 30% currently employed by NASA was found to be insufficient for entry into the cold-dense atmosphere. (Author)

A80-44128 * # An implicit finite-difference code for inviscid and viscous cascade flow. J. L. Steger (Flow Simulations, Inc., Sunnyvale, Calif.), T. H. Pulliam (NASA, Ames Research Center, Moffett Field, Calif.), and R. V. Chima (NASA, Lewis Research Center, Cleveland, Ohio). *American Institute of Aeronautics and Astronautics, Fluid and Plasma Dynamics Conference, 13th, Snowmass, Colo., July 14-16, 1980, Paper 80-1427.* 15 p. 32 refs.

An implicit finite-difference code is developed to solve either inviscid or viscous flow about two-dimensional cascade blade elements. General coordinate transformations are used so that boundaries can coincide with coordinate lines, and an automatic grid generation routine based on elliptic partial differential equations is employed to mesh arbitrary cascade elements. Characteristic combinations of the differential equations are used at inflow and outflow boundaries. Computed results for both inviscid and viscous flow are compared with other existing cascade solutions and experimental data. (Author)

A80-44132 * # Numerical simulation of three-dimensional boattail afterbody flow fields. G. S. Deiwert (NASA, Ames Research Center, Moffett Field, Calif.). *American Institute of Aeronautics and*

Astronautics, Fluid and Plasma Dynamics Conference, 13th, Snowmass, Colo., July 14-16, 1980, Paper 80-1347. 12 p. 30 refs.

The thin shear layer approximations of the three-dimensional, compressible Navier-Stokes equations are solved for subsonic, transonic, and supersonic flow over axisymmetric boattail bodies at moderate angles of attack. The plume is modeled by a solid body configuration identical to those used in experimental tests. An implicit algorithm of second-order accuracy is used to solve the equations on the ILLIAC IV computer. The turbulence is expressed by an algebraic model applicable to three-dimensional flow fields with moderate separation. The computed results compare favorably with three different sets of experimental data reported by Reubush, Shrewsbury, and Benek, respectively. (Author)

A80-44151 * # Asymmetric trailing-edge flows at high Reynolds number. J. W. Cleary, C. C. Horstman, H. L. Seegmiller (NASA, Ames Research Center, Moffett Field, Calif.), and P. R. Viswanath (Stanford University, Stanford, Calif.). *American Institute of Aeronautics and Astronautics, Fluid and Plasma Dynamics Conference, 13th, Snowmass, Colo., July 14-16, 1980, Paper 80-1396.* 17 p. 25 refs.

Results from an experimental investigation of asymmetric trailing-edge flows at high Reynolds numbers and subsonic Mach numbers are presented. Measurements include skin friction; surface and flow-field pressures; and mean-velocity, turbulent shear-stress, and turbulent kinetic-energy profiles in the trailing-edge region. Comparisons are made with computed solutions using Reynolds averaged Navier-Stokes and boundary-layer equations; two different turbulence models are used. Two attached flow are considered, one having a moderate adverse pressure gradient and the other a more severe gradient. From the comparisons, an evaluation is made of the predictions for these two pressure-gradient cases. Although the comparisons demonstrate reasonable agreement for the moderate pressure-gradient case, some differences are noted for the severe pressure-gradient case. (Author)

A80-44639 * Integrated infrared detector arrays for low-background astronomy. C. R. McCreight (NASA, Ames Research Center, Moffett Field, Calif.). In: Recent advances in TV sensors and systems; Proceedings of the Seminar, San Diego, Calif., August 27, 28, 1979. (A80-44626 19-35) Bellingham, Wash., Society of Photo-Optical Instrumentation Engineers, 1979, p. 109-116. 12 refs.

Existing integrated infrared detector array technology is being evaluated under low-background conditions to determine its applicability in orbiting astronomical applications where extended integration times and photometric accuracy are of interest. Preliminary performance results of a 1×20 elements InSb CCD array under simulated astronomical conditions are presented. Using the findings of these tests, improved linear- and area-array technology will be developed for use in NASA programs such as the Shuttle Infrared Telescope Facility. For wavelengths less than 30 microns, extrinsic silicon and intrinsic arrays with CCD readout will be evaluated and improved as required, while multiplexed arrays of Ge:Ga for wavelengths in the range 30 to 120 microns will be developed as fundamental understanding of this material improves. Future efforts will include development of improved drive and readout circuitry, and consideration of alternate multiplexing schemes. (Author)

A80-48079 * Thermophysical and flammability characterization of phosphorylated epoxy adhesives. D. A. Kourtidis, J. A. Parker (NASA, Ames Research Center, Moffett Field, Calif.), T. W. Giants, N. Bilow (Hughes Aircraft Co., Culver City, Calif.), and M.-T. Hsu (San Jose State University, San Jose, Calif.). In: Adhesives for industry; Proceedings of the Conference, El Segundo, Calif., June 24, 25, 1980. (A80-48076 21-27) El Segundo, Calif., Technology Conferences, 1980, p. 92-107. 5 refs.

Some of the thermophysical and flammability properties of a phosphorylated epoxy adhesive, which has potential applications in aircraft interior panels, are described. The adhesive consists of stoichiometric ratios of bis(3-glycidyloxyphenyl)methylphosphine oxide and bis(3-aminophenyl)methylphosphine oxide containing approximately 7.5% phosphorus. Preliminary data are presented from adhesive bonding studies conducted utilizing this adhesive with polyvinyl fluoride (PVF) film and phenolic-glass laminates. Limiting oxygen index and smoke density data are presented and compared with those of the tetraglycidyl methylene dianiline epoxy resin-adhesive system currently used in aircraft interiors. Initial results indicate that the phosphorylated epoxy compound has excellent adhesive properties when used with PVF film and that desirable fire-resistant properties are maintained. (Author)

A80-49296 * # **Vortex simulation of three-dimensional, spot-like disturbances in a laminar boundary layer.** A. Leonard (NASA, Ames Research Center, Moffett Field, Calif.). In: Symposium on Turbulent Shear Flows, 2nd, London, England, July 2-4, 1979, Proceedings. (A80-49226 21-34) London, Imperial College of Science and Technology, 1979, p. 14.7-14.12. 20 refs.

The growth of a turbulent spot in a laminar boundary layer, as the spot evolves from a localized disturbance in the layer, is simulated numerically using a three-dimensional vortex filament description of the vorticity field. The filaments are marked with a sequence of mode points which are tracked in a Lagrangian reference frame. Velocity computation is done by Biot-Savart integration. Although some discrepancies with experiment appear to exist in the near wall region, the gross properties of the spot, including the velocities of the leading and trailing edges and the velocity perturbations away from the wall, are in good agreement with experiment. (Author)

A80-49300 * # **Three-dimensional simulation of the free shear layer using the vortex-in-cell method.** B. Couet, O. Buneman (Stanford University, Stanford, Calif.), and A. Leonard (NASA, Ames Research Center, Moffett Field, Calif.). In: Symposium on Turbulent Shear Flows, 2nd, London, England, July 2-4, 1979, Proceedings. (A80-49226 21-34) London, Imperial College of Science and Technology, 1979, p. 14.29-14.34. 14 refs.

We present numerical simulations of the evolution of a mixing layer from an initial state of uniform vorticity with simple two- and three-dimensional small perturbations. A new method for tracing a large number of three-dimensional vortex filaments is used in the simulations. Vortex tracing by Biot-Savart interaction originally implied ideal (non-viscous) flow, but we use a 3-d mesh, Fourier transforms and filtering for vortex tracing, which implies 'modeling' of subgrid scale motion and hence some viscosity. Streamwise perturbations lead to the usual roll-up of vortex patterns with spanwise uniformity maintained. Remarkably, spanwise perturbations generate streamwise distortions of the vortex filaments and the combination of both perturbations leads to patterns with interesting features discernable in the movies and in the records of enstrophy and energy for the three components of the flow. (Author)

A80-49842 * **Simulation of the Infrared Astronomical Satellite (IRAS) telescope system.** E. Henderson (NASA, Ames Research Center, Moffett Field; Informatics, Inc., Palo Alto, Calif.), H. Lum, and R. Walker (NASA, Ames Research Center, Moffett Field, Calif.). In: Summer Computer Simulation Conference, Newport Beach, Calif., July 24-26, 1978, Proceedings. (A80-49826 22-66) Montvale, N.J., AFIPS Press, 1978, p. 838-843.

The Infrared Astronomical Satellite (IRAS), a joint Dutch-British-U.S. project scheduled for launch in February 1981, will

conduct the first all-sky infrared survey between 8 and 120 microns using a 60-cm aperture, cryogenically-cooled telescope. A computer simulation program has been developed at Ames Research Center to aid in the design of this complex telescope. The development and implementation of the IRAS Telescope Simulator (IRTS), its input data sources, and its output data products are described. (Author)

A80-52280 * **SOLARES orbiting mirror system.** K. Billman (NASA, Ames Research Center, Moffett Field, Calif.). In: Remember the future - The Apollo legacy; Proceedings of the Meeting, San Francisco, Calif., July 20, 21, 1979. (A80-52279 23-12) San Diego, Calif., American Astronautical Society, 1980, p. 15-26. (AAS 79-304)

Hardware characteristics and applications opportunities of large orbital mirrors, as determined to date by NASA's 'SOLARES' program are assessed. Assuming Space Shuttle availability, methods and timetables for the deployment of these thin film-covered structures are presented and comparisons are made between electricity-production values of terrestrial solar-energy systems to which SOLARES units deliver high-intensity insolation, on one hand, and on the other the various conventional generation systems. Electrolytic and photochemical production of gaseous and liquid fuels is also compared to synthetic hydrocarbon fuels derived from fossil sources, with considerable attention to project economics and overall process efficiencies. O.C.

AMES FUNDED RESEARCH JOURNAL ARTICLES

A80-10460 * **A model of the neutral and ion nitrogen chemistry in the daytime thermosphere of Venus.** D. W. Rusch (Colorado, University, Boulder, Colo.) and T. E. Cravens (Michigan, University, Ann Arbor, Mich.). *Geophysical Research Letters*, vol. 6, Oct. 1979, p. 791-794. 25 refs. Contracts No. NAS2-9130; No. NAS2-9477; Grant No. NGR-23-005-015.

Density profiles of N(4S), NO, N(2D), NO(+), and N(+) are calculated for the thermosphere of Venus. The results show that N(4S) is the dominant odd nitrogen species throughout the thermosphere and has a maximum density of 18 million atoms/cu cm at 132 km. The calculated NO(+) density agrees well with recent Pioneer Venus measurements, but the calculated N(+) densities are a factor of two to five less than the measurements. The production of N(4S) atoms generated in the model is adequate to explain recent measurements of the nitric oxide chemiluminescent emission on the night side of Venus. (Author)

A80-10526 * **The phase of the ten-hour modulation in the Jovian magnetosphere /Pioneers 10 and 11/. W. Fillius and P. Knickerbocker (California, University, La Jolla, Calif.). *Journal of Geophysical Research*, vol. 84, Oct. 1, 1979, p. 5763-5772. 28 refs. Contract No. NAS2-6552; Grant No. NGL-05-005-007.**

The paper describes the study of the phase of the 10-hour modulation of energetic electrons seen by Pioneers 10 and 11 in the Jovian magnetosphere. Attention is given to the peaks rather than the valleys of each cycle because the peaks are where physically interesting features occur, such as particle acceleration, current sheets, etc. To identify the peaks, it is required that the instantaneous intensity be higher than the 5-hour running average and the 5-hour running average be greater than the 10-hour running average. These criteria select an interval rather than a point and it is determined that this interval is an appropriate estimate of the experimental uncertainty. When the phases of the peaks are plotted together, they create patterns which are discussed in terms of

disk-like, clock-like, and rotating anomaly models of the magnetosphere. Each model fits some of the data, but no model explains all of the data convincingly. It is concluded that there is still no understanding of the configuration of the outer Jovian magnetosphere. (Author)

A80-11489 * Far infrared, near infrared, and radio molecular line studies of HFE 2, HFE 3, and FJM 6. J. Fischer (New York, State University, Stony Brook, N.Y.), L. Cassar (U.S. Merchant Marine Academy, Kings Point, N.Y.), G. Righini-Cohen, and M. Simon. *Astronomical Journal*, vol. 84, Oct. 1979, p. 1574-1580. 21 refs. Research supported by the Aerospace Corp.; NSF Grant No. MPS-73-04554; Grants No. NSG-2173; No. NSG-2264; No. NATO-1100.

Far-infrared, near-infrared, and radio molecular-line observations of the regions of HFE 2, HFE 3, and FJM 6 are described. At positions of high molecular column density nearest to the reported positions of these sources, their infrared emission cannot be confirmed at upper bounds below those of the original detection. Near-infrared observations of the FJM 6 region (which includes the Bok globule Barnard 361) reveal a number of stellar sources, most of which are behind the molecular cloud and are reddened by it. Visual extinction through B 361 estimated by star counts yields $A_{\text{sub V/N(C-13/O)}} = 3.7 \pm 1.6 \times 10$ to the -16th mag sq cm. The gas temperature and the upper bound on the dust temperature in the FJM 6 region are consistent with cosmic-ray heating of the cloud, while the values of these parameters for the clouds in the HFE 2 and HFE 3 regions do not appear consistent with either cosmic-ray or radiative heating. (Author)

A80-12012 * F + H₂ collisions on two electronic potential energy surfaces - Quantum-mechanical study of the collinear reaction. I. H. Zimmerman (Clarkson College of Technology, Potsdam, N.Y.), M. Baer (Atomic Energy Commission, Soreq Nuclear Research Centre, Yavne; Weizmann Institute of Science, Rehovot, Israel), and T. F. George. *Journal of Chemical Physics*, vol. 71, Nov. 15, 1979, p. 4132-4138. 26 refs. Research sponsored by the U.S.-Israel Binational Science Foundation, Camille and Henry Dreyfus Foundation, and Alfred P. Sloan Foundation; NSF Grant No. CHE-77-27826; Contract No. F49620-78-C-0005; Grant No. NSG-2198.

Collinear quantum calculations are carried out for reactive F + H₂ collisions on two electronic potential energy surfaces. The resulting transmission and reflection probabilities exhibit much greater variation with energy than single-surface studies would lead us to anticipate. Transmission to low-lying product channels is increased by orders of magnitude by the presence of the second surface; however, branching ratios among product states are found to be independent of the initial electronic state of the reactants. These apparently contradictory aspects of the calculation are discussed and a tentative explanation put forward to resolve them. (Author)

A80-13534 * A calculation of the diffusion energies for adatoms on surfaces of F.C.C. metals. T. Halicioglu (NASA/Stanford Joint Institute for Surface and Microstructural Research, Moffett Field, Calif.) and G. M. Pound (Stanford University, Stanford, Calif.). (*International Congress on Thin Films, 4th, Loughborough, Leics., England, Sept. 11-15, 1978.*) *Thin Solid Films*, vol. 57, 1979, p. 241-245. 11 refs. Grant No. NATO-858.

The activation energies for diffusion were determined for gold, platinum and iridium adatoms on plane and plane PT surfaces and were found to be in good agreement with the measurements reported by Bassett and Webber. The Lennard-Jones pair potentials were used to model the interatomic forces, and relaxation of the substrate atoms in near proximity to the adatom was considered in detail. The

present calculations clarify the mechanism of the observed two-dimensional diffusion of platinum and iridium atoms on a plane PT surface. The results are compared with those obtained using Morse potential functions and different relaxation techniques. (Author)

A80-13969 * Eolian sedimentation on earth and Mars - Some comparisons. I. J. Smalley (Department of Scientific and Industrial Research, Soil Bureau, Lower Hutt, New Zealand) and D. H. Krinsley (Arizona State University, Tempe, Ariz.). *Icarus*, vol. 40, Nov. 1979, p. 276-288. 51 refs. Grants No. NCA2-ORO35-801; No. NCA2-ORO35-901.

Eolian sediments on earth are mostly formed from quartz. The quartz particles originally came from a granitic source. With respect to eolian sediments on Mars, it appears that an entirely different set of criteria must apply, but some critical parameters can be usefully compared. Impact experiments with basalt in eolian abrasion devices suggest that basalt sand-sized particles fragment rapidly to produce silt and clay-sized detritus. Cohesive forces must be more effective on Mars since the gravitational contribution to the bond/weight ratio is lower. Compared to the terrestrial situation, both larger and smaller particles can be expected to make significant contributions to eolian sediments on Mars. The low gravity and the high speed of moving particles and the relative weak rock material of which they are composed will allow large-scale fine particle production. V.T.

A80-14397 * Pressure and temperature dependence kinetics study of the NO + BrO yielding NO₂ + Br reaction - Implications for stratospheric bromine photochemistry. R. T. Watson, S. P. Sander (California Institute of Technology, Jet Propulsion Laboratory, Molecular Physics and Chemistry Section, Pasadena, Calif.), and Y. L. Yung (California Institute of Technology, Pasadena, Calif.). *Journal of Physical Chemistry*, vol. 83, Nov. 15, 1979, p. 2936-2944. 36 refs. Contract No. NAS7-100; Grant No. NSG-2229.

The reactivity of NO with BrO radicals over a wide range of pressure (100-700 torr) and temperature (224-398 K) is investigated using the flash photolysis-ultraviolet absorption technique. The flash photolysis system consists of a high-pressure xenon arc light source, a reaction cell/gas filter/flash lamp combination, and a 216.5 half-meter monochromator/polychromator/spectrography for wavelength selectivity. The details of the reaction and its corresponding Arrhenius expression are identified. The results are compared with previous measurements, and atmospheric implications of the reaction are discussed. The NO + BrO yielding NO₂ + Br reaction is shown to be important in controlling the concentration ratios of BrO/Br and BrO/HBr in the stratosphere, but this reaction does not affect the catalytic efficiency of BrO_x in ozone destruction. S.D.

A80-15221 * Quantum-mechanical calculation of three-dimensional atom-diatom collisions in the presence of intense laser radiation. P. L. DeVries (Rochester, University, Rochester, N.Y.) and T. F. George. *Journal of Chemical Physics*, vol. 71, Aug. 15, 1979, p. 1543-1549. 17 refs. NSF Grant No. CHE-77-27826; Grant No. NSG-2198; Contract No. F49620-78-C-0005.

A formalism is presented for describing the collision of fluorine with the hydrogen molecule in the presence of intense radiation. For a laser frequency on the order of the spin-orbit splitting of fluorine, the interaction of the molecular system with the radiation occurs at relatively long range where, for this system, the electric dipole is vanishingly small. Hence the interaction occurs due to the magnetic dipole coupling. Even so, at low collision energies a substantial enhancement of the quenching cross section is found for a radiation intensity of 10 to the 11th W/sq cm. (Author)

A80-15293 * # On the inference of properties of Saturn's Ring E from energetic charged particle observations. M. F. Thomsen and J. A. Van Allen (Iowa, University, Iowa City, Iowa). *Geophysical Research Letters*, vol. 6, Nov. 1979, p. 893-896. 12 refs. Contracts No. NAS2-6553; No. N00014-76-C-0016.

The paper demonstrates that information about Saturn's Ring E particle size is potentially obtainable from observations of Saturnian trapped radiation. It is shown that observations of the radial dependence of the intensities, energy spectra, electron-to-proton intensity ratio, and pitch angle distributions of energetic charged particles trapped outside of Ring A can potentially provide information (1) on the existence of Ring E, (2) on the effective size of the particulate matter therein, and (3) on the magnitude of the radial diffusion coefficient for energetic particles. A parametric study of these possibilities is specialized to the characteristics of the University of Iowa detectors on Pioneer 11 which was scheduled to make a close encounter with Saturn in 1979. A.T.

A80-15296 * A comparison of Pioneer Venus and Venera bow shock observations - Evidence for a solar cycle variation. J. A. Slavin, R. C. Elphic, and C. T. Russell (California, University, Los Angeles, Calif.). *Geophysical Research Letters*, vol. 6, Nov. 1979, p. 905-908. 30 refs. Contract No. NAS2-9491.

Observations by the Venera 9 and 10 orbiters in 1975-76 have been used in previous studies to determine the mean location and shape of the Cytherean bow shock. In addition it has also been reported that the shock is found to be more distant from the planet above regions of the ionosheath where draped IMF field lines are oriented perpendicular to the flow as opposed to parallel. An examination of the dependence of shock altitude in the terminator plane on upstream IMF direction using 86 Pioneer Venus orbiter bow shock crossings in 1978-79 sets an upper limit on this asymmetry of 12% or approximately half that derived earlier from the Venera data. More significantly, the mean distance to the bow shock observed by Pioneer Venus Orbiter is 35% greater than was the case in 1975-76 near solar minimum. As the growth in effective obstacle radius is an order of magnitude larger than can be accounted for in terms of varying ionopause altitude due to all causes, these results strongly suggest that Venus can absorb significantly more of the incident solar wind plasma during solar minimum when EUV flux is low than during the current epoch in which maximum is approaching. (Author)

A80-15609 * A reconsideration of nucleation phenomena in light of recent findings concerning the properties of small clusters, and a brief review of some other particle growth processes. A. W. Castleman, Jr. (Colorado, University, Boulder, Colo.). (*Workshop on Thermodynamics and Kinetics of Dust Formation in the Space Medium, Houston, Tex., Sept. 6-8, 1978.*) *Astrophysics and Space Science*, vol. 65, no. 2, Oct. 1979, p. 337-349. 41 refs. NSF Grant No. ATM-76-14914; Contract No. EP-78-S-02-4776; Grants No. NSG-2248; No. DA-ARO(D)-29-76-G0276.

The paper examines mechanisms of nucleation and growth by condensation and coagulation in the light of recent research on properties of small clusters. Homogeneous, hetero-molecular, and heterogeneous nucleation is analyzed, and expressions for the rate of formation of a stable condensed phase and evaluation of the free energy of formation of charged droplets are given. Application of high-pressure mass spectrometry which makes possible a direct determination of intensity spectra for cluster distributions, measurement of the thermodynamic properties of individual ion clusters and determination of cluster entropy and bond energy is discussed. Finally, coagulation of the condensed phase is considered, noting that concentration and mean particle size vary during coagulation, but the shape distribution is time independent, leading to the concept of a self-preserving aerosol size distribution. A.T.

A80-15673 * An angular momentum approximation for molecular collisions in the presence of intense laser radiation. P. L. Devries and T. F. George (Rochester, University, Rochester, N.Y.). *Molecular Physics*, vol. 38, no. 2, 1979, p. 561-576. 15 refs. NSF Grants No. CHE-75-06775; No. CHE-77-27826; Grant No. NSG-2198; Contract No. F49620-78-C-0005.

An approximation to a previously presented rigorous description of molecular (atom-atom) collisions occurring in the presence of intense radiation is investigated. This rigorous description explicitly considers the angular momentum transferred between the molecule and the radiation field in the absorption or emission of a photon, but involves a complicated system of close-coupled equations which must be solved independently for each projection M of the initial, total molecular angular momentum. (This is a direct consequence of the lack of rotational invariance in the molecule-field problem). These equations are solved for a model system which mimics the collision of a halogen with a rare gas atom. Empirical observations made in the course of performing these calculations lead to the development of an approximation which avoids the repeated calculations for each initial M. This orientational average approximation greatly reduces the effort required to describe the system, and for the model calculation, yields accurate results for field intensities as high as 10 GW/sq cm. (Author)

A80-15768 * A new propagation method for the radial Schrödinger equation. P. L. Devries (Rochester, University, Rochester, N.Y.). *Chemical Physics Letters*, vol. 66, Oct. 1, 1979, p. 258-261. 6 refs. NSF Grant No. CHE-77-27826; Grant No. NSG-2198; Contract No. F49620-78-C-0005.

A new method for propagating the solution of the radial Schrödinger equation is derived from a Taylor series expansion of the wavefunction and partial re-summation of the infinite series. Truncation of the series yields an approximation to the exact propagator which is applied to a model calculation and found to be highly convergent. (Author)

A80-16697 * On the limitations of the concept of space frequency equivalence. R. H. MacPhie (Waterloo, University, Waterloo, Ontario, Canada). *Radio Science*, vol. 14, Nov.-Dec. 1979, p. 1185-1187. Grant No. NCA2-OR745-716.

A narrow-band correlation interferometer using directive (large) antennas is equivalent to a wideband correlation interferometer employing isotropic (small) antennas. This concept of space frequency equivalence, due to Kock and Stone, is reexamined and is shown to hold exactly only for the mean or expected values of the correlation interferometer outputs. If their variances are considered, the equivalence disappears, with the variance for the wideband system always equal to or greater than that of the narrow-band system. (Author)

A80-16862 * Infrared spectra of IC 418 and NGC 6572. S. P. Willner, B. Jones, R. W. Russell (California, University, La Jolla, Calif.), R. C. Puetter (Minnesota, University, Minneapolis, Minn.), and B. T. Soifer (California, University, La Jolla; California Institute of Technology, Pasadena, Calif.). *Astrophysical Journal, Part 1*, vol. 234, Dec. 1, 1979, p. 496-502. 51 refs. NSF Grants No. AST-76-82890; No. AST-76-21458; Grant No. NGR-05-005-055.

Spectrophotometric observations from 2 to 4 and 8 to 13 microns of NGC 6572 and from 4 to 13 microns of IC 418 are reported. Also reported are observations of the size of IC 418 in the optical and at 1.65 and 2.2 microns. Both planetary nebulae emit more radiation than expected from recombination at wavelengths longer than 4 microns; this radiation is attributed to heated dust.

The spectra show a plateau from 10.5 to 13 microns, and this peak is tentatively attributed to emission from large silicon carbide particles. Fine-structure emission lines are also discussed; the presence of (forbidden Ar III) but not (forbidden Ne II) in NGC 6572 suggests that ions having the same ionization potential can nevertheless have different fractional abundances. (Author)

A80-18943 * Hot hydrogen in the exosphere of Venus. T. E. Cravens, A. F. Nagy (Michigan, University, Ann Arbor, Mich.), and T. I. Gombosi (Michigan, University, Ann Arbor, Mich.; Magyar Tudományok Akadémia, Központi Fizikai Kutató Intézet, Budapest, Hungary). *Nature*, vol. 283, Jan. 10, 1980, p. 178-180. Contract No. NAS2-9130; Grant No. NGR-23-005-015.

Lyman-alpha measurements of the hydrogen corona of Venus by Mariners 5 and 10 have been shown to be consistent with a two-temperature component model. Bertaux et al. (1978) have successfully fitted the Venera 9 exospheric Lyman-alpha data to an elevated (500 K) single temperature. Various source mechanisms have been proposed to explain the 'hot' (1000 K) energetic component of the hydrogen corona. In the present paper recent results from the Pioneer Venus Orbiter are used to establish the major sources of this hot hydrogen population. B.J.

A80-19118 * Saturnian trapped radiation and its absorption by satellites and rings - The first results from Pioneer 11. J. A. Simpson, T. S. Bastian, D. L. Chenette, G. A. Lentz, R. B. McKibben, K. R. Pyle, and A. J. Tuzzolino (Chicago, University, Chicago, Ill.). *Science*, vol. 207, Jan. 25, 1980, p. 411-415. 26 refs. NSF Grant No. ATM-77-24494; Contract No. NAS2-6551; Grant No. NGL-14-001-006.

Preliminary results from Pioneer 11 concerning the acceleration and trapping of charged particles in the magnetic field of Saturn are reported. The identification and measurement of the intensities and spectra of charged particle species was performed by an experiment including four charged particle sensor systems, within 20 Saturn radii of the planet. Increases in the intensity of 0.5- to 1.8-MeV protons within 15 Saturn radii indicate the trapping and acceleration of particles in the dipole field region, while a decrease in proton intensity between seven and four Saturn radii is attributed to absorption by Dione and Enceladus and possibly ring material as well. Proton and electron intensity distributions are found to be axially symmetric within four Saturn radii, indicating a centered dipole aligned with the planetary rotation axis. Trapped radiation absorption at the orbit of Mimas is analyzed to obtain an upper limit of 4×10 to the 8th Saturn radii-squared/sec to the inward diffusion coefficient; an absorption-like feature observed at $L = 2.5$ is attributed to a previously unidentified satellite of diameter less than 200 km and semimajor axis 2.51 Saturn radii. Radiation absorption by the newly discovered F ring was also observed, however beneath the A, B and C rings a low flux of high-energy electrons was detected. A.L.W.

A80-19119 * Saturn's magnetosphere, rings, and inner satellites. J. A. Van Allen, M. F. Thomsen, B. A. Randall, R. L. Rairden, and C. L. Grosskreutz (Iowa, University, Iowa City, Iowa). *Science*, vol. 207, Jan. 25, 1980, p. 415-421. 20 refs. Navy-supported research; Contract No. NAS2-6553.

The discovery of the Saturn magnetosphere and its characterization by Pioneer 11 are reported, and findings on the planet's rings and satellites obtained by energetic charged particle measurements within the inner magnetosphere are presented. Bow shock crossings identified by the Pioneer plasma analyzer and magnetometer at

distances of 24.1, 23.1 and 20.0 Saturn radii indicate the presence of a magnetosphere with physical dimensions and charged particle populations intermediate between those of the earth and Jupiter, with a scale more similar to that of the earth. Particle angular distributions on the inbound leg of the trajectory are consistent with a dipole magnetic field approximately perpendicular to the planet's equator, while on the outbound leg the distributions indicate the presence of an equatorial current sheet. Charged particle absorption features are detected at the orbits of Dione and Mimas, encompassing the orbits of Tethys and Enceladus, and at 2.534 and 2.343 Saturn radii indicating the presence of satellites of diameters greater than 170 km. Charged particle measurements also confirm the Pioneer division in the rings between 2.292 and 2.336 Saturn radii, a suspected satellite at 2.82 Saturn radii, the presence of the F ring between 2.336 and 2.371 Saturn radii and the outer radius of the A ring at 2.292 Saturn radii. A.L.W.

A80-19121 * Trapped radiation belts of Saturn - First look. W. Fillius (California, University, La Jolla, Calif.), W. H. Ip (Max-Planck-Institut für Aeronomie, Katlenburg, West Germany), and C. E. McIlwain (California, University, San Diego, Calif.). *Science*, vol. 207, Jan. 25, 1980, p. 425-431. 25 refs. Contract No. NAS2-6552; Grant No. NGL-05-005-007.

Data on the magnetosphere of Saturn obtained with the trapped radiation detector package on board the Pioneer 11 spacecraft is reported. Radiation belt profiles determined by the trapped radiation detectors on Pioneer 10 and 11 indicate that Saturn's magnetosphere is intermediate in size between those of the earth and Jupiter, with particle intensities similar to those of the earth. The outer region of the Saturn magnetosphere is found to contain particles of lower energy than the outer region, being strongly influenced by the time-varying solar wind. The moons and rings of Saturn are observed to be effective absorbers of trapped particles, confirming the discoveries of the F ring, the Pioneer ring division and the moon 1979 S 2. Particle diffusion rates are used to estimate a cross-sectional area of greater than 7×10 to the 13th sq cm and an opacity greater than 0.00001 for the F ring. It is suggested that cosmic-ray albedo neutron decay be studied as a possible source of energetic particles in the inner magnetosphere of Saturn. A.L.W.

A80-19122 * Ultraviolet photometer observations of the Saturnian system. D. L. Judge, F.-M. Wu (Southern California, University, Los Angeles, Calif.), and R. W. Carlson (California Institute of Technology, Jet Propulsion Laboratory, Pasadena, Calif.). *Science*, vol. 207, Jan. 25, 1980, p. 431-434. 12 refs. Contract No. NAS2-6558.

Several interesting cloud and atmospheric features of the Saturn system have been observed by the long-wavelength channel of the two-channel ultraviolet photometer aboard the Pioneer Saturn spacecraft. Reported are observations of the most obvious features, including a Titan-associated cloud, a ring cloud, and the variation of atmospheric emission across Saturn's disk. The long-wavelength data for Titan suggest that a cloud of atomic hydrogen extends at least 5 Saturn radii along its orbit and about 1.5 Saturn radii vertically. A ring cloud, thought to be atomic hydrogen, has also been observed by the long-wavelength channel of the photometer; it shows significant enhancement in the vicinity of the B ring. Finally, spatially resolved observations of Saturn's disk show significant latitudinal variation. Possible explanations of the variation include aurora or limb brightening. (Author)

A80-19956 * Low-pass interference filters for submillimeter astronomy. S. E. Whitcomb and J. Keene (Chicago, University, Chicago, Ill.). *Applied Optics*, vol. 19, Jan. 15, 1980, p. 197, 198. 9

refs. Research supported by the Fannie and John Hertz Foundation; Grants No. NSG-2057; No. NGR-14-001-227.

Low-pass (long-wave transmitting) interference filters, suitable for broadband photometric observations, previously have been constructed from series of capacitive grids stretched on thin Mylar. These filters have the desired optical properties of high transmission, sharp cut-ons, and good blocking at short wavelengths. Their designs, however, do not scale from one wavelength to another and their performance can deteriorate at low temperatures due to differential contraction of the dielectric backing and the supporting structure. The deviation of these early filters from the predicted scaling was due primarily to the difference in refractive index between the backing material and the medium between the grids. In the present paper, filters are described in which dielectric spacers are used, instead of air, as the medium between the grids. This technique has improved the scaling and has reduced the distortion from differential contraction. V.P.

A80-20331 * **Lifting three-dimensional wings in transonic flow.** M. S. Cramer (Virginia Polytechnic Institute and State University, Blacksburg, Va.). *Journal of Fluid Mechanics*, vol. 95, Nov. 28, 1979, p. 223-240. 13 refs. Grants No. NSG-2112; No. AF-AFOSR-76-2954.

The far field of a lifting three-dimensional wing in transonic flow is analysed. The boundary-value problem governing the flow far from the wing is derived by the method of matched asymptotic expansions. The main result is to show that corrections which are second order in the near field make a first-order contribution to the far field. The present study corrects and simplifies the work of Cheng and Hafez (1975) and Barnwell (1975). (Author)

A80-21183 * **Acceleration of energetic protons by interplanetary shocks.** M. E. Pesses (Maryland, University, College Park, Md.), B. T. Tsurutani, E. J. Smith (California Institute of Technology, Jet Propulsion Laboratory, Pasadena, Calif.), and J. A. Van Allen (Iowa, University, Iowa City, Iowa). *Journal of Geophysical Research*, vol. 84, Dec. 1, 1979, p. 7297-7301. 16 refs. Contracts No. NAS2-6553; No. NAS7-100.

The University of Iowa instrument aboard Pioneer 11 detected 69 energetic proton events (EPE) (in the 0.6-3.4 MeV energy range) during 1973-1974 in the heliocentric radial range 1-5 AU. Sixty percent of the EPE peak within plus or minus 5 hours of a corotating interaction region (CIR) boundary, while 19% peak inside and 21% peak outside the interaction regions. Of the CIR boundaries at which an EPE peaks with plus or minus 5 hours, 80% have associated shocks. The observed intensities and pitch angle distributions of protons near shock fronts are consistent with a theoretical simulation of the acceleration of protons by a drift in the electric field at the shock front. (Author)

A80-21765 * **High-resolution Martian atmosphere modeling.** W. G. Egan, W. L. Fischbein, L. L. Smith, and T. Hilgeman (Grumman Aerospace Corp., Research Dept., Bethpage, N.Y.). *Icarus*, vol. 41, Jan. 1980, p. 166-174. 16 refs. Contract No. NAS2-8664.

A multilayer radiative transfer, high-spectral-resolution infrared model of the lower atmosphere of Mars has been constructed to assess the effect of scattering on line profiles. The model takes into account aerosol scattering and absorption and includes a line-by-line treatment of scattering and absorption by CO₂ and H₂O. The aerosol complex indices of refraction used were those measured on montmorillonite and basalt chosen on the basis of Mars in data from the

NASA Lear Airborne Observatory. The particle sizes and distribution were estimated using Viking data. The molecular line treatment employs the AFGL line parameters and Voigt profiles. The modeling results indicate that the line profiles are only slightly affected by normal aerosol scattering and absorption, but the effect could be appreciable for heavy loading. The technique described permits a quantitative approach to assessing and correcting for the effect of aerosols on lineshapes in planetary atmospheres. (Author)

A80-22207 * **The upper atmosphere of Uranus - Mean temperature and temperature variations.** E. Dunham, J. L. Elliot (MIT, Cambridge, Mass.), and P. J. Gierasch (Cornell University, Ithaca, N.Y.). *Astrophysical Journal, Part 1*, vol. 235, Jan. 1, 1980, p. 274-284. 45 refs. NSF Grant No. AST-79-08376; Grant No. NSG-2342.

The number-density, pressure, and temperature profiles of the Uranian atmosphere in the pressure interval from 0.3 to 30 dynes/sq cm are derived from observations of the occultation of SAO 158687 by Uranus on 1977 March 10, observations made from the Kuiper Airborne Observatory and the Cape Town station of the South African Astronomical Observatory. The mean temperature is found to be about 95 K, but peak-to-peak variations from 10 K to 20 K or more exist on a scale of 150 km or 3 scale heights. The existence of a thermal inversion is established, but the inversion is much weaker than the analogous inversion on Neptune. The mean temperature can be explained by solar heating in the 3.3 micron methane band with a methane mixing ratio of 4×10^{-6} to the -6th combined with the cooling effect of ethane with a mixing ratio of not greater than 4×10^{-6} to the -6th. The temperature variations are probably due to a photochemical process that has formed a Chapman layer. (Author)

A80-22987 * **Part-body and multibody effects on absorption of radio-frequency electromagnetic energy by animals and by models of man.** O. P. Gandhi, M. J. Hagmann, and J. A. D'Andrea (Utah, University, Salt Lake City, Utah). *Radio Science*, vol. 14, Nov.-Dec. 1979, Supplement, p. 15-21. 10 refs. Grant No. DAMD17-74-C-4092; Contract No. NAS2-9555.

Fine structure in the whole-body resonant curve for radio-frequency energy deposition in man can be attributed to part-body resonances. As for head resonance, which occurs near 350 MHz in man, the absorptive cross section is nearly three times the physical cross section of the head. The arm has a prominent resonance at 150 MHz. Numerical solutions, antenna theory, and experimental results on animals have shown that whole-body energy deposition may be increased by 50 percent or more because of multiple bodies that are strategically located in the field. Empirical equations for SARs are also presented along with test data for several species of laboratory animals. Barbiturate anesthesia is sufficiently disruptive of thermoregulation that delta Ts of colonic temperature yield energy dose values in several mammals that compare quite favorably with those based on whole-body calorimetry. (Author)

A80-24625 * **Toxicity of pyrolysis gases from foam plastics.** C. J. Hilado, H. J. Cumming, and C. J. Casey (San Francisco, University, San Francisco, Calif.). *SAMPE Quarterly*, vol. 11, Jan. 1980, p. 32-35. 9 refs. Grant No. NSG-2039.

Twenty-three samples of flexible foams and twelve samples of rigid foams were evaluated for toxicity of pyrolysis gases, using the USF toxicity screening test method. Polychloroprene among the flexible foams, and polystyrene among the rigid foams, appeared to exhibit the least toxicity under these particular test conditions. (Author)

S

A80-26111 * A far-infrared study of the reflection nebula NGC 2023. P. M. Harvey, H. A. Thronson, Jr. (Steward Observatory, Tucson, Ariz.), and I. Gatley (California Institute of Technology, Pasadena, Calif.). *Astrophysical Journal, Part 1*, vol. 235, Feb. 1, 1980, p. 894-898. 21 refs. Grants No. NGR-03-002-390; No. NGR-05-002-281.

Multicolor mapping of the reflection nebula NGC 2023 from 40 to 160 microns is presented. These data show the shorter wavelength emission to peak on or close to the exciting star HD 37903. The longest wavelength emission, however, peaks about 1 arcmin south of HD 37903, at a position coincident with the C II recombination line peak. The dust temperature appears to peak close to HD 37903 suggesting that it is probably the most luminous heating source for the cloud. The far-infrared data together with 10 microns photometry of HD 37903 imply a roughly uniform dust mass density within 0.1 pc of the star with no significant density increase toward the star. The results imply that the gas and dust column density increase slightly to the south of HD 37903 and that the bulk of the molecular cloud lies behind the star and the reflection nebula. (Author)

A80-26173 * Spectroscopic evidence for two achondrite parent bodies - Asteroids 349 Dembowska and 4 Vesta. M. A. Feierberg, H. P. Larson, U. Fink, and H. A. Smith (Arizona, University, Tucson, Ariz.). *Geochimica et Cosmochimica Acta*, vol. 44, Mar. 1980, p. 513-524. 40 refs. Grants No. NSG-7070; No. NGR-03-002-332.

A Fourier spectrometer was used to obtain IR spectra of asteroids 349 Dembowska and 4 Vesta. The spectrum of Dembowska shows olivine and pyroxene with an olivine/pyroxene abundance ratio greater than 2, and possibly as high as 10. This is probably an unsampled achondritic composition, similar to the unique achondrite ALHA 77005. Dembowska's mineralogy therefore appears related to the achondrites; pyroxene and plagioclase feldspar are seen, with a pyroxene/feldspar abundance ratio between 1.5 and 2.0. Time-resolved observations over one-half of the rotation period indicate compositional homogeneity; both 349 Dembowska and 4 Vesta can be considered as candidates for the parent bodies of igneous meteorites. (Author)

A80-26437 * Wave propagation and transport in the middle atmosphere. J. R. Holton (Washington, University, Seattle, Wash.). (Royal Society, Discussion on the Middle Atmosphere as Observed from Balloons, Rockets and Satellites, London, England, Dec. 12, 13, 1978.) *Royal Society (London), Philosophical Transactions, Series A*, vol. 296, no. 1418, Mar. 6, 1980, p. 73-85. 27 refs. Grant No. NSG-2228.

The paper reviews the dynamics of wave propagation and wave transport for vertically propagating, planetary scale waves in the middle atmosphere. Such waves are divided into two major classes: extratropical planetary waves and equatorial waves. The most significant extratropical modes are the quasi-stationary Rossby waves, while the most significant equatorial modes are the Kelvin wave and the mixed Rossby-gravity wave. Both types of waves are capable of generating mean flow changes through wave-mean flow interaction. B.J.

A80-27013 * The implications of hydrogen emission line ratios in quasi-stellar objects. R. C. Canfield and R. C. Puetter (California, University, La Jolla, Calif.). *Astrophysical Journal, Part 2 - Letters to the Editor*, vol. 236, Feb. 15, 1980, p. L7-L11. 24 refs. NSF Grant No. AST-76-82890; Grants No. NGR-05-005-055; No. AF-AFOSR-76-3071.

The results of multilevel, depth-dependent, fully interlocked radiative transfer calculations for hydrogen emission line strengths in

a single QSO emission line cloud (ELC) are summarized. The hydrogen-line forming region of the ELC is found to be quite thick (tau sub el between 1,000 and 100,000), which is consistent with heating of a pure hydrogen cloud by photoionization. Results indicate that the volume-averaged escape probability approach introduces large errors by assuming, in effect, that a single point in the ELC is representative of the emergent radiation; that the influence of frequency redistribution on the photon escape probability in resonance and subordinate lines must be explicitly recognized, and that full consistency between excitation and ionization processes must be maintained. J.P.B.

A80-28244 * A comparative study of cosmic ray intensity variations during 1972-1977 using spacecraft and ground-based observations. D. Venkatesan, S. P. Agrawal (Calgary, University, Calgary, Alberta, Canada), and J. A. Van Allen (Iowa, University, Iowa City, Iowa). *Journal of Geophysical Research*, vol. 85, Mar. 1, 1980, p. 1328-1334. 11 refs. National Research Council Grants No. A-1565; No. A-1096; Contract No. NAS2-6553.

A study of cosmic ray intensity variations using data registered by Detector C on Pioneer 10 and the Sulphur Mountain neutron monitor is presented. The spacecraft data were corrected for temperature, Radioisotope Thermoelectric Generator background, and contamination by energetic solar particle events. A consistent long-term solar cycle variation intensity is observed, but additional contribution is observed in the neighborhood of 5.1 AU which is attributed to energetic electrons of Jovian origin. The spectral variation in long-term changes of the cosmic ray intensity is studied by comparing the low-energy and high-energy data, and an average value of their ratio during 1972-1977 was found to agree with the value for the 1965-1972 interval. A.T.

A80-29697 * Degradation of tensile and shear properties of composites exposed to fire or high temperature. G. A. Pering, P. V. Farrell, and G. S. Springer (Michigan, University, Ann Arbor, Mich.). *Journal of Composite Materials*, vol. 14, Jan. 1980, p. 54-68. 8 refs. Grant No. NSG-2333.

The decrease in ultimate tensile strength, shear strength, tensile modulus, and shear modulus of fiber reinforced composites exposed to fire or to high temperature was investigated. A simple model was developed for calculating the mass loss of the material and the thickness of the char layer. The mass loss as well as the degradation in tensile and shear properties of Fiberite T300/1034 and Hercules AS/3501-6 graphite epoxy composites exposed to fire were measured. A correlation between the degradation in properties and the calculated mass loss and the char layer thickness was developed. A technique was proposed for predicting material damage through the use of such correlations. (Author)

A80-30835 * The Pioneer Venus Orbiter plasma wave investigation. F. L. Scarf, W. W. L. Taylor, and P. F. Virobik (TRW Defense and Space Systems Group, Redondo Beach, Calif.). *IEEE Transactions on Geoscience and Remote Sensing*, vol. GE-18, Jan. 1980, p. 36-38. Contracts No. NAS2-8809; No. NAS2-9842. Project PIONEER.

The Pioneer Venus plasma wave instrument has a self-contained balanced electric dipole (effective length = 0.75 m) and a 4-channel spectrum analyzer (30% bandwidth filters with center frequencies at 100 Hz, 730 Hz, and 30 kHz). The channels are continuously active and the highest Orbiter telemetry rate (2048 bits/sec) yields 4 spectral scans/sec. The total mass of 0.55 kg includes the electronics, the antenna, and the antenna deployment mechanism. This report contains a brief description of the instrument design and a discussion of the in-flight performance. (Author)

A80-30839 * Pioneer Venus Orbiter planar retarding potential analyzer plasma experiment. W. C. Knudsen, J. Bakke (Lockheed Research Laboratories, Palo Alto, Calif.), K. Spinner, and V. Novak (Fraunhofer-Gesellschaft zur Förderung der angewandten Forschung, Institut für physikalische Weltraumforschung, Freiburg im Breisgau, West Germany). *IEEE Transactions on Geoscience and Remote Sensing*, vol. GE-18, Jan. 1980, p. 54-59. 16 refs. Bundesministerium für Forschung und Technologie Contract No. DO-238/RV-B-28/73; Contract No. NAS2-8811.

The retarding potential analyzer (RPA) on the Pioneer Venus Orbiter Mission measures most of the thermal plasma parameters within and near the Venusian ionosphere. Parameters include total ion concentration, concentrations of the more abundant ions, ion temperatures, ion drift velocity, electron temperature, and low-energy (0-50 eV) electron distribution function. Several functions not previously used in RPA's were developed and incorporated into this instrument to accomplish these measurements on a spinning spacecraft with a small bit rate. The more significant functions include automatic electrometer ranging with background current compensation; digital, quadratic retarding potential step generation for the ion and low-energy electron scans; a current sampling interval of 2 ms throughout all scans; digital logic inflection point detection and data selection; and automatic ram direction detection. (Author)

A80-30841 * Design and operation of the Pioneer Venus Orbiter ultraviolet spectrometer. A. I. F. Stewart (Colorado, University, Boulder, Colo.). *IEEE Transactions on Geoscience and Remote Sensing*, vol. GE-18, Jan. 1980, p. 65-70. Contract No. NAS2-9477.

The University of Colorado's ultraviolet spectrometer instrument carried on the Pioneer Venus Orbiter spacecraft is a 125-mm f/5 Ebert-Fastie design with a 250-mm Cassegrain telescope. The instrument has extensive logic to control the grating motor drive and to adapt the basic spectrometer to the constraints and opportunities of the mission. Success has been achieved in reconciling the conflicting requirements of spectroscopic, limb profile, and imaging observations. A description of the instrument operating techniques is given together with representative results of all three types. (Author)

A80-30844 * Pioneer Venus Sounder Probe Neutral Gas Mass Spectrometer. J. H. Hoffman, R. R. Hodges, Jr., W. W. Wright, V. A. Blevins, K. D. Duerksen, and L. D. Brooks (Texas, University, Richardson, Tex.). *IEEE Transactions on Geoscience and Remote Sensing*, vol. GE-18, Jan. 1980, p. 80-84. 9 refs. Contracts No. NAS2-8802; No. NAS2-9485.

A neutral gas mass spectrometer was flown to Venus as part of the Pioneer Venus Multiprobe to measure the composition of its lower atmosphere. The instrument, mounted in the Sounder Probe, was activated after the probe entered the top of the atmosphere, and it obtained data during the descent from 62 km to the surface. Atmospheric gases were sampled through a pair of microleaks, the effluent from which was pumped by a combination of ion and getter pumping. A pneumatically operated valve, controlled by the ambient atmospheric pressure, maintained the ion source pressure at a nearly constant value during descent while the atmospheric pressure varied by three orders of magnitude. A single focusing magnetic sector field mass spectrometer with mass resolution sufficient to reasonably separate argon from C₃H₄ at 40 amu provided the mass analysis and relative abundance measurements. A microprocessor controlled the operation of the mass spectrometer through a highly efficient peak-tip stepping routine and data compression algorithm that effected a scan of the mass spectrum from 1 to 208 amu in 64 sec while requiring an information rate of only 40 bits/sec to return the data to earth. A subscale height altitude resolution was thus obtained. Weight, size, and power requirements were minimized to be consistent with interplanetary flight constraints. (Author)

A80-30846 * Pioneer Venus Sounder Probe Solar Flux Radiometer. M. G. Tomasko, L. R. Doose, J. M. Palmer, A. Holmes, W. L. Wolfe, A. G. DeBell, L. G. Brod, and R. R. Sholes (Arizona, University, Tucson, Ariz.). *IEEE Transactions on Geoscience and Remote Sensing*, vol. GE-18, Jan. 1980, p. 93-97. Contract No. NAS2-8818.

The Solar Flux Radiometer aboard the Pioneer Venus Sounder Probe operated successfully during its descent through the atmosphere of Venus. The instrument measured atmospheric radiance over the spectral range from 400 to 1800 nm as a function of altitude. Elevation and azimuthal measurements on the radiation field were made with five optical channels. Twelve filtered Si and Ge photovoltaic detectors were maintained near 30 C with a phase-change material. The detector output currents were processed with logarithmic transimpedance converters and digitized with an 11-bit A/D converter. Atmospheric sampling in both elevation and azimuth was done according to a Gaussian integration scheme. The serial output data averaged 20 bits/sec, including housekeeping (sync, spin period, sample timing and mode). The data were used to determine the deposition of solar energy in the atmosphere of Venus between 67 km and the surface along with upward and downward fluxes and radiances with an altitude resolution of several hundred meters. The results allow for more accurate modeling of the radiation balance of the atmosphere than previously possible. (Author)

A80-30850 * Pioneer Venus small probes net flux radiometer experiment. L. A. Sromovsky, H. E. Revercomb, and V. E. Suomi (Wisconsin, University, Madison, Wis.). *IEEE Transactions on Geoscience and Remote Sensing*, vol. GE-18, Jan. 1980, p. 117-122. 7 refs. Contracts No. NAS2-7882; No. NAS2-8813; No. NAS2-9480.

The University of Wisconsin net flux experiment on the Pioneer Venus mission investigated the distribution of radiative energy deposition and loss which drives atmospheric circulation on Venus. The instrument used an external sensor and a novel method of chopping to measure the net flux of solar and planetary radiation during descent through the thick Venus atmosphere. The sensor, consisting of a high temperature flux plate detector and protective diamond windows, was designed to make accurate flux measurements while exposed to the severe Venus environment. (Author)

A80-31937 * The radius and ellipticity of Uranus from its occultation of SAO 158687. J. L. Elliot, E. Dunham, D. J. Mink (MIT, Cambridge, Mass.), and J. Churms (South African Astronomical Observatory, Cape Town, Republic of South Africa). *Astro physical Journal, Part 1*, vol. 236, Mar. 15, 1980, p. 1026-1030. 35 refs. NSF Grant No. AST-79-08376; Grant No. NSG-2342.

From occultation timings obtained from the Kuiper Airborne Observatory and from Cape Town for Mar. 10, 1977 occultation of SAO 158687 by Uranus, the equatorial radius, R_e , of the planet has been determined to be $26,228 \pm 30$ km and its ellipticity $\epsilon = 1 - R_p/R_e = 0.033 \pm 0.007$. These values refer to the 1.0×10 to the 14th/cu cm number-density level, under the assumption that the upper atmosphere is composed of H₂ and He with a mean molecular weight $\mu = 2.20$. The dominant source of uncertainty is the position of the center of the ring system, which was used to define the center of Uranus in our analysis. A rotation rate of 12.8 ± 1.7 hours for the planet is implied by our value for the ellipticity, under the assumption that Uranus is in hydrostatic equilibrium below the 1.0×10 to the 14th/cu cm number density level. (Author)

A80-34443 * A numerical model of the zonal mean circulation of the middle atmosphere. J. R. Holton and W. M. Wehrbein (Washington, University, Seattle, Wash.). *Pure and Applied Geo-*

S

physics, vol. 118, no. 1-2, 1980, p. 284-306, 30 refs. Grant No. NsG-2228.

The paper presents a simulation of the zonally averaged circulation in the middle atmosphere using a numerical model based on the primitive equations in log pressure coordinates. The circulation is driven radiatively by heating due to solar ultraviolet absorption by ozone and infrared cooling due to carbon dioxide and ozone; Rayleigh friction with a short time constant above 70 km is included to simulate the strong mechanical dissipation which is hypothesized to exist in the vicinity of the mesopause due to turbulence associated with gravity waves and tides near the mesopause.

A.T.

A80-34445 * Preliminary calculations concerning the maintenance of the zonal mean ozone distribution in the Northern Hemisphere. D. M. Cunnold, F. N. Alyea (Georgia Institute of Technology, Atlanta, Ga.), and R. G. Prinn (MIT, Cambridge, Mass.). *Pure and Applied Geophysics*, vol. 118, no. 1-2, 1980, p. 329-354, 39 refs. Grants No. NsG-2010; No. NGR-22-009-729.

Results from a three-dimensional photochemical-dynamical model of ozone are presented and a qualitative description of the maintenance of the ozone distribution and its seasonal variations below 1 mb is given. The transition between photochemical and transport control of the ozone distribution is emphasized. Between 1 and 10 mb, transport by the eddies seems to play only a minor role at mid-latitudes in producing the observed ozone distribution despite the zero correlation between ozone and temperature which occurs in that region. In the lower stratosphere, mean and eddy contributions to ozone change generally strongly offset one another. The buildup and decay of the springtime ozone maximum is discussed. Emphasis is given to the mechanism of ozone transport by the mid-latitude eddies, which play an important role in the springtime accumulation of ozone.

(Author)

A80-34449 * The observed ozone flux by transient eddies, 0-30 km. R. W. Wilcox (Control Data Corp., Minneapolis, Minn.). *Pure and Applied Geophysics*, vol. 118, no. 1-2, 1980, p. 401-415, 28 refs. USAF-supported research; Contract No. NAS2-9578.

Ozone sonde data are matched with concomitant rawinsonde data to provide a direct determination of horizontal, meridional, flux of ozone by the transient eddies. Data are from 27 stations in 4 regions: eastern and western North America, western Europe, and Japan. Results confirm the existence of significant northward flux near 40 deg N, 10-18 km, in winter and spring, as shown by previous investigators. However, areas of significant equatorward flux are found at high mid-latitudes, 10-16 km, over North America in winter and spring, and at all 3 Japanese stations, 10-18 km, in spring. Transient eddy fluxes are typically small in summer, and are also small throughout the troposphere and most of the middle stratosphere.

(Author)

A80-34729 * Simple Cassegrain scanning system for infrared astronomy. J. Apt (California Institute of Technology, Jet Propulsion Laboratory, Earth and Space Sciences Div., Pasadena, Calif.), R. Goody (Harvard University, Cambridge, Mass.), and L. Mertz (Lockheed Solar Observatory, Palo Alto, Calif.). *Applied Optics*, vol. 19, May 15, 1980, p. 1590-1592, 11 refs. Contract No. NAS2-9127; Grant No. NGL-22-007-228.

To meet the need for a reliable, fast imaging system capable of being taken rapidly on and off the telescope, a simple, inexpensive, and compact Cassegrain reimaging system for scanning IR images was constructed. Using commercially available components without requiring close mechanical tolerances, the design solves the problem

of beam stability pointed out by Koornneef and van Overbeeke (1976). For the moving-iron galvanometer scanner, it is noted that at the imaging frequency of 0.5 Hz, hysteresis in image plane motion was found to be less than 0.2 arc sec for a 64-arc sec scan, and the deviation from linearity with a triangular wave input was found to be less than 0.3 arc sec. This system and a scanning secondary were used to image Venus at 11.5 microns, and compared with the scanning secondary, the reimaging system did not appear to contribute any additional noise, considerably improved mechanical reliability, and eliminated cross-scan motion.

J.P.B.

A80-35114 * Two micron spectroscopy and 2.7 mm CO line observations of V645 Cygni. P. M. Harvey and C. J. Lada (Steward Observatory, Tucson, Ariz.). *Astrophysical Journal, Part 1*, vol. 237, Apr. 1, 1980, p. 61-65, 21 refs. Grant No. NGR-03-002-390.

Spectroscopy of V645 Cyg from 1.5 to 2.5 microns and CO line observations at 2.7 mm are presented. A kinematic distance of 6 kpc is derived from the CO line velocity. The strengths of the observed members of the hydrogen Brackett recombination line series are consistent with a spectral type of O9 and an extinction of 4-5 mag to both the line-emitting region and to the exciting star. The infrared continuum is probably produced by thermal emission from hot (about 1000 K) dust. The star is embedded in a 20 pc diameter molecular cloud with a mass not less than 2500 solar masses. The cloud shows CO line broadening in the vicinity of the star and a velocity gradient perpendicular to the plane of polarization of the stellar optical emission. The system has many similarities to R Mon.

(Author)

A80-35234 * The 16- to 38-micron spectrum of Callisto. W. J. Forrest, J. R. Houck, and J. F. McCarthy (Cornell University, Ithaca, N.Y.). *Icarus*, vol. 41, Mar. 1980, p. 340-342, 11 refs. Research supported by the Guggenheim Foundation; Grant No. NGR-33-010-081.

The emission spectrum of Callisto was measured between 16 and 38 microns with a spectral resolution of 1/30 of a wavelength, using the NASA Kuiper Airborne Observatory on the night of October 30-31, 1975. Within the errors, the observed spectrum is like that of a 155 K blackbody, in both shape and absolute intensity. The infrared emission and diameter of Callisto indicate a bolometric Bond albedo of 0.05 ± 0.14 , which is consistent with heating of the surface by absorbed sunlight.

(Author)

A80-36356 * The propagation of Jovian electrons to earth. D. L. Chenette (Chicago, University, Chicago, Ill.). *Journal of Geophysical Research*, vol. 85, May 1, 1980, p. 2243-2256, 43 refs. Contract No. NAS2-6551; Grant No. NGL-14-001-006.

An analysis of the Jovian electron flux increases observed by the earth-orbiting satellite Imp 8 throughout five 13 month Jovian synodic years during the period from launch of the satellite in 1973 to 1979 is presented. The analysis defines the characteristics of Jovian propagation to earth. Corotating interaction regions (CIR) that form at the leading edges of fast solar wind streams continue to modulate the propagation of MeV electrons from Jupiter to the orbit of the earth to produce approximately 27 day recurrent variations in the Jovian electron density. The new and significant result of this study is that these time-intensity profiles are more accurately described not by assumption that Jupiter is a constant source of electrons, but rather by assuming that electron emission is initiated with each passage of CIR by Jupiter with the emission continuing for only several days.

A.T.

A80-36473 * **A Lagrangian mean theory of wave, mean-flow interaction with applications to nonacceleration and its breakdown.** T. Dunkerton (Washington, University, Seattle, Wash.). *Reviews of Geophysics and Space Physics*, vol. 18, May 1980, p. 387-400. 85 refs. Grant No. NSG-2228.

A review is given of new Lagrangian mean theory of wave transport. Attention is focused on the so-called 'nonacceleration' theorem, and it is shown that such a theorem arises naturally in the Lagrangian mean framework. Also discussed is a simple example of the Stokes drift, a concept which is central to nonacceleration. The Lagrangian mean theory substantially simplifies and unifies the understanding of wave driving in cases where nonacceleration is violated because of wave transience and dissipation. Moreover, the theory has given new insights in one particular case, that of Rossby gravity wave, mean-flow interaction. These insights have successfully explained some hitherto unresolved paradoxes in the theory of the quasi-biennial oscillation of zonal wind in the equatorial stratosphere. Some brief remarks are also made concerning some of the outstanding difficulties of the theory in need of future investigation.

(Author)

A80-37277 * **High-resolution Lyman-alpha filtergrams of the sun.** R. M. Bonnet, M. Decaudin (CNRS, Laboratoire de Physique Stellaire et Planétaire, Verrières-le-Buisson, Essonne, France), E. C. Bruner, Jr., L. W. Acton, and W. A. Brown (Lockheed Research Laboratories, Palo Alto, Calif.). *Astrophysical Journal, Part 2 - Letters to the Editor*, vol. 237, Apr. 15, 1980, p. L47-L50. 8 refs. Centre National d'Etudes Spatiales Contracts No. 75-202; No. 79-202; Contract No. NAS2-9181.

The results of an experiment, conducted jointly by the Lockheed Palo Alto Research Laboratory and the Laboratoire de Physique Stellaire et Planétaire du CNRS, which investigated the transition-region plasma and the geometry of coronal active regions, in relation to models of the high-temperature layers, are presented. A Black Brant rocket was used to obtain 1-arc sec resolution L-alpha pictures of the sun, which revealed small scale features not seen previously at this wavelength, that delineate the geometry of the magnetic field in the chromosphere and in the corona. It is concluded that these observations might provide a new way of observing the upper chromosphere and corona, and that they provide direct evidence of the inhomogeneous character of the chromosphere and of the dominant role of the magnetic field.

M.E.P.

A80-37510 * **New gas phase inorganic ion cluster species and their atmospheric implications.** T. D. Märk (Colorado, University, Boulder, Colo.; Innsbruck, Universität, Austria), K. I. Peterson, and A. W. Castleman, Jr. (Colorado, University, Boulder, Colo.). *Nature*, vol. 285, June 5, 1980, p. 392, 393. 8 refs. Österreichischer Fonds zur Förderung der Wissenschaftlichen Forschung Grant No. S-18/08; NSF Grant No. ATM-79-13801; Grant No. NSG-2248.

Recent experimental laboratory observations, with high-pressure mass spectroscopy, have revealed the existence of previously unreported species involving water clustered to sodium dimer ions, and alkali metal hydroxides clustered to alkali metal ions. The important implications of these results concerning the existence of such species are here discussed, as well as how from a practical aspect they confirm the stability of certain cluster species proposed by Ferguson (1978) to explain masses recently detected at upper altitudes using mass spectrometric techniques.

(Author)

A80-40508 * # **Note on the eigensolution of a homogeneous equation with semi-infinite domain.** A. R. Wadia (Texas, University, Arlington, Tex.). *Journal of Computational and Applied Mathematics*, vol. 6, June 1980, p. 161-165. 7 refs. Grant No. NSG-2077.

The 'variation-iteration' method using Green's functions to find the eigenvalues and the corresponding eigenfunctions of a homogeneous Fredholm integral equation is employed for the stability analysis of fluid hydromechanics problems with a semiinfinite (infinite) domain of application. The objective of the study is to develop a suitable numerical approach to the solution of such equations in order to better understand the full set of equations for 'real-world' flow models. The study involves a search for a suitable value of the length of the domain which is a fair finite approximation to infinity, which makes the eigensolution an approximation dependent on the length of the interval chosen. In the examples investigated $\gamma = 1$ seems to be the best approximation of infinity; for γ greater than unity this method fails due to the polynomial nature of Green's functions.

V.L.

A80-40843 * **Relaminarization of fluid flows.** R. Narasimha and K. R. Sreenivasan (Indian Institute of Science, Bangalore, India). In: *Advances in applied mechanics*. Volume 19. (A80-40840 17-31) New York, Academic Press, Inc., 1979, p. 221-309. 140 refs. Research supported by the Indian National Science Academy; Grant No. NSG-2303.

The mechanisms of the relaminarization of turbulent flows are investigated with a view to establishing any general principles that might govern them. Three basic archetypes of reverting flows are considered: the dissipative type, the absorptive type, and the Richardson type exemplified by a turbulent boundary layer subjected to severe acceleration. A number of other different reverting flows are then considered in the light of the analysis of these archetypes, including radial Poiseuille flow, convex boundary layers, flows reverting by rotation, injection, and suction, as well as heated horizontal and vertical gas flows. Magnetohydrodynamic duct flows are also examined. Applications of flow reversion for turbulence control are discussed.

V.L.

A80-45153 * **Modeling Jupiter's current disc - Pioneer 10 outbound.** D. E. Jones (Brigham Young University, Provo, Utah), J. G. Melville, II (U.S. Naval Ocean Systems Center, San Diego, Calif.), and M. L. Blake (Stanford University, Stanford, Calif.). *Journal of Geophysical Research*, vol. 85, July 1, 1980, p. 3329-3336. 33 refs. Contract No. NAS2-7358; Grant No. NSG-2082.

A model of the magnetic field of the Jovian current disk is presented. The model uses Euler functions and the Biot-Savart law applied to a series of concentric, but not necessarily coplanar current rings. It was found that the best fit to the Pioneer 10 outbound perturbation magnetic field data is obtained if the current disk is twisted, and also bent to tend toward parallelism with the Jovigraphic equator. The inner and outer radii of the disk appear to be about 7 and 150 Jovian radii, respectively; because of the observed current disk penetrations, the bent disk also requires a deformation in the form of a bump or wrinkle whose axis tends to exhibit spiraling. Modeling of the azimuthal field shows that it is due to a thin radial

A80-45227 * **The evolution of rapid oscillations in an outburst of a dwarf nova.** R. H. Hildebrand, E. J. Spillar (Chicago, University, Chicago, Ill.), J. Middleditch (California, University, Berkeley, Calif.), J. J. Patterson (Michigan, University, Ann Arbor, Mich.), and R. F. Stiening (Stanford Linear Accelerator Center, Stanford, Calif.). *Astrophysical Journal, Part 2 - Letters to the Editor*, vol. 238, June 15, 1980, p. L145-L148. 14 refs. Research supported by the University of Chicago and U.S. Department of Energy; Grant No. NSG-2057.

High-speed photometric observations of the dwarf nova AH Her on nine consecutive days during an outburst have been made, and rapid coherent oscillations on every day except two near maximum light have been detected. The period, amplitude, and luminosity for

S

each day is presented and the progression of the periods is discussed.
(Author)

A80-45996 * **Eddy diffusion coefficients and the variance of the atmosphere 30-60 km.** G. D. Nastrom, A. D. Belmont (Control Data Corp., Minneapolis, Minn.), and D. E. Brown (Purdue University, West Lafayette, Ind.). *Pure and Applied Geophysics*, vol. 118, no. 5, 1980, p. 1015-1031. 31 refs. Contract No. NAS2-9578.

The results of numerical models or of new observational programs are checked by comparing them with past observations. In view of the differing analysis techniques or differing data samples, the eddy diffusivities presented here agree remarkably well with past estimates. However, in the application of K-values to two-dimensional models, the actual magnitude of the diffusivities is no more important than their spatial patterns, i.e., their gradients with height and latitude. It should thus be noted that the present patterns are often much different from those of past results. T.M.

A80-48811 * **The location of the dayside ionopause of Venus - Pioneer Venus Orbiter magnetometer observations.** R. C. Elphic, C. T. Russell, J. A. Slavin (California, University, Los Angeles, Calif.), L. H. Brace (NASA, Goddard Space Flight Center, Greenbelt, Md.), and A. F. Nagy (Michigan, University, Ann Arbor, Mich.). *Geophysical Research Letters*, vol. 7, Aug. 1980, p. 561-564. 21 refs. Contract No. NAS2-9491.

The location of the dayside Venus ionopause, as observed by the Pioneer Venus Orbiter, is shown to depend on the magnetic pressure in the shocked, highly compressed solar wind plasma just outside the ionopause. Assuming a balance exclusively between this external magnetic pressure and internal ionospheric thermal pressure, invariance of ionospheric conditions, and an isothermal ionosphere, it is possible to determine pressure scale heights for various solar zenith angle intervals. These scale heights yield ionospheric temperatures which agree with direct measurements obtained independently. Not surprisingly, the average ionopause altitude is higher near the terminator, where the average external magnetic pressure is lower. The near-terminator ionopause has much greater positional variability than that at lower solar zenith angles; this appears to be due principally to concomitant variations in the external magnetic pressure, presumably related to solar wind pressure changes. (Author)

A80-48877 * **21 cm maps of Jupiter's radiation belts from all rotational aspects.** I. de Pater (Leiden, Sterrewacht, Leiden, Netherlands). *Astronomy and Astrophysics*, vol. 88, no. 1-2, Aug. 1980, p. 175-183. 28 refs. Grant No. NSG-7264.

Two-dimensional maps of the radio emission from Jupiter were made in December 1977 at a frequency of 1,412 MHz using the Westerbork telescope. Pictures in all four Stokes parameters have been obtained every 15 deg in longitude, each smeared over 15 deg of the planet's rotation. The maps have an E-W resolution of about 1/3 of the diameter of the disk and a N-S resolution 3 times less. The total intensity and linear polarization maps are accurate to 0.5% and the circularly polarized maps to 0.1% of the maximum intensities in I. The whole set of maps clearly shows the existence of higher order terms in the magnetic field of Jupiter. (Author)

A80-49037 * **On the calculation of turbulent heat transport downstream from an abrupt pipe expansion.** C. C. Chieng and B. E. Launder (California, University, Davis, Calif.). *Numerical Heat Transfer*, vol. 3, Apr.-June 1980, p. 189-207. 21 refs. Grant No. NSG-2256.

A numerical study of flow and heat transfer in the separated

flow region produced by an abrupt pipe explosion is reported, with emphasis on the region in the immediate vicinity of the wall where turbulent transport gives way to molecular conduction and diffusion. The analysis is based on a modified TEACH-2E program with the standard k-epsilon model of turbulence. Predictions of the experimental data of Zemanick and Dougall (1970) for a diameter ratio of 0.54 show generally encouraging agreement with experiment. At a diameter ratio of 0.43 different trends are discernable between measurement and calculation, though this appears to be due to effects unconnected with the wall region studied here. B.J.

A80-49185 * **Azimuthal magnetic field at Jupiter.** J. L. Parish, C. K. Goertz, and M. F. Thomsen (Iowa, University, Iowa City, Iowa). *Journal of Geophysical Research*, vol. 85, Aug. 1, 1980, p. 4152-4156. 7 refs. NSF Grant No. ATM-76-82739; Contract No. NAS2-6553.

The azimuthal component of the magnetic field at Jupiter is modeled. A current distribution which is the sum of two currents, one flowing along the magnetic field lines and another injected into the current sheet at $r(0)$ (about 10 Jupiter radii). Two cases are examined, one in which current flows along the field lines into the equatorial plane and then radially outward and a second case in which the only current is that injected into the current sheet at $r(0)$. Each of these two cases results in an azimuthal magnetic field which fits the magnetic field data. (Author)

A80-49217 * **Survival probabilities for interstellar hydrogen flowing into the interplanetary system from far regions of the heliosphere.** J. A. Kunc (Southern California, University, Los Angeles, Calif.). *Planetary and Space Science*, vol. 28, Aug. 1980, p. 815-821. 21 refs. Contract No. NAS2-6558.

The expressions for 'survival' probabilities are presented for an atomic hydrogen particle moving on a trajectory from far regions of the heliosphere to the vicinity of the sun. Three 'destroying' processes have been considered; photoionization, charge transfer and electron ionization. The solar wind has been assumed to be a two-flux steady stream radially expanding with constant flow velocity. Recent profiles of solar-wind electron temperature have been used. The results can be useful for theoretical analyses as well as for analysis of spaceflight observations. (Author)

A80-49362 * **A reanalysis of the observed interplanetary hydrogen L alpha emission profiles and the derived local interstellar gas temperature and velocity.** F. M. Wu and D. L. Judge (Southern California, University, Los Angeles, Calif.). *Astrophysical Journal, Part 1*, vol. 239, July 1, 1980, p. 389-394. 16 refs. Contract No. NAS2-6558.

AMES FUNDED RESEARCH CONFERENCE PAPERS

N80-13561*# California Univ., Los Angeles.
THE SOLAR WIND INTERACTION WITH VENUS c92
C. T. Russell, R. C. Elphic, and J. A. Slavin /in ESA Magnetospheric Boundary Layers Aug. 1979 p 231-239 refs (For primary document see N80-13529 04-42)
(Contract NAS2-9491)

Avail: NTIS HC A18/MF A01; ESA, Paris FF 120 CSDL 03B
The Pioneer Venus orbiter reveals that Venus has a well developed bow shock like the Earth's but on that is significantly

weaker than the Earth's shock. The location of the bow shock is highly variable, more so than would have been expected for an obstacle of essentially fixed size. The altitude of the ionopause is also highly variable in response to changes in the solar wind. In the ionosphere, the field is often low. However, on some orbits, very large fields are seen as low as 150 km, and on most dayside orbits, thin magnetic structures of flux ropes are observed. At night, large fields are often observed which vary from orbit to orbit. Venus has a much smaller intrinsic magnetic moment than expected from scaling the terrestrial moment.

Author (ESA)

N80-17950*# American Science and Engineering, Inc., Cambridge, Mass.

X-RAY BRIGHT POINTS AND THE SOLAR CYCLE DEPENDENCE OF EMERGING MAGNETIC FLUX

John M. Davis. In NASA. Goddard Space Flight Center Study of the Solar Cycle from Space. Feb. 1980 p 65-73 refs (For primary document see N80-17944 08-92)

(Contracts NAS2-8683; NAS5-25496; NAS2-7758)

Avail: NTIS HC A16/MF A01 CSCL 03B

Soft X-ray imaging of the solar corona during the period 1970 to 1978 resulted in significant modifications to the view of the solar cycle with respect to both the properties of the large scale (coronal holes) and small scale (X-ray Bright Points) solar magnetic field. In the latter case, the particular contribution is to the emerging magnetic flux. Sounding rocket observations combined with the Skylab data indicate that the XBP are anticorrelated with sunspot number and are the dominant contributors to the solar cycle. A continuous data set covering a complete cycle would enable the validity of this result which has serious implications for the nature of the solar dynamo, to be confirmed.

Author

N80-27660*# California Univ., Davis.

REYNOLDS STRESS CLOSURES: STATUS AND PROSPECTS

Brian E. Launder. In AGARD Turbulent Boundary Layers Jan. 1980 13 p refs (For primary document see N80-27647 18-34) (Grant NsG-2256)

Avail: NTIS HC A17/MF A01 CSCL 20D

The basic pattern of Reynolds closures and the reason they look as an attractive type of model for practical shear flow calculations is summarized. The relationship between the organized structures and Reynolds stress closures is discussed. An outline given of fundamental developments that are being introduced to extend the modest reliability of Reynolds stress closures. R.C.T.

A80-15225 * Problems and potentialities of cultured plant cells in retrospect and prospect. F. C. Steward and A. D. Krikorian (New York, State University, Stony Brook, N.Y.). In: Plant cell and tissue culture: Principles and applications. Columbus, Ohio State University Press, 1979, p. 221-262. 125 refs. Grants No. NIH-GM-09609; No. NsG-7270; Contract No. NAS2-7846.

The past, present and expected future accomplishments and limitations of plant cell and tissue culture are reviewed. Consideration is given to the pioneering insights of Haberlandt in 1902, the development of culture techniques, and past work on cell division, cell and tissue growth and development, somatic embryogenesis, and metabolism and respiration. Current activity in culture media and technique development for plant regions, organs, tissues, cells, protoplasts, organelles and embryos, totipotency, somatic embryogenesis and clonal propagation under normal and space conditions, biochemical potentialities, and genetic engineering is surveyed. Prospects for the investigation of the induced control of somatic cell division, the division of isolated protoplasts, the improvement of haploid cell cultures, liquid cultures for somatic embryogenesis, and the genetic control of development are outlined.

A.L.W.

A80-15247 * # Design of a one-year lifetime, spaceborne superfluid helium dewar. R. A. Hopkins (Ball Aerospace Systems, Boulder, Colo.). American Society of Mechanical Engineers, Inter-society Conference on Environmental Systems, 9th, San Francisco, Calif., July 16-19, 1979, Paper 79-ENAS-23. 11 p. Members, \$1.50; nonmembers, \$3.00. Contract No. NAS2-9700.

The Infrared Astronomical Satellite is an Explorer Mission and a joint venture of the Netherlands, the United Kingdom, and the United States scheduled for launch into earth orbit in 1981. The cryogenic system is a major part of the satellite; it incorporated many unique and state-of-the-art design features to satisfy the requirements of a one-year orbital lifetime, a focal plane temperature less than 4K, minimal launch weight, and zero-gravity operation. The 60-centimeter diameter telescope is contained within a superfluid helium dewar having a capacity of 540 liters. The telescope aperture cover employs an independent cryogenic system containing a 54-liter supercritical helium tank. The aperture cover, which is ejected two weeks after launch, protects the telescope from contamination and provides the low-temperature background needed to perform focal plane health checks. Design and predicted performance of the cryogenic systems are discussed in detail.

(Author)

A80-17468 * Pioneer-Venus solar flux radiometer. J. M. Palmer (Arizona, University, Tucson, Ariz.) In: Space optics; Proceedings of the Seminar, Huntsville, Ala., May 22-24, 1979. (A80-17432 05-89) Bellingham, Wash., Society of Photo-Optical Instrumentation Engineers, 1979, p. 305-311. Contract No. NAS2-8818.

The paper presents the design and performance characteristics of the Solar Flux Radiometer flown on the Large Probe of the Pioneer-Venus Multiprobe spacecraft. Radiance measurements of the Venusian atmosphere in spectral channels between 400 and 1800 nm as a function of altitude were made, along with elevation and azimuthal measurements of the radiation field performed with five optical channels. Filtered Si and Ge photovoltaic detector output currents were processed with logarithmic transimpedance converters prior to being multiplexed and digitized. Atmospheric sampling in elevation and azimuth was done according to a Gaussian integration scheme; the received data were used to determine the deposition of solar energy in the Venus atmosphere along with upward and downward fluxes and radiances with an altitude resolution of several hundred meters between 67 km and the surface.

A.T.

A80-17502 * X-ray spectrometer spectrograph telescope system. E. C. Bruner, Jr., L. W. Acton, W. A. Brown, S. W. Salat (Lockheed Research Laboratories, Palo Alto, Calif.), A. Franks (Aeronautical Research Council, National Physical Laboratory, Teddington, Middx., England), G. Schmidtke, W. Schweizer (Fraunhofer-Gesellschaft zur Förderung der angewandten Forschung, Institut für physikalische Weltraumforschung, Freiburg im Breisgau, West Germany), and R. J. Speer (Imperial College of Science and Technology, London, England). In: Space optics: Imaging X-ray optics workshop; Proceedings of the Seminar, Huntsville, Ala., May 22-24, 1979. (A80-17469 05-89) Bellingham, Wash., Society of Photo-Optical Instrumentation Engineers, 1979, p. 270-277. Research supported by the Lockheed Independent Research Program; Contract No. NAS2-9181.

A new sounding rocket payload that has been developed for X-ray spectroscopic studies of the solar corona is described. The instrument incorporates a grazing incidence Rowland mounted grating spectrograph and an extreme off-axis parabolic sector feed system to isolate regions of the sun of order 1×10 arc seconds in size. The focal surface of the spectrograph is shared by photographic and photoelectric detection systems, with the latter serving as a part of the rocket pointing system control loop. Fabrication and alignment of the optical system is based on high precision machining and mechanical metrology techniques. The spectrograph has a

resolution of 16 milliangstroms and modifications planned for future flights will improve the resolution to 5 milliangstroms, permitting line widths to be measured. (Author)

A80-17503 * Paraboloidal X-ray telescope mirror for solar coronal spectroscopy. W. A. Brown, E. C. Bruner, Jr., L. W. Acton (Lockheed Research Laboratories, Palo Alto, Calif.), A. Franks, M. Stedman (Aeronautical Research Council, National Physical Laboratory, Teddington, Middx., England), and R. J. Speer (Imperial College of Science and Technology, London, England). In: Space optics: Imaging X-ray optics workshop; Proceedings of the Seminar, Huntsville, Ala., May 22-24, 1979. (A80-17469 05-89) Bellingham, Wash., Society of Photo-Optical Instrumentation Engineers, 1979, p. 278-284. Research supported by the Lockheed Independent Research Program; Contract No. NAS2-9181.

The telescope mirror for the X-ray Spectrograph Spectrometer Telescope System is a sixty degree sector of an extreme off-axis paraboloid of revolution. It was designed to focus a coronal region 1 by 10 arc seconds in size on the entrance slit of the spectrometer after reflection from the gold surface. This paper discusses the design, manufacture, and metrology of the mirror, the methods of precision mechanical metrology used to focus the system, and the mounting system which locates the mirror and has proven itself through vibration tests. In addition, the results of reflection efficiency measurements, alignment tolerances, and ray trace analysis of the effects of misalignment are considered. (Author)

A80-18618 * # Evaluation of the time dependent surface shear stress in turbulent flows. V. A. Sandborn (Colorado State University, Fort Collins, Colo.). *American Society of Mechanical Engineers, Winter Annual Meeting, New York, N.Y., Dec. 2-7, 1979, Paper 79-WA/FE-17.* 7 p. 11 refs. Members, \$1.50; nonmembers, \$3.00. U.S. Department of Agriculture Contract No. 16-477-CA; NSF Grant No. ENG-76-05-896; Grant No. NCA2-OR165-604.

The time dependent surface shear stress has been evaluated using surface heat transfer measurements. For fully developed turbulent pipe and open channel water flows, and incompressible and compressible turbulent boundary layer air flows the measurements indicate the absolute magnitude of the surface shear stress fluctuations will be greater than two times the mean values. The root-mean-square shear stress fluctuations were of the order of 0.2 to 0.4 times the mean surface shear values. Due to these large surface shear stress fluctuations and the nonlinear relation between heat transfer and shear stress, a special technique has been developed to evaluate the measurements. It was found that the non-linear averaging errors for a hot film-surface shear stress gauge in a fully developed pipe flow was of the order of 10 percent at low velocities. A hot wire-surface shear stress gauge was employed for measurements of turbulent boundary layers in air. (Author)

A80-21141 * Time-temperature behavior of a unidirectional graphite/epoxy composite. Y. T. Yeow (Allied Chemical Corp., Morristown, N.J.), D. H. Morris, and H. F. Brinson (Virginia Polytechnic Institute and State University, Blacksburg, Va.). In: Composite materials: Testing and design; Proceedings of the Fifth Conference, New Orleans, La., March 20-22, 1978. (A80-21126 07-24) Philadelphia, Pa., American Society for Testing and Materials, 1979, p. 263-281. 19 refs. Grant No. NSG-2038.

A testing program to determine the time-temperature response of unidirectional T300/934 graphite/epoxy materials is presented. The short-term creep test results of tension specimens with the load

at various angles to the fiber direction and at various temperatures are reported, showing that the material is elastic at all temperatures when the fiber is in the load direction. However, when the load is transverse to the fibers, the viscoelastic response varies from small amounts at room temperature to large amounts at temperatures above the 180 C transition temperature. The time-temperature superposition principle or the method of reduced variables were used to determine compliance master curves for each fiber angle, and a viscoelastic analog to the elastic orthotropic transformation equation was used incrementally to predict the master curves for the tensile compliance of the off-axis specimen. A.T.

A80-23690 * Initial Pioneer Venus magnetometer observations. C. T. Russell, R. C. Elphic, and J. A. Slavin (California, University, Los Angeles, Calif.). In: Lunar and Planetary Science Conference, 10th, Houston, Tex., March 19-23, 1979, Proceedings. Volume 3. (A80-23677 08-91) New York, Pergamon Press, Inc., 1979, p. 2277-2290. 20 refs. Contract No. NAS2-9491.

Initial Pioneer Venus magnetometer observations reveal a highly dynamic interaction between the solar wind and the ionosphere and a very weak and possibly absent intrinsic magnetic field. The bow shock position and the altitude of the ionopause vary markedly from day to day. The magnetic pressure in the magnetosheath just outside the ionopause is in near balance with the thermal ionospheric pressure inside. Although the ionospheric magnetic field strength is generally low, occasional enhancements are observed with field strengths exceeding that in the magnetosheath. These bundles of magnetic flux, or flux ropes, may be convected to the night side ionosphere in which large field strengths (compared to the dayside) are common. The magnetic field magnitude and direction in this region are quite variable, suggesting that the field is not due to an intrinsic planetary source, but rather due to induced ionospheric currents. The magnetic moment is probably much less than 10 to the 22nd Gauss-cu cm. (Author)

A80-25595 * Using guided clustering techniques to analyze Landsat data for mapping forest land cover in northern California. L. Fox, III and K. E. Mayer (Humboldt State University, Arcata, Calif.). In: Machine processing of remotely sensed data; Proceedings of the Fifth Annual Symposium, West Lafayette, Ind., June 27-29, 1979. (A80-25561 09-43) New York, Institute of Electrical and Electronics Engineers, Inc., 1979, p. 364-367. 8 refs. Grants No. NSG-2244; No. NSG-2341.

A80-26694 * Application of the method of integral relations to unsteady fluid flow problems with shocks. A. R. Wadia and F. R. Payne (Texas, University, Arlington, Tex.). In: Advances in computer methods for partial differential equations - III; Proceedings of the Third International Symposium, Bethlehem, Pa., June 20-22, 1979. (A80-26663 09-64) New Brunswick, N.J., International Association for Mathematics and Computers in Simulation, 1979, p. 205-213. 16 refs. Grant No. NSG-2077.

A mixed method using both the method of integral relations and the finite difference technique is developed for the solution of unsteady flow problems. The integral relations method is based upon a chosen interpolating function dependent only on the time domain. The resulting local semidiscrete finite element equations obtained are assembled into a global form. The spatial derivatives at the nodes are replaced by finite difference operators and the discretized nonlinear algebraic system is solved by an iterative scheme. Solutions are obtained for the one-dimensional gasdynamics equation, the one-dimensional wave equation and Burger's model of turbulence. Agreement with other numerical and analytical solutions is excellent for the gasdynamics problem and satisfactory for the Burger equation in cases of small viscous effects. (Author)

A80-27435 * Landsat-based multiphase estimation of California's irrigated lands. S. L. Wall, R. W. Thomas (California, University, Berkeley, Calif.), and L. R. Tinney (California, University, Santa Barbara, Calif.). In: American Society of Photogrammetry and American Congress on Surveying and Mapping, Fall Technical Meeting, Sioux Falls, S. Dak., September 17-21, 1979, Joint Proceedings. (A80-27426 10-43) Falls Church, Va., American Society of Photogrammetry, 1979, p. 221-236. 6 refs. Grant No. NSG-2207; Contract No. NAS5-20969.

Currently, inventory of California's irrigated lands is performed on a seven year cycle. Since 1975, the University of California in cooperation with NASA and the California Department of Water Resources has been developing and testing techniques to utilize a Landsat based remote sensing system to produce statewide estimates in a single year. The proposed system utilizes multiphase sampling, stratification and multitemporal Landsat imagery to produce the estimate. Early research concentrated on regional estimates to develop the techniques. This year, an inventory of the entire state of California is being performed. In addition, research on the utilization of digital analysis for estimating irrigated acreage and the determination of specific crop types (manual and digital analysis) is also underway. (Author)

A80-34757 * Studies for improved high temperature coatings for Space Shuttle application. J. Creedon, R. Banas, and S. H. Garofalini (Lockheed Missiles and Space Co., Inc., Space Systems Div., Sunnyvale, Calif.). In: New horizons - Materials and processes for the eighties; Proceedings of the Eleventh National Conference, Boston, Mass., November 13-15, 1979. (A80-34751 14-23) Azusa, Calif., Society for the Advancement of Material and Process Engineering, 1979, p. 82-93. 7 refs. Contract No. NAS2-9809.

Improvement of the current Class 2 Space Shuttle Orbiter RCG coating was experimentally investigated. Coatings, which are applied to LI-900 or LI-2200 tiles, were prepared to provide increased performance in thermal expansion, impact, residual strain and increased viscosity. Turbulent duct arc-plasma tests at NASA/Ames Research Center are continuing on two candidates that show improved low residual strain and increased high temperature viscosity. A coating system with lower fusion-temperature (1950 F) was identified which has the potential of improving tile yield through reduced LI-900 shrinkage and distortion since it can be fused at 250 F lower than the present Class 2 coating. (Author)

A80-34760 * Development of high viscosity coatings for advanced Space Shuttle applications. S. H. Garofalini, R. Banas, and J. Creedon (Lockheed Missiles and Space Co., Space Systems Div., Sunnyvale, Calif.). In: New horizons - Materials and processes for the eighties; Proceedings of the Eleventh National Conference, Boston, Mass., November 13-15, 1979. (A80-34751 14-23) Azusa, Calif., Society for the Advancement of Material and Process Engineering, 1979, p. 114-124. 6 refs. Contract No. NAS2-9809.

Laboratory studies for increasing the thermal resistance of high viscosity coatings for silica reusable surface insulation are presented. The coatings are intended for the reentry temperature associated with advanced Space Shuttle applications which will involve aerodynamic shear forces during entry from earth orbits. Coating viscosity was increased by (1) reduction in the concentration of the low viscosity additive B2O3; (2) reduction in the particle size of the constituent powders in coatings; and (3) addition of a high viscosity glass former (GeO2). A coating system was produced by combining the three methods which showed apparent higher viscosity than the current coating, while satisfying all the current Shuttle Orbiter coating requirements. A.T.

A80-40233 * Narrow-field radiometry in a quasi-isotropic atmosphere. A. Holmes, J. M. Palmer, and M. G. Tomasko (Arizona, University, Tucson, Ariz.). In: Measurements of optical radiations; Proceedings of the Seminar, San Diego, Calif., August 29, 30, 1979. (A80-40229 16-35) Bellingham, Wash., Society of Photo-Optical Instrumentation Engineers, 1979, p. 27-32. 9 refs. Contract No. NAS2-9486.

If a radiometer having a narrow field of view is used to measure the radiance of a source such as a quasi-isotropic atmosphere, a knowledge of the out-of-field responsivity is critical. For example, if a radiometer with a field of view of 5 deg (full-angle) has a relative responsivity of 0.0001 for the out-of-field radiation, the contribution of the out-of-field radiation (assuming an isotropic source subtending 2 steradians) is 10.5% of the total signal. Either the stray light suppression of the radiometer must be extremely high or methods of determining the out-of-field response must be developed. A description of one method of determining the effect of out-of-field response and its application to a planetary atmospheric radiometer is presented. (Author)

A80-41466 * # Thermal design of a Shuttle infrared telescope facility (SIRTF). R. Stoll (Perkin-Elmer Corp., Optical Technology Div., Danbury, Conn.) and S. Willen (Beach Aircraft Corp., Boulder, Colo.). American Institute of Aeronautics and Astronautics, Thermophysics Conference, 15th, Snowmass, Colo., July 14-16, 1980, Paper 80-1502. 6 p. Contract No. NAS2-10066.

A thermal design concept has been developed for a cryogenically-cooled infrared telescope facility which will be carried aboard the Space Shuttle for missions of 14 to 30 days. Supercritical helium at 6 K is the principal coolant. Auxiliary tanks of superfluid helium at 2 K are utilized to provide additional low-temperature cooling requirements of specific instruments. The preliminary thermal design described enables SIRTF to provide the low-temperature environment for the telescope and instruments, while maintaining thermally-induced optical degradations within acceptable limits with a cryogen utilization rate compatible with weight and volumetric constraints. (Author)

A80-41495 * # Free convection in enclosures exposed to compressive heating. R. P. Bobco (Hughes Aircraft Co., Space and Communications Group, Los Angeles, Calif.). American Institute of Aeronautics and Astronautics, Thermophysics Conference, 15th, Snowmass, Colo., July 14-16, 1980, Paper 80-1536. 12 p. 8 refs. Contract No. NAS2-10000.

An experimental study of heat transfer in a vertical annulus and a three-dimensional gap used to establish the influence of compressive heating on the convective process in enclosures is presented. Test runs were made using helium gas with compressive rates of 6, 15, and 30 psi/min. Temperature and pressure histories were reduced to film coefficients based on nodal modeling of the test geometries. The data are correlated in terms of free convection parameters. The heat transfer correlations show virtually no influence of compression rate and only a slight dependence on geometry. The correlations will be applied to the design of a vented Galileo mission descent module parachuting into the Jupiter atmosphere. M.E.P.

A80-48179 * # Photocell heat engine solar power systems. R. T. Taussig, T. S. Vaidyanathan, S. Hoverson, C. Bruzzone (Mathematical Sciences Northwest, Inc., Bellevue, Wash.), and W. Christiansen (Washington, University, Seattle, Wash.). In: Energy to the 21st

century; Proceedings of the Fifteenth Intersociety Energy Conversion Engineering Conference, Seattle, Wash., August 18-22, 1980. Volume 1. (A80-48165 21-44) New York, American Institute of Aeronautics and Astronautics, Inc., 1980, p. 119-124. 12 refs. Contract No. NAS2-10079.

A combined photocell heat engine concept is proposed for high efficiency solar energy conversion in space. In this concept the short wavelength portion of the solar spectrum is split by a dichroic filter and sent to a bank of photocells. The long wave-length remainder of the spectrum is used by the heat engine. This technique allows the photocells to operate with the minimum amount of waste heat, increasing their efficiency and reducing the amount of cooling

A80-48757 * # Materials for fire resistant passenger seats in aircraft. G. Tesoro and A. Moussa (MIT, Cambridge, Mass.). In: Fire retardants; Proceedings of the European Conference on Flammability and Fire Retardants, Copenhagen, Denmark, July 13, 14, 1978. (A80-48751 21-27) Westport, Conn., Technomic Publishing Co., Inc., 1980, p. 159-173. 11 refs. Contract No. NAS2-9610.

The paper considers the selection of cushioning foam and upholstery fabric materials for aircraft passenger seats. Polyurethane, polychloroprene, polyimide, and polyphosphazene are the foam materials considered; and a variety of commercial and developmental fabrics (including wool, cotton, synthetics, and blends) are examined. Viable approaches to the design of fire-resistant seat assemblies are indicated. Results of an experimental laboratory study of fabrics and fabric/foam assemblies exposed to external point-source radiative heat flux are discussed. B.J.

A80-49235 * # Direct numerical simulations of the turbulent wake of an axisymmetric body. J. J. Riley and R. W. Metcalfe (Flow Research Co., Kent, Wash.). In: Symposium on Turbulent Shear Flows, 2nd, London, England, July 2-4, 1979, Proceedings. (A80-49226 21-34) London, Imperial College of Science and Technology, 1979, p. 2.18-2.23. 14 refs. Contract No. NAS2-9855.

The paper presents comparisons of results of direct numerical simulations of turbulence with both laboratory data and self-similarity theory for the case of the turbulent wakes of towed, axisymmetric bodies. In general, the agreement of the simulation results with both the laboratory data and the self-similarity theory is good, although the comparisons are hampered by inadequate procedures for initializing the numerical simulations. (Author)

A80-49277 * # Multiple-time-scale concepts in turbulent transport modelling. K. Hanjalic, B. E. Launder, and R. Schiestel (California, University, Davis, Calif.). In: Symposium on Turbulent Shear Flows, 2nd, London, England, July 2-4, 1979, Proceedings. (A80-49226 21-34) London, Imperial College of Science and Technology, 1979, p. 10.31-10.36. 15 refs. Grant No. NSG-2256.

The paper reports progress in developing a closure employing two or more independently calculated time scales with which to characterize the rates of progress of different turbulent interactions. The approach contrasts with that used by earlier single-point models which adopt just a single time scale, proportional to the turbulence energy turnover time. The present treatment divides the energy containing part of the spectrum into two regions which respond at different rates and in different ways to changes in the environment. Computational results are reported for several thin shear flows which show striking improvement in the level of agreement with experiment over that obtained with models employing only one time scale. (Author)

A80-53209 * The acceleration of energetic charged particles by interplanetary and supernova shock waves. M. E. Pesses (Iowa, University, Iowa City, Iowa). In: Particle acceleration mechanisms in astrophysics; Proceedings of the Workshop, La Jolla, Calif., January 3-5, 1979. (A80-53201 24-90) New York, American Institute of Physics, 1979, p. 107-113. 11 refs. Contract No. NAS2-6553.

PATENTS

N80-16116* National Aeronautics and Space Administration. Ames Research Center, Moffett Field, Calif.

CATALYSTS FOR POLYIMIDE FOAMS FROM AROMATIC ISOCYANATES AND AROMATIC DIANHYDRIDES Patent Salvatore R. Riccitiello, Paul M. Sawko, and Carlos A. Estrella, inventors (to NASA) Issued 4 Dec. 1979 5 p Filed 24 Feb. 1978 Supersedes N78-221156 (16 - 13, p 1674) (NASA-Case-ARC-11107-1; US-Patent-4,177,333; US-Patent-Appl-SN-883961; US-Patent-Class-521-124; US-Patent-Class-521-125; US-Patent-Class-521-127; US-Patent-Class-521-157; US-Patent-Class-528-73) Avail: US Patent and Trademark Office CSCL 07D

Polyimide foam products having greatly improved burn-through and flame-spread resistance are prepared by the reaction of aromatic polyisocyanates with aromatic dianhydrides in the presence of metallic salts of octoic acid. The salts, for example stannous octoate, ferric octoate and aluminum octoate, favor the formation of imide linkages at the expense of other possible reactions.

Official Gazette of the U.S. Patent and Trademark Office

N80-18393* National Aeronautics and Space Administration. Ames Research Center, Moffett Field, Calif.

CRYOGENIC CONTAINER COMPOUND SUSPENSION STRAP Patent

John W. Vorreiter, inventor (to NASA) Issued 22 Jan. 1980 5 p Filed 22 Aug. 1978 Supersedes N79-18087 (17 - 09, p 1109) (NASA-Case-ARC-11157-1; US-Patent-4,184,609; US-Patent-Appl-SN-935827; US-Patent-Class-220-445; US-Patent-Class-220-423; US-Patent-Class-220-901) Avail: US Patent and Trademark Office CSCL 13I

A support strap for use in a cryogenic storage vessel for supporting the inner shell from the outer shell with a minimum heat leak is presented. The compound suspension strap is made from a unidirectional fiberglass epoxy composite material with an ultimate tensile strength and fatigue strength which are approximately doubled when the material is cooled to a cryogenic temperature.

Official Gazette of the U.S. Patent and Trademark Office

N80-26298* National Aeronautics and Space Administration. Ames Research Center, Moffett Field, Calif.

REDUCTION OF NITRIC OXIDE EMISSIONS FROM A COMBUSTOR Patent

Roger A. Craig and Huw O. Pritchard, inventors (to NASA) Issued 27 May 1980 6 p Filed 8 Sep. 1977 Supersedes N77-31260 (15 - 22, p 2912) Continuation of abandoned US Patent Appl. SN-684045, filed 7 May 1976 (NASA-Case-ARC-10814-2; US-Patent-4,204,402; US-Patent-Appl-SN-831632; US-Patent-Class-60-39.06; US-Patent-Class-60-733; US-Patent-Class-60-746; US-Patent-Appl-SN-684045) Avail: US Patent and Trademark Office CSCL 21E

A turbojet combustor and method for controlling nitric oxide emissions by employing successive combustion zones is described.

After combustion of an initial portion of the fuel in a primary combustion zone, the combustion products of the primary zone are combined with the remaining portion of fuel and additional plenum air and burned in a secondary combustion zone under conditions that result in low nitric oxide emissions. Low nitric oxide emissions are achieved by a novel turbojet combustor arrangement which provides flame stability by allowing stable combustion to be accompanied by low nitric oxide emissions resulting from controlled fuel-lean combustion (ignited by the emission products from the primary zone) in a secondary combustion zone at a lower combustion temperature resulting in low emission of nitric oxide.

Official Gazette of the U.S. Patent and Trademark Office

S

LIFE SCIENCES

NASA FORMAL REPORTS

N80-15821*# National Aeronautics and Space Administration. Ames Research Center, Moffett Field, Calif.

SOME HUMAN FACTORS ISSUES IN THE DEVELOPMENT AND EVALUATION OF COCKPIT ALERTING AND WARNING SYSTEMS

Robert J. Randle, Jr., William E. Larsen, and Douglas H. Williams
Washington Jan. 1980 65 p refs
(NASA-RP-1055; A-7696) Avail: NTIS HC A04/MF A01 CSCL 05H

A set of general guidelines for evaluating a newly developed cockpit alerting and warning system in terms of human factors issues are provided. Although the discussion centers around a general methodology, it is made specifically to the issues involved in alerting systems. An overall statement of the current operational problem is presented. Human factors problems with reference to existing alerting and warning systems are described. The methodology for proceeding through system development to system test is discussed. The differences between traditional human factors laboratory evaluations and those required for evaluation of complex man-machine systems under development are emphasized. Performance evaluation in the alerting and warning subsystem using a hypothetical sample system is explained. R.C.T.

interaction in mean decision time between wind shear, day-night, and ceiling RVR variables occurred; (4) mean number of head-up transitions to VFR conditions after breakout ranged from 4.6 to 13.4 and increased as a function of ceiling and severity of wind shear; the typical duration of fixation out the window was 1.5 sec; and (5) subjective pilot ratings of controllability and precision of control as well as amount of skill, attention, or effort required to make the landing were influenced significantly by the wind shear, night conditions, and low breakout ceiling conditions.

R.E.S.

N80-28349*# National Aeronautics and Space Administration. Ames Research Center, Moffett Field, Calif.

AN EXPERIMENTAL EVALUATION OF HEAD-UP DISPLAY FORMATS

J. M. Naish and Donna L. Miller (Informatics, Inc., Palo Alto, Calif.) Jul. 1980 78 p refs
(NASA-TP-1550; A-7970) Avail: NTIS HC A05/MF A01 CSCL 01D

Three types of head-up display format are investigated. Type 1 is an unreferenced (conventional) flight director, type 2 is a ground referenced flight path display, and type 3 is a ground referenced director. Formats are generated by computer and presented by reflecting collimation against a simulated forward view in flight. Pilots, holding commercial licenses, fly approaches in the instrument flight mode and in a combined instrument and visual flight mode. The approaches are in wind shear with varied conditions of visibility, offset, and turbulence. The displays are equivalent in pure tracking but there is a slight advantage for the unreferenced director in poor conditions. Flight path displays are better for tracking in the combined flight mode, possibly because of poor director control laws and the division of attention between superimposed fields. Workloads is better for the type 2 displays. The flight path and referenced director displays are criticized for effects of symbol motion and field limiting. In the subjective judgment of pilots familiar with the director displays, they are rated clearly better than path displays, with a preference for the unreferenced director. There is a fair division of attention between superimposed fields. Author

N80-22283*# National Aeronautics and Space Administration. Ames Research Center, Moffett Field, Calif.

RESOURCE MANAGEMENT ON THE FLIGHT DECK

George E. Cooper, ed., Maurice D. White, ed. (Cooper (George E.), Saratoga, Calif.), and John K. Lauber, ed. Mar. 1980 247 p ref Proceedings of a NASA/Industry Workshop, San Francisco, 26-28 Jun. 1979
(NASA-CP-2120) Avail: NTIS HC A11/MF A01 CSCL 05J

Several approaches to the training and selection of aircrew are presented including both industry and nonindustry perspectives. Human factor aspects of the problem are also examined with specific emphasis on the psychology of the flight deck situation. For individual titles, see N80-22284 through N80-22292.

N80-26039*# National Aeronautics and Space Administration. Ames Research Center, Moffett Field, Calif.

HEAD-UP TRANSITION BEHAVIOR OF PILOTS DURING SIMULATED LOW-VISIBILITY APPROACHES

Richard F. Haines Jun. 1980 35 p refs
(NASA-TP-1618; A-8057) Avail: NTIS HC A03/MF A01 CSCL 05H

Each of 13 commercial pilots from four airlines flew a total of 108 manual flight director approaches in a moving base simulation of a medium-sized turbojet (95,000 lb gross weight) which had a day and night Redifon external scene. Three levels of runway visual range (RVR) (1,600; 2,400; and greater than 8,000 ft), three wind-shear profiles, nine ceiling heights, and continuous and intermittent visibility after initial breakout were tested. The results indicated that: (1) mean decision time ranged from 2 to 4.6 sec for ceilings under 380 ft across the three RVR conditions; (2) mean vertical distance traveled during the visual-cue assessment period was a relatively constant proportion below the existing ceiling; (3) a significant three way

N80-34099*# National Aeronautics and Space Administration. Ames Research Center, Moffett Field, Calif.

EFFECTS OF MAGNIFICATION AND VISUAL ACCOMMODATION ON AIMPOINT ESTIMATION IN SIMULATED LANDINGS WITH REAL AND VIRTUAL IMAGE DISPLAYS

Robert J. Randle, Stanley N. Roscoe (New Mexico State Univ., Las Cruces), and John C. Pettitt (California Univ., San Diego) Oct. 1980 29 p refs
(NASA-TP-1635; A-8104) Avail: NTIS HC A03/MF A01 CSCL 05I

Twenty professional pilots observed a computer-generated airport scene during simulated autopilot-coupled night landing approaches and at two points (20 sec and 10 sec before touchdown) judged whether the airplane would undershoot or overshoot the aimpoint. Visual accommodation was continuously measured using an automatic infrared optometer. Experimental variables included approach slope angle, display magnification, visual focus demand (using ophthalmic lenses), and presentation

of the display as either a real (direct view) or a virtual (collimated) image. Aimpoint judgments shifted predictably with actual approach slope and display magnification. Both pilot judgments and measured accommodation interacted with focus demand with real-image displays but not with virtual-image displays. With either type of display, measured accommodation lagged far behind focus demand and was reliably less responsive to the virtual images. Pilot judgments shifted dramatically from an overwhelming perceived-overshoot bias 20 sec before touchdown to a reliable undershoot bias 10 sec later. Author

NASA TECHNICAL MEMORANDA

N80-18010*# National Aeronautics and Space Administration. Ames Research Center, Moffett Field, Calif.

NASA AVIATION SAFETY REPORTING SYSTEM Quarterly Report, 1 Apr. - 30 Jun. 1978

Jun. 1979 54 p refs Prepared in cooperation with Battelle Columbus Labs., Mountain View, Calif.

(NASA-TM-78608; A-7904; QR-9) Avail: NTIS HC A04/MF A01 CSCL 01C

The human factors frequency considered a cause of or contributor to hazardous events onboard air carriers are examined with emphasis on distractions. Safety reports that have been analyzed, processed, and entered into the aviation safety reporting system data base are discussed. A sampling of alert bulletins and responses to them is also presented. J.M.S.

N80-18038*# National Aeronautics and Space Administration. Ames Research Center, Moffett Field, Calif.

THE EFFECT OF VIEWING TIME, TIME TO ENCOUNTER, AND PRACTICE ON PERCEPTION OF AIRCRAFT SEPARATION ON A COCKPIT DISPLAY OF TRAFFIC INFORMATION

Sharon O'Connor, Everett Palmer, Daniel Baty, and Sharon Jago Feb. 1980 17 p refs Prepared in cooperation with San Jose State Univ., Calif.

(Grant NSG-2269) (NASA-TM-81173; A-8072) Avail: NTIS HC A02/MF A01 CSCL 01D

The concept of a cockpit display of traffic information (CDTI) includes the integration of air traffic, navigation, and other pertinent information in a single electronic display in the cockpit. Two studies were conducted to develop a clear and concise display format for use in later full-mission simulator evaluations of the CDTI concept. Subjects were required to monitor a CDTI for specified periods of time and to make perceptual judgments concerning the future position of a single intruder aircraft in relationship to their own aircraft. Experimental variables included: type of predictor information displayed on the two aircraft symbols; time to encounter point; length of time subjects viewed the display; amount of practice; and type of encounter (straight or turning). Results show that length of viewing time had little or no effect on performance; time to encounter influenced performance with the straight predictor but did not with the curved predictor; and that learning occurred under all conditions. R.E.S.

N80-18680*# National Aeronautics and Space Administration. Ames Research Center, Moffett Field, Calif.

THE CARBON ISOTOPE BIOGEOCHEMISTRY OF THE INDIVIDUAL HYDROCARBONS IN BAT GUANO AND THE ECOLOGY OF INSECTIVOROUS BATS IN THE REGION OF CARLSBAD, NEW MEXICO

David J. DesMarais, J. M. Mitchell (Indiana Univ., Bloomington), W. G. Meinschein (Indiana Univ., Bloomington), and J. M. Hayes Feb. 1980 46 p refs

(NASA-TM-81164; A-8056) Avail: NTIS HC A03/MF A01 CSCL 06C

The structures and C-13 contents of individual alkanes extracted from bat guano found in the Carlsbad region of New Mexico can be related to both the photosynthetic pathways of the local plants and the feeding habits of the insects that support the bats. Carbon isotopic analyses of the 62 most important plant species in the Pecos River Valley, the most significant feeding area for the Carlsbad bats, reveal the presence of 29 species with C3 photosynthesis and 33 species, mostly grasses, with C4 photosynthesis. Although the abundances of nonagricultural C3 and C4 plants are similar, alfalfa and cotton, both C3 plants, constitute over 95 per cent of the crop biomass. The molecular composition of the bat guano hydrocarbons is fully consistent with an insect origin. Two isotopically distinct groups of insect branched alkanes were discerned. These two groups of alkanes derived from two chemotaxonomically distinct populations of insects possessing distinctly different feeding habits. It is likely that one population grazes predominantly on crops whereas the other population prefers native vegetation. This and other isotopic evidence supports the notion that crop pests constitute a major percentage of the bats' diet. Author

N80-18710*# National Aeronautics and Space Administration. Ames Research Center, Moffett Field, Calif.

COSMOS 81 US/USSR CARDIOVASCULAR STUDY: EXPERIMENT IMPLEMENTATION PLAN

John W. Hines Feb. 1980 14 p

(NASA-TM-81178) Avail: NTIS HC A02/MF A01 CSCL 06B

The experimental activities to be undertaken in the accomplishment of the Cosmos 81 Primate Study are discussed. A detailed description of the specific tasks to be performed, approaches, options, and tradeoffs to be considered, and personnel assigned is presented. The main project is to chronically instrument the carotid artery (flow, pressure) using Rhesus monkeys and interpret the results. R.E.S.

N80-19792*# National Aeronautics and Space Administration. Ames Research Center, Moffett Field, Calif.

EFFECT OF FIELD OF VIEW AND MONOCULAR VIEWING ON ANGULAR SIZE JUDGEMENTS IN AN OUTDOOR SCENE

Edward A. Denz (San Jose State Univ., Calif.), Everett A. Palmer, and Stephen R. Ellis Feb. 1980 20 p refs

(Grant NSG-2269) (NASA-TM-81176; A-8083) Avail: NTIS HC A02/MF A01 CSCL 05I

Observers typically overestimate the angular size of distant objects. Significantly, overestimations are greater in outdoor settings than in aircraft visual-scene simulators. The effect of field of view and monocular and binocular viewing conditions on angular size estimation in an outdoor field was examined. Subjects adjusted the size of a variable triangle to match the angular size of a standard triangle set at three greater distances. Goggles were used to vary the field of view from 11.5 deg to 90 deg for both monocular and binocular viewing. In addition, an unrestricted monocular and binocular viewing condition was used. It is concluded that neither restricted fields of view similar to those present in visual simulators nor the restriction of monocular viewing causes a significant loss in depth perception in outdoor settings. Thus, neither factor should significantly affect the depth realism of visual simulators. Author

N80-25108*# National Aeronautics and Space Administration. Ames Research Center, Moffett Field, Calif.

MODIFIED ITERATIVE EXTENDED HUECKEL 1: THEORY

S. Aronowitz Apr. 1980 26 p refs 2 Vol.

(NASA-TM-81200; A-8183) Avail: NTIS HC A03/MF A01 CSCL 20H

Iterative Extended Hueckel is modified by inclusion of explicit effective internuclear and electronic interactions. The one electron energies are shown to obey a variational principle because of the form of the effective electronic interactions. The modifications permit mimicking of aspects of valence bond theory with the additional feature that the energies associated with valence bond type structures are explicitly calculated. In turn, a hybrid molecular, orbital valence, bond scheme is introduced which incorporates variant total molecular electronic density distributions similar to the way that Iterative Extended Hueckel incorporates atoms.

Author

N80-25109*# National Aeronautics and Space Administration. Ames Research Center, Moffett Field, Calif.

MODIFIED ITERATIVE EXTENDED HUECKEL. 2: APPLICATION TO THE INTERACTION OF $\text{Na}(+)$, $\text{Na}(+)(\text{aq.})$, $\text{Mg}(+)-2(\text{aq.})$ WITH ADENINE AND THYMINE

S. Aronowitz, R. MacElroy, and S. Chang Apr. 1980 28 p refs 2 Vol.

(NASA-TM-81201; A-8184) Avail: NTIS HC A03/MF A01 CSCL 20H

Modified Iterative Extended Hueckel, which includes explicit effective internuclear and electronic interactions, is applied to the study of the energetics of $\text{Na}(+)$, $\text{Mg}(+)$, $\text{Na}(+)$ (aqueous), and $\text{Mg}(+2)$ (aqueous) ions approaching various possible binding sites on adenine and thymine. Results for the adenine + ion and thymine + ion are in good qualitative agreement with ab initio work on analogous systems. Energy differences between competing sites are in excellent agreement. Hydration appears to be a critical factor in determining favorable binding sites. That the adenine N1 and N3 sites cannot displace a water molecule from the hydrated cation indicates that they are not favorable binding sites in aqueous media. Of those sites investigated, O4 was the most favorable binding site on the thymine for the bare $\text{Na}(+)$. However, the O2 site was the most favorable binding site for either hydrated cation.

Author

N80-25110*# National Aeronautics and Space Administration. Ames Research Center, Moffett Field, Calif.

QUANTUM THEORY AND CHEMISTRY: TWO PROPOSITIONS

S. Aronowitz May 1980 13 p refs

(NASA-TM-81202) Avail: NTIS HC A02/MF A01 CSCL 20J

Two propositions concerning quantum chemistry are proposed. First, it is proposed that the nonrelativistic Schrodinger equation, where the Hamiltonian operator is associated with an assemblage of nuclei and electrons, can never be arranged to yield specific molecules in the chemists' sense. It is argued that this result is a necessary condition if the Schrodinger has relevancy to chemistry. Second, once a system is in a particular state with regard to interactions among its components (the assemblage of nuclei and electrons), it cannot spontaneously eliminate any of those interactions. This leads to a subtle form of irreversibility.

J.M.S.

N80-26040*# National Aeronautics and Space Administration. Ames Research Center, Moffett Field, Calif.

FLIGHT-DECK AUTOMATION: PROMISES AND PROBLEMS

Earl L. Wiener (Miami Univ., Coral Gables, Fla.) and Renwick E. Curry Jun. 1980 27 p refs

(NASA-TM-81206; A-8210) Avail: NTIS HC A03/MF A01 CSCL 05H

The state of the art in human factors in flight-deck automation is presented. A number of critical problem areas are identified and broad design guidelines are offered. Automation-related aircraft accidents and incidents are discussed as examples of human factors problems in automated flight.

R.E.S.

N80-26296*# National Aeronautics and Space Administration. Ames Research Center, Moffett Field, Calif.

HEAD-UP DISPLAY IN THE NON-PRECISION APPROACH

J. M. Naish May 1980 20 p refs

(NASA-TM-81167; A-8061) Avail: NTIS HC A02/MF A01 CSCL 01D

The problem of head-up guidance for an aircraft making an instrument approach without glide slope information is discussed. Requirements for path control are considered for each section of the approach profile and a head-up display is developed to meet these needs. The display is an unreferenced flight director which is modified by adding a ground referenced symbol as an alternative guidance component. The director is used for holding altitude in the first segment and for descent at a controlled rate in the second segment. It is used in the third segment to maintain the minimum decision altitude while assessing the approach situation. This is done by means of occasional brief changes to the referenced symbol. In the final segment a visual approach is made with the referenced symbol used continuously for path control. The display is investigated experimentally in simulated approaches made by three pilots. The results show a fair agreement between objective and subjective estimates of the quality of landing decisions.

E.D.K.

N80-27164*# National Aeronautics and Space Administration. Ames Research Center, Moffett Field, Calif.

DIFFERENTIATION OF OPTICAL ISOMERS THROUGH ENHANCED WEAK-FIELD INTERACTIONS

S. Aronowitz Jun. 1980 13 p refs

(NASA-TM-81208; A-8212) Avail: NTIS HC A02/MF A01 CSCL 20 H

The influence of weak field interaction terms due to the cooperative effects which arise from a macroscopic assemblage of interacting sites is studied. Differential adsorption of optical isomers onto an achiral surface is predicted to occur if the surface was continuous and sufficiently large. However, the quantity of discontinuous crystal surfaces did not enhance the percentage of differentiation and thus the procedure of using large quantities of small particles was not a viable technique for obtaining a detectable differentiation of optical isomers on an achiral surface.

B.D.

N80-31397*# National Aeronautics and Space Administration. Ames Research Center, Moffett Field, Calif.

PERCEPTION OF AIRCRAFT SEPARATION WITH PILOT-PREFERRED SYMBOLOGY ON A COCKPIT DISPLAY OF TRAFFIC INFORMATION

Sharon O'Connor (San Jose State Univ.), Sharon Jago (San Jose State Univ.), Daniel Baty, and Everett Palmer Sep. 1980 16 p refs

(Grant NsG-2269)

(NASA-TM-81172; A-8107) Avail: NTIS HC A02/MF A01 CSCL 01D

The concept of a cockpit display of traffic information (CDTI) was developed for use in later full mission simulator evaluations of the CDTI concept. Pilots chose their preferred method of displaying air traffic information for several variables. Variables included: type of background, update rate, update type, predictor type, and history type. Each pilot designed a display he felt would be most useful in flight operations. After a series of test trials, each pilot was given the opportunity to modify the display for the experimental task. For a second day of testing, they repeated the experimental task using their display as well as displays chosen by other pilots. Results indicated a variety of individual preferences in symbology and differences in the accuracy of judgments. Pilots indicated concern for clutter of the display, relationship of the displayed symbology to physical reality, and a need to perceive the relative motion of the intruder aircraft. Analysis of data indicated that pilots were able to improve their performance with practice.

R.K.G.

N80-32352*# National Aeronautics and Space Administration. Ames Research Center, Moffett Field, Calif.
NASA AVIATION SAFETY REPORTING SYSTEM Quarterly Report, 1 Oct. - 31 Dec. 1978
 Apr. 1980 39 p refs Prepared in cooperation with Battelle Columbus Labs., Mountain View, Calif.
 (NASA-TM-81197; A-8176; QR-10) Avail: NTIS HC A03/MF A01 CSCL 01C

Knowledge of limitations of the Air Traffic Control system in conflict avoidance capabilities is discussed. Assumptions and expectations held by airmen regarding the capabilities of the system are presented. Limitations related to communication are described and problems associated with visual approaches, airspace configurations, and airport layouts are discussed. A number of pilot and controller reports illustrative of three typical problem types: occurrences involving pilots who have limited experience; reports describing inflight calls for assistance; and flights in which pilots have declined to use available radar services are presented. Examples of Alert Bulletins and the FAA responses to them are included. T.M.

N80-34056*# National Aeronautics and Space Administration. Ames Research Center, Moffett Field, Calif.
HUMAN ACCLIMATION AND ACCLIMATIZATION TO HEAT: A COMPENDIUM OF RESEARCH, 1968-1978
 Deanna Sciaraffa, Stephen C. Fox, Ralph Stockmann, and John E. Greenleaf Aug. 1980 104 p refs
 (NASA-TM-81181; A-8099) Avail: NTIS HC A06/MF A01 CSCL 06P

Abstracts and annotations of the majority of scientific works that elucidate the mechanisms of short-term acclimation to heat in men and women are presented. The compendium includes material from 1968 through 1977. Subject and author indexes are provided and additional references of preliminary research findings or work of a peripheral nature are included in a bibliography. T.M.

NASA CONTRACTOR REPORTS

N80-11103*# San Jose State Univ., Calif. Dept. of Psychology.
PERCEPTION AND PERFORMANCE IN FLIGHT SIMULATORS: THE CONTRIBUTION OF VESTIBULAR, VISUAL, AND AUDITORY INFORMATION Final Report
 Oct. 1979 20 p refs
 (Grant NSG-2269)
 (NASA-CR-162129) Avail: NTIS HC A02/MF A01 CSCL 14B

The pilot's perception and performance in flight simulators is examined. The areas investigated include: vestibular stimulation, flight management and man cockpit information interfacing, and visual perception in flight simulation. The effects of higher levels of rotary acceleration on response time to constant acceleration, tracking performance, and thresholds for angular acceleration are examined. Areas of flight management examined are cockpit display of traffic information, work load, synthetic speech call outs during the landing phase of flight, perceptual factors in the use of a microwave landing system, automatic speech recognition, automation of aircraft operation, and total simulation of flight training. A.W.H.

N80-12735*# Georgia Inst. of Tech., Atlanta.
GUIDING THE DEVELOPMENT OF A CONTROLLED ECOLOGICAL LIFE SUPPORT SYSTEM
 Robert M. Mason, ed. (Metrics, Inc., Atlanta) and John L. Carden, ed. Nov. 1979 98 p refs Report on workshop held at NASA/Ames, 8-12 Jan. 1979

(Grant N 0023)
 (NASA-CR-162452) Avail: NTIS HC A05/MF A01 CSCL 06K

The workshop is reported which was held to establish guidelines for future development of ecological support systems, and to develop a group of researchers who understand the interdisciplinary requirements of the overall program. For individual titles, see N80-12736 through N80-12738.

N80-19800*# Life Systems, Inc., Cleveland, Ohio.
DEVELOPMENT OF A NITROGEN GENERATION SYSTEM Final Report
 D. B. Heppner, R. D. Marshall, J. D. Powell, III, and F. H. Schubert Jan. 1980 63 p refs
 (Contract NAS2-10096)
 (NASA-CR-152333; LSI-TR-353-4) Avail: NTIS HC A04/MF A01 CSCL 06K

An eight-stage nitrogen generation module was developed. The design integrated a hydrazine catalytic dissociator, three ammonia dissociation stages and four palladium/silver hydrogen separator stages. Alternating ammonia dissociation and hydrogen separation stages are used to remove hydrogen and ammonia formed in the dissociation of hydrazine which results in negligible ammonia and hydrogen concentrations in the product nitrogen stream. An engineering breadboard nitrogen supply subsystem was also developed. It was developed as an integratable subsystem for a central spacecraft air revitalization system. The subsystem consists of the hydrazine storage and feed mechanism, the nitrogen generation module, the peripheral mechanical and electrical components required to control and monitor subsystem performance, and the instrumentation required to interface with other subsystems of an air revitalization system. The breadboard nitrogen supply subsystem was integrated and tested with a one-person capacity experimental air revitalization system. The integration, checkout and testing was successfully accomplished. R.E.S.

N80-22987*# Life Systems, Inc., Cleveland, Ohio.
PERFORMANCE CHARACTERIZATION OF A BOSCH CO SUB 2 REDUCTION SUBSYSTEM Final Report
 D. B. Heppner, T. M. Hallick, and F. H. Schubert Feb. 1980 40 p refs
 (Contract NAS2-10204)
 (NASA-CR-152342; LST-TR-379-11) Avail: NTIS HC A03/MF A01 CSCL 06K

The performance of Bosch hardware at the subsystem level (up to five-person capacity) in terms of five operating parameters was investigated. The five parameters were: (1) reactor temperature, (2) recycle loop mass flow rate, (3) recycle loop gas composition (percent hydrogen), (4) recycle loop dew point and (5) catalyst density. Experiments were designed and conducted in which the five operating parameters were varied and Bosch performance recorded. A total of 12 carbon collection cartridges provided over approximately 250 hours of operating time. Generally, one cartridge was used for each parameter that was varied. The Bosch hardware was found to perform reliably and reproducibly. No startup, reaction initiation or carbon containment problems were observed. Optimum performance points/ranges were identified for the five parameters investigated. The performance curves agreed with theoretical projections. R.E.S.

N80-29023*# GARD, Inc., Niles, Ill.
DESIGN, FABRICATION AND TESTING OF A DUAL CATALYST AMMONIA REMOVAL SYSTEM FOR A URINE VCD UNIT Final Report
 P. Budinikas Jun. 1980 43 p ref
 (Contract NAS2-10237)
 (NASA-CR-152372) Avail: NTIS HC A03/MF A01 CSCL 06B

A three-man capacity catalytic system for the recovery of water from urine was designed, constructed, and tested, it was designed to operate with feed streams containing high concentrations of urine vapor and only 5 to 7% of oxygen for the oxidation of ammonia and volatile organic vapor. It can operate either in a flow-through or a recycle mode and is capable of accepting the urine vapor produced by a vapor compression distillation evaporator. Testing consisted of short preliminary and optimization test, an endurance test of 74 hours continuous operation, and recycle tests using both air and oxygen. The system was designed for a urine processing rate of 0.86 liters/hr; however, it was tested at rates up to 1.2 liter/hr. Untreated urine evaporated by an electrically heated evaporator was used. The quality of the recovered water meets the U.S. Drinking Water Standards, with the exception of a low pH. Accumulation of solids in the urine sludge is reduced to approximately 65% of the anticipated value. L.F.M.

N80-33086*# Webb Associates, Yellow Springs, Ohio.
THE DEVELOPMENT OF AN ELASTIC REVERSE GRADIENT GARMENT TO BE USED AS A COUNTERMEASURE FOR CARDIOVASCULAR DECONDITIONING
 James F. Annis and Paul Webb [1980] 69 p refs
 (Contract NAS2-7156)
 (NASA-CR-152379) Avail: NTIS HC A04/MF A01 CSCL 06P

Using a new nomex lycra elastic fabric and individualized garment engineering techniques, reverse gradient garments (RGG's) were designed, constructed, and tested for effectiveness as a countermeasure against cardiovascular deconditioning. By combining torso compensated positive pressure breathing with a distally diminishing gradient of counterpressure supplied by the elastic fabric on the limbs, the RGG acts to pool blood in the extremities of recumbent persons much as though they were standing erect in 1 g. The RGG stresses the vasculature in a fashion similar to that experienced by the normally active man, hence preventing or limiting the development of post weightlessness orthostatic intolerance and related conditions. Four male, college age subjects received daily treatments with the RGG during a 15 day bedrest study. Four additional subjects also underwent the bedrest, but received no treatments; they served as controls. The preliminary indication was that the RGG was somewhat effective in limiting the deconditioning process. R.K.G.

JOURNAL ARTICLES

A80-10738 * # The Viking mission and the search for life on Mars. H. P. Klein (NASA, Ames Research Center, Directorate of Life Sciences, Moffett Field, Calif.). (*International Union of Geodesy and Geophysics, General Assembly, 17th, Canberra, Australia, Dec. 2-15, 1979.*) *Reviews of Geophysics and Space Physics*, vol. 17, Oct. 1979, p. 1655-1662. 80 refs.

Experiments conducted by the Viking mission to search for life on Mars are examined and the results of direct chemical analyses are surveyed to determine the presence of any complex organic compound. Observations taken from lander imaging and experiments from biological investigation are analyzed for pyrolytic release, gas exchange (both humid and nutrient) and labeled release (LR). Attention is given to the results in an attempt to simulate LR initial reaction, and to the implications and extrapolations of the Viking mission. C.F.W.

A80-11473 * Aldocyanoin microspheres - Partial amino acid analysis of the microparticulates formed from simple reactants under various conditions. G. E. Pollock and R. Heiderer (NASA, Ames

Research Center, Moffett Field, Calif.). *Journal of Molecular Evolution*, vol. 13, no. 3, 1979, p. 253-263. 22 refs.

A80-12229 * Oxygen as a factor in eukaryote evolution - Some effects of low levels of oxygen on *Saccharomyces cerevisiae*. L. Jahnke and H. P. Klein (NASA, Ames Research Center, Exobiology Research Div., Moffett Field, Calif.). *Origins of Life*, vol. 9, Sept. 1979, p. 329-334. 23 refs.

A comparative study of the effects of varying levels of oxygen on some of the metabolic functions of the primitive eukaryote, *Saccharomyces cerevisiae*, has shown that these cells are responsive to very low levels of oxygen: the level of palmitoyl-Co A desaturase was greatly enhanced by only 0.03 vol % oxygen. Similarly, an acetyl-CoA synthetase associated predominantly with anaerobic growth was stimulated by as little as 0.1% oxygen, while an isoenzyme correlated with aerobic growth was maximally active at much higher oxygen levels (greater than 1%). Closely following this latter pattern were three mitochondrial enzymes that attained maximal activity only under atmospheric levels of oxygen. (Author)

A80-13013 * Carbonaceous chondrites. I - Characterization and significance of carbonaceous chondrite /CM/ xenoliths in the Jodzie howardite. T. E. Bunch, S. Chang (NASA, Ames Research Center, Moffett Field, Calif.), U. Frick, J. Neil (California, University, Berkeley, Calif.), and G. Moreland (Smithsonian Institution, Div. of Meteorites, Washington, D.C.). *Geochimica et Cosmochimica Acta*, vol. 43, Nov. 1979, p. 1727-1729, 1731-1742. 83 refs. Grants No. NGL-75-003-409; No. NGL-24-005-225.

Mineralogical, chemical, textural, and isotopic studies of the abundant carbonaceous inclusions in the Jodzie howardite which are consistent with carbonaceous chondrite (CM) characteristics are examined. These CM xenoliths show regolith alteration comparable to the Murray and Murchison meteorites but less than Nogoya, flow-oriented development of phyllosilicates and 'poorly characterized phases', and partial oxidation of sulfides. Temperature-programmed pyrolysis mass spectrometry indicates that gas release patterns of volatiles and hydrocarbons, and N, C, and S contents are typical of CM meteorites. The fact that the Ne content is typical for 'solar' values and the isotopic structure of Xe is 'planetary' indicates that these gases were entrapped by different mechanisms, and cosmic ray exposure ages for the xenoliths agree with the reported exposure age for the eucritic host. A.T.

A80-13018 * The radioracemization of isovaline - Cosmochemical implications. W. A. Bonner, N. E. Blair, R. M. Lemmon, J. J. Flores, and G. E. Pollock (NASA, Ames Research Center, Moffett Field; Stanford University, Stanford; California, University, Lawrence Berkeley Laboratory, Berkeley, Calif.). *Geochimica et Cosmochimica Acta*, vol. 43, Nov. 1979, p. 1841-1846. 30 refs. Research supported by the U.S. Department of Energy and NASA.

The optically pure D- and L-enantiomers of isovaline, which cannot be racemized by ordinary chemical mechanisms involving alpha-hydrogen removal and which has been isolated in apparently racemic form from the Murchison meteorite, have been subjected to partial radiolysis by the ionizing radiation from a 3000-Ci Co-60 gamma-ray source. Both in the anhydrous and hydrated solid states and as solid sodium or hydrochloride salts each enantiomer suffered significant radioracemization of the undestroyed residue during its partial radiolysis. The sodium salt of isovaline in 0.1-M aqueous solution suffered extensive radiolysis with relatively small radiation doses, but showed no detectable radioracemization. The significance of these observations with respect to the primordial enantiomeric composition of the isovaline (and other amino acids) indigenous to meteorites is discussed. (Author)

A80-13506 * Plasma volume during stress in man - Osmolality and red cell volume. J. E. Greenleaf, V. A. Convertino, and G. R. Mangseth (NASA, Ames Research Center, Biomedical Research Div., Moffett Field, Calif.). *Journal of Applied Physiology: Respiratory, Environmental and Exercise Physiology*, vol. 47, Nov. 1979, p. 1031-1038. 30 refs.

The purpose was (1) to test the hypothesis that in man there is a range of plasma osmolality within which the red cell volume (RCV) and mean corpuscular volume (MCV) remain essentially constant and (2) to determine the upper limit of this range. During a variety of stresses - submaximal and maximal exercise, heat and altitude exposure, +Gz acceleration, and tilting - changes in plasma osmolality between -1 and +13 mosmol/kg resulted in essentially no change in the regression of percent change in plasma volume (PV) calculated from a change in hematocrit (Hct) on that calculated from a change in Hct + hemoglobin (Hb), i.e., the RCV and MCV were constant. Factors that do not influence RCV are the level of metabolism, heat exposure at rest, and short-term orthostasis (heat-to-foot acceleration). Factors that may influence RCV are exposure to high altitude and long-term orthostasis (head-up tilting). Factors that definitely influence RCV are prior dehydration and extended periods of stress. Thus, either the Hct or the Hct + Hb equations can be used to calculate percent changes in PV under short-term periods of stress when the change in plasma osmolality is less than 13 mosmol/kg.

(Author)

A80-13549 * Quantification of monocarboxylic acids in the Murchison carbonaceous meteorite. J. G. Lawless (NASA, Ames Research Center, Extraterrestrial Research Div., Moffett Field, Calif.) and G. U. Yuen (Arizona State University, Tempe, Ariz.). *Nature*, vol. 282, Nov. 22, 1979, p. 396-398. 30 refs.

The abundances of some of the straight- and branched-chain isomers of the monocarboxylic acids found in the Murchison carbonaceous chondrite are determined. Monocarboxylic acids extracted from a crushed sample of Murchison interior were quantified by means of gas chromatography and mass spectroscopy after a spiking solution of deuterated analogues of 11 carboxylic acids had been added. Monocarboxylic acid abundances are found to range between 1.83 and 0.01 micromole/g, which is significantly higher than Murchison amino acid concentrations, and to decrease with increasing carbon number for both branched and unbranched molecules. The results are interpreted to support the abiotic extraterrestrial synthesis of monocarboxylic acids. Possible mechanisms leading to the equal synthesis of branched and each unbranched carboxylic acid with the same carbon number are considered, noting that the Fischer-Tropsch Type mechanism by itself is incapable of accounting for the observed distributions. A.L.W.

A80-15295 * Position and shape of the Venus bow shock - Pioneer Venus Orbiter observations. J. A. Slavin, R. C. Elphic, C. T. Russell, D. S. Intriligator (California, University, Los Angeles, Calif.), and J. H. Wolfe (NASA, Ames Research Center, Moffett Field, Calif.). *Geophysical Research Letters*, vol. 6, Nov. 1979, p. 901-904. 32 refs. Contract No. NAS2-9491.

Magnetometer data from the Pioneer Venus Orbiter is used to examine the position and shape of this planet's bow shock. Utilizing crossings identified on 86 occasions during the first 65 orbits a mean shock surface is defined for sun-Venus-satellite angles of 60-110 deg. Both the shock shape and variance in location are found to be very similar to the terrestrial case for the range in SVS angle considered. However, while the spread in shock positions at the earth is due predominantly to the magnetopause location varying in response to solar wind dynamic pressure, ionopause altitude variations can have little effect on total obstacle radius. Thus, the Cytherean shock is sometimes observed much closer to or farther from the planet than previously predicted by gasdynamic theory applied to the deflection of flow about a blunt body which acts neither as source nor sink for any portion of the flow. (Author)

A80-17686 * Proton movements in response to a light-driven electrogenic pump for sodium ions in *Halobacterium halobium* membranes. R. V. Greene (Cornell University, Ithaca, N.Y.) and J. K. Lanyi (NASA, Ames Research Center, Moffett Field, Calif.). *Journal of Biological Chemistry*, vol. 254, Nov. 10, 1979, p. 10986-10994. 35 refs. NSF Grant No. 76-09718; Grant No. NIH-GM-23225A.

A80-17741 * Review of cell aging in *Drosophila* and mouse. J. Miquel (NASA, Ames Research Center, Biomedical Research Div., Moffett Field, Calif.), A. C. Economos (San Jose State University, San Jose, Calif.), K. G. Bensch (Stanford University, Stanford, Calif.), H. Atlan (Paris VI, Université, Paris, France), and J. E. Johnson, Jr. (National Institutes of Health, National Institute on Aging, Baltimore, Md.). *Age*, vol. 2, July 1979, p. 78-88. 70 refs.

A80-20340 * // Organic chemistry on Titan. S. Chang, T. Scattergood, S. Aronowitz, and J. Flores (NASA, Ames Research Center, Extraterrestrial Research Div., Moffett Field, Calif.). *Review of Geophysics and Space Physics*, vol. 17, Nov. 1979, p. 1923-1933. 71 refs. NASA Order A-39942-B.

Features taken from various models of Titan's atmosphere are combined in a working composite model that provides environmental constraints within which different pathways for organic chemical synthesis are determined. Experimental results and theoretical modeling suggest that the organic chemistry of the satellite is dominated by two processes: photochemistry and energetic particle bombardment. Photochemical reactions of CH₄ in the upper atmosphere can account for the presence of C₂ hydrocarbons. Reactions initiated at various levels of the atmosphere by cosmic rays, Saturn 'wind', and solar wind particle bombardment of a CH₄-N₂ atmospheric mixture can account for the UV-visible absorbing stratospheric haze, the reddish appearance of the satellite, and some of the C₂ hydrocarbons. In the lower atmosphere photochemical processes will be important if surface temperatures are sufficiently high for gaseous NH₃ to exist. It is concluded that the surface of Titan may contain ancient or recent organic matter (or both) produced in the atmosphere. B.J.

A80-21780 * On the significance of the apparent absence of extraterrestrials on earth. M. A. Stull (NASA, Ames Research Center, Moffett Field, Calif.). *British Interplanetary Society, Journal (Interstellar Studies)*, vol. 32, June 1979, p. 221, 222. 6 refs.

The paper considers arguments on the existence or absence of extraterrestrial civilizations. It is suggested that arguments that even a single extraterrestrial civilization would have long ago colonized the Galaxy are not compelling. Attention is given to factors such as intraspecific competition, which could have prevented complete colonization, noting that an exception perhaps would be on time scales much greater than 10 to the 10 years. It is concluded that the fact that extraterrestrial civilizations do not appear to be represented on earth is irrelevant to the formulation of plans to search for them. M.E.P.

A80-21982 * Microbial sulfate reduction measured by an automated electrical impedance technique. R. S. Oremland and M. P. Silverman (NASA, Ames Research Center, Extraterrestrial Biology Div., Moffett Field, Calif.). *Geomicrobiology Journal*, vol. 1, no. 4, 1979, p. 355-372. 27 refs.

Electrical impedance measurements are used to investigate the rates of sulfate reduction by pure cultures of and sediments containing sulfur-reducing bacteria. Changes in the electrical impedance ratios of pure cultures of *Desulfovibrio aestuarii* and samples of reduced sediments from San Francisco Bay were measured by a Bactometer 32, and sulfate reduction was followed by measuring the incorporation of (S-35) sulfate into metal sulfides. The growth of the bacteria in pure culture is found to result in an increase of 0.2200 in the impedance ratio within 24 h, accompanied by increases in protein, ATP, sulfide and absorbance at 660 nm, all of which are inhibited by the addition of molybdate. Similar responses were observed in the sediments, although impedance ratio responses were not completely inhibited upon the addition of molybdate, due to the presence of nonsulfate-respiring microorganisms. Experiments conducted with sterile media and autoclaved sediments indicate that the presence of H₂S together with iron is responsible for the impedance effect, and sulfate reduction rates ranging between 0.85 and 1.78 mmol/l per day are estimated for the sediments by the impedance technique.

A.L.W.

A80-21988 * **Noninvasive measures of bone bending rigidity in the monkey /M. nemestrina/.** D. R. Young, W. H. Howard, C. Cann (NASA, Ames Research Center, Biomedical Research Div., Moffett Field, Calif.), and C. R. Steele (Stanford University, Stanford, Calif.). *Calcified Tissue International*, vol. 27, Mar. 1979, p. 109-115. 23 refs.

The in vivo bending rigidity and bone mineral content of monkey ulnae and tibiae were measured. Bending rigidity in the anteroposterior plane was measured by an impedance probe technique. Forced vibrations of the bones were induced with an electromechanical shaker, and force and velocity at the driving point were determined. The responses over the range of 100-250 Hz were utilized to compute the bending rigidity. Bone mineral content in the cross section was determined by a photon absorption technique. Seventeen male monkeys (*Macaca nemestrina*) weighing 6-14 kg were evaluated. Bending rigidity was correlated with the mineral content of the cross section, with a correlation coefficient of 0.899. Two monkeys were evaluated during prolonged hypodynamic restraint. Restraint produced regional losses of bone most obviously in the proximal tibia. The local bone mineral content declines 17 to 24% and the average bending rigidity declines 12 to 22%. Changes in bones leading to a reduction in mineral content and stiffness are discussed.

(Author)

A80-24222 * **Growth hormone control of glucose oxidation pathways in hypophysectomized rats.** D. D. Feller, E. D. Neville, L. C. Keil, and S. Ellis (NASA, Ames Research Center, Moffett Field, Calif.). *Physiological Chemistry and Physics*, vol. 11, no. 3, 1979, p. 205-215. 12 refs.

A80-25894 * **Effect of simulated weightlessness on the immune system in rats.** L. D. Caren, A. D. Mandel, and J. A. Nunes (NASA, Ames Research Center, Moffett Field; Santa Clara, University, Santa Clara, Calif.). *Aviation, Space, and Environmental Medicine*, vol. 51, Mar. 1980, p. 251-255. 14 refs. Grant No. NCA2-OR685-813.

Rats suspended in a model system designed to simulate many aspects of weightlessness were immunized with sheep red blood cells. Parameters measured on these and control rats included titers of anti-sheep red blood cell antibodies, serum immunoglobulin levels, spleen and thymus weights, hematocrits, and leukocyte differential counts on peripheral blood. No significant differences were found between test and weight-bearing, harnessed controls; however, the

thymuses of animals in both these groups were significantly smaller than untreated cage controls. The lack of an effect of simulated weightlessness on the immune system is an interesting result, and its significance is discussed.

(Author)

A80-25989 * **Exercise thermoregulation after 14 days of bed rest.** J. E. Greenleaf and R. D. Reese (NASA, Ames Research Center, Laboratory of Human Environmental Physiology, Moffett Field, Calif.). *Journal of Applied Physiology: Respiratory, Environmental and Exercise Physiology*, vol. 48, Jan. 1980, p. 72-78. 32 refs.

The effects of bed rest and exercise training during bed rest on body temperature and thermoregulatory responses at rest and during exercise are investigated. Seven male subjects underwent three two-week periods of bed rest during which isometric, isotonic, or no exercises were performed, separated by two ambulatory control periods and preceded by a two-week control period, during which they exercised regularly. Rectal and mean skin temperatures and sweating responses were determined during 70-min submaximal supine exercise during the bed rest and recovery periods. Measurements reveal a reduction in basal oral temperature during the control-recovery periods, with a relatively constant level during bed rest periods, and a significant increase in the rectal temperature elevation brought on by exercise following all three bed-rest regimes. It is concluded that the excessive increase in rectal temperature could be influenced by changes in skin heat conductance or the inhibition of sweating.

A.L.W.

A80-25990 * **Fluid shifts and endocrine responses during chair rest and water immersion in man.** J. E. Greenleaf, E. Shvartz, S. Kravik, and L. C. Keil (NASA, Ames Research Center, Laboratory of Human Environmental Physiology, Moffett Field, Calif.). *Journal of Applied Physiology: Respiratory, Environmental and Exercise Physiology*, vol. 48, Jan. 1980, p. 79-88. 45 refs.

The effects of external water pressure on intercompartmental fluid volume shifts and endocrine responses in man are investigated. Extracellular fluid volumes and plasma and urine electrolyte and endocrine responses of four male subjects were measured during eight hours of head-out water immersion and 16 hours of recovery bed rest and compared to responses obtained during eight hours of chair rest and 16 hours of bed rest without external hydrostatic pressure obtained in the same subjects five months later. Immersion is found to result in a substantial diuresis with respect to chair rest, accounted for by decreases in extracellular volume. A negative water balance during immersion and a positive water balance during chair rest were observed to be accompanied by a shift of extracellular volume to the intracellular compartment, as well as the suppression of plasma arginine vasopressin and renin activities in both regimes. The vasopressin and renin activity decreases are attributed to the increased central blood volume, and half of the plasma loss in immersed subjects is attributed to the effects of external water pressure.

A.L.W.

A80-26015 **Spectrophotometric identification of the pigment associated with light-driven primary sodium translocation in *Halobacterium halobium*.** J. K. Lanyi (NASA, Ames Research Center, Moffett Field, Calif.) and H. J. Weber (California, University, Berkeley, Calif.). *Journal of Biological Chemistry*, vol. 255, Jan. 10, 1980, p. 243-250. 22 refs. NIH-supported research.

A80-27077 * **The role of Na⁺/K⁺ in transport processes of bacterial membranes.** J. K. Lanyi (NASA, Ames Research Center, Extraterrestrial Research Div., Moffett Field, Calif.). *Biochimica et Biophysica Acta*, vol. 559, 1979, p. 377-397. 140 refs.

Until recently it was generally held that transport in bacteria was linked exclusively to proton circulation, in contrast to most eucaryotic systems, which depended on Na(+) circulation. The present review is intended to trace recent developments which have led to the discarding of this idea. The discussion covers transport of Na(+) and other cations, effects of Na(+) and Na(+) gradients on metabolite transport, properties of Na(+) dependent transport carriers, and evolutionary considerations of Na(+) transport. It is now apparent that the transport of Na(+) is an important part of energy metabolism in bacteria, and that Na(+) gradients as well as H(+) gradients are used in these systems for the conservation and transmission of energy. Two hypotheses are proposed to explain the evolution of Na/K systems, and it is presently difficult to decide between them. S.D.

A80-29085 * **Favorable effects of the antioxidants sodium and magnesium thiazolidine carboxylate on the vitality and life span of *Drosophila* and mice.** J. Miquel (NASA, Ames Research Center, Moffett Field, Calif.) and A. C. Economos (San Jose State University, San Jose, Calif.). *Experimental Gerontology*, vol. 14, 1979, p. 279-285. 30 refs.

A80-30845 * **Pioneer Venus Sounder Probe gas chromatograph.** V. I. Oyama, G. C. Carle, F. Woeller (NASA, Ames Research Center, Moffett Field, Calif.), S. Rocklin, J. Vogrin, W. Potter, G. Rosiak (TRW Defense and Space Systems Group, Redondo Beach, Calif.), and C. Reichwein (Technology, Inc., Houston, Tex.). *IEEE Transactions on Geoscience and Remote Sensing*, vol. GE-18, Jan. 1980, p. 85-93. 10 refs.

The design logic, construction, function, and data processing of the Pioneer Venus Sounder Probe gas chromatograph instrument are discussed. A gas chromatograph for the analysis of the chemical composition of the lower atmosphere of Venus was included in the Sounder Probe of the Pioneer Venus mission. This paper describes the design logic of the gas chromatograph as constrained by the mission; attention is given to instrument construction, function, and data reduction. B.J.

A80-30875 * **Corrections in the Pioneer Venus sounder probe gas chromatographic analysis of the lower Venus atmosphere.** V. I. Oyama, G. C. Carle, and F. Woeller (NASA, Ames Research Center, Moffett Field, Calif.). *Science*, vol. 208, Apr. 25, 1980, p. 399-401. 8 refs.

Misidentification of two peaks from the Pioneer Venus sounder probe gas chromatograph (SPGC), also formerly known as the LGC, gave rise to quantitative errors in the abundances of oxygen, argon, and carbon monoxide. The argon abundance is estimated at 67 parts per million and that of carbon monoxide at 20 parts per million. At this time, no estimates for the oxygen abundance can be made.

(Author)

A80-32748 * **Role of thermal and exercise factors in the mechanism of hypervolemia.** V. A. Convertino, J. E. Greenleaf, and E. M. Bernauer (NASA, Ames Research Center, Biomedical Research Div., Moffett Field, Calif.). *Journal of Applied Physiology: Respiratory Environmental and Exercise Physiology*, vol. 48, Apr. 1980, p. 657-664. 40 refs.

The present study was undertaken to determine whether the chronic increase in plasma volume, resulting from heat exposure and exercise training, was due only to elevated rectal temperature or

whether there were additional nonthermal factors related to the exercise. The study was conducted on eight volunteer, healthy, moderately trained male college subjects (18-26 yr). Exercise-induced hypervolemia was associated with thermal factor(s) that contributed 40% and nonthermal factors that accounted for the remaining 60%. In addition, some nonthermal, exercise-induced factors were twofold increases in plasma osmotic and vasopressin levels during exercise, and a fivefold increase in resting plasma protein content. S.D.

A80-32749 * **Exercise training-induced hypervolemia - Role of plasma albumin, renin, and vasopressin.** V. A. Convertino, P. J. Brock, L. C. Keil, E. M. Bernauer, and J. E. Greenleaf (NASA, Ames Research Center, Biomedical Research Div., Moffett Field, Calif.). *Journal of Applied Physiology: Respiratory Environmental and Exercise Physiology*, vol. 48, Apr. 1980, p. 665-669. 32 refs.

The purpose of the present study was twofold: (1) to determine the rate of induction and decay of exercise-training hypervolemia with a short-duration high-intensity training regimen; and (2) to assess the protein, osmotic, and endocrine responses that contribute to that mechanism. The test subjects were eight volunteer, healthy, trained college men (20-22 yr) engaged in isotonic exercise on a bicycle ergometer. Factors associated with plasma hypervolemia during training are identified. The results suggest that an efficient procedure for increasing plasma volume is the daily performance of high-intensity isotonic leg exercise for 2 h/day. S.D.

A80-32834 * **Microbial mobilization of calcium and magnesium in waterlogged soils.** M. P. Silverman and E. F. Munoz (NASA, Ames Research Center, Extraterrestrial Research Div., Moffett Field, Calif.). *Journal of Environmental Quality*, vol. 9, Jan.-Mar. 1980, p. 9-12. 18 refs.

A80-35751 * **Insulin binding and glucose uptake of adipocytes in rats adapted to hypergravitational force.** M. Kobayashi, C. E. Mondon, and J. Oyama (NASA, Ames Research Center, Biomedical Research Div., Moffett Field; Stanford University, Palo Alto, Calif.). *American Journal of Physiology*, vol. 238, Apr. 1980, p. E330-E335. 27 refs. NASA-supported research; Grant No. NIH-AM-07217.

Rats were exposed to 4.15 g for 1 yr and weight and age matched, and lean noncentrifuged rats were used as control groups. Rats exposed to chronic hypergravity (hypergravic rats) were found to show lower ambient insulin levels, greater food intake with smaller body weight gain, and decreased size of isolated adipocytes. The ability of adipocytes from the hypergravic rats to bind insulin was increased. With Scatchard analysis, both number and affinity of receptors were increased. In contrast to the increased binding, glucose transport was found to be decreased in adipocytes from these animals. However, when the data were expressed as a percentage of maximal effect, the half maximal insulin effect for both the hypergravic and lean control groups was produced at an insulin concentration of 0.23 + or - 0.02 ng/ml, which was lower than the insulin concentration of 0.31 + or - 0.02 ng/ml for the weight-matched control group (P less than 0.05). This increased insulin sensitivity in the hypergravic group was accounted for by an increased number of receptors. (Author)

A80-36061 * **Mars ultraviolet simulation facility.** L. P. Zill, R. Mack, and D. L. DeVincenzi (NASA, Ames Research Center, Extraterrestrial Research Div., Moffett Field, Calif.). *Journal of*

Molecular Evolution, vol. 14, Dec. 1979, p. 79-89. 9 refs.

A facility was established for long-duration ultraviolet (UV) radiation exposure of natural and synthetic materials in order to test hypotheses concerning Martian soil chemistry observed by the Viking Mars landers. The system utilized a 2500 watt xenon lamp as the radiation source, with the beam passing through a heat-dissipating water filter before impinging upon an exposure chamber containing the samples to be irradiated. The chamber was designed to allow for continuous tumbling of the samples, maintenance of temperatures below 0 C during exposure, and monitoring of beam intensity. The facility also provided for sample preparation under a variety of atmospheric conditions, in addition to the Mars nominal. As many as 33 sealed sample ampules have been irradiated in a single exposure. Over 100 samples have been irradiated for approximately 100 to 700 h. The facility has performed well in providing continuous UV irradiation of multiple samples for long periods of time under simulated Mars atmospheric and thermal conditions. (Author)

A80-36062 * **Heterogeneous phase reactions of Martian volatiles with putative regolith minerals.** B. C. Clark, S. L. Kenley, D. L. O'Brien (Martin Marietta Aerospace, Planetary Sciences Laboratory, Denver, Colo.), G. R. Huss (New Mexico, University, Albuquerque, N. Mex.), R. Mack (NASA, Ames Research Center, Moffett Field, Calif.), and A. K. Baird (Pomona College, Claremont, Calif.). *Journal of Molecular Evolution*, vol. 14, Dec. 1979, p. 91-102. 17 refs. Contracts No. NAS1-9000; No. NAS1-11855; No. NAS1-11858.

The chemical reactivity of several minerals thought to be present in Martian fines is tested with respect to gases known in the Martian atmosphere. In these experiments, liquid water is excluded from the system, environmental temperatures are maintained below 0 C, and the solar illumination spectrum is simulated in the visible and UV using a xenon arc lamp. Reactions are detected by mass spectrometric analysis of the gas phase over solid samples. No reactions were detected for Mars nominal gas over sulfates, nitrates, chloride, nontronite clay, or magnetite. Oxidation was not observed for basaltic glass, nontronite, and magnetite. However, experiments incorporating SO₂ gas - an expected product of volcanism and intrusive volatile release - gave positive results. Displacement of CO₂ by SO₂ occurred in all four carbonates tested. These reactions are catalyzed by irradiation with the solar simulator. A calcium nitrate hydrate released NO₂ in the presence of SO₂. These results have implications for the cycling of atmospheric CO₂, H₂O, and N₂ through the regolith. (Author)

A80-36066 * **Simulation of the Viking biology experiments - An overview.** H. P. Klein (NASA, Ames Research Center, Moffett Field, Calif.). *Journal of Molecular Evolution*, vol. 14, Dec. 1979, p. 161-165. 24 refs.

In the present paper, ground-based investigations of the Viking Martian biology data, which have resulted in reasonable simulations of these data, are reviewed. These simulations, which in strong oxidants, UV-treated materials, iron-containing clays, or iron salts were used as Martian analogs, are capable of explaining the ambiguity between the GCMS (gas-chromatography mass-spectrometry) experiments, in which no organic compounds were found on Mars, and the Labeled Release experiments, in which added organics were decomposed. V.P.

A80-36069 * **A model of Martian surface chemistry.** V. I. Oyama and B. J. Berdahl (NASA, Ames Research Center, Extraterrestrial Research Div., Moffett Field, Calif.). *Journal of Molecular Evolution*, vol. 14, Dec. 1979, p. 199-210. 46 refs.

Alkaline earth and alkali metal superoxides and peroxides, gamma-Fe₂O₃ and carbon suboxide polymer, are proposed to be

constituents of the Martian surface material. These reactive substances explain the water modified reactions and thermal behaviors of the Martian samples demonstrated by all of the Viking Biology Experiments. It is also proposed that the syntheses of these substances result mainly from electrical discharges between wind-mobilized particles at Martian pressures; plasmas are initiated and maintained by these discharges. Active species in the plasma either combine to form or react with inorganic surfaces to create the reactive constituents. (Author)

A80-36195 * **The role of metal ions in chemical evolution - Polymerization of alanine and glycine in a cation-exchanged clay environment.** J. G. Lawless and N. Levi (NASA, Ames Research Center, Moffett Field, Calif.). *Journal of Molecular Evolution*, vol. 13, Nov. 1979, p. 281-286. 33 refs.

The effect of the exchangeable cation on the condensation of glycine and alanine was investigated using a series of homoionic bentonites. A cycling procedure of drying, warming and wetting was employed. Peptide bond formation was observed, and the effectiveness of metal ions to catalyze the condensation was Cu(2+) greater than Ni(2) approximately equals Zn(2+) greater than Na(+). Glycine showed 6% of the monomer incorporated into oligomers with the largest detected being the pentamer. Alanine showed less peptide bond formation (a maximum of 2%) and only the dimer was observed. (Author)

A80-37933 * **A high-sensitivity search for extraterrestrial intelligence at lambda 18 cm.** J. Tarter (California, University, Berkeley, Calif.), J. Cuzzi, D. Black (NASA, Ames Research Center, Moffett Field, Calif.), and T. Clark (NASA, Goddard Space Flight Center, Radioastronomy Branch, Greenbelt, Md.). *Icarus*, vol. 42, Apr. 1980, p. 136-144. 13 refs. Grants No. NSG-2271; No. NCA2-OR-050-702.

A targeted high-sensitivity search for narrow-band signals near a wavelength of 18 cm has been conducted using the 91-m radiotelescope of the National Radio Astronomy Observatory. The search included 201 nearby solar-type stars and achieved a frequency resolution of 5.5 Hz over a 1.4-MHz bandwidth. This high spectral resolution was obtained through a non-real-time reduction procedure using a Mark I VLB recording terminal in conjunction with the CDC 7600 computational facility at the NASA-Ames Research Center. This is the first high-resolution search for narrow-band signals in this wavelength regime. To date it is the most sensitive search per unit observing time of any search strategy which does not postulate a unique magic frequency. Data show no evidence for narrow-band signals due to extraterrestrial intelligence at a 12-standard-deviation upper limit on signal strength of 1.1×10^{-23} W/sq m. (Author)

A80-40383 * **Physical chemistry and evolution of salt tolerance in halobacteria.** J. K. Lanyi (NASA, Ames Research Center, Moffett Field, Calif.). (*College Park Colloquium on Chemical Evolution: Limits of Life, 4th, College Park, Md., Oct. 18-20, 1978.*) *Origins of Life*, vol. 10, June 1980, p. 161-167. 35 refs.

The cellular constituents of extremely halophilic bacteria not only tolerate high salt concentration, but in many cases require it for optical functioning. The characteristics affected by salt include enzyme activity, stability, allosteric regulation, conformation and subunit association. The salt effects are of two major kinds: electrostatic shielding of negative charges by cations at low salt concentration, and hydrophobic stabilization by salting-out type salts at high salt concentration. The composition of halobacterial proteins shows an excess of acidic amino acids and a deficiency of nonpolar amino acids, which accounts for these effects. Since the

cohesive forces are weaker and the repulsing forces are stronger in these proteins, preventing aggregation in salt, these structures are no longer suited for functioning in the absence of high salt concentrations. Unlike these nonspecific effects, ribosomes in halobacteria show marked preference for potassium over sodium ions. To ensure the proper intracellular ionic composition, powerful ion transport systems have evolved in the halobacteria, resulting in the extrusion of sodium ions and their replacement by potassium. It is likely that such membrane transport system for ionic movements is a necessary requisite for salt tolerance. (Author)

A80-41250 * The intracellular Na⁺/ and K⁺/ composition of the moderately halophilic bacterium, *Paracoccus halodenitrificans*. M. Sadler, M. McAninch, L. I. Hochstein (NASA, Ames Research Center, Extraterrestrial Research Div., Moffett Field, Calif.), and R. Alico. *Canadian Journal of Microbiology*, vol. 26, no. 4, 1980, p. 496-502. 24 refs.

A80-41661 * Na⁺ and Ca²⁺ ingestion - Plasma volume-electrolyte distribution at rest and exercise. J. E. Greenleaf and P. J. Brock (NASA, Ames Research Center, Biomedical Research Div., Moffett Field, Calif.). *Journal of Applied Physiology: Respiratory, Environmental and Exercise Physiology*, vol. 48, May 1980, p. 838-847. 24 refs.

The effects of hypernatremia and hypercalcemia on plasma volume and electrolyte distribution during rest, exercise and recovery in cool and hot environments are investigated. Plasma volume, protein and electrolytes were measured in two groups of five men in the supine position during rest, exercise at 40-47% maximal oxygen consumption and recovery in 26.5 C and 39.4 C environments, after ingestion in the rest period of 16-17 ml/kg hypertonic NaCl, isotonic NaCl or hypertonic calcium gluconate solutions. During the rest period, it is found that the hypertonic Ca drink prevents any rise in plasma volume in both cool and hot environments, while hypertonic Na retarded hypervolemia only in the cool environment and consumption of both isotonic and hypertonic Na in the heat resulted in a hypervolemic response twice as great as that in the cool environment. During exercise and recovery, plasma volume is found to be greatest after drinking hypertonic Na in the heat, while the normal hypervolemic responses during exercise were not influenced by drink composition. Results suggest that hypertonic drinks may be better for maintaining plasma volumes during exercise in the heat.

A.L.W.

A80-41995 * Retinal changes in rats flown on Cosmos 936 - A cosmic ray experiment. D. E. Philpott, R. Corbett, C. Turnbull, S. Black, D. Dayhoff, J. McGourty, R. Lee, G. Harrison (NASA, Ames Research Center, Ultrastructural Research Laboratory and Biomedical Research Div., Moffett Field, Calif.), and L. Savik (Ministerstvo Zdravookhraneniia SSSR, Institut Mediko-Biologicheskikh Problem, Moscow, USSR). *Aviation, Space, and Environmental Medicine*, vol. 51, June 1980, p. 556-562. 27 refs.

Ten rats, five centrifuged during flight to simulate gravity and five stationary in flight and experiencing hypogravity, orbited the Earth. No differences were noted between flight-stationary and flight-centrifuged animals, but changes were seen between these two groups and ground controls. Morphological alterations were observed comparable to those in the experiment flown on Cosmos 782 and to the retinal cells exposed to high-energy particles at Berkeley. Affected cells in the outer nuclear layer showed swelling, clearing of cytoplasm, and disruption of the membranes. Tissue channels were again found, similar to those seen on 782. After space flight, preliminary data indicated an increase in cell size in montages of the

nuclear layer of both groups of flight animals. This experiment shows that weightlessness and environmental conditions other than cosmic radiation do not contribute to the observed damage of retinal cells. (Author)

A80-42003 * Thresholds for detection of constant rotary acceleration during vibratory rotary acceleration. B. Clark, J. D. Stewart, and N. H. Phillips (NASA, Ames Research Center, Moffett Field; San Jose State University, San Jose, Calif.). *Aviation, Space, and Environmental Medicine*, vol. 51, June 1980, p. 603-606. 19 refs. Grant No. NCC2-35.

The effects of vibratory angular acceleration on detection thresholds for constant angular acceleration in a dynamic flight simulator are reported in three experiments. Detection thresholds were determined for 10 pilots and four nonpilots using a random, double-staircase procedure while the subjects sat erect in a device which rotated about an earth-vertical axis. Constant angular acceleration were presented for 0.5 and 1.0 s with concurrent, vibratory angular acceleration at 1 and 5 Hz, and thresholds with no vibratory angular acceleration were established. The thresholds were obtained while the subjects observed a visual reference in the enclosed cockpit in two experiments and in total darkness in a third. The results confirmed earlier experiments showing an inverse relationship between the duration of constant angular acceleration and detection threshold and showed that the detection thresholds in darkness were higher than with a visual reference present. Two analyses of variance revealed no significant differences in thresholds across the three vibration conditions. These results indicate that vibratory angular acceleration of fairly high levels can be present in a dynamic flight simulator without masking the pilot's ability to detect either maneuver or disturbance motions. (Author)

A80-46196 * Extremes of urine osmolality - Lack of effect on red blood cell survival. H. A. Leon and J. E. Fleming (NASA, Ames Research Center, Biomedical Research Div., Moffett Field, Calif.). *American Journal of Physiology*, vol. 239, July 1980, p. C27-C31. 13 refs.

Rats were allowed a third of normal water intake for 20 days, and food consumption decreased. The reticulocyte count indicated a suppression of erythropoiesis. Urine osmolality increased from 2,000 mosmol/kg to 3,390 mosmol/kg. Random hemolysis and senescence of a cohort of red blood cell (RBC) previously labeled with (2-C-14) glycine was monitored via the production of (C-14)O. Neither hemolysis nor senescence was affected. Following water restriction, the polydipsic rats generated a hypotonic urine. Urine osmolality decreased to 1,300 mosmol/kg for at least 6 days; a include the different types of natural boundary conditions. Finite element equations corresponding to the various formulations are then presented and applied to a simple one-dimensional bore propagation problem to examine the consequences of the different weighted residual formulations, and to the computation of current velocity and water elevation in an idealized closed basin excited periodically at its entrance. Finally, a finite element analysis of the storm surge accompanying the attack of a moderate-scale typhoon on Surugawan Bay, on the Pacific coast of Japan, is presented and shown to be in reasonably good agreement with tide measurements.

A.L.W.

A80-48086 * # Fluid-electrolyte shifts and thermoregulation - Rest and work in heat with head cooling. J. E. Greenleaf, W. Van Beaumont, P. J. Brock, L. D. Montgomery, J. T. Morse, E. Shvartz, and S. Kravik (NASA, Ames Research Center, Biomedical Research Div., Moffett Field, Calif.). *Aviation, Space, and Environmental Medicine*, vol. 51, Aug. 1980, p. 747-753. 28 refs.

The effects of head cooling on thermoregulation and associated plasma fluid and electrolyte shifts during rest and submaximal exercise in the heat are investigated. Thermoregulatory responses and plasma volume were measured in four male subjects fitted with liquid-cooled neoprene headgear during 80 min of rest, 60 min of ergometer exercise at 45% maximal oxygen uptake and 30 min of recovery in the supine position at 40.1 C and 40% relative humidity. It is found that, compared to control responses, head cooling decreased thigh sweating and increased mean skin temperature at rest and attenuated increases in thigh sweating, heart rate, rectal temperature and ventilation during exercise. During recovery, cooling is observed to facilitate decreases in sweat rate, heart rate, rectal temperature and forearm blood flow and enhance the increase in average temperature. Cooling had no effect on plasma protein, osmotic or electrolyte shifts, and decreased plasma volume losses. The findings indicate the effectiveness of moderate head cooling for the improvement of human performance during exercise in heat.

A.L.W.

A80-54076 * **Extracellular hyperosmolality and body temperature during physical exercise in dogs.** S. Kozlowski, J. E. Greenleaf, E. Turlejska, and K. Nazar (NASA, Ames Research Center, Biomedical Research Div., Moffett Field, Calif.; Polish Academy of Sciences, Medical Research Centre, Warsaw, Poland). *American Journal of Physiology*, vol. 239, July 1980, p. R180-R183. 23 refs.

The purpose of this study was to test the hypothesis that thermoregulation during exercise can be affected by extracellular fluid hyperosmolality without changing the plasma Na(+) concentration. The effects of preexercise venous infusions of hypertonic mannitol and NaCl solutions on rectal temperature responses were compared in dogs running at moderate intensity for 60 min on a treadmill. Plasma Na(+) concentration was increased by 12 meq after NaCl infusion, and decreased by 9 meq after mannitol infusion. Both infusions increased plasma by 15 mosmol/kg. After both infusions, rectal temperature was essentially constant during 60 min rest. However, compared with the noninfusion exercise increase in osmolality of 1.3 C, rectal temperature increased by 1.9 C after both postinfusion exercise experiments. It was concluded that inducing extracellular hyperosmolality, without elevating plasma, can induce excessive increases in rectal temperature during exercise but not at rest.

(Author)

CONFERENCE PAPERS

N80-11975*# National Aeronautics and Space Administration. Ames Research Center, Moffett Field, Calif.
COMETS: COSMIC CONNECTIONS WITH CARBONACEOUS METEORITES, INTERSTELLAR MOLECULES AND THE ORIGIN OF LIFE
Sherwood Chang *In* NASA. Goddard Space Flight Center Space Missions to Comets 1979 p 59-111 refs (For primary document see N80-11972 02-91)
Avail: NTIS HC A11/MF A01 CSDL 03B

The ions, radicals, and molecules observed in comets may be derived intact or by partial decomposition from parent compounds of the sort found either in the interstellar medium or in carbonaceous meteorites. The early loss of highly reducing primitive atmosphere and its replacement by a secondary atmosphere dominated by H₂O, CO₂, and N₂, as depicted in current models of the earth's evolution, pose a dilemma for the origin of life: the synthesis of organic compounds necessary for life from components of the secondary atmosphere appears to be difficult, and plausible mechanisms have not been evaluated. Both comets and carbonaceous meteorites are implicated as sources for the earth's atmophilic and organogenic elements. A mass balance argument involving the estimated ratios of hydrogen to carbon in carbonaceous meteorites, comets, and the crust

and upper mantle suggests that comets supplied the earth with a large fraction of its volatiles. The probability that comets contributed significantly to the earth's volatile inventory suggests a chemical evolutionary link between comets, prebiotic organic synthesis, and the origin of life.

A.R.H.

A80-15240 * # **High-pressure protective systems technology.** H. C. Vykukap' and B. W. Webbon (NASA, Ames Research Center, Moffett Field, Calif.). *American Society of Mechanical Engineers, Intersociety Conference on Environmental Systems, 9th, San Francisco, Calif., July 16-19, 1979, Paper 79-ENAS-15.* 16 p. 14 refs. Members, \$1.50; nonmembers, \$3.00.

Space suit assemblies developed in the past provide candidate concepts to meet future extravehicular-activity requirements. The paper is concerned with the development of the modular 8-psi Ames AX-3 high-pressure suit assembly on the basis of a review of existing suit assemblies, component developments, and mobility exercises. The discussion covers description of the AX-3 suit, its performance, and technology developments. In conclusion, high-pressure space suit technology is demonstrated with the development of the Ames AX-3 suit assembly. Several photographs and diagrams supplement the text.

S.D.

A80-15256 * # **Bosch - An alternate CO₂ reduction technology.** D. B. Heppner, T. M. Hallick (Life Systems, Inc., Cleveland, Ohio), D. C. Clark (NASA, Marshall Space Flight Center, Huntsville, Ala.), and P. D. Quattrone (NASA, Ames Research Center, Moffett Field, Calif.). *American Society of Mechanical Engineers, Intersociety Conference on Environmental Systems, 9th, San Francisco, Calif., July 16-19, 1979, Paper 79-ENAS-32.* 9 p. 11 refs. Members, \$1.50; nonmembers, \$3.00. Contracts No. NAS8-30891; No. NAS8-32492; No. NAS2-8666.

The Bosch process is the most promising CO₂ reduction concept for future prolonged space missions. The paper presents the design of a three-person-capacity preprototype B-CRS (Bosch-based CO₂ Reduction Subsystem). It is sized to reduce 3.0 kg/d CO₂ generated by the crew and to supply the product water to an O₂ generation subsystem to obtain O₂. The design supports future development of the B-CRS as an alternative CO₂ reduction subsystem to the Sabatier-based process presently under test at NASA. The discussion covers the Bosch CO₂ reduction concept, process and hardware description, performance parameters, design specifications, subsystem schematic and operation, mechanical subsystem summary, control/monitor instrumentation, and subsystem packaging. A B-CRS with a proven technological base is an attractive CO₂ reduction subsystem that eliminates overboard venting.

S.D.

A80-15257 * # **Development of the electrochemically regenerable carbon dioxide absorber for portable life support system application.** R. R. Woods, D. B. Heppner, R. D. Marshall (Life Systems, Inc., Cleveland, Ohio), and P. D. Quattrone (NASA, Ames Research Center, Moffett Field, Calif.). *American Society of Mechanical Engineers, Intersociety Conference on Environmental Systems, 9th, San Francisco, Calif., July 16-19, 1979, Paper 79-ENAS-33.* 9 p. 12 refs. Members, \$1.50; nonmembers, \$3.00. Contract No. NAS2-8666.

As the length of manned space missions increase, more ambitious extravehicular activities (EVAs) are required. For the projected longer mission the use of expendables in the portable life support system (PLSS) will become prohibited due to high launch weight and volume requirements. Therefore, the development of a regenerable CO₂ absorber for the PLSS application is highly desirable. The paper discusses the concept, regeneration mechanism, performance, system design, and absorption/regeneration cycle

testing of a most promising concept known as ERCA (Electrochemically Regenerable CO₂ Absorber). This concept is based on absorbing CO₂ into an alkaline absorbent similar to LiOH. The absorbent is an aqueous solution supported in a porous matrix which can be electrochemically regenerated on board the primary space vehicle. With the metabolic CO₂ recovery the ERCA concept results in a totally regenerable CO₂ scrubber. The ERCA test hardware has passed 200 absorption/regeneration cycles without performance degradation. S.D.

A80-19895 * On the design of a postprocessor for a search for extraterrestrial intelligence /SETI/ system. T. J. Healy (Santa Clara, University, Santa Clara, Calif.), C. L. Seeger (NASA, Ames Research Center, SETI Program Office, Moffett Field; San Francisco State University, San Francisco, Calif.), and M. A. Stull (NASA, Ames Research Center, SETI Program Office, Moffett Field, Calif.). *International Astronautical Federation, International Astronautical Congress, 30th, Munich, West Germany, Sept. 17-22, 1979, Paper 79-A-39*. 12 p. Research sponsored by the American Society for Engineering Education, University of Santa Clara, and NASA.

The design of an on-line postprocessor for a search for extraterrestrial intelligence (SETI) system is described. Signal processing tasks of the postprocessor include: (1) analysis of power level, phase coherence, and state of polarization of single-channel signals in a search for significant signals; (2) grouping or aggregation of adjacent channel data, time averaging of data; and (3) the detection of drifting and modulated signals. Control functions include multichannel spectrum analyzer frequency and clock control, system calibration and selfdiagnostic, control of data flow to and from short-term and long-term (archival) memories, and operation of detection subsystems, such as a visual display and a tunable receiver. V.T.

A80-23669 * Noble gas trapping and fractionation during synthesis of carbonaceous matter. U. Frick (Minnesota, University, Minneapolis, Minn.), R. Mack, and S. Chang (NASA, Ames Research Center, Extraterrestrial Research Div., Moffett Field, Calif.). In: *Lunar and Planetary Science Conference, 10th, Houston, Tex., March 19-23, 1979, Proceedings. Volume 2*. (A80-23617 08-91) New York, Pergamon Press, Inc., 1979, p. 1961-1972. 40 refs. Grants No. NGL-75-003-409; No. NGL-24-005-225.

An investigation of noble gas entrapment during synthesis of carbonaceous, macromolecular, and kerogen-like substances is presented. High molecular weight organic matter synthesized in aqueous condensation reactions contained little gas, and the composition was consistent with fractionation due to noble gas solubility in water; however, propane soot produced during a modified Miller-Urey experiment in an artificial gas mixture contained high concentrations of trapped noble gases that displayed strong elemental fractionation from their reservoirs. It is concluded that these experiments show that processes exist for synthesis of carbonaceous carriers that result in high noble gas concentrations and strong elemental fractionation at temperatures well above those required by absorption to achieve similar effects. A.T.

A80-24158 * Plasma etching of poly(N,N'-p,p'-oxydiphenylene/pyromellitimide/ film and photo/thermal degradation of etched and unetched film. T. Wydeven, C. C. Johnson, M. A. Golub, M. S. Hsu, and N. R. Lerner (NASA, Ames Research Center, Moffett Field, Calif.). In: *Plasma Polymerization*. Washington, D.C., American Chemical Society (ACS Symposium Series, No. 108), 1979, p. 299-314. 17 refs.

A80-24265 * Optimal estimator model for human spatial orientation. J. Borah (G & W Applied Science Laboratories, Waltham, Mass.), L. R. Young (MIT, Cambridge, Mass.), and R. E. Curry (NASA, Ames Research Center, Moffett Field, Calif.). In: *Joint Automatic Control Conference, Denver, Colo., June 17-21, 1979, Proceedings*. (A80-24226 08-63) New York, American Institute of Chemical Engineers, 1979, p. 800-805. 17 refs. Contract No. F33615-76-C-0039.

A model is being developed to predict pilot dynamic spatial orientation in response to multisensory stimuli. Motion stimuli are first processed by dynamic models of the visual, vestibular, tactile, and proprioceptive sensors. Central nervous system function is then modeled as a steady-state Kalman filter which blends information from the various sensors to form an estimate of spatial orientation. Where necessary, this linear central estimator has been augmented with nonlinear elements to reflect more accurately some highly nonlinear human response characteristics. Computer implementation of the model has shown agreement with several important qualitative characteristics of human spatial orientation, and it is felt that with further modification and additional experimental data the model can be improved and extended. Possible means are described for extending the model to better represent the active pilot with varying skill and work load levels. (Author)

A80-27078 * Changes in body temperature and metabolic rate after injection of calcium into the caudal hypothalamus of the rabbit. P. E. Penn, R. L. Gerber, and B. A. Williams (NASA, Ames Research Center, Biosystems Div., Moffett Field, Calif.). In: *Thermoregulatory mechanisms and their therapeutic implications*. Basel, S. Karger AG, 1980, p. 212, 213. 5 refs.

A80-40340 * # Analysis of eighty-four commercial aviation incidents - Implications for a resource management approach to crew training. M. R. Murphy (NASA, Ames Research Center, Moffett Field, Calif.). In: *Annual Reliability and Maintainability Symposium, San Francisco, Calif., January 22-24, 1980, Proceedings*. (A80-40301 16-38) New York, Institute of Electrical and Electronics Engineers, Inc., 1980, p. 298-306. 9 refs.

A resource management approach to aircrew performance is defined and utilized in structuring an analysis of 84 exemplary incidents from the NASA Aviation Safety Reporting System. The distribution of enabling and associated (evolutionary) and recovery factors between and within five analytic categories suggests that resource management training be concentrated on: (1) interpersonal communications, with air traffic control information of major concern; (2) task management, mainly setting priorities and appropriately allocating tasks under varying workload levels; and (3) planning, coordination, and decisionmaking concerned with preventing and recovering from potentially unsafe situations in certain aircraft maneuvers. (Author)

A80-43192 * # Water recovery by catalytic treatment of urine vapor. P. Budininkas (Gard, Inc., Niles, Ill.), P. D. Quattrone, and M. I. Leban (NASA, Ames Research Center, Moffett Field, Calif.). *American Society of Mechanical Engineers, Intersociety Environmental Systems Conference, San Diego, Calif., July 14-17, 1980, Paper 80-ENAS-16*. 6 p. Members, \$1.50; nonmembers, \$3.00. Contracts No. NAS2-9715; No. NAS2-10237.

The objective of this investigation was to demonstrate the feasibility of water recovery on a man-rated scale by the catalytic processing of untreated urine vapor. For this purpose, two catalytic systems, one capable of processing an air stream containing low urine vapor concentrations and another to process streams with high urine vapor concentrations, were designed, constructed, and tested to establish the quality of the recovered water. (Author)

A80-43194 * # The preparation of calcium superoxide in a flowing gas stream and fluidized bed. P. C. Wood, E. V. Ballou, L. A. Spitze (San Jose State University, San Jose, Calif.), and T. Wydeven (NASA, Ames Research Center, Moffett Field, Calif.). *American Society of Mechanical Engineers, Intersociety Environmental Systems Conference, San Diego, Calif., July 14-17, 1980, Paper 80-ENAS-18*. 6 p. 11 refs. Members, \$1.50; nonmembers, \$3.00. Research supported by the U.S. Bureau of Mines.

Superoxides can be used as sources of chemically stored oxygen in emergency breathing apparatus. The work reported here describes the use of a low-pressure nitrogen gas sweep through the reactant bed, for temperature control and water vapor removal. For a given set of gas temperature, bed thickness, and reaction time values, the highest purity calcium superoxide, $\text{Ca}(\text{O}_2)_2$, was obtained at the highest space velocity of the nitrogen gas sweep. The purity of the product was further increased by flow conditions that resulted in the fluidization of the reactant bed. However, scale-up of the low-pressure fluidized bed process was limited to the formation of agglomerates of reactant particles, which hindered thermal control by the flowing gas stream. A radiofrequency flow discharge inside the reaction chamber prevented agglomeration, presumably by dissipation of the static charges on the fluidized particles. (Author)

A80-43209 * # NASA-Ames Life Sciences Flight Experiments program - 1980 status report. W. E. Berry, C. C. Dant, G. MacLeod (GE Management and Technical Services Co., Moffett Field, Calif.), and B. A. Williams (NASA, Ames Research Center, Moffett Field, Calif.). *American Society of Mechanical Engineers, Intersociety Environmental Systems Conference, San Diego, Calif., July 14-17, 1980, Paper 80-ENAS-34*. 3 p. Members, \$1.50; nonmembers, \$3.00.

The paper deals with the ESA's Spacelab LSFE (Life Sciences Flight Experiments) program which, once operational, will provide new and unique opportunities to conduct research into the effects of spaceflight and weightlessness on living organisms under conditions approximating ground-based laboratories. Spacelab missions, launched at 18-month intervals, will enable scientists to test hypotheses from such disciplines as vestibular physiology, developmental biology, biochemistry, cell biology, plant physiology, and similar life sciences. V.P.

A80-43212 * # Evaluation of biological models using Space-lab. D. Tollinger (GE Management and Technical Services Co., Moffett Field, Calif.) and B. A. Williams (NASA, Ames Research Center, Moffett Field, Calif.). *American Society of Mechanical Engineers, Intersociety Environmental Systems Conference, San Diego, Calif., July 14-17, 1980, Paper 80-ENAS-38*. 7 p. 30 refs. Members, \$1.50; nonmembers, \$3.00. Contract No. NAS9-15850.

Biological models of hypogravity effects are described, including the cardiovascular-fluid shift, musculoskeletal, embryological and space sickness models. These models predict such effects as loss of extracellular fluid and electrolytes, decrease in red blood cell mass, and the loss of muscle and bone mass in weight-bearing portions of the body. Experimentation in Spacelab by the use of implanted electromagnetic flow probes, by fertilizing frog eggs in hypogravity and fixing the eggs at various stages of early development and by assessing the role of the vestibulocular reflex arc in space sickness is suggested. It is concluded that the use of small animals eliminates the uncertainties caused by corrective or preventive measures employed with human subjects. J.P.B.

A80-50053 * Organic compounds in meteorites. J. G. Lawless (NASA, Ames Research Center, Moffett Field, Calif.). In: *Life sciences and space research. Volume 18 - Proceedings of the Open*

Meeting of the Working Group on Space Biology, Bangalore, India, May 29-June 9, 1979. (A80-50051 22-51) Oxford and Elmsford, N.Y., Pergamon Press, 1980, p. 19-27. 29 refs.

Recent studies of carbonaceous chondrites provide evidence that certain organic compounds are indigenous and the result of an abiotic, chemical synthesis. The results of several investigators have established the presence of amino acids and precursors, mono- and dicarboxylic acids, N-heterocycles, and hydrocarbons as well as other compounds. For example, studies of the Murchison and Murray meteorites have revealed the presence of at least 40 amino acids with nearly equal abundances of D and L isomers. The population consists of both protein and nonprotein amino acids including a wide variety of linear, cyclic, and polyfunctional types. Results show a trend of decreasing concentration with increasing carbon number, with the most abundant being glycine (41 n Moles/g). These and other results to be reviewed provide persuasive support for the theory of chemical evolution and provide the only natural evidence for the protobiological subset of molecules from which life on earth may have arisen. (Author)

A80-50060 * The possible role of metal ions and clays in prebiotic chemistry. J. G. Lawless (NASA, Ames Research Center, Extraterrestrial Research Div., Moffett Field, Calif.) and E. H. Edelson (Southern California, University, Los Angeles, Calif.). In: *Life sciences and space research. Volume 18 - Proceedings of the Open Meeting of the Working Group on Space Biology, Bangalore, India, May 29-June 9, 1979. (A80-50051 22-51) Oxford and Elmsford, N.Y., Pergamon Press, 1980, p. 83-88. 17 refs.*

Eight homoionic bentonites were prepared using alkali, alkaline earth, and transition metal ions as counterions. The interaction of the clays with 5'-AMP was studied and it was found that the alkali metal-substituted clays did not remove any nucleotide from dilute solution, and that zinc-bentonite adsorbed the most (98%). In addition, study of the interaction of seven other nucleotides with zinc-bentonite showed that the purine nucleotides were more strongly absorbed than the pyrimidine nucleotides. Langmuir isotherms were obtained for these systems and the adsorption data were explained by the adsorption coefficient and the accessibility of metal for binding. (Author)

AMES FUNDED RESEARCH JOURNAL ARTICLES

A80-20447 * Hypergravity and estrogen effects on avian anterior pituitary growth hormone and prolactin levels. R. P. Fiorindo and J. A. Negulesco (Ohio State University, Columbus, Ohio). *Aviation, Space, and Environmental Medicine*, vol. 51, Jan. 1980, p. 35-40. 26 refs. Research supported by the Ohio State University; Contract No. NAS2-6634.

Developing female chicks with fractured right radii were maintained for 14 d at either earth gravity (1 g) or a hypergravity state (2 g). The birds at 1 g were divided into groups which received daily injections of (1) saline, (2) 200 micrograms estrone, and (3) 400 micrograms estrone for 14 d. The 2-g birds were divided into three similarly treated groups. All 2-g birds showed significantly lower body weights than did 1-g birds. Anterior pituitary (AP) glands were excised and analyzed for growth hormone and prolactin content by analytical electrophoresis. The 1-g chicks receiving either dose of daily estrogen showed increased AP growth hormone levels, whereas hypergravity alone did not affect growth hormone content. Chicks exposed to daily estrogen and hypergravity displayed reduced growth hormone levels. AP prolactin levels were slightly increased by the lower daily estrogen dose in 1-g birds, but markedly reduced in birds exposed only to hypergravity. Doubly-treated chicks displayed normal prolactin levels. Reduced growth in 2-g birds might be due, in part, to reduced AP levels of prolactin and/or growth hormone. (Author)

A80-21544 * Simulated weightlessness - Effects on bioenergetic balance. J. P. Jordan, H. A. Sykes, J. C. Crownover, C. L. Schatte, J. B. Simmons, II, and D. P. Jordan (Colorado State University, Fort Collins, Colo.). *Aviation, Space, and Environmental Medicine*, vol. 51, Feb. 1980, p. 132-136. 35 refs. Grant No. NsG-2232.

As a prelude to a flight experiment, an attempt was made to separate energy requirements associated with gravity from all other metabolic needs. The biological effects of weightlessness were simulated by suspending animals in a harness so that antigravity muscles were not supporting the body. Twelve pairs of rats were allowed to adapt to wearing a harness for 5 d. Experimental animals were then suspended in harness for 7 d followed by recovery for 7 d. Control animals were harnessed but never suspended. Oxygen consumption, carbon dioxide production and rate of (C-14)O₂ expiration from radio-labeled glucose were monitored on selected days. Food intake and body mass were recorded daily. Metabolic rate decreased in experimental animals during 7 d of suspension and returned to normal during recovery. Although some of the metabolic changes may have related to variation in food intake, simulated weightlessness appears to directly affect bioenergetic balance.

(Author)

A80-21547 * Physiological response to hyper- and hypogravity during rollercoaster flight. R. J. von Baumgarten, H. Vogel (Mainz, Universität, Mainz, West Germany), G. Baldrighi (Michigan, University, Ann Arbor, Mich.), and R. Thümler (Michigan, University, Ann Arbor, Mich.; Mainz, Universität, Mainz, West Germany). *Aviation, Space, and Environmental Medicine*, vol. 51, Feb. 1980, p. 145-154. 27 refs. Contract No. NAS2-9466.

Twenty-six healthy male subjects were flown in a Lear jet aircraft through rollercoaster and parabolic weightlessness flight. Eye movements, respiration, and blood volume pulse were recorded on magnetic tape. The same subjects underwent a battery of five vestibular tests in the laboratory on the ground. One subject in each flight was flown in an upright position, the other in a 90 deg forward tilted head position. The forward tilted subjects always reported motion sickness earlier and after fewer rollercoaster maneuvers than the upright-sitting subjects. It is concluded that the susceptibility to changes of X-axis acceleration is higher than to changes of Z-axis acceleration. Correlation was found between the ability to estimate the subjective vertical (modified Müller-Aubert-test), optokinetic nystagmus asymmetries, and susceptibility to rollercoaster flight sickness.

(Author)

A80-25891 * Motion sickness in the squirrel monkey. J. M. Ordy and K. R. Brizzee (Tulane University, Covington, La.). *Aviation, Space, and Environmental Medicine*, vol. 51, Mar. 1980, p. 215-223. 42 refs. Grants No. NIH-R-00164; No. NsG-2139.

In this study of susceptibility to motion sickness the specific aims were to examine the effects of combined vertical rotation and horizontal acceleration, phenotype, sex, visual cues, morning and afternoon testing, and repeated test exposures on incidence, frequency, and latency of emetic responses. The highest emetic incidence of 89% with an emetic frequency of 2.0 during 60 min and a latency of 19 min from onset of testing occurred at 25 rpm and 0.5 Hz linear acceleration. Since the emetic responses were quite similar to man in eliciting motion stimuli it was concluded that the squirrel monkey represents a very suitable primate model for studies of motion and space sickness.

B.J.

A80-28188 * A model for hypokinesia: Effects on muscle atrophy in the rat. X. J. Musacchia, D. R. Deavers, G. A. Meininger, and T. P. Davis (Louisville, University, Louisville, Ky.; Missouri, University, Columbia, Mo.). *Journal of Applied Physiology: Respira-*

tory, Environmental and Exercise Physiology, vol. 48, Mar. 1980, p. 479-486. 28 refs. Grants No. NsG-2191; No. NsG-2325.

Hypokinesia in the hindlimbs of rats was induced by suspension; a newly developed harness system was used. The animal was able to use its forelimbs to maneuver, within a 140 deg arc, to obtain food and water and to permit limited grooming of the forequarters. The hindlimbs were nonload bearing for 7 days; following a 7-day period of hypodynamia, selected animals were placed in metabolic cages for 7 days to study recovery from hypokinesia. During the 7-day period of hypokinesia there was evidence of muscle atrophy. Gastrocnemius weight decreased, renal papillary urea content increased, and daily urinary losses of NH₃ and 3-methylhistidine increased. During the 7-day recovery period muscle mass and excretion rate of urea, NH₃ and 3-methylhistidine returned to control levels. Calcium balance was positive throughout the 7-day period of hypokinesia. Hypertrophy of the adrenals suggested the occurrence of some level of stress despite the apparent behavioral adjustment to the suspension harness. It was concluded that significant muscle atrophy and parallel changes in nitrogen metabolism occur in suspended rats and these changes are readily reversible.

(Author)

A80-40898 * Dynamic decisions and work load in multitask supervisory control. M. K. Tulga (Commercial Information Corp., Woburn, Mass.) and T. B. Sheridan (MIT, Cambridge, Mass.). *IEEE Transactions on Systems, Man, and Cybernetics*, vol. SMC-10, May 1980, p. 217-232. 38 refs. Grant No. NsG-2118.

A paradigm is developed for the problem of allocating in time a single resource to multiple simultaneous task demands which appear randomly, last for various periods, and offer varying rewards for service. Based upon a dynamic optimizing algorithm plus an estimator, and including response time and future discounting constraints, a model of the human decisionmaker is compared to experimental results for human subjects performing such a task at a computer-graphics terminal. Results indicate a reasonable fit, under various model parameters and task conditions, and suggest interesting hypotheses about the nature of human 'planning ahead' and mental work load.

(Author)

A80-40899 * Optimal control model predictions of system performance and attention allocation and their experimental validation in a display design study. G. Johannsen and T. Govindaraj (Purdue University, Lafayette, Ind.). *IEEE Transactions on Systems, Man, and Cybernetics*, vol. SMC-10, May 1980, p. 249-261. 25 refs. Grant No. NsG-2119.

The influence of different types of predictor displays in a longitudinal vertical takeoff and landing (VTOL) hover task is analyzed in a theoretical study. Several cases with differing amounts of predictive and rate information are compared. The optimal control model of the human operator is used to estimate human and system performance in terms of root-mean-square (rms) values and to compute optimized attention allocation. The only part of the model which is varied to predict these data is the observation matrix. Typical cases are selected for a subsequent experimental validation. The rms values as well as eye-movement data are recorded. The results agree favorably with those of the theoretical study in terms of relative differences. Better matching is achieved by revised model input data.

(Author)

A80-41532 * Improved characterization of the Si-SiO₂ interface. P. Su, A. Sher, Y. H. Tsuo, J. A. Moriarty (College of William and Mary, Williamsburg, Va.), and W. E. Miller (NASA, Langley Research Center, Hampton, Va.). *Applied Physics Letters*, vol. 36, June 15, 1980, p. 991-993. 9 refs. Grant No. NsG-2385.

Refined quasi-static and conductance methods, based on effec-

tively thin composite insulating layers, low-carrier-concentration bulk semiconductors, and low-level illumination, have been applied to an improved characterization of the (100) Si-SiO₂ interface. Accurate measurement of both the total density of interface states and its major components as a function of energy in the forbidden gap have been made over four decades (10-billion to 100-trillion states/eV sq cm) on a single sample. The normal U-shaped density of states is resolved into separate valence- and conduction-band-derived contributions as well as impurity-derived contributions corresponding to concentrations on the order of 20 ppm at the interface.

(Author)

A80-41983 * **Effects of chronic centrifugation on skeletal muscle fibers in young developing rats.** W. D. Martin (Albert B. Chandler Medical Center, Lexington, Ky.). *Aviation, Space, and Environmental Medicine*, vol. 51, May 1980, p. 473-479. 22 refs. Grant No. NsG-2187.

Three groups of 30-d old male and female rats were centrifuged for 2, 4, 8, and 16 weeks, after which their soleus and plantaris muscles were analysed for changes in proportions of muscle fiber types. The groups were: earth control, maintained at earth gravity without rotation; rotation control, subjected to a gravitational force of 1.05 G and 28 rpm; and rotation experimental, subjected to a gravitational force of 2 G and 28 rpm. Muscle fibers were classified into four fiber types on the basis of actomyosin ATPase activity as slow oxidative, fast oxidative glycolytic and either fast glycolytic (plantaris) or intermediate (soleus). Hypergravity resulted in an increase in slow oxidative fibers in soleus relative to the earth control, but not of females treated similarly. The relationship of body weight to the changes in proportion of slow oxidative fibers is discussed.

(Author)

A80-42013 * **The architecture of the avian retina following exposure to chronic 2 G.** R. G. Orlando and J. A. Negulesco (Ohio State University, Columbus, Ohio). *Aviation, Space, and Environmental Medicine*, vol. 51, July 1980, p. 704-708. 18 refs. Research supported by the Ohio State University; Contract No. NAS2-6634.

Rhode Island Red female chicks at 2 weeks posthatch were subjected, for 7 d, to either earth gravity of 1 G or a 2-G hypergravity environment by chronic whole-body centrifugation. Animals were sacrificed at 3 weeks posthatch and the eyes were enucleated, fixed in 10% BNF, doubly embedded, sectioned at 7-8 microns and routinely processed with H & E for histological examination. Compared to normogravity controls, animal exposure for 1 week to the chronic effects of 2-G resulted in a significantly decreased mean width of the photoreceptor, inner nuclear, and inner plexiform retinal layers. The outer nuclear, outer plexiform, and ganglion cell layers of the retina appeared minimally affected by the hypergravity state since the mean width of these layers showed no noticeable differences from earth gravity control animals. The present anatomic findings suggest a reduction in the detection of motion or rapid changes in illumination by the avian retina when the animal is exposed at a 2-G environment.

(Author)

A80-44213 * **Visually induced self-motion sensation adapts rapidly to left-right visual reversal.** C. M. Oman, O. L. Bock, and J.-K. Huang (MIT, Cambridge, Mass.). *Science*, vol. 209, Aug. 8, 1980, p. 706-708. 16 refs. Grant No. NsG-2032; Contract No. NAS9-15343.

The experimental demonstration of a reversal of the circularvection (CV) phenomenon is reported. After one to three hours of active movement while wearing vision-reversing goggles, 9 of 12 stationary human subjects viewing a moving stripe display experienced a self-rotation illusion in the same direction as the seen stripe motion. In addition, the subjects showed a 17% reduction in

vestibulo-ocular reflex slow phase gain over their brief exposure period. It is noted that whether a subject demonstrated reversed CV within the allowed exposure period appeared to be correlated with CV strength produced with a narrow field stimulus.

J.P.B.

A80-50427 * **Computer-based manuals for procedural information.** S. H. Rouse and W. B. Rouse. *IEEE Transactions on Systems, Man, and Cybernetics*, vol. SMC-10, Aug. 1980, p. 506-510. 9 refs. Grant No. NsG-2119.

Display of procedural information as found in aircraft operating manuals is discussed. The problem of converting hardcopy manuals to a computer-based presentation is considered. The trade-off of faster retrieval and display integration possible with a cathode-ray tube (CRT) versus the limited size of a CRT is emphasized. Nine subjects participated in an experimental study of the effectiveness of three alternative displays. Displays were evaluated for the task of retrieving and carrying out emergency procedures in an environment where task interruptions were prevalent. It was found that an on-line manual which provided considerable user assistance was superior to a hardcopy manual in terms of both task completion time and errors. However, an on-line manual without user assistance was inferior to a hardcopy manual in terms of errors.

(Author)

AMES FUNDED RESEARCH CONFERENCE PAPERS

A80-43193 * # **Adsorption interference in mixtures of trace contaminants flowing through activated carbon adsorber beds.** R. Madey and P. J. Photinos (Kent State University, Kent, Ohio). *American Society of Mechanical Engineers, Intersociety Environmental Systems Conference, San Diego, Calif., July 14-17, 1980, Paper 80-ENAs-17*. 6 p. 22 refs. Members, \$1.50; nonmembers, \$3.00. Grant No. NsG-2013.

Adsorption interference in binary and ternary mixtures of trace contaminants in a helium carrier gas flowing through activated carbon adsorber beds are studied. The isothermal transmission, which is the ratio of the outlet to the inlet concentration, of each component is measured. Interference between co-adsorbing gases occurs when the components are adsorbed strongly. Displacement of one component by another is manifested by a transmission greater than unity for the displaced component over some range of eluted volume. Interference is evidenced not only by a reduction of the adsorption capacity of each component in the mixture in comparison with the value obtained in a single-component experiment, but also by a change in the slope of the transmission curve of each component experiment.

(Author)

A80-43213 * # **The development of a Space Shuttle Research Animal Holding Facility.** R. B. Jagow (Lockheed Missiles and Space Co., Inc., Sunnyvale, Calif.). *American Society of Mechanical Engineers, Intersociety Environmental Systems Conference, San Diego, Calif., July 14-17, 1980, Paper 80-ENAs-39*. 6 p. Members, \$1.50; nonmembers, \$3.00. Contract No. NAS2-10128.

The ability to maintain the well being of experiment animals is of primary importance to the successful attainment of life sciences flight experiment goals. To assist scientists in the conduct of life sciences flight experiments, a highly versatile Research Animal Holding Facility (RAHF) is being developed for use on Space Shuttle/Spacelab missions. This paper describes the design of the RAHF system, which in addition to providing general housing for various animal species, approximating the environment found in ground based facilities, is designed to minimize disturbances of the

specimens by vehicle and mission operations. Life-sustaining capabilities such as metabolic support and environmental control are provided. RAHF is reusable and is a modular concept to accommodate animals of different sizes. The basic RAHF system will accommodate a combination of 24 500-g rats or 144 mice or a mixed number of rats and mice. An alternative design accommodates four squirrel monkeys. The entire RAHF system is housed in a single ESA rack. The animal cages are in drawers which are removable for easy access to the animals. Each cage contains a waste management system, a feeding system and a watering system all of which will operate in zero or one gravity. (Author)

PATENTS

N80-23383* National Aeronautics and Space Administration. Ames Research Center, Moffett Field, Calif.

CHELATE-MODIFIED POLYMERS FOR ATMOSPHERIC GAS CHROMATOGRAPHY Patent

Warren W. Christensen (San Jose State Univ.), Ludwig A. Mayer (San Jose State Univ.), and Fritz H. Woeller, inventors (to NASA) (San Jose State Univ.) Issued 22 Apr. 1980 9 p Filed 30 Jun. 1978 Supersedes N78-27275 (16 - 18, p 2375) Sponsored by NASA

(NASA-Case-ARC-11154-1; US-Patent-4,198,792;

US-Patent-Appl-SN-921626; US-Patent-Class-521-55;

US-Patent-Class-55-66; US-Patent-Class-55-67;

US-Patent-Class-55-68; US-Patent-Class-55-72;

US-Patent-Class-521-146; US-Patent-Class-521-918;

US-Patent-Class-525-4) Avail: US Patent and Trademark Office CSCL 07D

Chromatographic materials were developed to serve as the stationary phase of columns used in the separation of atmospheric gases. These materials consist of a crosslinked porous polymer matrix, e.g., a divinylbenzene polymer, into which has been embedded an inorganic complexed ion such as N,N'-ethylene-bis-(acetylacetoniminato)-cobalt (2). Organic nitrogenous bases, such as pyridine, may be incorporated into the chelate polymer complexes to increase their chromatographic utility. With such materials, the process of gas chromatography is greatly simplified, especially in terms of time and quantity of material needed for a gas separation.

Official Gazette of the U.S. Patent and Trademark Office

N80-23452* National Aeronautics and Space Administration. Ames Research Center, Moffett Field, Calif.

REVERSE OSMOSIS MEMBRANE OF HIGH UREA REJECTION PROPERTIES Patent

Catherine C. Johnson and Theodore J. Wydeven, inventors (to NASA) Issued 22 Apr. 1980 6 p Filed 9 Jun. 1976 Supersedes N77-18265 (15 - 09, p1152)

(NASA-Case-ARC-10980-1; US-Patent-4,199,448;

US-Patent-Appl-SN-694407; US-Patent-Class-210-23H;

US-Patent-Class-204-171; US-Patent-Class-210-500M;

US-Patent-Class-427-41; US-Patent-Class-427-245) Avail: US Patent and Trademark Office CSCL 11G

Polymeric membranes suitable for use in reverse osmosis water purification because of their high urea and salt rejection properties are prepared by generating a plasma of an unsaturated hydrocarbon monomer and nitrogen gas from an electrical source. A polymeric membrane is formed by depositing a polymer of the unsaturated monomer from the plasma onto a substrate, so that nitrogen from the nitrogen gas is incorporated within the polymer in a chemically combined form.

Official Gazette of the U.S. Patent and Trademark Office

RESEARCH SUPPORT

NASA TECHNICAL MEMORANDA

N80-18709*# National Aeronautics and Space Administration. Ames Research Center, Moffett Field, Calif.

OBJECTIVE MEASUREMENT OF HUMAN TOLERANCE TO +G SUB 2 ACCELERATION STRESS Ph.D. Thesis - Univ. of N. Indiana

Salvadore A. Rositano Washington Feb. 1980 100 p refs (NASA-TM-81166; A-8059) Avail: NTIS HC A05/MF A01 CSCL 06S

The efficacy of a new objective technique using a transcutaneous Doppler flowmeter to monitor superficial temporal artery blood flow velocity during acceleration was investigated. The results were correlated with current objective and subjective G tolerance end points. In over 1300 centrifuge runs, retrograde eye level blood flow leading to total flow cessation was consistently recorded and preceded visual field deterioration leading to blackout by 3 to 23 seconds. The new method was successfully applied as an objective indication of tolerance in a variety of test situations including evaluation of g-suits, straining maneuvers, and 13 deg, 45 deg and 65 deg set back angles.

R.E.S.

N80-19471*# National Aeronautics and Space Administration. Ames Research Center, Moffett Field, Calif.

TEXTURE EXTRACTION ON THE ILLIAC 4 Final Report Richard M. Brown and Marsha Jo Hannah 15 May 1979 40 p refs

(AD-A070523; NASA-TM-81002; IAC-TM-5768;

IAC-Ref-77-15/1; ETL-0191) Avail: NTIS HC A03/MF A01 CSCL 14E

IAC has developed texture extraction programs that run on the ILLIAC IV parallel processor. It has used these programs to extract two different texture measures from 32 aerial images provided by ETL. These textures are based on the MAX-MIN technique on the computation of spatial dependence matrices. This report provides high-level descriptions of the texture algorithms, the software system created to implement these algorithms, the test and verification efforts and the results and conclusions.

GRA

NASA CONTRACTOR REPORTS

N80-16070*# Franklin Inst. Research Labs., Philadelphia, Pa. **FEASIBILITY AND CONCEPT STUDY TO CONVERT THE NASA/AMES VERTICAL MOTION SIMULATOR TO A HELICOPTER SIMULATOR** Final Report

C. A. Belsterling, R. C. Chou, E. G. Davies, and K. C. Tsui Sep. 1978 150 p

(Contract NAS2-9884; NASA Order C-4952-1)

(NASA-CR-152193) Avail: NTIS HC A07/MF A01 CSCL 14B

The conceptual design for converting the vertical motion simulator (VMS) to a multi-purpose aircraft and helicopter simulator is presented. A unique, high performance four degrees of freedom (DOF) motion system was developed to permanently replace the present six DOF synergistic system. The new four DOF system has the following outstanding features: (1) will integrate with the two large VMS translational modes and their associated subsystems; (2) can be converted from helicopter to

fixed-wing aircraft simulation through software changes only; (3) interfaces with an advanced cab/visual display system of large dimensions; (4) makes maximum use of proven techniques, convenient materials and off-the-shelf components; (5) will operate within the existing building envelope without modifications; (6) can be built within the specified weight limit and avoid compromising VMS performance; (7) provides maximum performance with a minimum of power consumption; (8) simple design minimizes coupling between motions and maximizes reliability; and (9) can be built within existing budgetary figures.

R.E.S.

JOURNAL ARTICLES

A80-15750 * A solar-heated water system for a photographic processing laboratory. R. P. Michaelis and H. Nitta (NASA, Ames Research Center, Moffett Field, Calif.). (*Society of Photographic Scientists and Engineers and U.S. Geological Survey, Seminar on Chemical and Efficient Management, Sioux Falls, S. Dak., Oct. 1978.*) *Journal of Applied Photographic Engineering*, vol. 5, Summer 1979, p. 127-131. Contract No. NAS2-9925.

A80-50322 * A microprocessor-based instrument for neural pulse wave analysis. G. K. Kojima (NASA, Ames Research Center, Moffett Field, Calif.) and F. Bracchi (Milano, Università, Milan, Italy). *IEEE Transactions on Biomedical Engineering*, vol. BME-27, Sept. 1980, p. 515-519. 12 refs.

CONFERENCE PAPERS

A80-22382 * # The suitability of the ILLIAC IV architecture for image processing. D. K. Stevenson and R. M. Hord (NASA, Ames Research Center, Moffett Field, Calif.). In: *International Symposium on Remote Sensing of Environment*, 13th, Ann Arbor, Mich., April 23-27, 1979, Proceedings. Volume 1. (A80-22376 07-43) Ann Arbor, Mich., Environmental Research Institute of Michigan, 1979, p. 61-71. 10 refs.

The major architectural features of the ILLIAC IV large scale, array processor are summarized along with their applicability to image processing. Several image processing algorithms are considered, including multispectral classification, texture feature extraction, two-dimensional Fourier transform, and synthetic aperture radar processing. The basic parallelism of the ILLIAC IV (64 processing elements acting in lock-step) is usually fully utilized by the image processing applications. The major architectural aspect of the system with respect to image processing is the relatively small local scratch-pad memory and the long latency time to access the main storage device. The major precision used for the image processing applications is the 32-bit floating point, given a choice of 8-bit integers and 64-bit floating point.

B.J.

A80-27432 * Error detection and rectification in digital terrain models. M. J. Hannah (NASA, Ames Research Center, Institute for Advanced Computation, Moffett Field, Calif.). In: American Society of Photogrammetry and American Congress on Surveying and Mapping, Fall Technical Meeting, Sioux Falls, S. Dak., September 17-21, 1979, Joint Proceedings. (A80-27426 10-43) Falls Church, Va., American Society of Photogrammetry, 1979, p. 152-164. 5 refs.

Digital terrain models produced by computer correlation of stereo images are likely to contain occasional gross errors in terrain elevation. These errors typically result from having mismatched sub-areas of the two images, a problem which can occur for a variety of image- and terrain-related reasons. Such elevation errors produce undesirable effects when the models are further processed, and should be detected and corrected as early in the processing as possible. Algorithms have been developed to detect and correct errors in digital terrain models. These algorithms focus on the use of constraints on both the allowable slope and the allowable change in slope in local areas around each point. Relaxation-like techniques are employed in the iteration of the detection and correction phases to obtain best results. (Author)

A80-29480 * # Calorimeter probes for measuring high thermal flux. L. D. Russell (NASA, Ames Research Center, Moffett Field, Calif.). In: ICIASF '79; International Congress on Instrumentation in Aerospace Simulation Facilities, 8th, Monterey, Calif., September 24-26, 1979, Record. (A80-29476 11-35) New York, Institute of Electrical and Electronics Engineers, Inc., 1979, p. 33-36.

The paper describes expendable, slug-type calorimeter probes developed for measuring high heat-flux levels of 10-30 kW/sq cm in electric-arc jet facilities. The probes are constructed with thin tungsten caps mounted on Teflon bodies; the temperature of the back surface of the tungsten cap is measured, and its rate of change gives the steady-state, absorbed heat flux as the calorimeter probe heats to destruction when inserted into the arc jet. It is concluded that the simple construction of these probes allows them to be expendable and heated to destruction to obtain a measurable temperature slope at high heating rates. A.T.

R

PATENTS

N80-18691* National Aeronautics and Space Administration. Ames Research Center, Moffett Field, Calif.

INDUCTION POWERED BIOLOGICAL RADIOSONDE Patent

Thomas B. Fryer, inventor (to NASA) Issued 5 Feb. 1980
12 p Filed 12 May 1977 Supersedes N77-23743 (16 - 14, p 1894)

(NASA-Case-ARC-11120-1; US-Patent-4,186,749;

US-Patent-Appl-SN-796256; US-Patent-Class-128-748;

US-Patent-Class-128-903; US-Patent-Class-73-724) Avail: US Patent and Trademark Office CSCL 06B

An induction powered implanted monitor for epidurally measuring intracranial pressure and telemetering the pressure information to a remote readout is disclosed. The monitor utilizes an inductance-capacitance (L-C) oscillator in which the C comprises a variable capacitance transducer, one electrode of which is a small stiff pressure responsive diaphragm. The oscillator is isolated from a transmitting tank circuit by a buffer circuit and all electric components in the implanted unit except an input and an output coil are shielded by a metal housing.

Official Gazette of the U.S. Patent and Trademark Office

ARMY RESEARCH AND TECHNOLOGY LABORATORIES (AVRADCOM)

NASA FORMAL REPORTS

N80-33356*# National Aeronautics and Space Administration.
Ames Research Center, Moffett Field, Calif.

CALCULATION OF THREE-DIMENSIONAL UNSTEADY TRANSONIC FLOWS PAST HELICOPTER BLADES

J. J. Chattot Oct. 1980 32 p refs Prepared in cooperation
with Army Aviation Research and Development Command, Moffett
Field, Calif.

(NASA-TP-1721; A-8024) Avail: NTIS HC A03/MF A01 CSCL
01A

A finite difference code for predicting the high speed flow
over the advancing helicopter rotor is presented. The code solves
the low frequency, transonic small disturbance equation and is
suitable for modeling the effects of advancing blade unsteadiness
on blades of nearly arbitrary planform. The method employs a
quasi-conservative mixed differencing scheme and solves the
resulting difference equations by an alternating direction scheme.
Computed results showed good agreement with experimental
blade pressure data and illustrate some of the effects of varying
the rotor planform. The flow unsteadiness is shown to be an
indispensible part of a transonic solution. Close to the tip at
high advance ratio, cross flow effects can significantly affect the
solution.

Author

X

NASA CONTRACTOR REPORTS

N80-16737*# Ohio State Univ., Columbus. Human Performance
Center and Aviation Psychology Lab.

MULTI-MODAL INFORMATION PROCESSING FOR VISUAL WORKLOAD RELIEF

Michael W. Burke, Richard D. Gilson, and Richard J. Jagacinski
1980 28 p refs

(Grant NsG-2179)

(NASA-CR-162720) Avail: NTIS HC A03/MF A01 CSCL
05H

The simultaneous performance of two single-dimensional
compensatory tracking tasks, one with the left hand and one
with the right hand, is discussed. The tracking performed with
the left hand was considered the primary task and was performed
with a visual display or a quickened kinesthetic-tactual (KT) display.
The right-handed tracking was considered the secondary task
and was carried out only with a visual display. Although the
two primary task displays had afforded equivalent performance
in a critical tracking task performed alone, in the dual-task situation
the quickened KT primary display resulted in superior secondary
visual task performance. Comparisons of various combinations
of primary and secondary visual displays in integrated or separated
formats indicate that the superiority of the quickened KT
display is not simply due to the elimination of visual scanning.
Additional testing indicated that quickening per se also is not
the immediate cause of the observed KT superiority. R.E.S.

AEROMECHANICS LABORATORY

NASA FORMAL REPORTS

N80-20619*# National Aeronautics and Space Administration. Ames Research Center, Moffett Field, Calif.
ON THE NONLINEAR DEFORMATION GEOMETRY OF EULER-BERNOULLI BEAMS
Dewey H. Hodges, Robert A. Ormiston, and David A. Peters
Apr. 1980 57 p refs
(NASA-TP-1566; A-7985; AVRADCOM-TR-80-A-1) Avail: NTIS HC A04/MF A01 CSCL 20K

Nonlinear expressions are developed to relate the orientation of the deformed beam cross section, torsion, local components of bending curvature, angular velocity, and virtual rotation to deformation variables. The deformed beam kinematic quantities are proven to be equivalent to those derived from various rotation sequences by identifying appropriate changes of variable based on fundamental uniqueness properties of the deformed beam geometry. The torsion variable used is shown to be mathematically analogous to an axial deflection variable commonly used in the literature. Rigorous applicability of Hamilton's principle to systems described by a class of quasi-coordinates that includes these variables is formally established. K.L.

NASA CONTRACTOR REPORTS

N80-27397*# Northrop Corp., Hawthorne, Calif. Aerosciences Lab.
SYSTEM DESCRIPTION AND ANALYSIS. PART 1: FEASIBILITY STUDY FOR HELICOPTER/VTOL WIDE-ANGLE SIMULATION IMAGE GENERATION DISPLAY SYSTEM Final Report
Oct. 1977 198 p Sponsored in part by Army Air Mobility and Research and Development Lab. and Ames Research Center, Mountain View, Calif.
(Contract NAS2-9351)
(NASA-CR-152376; NOR-77-102-Pt-1) Avail: NTIS HC A09/MF A01 CSCL 14B

A preliminary design for a helicopter/VSTOL wide angle simulator image generation display system is studied. The visual system is to become part of a simulator capability to support Army aviation systems research and development within the near term. As required for the Army to simulate a wide range of aircraft characteristics, versatility and ease of changing cockpit configurations were primary considerations of the study. Due to the Army's interest in low altitude flight and descents into and landing in constrained areas, particular emphasis is given to wide field of view, resolution, brightness, contrast, and color. The visual display study includes a preliminary design, demonstrated feasibility of advanced concepts, and a plan for subsequent detail design and development. Analysis and tradeoff considerations for various visual system elements are outlined and discussed. E.D.K.

CONFERENCE PAPERS

N80-29252# Army Research and Technology Labs., Moffett Field, Calif.
DYNAMIC STALL ON ADVANCED AIRFOIL SECTIONS
W. J. McCroskey, K. W. McAlister, L. W. Carr, S. L. Pucci, O.

Lambert (Service Technique des Construction Aeronautiques, Paris), and R. F. Indergand (Mather AFB, Calif.) May 1980 26 p refs Presented at the 36th Annual Forum of the Am. Helicopter Soc., Washington, D.C., May 1980
(AD-A085809) Avail: NTIS HC A03/MF A01 CSCL 01/2

The dynamic stall characteristics of eight airfoils have been investigated in sinusoidal pitch oscillations over a wide range of two dimensional unsteady flow conditions. The results provide a unique comparison of the effects of section geometry in a simulated rotor environment. Important differences between the various airfoils were observed, particularly when the stall regimes were penetrated only slightly. Under these circumstances, the profiles that stall gradually from the trailing edge appear to offer an advantage. However, all of the airfoils tended increasingly toward leading-edge stall when both the severity of dynamic stall and the free-stream Mach number increased. In all cases, the parameters of the unsteady motion appear to be more important than airfoil geometry for configurations that are appropriate for helicopter rotors. GRA

N80-29294# Army Research and Technology Labs., Moffett Field, Calif. Aeromechanics Lab.
AN EXPERIMENTAL INVESTIGATION OF THE EFFECTS OF AEROELASTIC COUPLINGS ON AEROMECHANICAL STABILITY OF A HINGELESS ROTOR HELICOPTER
William G. Bousman 1980 14 p refs Presented at the Ann. Forum of the Am. Helicopter Soc., Washington, D.C., May 1980
(AD-A085819) Avail: NTIS HC A02/MF A01 CSCL 20/4

A 1.62 m diameter rotor model was used to investigate aeromechanical stability, and the results were compared to theory. Configurations tested included: (1) a nonmatched stiffness rotor as a baseline, (2) the baseline rotor with negative pitch-lag coupling, (3) the combination of negative pitch-lag and structural flap-lag coupling on the baseline rotor, (4) a matched stiffness rotor, and (5) a matched stiffness rotor with negative pitch-lag coupling. The measured lead-lag regressing mode damping of the five configurations agreed well with theory, but only the matched stiffness case with negative pitch-lag coupling was able to stabilize the air resonance mode. Comparison of theory and experiment for the damping of the body modes showed significant differences that may be related to rotor inflow dynamics. GRA

N80-29370# Army Research and Technology Labs., Moffett Field, Calif. Aeromechanics Lab.
RESULTS OF A SIMULATOR INVESTIGATION OF CONTROL SYSTEM AND DISPLAY VARIATIONS FOR AN ATTACK HELICOPTER MISSION
Edwin W. Aiken and Robert K. Merrill May 1980 25 p refs Presented at 36th Ann. Natl. Forum of the AHS, Washington, D.C., May 1980
(AD-A085812) Avail: NTIS HC A02/MF A01 CSCL 01/2

A piloted simulator experiment designed to assess the effects on overall system performance and pilot workload of variations in control system characteristics and display format and logic for a nighttime attack helicopter mission is described. The simulation facility provided a representation of a helmet-mounted display image consisting of flight-control and fire-control symbology superimposed on the background video from a

simulated forward-looking infrared sensor. Control systems ranging from the baseline stability and control augmentation system to various hover augmentation schemes were investigated together with variations in the format and logic of the superimposed symbology. Selected control system and display failures were also simulated. The results of the experiment indicate that the baseline control/display system is unsatisfactory without improvement for the evaluation task which included a hovering target search and acquisition. Significant improvements in pilot rating were achieved by both control system and display variations.

GRA

PATENTS

N80-14107* National Aeronautics and Space Administration, Ames Research Center, Moffett Field, Calif.

ACOUSTICALLY SWEEPED ROTOR Patent

Fredric H. Schmitz, Donald A. Boxwell, and Rande Vause, inventors (to NASA) Issued 25 Sep. 1979 23 p Filed 8 Sep. 1977 Supersedes N77-31130 (15 - 22, p 2893)

(NASA-Case-ARC-11106-1; US-Patent-4,168,939;

US-Patent-Appl-SN-831633; US-Patent-Class-416-228;

US-Patent-Class-416-238; US-Patent-Class-415-199) Avail: US Patent and Trademark Office CSCL 01C

Impulsive noise reduction is provided in a rotor blade by acoustically sweeping the chord line from root to tip so that the acoustic radiation resulting from the summation of potential singularities used to model the flow about the blade tend to cancel for all times at an observation point in the acoustic far field. Official Gazette of the U.S. Patent and Trademark Office

Y

AIR FORCE HUMAN RESOURCES LABORATORY TECHNOLOGY OFFICE

NASA TECHNICAL MEMORANDA

N80-22984*# National Aeronautics and Space Administration.
Ames Research Center, Moffett Field, Calif.

THEORY OF THE DECISION/PROBLEM STATE

Duncan L. Dieterly Apr. 1980 21 p refs
(NASA-TM-81192; AFHRL/H80-104; A-8161) Avail: NTIS
HC A02/MF A01 CSCL 05J

A theory of the decision-problem state was introduced and elaborated. Starting with the basic model of a decision-problem condition, an attempt was made to explain how a major decision-problem may consist of subsets of decision-problem conditions composing different condition sequences. In addition, the basic classical decision-tree model was modified to allow for the introduction of a series of characteristics that may be encountered in an analysis of a decision-problem state. The resulting hierarchical model reflects the unique attributes of the decision-problem state. The basic model of a decision-problem condition was used as a base to evolve a more complex model that is more representative of the decision-problem state and may be used to initiate research on decision-problem states.

R.E.S.

N80-22985*# National Aeronautics and Space Administration.
Ames Research Center, Moffett Field, Calif.

PROBLEM SOLVING AND DECISIONMAKING: AN INTEGRATION

Duncan L. Dieterly Apr. 1980 20 p refs Prepared in cooperation with Air Force Human Resources Lab., Moffett Field, Calif.
(NASA-TM-81191; AFHRL/H80-103; A-8160) Avail: NTIS
HC A02/MF A01 CSCL 05J

An attempt was made to redress a critical fault of decisionmaking and problem solving research-a lack of a standard method to classify problem or decision states or conditions. A basic model was identified and expanded to indicate a possible taxonomy of conditions which may be used in reviewing previous research or for systematically pursuing new research designs. A generalization of the basic conditions was then made to indicate that the conditions are essentially the same for both concepts, problem solving and decisionmaking.

R.E.S.

N80-23985*# National Aeronautics and Space Administration.
Ames Research Center, Moffett Field, Calif.

CLARIFICATION PROCESS: RESOLUTION OF DECISION-PROBLEM CONDITIONS

Duncan L. Dieterly May 1980 24 p refs
(NASA-TM-81193; AFHRL-H-80-101; A-8162) Avail: NTIS
HC A02/MF A01 CSCL 05J

A model of a general process which occurs in both decisionmaking and problem-solving tasks is presented. It is called the clarification model and is highly dependent on information flow. The model addresses the possible constraints of individual indifferences and experience in achieving success in resolving decision-problem conditions. As indicated, the application of the clarification process model is only necessary for certain classes of the basic decision-problem condition. With less complex decision problem conditions, certain phases of the model may be omitted. The model may be applied across a wide range of decision problem conditions. The model consists of two major components: (1) the five-phase prescriptive sequence (based on previous approaches to both concepts) and (2) the information

manipulation function (which draws upon current ideas in the areas of information processing, computer programming, memory, and thinking). The two components are linked together to provide a structure that assists in understanding the process of resolving problems and making decisions.

R.E.S.

N80-25002*# National Aeronautics and Space Administration.
Ames Research Center, Moffett Field, Calif.

DECISION-PROBLEM STATE ANALYSIS METHODOLOGY

Duncan L. Dieterly May 1980 21 p refs Prepared in cooperation with AFHRL, Moffett Field, Calif.
(NASA-TM-81194; AFHRL/H/80-102) Avail: NTIS
HC A02/MF A01 CSCL 05J

A methodology for analyzing a decision-problem state is presented. The methodology is based on the analysis of an incident in terms of the set of decision-problem conditions encountered. By decomposing the events that preceded an unwanted outcome, such as an accident, into the set of decision-problem conditions that were resolved, a more comprehensive understanding is possible. All human-error accidents are not caused by faulty decision-problem resolutions, but it appears to be one of the major areas of accidents cited in the literature. A three-phase methodology is presented which accommodates a wide spectrum of events. It allows for a systems content analysis of the available data to establish: (1) the resolutions made, (2) alternatives not considered, (3) resolutions missed, and (4) possible conditions not considered. The product is a map of the decision-problem conditions that were encountered as well as a projected, assumed set of conditions that should have been considered. The application of this methodology introduces a systematic approach to decomposing the events that transpired prior to the accident. The initial emphasis is on decision and problem resolution. The technique allows for a standardized method of accident into a scenario which may be used for review or the development of a training simulation.

R.E.S.

N80-34097*# National Aeronautics and Space Administration.
Ames Research Center, Moffett Field, Calif.

AUTOMATION LITERATURE: A BRIEF REVIEW AND ANALYSIS

Dianne Smith and Duncan L. Dieterly Oct. 1980 17 p refs
(NASA-TM-81245; A-8369) Avail: NTIS HC A02/MF A01
CSCL 05E

Current thought and research positions which may allow for an improved capability to understand the impact of introducing automation to an existing system are established. The orientation was toward the type of studies which may provide some general insight into automation; specifically, the impact of automation in human performance and the resulting system performance. While an extensive number of articles were reviewed, only those that addressed the issue of automation and human performance were selected to be discussed. The literature is organized along two dimensions: time, Pre-1970, Post-1970; and type of approach, Engineering or Behavioral Science. The conclusions reached are not definitive, but do provide the initial stepping stones in an attempt to begin to bridge the concept of automation in a systematic progression.

L.F.M.

CONFERENCE PAPERS

A80-44492 * # A computational and experimental study of high Reynolds number viscous/inviscid interaction about a cone at high angle of attack. D. S. McRae (NASA, Ames Research Center, Moffett Field, Calif.; USAF, Flight Dynamics Laboratory, Wright-Patterson AFB, Ohio), D. F. Fisher (NASA, Ames Research Center, Moffett Field; NASA, Flight Research Center, Edwards, Calif.), and D. J. Peake. *American Institute of Aeronautics and Astronautics, Fluid and Plasma Dynamics Conference, 13th, Snowmass, Colo., July 14-16, 1980, Paper 80-1422.* 14 p. 21 refs. Contract No. NAS2-10578.

The flow over a 5 deg semi-angle cone at incidence in supersonic flow is studied as a model problem for the flow over aircraft forebodies. A computational method utilizing the conically symmetric Navier-Stokes equations is used to obtain theoretical flow results which are compared with experimental data from the Ames Research Center 6- by 6-Foot Wind Tunnel and with results from a cone model sting mounted on an F-15 aircraft. The computed results agree well with the wind-tunnel data but less well with the flight data. Modification of the algebraic turbulence model was necessary to reflect an apparent lower turbulence level in flight than was present in the wind tunnel.

(Author)

H

COMPUTER PROGRAMS

M80-10004* National Aeronautics and Space Administration.
Ames Research Center, Moffett Field, Calif.

OPTIMAL AIRCRAFT TRAJECTORIES FOR SPECIFIED RANGES

FORTTRAN IV 2,583 source statements

CDC 6000

ARC-11282 Price: Program \$590.00/Documentation \$17.50

For an aircraft operating over a fixed range, the operating costs are basically a sum of fuel cost and time cost. While minimum fuel and minimum time trajectories are relatively easy to calculate, the determination of a minimum cost trajectory can be a complex undertaking. This computer program was developed to optimize trajectories with respect to a cost function based on a weighted sum of fuel cost and time cost. As a research tool, the program could be used to study various characteristics of optimum trajectories and their comparison to standard trajectories. It might also be used to generate a model for the development of an airborne trajectory optimization system. The program could be incorporated into an airline flight planning system, with optimum flight plans determined at takeoff time for the prevailing flight conditions. The use of trajectory optimization could significantly reduce the cost for a given aircraft mission. The algorithm incorporated in the program assumes that a trajectory consists of climb, cruise, and descent segments. The optimization of each segment is not done independently, as in classical procedures, but is performed in a manner which accounts for interaction between the segments. This is accomplished by the application of optimal control theory. The climb and descent profiles are generated by integrating a set of kinematic and dynamic equations, where the total energy of the aircraft is the independent variable. At each energy level of the climb and descent profiles, the air speed and power setting necessary for an optimal trajectory are determined. The variational Hamiltonian of the problem consists of the rate of change of cost with respect to total energy and a term dependent on the adjoint variable, which is identical to the optimum cruise cost at a specified altitude. This variable uniquely specifies the optimal cruise energy, cruise altitude, cruise Mach number, and, indirectly, the climb and descent profiles. If the optimum cruise cost is specified, an optimum trajectory can easily be generated; however, the range obtained for a particular optimum cruise cost is not known a priori. For short range flights, the program iteratively varies the optimum cruise cost until the computed range converges to the specified range. For long-range flights, iteration is unnecessary since the specified range can be divided into a cruise segment distance and full climb and descent distances. The user must supply the program with engine fuel flow rate coefficients and an aircraft aerodynamic model. The program currently includes coefficients for the Pratt-Whitney JT8D-7 engine and an aerodynamic model for the Boeing 727. Input to the program consists of the flight range to be covered and the prevailing flight conditions including pressure, temperature, and wind profiles. Information output by the program includes: optimum cruise tables at selected weights, optimal cruise quantities as a function of cruise weight and cruise distance, climb and descent profiles, and a summary of the complete synthesized optimal trajectory. This program is written in FORTTRAN IV for batch execution and has been implemented on a CDC 6000 series computer with a central memory requirement of approximately 100K (octal) of 60 bit words. This aircraft trajectory optimization program was developed in 1979.

M80-10034* National Aeronautics and Space Administration.
Ames Research Center, Moffett Field, Calif.

AEROELASTIC ANALYSIS FOR ROTORCRAFT IN FLIGHT OR IN A WIND TUNNEL

FORTTRAN IV 13,793 source statements

IBM 360

ARC-11150 Price: Program \$1200.00/Documentation \$28.50

The testing of rotorcraft, either in flight or in a wind tunnel, requires a consideration of the coupled aeroelastic stability of the rotor and airframe, or the rotor and support system. Even if the primary purpose of a test is to measure rotor performance, ignoring the question of dynamic stability introduces the risk of catastrophic failure of the aircraft. This computer program was developed to incorporate an analytical model of the aeroelastic behavior of a wide range of rotorcraft. Such an analytical model is desirable for both pre-test predictions and post-test correlations. The program is also applicable in investigations of isolated rotor aeroelasticity and helicopter flight dynamics and could be employed as a basis for more extensive investigations of aeroelastic behavior, such as automatic control system design. The program incorporates an analytical model which is applicable to a wide range of rotors, helicopters, and operating conditions. The equations of motion used in the model were derived using an integral Newtonian method, which provides considerable insight into the blade inertial and aerodynamic forces. The rotor model includes coupled flap-lag bending and blade torsion degrees of freedom, and is applicable to articulated, hingeless, gimbaled, and teetering rotors with an arbitrary number of blades. The aerodynamic model is valid for both high and low inflow, and for both axial and nonaxial flight. Rotor rotational speed dynamics, including engine inertia and damping, and perturbation inflow dynamics are included in the aerodynamic model. For a rotor on a wind tunnel support, a normal mode representation of the test module, strut, and balance is used. The aeroelastic analysis for rotorcraft in flight is applicable to a general two-rotor aircraft, including single main-rotor and tandem helicopter configurations, and side-by-side or tilting proprotor aircraft configurations. The rotor model includes rotor-rotor aerodynamic interference and ground effect. The aircraft model includes rotor-fuselage-tail aerodynamic interference, engine dynamics, and control dynamics. A constant-coefficient approximation is used for nonaxial flow and a quasistatic approximation is used for the low frequency dynamics. The coupled system dynamics results in a set of linear differential equations which are used to determine the stability and aeroelastic response of the system. This program is written in FORTTRAN IV for batch execution and has been implemented on an IBM 360 series computer with a central memory requirement of approximately 624K of 8 bit bytes. This program was developed in 1977.

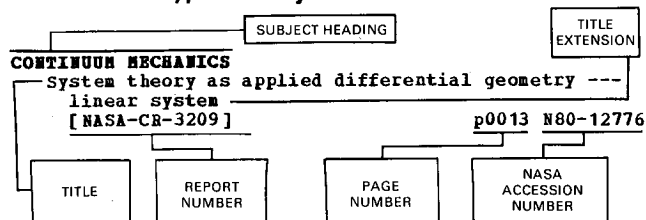
SECTION II

INDEXES

PUBLICLY AVAILABLE PUBLICATIONS

SUBJECT INDEX

Typical Subject Index Listing



The title is used to provide a description of the subject matter. When the title is insufficiently descriptive of the document content, a title extension is added, separated from the title by three hyphens. The *STAR* or *IAA* accession number is included in each entry to assist the user in locating the abstract in the abstract section. If applicable a report number is also included as an aid in identifying the document. The page and accession numbers are located beneath and to the right of the title. Under any one subject heading the accession numbers are arranged in sequence with the *IAA* accession numbers appearing first.

A

ABIOGENESIS

Aldocyanoin microspheres - Partial amino acid analysis of the microparticulates formed from simple reactants under various conditions
p0086 A80-11473

ABLATION

Shape change of Galileo probe models in free-flight tests
[NASA-TM-81209] p0037 N80-27418

ABLATIVE NOSE CONES

Supersonic flow over three-dimensional ablated nosetips using an unsteady implicit numerical procedure
[AIAA PAPER 80-0063] p0060 A80-19271

ABSORBERS (EQUIPMENT)

Development of the electrochemically regenerable carbon dioxide absorber for portable life support system application
[ASME PAPER 79-ENAS-33] p0092 A80-15257

ABSORBERS (MATERIALS)

Adsorption interference in mixtures of trace contaminants flowing through activated carbon adsorber beds
[ASME PAPER 80-ENAS-17] p0096 A80-43193

ABSORPTION BANDS

U ABSORPTION SPECTRA

ABSORPTION CROSS SECTIONS

Part-body and multibody effects on absorption of radio-frequency electromagnetic energy by animals and by models of man
p0071 A80-22987

Na + Xe collisions in the presence of two nonresonant lasers
p0051 A80-32416

ABSORPTION SPECTRA

A new atlas of infrared methane spectra between 1120 per cm and 1800 per cm --- Book
p0042 A80-15655

Integrated band intensities of gaseous N₂O/5/
p0047 A80-25660

ABUNDANCE

Carbonaceous chondrites. I - Characterization and significance of carbonaceous chondrite /CM/ xenoliths in the Jodzie howardite
p0086 A80-13013

ACCELERATED LIFE TESTS

The accelerated characterization of viscoelastic composite materials
[NASA-CR-163188] p0039 N80-24370

ACCELERATION (PHYSICS)

NT ANGULAR ACCELERATION

NT HIGH GRAVITY ENVIRONMENTS

NT PARTICLE ACCELERATION

The effects of motion and g-seat cues on pilot simulator performance of three piloting tasks
[NASA-TP-1601] p0004 N80-15069

ACCELERATION PROTECTION

A new approach to active control of rotorcraft vibration
[AIAA 80-1778] p0027 A80-45556

ACCELERATION STRESSES (PHYSIOLOGY)

NT CENTRIFUGING STRESS

The architecture of the avian retina following exposure to chronic 2 G
p0096 A80-42013

Objective measurement of human tolerance to +G sub z acceleration stress
[NASA-TM-81166] p0098 N80-18709

ACCIDENT INVESTIGATION

NT AIRCRAFT ACCIDENT INVESTIGATION

Equations for determining aircraft motions for accident data
[NASA-TM-78609] p0010 N80-25306

ACCIDENT PREVENTION

Decision-problem state analysis methodology
[NASA-TM-81194] p0103 N80-25002

ACCLIMATIZATION

NT HEAT ACCLIMATIZATION

ACCOMMODATION COEFFICIENT

An extended soft-cube model for the thermal accommodation of gas atoms on solid surfaces
[NASA-TM-81163] p0035 N80-14941

ACCRETION

U DEPOSITION

ACCUMULATORS

NT SOLAR COLLECTORS

NT SOLAR REFLECTORS

ACHONDRITES

Spectroscopic evidence for two achondrite parent bodies - Asteroids 349 Dembowska and 4 Vesta
p0072 A80-26173

ACIDS

NT AMINO ACIDS

NT CARBOXYLIC ACIDS

ACOUSTIC ATTENUATION

Evaluation of approximate methods for the prediction of noise shielding by airframe components
[NASA-TP-1004] p0004 N80-15129

ACOUSTIC EMISSION

On the output of acoustical sources
[NASA-CR-162576] p0014 N80-15872

ACOUSTIC EXCITATION

A note of sound radiation from distributed sources
p0030 A80-31805

ACOUSTIC GENERATORS

U SOUND GENERATORS

ACOUSTIC INSTABILITY

Characterization of acoustic disturbances in linearly sheared flows
[NASA-CR-162577] p0014 N80-15869

ACOUSTIC MEASUREMENTS

NT NOISE MEASUREMENT

Acoustic characteristics of two hybrid inlets at forward speed
[AIAA PAPER 79-0678] p0021 A80-20828

An experimental study of the structure and acoustic field of a jet in a cross stream --- Ames 7-ft by 10-ft wind tunnel tests
[NASA-CR-162464] p0014 N80-15871

ACOUSTIC PROPAGATION

Characterization of acoustic disturbances in linearly sheared flows
p0030 A80-31804

Modal content of noise generated by a coaxial jet in a pipe

ACOUSTIC PROPERTIES

SUBJECT INDEX

[NASA-CR-163575] p0019 N80-33177

ACOUSTIC PROPERTIES

NT ACOUSTIC INSTABILITY

NT ACOUSTIC SCATTERING

ACOUSTIC RADIATION

U SOUND WAVES

ACOUSTIC SCATTERING

Acoustic resonances and sound scattering by a shear layer

[NASA-CR-166181] p0014 N80-15873

ACOUSTIC VIBRATIONS

U SOUND WAVES

ACOUSTICS

NT AEROACOUSTICS

Output of acoustical sources --- effects of structural elements and background flow on immobile multipolar point radiation p0030 A80-37806

ACQUISITION

NT DATA ACQUISITION

ACTINIDE SERIES COMPOUNDS

NT URANIUM FLUORIDES

ACTINOMETERS

NT INFRARED DETECTORS

NT INFRARED SCANNERS

NT RADIOMETERS

NT SPECTORADIOMETERS

NT ULTRAVIOLET SPECTROMETERS

ACTIVATED CARBON

Adsorption interference in mixtures of trace contaminants flowing through activated carbon adsorber beds

[ASME PAPER 80-ENAS-17] p0096 A80-43193

ACTIVATION ENERGY

A calculation of the diffusion energies for adatoms on surfaces of P.C.C. metals p0068 A80-13534

ACTIVE CONTROL

Analytical design and evaluation of an active control system for helicopter vibration reduction and gust response alleviation

[NASA-CR-152377] p0017 N80-28369

Application of advanced technologies to small, short-haul transport aircraft

[NASA-CR-152363] p0018 N80-32353

ACTIVE VOLCANOES

U VOLCANOES

ADAPTATION

NT HEAT ACCLIMATIZATION

ADAPTIVE CONTROL

NT ACTIVE CONTROL

ADDITIVES

NT ANTIOXIDANTS

ADHESIVE BONDING

Thermophysical and flammability characterization of phosphorylated epoxy adhesives p0066 A80-48079

ADHESIVES

Thermophysical and flammability characterization of phosphorylated epoxy adhesives p0066 A80-48079

ADIPOSE TISSUES

Insulin binding and glucose uptake of adipocytes in rats adapted to hypergravitational force p0089 A80-35751

ADMITTANCE

U ELECTRICAL IMPEDANCE

ADSORPTION

NT CHEMISORPTION

AERIAL IMAGERY

U AERIAL PHOTOGRAPHY

AERIAL PHOTOGRAPHY

Texture extraction on the ILLIAC 4 --- aerial images

[AD-A070523] p0098 N80-19471

AEROACOUSTICS

Acoustic characteristics of two hybrid inlets at forward speed

[AIAA PAPER 79-0678] p0021 A80-20828

Upper surface blowing noise of the NASA-Ames quiet short-haul research aircraft

[AIAA PAPER 80-1064] p0026 A80-36002

Unified aerodynamic-acoustic theory for a thin rectangular wing encountering a gust p0030 A80-36401

Acoustically swept rotor --- helicopter noise reduction

[NASA-CASE-ARC-11106-1] p0102 N80-14107

AEROBIOLOGY

Oxygen as a factor in eukaryote evolution - Some

effects of low levels of oxygen on *Saccharomyces cerevisiae* p0086 A80-12229

AERODYNAMIC AXIS

U AERODYNAMIC BALANCE

AERODYNAMIC BALANCE

Total aircraft flight-control system - Balanced open- and closed-loop control with dynamic trim maps p0025 A80-32448

A comprehensive analytical model of rotorcraft aerodynamics and dynamics. Part 2: User's manual [NASA-TM-81183] p0010 N80-28297

AERODYNAMIC BRAKES

NT WING FLAPS

AERODYNAMIC CENTER

U AERODYNAMIC BALANCE

AERODYNAMIC CHARACTERISTICS

NT AERODYNAMIC BALANCE

NT AERODYNAMIC DRAG

NT AERODYNAMIC STABILITY

NT INTERFERENCE DRAG

NT INTERFERENCE LIFT

NT LIFT

NT ROTOR LIFT

Computer/experiment integration for unsteady aerodynamic research p0025 A80-29501

Analysis of two-dimensional incompressible flows by a subsurface panel method p0029 A80-30566

Types of leeside flow over delta wings p0052 A80-34652

Test section configuration for aerodynamic testing in shock tubes p0026 A80-38085

A vortex-lattice method for the calculation of the nonsteady separated flow over delta wings

[AIAA PAPER 80-1803] p0027 A80-43286

A computational and experimental study of high Reynolds number viscous/inviscid interaction about a cone at high angle of attack

[AIAA PAPER 80-1422] p0104 A80-44492

A variational technique for smoothing flight-test and accident data p0028 A80-45894

Wind-tunnel/flight correlation study of aerodynamic characteristics of a large flexible supersonic cruise airplane CXB-70-1). 1: Wind-tunnel tests of a 0.03-scale model at Mach numbers from 0.6 to 2.53

[NASA-TP-1514] p0004 N80-11068

Quiet short-haul research aircraft familiarization document --- STOL p0007 N80-14108

Investigation of ground effects on large and small scale models of a three fan V/STOL aircraft configuration

[NASA-CR-152240] p0015 N80-16030

An experimental investigation of two large annular diffusers with swirling and distorted inflow

[NASA-TP-1628] p0005 N80-17984

Wind-tunnel tests of the XV-15 tilt rotor aircraft

[NASA-TM-81177] p0009 N80-24294

AERODYNAMIC CHORDS

U AIRFOIL PROFILES

AERODYNAMIC COEFFICIENTS

Aerodynamic coefficients in generalized unsteady thin airfoil theory p0030 A80-38034

A comparison of calculated and experimental lift and pressure distributions for several helicopter rotor sections

[NASA-TM-81160] p0007 N80-16036

Leeward flow over delta wings at supersonic speeds

[NASA-TM-81187] p0036 N80-23250

AERODYNAMIC CONFIGURATIONS

Three-dimensional interactions and vortical flows with emphasis on high speeds

[NASA-TM-81169] p0008 N80-21286

A general panel method for the analysis and design of arbitrary configurations in incompressible flows --- boundary value problem

[NASA-CR-3079] p0017 N80-24268

An advanced panel method for analysis of arbitrary configurations in unsteady subsonic flow

[NASA-CR-152323] p0017 N80-26270

AERODYNAMIC DRAG

Effect of propeller slipstream on the drag and

SUBJECT INDEX

AEROSPACE ENVIRONMENTS

- performance of the engine cooling system for a general aviation twin-engine aircraft
[AIAA PAPER 80-1872] p0027 A80-43315
- AERODYNAMIC FORCES**
NT AERODYNAMIC DRAG
NT AERODYNAMIC INTERFERENCE
NT AERODYNAMIC LOADS
NT GUST LOADS
NT INTERFERENCE LIFT
NT LIFT
NT ROTOR LIFT
Control of forebody vortex orientation to alleviate side forces
[AIAA PAPER 80-0183] p0024 A80-23955
Classical aerodynamic theory
[NASA-RP-1050] p0001 N80-15033
- AERODYNAMIC HEATING**
NT SHOCK HEATING
The 60-MW Shuttle interaction heating facility
p0059 A80-12603
A technique for evaluating the Jovian entry-probe heat-shield material with a gasdynamic laser
p0063 A80-29479
- AERODYNAMIC INTERFERENCE**
Reformulation of Possio's kernel with application to unsteady wind tunnel interference
p0031 A80-43129
- AERODYNAMIC LIFT**
U LIFT
- AERODYNAMIC LOADS**
NT GUST LOADS
Propeller slipstream/wing interaction in the transonic regime
[AIAA PAPER 80-0125] p0032 A80-22733
Multicyclic control of a helicopter rotor considering the influence of vibration, loads, and control motion
[AIAA 80-0673] p0025 A80-34998
Unsteady aerodynamics of conventional and supercritical airfoils
[AIAA 80-0734] p0026 A80-35038
A comprehensive analytical model of rotorcraft aerodynamics and dynamics. Part 3: Program manual
[NASA-TM-81184] p0010 N80-28298
- AERODYNAMIC NOISE**
Acoustic characteristics of two hybrid inlets at forward speed
[AIAA PAPER 79-0678] p0021 A80-20828
Noise generation by a lifting wing/flap combination at Reynolds numbers to 2.8×10^6 to the 6th
[AIAA PAPER 80-0035] p0024 A80-22729
Output of acoustical sources --- effects of structural elements and background flow on immobile multipolar point radiation
p0030 A80-37806
Acoustically swept rotor --- helicopter noise reduction
[NASA-CASE-ARC-11106-1] p0102 N80-14107
- AERODYNAMIC STABILITY**
Formulation of coupled rotor/fuselage equations of motion
p0021 A80-17717
An experimental investigation of the effects of aeroelastic couplings on aeromechanical stability of a hingeless rotor helicopter
[AD-A085819] p0101 N80-29294
- AERODYNAMIC STALLING**
Dynamic stall on advanced airfoil sections
[AD-A085809] p0101 N80-29252
- AERODYNAMICS**
NT ROTOR AERODYNAMICS
Computational aerodynamics on large computers
p0048 A80-27415
Unsteady aerodynamics of conventional and supercritical airfoils
[AIAA 80-0734] p0026 A80-35038
Nonreflecting far-field boundary conditions for unsteady transonic flow computation
[AIAA PAPER 80-1393] p0065 A80-41597
Computation of supersonic turbulent flows over an inclined ogive-cylinder-flare
[AIAA PAPER 80-1410] p0066 A80-41608
Numerical simulation of three-dimensional boattail afterbody flow fields
[AIAA PAPER 80-1347] p0066 A80-44132
Mathematical modeling of the aerodynamics of high-angle-of-attack maneuvers
- [AIAA 80-1583] p0028 A80-45879
Computations of the Magnus effect for slender bodies in supersonic flow
[AIAA 80-1586] p0028 A80-45882
Aerodynamic interactions from reaction controls for lateral control of the M2-P2 lifting-body entry configuration at transonic and supersonic and supersonic Mach numbers --- wind tunnel tests
[NASA-TM-78534] p0006 N80-11033
Classical aerodynamic theory
[NASA-RP-1050] p0001 N80-15033
Workshop on Aircraft Surface Representation for Aerodynamic Computation
[NASA-TM-81170] p0008 N80-19025
Proceedings of the Aero-Optics Symposium on Electromagnetic Wave Propagation from Aircraft
[NASA-CR-2121] p0006 N80-25588
Overview of 6- X 6-foot wind tunnel aero-optics tests --- transonic wind tunnel tests
p0023 N80-25590
Experimental unsteady aerodynamics of conventional and supercritical airfoils --- conducted in the Ames 11 foot transonic wind tunnel
[NASA-TM-81221] p0012 N80-33345
- AEROELASTICITY**
Formulation of coupled rotor/fuselage equations of motion
p0021 A80-17717
Wind-tunnel tests of the XV-15 tilt rotor aircraft
[NASA-TM-81177] p0009 N80-24294
A comprehensive analytical model of rotorcraft aerodynamics and dynamics. Part 1: Analysis development
[NASA-TM-81182] p0010 N80-28296
Analysis and correlation of test data from an advanced technology rotor system --- helicopter performance prediction
[NASA-CR-152366] p0019 N80-33351
- AERONAUTICAL ENGINEERING**
NASA overview
p0022 N80-10109
Documentation of the analysis of the benefits and costs of aeronautical research and technology models, volume 1
[NASA-CR-152278] p0001 N80-15865
- AEROSOLS**
OCS, stratospheric aerosols and climate
p0044 A80-19741
Titan aerosols - Optical properties and vertical distribution
p0045 A80-21759
High-resolution Martian atmosphere modeling
p0071 A80-21765
Stratospheric aerosol modification by supersonic transport and space shuttle operations - Climate implications
p0047 A80-26088
Scattering by non-spherical particles of size comparable to a wavelength - A new semi-empirical theory
p0063 A80-34050
The stratospheric sulfate aerosol layer - Processes, models, observations, and simulations
p0051 A80-34435
Scattering by nonspherical particles of size comparable to wavelength - A new semi-empirical theory and its application to tropospheric aerosols
p0052 A80-36040
Atmospheric aerosols and climate
p0052 A80-36305
Efficiency of aerosol collection on wires exposed in the stratosphere
[NASA-TM-81147] p0035 N80-11676
Stratospheric aerosol modification by supersonic transport operations with climate implications
[NASA-RP-1058] p0034 N80-15726
- AEROSPACE ENGINEERING**
NT AERONAUTICAL ENGINEERING
Space applications of superconductivity
p0044 A80-20126
Cryogenic systems for spacecraft
p0055 A80-42902
Performance characterization of a Bosch CO sub 2 reduction subsystem
[NASA-CR-152342] p0085 N80-22987
- AEROSPACE ENVIRONMENTS**
High-pressure protective systems technology
[ASME PAPER 79-ENAS-15] p0092 A80-15240

AEROSPACE MEDICINE

SUBJECT INDEX

AEROSPACE MEDICINE

Physiological response to hyper- and hypogravity during rollercoaster flight p0095 A80-21547

Noninvasive measures of bone bending rigidity in the monkey /M. nemestrina/ p0088 A80-21988

Motion sickness in the squirrel monkey p0095 A80-25891

Insulin binding and glucose uptake of adipocytes in rats adapted to hypergravitational force p0089 A80-35751

Retinal changes in rats flown on Cosmos 936 - A cosmic ray experiment p0091 A80-41995

Fluid-electrolyte shifts and thermoregulation - Rest and work in heat with head cooling p0091 A80-48086

Objective measurement of human tolerance to +G sub z acceleration stress [NASA-TM-81166] p0098 N80-18709

AEROSPACE SYSTEMS

The development and use of large-motion simulator systems in aeronautical research and development p0001 A80-10765

AEROSPACE VEHICLES

Unified treatment of lifting atmospheric entry p0048 A80-28027

AEROSTATS

U AIRSHIPS

AFCS (CONTROL SYSTEM)

U AUTOMATIC FLIGHT CONTROL

AFTERBODIES

Numerical simulation of three-dimensional boattail afterbody flow fields [AIAA PAPER 80-1347] p0066 A80-44132

AGGREGATES

Silt-clay aggregates on Mars p0041 A80-10366

AGING (BIOLOGY)

Review of cell aging in Drosophila and mouse p0087 A80-17741

Favorable effects of the antioxidants sodium and magnesium thiazolidine carboxylate on the vitality and life span of Drosophila and mice p0089 A80-29085

AGRICULTURE

Landsat-based multiphase estimation of California's irrigated lands p0079 A80-27435

Irrigated lands assessment for water management Applications Pilot Test (APT) --- California [E80-10324] p0019 N80-32815

Infrared-temperature variability in a large agricultural field --- Dunnigan, California [E80-10331] p0038 N80-32822

AIR BREATHING ENGINES

NT BRISTOL-SIDDELEY BS 53 ENGINE

NT TURBOFAN ENGINES

NT TURBOJET ENGINES

NT TURBOPROP ENGINES

AIR COOLING

Study of cooling air inlet and exit geometries for horizontally opposed piston aircraft engines [AIAA PAPER 80-1242] p0027 A80-38984

AIR FLOW

Modal content of noise generated by a coaxial jet in a pipe [NASA-CR-163575] p0019 N80-33177

AIR INTAKES

NT ENGINE INLETS

AIR NAVIGATION

NT NAP-OF-THE-EARTH NAVIGATION

AIR POLLUTION

Nitrogen fertiliser and stratospheric ozone - Latitudinal effects p0043 A80-18948

The stratospheric sulfate aerosol layer - Processes, models, observations, and simulations p0051 A80-34435

Meteorological and air pollution modeling for an urban airport p0055 A80-42659

AIR PURIFICATION

Development of a nitrogen generation system [NASA-CR-152333] p0085 N80-19800

AIR SICKNESS

U MOTION SICKNESS

AIR TRAFFIC

Perception of aircraft separation with pilot-preferred symbology on a cockpit display of traffic information [NASA-TM-81172] p0084 N80-31397

AIR TRAFFIC CONTROL

The effect of viewing time, time to encounter, and practice on perception of aircraft separation on a cockpit display of traffic information [NASA-TM-81173] p0083 N80-18038

Effectiveness of advanced fuel-conservative procedures in the transitional ATC environment p0023 N80-27347

NASA aviation safety reporting system [NASA-TM-81197] p0085 N80-32352

AIR TRANSPORTATION

Toward new small transports for commuter airlines p0021 A80-21224

AIRBORNE EQUIPMENT

NT AIRBORNE/SPACEBORNE COMPUTERS

Airborne stellar spectrophotometry from 1.2 to 5.5 microns - Absolute calibration and spectra of stars earlier than M3 p0043 A80-16407

Computer-based manuals for procedural information p0096 A80-50427

AIRBORNE/SPACEBORNE COMPUTERS

A comparison of computer architectures for the NASA demonstration advanced avionics system p0032 A80-32427

Comet nucleus impact probe feasibility study [NASA-CR-152375] p0040 N80-26364

AIRCRAFT ACCIDENT INVESTIGATION

Aircraft motion analysis using limited flight and radar data p0025 A80-27241

Analysis of eighty-four commercial aviation incidents - Implications for a resource management approach to crew training p0093 A80-40340

Civil helicopter wire strike assessment study. Volume 1: Findings and recommendations [NASA-CR-152389] p0019 N80-33381

AIRCRAFT ACCIDENTS

A variational technique for smoothing flight-test and accident data p0028 A80-45894

Some human factors issues in the development and evaluation of cockpit alerting and warning systems [NASA-RP-1055] p0082 N80-15821

Equations for determining aircraft motions for accident data [NASA-TM-78609] p0010 N80-25306

AIRCRAFT APPROACH SPACING

NASA aviation safety reporting system [NASA-TM-81197] p0085 N80-32352

AIRCRAFT BRAKES

NT WING FLAPS

AIRCRAFT CABINS

U AIRCRAFT COMPARTMENTS

AIRCRAFT CARRIERS

A piloted simulator analysis of the carrier landing capability of the quiet short-haul research aircraft [NASA-TM-78508] p0011 N80-28338

AIRCRAFT COMPARTMENTS

Fire-resistant materials for aircraft passenger seat construction [NASA-TM-78617] p0035 N80-13255

AIRCRAFT CONFIGURATIONS

Investigation of ground effects on large and small scale models of a three fan V/STOL aircraft configuration [NASA-CR-152240] p0015 N80-16030

Workshop on Aircraft Surface Representation for Aerodynamic Computation [NASA-TM-81170] p0008 N80-19025

Application of advanced technologies to small, short-haul air transports [NASA-CR-152364] p0019 N80-33396

AIRCRAFT CONSTRUCTION

U AIRCRAFT STRUCTURES

AIRCRAFT CONSTRUCTION MATERIALS

NT AIRFRAME MATERIALS

Release-rate calorimetry of multilayered materials for aircraft seats p0051 A80-34223

Performance properties of graphite reinforced composites with advanced resin matrices --- for

SUBJECT INDEX

AIRCRAFT STABILITY

aircraft p0052 A80-35330

AIRCRAFT CONTROL

NT HELICOPTER CONTROL

Constrained optimum trajectories with specified range p0021 A80-18538

Implicit model following and parameter identification of unstable aircraft p0022 A80-28019

Optimal control model predictions of system performance and attention allocation and their experimental validation in a display design study p0095 A80-40899

A new approach to active control of rotorcraft vibration [AIAA 80-1778] p0027 A80-45556

A pilot modeling technique for handling-qualities research [AIAA 80-1624] p0028 A80-45912

Static calibration of a two-dimensional wedge nozzle with thrust vectoring and spanwise blowing [NASA-TM-81161] p0009 N80-23317

AIRCRAFT DESIGN

NT HELICOPTER DESIGN

Small Transport Aircraft Technology p0021 A80-21225

The Quiet Short-Haul Research Aircraft /Qsra/ p0021 A80-27384

Some observations on supersonic wing design [AIAA 80-3040] p0001 A80-31009

Quiet short-haul research aircraft familiarization document --- STOL [NASA-TM-81149] p0007 N80-14108

An acceptable role for computers in the aircraft design process p0023 N80-21246

Parametric study of helicopter aircraft systems costs and weights [NASA-CR-152315] p0016 N80-22305

A candidate V/STOL research aircraft design concept using an S-3A aircraft and 2 Pegasus 11 engines [NASA-TM-81204] p0009 N80-24293

Application of advanced technologies to small, short-haul transport aircraft [NASA-CR-152363] p0018 N80-32353

Application of advanced technologies to small, short-haul air transports [NASA-CR-152364] p0019 N80-33396

AIRCRAFT ENGINES

A measurement of forward-flight effects on the noise from a JT15D-1 turbofan engine in the NASA-Ames 40- by 80-Foot Wind Tunnel [AIAA PAPER 80-1026] p0026 A80-38641

Study of cooling air inlet and exit geometries for horizontally opposed piston aircraft engines [AIAA PAPER 80-1242] p0027 A80-38984

Effect of propeller slipstream on the drag and performance of the engine cooling system for a general aviation twin-engine aircraft [AIAA PAPER 80-1872] p0027 A80-43315

Aircraft engine nozzle [NASA-CASE-ARC-10977-1] p0033 N80-32392

AIRCRAFT EQUIPMENT

Release-rate calorimetry of multilayered materials for aircraft seats p0051 A80-34223

AIRCRAFT GUIDANCE

Model development for automatic guidance of a VTOL aircraft to a small aviation ship [AIAA 80-1617] p0028 A80-45907

A new algorithm for horizontal capture trajectories [NASA-TM-81186] p0009 N80-22297

Head-up display in the non-precision approach [NASA-TM-81167] p0084 N80-26296

AIRCRAFT INSTRUMENTS

NT ATTITUDE INDICATORS

NT AUTOMATIC PILOTS

NT FLIGHT RECORDERS

NT SPEED INDICATORS

AIRCRAFT LANDING

Optimal washout for control of a moving base simulator --- vertical motion flight simulation using linear filter p0031 A80-14833

An exploratory investigation of the STOL landing maneuver [NASA-CR-3191] p0014 N80-12996

Application of the concept of dynamic trim control to automatic landing of carrier aircraft --- utilizing digital feedforward control [NASA-TP-1512] p0005 N80-19126

A head-up display format for application to transport aircraft approach and landing [NASA-TM-81199] p0012 N80-29295

A comparison of flight and simulation data for three automatic landing system control laws for the Augmentor wing jet STOL research airplane [NASA-CR-152365] p0018 N80-32338

AIRCRAFT MANEUVERS

Mathematical modeling of the aerodynamics of high-angle-of-attack maneuvers [AIAA 80-1583] p0028 A80-45879

Flying-qualities criteria for wings-level-turn maneuvering during an air-to-ground weapon delivery task [AIAA 80-1628] p0029 A80-45916

An exploratory investigation of the STOL landing maneuver [NASA-CR-3191] p0014 N80-12996

Results of a simulator investigation of control system and display variations for an attack helicopter mission [AD-A085812] p0101 N80-29370

AIRCRAFT MODELS

Wind-tunnel/flight correlation study of aerodynamic characteristics of a large flexible supersonic cruise airplane CXB-70-1). 1: Wind-tunnel tests of a 0.03-scale model at Mach numbers from 0.6 to 2.53 [NASA-TP-1514] p0004 N80-11068

AIRCRAFT NOISE

NT JET AIRCRAFT NOISE

Fan noise caused by the ingestion of anisotropic turbulence - A model based on axisymmetric turbulence theory [AIAA PAPER 80-1021] p0032 A80-35977

Distortion-rotor interaction noise produced by a drooped inlet [AIAA PAPER 80-1050] p0033 A80-35994

Upper surface blowing noise of the NASA-Ames quiet short-haul research aircraft [AIAA PAPER 80-1064] p0026 A80-36002

Effect of tip vortex structure on helicopter noise due to blade-vortex interaction p0031 A80-52645

A closed-form solution for noise contours [NASA-TP-1432] p0004 N80-11869

A comprehensive analytical model of rotorcraft aerodynamics and dynamics. Part 3: Program manual [NASA-TM-81184] p0010 N80-28298

AIRCRAFT NOISE PREDICTION

U NOISE PREDICTION (AIRCRAFT)

AIRCRAFT PERFORMANCE

NT HELICOPTER PERFORMANCE

The Quiet Short-Haul Research Aircraft /Qsra/ p0021 A80-27384

Wind-tunnel tests of the XV-15 tilt rotor aircraft [NASA-TM-81177] p0009 N80-24294

AIRCRAFT PILOTS

Thresholds for detection of constant rotary acceleration during vibratory rotary acceleration p0091 A80-42003

Perception of aircraft separation with pilot-preferred symbology on a cockpit display of traffic information [NASA-TM-81172] p0084 N80-31397

AIRCRAFT POWER SOURCES

U AIRCRAFT ENGINES

AIRCRAFT PRODUCTION COSTS

NT AIRPLANE PRODUCTION COSTS

AIRCRAFT SAFETY

Materials for fire resistant passenger seats in aircraft p0080 A80-48757

NASA aviation safety reporting system [NASA-TM-78608] p0083 N80-18010

AIRCRAFT STABILITY

NT HOVERING STABILITY

Measurements of control stability characteristics of a wind-tunnel model using a transfer function method [AIAA 80-0457] p0024 A80-26957

Implicit model following and parameter identification of unstable aircraft p0022 A80-28019

AIRCRAFT STRUCTURES

SUBJECT INDEX

AIRCRAFT STRUCTURES

NT AFTERBODIES
 NT FOREBODIES
 NT FUSELAGES
 NT NOSES (FOREBODIES)
 Measurements of control stability characteristics of a wind-tunnel model using a transfer function method
 [AIAA 80-0457] p0024 A80-26957
 Release-rate calorimetry of multilayered materials for aircraft seats
 [AIAA 80-0759] p0064 A80-35052
 Evaluation of approximate methods for the prediction of noise shielding by airframe components
 [NASA-TP-1004] p0004 N80-15129
 A general panel method for the analysis and design of arbitrary configurations in incompressible flows --- boundary value problem
 [NASA-CR-3079] p0017 N80-24268
 Optimized laser turrets for minimum phase distortion
 p0023 N80-25600

AIRCRAFT WAKES

NT HELICOPTER WAKES
 NT PROPELLER SLIPSTREAMS
 A vortex-lattice method for the calculation of the nonsteady separated flow over delta wings
 [AIAA PAPER 80-1803] p0027 A80-43286

AIRCRAFTS

U FLIGHT CREWS

AIRFIELDS

U AIRPORTS

AIRFOIL CHARACTERISTICS

U AIRFOILS

AIRFOIL PROFILES

NT WING PROFILES
 Experimental and computational study of transonic flow about swept wings
 [AIAA PAPER 80-0005] p0060 A80-18235
 High-resolution LDA measurements of Reynolds stress in boundary layers and wakes
 [AIAA 80-0436] p0025 A80-26967
 Unsteady aerodynamics of conventional and supercritical airfoils
 [AIAA 80-0734] p0026 A80-35038
 Calculations of transonic flow about an airfoil in a wind tunnel
 [AIAA PAPER 80-1366] p0027 A80-44142
 Classical aerodynamic theory
 [NASA-RP-1050] p0001 N80-15033
 Experimental studies of scale effects on oscillating airfoils at transonic speeds
 [NASA-TM-81216] p0010 N80-27287

AIRFOIL SECTIONS

U AIRFOIL PROFILES

AIRFOIL THICKNESS

U AIRFOIL PROFILES

AIRFOILS

NT DELTA WINGS
 NT FLAPS (CONTROL SURFACES)
 NT INFINITE SPAN WINGS
 NT LIFTING ROTORS
 NT OBLIQUE WINGS
 NT RECTANGULAR WINGS
 NT RIGID ROTORS
 NT ROTARY WINGS
 NT SUPERCRITICAL WINGS
 NT SWEEP WINGS
 NT THIN AIRFOILS
 NT THIN WINGS
 NT UPPER SURFACE BLOWN FLAPS
 NT WING FLAPS
 NT WINGS

Integral equations for flows in wind tunnels
 p0029 A80-21906

Computer/experiment integration for unsteady aerodynamic research
 p0025 A80-29501

Test section configuration for aerodynamic testing in shock tubes
 p0026 A80-38085

Simple turbulence models and their application to boundary layer separation
 [NASA-CR-3283] p0017 N80-24269

A computer program to generate two-dimensional grids about airfoils and other shapes by the use of Poisson's equation
 [NASA-TM-81198] p0036 N80-26266

Dynamic stall on advanced airfoil sections
 [AD-A085809] p0101 N80-29252
 Experimental unsteady aerodynamics of conventional and supercritical airfoils --- conducted in the Ames 11 foot transonic wind tunnel
 [NASA-TM-81221] p0012 N80-33345

AIRFRAME MATERIALS

Documentation of the analysis of the benefits and costs of aeronautical research and technology models, volume 1
 [NASA-CR-152278] p0001 N80-15865

AIRLINE OPERATIONS

Toward new small transports for commuter airlines
 p0021 A80-21224
 Factors affecting the retirement of commercial transport jet aircraft
 [NASA-CR-152308] p0013 N80-10148

AIRPLANE PRODUCTION COSTS

Application of parametric weight and cost estimating relationships to future transport aircraft
 [SAWE PAPER 1292] p0024 A80-20637

AIRPORTS

Meteorological and air pollution modeling for an urban airport
 p0055 A80-42659

AIRSHIPS

In depth review of the 1979 AIAA Lighter-Than-Air Systems Technology Conference
 [NASA-TM-81158] p0006 N80-12991
 Parametric study of modern airship productivity
 [NASA-TM-81151] p0011 N80-28340

ALARMS

U WARNING SYSTEMS

ALBUMINS

Exercise training-induced hypervolemia - Role of plasma albumin, renin, and vasopressin
 p0089 A80-32749

ALDEHYDES

NT FORMALDEHYDE

Aldocyanoin microspheres - Partial amino acid analysis of the microparticulates formed from simple reactants under various conditions
 p0086 A80-11473

ALGEBRA

NT EIGENVALUES

NT GROUP THEORY

NT LINEAR EQUATIONS

NT MATRICES (MATHEMATICS)

NT VORTICITY

ALGORITHMS

An explicit algorithm for a fluid approach to nonlinear optics propagation using splitting and rezoning techniques
 p0059 A80-14987

A new algorithm for horizontal capture trajectories
 [NASA-TM-81186] p0009 N80-22297

Algorithm for fixed-range optimal trajectories
 [NASA-TP-1565] p0006 N80-28329

ALIPHATIC COMPOUNDS

NT ALKYL COMPOUNDS

NT CARBOXYLATES

NT GLUCOSE

NT HEXADIENE

NT METHANE

ALKALI METALS

NT POTASSIUM

NT SODIUM

Computational study of alkali-metal-noble gas collisions in the presence of nonresonant lasers
 - Na + Xe + h/2/pi/omega sub 1 + h/2/pi/omega sub 2 system
 p0056 A80-48762

ALKALIES

NT SODIUM HYDROXIDES

ALKALINE EARTH OXIDES

NT CALCIUM OXIDES

ALKANES

NT METHANE

ALKYL COMPOUNDS

Perfluoroether triazine elastomers
 [NASA-CR-162748] p0039 N80-16166

AMIDES

NT POLYIMIDES

NT UREAS

AMINO ACIDS

Aldocyanoin microspheres - Partial amino acid analysis of the microparticulates formed from simple reactants under various conditions

SUBJECT INDEX

ARCHITECTURE (COMPUTERS)

- The radioracemization of isovaline - Cosmochemical implications --- gamma ray effects on Murchison meteorite primordial composition p0086 A80-11473
- The role of metal ions in chemical evolution - Polymerization of alanine and glycine in a cation-exchanged clay environment p0086 A80-13018
- AMMONIA** p0090 A80-36195
Design, fabrication and testing of a dual catalyst ammonia removal system for a urine VCD unit [NASA-CR-152372] p0085 N80-29023
- AMORPHOUS MATERIALS**
Direct /TEM/ observation of the catalytic oxidation of amorphous carbon by Pd particles p0053 A80-37180
- ANAEROBES**
Microbial sulfate reduction measured by an automated electrical impedance technique p0087 A80-21982
- ANALYSIS (MATHEMATICS)**
NT APPROXIMATION
NT CHEBYSHEV APPROXIMATION
NT COMPUTATIONAL FLUID DYNAMICS
NT DIFFERENTIAL EQUATIONS
NT ELLIPTIC DIFFERENTIAL EQUATIONS
NT ERROR ANALYSIS
NT FINITE DIFFERENCE THEORY
NT GREEN FUNCTION
NT HARMONIC ANALYSIS
NT HYPERGEOMETRIC FUNCTIONS
NT ITERATION
NT KERNEL FUNCTIONS
NT LEAST SQUARES METHOD
NT LINEAR EQUATIONS
NT MONTE CARLO METHOD
NT NUMERICAL ANALYSIS
NT NUMERICAL DIFFERENTIATION
NT PARABOLIC DIFFERENTIAL EQUATIONS
NT PARTIAL DIFFERENTIAL EQUATIONS
NT POISSON EQUATION
NT SINGULAR INTEGRAL EQUATIONS
NT SINGULARITY (MATHEMATICS)
NT TAYLOR SERIES
NT VORTICITY
- ANATOMY**
NT BONES
NT CARDIOVASCULAR SYSTEM
NT ERYTHROCYTES
NT HEAD (ANATOMY)
NT HUMAN BODY
NT MUSCULOSKELETAL SYSTEM
NT PITUITARY GLAND
NT RETINA
- ANECHOIC CHAMBERS**
Evaluation of approximate methods for the prediction of noise shielding by airframe components [NASA-TP-1004] p0004 N80-15129
- ANEMOMETERS**
NT LASER ANEMOMETERS
- ANEMOMETRY**
U VELOCITY MEASUREMENT
- ANGLE OF ATTACK**
A three dimensional vortex wake model for missiles at high angles on attack [NASA-CR-3208] p0014 N80-14048
Experimental unsteady aerodynamics of conventional and supercritical airfoils --- conducted in the Ames 11 foot transonic wind tunnel [NASA-TM-81221] p0012 N80-33345
- ANGLES (GEOMETRY)**
NT ANGLE OF ATTACK
Effect of field of view and monocular viewing on angular size judgements in an outdoor scene [NASA-TM-81176] p0083 N80-19792
- ANGULAR ACCELERATION**
Thresholds for detection of constant rotary acceleration during vibratory rotary acceleration p0091 A80-42003
- ANGULAR MOMENTUM**
An angular momentum approximation for molecular collisions in the presence of intense laser radiation p0069 A80-15673
- ANHYDRIDES**
NT INORGANIC PEROXIDES
- Catalysts for polyimide foams from aromatic isocyanates and aromatic dianhydrides --- flame retardant foams [NASA-CASE-ARC-11107-1] p0080 N80-16116
- ANIMALS**
NT DOGS
NT DROSOPHILA
NT MICE
The development of a Space Shuttle Research Animal Holding Facility [ASME PAPER 80-ENAS-39] p0096 A80-43213
- ANNUAL VARIATIONS**
A numerical model of the zonal mean circulation of the middle atmosphere p0073 A80-34443
Preliminary calculations concerning the maintenance of the zonal mean ozone distribution in the Northern Hemisphere p0074 A80-34445
- ANOMALIES**
NT MAGNETIC ANOMALIES
- ANTENNAS**
NT RADIO ANTENNAS
- ANTIMONIDES**
NT INDIUM ANTIMONIDES
- ANTIMONY COMPOUNDS**
NT INDIUM ANTIMONIDES
- ANTIOXIDANTS**
Favorable effects of the antioxidants sodium and magnesium thiazolidine carboxylate on the vitality and life span of Drosophila and mice p0089 A80-29085
- ANTISUBMARINE WARFARE AIRCRAFT**
NT S-3 AIRCRAFT
- APPROACH**
NT INSTRUMENT APPROACH
Analysis of fuel-conservative curved decelerating approach trajectories for powered-lift and CTOL jet aircraft [NASA-TP-1650] p0005 N80-19022
Flight evaluation of configuration management system concepts during transition to the landing approach for a powered-lift STOL aircraft [NASA-TM-81146] p0008 N80-19127
- APPROACH CONTROL**
Model development for automatic guidance of a VTOL aircraft to a small aviation ship [AIAA 80-1617] p0028 A80-45907
Head-up transition behavior of pilots during simulated low-visibility approaches [NASA-TP-1618] p0082 N80-26039
Analytical methodology for determination of helicopter IFR precision approach requirements --- pilot workload and acceptance level [NASA-CR-152367] p0040 N80-28330
- APPROXIMATION**
NT CHEBYSHEV APPROXIMATION
NT FINITE DIFFERENCE THEORY
NT LEAST SQUARES METHOD
NT NUMERICAL DIFFERENTIATION
A new propagation method for the radial Schroedinger equation p0069 A80-15768
Evaluation of approximate methods for the prediction of noise shielding by airframe components [NASA-TP-1004] p0004 N80-15129
- APPROXIMATION METHODS**
U APPROXIMATION
- ARC DISCHARGES**
'GAIN' - Gas-addition, impedance-matched arc driver --- shock tube gas dynamics p0064 A80-38131
- ARC JET ENGINES**
Calorimeter probes for measuring high thermal flux --- in electric-arc jet facilities for planetary entry heating simulation p0099 A80-29480
- ARCHITECTURE (COMPUTERS)**
The suitability of the ILLIAC IV architecture for image processing p0098 A80-22382
A comparison of computer architectures for the NASA demonstration advanced avionics system p0032 A80-32427
An assessment of future computer system needs for large-scale computation [NASA-TM-78613] p0008 N80-17717

ARIP (IMPACT PREDICTION)

SUBJECT INDEX

- ARIP (IMPACT PREDICTION)
 U COMPUTERIZED SIMULATION
 U IMPACT PREDICTION
- ARTHOPODS
 NT DROSOPHILA
- ARTIFICIAL SATELLITES
 NT ATS 3
 NT COSMOS SATELLITES
 NT INFRARED ASTRONOMY SATELLITE
 NT NIMBUS 4 SATELLITE
 NT VENERA SATELLITES
- ASSESSMENTS
 NT TECHNOLOGY ASSESSMENT
- ASTEROID BELTS
 NT ASTEROIDS
- ASTEROIDS
 Aqueous activity on asteroids - Evidence from carbonaceous meteorites p0062 A80-24586
 Primordial heating of asteroidal parent bodies p0062 A80-24590
 Spectroscopic evidence for two achondrite parent bodies - Asteroids 349 Dembowska and 4 Vesta p0072 A80-26173
- ASTROBIOLOGY
 U EXOBIOLOGY
- ASTROMETRY
 An assessment of ground-based techniques for detecting other planetary systems. Volume 1: An overview --- workshop conclusions [NASA-CP-2124-VOL-1] p0034 N80-18997
 An Assessment of Ground-Based Techniques for Detecting Other Planetary Systems. Volume 2: Position papers [NASA-CP-2124-VOL-2] p0034 N80-25224
- ASTRONOMICAL CATALOGS
 Infrared methane spectra between 1120 per cm and 1800 per cm - A new atlas p0042 A80-13143
 A new atlas of infrared methane spectra between 1120 per cm and 1800 per cm --- Book p0042 A80-15655
- ASTRONOMICAL MODELS
 NT DENSITY WAVE MODEL
 NT STELLAR MODELS
 Galaxy collisions - A preliminary study p0046 A80-23420
 Protostellar formation in rotating interstellar clouds. III - Nonaxisymmetric collapse p0054 A80-39375
 Modeling Jupiter's current disc - Pioneer 10 outbound p0075 A80-45153
- ASTRONOMICAL OBSERVATORIES
 Quest for ultrahigh resolution in X-ray optics --- for solar astronomy p0032 A80-17480
- ASTRONOMICAL PHOTOGRAPHY
 Red and nebulous objects in dark clouds - A survey p0044 A80-20662
- ASTRONOMICAL PHOTOMETRY
 NT STELLAR SPECTROPHOTOMETRY
 Ultraviolet photometer observations of the Saturnian system p0070 A80-19122
 An investigation of previously derived Hyades, Coma, and M67 reddenings p0049 A80-29959
 Integrated infrared detector arrays for low-background astronomy p0066 A80-44639
 Discovery of optical molecular emission from the bipolar nebula surrounding HD 44179 p0058 A80-52399
- ASTRONOMICAL SPECTROSCOPY
 Far infrared, near infrared, and radio molecular line studies of HFE 2, HFE 3, and FJM 6 p0068 A80-11489
 16-30 micron spectroscopy of Titan p0049 A80-29321
- ASTRONOMICAL TELESCOPES
 NT INFRARED TELESCOPES
 NT SPECTROSCOPIC TELESCOPES
 NT X RAY TELESCOPES
 An Assessment of Ground-Based Techniques for Detecting Other Planetary Systems. Volume 2: Position papers [NASA-CP-2124-VOL-2] p0034 N80-25224
- Project Orion: A design study of a system for detecting extrasolar planets [NASA-SP-436] p0035 N80-27260
 Large Deployable Reflector (LDR) [NASA-CR-152402] p0040 N80-33319
- ASTRONOMY
 NT INFRARED ASTRONOMY
 NT RADIO ASTRONOMY
 NT SPACEBORNE ASTRONOMY
 NT X RAY ASTRONOMY
 In search of other planetary systems p0046 A80-22978
- ASTROPHYSICS
 Molecule formation and infrared emission in fast interstellar shocks. I Physical processes p0043 A80-16410
 Studies in astronomical time series analysis: Modeling random processes in the time domain [NASA-TM-81148] p0036 N80-15854
- ASYMPTOTIC METHODS
 Transonic swept-wing analysis using asymptotic and other numerical methods [AIAA PAPER 80-0342] p0024 A80-22751
 Asymptotic features of shock-wave boundary-layer interaction p0055 A80-43135
 Asymptotic behavior of the efficiencies in Mie scattering p0031 A80-47048
 Analysis of transonic swept wings using asymptotic and other numerical methods [NASA-TM-80762] p0011 N80-29255
- ATMOSPHERIC CHEMISTRY
 Pressure and temperature dependence kinetics study of the NO + BrO yielding NO2 + Br reaction - Implications for stratospheric bromine photochemistry p0068 A80-14397
 OCS, stratospheric aerosols and climate p0044 A80-19741
 Organic chemistry on Titan p0087 A80-20340
 Temperature dependence of intensities of the 8-12 micron bands of CFC13 p0045 A80-21559
 Band model calculations for CFC13 in the 8-12 micron region p0045 A80-21560
 The properties of clusters in the gas phase. IV - Complexes of H2O and HNOx clustering on NOx/-/ p0046 A80-23322
 Stratospheric ozone decrease due to chlorofluoromethane photolysis - Predictions of latitude dependence p0049 A80-29762
 Corrections in the Pioneer Venus sounder probe gas chromatographic analysis of the lower Venus atmosphere p0089 A80-30875
 New gas phase inorganic ion cluster species and their atmospheric implications p0075 A80-37510
- ATMOSPHERIC CIRCULATION
 Wave propagation and transport in the middle atmosphere p0072 A80-26437
 Pioneer Venus small probes net flux radiometer experiment p0073 A80-30850
 A numerical model of the zonal mean circulation of the middle atmosphere p0073 A80-34443
 Preliminary calculations concerning the maintenance of the zonal mean ozone distribution in the Northern Hemisphere p0074 A80-34445
 The observed ozone flux by transient eddies, 0-30 km p0074 A80-34449
- ATMOSPHERIC COMPOSITION
 NT IONOSPHERIC COMPOSITION
 A model of the neutral and ion nitrogen chemistry in the daytime thermosphere of Venus p0067 A80-10460
 Organic chemistry on Titan p0087 A80-20340
 Temperature dependence of intensities of the 8-12 micron bands of CFC13 p0045 A80-21559

SUBJECT INDEX

AUTOMATIC CONTROL

- Band model calculations for CFC13 in the 8-12 micron region p0045 A80-21560
- Titan aerosols - Optical properties and vertical distribution p0045 A80-21759
- 16-30 micron spectroscopy of Titan p0049 A80-29321
- Atmosphere structure instruments on the four Pioneer Venus entry probes p0051 A80-30849
- Preliminary calculations concerning the maintenance of the zonal mean ozone distribution in the Northern Hemisphere p0074 A80-34445
- Atmospheric aerosols and climate p0052 A80-36305
- New gas phase inorganic ion cluster species and their atmospheric implications p0075 A80-37510
- Measurements of NO, O3, and temperature at 19.8 km during the total solar eclipse of 26 February 1979 p0055 A80-43638
- Chelate-modified polymers for atmospheric gas chromatography [NASA-CASE-ARC-11154-1] p0097 N80-23383
- ATMOSPHERIC DIFFUSION**
Eddy diffusion coefficients and the variance of the atmosphere 30-60 km p0076 A80-45996
- ATMOSPHERIC EFFECTS**
Stratospheric aerosol modification by supersonic transport operations with climate implications [NASA-RP-1058] p0034 N80-15726
- ATMOSPHERIC ENTRY**
NT SPACECRAFT REENTRY
Forebody and base region real-gas flow in severe planetary entry by a factored implicit numerical method. I - Computational fluid dynamics [AIAA PAPER 80-0065] p0061 A80-22731
Unified treatment of lifting atmospheric entry p0048 A80-28027
A technique for evaluating the Jovian entry-probe heat-shield material with a gasdynamic laser p0063 A80-29479
Calorimeter probes for measuring high thermal flux --- in electric-arc jet facilities for planetary entry heating simulation p0099 A80-29480
Pioneer Venus Multiprobe entry telemetry recovery p0050 A80-30831
Shock-tube studies of radiative base heating of Jovian probe p0064 A80-38114
- ATMOSPHERIC ENTRY SIMULATION**
Galileo probe thermal protection: Entry heating environments and spallation experiments design [NASA-CR-152334] p0038 N80-14184
- ATMOSPHERIC IMPURITIES**
U AIR POLLUTION
- ATMOSPHERIC MODELS**
NT DYNAMIC MODELS
Are solar spectral variations a drive for climatic change p0042 A80-15488
High-resolution Martian atmosphere modeling p0071 A80-21765
The stratospheric sulfate aerosol layer - Processes, models, observations, and simulations p0051 A80-34435
A numerical model of the zonal mean circulation of the middle atmosphere p0073 A80-34443
A Lagrangian mean theory of wave, mean-flow interaction with applications to nonacceleration and its breakdown --- large-scale atmospheric dynamics p0075 A80-36473
Meteorological and air pollution modeling for an urban airport p0055 A80-42659
- ATMOSPHERIC OPTICS**
Titan aerosols - Optical properties and vertical distribution p0045 A80-21759
- ATMOSPHERIC RADIATION**
NT STRATOSPHERE RADIATION
Narrow-field radiometry in a quasi-isotropic atmosphere
- ATMOSPHERIC SCATTERING**
NT TROPOSPHERIC SCATTERING
Scattering by non-spherical particles of size comparable to a wavelength - A new semi-empirical theory p0079 A80-40233
- ATMOSPHERIC TEMPERATURE**
The upper atmosphere of Uranus - Mean temperature and temperature variations p0071 A80-22207
Measurements of NO, O3, and temperature at 19.8 km during the total solar eclipse of 26 February 1979 p0055 A80-43638
- ATMOSPHERIC TURBULENCE**
Analytical study of the effects of wind tunnel turbulence on turbofan rotor noise --- NASA Ames 40 by 80 foot wind tunnel [NASA-CR-152359] p0016 N80-23099
- ATOMIC COLLISIONS**
F + H2 collisions on two electronic potential energy surfaces - Quantum-mechanical study of the collinear reaction p0068 A80-12012
Quantum-mechanical calculation of three-dimensional atom-diatom collisions in the presence of intense laser radiation p0068 A80-15221
Computational study of alkali-metal-noble gas collisions in the presence of nonresonant lasers - Na + Xe + $h/2\pi/\omega$ sub 1 + $h/2\pi/\omega$ sub 2 system p0056 A80-48762
- ATOMIC STRUCTURE**
Relativistic scattered wave calculations on Uf6 p0049 A80-30458
- ATOMS**
NT HYDROGEN ATOMS
NT NITROGEN ATOMS
- ATS**
NT ATS 3
ATS 3
Operational procedures for ground station operation: ATS-3 Hawaii-Ames satellite link experiment [NASA-TM-81155] p0035 N80-13333
- ATTACK AIRCRAFT**
NT B-70 AIRCRAFT
NT BOMBER AIRCRAFT
NT FIGHTER AIRCRAFT
Results of a simulator investigation of control system and display variations for an attack helicopter mission [AD-A085812] p0101 N80-29370
- ATTENUATION**
NT ACOUSTIC ATTENUATION
NT MICROWAVE ATTENUATION
- ATTITUDE CONTROL**
NT LATERAL CONTROL
NT LONGITUDINAL CONTROL
NT THRUST VECTOR CONTROL
Control system designs for the shuttle infrared telescope facility [NASA-TM-81159] p0036 N80-18869
A pilot's assessment of helicopter handling-quality factors common to both agility and instrument flying tasks [NASA-TM-81217] p0011 N80-28341
- ATTITUDE INDICATORS**
A simulator study of control and display augmentations for helicopters [NASA-CR-163451] p0018 N80-31408
- ATTITUDE STABILITY**
Internal image motion compensation system for the Shuttle Infrared Telescope Facility p0064 A80-37427
- AUDITORY PERCEPTION**
Perception and performance in flight simulators: The contribution of vestibular, visual, and auditory information [NASA-CR-162129] p0085 N80-11103
- AUGMENTATION**
NT THRUST AUGMENTATION
- AUTOMATA THEORY**
Automation literature: A brief review and analysis [NASA-TM-81245] p0103 N80-34097
- AUTOMATIC CONTROL**
NT ACTIVE CONTROL
NT AUTOMATIC FLIGHT CONTROL

AUTOMATIC DATA PROCESSING

NT AUTOMATIC LANDING CONTROL
 NT DYNAMIC CONTROL
 NT FEEDBACK CONTROL
 NT FEEDFORWARD CONTROL
 NT OPTIMAL CONTROL
 Automation literature: A brief review and analysis
 [NASA-TM-81245] p0103 N80-34097

AUTOMATIC DATA PROCESSING
 U DATA PROCESSING

AUTOMATIC FLIGHT CONTROL
 NT AUTOMATIC LANDING CONTROL
 Total aircraft flight-control system - Balanced
 open- and closed-loop control with dynamic trim
 maps
 p0025 A80-32448
 Pilot control through the TAPCOS automatic flight
 control system
 [NASA-TM-81152] p0007 N80-14138
 Flight tests of the total automatic flight control
 system (Tafcos) concept on a DHC-6 Twin Otter
 aircraft
 [NASA-TP-1513] p0005 N80-17081
 Flight-deck automation: Promises and problems
 [NASA-TM-81206] p0084 N80-26040

AUTOMATIC LANDING CONTROL
 Model development for automatic guidance of a VTOL
 aircraft to a small aviation ship
 [AIAA 80-1617] p0028 A80-45907
 Application of the concept of dynamic trim control
 to automatic landing of carrier aircraft ---
 utilizing digital feedforward control
 [NASA-TP-1512] p0005 N80-19126
 A comparison of flight and simulation data for
 three automatic landing system control laws for
 the Augmentor wing jet STOL research airplane
 [NASA-CR-152365] p0018 N80-32338

AUTOMATIC PATTERN RECOGNITION
 U PATTERN RECOGNITION

AUTOMATIC PILOTS
 Model development for automatic guidance of a VTOL
 aircraft to a small aviation ship
 [AIAA 80-1617] p0028 A80-45907
 Pilot control through the TAPCOS automatic flight
 control system
 [NASA-TM-81152] p0007 N80-14138
 A summary of joint US-Canadian augmentor wing
 powered-lift STOL research programs at the Ames
 Research Center, NASA, 1975-1980
 [NASA-TM-81215] p0011 N80-28373

AUTOMATIC ROCKET IMPACT PREDICTORS
 U COMPUTERIZED SIMULATION
 U IMPACT PREDICTION

AUTOPILOTS
 U AUTOMATIC PILOTS

AVIATORS
 U AIRCRAFT PILOTS

AVIONICS
 A comparison of computer architectures for the
 NASA demonstration advanced avionics system
 p0032 A80-32427
 Flight test of navigation and guidance sensor
 errors measured on STOL approaches
 [NASA-TM-81154] p0007 N80-13041
 Navigation systems for approach and landing of
 VTOL aircraft
 [NASA-CR-152335] p0016 N80-19055
 Parametric study of helicopter aircraft systems
 costs and weights
 [NASA-CR-152315] p0016 N80-22305

AVOIDANCE
 NT COLLISION AVOIDANCE

AXISYMMETRIC BODIES
 Experimental investigation of the asymmetric body
 vortex wake
 [AIAA PAPER 80-0174] p0032 A80-23937
 Direct numerical simulations of the turbulent wake
 of an axisymmetric body
 p0080 A80-49235

AXISYMMETRIC FLOW
 Forebody and base region real-gas flow in severe
 planetary entry by a factored implicit numerical
 method. I - Computational fluid dynamics
 [AIAA PAPER 80-0065] p0061 A80-22731
 Fan noise caused by the ingestion of anisotropic
 turbulence - A model based on axisymmetric
 turbulence theory
 [AIAA PAPER 80-1021] p0032 A80-35977

AZINES
 NT METHYLENE BLUE

SUBJECT INDEX

Perfluoroether triazine elastomers
 [NASA-CR-162748] p0039 N80-16166

AZOLES
 NT OXAZOLE

B

B STARS
 High-frequency continuum observations of young stars
 p0047 A80-25365

B-70 AIRCRAFT
 Wind-tunnel/flight correlation study of
 aerodynamic characteristics of a large flexible
 supersonic cruise airplane CXB-70-1). 1:
 Wind-tunnel tests of a 0.03-scale model at Mach
 numbers from 0.6 to 2.53
 [NASA-TP-1514] p0004 N80-11068

BACKSCATTERING
 Comparison of the Nimbus-4 BUV ozone data with the
 Ames two-dimensional model
 [NASA-TM-81207] p0036 N80-24914

BACTERIA
 Proton movements in response to a light-driven
 electrogenic pump for sodium ions in
 Halobacterium halobium membranes
 p0087 A80-17686
 Spectrophotometric identification of the pigment
 associated with light-driven primary sodium
 translocation in Halobacterium halobium
 p0088 A80-26015
 The role of Na⁺/ in transport processes of
 bacterial membranes
 p0088 A80-27077
 Physical chemistry and evolution of salt tolerance
 in halobacteria
 p0090 A80-40383
 The intracellular Na⁺/ and K⁺/ composition of
 the moderately halophilic bacterium, Paracoccus
 halodenitrificans
 p0091 A80-41250

BACTERIOLOGY
 Microbial sulfate reduction measured by an
 automated electrical impedance technique
 p0087 A80-21982

BANDWIDTH
 NT BROADBAND
 NT SPECTRAL LINE WIDTH

BANKING FLIGHT
 U TURNING FLIGHT

BARCHANS
 U DUNES

BARDEEN APPROXIMATION
 U SURFACE PROPERTIES

BARLEY
 Infrared-temperature variability in a large
 agricultural field --- Dunnigan, California
 [E80-10331] p0038 N80-32822

BARRIED GALAXIES
 Gas dynamics in barred spirals - Gaseous density
 waves and galactic shocks
 p0041 A80-10685
 Self-gravitating gas flow in barred spiral galaxies
 p0055 A80-44959

BASALT
 Endogenic craters on basaltic lava flows - Size
 frequency distributions
 p0061 A80-23727

BASE FLOW
 Forebody and base region real-gas flow in severe
 planetary entry by a factored implicit numerical
 method. I - Computational fluid dynamics
 [AIAA PAPER 80-0065] p0061 A80-22731

BASE HEATING
 Shock-tube studies of radiative base heating of
 Jovian probe
 p0064 A80-38114

BED REST
 Exercise thermoregulation after 14 days of bed rest
 p0088 A80-25989

BEHAVIOR
 NT DECONDITIONING
 NT HUMAN BEHAVIOR

BELL AIRCRAFT
 NT UH-1 HELICOPTER
 NT XV-15 AIRCRAFT

BENCHES
 U SEATS

BENDING
 Noninvasive measures of bone bending rigidity in

SUBJECT INDEX

BODY TEMPERATURE

- the monkey /M. nemestrina/ p0088 A80-21988
- BENDING MOMENTS**
Wing flapping with minimum energy --- minimize the drag for a bending moment at the wing root
[NASA-TM-81174] p0001 N80-16035
Comparison of calculated and measured blade loads on a full-scale tilting propotor in a wind tunnel
[NASA-TM-81228] p0012 N80-31386
- BIBLIOGRAPHIES**
Ames Research Center publications: A continuing bibliography, 1978
[NASA-TM-81175] p0003 N80-18985
Chemical research projects office: An overview and bibliography, 1975-1980
[NASA-TM-81227] p0037 N80-31473
Human acclimation and acclimatization to heat: A compendium of research, 1968-1978 --- Bibliography
[NASA-TM-81181] p0085 N80-34056
- BINARY MIXTURES**
Adsorption interference in mixtures of trace contaminants flowing through activated carbon adsorber beds
[ASME PAPER 80-ENAS-17] p0096 A80-43193
- BINARY STARS**
The evolution of rapid oscillations in an outburst of a dwarf nova
p0075 A80-45227
- BINARY SYSTEMS (DIGITAL)**
U DIGITAL SYSTEMS
- BINARY SYSTEMS (MATHEMATICAL)**
NT BINARY MIXTURES
- BINDERS (ADHESIVES)**
U ADHESIVES
- BIOASTRONAUTICS**
Simulated weightlessness - Effects on bioenergetic balance
p0095 A80-21544
Evaluation of biological models using Spacelab
[ASME PAPER 80-ENAS-38] p0094 A80-43212
The development of a Space Shuttle Research Animal Holding Facility
[ASME PAPER 80-ENAS-39] p0096 A80-43213
- BIOCHEMISTRY**
NT BACTERIOLOGY
NT BIOGEOCHEMISTRY
Proton movements in response to a light-driven electrogenic pump for sodium ions in Halobacterium halobium membranes
p0087 A80-17686
Spectrophotometric identification of the pigment associated with light-driven primary sodium translocation in Halobacterium halobium
p0088 A80-26015
Favorable effects of the antioxidants sodium and magnesium thiazolidine carboxylate on the vitality and life span of Drosophila and mice
p0089 A80-29085
Evaluation of biological models using Spacelab
[ASME PAPER 80-ENAS-38] p0094 A80-43212
- BIODYNAMICS**
Optimal estimator model for human spatial orientation
p0093 A80-24265
- BIOENGINEERING**
NT BIOINSTRUMENTATION
- BIOGENESIS**
U BIOLOGICAL EVOLUTION
- BIOGEOCHEMISTRY**
The carbon isotope biogeochemistry of the individual hydrocarbons in bat guano and the ecology of insectivorous bats in the region of Carlsbad, New Mexico
[NASA-TM-81164] p0083 N80-18680
- BIOINSTRUMENTATION**
A microprocessor-based instrument for neural pulse wave analysis
p0098 A80-50322
Induction powered biological radiosonde
[NASA-CASE-ARC-11120-1] p0099 N80-18691
- BIOLOGICAL CELLS**
U CELLS (BIOLOGY)
- BIOLOGICAL EFFECTS**
Hypergravity and estrogen effects on avian anterior pituitary growth hormone and prolactin levels
p0094 A80-20447
- BIOLOGICAL EVOLUTION**
NT ABIOTIC EVOLUTION
- Oxygen as a factor in eukaryote evolution - Some effects of low levels of oxygen on Saccharomyces cerevisiae
p0086 A80-12229
Evaluation of biological models using Spacelab
[ASME PAPER 80-ENAS-38] p0094 A80-43212
- BIOLOGICAL MODELS**
U BIONICS
- BIOMASS**
Analysis of coastal upwelling and the production of a biomass
[NASA-TM-78614] p0035 N80-12720
- BIOMECHANICS**
U BIODYNAMICS
- BIONICS**
Optimal estimator model for human spatial orientation
p0093 A80-24265
Evaluation of biological models using Spacelab
[ASME PAPER 80-ENAS-38] p0094 A80-43212
- BIOPHYSICS**
NT HEALTH PHYSICS
Noninvasive measures of bone bending rigidity in the monkey /M. nemestrina/
p0088 A80-21988
- BIOREGENERATIVE LIFE SUPPORT SYSTEMS**
U CLOSED ECOLOGICAL SYSTEMS
- BIOSENSORS**
U BIOINSTRUMENTATION
- BIOSIMULATION**
U BIONICS
- BLADE TIPS**
Effect of tip planform on blade loading characteristics for a two-bladed rotor in hover
[NASA-TM-78615] p0007 N80-14049
- BLOOD**
NT ERYTHROCYTES
- BLOOD PLASMA**
Plasma volume during stress in man - Osmolality and red cell volume
p0087 A80-13506
Role of thermal and exercise factors in the mechanism of hypervolemia
p0089 A80-32748
Exercise training-induced hypervolemia - Role of plasma albumin, renin, and vasopressin
p0089 A80-32749
Na+ and Ca2+ ingestion - Plasma volume-electrolyte distribution at rest and exercise
p0091 A80-41661
Fluid-electrolyte shifts and thermoregulation - Rest and work in heat with head cooling
p0091 A80-48086
Extracellular hyperosmolality and body temperature during physical exercise in dogs
p0092 A80-54076
- BLOOD VOLUME**
Plasma volume during stress in man - Osmolality and red cell volume
p0087 A80-13506
- BO-105 HELICOPTER**
A compilation and analysis of helicopter handling qualities data. Volume 1: Data compilation
[NASA-CR-3144] p0013 N80-11097
- BOAT TAILS**
Numerical simulation of three-dimensional boat tail afterbody flow fields
[AIAA PAPER 80-1347] p0066 A80-44132
- BODIES OF REVOLUTION**
NT CYLINDRICAL BODIES
NT SPHERES
A three dimensional vortex wake model for missiles at high angles on attack
[NASA-CR-3208] p0014 N80-14048
A correlation method to predict the surface pressure distribution of an infinite plate or a body of revolution from which a jet is issuing
[NASA-CR-152345] p0018 N80-32339
- BODY FLUIDS**
NT ERYTHROCYTES
NT URINE
Fluid shifts and endocrine responses during chair rest and water immersion in man
p0088 A80-25990
Fluid-electrolyte shifts and thermoregulation - Rest and work in heat with head cooling
p0091 A80-48086
- BODY TEMPERATURE**
Exercise thermoregulation after 14 days of bed rest

BODY TEMPERATURE REGULATION

SUBJECT INDEX

- Changes in body temperature and metabolic rate after injection of calcium into the caudal hypothalamus of the rabbit p0088 A80-25989
- Role of thermal and exercise factors in the mechanism of hypervolemia p0093 A80-27078
- Extracellular hyperosmolality and body temperature during physical exercise in dogs p0089 A80-32748
- Human acclimation and acclimatization to heat: A compendium of research, 1968-1978 --- Bibliography [NASA-TM-81181] p0092 A80-54076
- BODY TEMPERATURE REGULATION**
U THERMOREGULATION p0085 N80-34056
- BODY-WING AND TAIL CONFIGURATIONS**
Large scale model tests of a new technology V/STOL concept [AIAA PAPER 80-0233] p0023 A80-19303
- Wind tunnel investigation of an oblique wing transport model at mach numbers between 0.6 and 1.4 [NASA-CR-137697] p0013 N80-12059
- BOEING AIRCRAFT**
NT C-135 AIRCRAFT
- BOLKOW AIRCRAFT**
NT BO-105 HELICOPTER
- BOLTZMANN TRANSPORT EQUATION**
Solution of Boltzmann equation for highly nonequilibrium diatomic gases rotational translational energy relaxation p0064 A80-34904
- BOMBER AIRCRAFT**
NT B-70 AIRCRAFT
- Flying-qualities criteria for wings-level-turn maneuvering during an air-to-ground weapon delivery task [AIAA 80-1628] p0029 A80-45916
- BONBS (SAMPLERS)**
U SAMPLERS
- BONDING**
NT ADHESIVE BONDING
NT METAL-METAL BONDING
- BONES**
Noninvasive measures of bone bending rigidity in the monkey /M. nemestrina/ p0088 A80-21988
- BOOST**
U ACCELERATION (PHYSICS)
- BOUNDARY LAYER CONTROL**
Control of forebody three-dimensional flow separations p0022 N80-15164
- BOUNDARY LAYER FLOW**
NT BOUNDARY LAYER SEPARATION
NT REATTACHED FLOW
NT SEPARATED FLOW
- The 60-MW Shuttle interaction heating facility p0059 A80-12603
- Investigation of a reattaching turbulent shear layer flow over a backward-facing step p0062 A80-27736
- Relaminarization of fluid flows p0075 A80-40843
- Computation of supersonic turbulent flows over an inclined ogive-cylinder-flare [AIAA PAPER 80-1410] p0066 A80-41608
- Overview of 6- X 6-foot wind tunnel aero-optics tests --- transonic wind tunnel tests p0023 N80-25590
- Pressure and temperature fields associated with aero-optics tests --- transonic wind tunnel tests p0031 N80-25591
- Unsteady density and velocity measurements in the 6 foot x 6 foot wind tunnel p0023 N80-25594
- A computer program to generate two-dimensional grids about airfoils and other shapes by the use of Poisson's equation [NASA-TM-81198] p0036 N80-26266
- BOUNDARY LAYER NOISE**
U AERODYNAMIC NOISE
- BOUNDARY LAYER SEPARATION**
An experimental and numerical investigation of a three-dimensional shock wave separated turbulent boundary layer [AIAA PAPER 80-0002] p0061 A80-22727
- Asymptotic features of shock-wave boundary-layer interaction p0055 A80-43135
- A comprehensive comparison between experiment and prediction for a transonic turbulent separated flow [AIAA PAPER 80-1407] p0027 A80-44154
- Three-dimensional interactions and vortical flows with emphasis on high speeds [NASA-TM-81169] p0008 N80-21286
- Simple turbulence models and their application to boundary layer separation [NASA-CR-3283] p0017 N80-24269
- BOUNDARY LAYER STABILITY**
Numerical experiments in boundary-layer stability [AIAA PAPER 80-0275] p0062 A80-23957
- BOUNDARY LAYER TRANSITION**
Study of boundary-layer transition using transonic-cone preston tube data [NASA-TM-81103] p0010 N80-28305
- BOUNDARY LAYERS**
NT LAMINAR BOUNDARY LAYER
NT THREE DIMENSIONAL BOUNDARY LAYER
NT TURBULENT BOUNDARY LAYER
NT TWO DIMENSIONAL BOUNDARY LAYER
- BOUNDARY VALUE PROBLEMS**
On the numerical solution of time-dependent viscous incompressible fluid flows involving solid boundaries p0052 A80-34980
- Nonreflecting far-field boundary conditions for unsteady transonic flow computation [AIAA PAPER 80-1393] p0065 A80-41597
- A general panel method for the analysis and design of arbitrary configurations in incompressible flows --- boundary value problem [NASA-CR-3079] p0017 N80-24268
- BOW SHOCK WAVES**
U BOW WAVES
U SHOCK WAVES
- BOW WAVES**
Position and shape of the Venus bow shock - Pioneer Venus Orbiter observations p0087 A80-15295
- A comparison of Pioneer Venus and Venera bow shock observations - Evidence for a solar cycle variation p0069 A80-15296
- BRAKES (FOR ARRESTING MOTION)**
NT WING FLAPS
- BREAKAWAY**
U BOUNDARY LAYER SEPARATION
- BRIGHTNESS**
X-ray bright points and the solar cycle dependence of emerging magnetic flux p0077 N80-17950
- BRIGHTNESS TEMPERATURE**
Saturn's rings - 3-mm observations and derived properties p0045 A80-21758
- BRISTOL-SIDDELEY BS 53 ENGINE**
A candidate V/STOL research aircraft design concept using an S-3A aircraft and 2 Pegasus 11 engines [NASA-TM-81204] p0009 N80-24293
- BROADBAND**
On the limitations of the concept of space frequency equivalence p0069 A80-16697
- BROMINE COMPOUNDS**
Pressure and temperature dependence kinetics study of the NO + BrO yielding NO2 + Br reaction - Implications for stratospheric bromine photochemistry p0068 A80-14397
- BROWNIAN MOVEMENTS**
Feasibility studies for light scattering experiments to determine the velocity relaxation of small particles in a fluid [NASA-CR-163214] p0040 N80-25586
- BUILDING MATERIALS**
U CONSTRUCTION MATERIALS
- BURNING RATE**
Flash-fire propensity and heat-release rate studies of improved fire resistant materials p0042 A80-15201

C

C-8A AUGMENTOR WING AIRCRAFT
NASA overview

p0022 N80-10109

C-135 AIRCRAFT

The effects of motion and g-seat cues on pilot simulator performance of three piloting tasks
[NASA-TP-1601] p0004 N80-15069

CABIN ATMOSPHERES

NT SPACECRAFT CABIN ATMOSPHERES

CAI

U COMPUTER ASSISTED INSTRUCTION

CALCIUM

Changes in body temperature and metabolic rate after injection of calcium into the caudal hypothalamus of the rabbit p0093 A80-27078

Microbial mobilization of calcium and magnesium in waterlogged soils p0089 A80-32834

Na+ and Ca2+ ingestion - Plasma volume-electrolyte distribution at rest and exercise p0091 A80-41661

CALCIUM COMPOUNDS

NT CALCIUM OXIDES

CALCIUM OXIDES

The preparation of calcium superoxide in a flowing gas stream and fluidized bed
[ASME PAPER 80-ENAS-18] p0094 A80-43194

CALCULUS

NT TAYLOR SERIES

NT VORTICITY

CALIBRATING

Airborne stellar spectrophotometry from 1.2 to 5.5 microns - Absolute calibration and spectra of stars earlier than M3 p0043 A80-16407

CALIFORNIA

Using guided clustering techniques to analyze Landsat data for mapping forest land cover in northern California p0078 A80-25595

Landsat-based multiphase estimation of California's irrigated lands p0079 A80-27435

Use of collateral information to improve LANDSAT classification accuracies --- Ventura County and Klamath National Forest, California [E80-10268] p0040 N80-29815

Irrigated lands assessment for water management Applications Pilot Test (APT) --- California [E80-10324] p0019 N80-32815

Infrared-temperature variability in a large agricultural field --- Dunnigan, California [E80-10331] p0038 N80-32822

CALLISTO

On the comparative evolution of Ganymede and Callisto p0048 A80-28080

The 16- to 38-micron spectrum of Callisto p0074 A80-35234

CALORIMETERS

Calorimeter probes for measuring high thermal flux --- in electric-arc jet facilities for planetary entry heating simulation p0099 A80-29480

CALORIMETRY

U HEAT MEASUREMENT

CANOPIES (VEGETATION)

Infrared-temperature variability in a large agricultural field --- Dunnigan, California [E80-10331] p0038 N80-32822

CANT

U SLOPES

CAWTLIVER WINGS

U WINGS

CAPACITORS

Transient solution for megajoule energy release in a lumped-parameter series RLC circuit p0051 A80-32826

CAPTURE CROSS SECTIONS

U ABSORPTION CROSS SECTIONS

CARBOHYDRATE METABOLISM

Growth hormone control of glucose oxidation pathways in hypophysectomized rats p0088 A80-24222

CARBOHYDRATES

NT GLUCOSE

CARBON

NT ACTIVATED CARBON

NT CARBON ISOTOPES

Direct /TEM/ observation of the catalytic oxidation of amorphous carbon by Pd particles p0053 A80-37180

CARBON COMPOUNDS

NT CHLOROCARBONS

NT FLUOROPOLYMERS

NT HALOCARBONS

Organic compounds in meteorites p0094 A80-50053

CARBON DIOXIDE

Absolute intensities and pressure broadening coefficients measured at different temperatures for the 201/II/-000 band of C-12/O2/-16 at 4978/cm p0048 A80-27125

CARBON DIOXIDE REMOVAL

Bosch - An alternate CO2 reduction technology [ASME PAPER 79-ENAS-32] p0092 A80-15256

Development of the electrochemically regenerable carbon dioxide absorber for portable life support system application [ASME PAPER 79-ENAS-33] p0092 A80-15257

Performance characterization of a Bosch CO sub 2 reduction subsystem [NASA-CR-152342] p0085 N80-22987

CARBON FIBERS

A small-scale test for fiber release from carbon composites p0062 A80-26881

A small-scale test for fiber release from carbon composites --- pyrolysis and impact [NASA-TM-81179] p0036 N80-18105

CARBON ISOTOPES

The carbon isotope biogeochemistry of the individual hydrocarbons in bat guano and the ecology of insectivorous bats in the region of Carlsbad, New Mexico [NASA-TM-81164] p0083 N80-18680

CARBON MONOXIDE

Two micron spectroscopy and 2.7 mm CO line observations of V645 Cygni p0074 A80-35114

CARBON STARS

The infrared spectrum of the carbon star Y Canum Venaticorum between 1.2 and 30 microns p0046 A80-22191

The spectrum of IRC + 10216 from 2.0 to 8.5 microns p0056 A80-44965

An optical emission-line phase of the extreme carbon star IRC +30219 p0056 A80-44993

CARBON SUBOXIDES

A model of Martian surface chemistry p0090 A80-36069

CARBON-CARBON COMPOSITES

Shape change of Galileo probe models in free-flight tests [NASA-TM-81209] p0037 N80-27418

CARBONACEOUS CHONDRITES

Carbonaceous chondrites. I - Characterization and significance of carbonaceous chondrite /CM/ xenoliths in the Jodzie howardite p0086 A80-13013

The radiocemization of isovaline - Cosmochemical implications --- gamma ray effects on Murchison meteorite primordial composition p0086 A80-13018

Quantification of monocarboxylic acids in the Murchison carbonaceous meteorite p0087 A80-13549

Meteoroid ablation spheres from deep-sea sediments p0046 A80-22948

Aqueous activity on asteroids - Evidence from carbonaceous meteorites p0062 A80-24586

Organic compounds in meteorites p0094 A80-50053

CARBONACEOUS METEORITES

Noble gas trapping and fractionation during synthesis of carbonaceous matter --- in meteorites p0093 A80-23669

Comets: Cosmic connections with carbonaceous meteorites, interstellar molecules and the origin of life p0092 N80-11975

CARBONYL COMPOUNDS

SUBJECT INDEX

CARBONYL COMPOUNDS

OCS, stratospheric aerosols and climate
p0044 A80-19741

CARBOXYLATES

Favorable effects of the antioxidants sodium and
magnesium thiazolidine carboxylate on the
vitality and life span of Drosophila and mice
p0089 A80-29085

CARBOXYLIC ACIDS

Quantification of monocarboxylic acids in the
Murchison carbonaceous meteorite
p0087 A80-13549

CARDIOVASCULAR SYSTEM

NT ERYTHROCYTES
Objective measurement of human tolerance to +G sub
z acceleration stress
[NASA-TM-81166]
p0098 N80-18709

CARGO AIRCRAFT

NT C-135 AIRCRAFT
Conceptual studies of a long-range transport with
an upper surface blowing propulsive lift system
[NASA-TM-81196]
p0009 N80-23249

CARTOGRAPHY

U MAPPING

CASCADE FLOW

An implicit finite-difference code for inviscid
and viscous cascade flow
[AIAA PAPER 80-1427]
p0066 A80-44128

CASCADES (FLUID DYNAMICS)

U FLUID DYNAMICS

CASSEGRAIN OPTICS

Simple Cassegrain scanning system for infrared
astronomy
p0074 A80-34729

CATABOLISM

A model for hypokinesia: Effects on muscle atrophy
in the rat
p0095 A80-28188

CATALOGS (PUBLICATIONS)

NT ASTRONOMICAL CATALOGS

CATALYSIS

Water recovery by catalytic treatment of urine vapor
[ASME PAPER 80-ENAS-16]
p0093 A80-43192
Design, fabrication and testing of a dual catalyst
ammonia removal system for a urine VCD unit
[NASA-CR-152372]
p0085 N80-29023

CATALYSTS

Catalysts for polyimide foams from aromatic
isocyanates and aromatic dianhydrides --- flame
retardant foams
[NASA-CASE-ARC-11107-1]
p0080 N80-16116

CATALYTIC ACTIVITY

Direct TEM/ observation of the catalytic
oxidation of amorphous carbon by Pd particles
p0053 A80-37180

CATIONS

NT METAL IONS

Modified Iterative Extended Hueckel. 2:
Application to the interaction of Na(+),
Na(+)(aq.), Mg(+)-2(aq.) with adenine and thymine
[NASA-TM-81201]
p0084 N80-25109

CCD

U CHARGE COUPLED DEVICES

CELESTIAL BODIES

NT ACHONDrites
NT ASTEROIDS
NT B STARS
NT BARRED GALAXIES
NT BINARY STARS
NT CALLISTO
NT CARBON STARS
NT CARBONACEOUS CHONDRITES
NT CARBONACEOUS METEORITES
NT COMET NUCLEI
NT COMETS
NT DWARF STARS
NT EARLY STARS
NT ELLIPTICAL GALAXIES
NT EXTRAGALACTIC RADIO SOURCES
NT EXTRASOLAR PLANETS
NT GALACTIC CLUSTERS
NT GANYMEDE
NT GAS GIANT PLANETS
NT GLOBULAR CLUSTERS
NT HOT STARS
NT JUPITER (PLANET)
NT JUPITER RINGS
NT LATE STARS
NT M STARS

NT MICROMETEORIDS

NT NATURAL SATELLITES

NT NEBULAE

NT NOVAE

NT O STARS

NT PLANETARY NEBULAE

NT PLUTO (PLANET)

NT PROTOPLANETS

NT PROTOSTARS

NT QUASARS

NT RADIO SOURCES (ASTRONOMY)

NT SATURN (PLANET)

NT SATURN RINGS

NT SOLAR SYSTEM

NT SPIRAL GALAXIES

NT STAR CLUSTERS

NT SUPERNOVAE

NT T TAURI STARS

NT TITAN

NT URANUS (PLANET)

NT VARIABLE STARS

CELESTIAL MECHANICS

On the three-dimensional shapes of elliptical
galaxies
p0047 A80-26101

CELESTIAL OBSERVATION

U ASTRONOMY

CELLS (BIOLOGY)

NT ERYTHROCYTES

NT HEMOGLOBIN

Oxygen as a factor in eukaryote evolution - Some
effects of low levels of oxygen on Saccharomyces
cerevisiae
p0086 A80-12229

Problems and potentialities of cultured plant
cells in retrospect and prospect
p0077 A80-15225

Review of cell aging in Drosophila and mouse
p0087 A80-17741

Insulin binding and glucose uptake of adipocytes
in rats adapted to hypergravitational force
p0089 A80-35751

CENTRIFUGING STRESS

Effects of chronic centrifugation on skeletal
muscle fibers in young developing rats
p0096 A80-41983

CERAMAL PROTECTIVE COATINGS

U PROTECTIVE COATINGS

CESIUM COMPOUNDS

NT CESIUM OXIDES

CESIUM OXIDES

The role of cesium suboxides in low-work-function
surface layers studied by X-ray photoelectron
spectroscopy - Ag-O-Cs
p0051 A80-33844

CH-53 HELICOPTER

U H-53 HELICOPTER

CHAIRS

U SEATS

CHALCOGENIDES

NT ANHYDRIDES

NT CALCIUM OXIDES

NT CARBON DIOXIDE

NT CARBON MONOXIDE

NT CARBON SUBOXIDES

NT CESIUM OXIDES

NT INORGANIC PEROXIDES

NT NITRIC OXIDE

NT NITROGEN OXIDES

NT OXIDES

NT SILICON DIOXIDE

NT SULFIDES

CHANNEL CAPACITY

Conditional replenishment using motion prediction
p0065 A80-39715

CHANNELS

Plains and channels in the Lunae Planum-Chryse
Planitia region of Mars
p0047 A80-26358

CHAPMAN SHEAR LAYER

U SHEAR LAYERS

CHAPMAN-JOUGET FLAME

U FLAME PROPAGATION

CHARACTERISTIC EQUATIONS

U EIGENVALUES

CHARACTERISTIC FUNCTIONS

U EIGENVALUES

CHARCOAL

NT ACTIVATED CARBON

CHARGE COUPLED DEVICES

Integrated infrared detector arrays for
low-background astronomy

p0066 A80-44639

CHARGE TRANSFER DEVICES

NT CHARGE COUPLED DEVICES

CHARGED PARTICLES

NT CATIONS

NT COSMIC PLASMA

NT ENERGETIC PARTICLES

NT METAL IONS

NT NEGATIVE IONS

NT PLASMA CLOUDS

NT POSITIVE IONS

NT PROTONS

NT RADIATION BELTS

NT RAREFIED PLASMAS

NT SOLAR WIND

NT STELLAR WINDS

NT THERMAL PLASMAS

On the inference of properties of Saturn's Ring E
from energetic charged particle observations

p0069 A80-15293

The acceleration of energetic charged particles by
interplanetary and supernova shock waves

p0080 A80-53209

CHEBYSHEV APPROXIMATION

On the numerical solution of time-dependent
viscous incompressible fluid flows involving
solid boundaries

p0052 A80-34980

CHELATE COMPOUNDS

U CHELATES

CHELATES

Chelate-modified polymers for atmospheric gas

chromatography

[NASA-CASE-ARC-11154-1]

p0097 N80-23383

CHEMICAL ANALYSIS

NT GAS SPECTROSCOPY

NT OZONOMETRY

NT SPECTROSCOPIC ANALYSIS

Carbonaceous chondrites. I - Characterization and
significance of carbonaceous chondrite /CH/
xenoliths in the Jodzie howardite

p0086 A80-13013

CHEMICAL BONDS

Modified Iterative Extended Hueckel. 2:

Application to the interaction of Na(+),

Na(+)(aq.), Mg(+)-2(aq.) with adenine and thymine

[NASA-TM-81201]

p0084 N80-25109

CHEMICAL COMPOSITION

Meteoroid ablation spheres from deep-sea sediments

p0046 A80-22948

Heterogeneous phase reactions of Martian volatiles

with putative regolith minerals

p0090 A80-36062

CHEMICAL ELEMENTS

NT ACTIVATED CARBON

NT ALKALI METALS

NT CALCIUM

NT CARBON

NT CARBON ISOTOPES

NT COPPER

NT FLUORINE

NT HELIUM

NT HYDROGEN

NT HYDROGEN ATOMS

NT HYDROGEN IONS

NT LIQUID HELIUM

NT LIQUID HELIUM 2

NT LIQUID NITROGEN

NT MAGNESIUM

NT MOLYBDENUM

NT NICKEL

NT NITROGEN

NT NITROGEN ATOMS

NT NITROGEN IONS

NT OXYGEN

NT PALLADIUM

NT POTASSIUM

NT RADIOACTIVE ISOTOPES

NT RARE GASES

NT SILICON

NT SILVER

NT SODIUM

NT XENON

CHEMICAL EVOLUTION

Aldocyanoin microspheres - Partial amino acid
analysis of the microparticulates formed from

simple reactants under various conditions

p0086 A80-11473

The radioracemization of isovaline - Cosmochemical
implications --- gamma ray effects on Murchison
meteorite primordial composition

p0086 A80-13018

The role of metal ions in chemical evolution -

Polymerization of alanine and glycine in a

cation-exchanged clay environment

p0090 A80-36195

The possible role of metal ions and clays in

prebiotic chemistry

p0094 A80-50060

CHEMICAL FRACTIONATION

Noble gas trapping and fractionation during

synthesis of carbonaceous matter --- in meteorites

p0093 A80-23669

CHEMICAL KINETICS

U REACTION KINETICS

CHEMICAL LASERS

Quantum-mechanical calculation of

three-dimensional atom-diatom collisions in the

presence of intense laser radiation

p0068 A80-15221

CHEMICAL PROPERTIES

NT THERMOCHEMICAL PROPERTIES

CHEMICAL REACTIONS

NT OXIDATION

NT OXYGENATION

NT PHOTOCHEMICAL REACTIONS

NT PHOTOLYSIS

NT PHOTOOXIDATION

NT PYROLYSIS

The properties of clusters in the gas phase. IV -

Complexes of H₂O and HNO_x clustering on NO_x-/-

p0046 A80-23322

CHEMICAL RELAXATION

U MOLECULAR RELAXATION

CHEMICAL TESTS

NT CHEMICAL ANALYSIS

NT GAS SPECTROSCOPY

NT OZONOMETRY

NT SPECTROSCOPIC ANALYSIS

CHEMISORPTION

Isothermal-desorption-rate measurements in the

vicinity of the Curie temperature for H₂

chemisorbed on nickel films

p0042 A80-16167

CHILLING

U COOLING

CHIRAL DYNAMICS

Differentiation of optical isomers through

enhanced weak-field interactions

[NASA-TM-81208]

p0084 N80-27164

CHLORINE COMPOUNDS

NT CHLOROCARBONS

CHLOROCARBONS

Band model calculations for CFC13 in the 8-12

micron region

p0045 A80-21560

Stratospheric ozone decrease due to

chlorofluoromethane photolysis - Predictions of

latitude dependence

p0049 A80-29762

CHONDRITES

NT CARBONACEOUS CHONDRITES

NT CARBONACEOUS METEORITES

CHROMATOGRAPHY

NT GAS CHROMATOGRAPHY

CHRONIC CONDITIONS

Effects of chronic centrifugation on skeletal

muscle fibers in young developing rats

p0096 A80-41983

CHROMOTRONS

U TIME LAG

CIRCUITS

NT INTEGRATED CIRCUITS

NT RLC CIRCUITS

CIRCULAR POLARIZATION

21 cm maps of Jupiter's radiation belts from all

rotational aspects

p0076 A80-48877

CIRCULATION

NT ATMOSPHERIC CIRCULATION

On the combination of kinematics with flow

visualization to compute total circulation -

Application to vortex rings in a tube

[AIAA PAPER 80-1330]

p0065 A80-41563

CIRCUMSTELLAR MATTER

SUBJECT INDEX

CIRCUMSTELLAR MATTER

U STELLAR ENVELOPES

CIVIL AVIATION

Analysis of eighty-four commercial aviation incidents - Implications for a resource management approach to crew training

p0093 A80-40340

Civil helicopter wire strike assessment study.

Volume 1: Findings and recommendations

[NASA-CR-152389]

p0019 N80-33381

CLARK Y AIRFOIL

U AIRFOIL PROFILES

CLASSICAL MECHANICS

NT CELESTIAL MECHANICS

CLAYS

Silt-clay aggregates on Mars

p0041 A80-10366

The possible role of metal ions and clays in prebiotic chemistry

p0094 A80-50060

CLIMATE

Stratospheric aerosol modification by supersonic transport operations with climate implications

[NASA-RP-1058]

p0034 N80-15726

CLIMATOLOGY

OCS, stratospheric aerosols and climate

p0044 A80-19741

Stratospheric aerosol modification by supersonic transport and space shuttle operations - Climate implications

p0047 A80-26088

Atmospheric aerosols and climate

p0052 A80-36305

CLOSED ECOLOGICAL SYSTEMS

Performance characterization of a Bosch CO sub 2 reduction subsystem

[NASA-CR-152342]

p0085 N80-22987

CLOSED LOOP SYSTEMS

U FEEDBACK CONTROL

CLOTHING

NT GARMENTS

NT SPACE SUITS

CLOUDS

NT HYDROGEN CLOUDS

NT PLASMA CLOUDS

NT VENUS CLOUDS

COAGULATION

A reconsideration of nucleation phenomena in light of recent findings concerning the properties of small clusters, and a brief review of some other particle growth processes --- for cosmic dust

p0069 A80-15609

COASTAL DUNES

U DUNES

COASTS

Analysis of coastal upwelling and the production of a biomass

[NASA-TM-78614]

p0035 N80-12720

COATINGS

NT METAL COATINGS

NT PROTECTIVE COATINGS

NT THERMAL CONTROL COATINGS

COAXIAL FLOW

Modal content of noise generated by a coaxial jet

in a pipe

[NASA-CR-163575]

p0019 N80-33177

COCKPIT SIMULATORS

Operations manual: Vertical Motion Simulator

(VMS) S.08

[NASA-TM-81180]

p0009 N80-23295

COCKPITS

The effect of viewing time, time to encounter, and practice on perception of aircraft separation on a cockpit display of traffic information

[NASA-TM-81173]

p0083 N80-18038

Perception of aircraft separation with pilot-preferred symbology on a cockpit display of traffic information

[NASA-TM-81172]

p0084 N80-31397

COEFFICIENTS

NT ACCOMMODATION COEFFICIENT

NT AERODYNAMIC COEFFICIENTS

NT DIFFUSION COEFFICIENT

COHERENT SOURCES

U RADIATION SOURCES

COLLISION AVOIDANCE

NASA aviation safety reporting system

[NASA-TM-81197]

p0085 N80-32352

COLLISION PARAMETERS

Galaxy collisions - A preliminary study

p0046 A80-23420

COLLISION WARNING DEVICES

U COLLISION AVOIDANCE

U WARNING SYSTEMS

COLLISIONS

NT ATOMIC COLLISIONS

NT MOLECULAR COLLISIONS

COLLOIDS

NT AEROSOLS

COMBUSTIBILITY

U FLAMMABILITY

COMBUSTION CHAMBERS

Reduction of nitric oxide emissions from a combustor

[NASA-CASE-ARC-10814-2]

p0080 N80-26298

COMBUSTION PRODUCTS

A small-scale test for fiber release from carbon composites

p0062 A80-26881

COMBUSTION WAVES

U FLAME PROPAGATION

COMBUSTORS

U COMBUSTION CHAMBERS

COMET NUCLEI

Comet nucleus impact probe feasibility study

[NASA-CR-152375]

p0040 N80-26364

COMETS

NT COMET NUCLEI

Comets: Cosmic connections with carbonaceous meteorites, interstellar molecules and the origin of life

p0092 N80-11975

COMMERCIAL AIRCRAFT

NT LIGHT TRANSPORT AIRCRAFT

Factors affecting the retirement of commercial transport jet aircraft

[NASA-CR-152308]

p0013 N80-10148

COMMERCIAL AVIATION

U CIVIL AVIATION

U COMMERCIAL AIRCRAFT

COMPARTMENTS

NT AIRCRAFT COMPARTMENTS

NT ANECHOIC CHAMBERS

COMPLEX VARIABLES

NT HYPERGEOMETRIC FUNCTIONS

NT SINGULARITY (MATHEMATICS)

COMPLEXITY

NT TASK COMPLEXITY

COMPONENT RELIABILITY

V/STOLAND avionics system flight-test data on a

UH-1H helicopter

[NASA-TM-78591]

p0008 N80-18047

COMPOSITE MATERIALS

NT CARBON-CARBON COMPOSITES

NT EPOXY MATRIX COMPOSITE MATERIALS

NT FIBER COMPOSITES

NT GLASS FIBER REINFORCED PLASTICS

NT GRAPHITE-EPOXY COMPOSITE MATERIALS

NT LAMINATES

NT POLYMER MATRIX COMPOSITE MATERIALS

Release-rate calorimetry of multilayered materials

for aircraft seats

[AIAA 80-0759]

p0064 A80-35052

A small-scale test for fiber release from carbon

composites --- pyrolysis and impact

[NASA-TM-81179]

p0036 N80-18105

The accelerated characterization of viscoelastic

composite materials

[NASA-CR-163188]

p0039 N80-24370

Application of advanced technologies to small,

short-haul transport aircraft

[NASA-CR-152363]

p0018 N80-32353

Influence of quality control variables on failure

of graphite/epoxy under extreme moisture

conditions

[NASA-TM-81246]

p0038 N80-33493

COMPOSITE STRUCTURES

NT LAMINATES

COMPOSITES

U COMPOSITE MATERIALS

COMPOSITION (PROPERTY)

NT ATMOSPHERIC COMPOSITION

NT CHEMICAL COMPOSITION

NT IONOSPHERIC COMPOSITION

NT METEORITIC COMPOSITION

NT MOISTURE CONTENT

NT PLANETARY COMPOSITION

NT PLASMA COMPOSITION

SUBJECT INDEX

COMPUTERIZED SIMULATION

COMPRESSIBLE FLOW

NT TRANSONIC FLOW

An efficient explicit-implicit-characteristic method for solving the compressible Navier-Stokes equations

p0062 A80-27408

Characterization of acoustic disturbances in linearly sheared flows

p0030 A80-31804

Progress in turbulence modeling for complex flow fields including effects of compressibility [NASA-TP-1517]

p0034 N80-20527

COMPUTATIONAL FLUID DYNAMICS

Supersonic flow over three-dimensional ablated noetips using an unsteady implicit numerical procedure

[AIAA PAPER 80-0063] p0060 A80-19271

Numerical simulation of steady supersonic flow over an ogive-cylinder-boattail body

[AIAA PAPER 80-0066] p0060 A80-19273

A diagonal form of an implicit approximate-factorization algorithm with application to a two dimensional inlet [AIAA PAPER 80-0067]

p0061 A80-19274

Automatic mesh-point clustering near a boundary in grid generation with elliptic partial differential equations

p0044 A80-20593

Forebody and base region real-gas flow in severe planetary entry by a factored implicit numerical method. I - Computational fluid dynamics [AIAA PAPER 80-0065]

p0061 A80-22731

Transonic swept-wing analysis using asymptotic and other numerical methods

[AIAA PAPER 80-0342] p0024 A80-22751

Implicit computations of unsteady transonic flow governed by the full-potential equation in conservation form

[AIAA PAPER 80-0150] p0062 A80-23935

Numerical experiments in boundary-layer stability [AIAA PAPER 80-0275]

p0062 A80-23957

Application of the method of integral relations to unsteady fluid flow problems with shocks

p0078 A80-26694

On the construction and application of implicit factored schemes for conservation laws --- in computational fluid dynamics

p0062 A80-27407

An efficient explicit-implicit-characteristic method for solving the compressible Navier-Stokes equations

p0062 A80-27408

Computational aerodynamics on large computers

p0048 A80-27415

Note on the eigensolution of a homogeneous equation with semi-infinite domain

p0075 A80-40508

Experimental investigation of a three dimensional turbulent boundary layer with a non disappearing pressure gradient

p0054 A80-40907

Nonreflecting far-field boundary conditions for unsteady transonic flow computation

[AIAA PAPER 80-1393] p0065 A80-41597

Computation of supersonic turbulent flows over an inclined ogive-cylinder-flare

[AIAA PAPER 80-1410] p0066 A80-41608

A vortex-lattice method for the calculation of the nonsteady separated flow over delta wings

[AIAA PAPER 80-1803] p0027 A80-43286

An implicit finite-difference code for inviscid and viscous cascade flow

[AIAA PAPER 80-1427] p0066 A80-44128

Calculations of transonic flow about an airfoil in a wind tunnel

[AIAA PAPER 80-1366] p0027 A80-44142

Computations of the Magnus effect for slender bodies in supersonic flow

[AIAA 80-1586] p0028 A80-45882

On the calculation of turbulent heat transport downstream from an abrupt pipe expansion

p0076 A80-49037

Direct numerical simulations of the turbulent wake of an axisymmetric body

p0080 A80-49235

Vortex simulation of three-dimensional, spotlike disturbances in a laminar boundary layer

p0067 A80-49296

Three-dimensional simulation of the free shear layer using the vortex-in-cell method

p0067 A80-49300

Use of advanced computers for aerodynamic flow simulation

p0058 N80-21257

COMPUTER ASSISTED INSTRUCTION

Computer-based manuals for procedural information

p0096 A80-50427

Conference of Remote Sensing Educators (CORSE-78) [NASA-CP-2102]

p0034 N80-20003

COMPUTER GRAPHICS

Dynamic decisions and work load in multitask supervisory control

p0095 A80-40898

COMPUTER METHODS

U COMPUTER PROGRAMS

COMPUTER NETWORKS

An assessment of future computer system needs for large-scale computation [NASA-TM-78613]

p0008 N80-17717

COMPUTER PROGRAMS

NT COMPUTER SYSTEMS PROGRAMS

NT SUBROUTINES

Fragmentation in a rotating protostar - A comparison of two three-dimensional computer codes

p0053 A80-38432

Recent improvements to the spinning body version of the EDDYBL computer program

[NASA-CR-152347] p0039 N80-19448

A computer program to generate two-dimensional grids about airfoils and other shapes by the use of Poisson's equation

[NASA-TM-81198] p0036 N80-26266

A comprehensive analytical model of rotorcraft aerodynamics and dynamics. Part 2: User's manual [NASA-TM-81183]

p0010 N80-28297

A comprehensive analytical model of rotorcraft aerodynamics and dynamics. Part 3: Program manual [NASA-TM-81184]

p0010 N80-28298

Algorithm for fixed-range optimal trajectories [NASA-TP-1565]

p0006 N80-28329

Experimental unsteady aerodynamics of conventional and supercritical airfoils --- conducted in the Ames 11 foot transonic wind tunnel [NASA-TM-81221]

p0012 N80-33345

COMPUTER SIMULATION

U COMPUTERIZED SIMULATION

COMPUTER SYSTEMS DESIGN

An assessment of future computer system needs for large-scale computation

[NASA-TM-78613] p0008 N80-17717

COMPUTER SYSTEMS PROGRAMS

The analysis of delays in simulator digital computing systems. Volume 1: Formulation of an analysis approach using a central example simulator model [NASA-CR-152340]

p0015 N80-17722

COMPUTER TECHNIQUES

Computational aerodynamics on large computers

p0048 A80-27415

Computer/experiment integration for unsteady aerodynamic research

p0025 A80-29501

COMPUTERIZED DESIGN

Automated design using numerical optimization [SAE PAPER 791061]

p0024 A80-26628

Application of numerical optimization to the design of wings with specified pressure distributions [NASA-CR-3238]

p0015 N80-16031

An acceptable role for computers in the aircraft design process

p0023 N80-21246

An experimental evaluation of a helicopter rotor section designed by numerical optimization [NASA-TM-78622]

p0009 N80-21287

COMPUTERIZED SIMULATION

NT DIGITAL SIMULATION

The stratospheric sulfate aerosol layer - Processes, models, observations, and simulations

p0051 A80-34435

Nonreflecting far-field boundary conditions for unsteady transonic flow computation

[AIAA PAPER 80-1393] p0065 A80-41597

Three-dimensional simulation of the free shear layer using the vortex-in-cell method

p0067 A80-49300

COMPUTERS

Aircraft simulation data management - A prototype system
p0029 A80-49832

Simulation of the Infrared Astronomical Satellite /IRAS/ telescope system
p0067 A80-49842

Pilot control through the TAFCOS automatic flight control system
[NASA-TM-81152] p0007 N80-14138

Use of advanced computers for aerodynamic flow simulation
p0058 N80-21257

Introductory study of the chemical behavior of jet emissions in photochemical smog --- computerized simulation
[NASA-CR-152345] p0016 N80-21891

Study of boundary-layer transition using transonic-cone preston tube data
[NASA-TM-81103] p0010 N80-28305

An experimental evaluation of head-up display formats
[NASA-TP-1550] p0082 N80-28349

Turbulent structures in wall-bounded shear flows observed via three-dimensional numerical simulators --- using the Illiac 4 computer
[NASA-TM-81219] p0037 N80-29622

A comparison of flight and simulation data for three automatic landing system control laws for the Augmentor wing jet STOL research airplane
[NASA-CR-152365] p0018 N80-32338

COMPUTERS
NT AIRBORNE/SPACEBORNE COMPUTERS
NT ILLIAC 4 COMPUTER
Use of advanced computers for aerodynamic flow simulation
p0058 N80-21257

CONCENTRATION (COMPOSITION)
NT MOISTURE CONTENT

CONDITIONS
NT CHRONIC CONDITIONS
NT FLIGHT CONDITIONS
NT NONEQUILIBRIUM CONDITIONS

CONDUCTORS
NT SUPERCONDUCTORS

CONES
NT ABLATIVE NOSE CONES
Study of boundary-layer transition using transonic-cone preston tube data
[NASA-TM-81103] p0010 N80-28305

CONFERENCES
Workshop on Thrust Augmenting Ejectors
[NASA-CP-2093] p0004 N80-10107

Guiding the development of a controlled ecological life support system
[NASA-CR-162452] p0085 N80-12735

In depth review of the 1979 AIAA Lighter-Than-Air Systems Technology Conference
[NASA-TM-81158] p0006 N80-12991

An assessment of ground-based techniques for detecting other planetary systems. Volume 1: An overview --- workshop conclusions
[NASA-CP-2124-VOL-1] p0034 N80-18997

Workshop on Aircraft Surface Representation for Aerodynamic Computation
[NASA-TM-81170] p0008 N80-19025

Conference of Remote Sensing Educators (CORSE-78)
[NASA-CP-2102] p0034 N80-20003

Data reduction by computer processing
p0058 N80-20016

Resource management on the flight deck --- conferences
[NASA-CP-2120] p0082 N80-22283

Proceedings of the Aero-Optics Symposium on Electromagnetic Wave Propagation from Aircraft
[NASA-CP-2121] p0006 N80-25588

CONFIGURATION INTERACTION
SCF and CI calculations of the dipole moment function of ozone --- Self-Consistent Field and Configuration-Interaction
p0043 A80-17111

CONFIGURATION MANAGEMENT
Flight evaluation of configuration management system concepts during transition to the landing approach for a powered-lift STOL aircraft
[NASA-TM-81146] p0008 N80-19127

CONICAL FLARE
U CONES

CONICAL FLOW
A computational and experimental study of high

SUBJECT INDEX

Reynolds number viscous/inviscid interaction about a cone at high angle of attack
[AIAA PAPER 80-1422] p0104 A80-44492

CONSERVATION
NT ENERGY CONSERVATION

CONSERVATION LAWS
On the construction and application of implicit factored schemes for conservation laws --- in computational fluid dynamics
p0062 A80-27407

CONSTELLATIONS
NT CYGNUS CONSTELLATION

CONSTRUCTION MATERIALS
Fire-resistant materials for aircraft passenger seat construction
[NASA-TM-78617] p0035 N80-13255

CONSUMABLES (SPACECREW SUPPLIES)
NT POTABLE WATER

CONSUMPTION
NT FUEL CONSUMPTION
NT WATER CONSUMPTION

CONTAMINANTS
NT TRACE CONTAMINANTS

CONTINUUM MECHANICS
System theory as applied differential geometry --- linear system
[NASA-CR-3209] p0013 N80-12776

One millimeter continuum observations of extragalactic thermal sources
[NASA-CR-163590] p0040 N80-33334

CONTOURS
A closed-form solution for noise contours
[NASA-TP-1432] p0004 N80-11869

CONTROL SIMULATION
A pilot modeling technique for handling-qualities research
[AIAA 80-1624] p0028 A80-45912

Flying-qualities criteria for wings-level-turn maneuvering during an air-to-ground weapon delivery task
[AIAA 80-1628] p0029 A80-45916

CONTROL STABILITY
Measurements of control stability characteristics of a wind-tunnel model using a transfer function method
[AIAA 80-0457] p0024 A80-26957

CONTROL SURFACES
NT FLAPS (CONTROL SURFACES)
NT GUIDE VANES
NT UPPER SURFACE BLOWN FLAPS
NT WING FLAPS

Force and moment data from a wind-tunnel test of a tilt-macelle V/STOL propulsion system with an attitude control vane --- conducted in Ames 40 by 80 foot wind tunnel
[NASA-TM-81157] p0006 N80-13003

CONTROLLABILITY
A pilot modeling technique for handling-qualities research
[AIAA 80-1624] p0028 A80-45912

Flying-qualities criteria for wings-level-turn maneuvering during an air-to-ground weapon delivery task
[AIAA 80-1628] p0029 A80-45916

Pilot control through the TAFCOS automatic flight control system
[NASA-TM-81152] p0007 N80-14138

Flight evaluation of configuration management system concepts during transition to the landing approach for a powered-lift STOL aircraft
[NASA-TM-81146] p0008 N80-19127

CONTROLLED ATMOSPHERES
NT SPACECRAFT CABIN ATMOSPHERES

CONTROLLERS
NT SERVOMECHANISMS

CONVECTION
NT FREE CONVECTION

CONVECTIVE HEAT TRANSFER
Core cooling by subsolidus mantle convection --- thermal evolution model of earth
p0044 A80-19391

Free convection in enclosures exposed to compressive heating --- Galileo descent module
[AIAA PAPER 80-1536] p0079 A80-41495

CONVERGENT-DIVERGENT NOZZLES
Aircraft engine nozzle
[NASA-CASE-ARC-10977-1] p0033 N80-32392

CONVERTAPLANES
U V/STOL AIRCRAFT

SUBJECT INDEX

CRYOGENIC EQUIPMENT

COOLING

- NT AIR COOLING
- NT LIQUID COOLING
- NT SURFACE COOLING
 - Core cooling by subsolidus mantle convection --- thermal evolution model of earth p0044 A80-19391
 - Fluid-electrolyte shifts and thermoregulation - Rest and work in heat with head cooling p0091 A80-48086

COOLING SYSTEMS

- Cryogenic systems for spacecraft p0055 A80-42902
- Effect of propeller slipstream on the drag and performance of the engine cooling system for a general aviation twin-engine aircraft [AIAA PAPER 80-1872] p0027 A80-43315

COORDINATE TRANSFORMATIONS

- Feedback invariants for nonlinear systems p0031 A80-14810

COPILOTS

- U AIRCRAFT PILOTS

COPPER

- Comparison of the early stages of condensation of Cu and Ag on Mo/100/ with Cu and Ag on W/100/ p0053 A80-37193

CORES

- NT EARTH CORE
- NT PLANETARY CORES

CORONAL HOLES

- X-ray bright points and the solar cycle dependence of emerging magnetic flux p0077 N80-17950

CORONAS

- NT CORONAL HOLES
- NT SOLAR CORONA

CORPUSCULAR RADIATION

- NT ENERGETIC PARTICLES
- NT RADIATION BELTS

CORRELATION

- NT DATA CORRELATION
- NT SPECTRAL CORRELATION
 - A correlation method to predict the surface pressure distribution of an infinite plate or a body of revolution from which a jet is issuing [NASA-CR-152345] p0018 N80-32339

CORRELATION FUNCTIONS

- U CORRELATION

COSMIC DUST

- A reconsideration of nucleation phenomena in light of recent findings concerning the properties of small clusters, and a brief review of some other particle growth processes --- for cosmic dust p0069 A80-15609
- A far-infrared study of the reflection nebula NGC 2023 p0072 A80-26111
- Excitation mechanisms for the unidentified infrared emission features p0054 A80-40642

COSMIC GASES

- NT INTERPLANETARY GAS
- NT INTERSTELLAR GAS
- NT NEUTRAL GASES

COSMIC PLASMA

- The Pioneer Venus Orbiter plasma analyzer experiment p0050 A80-30836

COSMIC RADIATION

- U COSMIC RAYS

COSMIC RAYS

- A comparative study of cosmic ray intensity variations during 1972-1977 using spacecraft and ground-based observations p0072 A80-28244
- Retinal changes in rats flown on Cosmos 936 - A cosmic ray experiment p0091 A80-41995

COSMOGONY

- U COSMOLOGY

COSMOLOGY

- The settling of helium and the ages of globular clusters p0052 A80-35151
- Origin and evolution of planetary atmospheres p0053 A80-37598
- Comets: Cosmic connections with carbonaceous meteorites, interstellar molecules and the origin of life p0092 A80-11975

COSMOS SATELLITES

- Retinal changes in rats flown on Cosmos 936 - A cosmic ray experiment p0091 A80-41995

COST ANALYSIS

- Documentation of the analysis of the benefits and costs of aeronautical research and technology models, volume 1 [NASA-CR-152278] p0001 N80-15865
- Application of advanced technologies to small, short-haul transport aircraft [NASA-CR-152363] p0018 N80-32353

COST EFFECTIVENESS

- An acceptable role for computers in the aircraft design process p0023 N80-21246

COST ESTIMATES

- Application of parametric weight and cost estimating relationships to future transport aircraft [SAWE PAPER 1292] p0024 A80-20637

COST REDUCTION

- Algorithm for fixed-range optimal trajectories [NASA-TP-1565] p0006 N80-28329

COSTS

- NT AIRPLANE PRODUCTION COSTS

COTTON

- Irrigated lands assessment for water management Applications Pilot Test (APT) --- California [E80-10324] p0019 N80-32815

COUNTERS

- NT NEUTRON COUNTERS

CRACKING (CHEMICAL ENGINEERING)

- NT PYROLYSIS

CRATERS

- NT LUNAR CRATERS
- NT PLANETARY CRATERS

CREEP ANALYSIS

- Some observations regarding the statistical determination of stress rupture regression lines p0041 A80-12828

CREEP RUPTURE STRENGTH

- Some observations regarding the statistical determination of stress rupture regression lines p0041 A80-12828

CREEP TESTS

- Time-temperature behavior of a unidirectional graphite/epoxy composite p0078 A80-21141
- The accelerated characterization of viscoelastic composite materials [NASA-CR-163188] p0039 N80-24370

CREWS

- NT FLIGHT CREWS

CRITICAL FLOW

- Second sound shock waves and critical velocities in liquid helium 2 [NASA-CR-162687] p0015 N80-16837

CRITICAL REYNOLDS NUMBER

- U REYNOLDS NUMBER

CROP IDENTIFICATION

- Landsat-based multiphase estimation of California's irrigated lands p0079 A80-27435

CROP INVENTORIES

- Irrigated lands assessment for water management Applications Pilot Test (APT) --- California [E80-10324] p0019 N80-32815

CROPLANDS

- U FARMLANDS

CROSS FLOW

- A note on sound radiation into a uniformly flowing medium p0031 A80-45488
- An experimental study of the structure and acoustic field of a jet in a cross stream --- Ames 7-ft by 10-ft wind tunnel tests [NASA-CR-162464] p0014 N80-15871
- Vorticity associated with multiple jets in a crossflow --- vertical takeoff aircraft [NASA-CR-162855] p0016 N80-19454

CROSSLINKING

- Study of crosslinking and degradation mechanisms in sealant polymer candidates [NASA-CR-152346] p0039 N80-22484

CRUSTS

- NT LUNAR CRUST

CRYOGENIC EQUIPMENT

- Design of a one-year lifetime, spaceborne

CRYOGENIC FLUID STORAGE

SUBJECT INDEX

superfluid helium dewar
[ASME PAPER 79-ENAS-23] p0077 A80-15247
Cryogenic systems for spacecraft p0055 A80-42902

CRYOGENIC FLUID STORAGE
Design of a one-year lifetime, spaceborne
superfluid helium dewar
[ASME PAPER 79-ENAS-23] p0077 A80-15247
Cryogenic container compound suspension strap
[NASA-CASE-ARC-11157-1] p0080 N80-18393

CRYOGENIC FLUIDS
NT LIQUID HELIUM
NT LIQUID HELIUM 2
NT LIQUID NITROGEN

CRYOGENICS
Cryogenic systems for spacecraft p0055 A80-42902

CRYSTAL LATTICES
NT FACE CENTERED CUBIC LATTICES

CRYSTAL STRUCTURE
Effect of three-body interactions on the structure
of small clusters p0057 A80-49383

CRYSTALLITES
Changes induced on the surfaces of small Pd
clusters by the thermal desorption of CO p0053 A80-37179

CRYSTALLOGRAPHY
Effect of three-body interactions on the structure
of small clusters p0057 A80-49383

CRYSTALS
NT CRYSTALLITES
NT MICROCRYSTALS

CUBIC LATTICES
NT FACE CENTERED CUBIC LATTICES

CULTURE TECHNIQUES
Problems and potentialities of cultured plant
cells in retrospect and prospect p0077 A80-15225

CURIE TEMPERATURE
Isothermal-desorption-rate measurements in the
vicinity of the Curie temperature for H2
chemisorbed on nickel films p0042 A80-16167

CURING
Ambient curing fire resistant foams p0063 A80-34790

CURL (VECTORS)
NT VORTICITY

CURVE FITTING
Synthesis of rotor test data for real-time
simulation
[NASA-CR-152311] p0015 N80-18029

CURVED PANELS
Analysis of two-dimensional incompressible flows
by a subsurface panel method p0029 A80-30566

CURVED SURFACES
U CONTOURS

CYANATES
Catalysts for polyimide foams from aromatic
isocyanates and aromatic dianhydrides --- flame
retardant foams
[NASA-CASE-ARC-11107-1] p0080 N80-16116

CYCLES
NT SOLAR CYCLES
NT SUNSPOT CYCLE

CYGNUS CONSTELLATION
Two micron spectroscopy and 2.7 mm CO line
observations of V645 Cygni p0074 A80-35114

CYLINDRICAL AFTERBODIES
U AFTERBODIES
U CYLINDRICAL BODIES

CYLINDRICAL BODIES
Numerical simulation of steady supersonic flow
over an ogive-cylinder-boattail body
[AIAA PAPER 80-0066] p0060 A80-19273

CYLINDROIDS
U CYLINDRICAL BODIES

CYTOLOGY
Oxygen as a factor in eukaryote evolution - Some
effects of low levels of oxygen on Saccharomyces
cerevisiae p0086 A80-12229

Proton movements in response to a light-driven
electrogenic pump for sodium ions in
Halobacterium halobium membranes

The role of Na⁺/ in transport processes of
bacterial membranes p0087 A80-17686
p0088 A80-27077

D

DAENO (DATA ANALYSIS)
U DATA PROCESSING
U DATA REDUCTION
U DATA TRANSMISSION

DAMAGE
NT FIRE DAMAGE

DAMPING
NT VIBRATION DAMPING

DAMPNESS
U MOISTURE CONTENT

DART TURBOPROP ENGINES
U TURBOPROP ENGINES

DATA ACQUISITION
Data acquisition for measuring the wind on Venus
from Pioneer Venus p0051 A80-30852
Data acquisition for measuring the wind on Venus
from Pioneer Venus p0058 N80-26361
Data acquisition techniques for exploiting the
uniqueness of the time-of-flight mass
spectrometer: Application to sampling pulsed
gas systems
[NASA-TM-81224] p0037 N80-31775

DATA ADAPTIVE EVALUATOR/MONITOR
U DATA PROCESSING
U DATA REDUCTION
U DATA TRANSMISSION

DATA ANALYSIS
U DATA PROCESSING
U DATA REDUCTION

DATA BASES
A comparison of flight and simulation data for
three automatic landing system control laws for
the Augmentor wing jet STOL research airplane
[NASA-CR-152365] p0018 N80-32338

DATA COMPACTION
U DATA COMPRESSION

DATA COMPRESSION
Conditional replenishment using motion prediction
p0065 A80-39715

DATA CONVERSION ROUTINES
NT SUBROUTINES

DATA CORRELATION
Analysis and correlation of test data from an
advanced technology rotor system --- helicopter
performance prediction
[NASA-CR-152366] p0019 N80-33351

DATA HANDLING SYSTEMS
U DATA SYSTEMS

DATA LINKS
Operational procedures for ground station
operation: ATS-3 Hawaii-Ames satellite link
experiment
[NASA-TM-81155] p0035 N80-13333

DATA MANAGEMENT
Aircraft simulation data management - A prototype
system p0029 A80-49832

DATA PROCESSING
NT DATA CORRELATION
NT DATA REDUCTION
NT DATA SMOOTHING
NT SIGNAL PROCESSING
The suitability of the ILLIAC IV architecture for
image processing p0098 A80-22382
Conference of Remote Sensing Educators (CORSE-78)
[NASA-CP-2102] p0034 N80-20003

DATA PROCESSING EQUIPMENT
NT AIRBORNE/SPACEBORNE COMPUTERS
NT COMPUTERS
NT ILLIAC 4 COMPUTER
NT INTEL 8080 MICROPROCESSOR

DATA READOUT SYSTEMS
U DATA SYSTEMS
U DISPLAY DEVICES

DATA REDUCTION
NT DATA SMOOTHING
Aircraft motion analysis using limited flight and
radar data p0025 A80-27241

SUBJECT INDEX

DIFFUSION

- Data reduction by computer processing p0058 N80-20016
- DATA SMOOTHING**
A variational technique for smoothing flight-test and accident data [AIAA 80-1601] p0028 A80-45894
- DATA SYSTEMS**
Computer/experiment integration for unsteady aerodynamic research p0025 A80-29501
Pioneer Venus Unified Abstract Data Library and Quick Look Data Delivery System p0050 A80-30832
- DATA TRANSMISSION**
Pioneer Venus Unified Abstract Data Library and Quick Look Data Delivery System p0050 A80-30832
Pioneer Venus multiprobe entry telemetry recovery p0058 N80-26347
- DAYTIME**
The location of the dayside ionopause of Venus - Pioneer Venus Orbiter magnetometer observations p0076 A80-48811
- DE LAVAL NOZZLES**
U CONVERGENT-DIVERGENT NOZZLES
- DECAY**
NT ACOUSTIC EMISSION
NT EXHAUST EMISSION
NT FLUORESCENCE
NT PHOTOELECTRIC EMISSION
NT PHOTOIONIZATION
NT RADIO EMISSION
NT THERMAL EMISSION
NT WEAK ENERGY INTERACTIONS
- DECISION MAKING**
Dynamic decisions and work load in multitask supervisory control p0095 A80-40898
Theory of the decision/problem state [NASA-TM-81192] p0103 N80-22984
Problem solving and decisionmaking: An integration [NASA-TM-81191] p0103 N80-22985
Clarification process: Resolution of decision-problem conditions [NASA-TM-81193] p0103 N80-23985
Decision-problem state analysis methodology [NASA-TM-81194] p0103 N80-25002
- DECOMPOSITION**
NT PHOTOLYSIS
- DECONDITIONING**
The development of an elastic reverse gradient garment to be used as a countermeasure for cardiovascular deconditioning [NASA-CR-152379] p0086 N80-33086
- DEEP SPACE NETWORK**
Pioneer Venus multiprobe entry telemetry recovery p0058 N80-26347
- DEFECTS**
NT INCLUSIONS
Influence of quality control variables on failure of graphite/epoxy under extreme moisture conditions [NASA-TM-81246] p0038 N80-33493
- DEFORMATION**
On the nonlinear deformation geometry of Euler-Bernoulli beams --- rotary wings [NASA-TP-1566] p0101 N80-20619
- DEGRADATION**
NT THERMAL DEGRADATION
Study of crosslinking and degradation mechanisms in sealant polymer candidates [NASA-CR-152346] p0039 N80-22484
- DELIVERY**
NT PAYLOAD DELIVERY (STS)
NT WEAPONS DELIVERY
- DELTA WINGS**
Types of leeside flow over delta wings p0052 A80-34652
A vortex-lattice method for the calculation of the nonsteady separated flow over delta wings [AIAA PAPER 80-1803] p0027 A80-43286
Leeward flow over delta wings at supersonic speeds [NASA-TM-81187] p0036 N80-23250
- DENDRITIC DRAINAGE**
U DRAINAGE PATTERNS
- DENSITY (RATE/AREA)**
U FLUX DENSITY
- DENSITY DISTRIBUTION**
A model of the neutral and ion nitrogen chemistry in the daytime thermosphere of Venus p0067 A80-10460
- DENSITY WAVE MODEL**
Gas dynamics in barred spirals - Gaseous density waves and galactic shocks p0041 A80-10685
- DEPENDENCE**
NT TEMPERATURE DEPENDENCE
NT TIME DEPENDENCE
- DEPERSONALIZATION**
Automation literature: A brief review and analysis [NASA-TM-81245] p0103 N80-34097
- DEPOSITION**
NT VAPOR DEPOSITION
Silt-clay aggregates on Mars p0041 A80-10366
- DEPTH PERCEPTION**
U SPACE PERCEPTION
- DESCENT TRAJECTORIES**
Analysis of fuel-conservative curved decelerating approach trajectories for powered-lift and CTOL jet aircraft [NASA-TP-1650] p0005 N80-19022
- DESIGN ANALYSIS**
Design alternatives for the Shuttle Infrared Telescope Facility p0060 A80-17435
Aircraft simulation data management - A prototype system p0029 A80-49832
- DESIGN OF EXPERIMENTS**
U EXPERIMENTAL DESIGN
- DESORPTION**
Isothermal-desorption-rate measurements in the vicinity of the Curie temperature for H₂ chemisorbed on nickel films p0042 A80-16167
Changes induced on the surfaces of small Pd clusters by the thermal desorption of CO p0053 A80-37179
- DESTRUCTIVE TESTS**
Release-rate calorimetry of multilayered materials for aircraft seats p0051 A80-34223
- DEUTERIUM COMPOUNDS**
Ground-state rotational constants of /C-13/H₃D p0054 A80-41175
- DEWAR SYSTEMS**
U CRYOGENIC EQUIPMENT
- DIAGRAMS**
NT S-N DIAGRAMS
- DIAMOND WINGS**
U SWEEP WINGS
- DIATOMIC GASES**
Solution of Boltzmann equation for highly nonequilibrium diatomic gases rotational translational energy relaxation p0064 A80-34904
- DIATOMIC MOLECULES**
Recommended conventions for defining transition moments and intensity factors in diatomic molecular spectra p0055 A80-41323
- DIELECTRIC CONSTANT**
U PERMITTIVITY
- DIELECTRIC PROPERTIES**
NT PERMITTIVITY
- DIENES**
NT HEXADIENE
- DIFFERENTIAL ALGEBRA**
U MATRICES (MATHEMATICS)
- DIFFERENTIAL EQUATIONS**
NT ELLIPTIC DIFFERENTIAL EQUATIONS
NT PARABOLIC DIFFERENTIAL EQUATIONS
NT PARTIAL DIFFERENTIAL EQUATIONS
NT POISSON EQUATION
Note on the eigensolution of a homogeneous equation with semi-infinite domain p0075 A80-40508
- DIFFERENTIAL GEOMETRY**
System theory as applied differential geometry --- linear system [NASA-CR-3209] p0013 N80-12776
- DIFFERENTIAL OPERATORS**
U DIFFERENTIAL EQUATIONS
- DIFRACTION TELESCOPES**
U SPECTROSCOPIC TELESCOPES
- DIFFUSION**
NT ATMOSPHERIC DIFFUSION

DIFFUSION COEFFICIENT

SUBJECT INDEX

NT SURFACE DIFFUSION
 NT TURBULENT DIFFUSION
DIFFUSION COEFFICIENT
 Eddy diffusion coefficients and the variance of the atmosphere 30-60 km p0076 A80-45996

DIFLUORO COMPOUNDS
 NT PERFLUOROALKANE

DIGITAL COMPUTERS
 NT ILLIAC 4 COMPUTER

DIGITAL NAVIGATION
 Navigation systems for approach and landing of VTOL aircraft [NASA-CR-152335] p0016 N80-19055

DIGITAL SIMULATION
 Numerical simulation of steady supersonic flow over an ogive-cylinder-boattail body [AIAA PAPER 80-0066] p0060 A80-19273
 Error detection and rectification in digital terrain models p0099 A80-27432
 On the numerical solution of time-dependent viscous incompressible fluid flows involving solid boundaries p0052 A80-34980
 Direct numerical simulations of the turbulent wake of an axisymmetric body p0080 A80-49235
 Vortex simulation of three-dimensional, spotlike disturbances in a laminar boundary layer p0067 A80-49296
 Math modeling and computer mechanization for real time simulation of rotary-wing aircraft [NASA-CR-162400] p0013 N80-10137
 The analysis of delays in simulator digital computing systems. Volume 1: Formulation of an analysis approach using a central example simulator model [NASA-CR-152340] p0015 N80-17722
 The analysis of delays in simulator digital computing systems. Volume 2: Formulation of discrete state transition matrices, an alternative procedure for multirate digital computations --- flight control [NASA-CR-152341] p0015 N80-18722

DIGITAL SYSTEMS
 NT DIGITAL NAVIGATION
 Total aircraft flight-control system - Balanced open- and closed-loop control with dynamic trim maps p0025 A80-32448
 V/STOLAND avionics system flight-test data on a UH-1H helicopter [NASA-TN-78591] p0008 N80-18047

DIGITAL TECHNIQUES
 Application of the concept of dynamic trim control to automatic landing of carrier aircraft --- utilizing digital feedforward control [NASA-TP-1512] p0005 N80-19126
 Data reduction by computer processing p0058 N80-20016

DIMENSIONAL ANALYSIS
 Multiple-time-scale concepts in turbulent transport modelling p0080 A80-49277

DIMENSIONLESS NUMBERS
 NT REYNOLDS NUMBER
 NT STROUHAL NUMBER

DIODES
 Long term tests of the HEPP liquid trap diode heat pipe prototype [NASA-CR-152358] p0039 N80-22635

DIOXIDES
 NT CARBON DIOXIDE
 NT SILICON DIOXIDE

DIPOLE MOMENTS
 SCF and CI calculations of the dipole moment function of ozone --- Self-Consistent Field and Configuration-Interaction p0043 A80-17111

DIRECTIONAL CONTROL
 NT THRUST VECTOR CONTROL

DIRIGIBLES
 U AIRSHIPS

DISPERSIONS
 NT AEROSOLS
 NT SMOKE

DISPLAY DEVICES
 NT HEAD-UP DISPLAYS

NT SPEED INDICATORS
 Optimal control model predictions of system performance and attention allocation and their experimental validation in a display design study p0095 A80-40899
 Computer-based manuals for procedural information p0096 A80-50427

Multi-modal information processing for visual workload relief [NASA-CR-162720] p0100 N80-16737
 The effect of viewing time, time to encounter, and practice on perception of aircraft separation on a cockpit display of traffic information [NASA-TN-81173] p0083 N80-18038
 System description and analysis. Part 1: Feasibility study for helicopter/VTOL wide-angle simulation image generation display system [NASA-CR-152376] p0101 N80-27397
 A mathematical representation of an advanced helicopter for piloted simulator investigations of control system and display variations [NASA-TN-81203] p0011 N80-28371
 A head-up display format for application to transport aircraft approach and landing [NASA-TN-81199] p0012 N80-29295
 A simulator study of control and display augmentations for helicopters [NASA-CR-163451] p0018 N80-31408

DISPLAY SYSTEMS
 U DISPLAY DEVICES

DISTANCE PERCEPTION
 U SPACE PERCEPTION

DISTILLATION
 Design, fabrication and testing of a dual catalyst ammonia removal system for a urine VCD unit [NASA-CR-152372] p0085 N80-29023

DISTORTION
 NT FLOW DISTORTION

DISTRIBUTION (PROPERTY)
 NT FLOW DISTRIBUTION
 NT FORCE DISTRIBUTION
 NT INTERFERENCE LIFT
 NT LOAD DISTRIBUTION (FORCES)
 NT PRESSURE DISTRIBUTION
 NT SPECTRAL ENERGY DISTRIBUTION
 NT TEMPERATURE DISTRIBUTION
 NT VELOCITY DISTRIBUTION

DISTURBANCE THEORY
 U PERTURBATION THEORY

DOCUMENTS
 NT ASTRONOMICAL CATALOGS
 NT BIBLIOGRAPHIES
 NT MANUALS
 NT USER MANUALS (COMPUTER PROGRAMS)

DOGS
 Extracellular hyperosmolality and body temperature during physical exercise in dogs p0092 A80-54076

DRAG
 NT AERODYNAMIC DRAG
 NT INTERFERENCE DRAG
 Phase 1 wind tunnel tests of the J-97 powered, external augmentor V/STOL model [NASA-CR-152255] p0017 N80-28303
 A comparison of flight and simulation data for three automatic landing system control laws for the Augmentor wing jet STOL research airplane [NASA-CR-152365] p0018 N80-32338

DRAG BALANCE
 U AERODYNAMIC BALANCE

DRAG COEFFICIENT
 U AERODYNAMIC COEFFICIENTS
 U AERODYNAMIC DRAG

DRAG DEVICES
 NT WING FLAPS

DRAG EFFECT
 U DRAG

DRAG REDUCTION
 Wing flapping with minimum energy --- minimize the drag for a bending moment at the wing root [NASA-TN-81174] p0001 N80-16035

DRAINAGE PATTERNS
 Irrigated lands assessment for water management Applications Pilot Test (APT) --- California [E80-10324] p0019 N80-32815

DRINKING
 Na+ and Ca2+ ingestion - Plasma volume-electrolyte distribution at rest and exercise p0091 A80-41661

SUBJECT INDEX

EDDY VISCOSITY

DRONE HELICOPTERS
U HELICOPTERS
DROSOPHILA
 Review of cell aging in Drosophila and mouse
 p0087 A80-17741

DRUGS
 NT INSULIN

DUCTED FLOW
 Examination of group-velocity criterion for
 breakdown of vortex flow in a divergent duct
 p0022 A80-38049

DUNES
 Mars - The north polar sand sea and related wind
 patterns
 p0047 A80-26370

DUST
 NT COSMIC DUST

DWARF STARS
 The evolution of rapid oscillations in an outburst
 of a dwarf nova
 p0075 A80-45227

DYE LASERS
 Computational study of alkali-metal-noble gas
 collisions in the presence of nonresonant lasers
 - Na + Xe + $h/2\pi\omega$ sub 1 + $h/2\pi\omega$
 sub 2 system
 p0056 A80-48762

Two-photon excitation of nitric oxide fluorescence
 as a temperature indicator in unsteady
 gas-dynamic processes
 [NASA-TN-81220]
 p0037 N80-32700

DYES
 NT METHYLENE BLUE

DYNAMIC CHARACTERISTICS
 NT AERODYNAMIC DRAG
 NT AERODYNAMIC STABILITY
 NT AIRCRAFT STABILITY
 NT ATTITUDE STABILITY
 NT BOUNDARY LAYER STABILITY
 NT CONTROL STABILITY
 NT DRAG
 NT DYNAMIC STABILITY
 NT FLOW CHARACTERISTICS
 NT FLOW DISTRIBUTION
 NT FLOW STABILITY
 NT FLOW VELOCITY
 NT HOVERING STABILITY
 NT INTERFERENCE DRAG
 NT INTERFERENCE LIFT
 NT LIFT
 NT ROTOR LIFT
 NT TRANSIENT RESPONSE
 Dynamic modal estimation using instrumental
 variables
 [NASA-CR-152396]
 p0019 N80-32777

DYNAMIC CONTROL
 Total aircraft flight-control system - Balanced
 open- and closed-loop control with dynamic trim
 maps
 p0025 A80-32448

The promise of multicyclic control --- for
 helicopter vibration reduction
 p0022 A80-33123

Application of the concept of dynamic trim control
 to automatic landing of carrier aircraft ---
 utilizing digital feedforward control
 [NASA-TP-1512]
 p0005 N80-19126

DYNAMIC LOADS
 NT AERODYNAMIC LOADS
 NT GUST LOADS
 NT VIBRATORY LOADS

DYNAMIC MODELS
 The dynamics and stability of radiatively driven
 gas clouds. I - Plane-parallel slabs
 p0042 A80-14058

DYNAMIC PROPERTIES
 U DYNAMIC CHARACTERISTICS

DYNAMIC RESPONSE
 NT TRANSIENT RESPONSE
 Dynamic stall on advanced airfoil sections
 [AD-A085809]
 p0101 N80-29252

DYNAMIC STABILITY
 NT AERODYNAMIC STABILITY
 NT AIRCRAFT STABILITY
 NT ATTITUDE STABILITY
 NT BOUNDARY LAYER STABILITY
 NT CONTROL STABILITY
 NT FLOW STABILITY
 NT HOVERING STABILITY

The dynamics and stability of radiatively driven
 gas clouds. I - Plane-parallel slabs
 p0042 A80-14058

DYNAMIC STRUCTURAL ANALYSIS
 A comprehensive analytical model of rotorcraft
 aerodynamics and dynamics. Part 1: Analysis
 development
 [NASA-TN-81182]
 p0010 N80-28296

E

EARLY STARS
 NT PROTOSTARS
 NT T TAURI STARS
 High-frequency continuum observations of young stars
 p0047 A80-25365

EARTH ATMOSPHERE
 NT IONOSPHERE
 NT MAGNETOSPHERE
 NT MESOSPHERE
 NT MIDDLE ATMOSPHERE
 NT MIDLATITUDE ATMOSPHERE
 NT OZONOSPHERE
 NT RADIATION BELTS
 NT STRATOSPHERE
 NT THERMOSPHERE
 NT TROPOSPHERE
 NT UPPER ATMOSPHERE
 Unified treatment of lifting atmospheric entry
 p0048 A80-28027

The propagation of Jovian electrons to earth
 p0074 A80-36356

EARTH CORE
 Core cooling by subsolidus mantle convection ---
 thermal evolution model of earth
 p0044 A80-19391

EARTH MANTLE
 Core cooling by subsolidus mantle convection ---
 thermal evolution model of earth
 p0044 A80-19391

Whole planet cooling and the radiogenic heat
 source contents of the earth and moon
 p0053 A80-36651

EARTH RESOURCES
 NT FORESTS

EARTH SATELLITES
 NT ATS 3
 NT COSMOS SATELLITES
 NT INFRARED ASTRONOMY SATELLITE
 NT NIMBUS 4 SATELLITE
 NT VENERA SATELLITES

EARTH SURFACE
 Eolian sedimentation on earth and Mars - Some
 comparisons
 p0068 A80-13969

EBERT SPECTROMETERS
 Design and operation of the Pioneer Venus Orbiter
 ultraviolet spectrometer
 p0073 A80-30841

ECLIPSES
 NT SOLAR ECLIPSES

ECOLOGICAL SYSTEMS
 U ECOLOGY

ECOLOGY
 Guiding the development of a controlled ecological
 life support system
 [NASA-CR-162452]
 p0085 N80-12735

The carbon isotope biogeochemistry of the
 individual hydrocarbons in bat guano and the
 ecology of insectivorous bats in the region of
 Carlsbad, New Mexico
 [NASA-TN-81164]
 p0083 N80-18680

ECONOMIC ANALYSIS
 Toward new small transports for commuter airlines
 p0021 A80-21224

Parametric study of modern airship productivity
 [NASA-TN-81151]
 p0011 N80-28340

ECONOMIC FACTORS
 Small Transport Aircraft Technology
 p0021 A80-21225

EDDIES
 U VORTICES

EDDY DIFFUSION
 U TURBULENT DIFFUSION

EDDY VISCOSITY
 Large eddy simulation of turbulent channel flow:
 ILLIAC 5 calculation
 p0059 N80-27661

EDGES

SUBJECT INDEX

EDGES
 NT TRAILING EDGES

EDUCATION
 NT FLIGHT TRAINING
 NT PILOT TRAINING
 Conference of Remote Sensing Educators (CORSE-78)
 [NASA-CP-2102] p0034 N80-20003
 NASA's western regional applications training
 activity p0058 N80-20010
 Data reduction by computer processing p0058 N80-20016

EFFECTIVENESS
 NT COST EFFECTIVENESS
 NT SYSTEM EFFECTIVENESS

EFFICIENCY
 NT ENERGY CONVERSION EFFICIENCY
 NT PROPULSIVE EFFICIENCY
 NT THERMODYNAMIC EFFICIENCY
 NT TRANSMISSION EFFICIENCY
 Parametric study of modern airship productivity
 [NASA-TN-81151] p0011 N80-28340

EFFUSIVES
 NT LAVA

EIGENVALUES
 Note on the eigensolution of a homogeneous
 equation with semi-infinite domain p0075 A80-40508

EJECTORS
 Workshop on Thrust Augmenting Ejectors
 [NASA-CP-2093] p0004 N80-10107
 NASA overview p0022 N80-10109

EKMAN LAYER
 U BOUNDARY LAYER TRANSITION

ELASTIC PROPERTIES
 NT AEROELASTICITY
 NT VISCOELASTICITY

ELASTIC WAVES
 NT AERODYNAMIC NOISE
 NT AIRCRAFT NOISE
 NT ENGINE NOISE
 NT JET AIRCRAFT NOISE
 NT PLASMA WAVES
 NT SHOCK WAVES
 NT SOUND WAVES

ELASTOMERS
 Synthesis of perfluoroalkylether oxadiazole
 elastomers p0045 A80-21992
 Synthesis of perfluoroalkylether triazine elastomers
 p0051 A80-32825
 Perfluoroether triazine elastomers
 [NASA-CR-162748] p0039 N80-16166

ELECTRIC ARCS
 Calorimeter probes for measuring high thermal flux
 --- in electric-arc jet facilities for planetary
 entry heating simulation p0099 A80-29480

ELECTRIC CURRENT
 NT ARC DISCHARGES
 NT ELECTRIC ARCS
 NT ELECTRIC DISCHARGES

ELECTRIC DISCHARGES
 NT ARC DISCHARGES
 NT ELECTRIC ARCS
 Transient solution for megajoule energy release in
 a lumped-parameter series RLC circuit p0051 A80-32826

ELECTRIC FILTERS
 NT MICROWAVE FILTERS

ELECTRIC ROCKET ENGINES
 NT ARC JET ENGINES

ELECTRICAL IMPEDANCE
 Microbial sulfate reduction measured by an
 automated electrical impedance technique p0087 A80-21982

ELECTRICAL PROPERTIES
 NT ELECTRICAL IMPEDANCE
 NT PERMITTIVITY
 NT SUPERCONDUCTIVITY

ELECTRICAL RESISTIVITY
 NT SUPERCONDUCTIVITY

ELECTROCHEMISTRY
 Development of the electrochemically regenerable
 carbon dioxide absorber for portable life
 support system application
 [ASME PAPER 79-ENAS-33] p0092 A80-15257

ELECTROCONDUCTIVITY
 Electrical conductivity anomalies associated with
 circular lunar maria p0061 A80-23691

ELECTROLYTE METABOLISM
 Na⁺ and Ca²⁺ ingestion - Plasma volume-electrolyte
 distribution at rest and exercise p0091 A80-41661

ELECTROMAGNETIC ABSORPTION
 NT INFRARED ABSORPTION
 NT MULTIPHOTON ABSORPTION
 NT PHOTOABSORPTION
 Part-body and multibody effects on absorption of
 radio-frequency electromagnetic energy by
 animals and by models of man p0071 A80-22987

ELECTROMAGNETIC FIELDS
 NT FAR FIELDS

ELECTROMAGNETIC INTERACTIONS
 Modified Iterative Extended Hueckel. 1: Theory
 [NASA-TN-81200] p0083 N80-25108

ELECTROMAGNETIC MEASUREMENT
 One millimeter continuum observations of
 extragalactic thermal sources
 [NASA-CR-163590] p0040 N80-33334

ELECTROMAGNETIC PROPAGATION
 U ELECTROMAGNETIC WAVE TRANSMISSION

ELECTROMAGNETIC PROPERTIES
 NT BRIGHTNESS
 NT ELECTROMAGNETIC ABSORPTION
 NT INFRARED ABSORPTION
 NT OPTICAL PROPERTIES
 NT PERMITTIVITY
 NT PHOTOELECTRIC EMISSION
 NT PHOTOIONIZATION
 NT STELLAR LUMINOSITY

ELECTROMAGNETIC RADIATION
 NT FAR INFRARED RADIATION
 NT GAMMA RAYS
 NT INFRARED RADIATION
 NT LYMAN ALPHA RADIATION
 NT NEAR INFRARED RADIATION
 NT PLANETARY RADIATION
 NT RADIO EMISSION
 NT SOLAR X-RAYS
 NT SUBMILLIMETER WAVES
 NT THERMAL RADIATION
 NT ULTRAVIOLET RADIATION
 Scattering by nonspherical particles of size
 comparable to wavelength - A new semi-empirical
 theory and its application to tropospheric
 aerosols p0052 A80-36040

ELECTROMAGNETIC SCATTERING
 NT LIGHT SCATTERING
 NT MIE SCATTERING

ELECTROMAGNETIC SPECTRA
 NT H LINES
 NT INFRARED SPECTRA
 NT LINE SPECTRA
 NT SOLAR SPECTRA
 NT STELLAR SPECTRA
 NT VIBRATIONAL SPECTRA

ELECTROMAGNETIC WAVE FILTERS
 NT INFRARED FILTERS
 NT MICROWAVE FILTERS

ELECTROMAGNETIC WAVE TRANSMISSION
 NT LIGHT SCATTERING
 NT LIGHT TRANSMISSION
 NT MICROWAVE ATTENUATION
 Proceedings of the Aero-Optics Symposium on
 Electromagnetic Wave Propagation from Aircraft
 [NASA-CP-2121] p0006 N80-25588

ELECTROMAGNETIC WAVES
 U ELECTROMAGNETIC RADIATION

ELECTRON EMISSION
 NT PHOTOELECTRIC EMISSION

ELECTRON ENERGY
 NT ELECTRON STATES

ELECTRON FLUX DENSITY
 The propagation of Jovian electrons to earth
 p0074 A80-36356

ELECTRON INTENSITY
 U ELECTRON FLUX DENSITY

ELECTRON RECOMBINATION
 NT RADIATIVE RECOMBINATION

ELECTRON SCATTERING
 NT CONFIGURATION INTERACTION

SUBJECT INDEX

ENVIRONMENT SIMULATION

ELECTRON STATES

F + H₂ collisions on two electronic potential energy surfaces - Quantum-mechanical study of the collinear reaction

p0068 A80-12012

ELECTRON TRANSITIONS

Photoexcitation and ionization in molecular oxygen - Theoretical studies of electronic transitions in the discrete and continuous spectral intervals

p0044 A80-20275

Recommended conventions for defining transition moments and intensity factors in diatomic molecular spectra

p0055 A80-41323

ELECTRON-ION RECOMBINATION

NT RADIATIVE RECOMBINATION

ELECTRONIC EQUIPMENT

NT CHARGE COUPLED DEVICES

NT DIODES

NT MIS (SEMICONDUCTORS)

NT PHOTOVOLTAIC CELLS

ELECTRONIC STRUCTURE

U ATOMIC STRUCTURE

ELECTROTHERMAL ENGINES

NT ARC JET ENGINES

ELEMENT ABUNDANCE

U ABUNDANCE

ELEMENTARY PARTICLES

NT PROTONS

ELLIPTIC DIFFERENTIAL EQUATIONS

Automatic mesh-point clustering near a boundary in grid generation with elliptic partial differential equations

p0044 A80-20593

ELLIPTICAL GALAXIES

On the three-dimensional shapes of elliptical galaxies

p0047 A80-26101

EMISSION

NT ACOUSTIC EMISSION

NT EXHAUST EMISSION

NT FLUORESCENCE

NT PHOTOELECTRIC EMISSION

NT PHOTOIONIZATION

NT RADIO EMISSION

NT THERMAL EMISSION

EMISSION SPECTRA

The 16- to 38-micron spectrum of Callisto

p0074 A80-35234

An optical emission-line phase of the extreme carbon star IRC +30219

p0056 A80-44993

A reanalysis of the observed interplanetary hydrogen I alpha emission profiles and the derived local interstellar gas temperature and velocity

p0076 A80-49362

ENCLOSURES

The development of a Space Shuttle Research Animal Holding Facility [ASME PAPER 80-ENAS-39]

p0096 A80-43213

ENDOCRINE GLANDS

NT PITUITARY GLAND

ENDOCRINE SECRETIONS

NT ESTROGENS

NT HORMONES

NT INSULIN

NT PITUITARY HORMONES

Exercise training-induced hypervolemia - Role of plasma albumin, renin, and vasopressin

p0089 A80-32749

ENDOCRINE SYSTEMS

Fluid shifts and endocrine responses during chair rest and water immersion in man

p0088 A80-25990

ENERGETIC PARTICLES

NT THERMAL PLASMAS

On the inference of properties of Saturn's Ring E from energetic charged particle observations

p0069 A80-15293

Acceleration of energetic protons by interplanetary shocks

p0071 A80-21183

The acceleration of energetic charged particles by interplanetary and supernova shock waves

p0080 A80-53209

ENERGY ABSORPTION

NT ELECTROMAGNETIC ABSORPTION

NT INFRARED ABSORPTION

NT MULTIPHOTON ABSORPTION

NT PHOTOABSORPTION

ENERGY CONSERVATION

Effectiveness of advanced fuel-conservative procedures in the transitional ATC environment

p0023 N80-27347

ENERGY CONVERSION

NT PHOTOTHERMAL CONVERSION

NT SOLAR ENERGY CONVERSION

Measurements of wind vectors, eddy momentum transports, and energy conversions in Jupiter's atmosphere from Voyager 1 images

A80-24159

ENERGY CONVERSION EFFICIENCY

Photocell heat engine solar power systems

p0079 A80-48179

ENERGY DENSITY

U FLUX DENSITY

ENERGY DISTRIBUTION

NT SPECTRAL ENERGY DISTRIBUTION

ENERGY EXCHANGE

U ENERGY TRANSFER

ENERGY LEVELS

NT ELECTRON STATES

NT GROUND STATE

NT MOLECULAR ENERGY LEVELS

ENERGY SPECTRA

On the inference of properties of Saturn's Ring E from energetic charged particle observations

p0069 A80-15293

ENERGY TECHNOLOGY

Potential benefits for propfan technology on derivatives of future short- to medium-range transport aircraft

p0026 A80-38905

[AIAA PAPER 80-1090]

ENERGY TRANSFER

Multiple-time-scale concepts in turbulent transport modelling

p0080 A80-49277

ENGINE DESIGN

Photocell heat engine solar power systems

p0079 A80-48179

ENGINE INLETS

Acoustic characteristics of two hybrid inlets at forward speed

p0021 A80-20828

Study of cooling air inlet and exit geometries for horizontally opposed piston aircraft engines

p0027 A80-38984

Top inlet system feasibility for transonic-supersonic fighter aircraft applications

p0033 A80-45735

Effects of free-stream turbulence on diffuser performance

p0017 N80-24264

[NASA-CR-163194]

ENGINE NOISE

Distortion-rotor interaction noise produced by a drooped inlet

p0033 A80-35994

A measurement of forward-flight effects on the noise from a JT15D-1 turbofan engine in the NASA-Ames 40- by 80-Foot Wind Tunnel

p0026 A80-38641

[AIAA PAPER 80-1026]

ENGINE TESTS

Acoustic characteristics of two hybrid inlets at forward speed

p0021 A80-20828

A measurement of forward-flight effects on the noise from a JT15D-1 turbofan engine in the NASA-Ames 40- by 80-Foot Wind Tunnel

p0026 A80-38641

Study of cooling air inlet and exit geometries for horizontally opposed piston aircraft engines

p0027 A80-38984

[AIAA PAPER 80-1242]

ENGINES

NT ARC JET ENGINES

NT BRISTOL-SIDDELEY BS 53 ENGINE

NT PISTON ENGINES

NT TURBOFAN ENGINES

NT TURBOJET ENGINES

NT TURBOPROP ENGINES

ENVIRONMENT EFFECTS

Equivalent-cone calculation of nitric oxide production rate during Space Shuttle re-entry

p0056 A80-45359

ENVIRONMENT POLLUTION

NT AIR POLLUTION

ENVIRONMENT SIMULATION

NT WEIGHTLESSNESS SIMULATION

ENVIRONMENTAL CHEMISTRY

SUBJECT INDEX

Threshold windspeeds for sand on Mars - Wind
tunnel simulations p0048 A80-27391

Mars ultraviolet simulation facility p0089 A80-36061

ENVIRONMENTAL CHEMISTRY
 NT ATMOSPHERIC CHEMISTRY
 NT BIOCHEMISTRY
 NT BIOGEOCHEMISTRY
 NT GEOCHEMISTRY

ENVIRONMENTAL TESTS
 NT HIGH TEMPERATURE TESTS

ENVIRONMENTS
 NT AEROSPACE ENVIRONMENTS
 NT HIGH GRAVITY ENVIRONMENTS
 NT IONOSPHERE
 NT JUPITER ATMOSPHERE
 NT MAGNETOSPHERE
 NT MARS ATMOSPHERE
 NT MARS ENVIRONMENT
 NT MESOSPHERE
 NT MIDLATITUDE ATMOSPHERE
 NT PLANETARY ATMOSPHERES
 NT ROTATING ENVIRONMENTS
 NT SATELLITE ATMOSPHERES
 NT SATURN ATMOSPHERE
 NT STELLAR ATMOSPHERES
 NT THERMAL ENVIRONMENTS
 NT URANUS ATMOSPHERE
 NT VENUS ATMOSPHERE

EPOXY MATRIX COMPOSITE MATERIALS
 Radiant panel tests on an epoxy/carbon fiber
 composite
 [NASA-TM-81185] p0037 N80-32435

EPOXY RESINS
 Thermal expansion and swelling of cured epoxy
 resin used in graphite/epoxy composite materials
 p0054 A80-40926

Thermophysical and flammability characterization
 of phosphorylated epoxy adhesives p0066 A80-48079

Influence of quality control variables on failure
 of graphite/epoxy under extreme moisture
 conditions
 [NASA-TM-81246] p0038 N80-33493

EQUATIONS OF MOTION
 NT NAVIER-STOKES EQUATION
 Formulation of coupled rotor/fuselage equations of
 motion p0021 A80-17717

Coupled rotor and fuselage equations of motion
 [NASA-TM-81153] p0006 N80-10516

Equations for determining aircraft motions for
 accident data
 [NASA-TM-78609] p0010 N80-25306

ERGONOMICS
 U HUMAN FACTORS ENGINEERING

ERROR ANALYSIS
 On the Routh approximation technique and least
 squares errors p0032 A80-20873

Separated skin-friction measurements - Source of
 error: An assessment and elimination
 [AIAA PAPER 80-1409] p0027 A80-44155

ERROR CORRECTING CODES
 Error detection and rectification in digital
 terrain models p0099 A80-27432

ERROR DETECTION CODES
 Error detection and rectification in digital
 terrain models p0099 A80-27432

ERRORS
 NT INSTRUMENT ERRORS
 NT PILOT ERROR
 NT TRUNCATION ERRORS

ERYTHROCYTES
 Plasma volume during stress in man - Osmolality
 and red cell volume p0087 A80-13506

Extremes of urine osmolality - Lack of effect on
 red blood cell survival p0091 A80-46196

ESTERS
 NT CARBOXYLATES
 Perfluoroether triazine elastomers
 [NASA-CR-162748] p0039 N80-16166

ESTIMATES
 NT COST ESTIMATES

ESTIMATING
 NT SYSTEM IDENTIFICATION

ESTROGENS
 Hypergravity and estrogen effects on avian
 anterior pituitary growth hormone and prolactin
 levels p0094 A80-20447

ETCHING
 Plasma etching of poly/N,N'-/p,p'-
 oxydiphenylene/pyromellitimide/ film and
 photo/thermal degradation of etched and unetched
 film p0093 A80-24158

EUCLIDEAN GEOMETRY
 NT ANGLE OF ATTACK
 NT ANGLES (GEOMETRY)

EULER-LAGRANGE EQUATION
 A Lagrangian mean theory of wave, mean-flow
 interaction with applications to nonacceleration
 and its breakdown --- large-scale atmospheric
 dynamics p0075 A80-36473

EVECTION
 U ORBIT PERTURBATION
 U SOLAR GRAVITATION

EVOLUTION (DEVELOPMENT)
 NT ABIOTIC GENESIS
 NT BIOLOGICAL EVOLUTION
 NT CHEMICAL EVOLUTION
 NT GALACTIC EVOLUTION
 NT LUNAR EVOLUTION
 NT PLANETARY EVOLUTION
 NT STELLAR EVOLUTION
 Comets: Cosmic connections with carbonaceous
 meteorites, interstellar molecules and the
 origin of life p0092 N80-11975

EXCITATION
 NT ACOUSTIC EXCITATION
 NT MOLECULAR EXCITATION

EXECUTIVE AIRCRAFT
 U GENERAL AVIATION AIRCRAFT
 U PASSENGER AIRCRAFT

EXERCISE (PHYSIOLOGY)
 U PHYSICAL EXERCISE

EXERCISE PHYSIOLOGY
 Human acclimation and acclimatization to heat: A
 compendium of research, 1968-1978 --- Bibliography
 [NASA-TM-81181] p0085 N80-34056

EXHAUST DIFFUSERS
 An experimental investigation of two large annular
 diffusers with swirling and distorted inflow
 [NASA-TP-1628] p0005 N80-17984

EXHAUST EMISSION
 Stratospheric aerosol modification by supersonic
 transport and space shuttle operations - Climate
 implications p0047 A80-26088

EXHAUST FLOW SIMULATION
 NT ATMOSPHERIC ENTRY SIMULATION
 NT FLIGHT SIMULATION

EXHAUST GASES
 Toxicity of pyrolysis gases from foam plastics
 p0071 A80-24625

Introductory study of the chemical behavior of jet
 emissions in photochemical smog --- computerized
 simulation
 [NASA-CR-152345] p0016 N80-21891

EXHAUST JETS
 U EXHAUST GASES

EXHAUST NOZZLES
 NT CONVERGENT-DIVERGENT NOZZLES

EXOBIOLOGY
 The Viking mission and the search for life on Mars
 p0086 A80-10738

Simulation of the Viking biology experiments - An
 overview p0090 A80-36066

EXPANSION
 NT THERMAL EXPANSION

EXPERIMENTAL DESIGN
 Galileo probe thermal protection: Entry heating
 environments and spallation experiments design
 [NASA-CR-152334] p0038 N80-14184

Feasibility studies for light scattering
 experiments to determine the velocity relaxation
 of small particles in a fluid
 [NASA-CR-163214] p0040 N80-25586

SUBJECT INDEX

FEEDFORWARD CONTROL

EXPERIMENTAL STOL TRANSPORT RSCH AIRPLANE

U QUESTOL

EXPLORATION

NT SPACE EXPLORATION

EXTERNALLY BLOWN FLAPS

NT UPPER SURFACE BLOWN FLAPS

EXTRAGALACTIC RADIO SOURCES

One millimeter continuum observations of

extragalactic thermal sources

[NASA-CR-163590]

p0040 N80-33334

EXTRASOLAR PLANETS

An Assessment of Ground-Based Techniques for
Detecting Other Planetary Systems. Volume 2:

Position papers

[NASA-CP-2124-VOL-2]

p0034 N80-25224

Project Orion: A design study of a system for
detecting extrasolar planets

[NASA-SP-436]

p0035 N80-27260

EXTRATERRESTRIAL COMMUNICATION

On the significance of the apparent absence of
extraterrestrials on earth

p0087 A80-21780

EXTRATERRESTRIAL ENVIRONMENTS

NT JUPITER ATMOSPHERE

NT MARS ATMOSPHERE

NT MARS ENVIRONMENT

NT PLANETARY ATMOSPHERES

NT SATELLITE ATMOSPHERES

NT SATURN ATMOSPHERE

NT STELLAR ATMOSPHERES

NT URANUS ATMOSPHERE

NT VENUS ATMOSPHERE

EXTRATERRESTRIAL INTELLIGENCE

On the design of a postprocessor for a search for
extraterrestrial intelligence /SETI/ system

[IAF PAPER 79-A-39]

p0093 A80-19895

A high-sensitivity search for extraterrestrial
intelligence at lambda 18 cm

p0090 A80-37933

EXTRATERRESTRIAL LIFE

The Viking mission and the search for life on Mars

p0086 A80-10738

On the significance of the apparent absence of
extraterrestrials on earth

p0087 A80-21780

Simulation of the Viking biology experiments - An
overview

p0090 A80-36066

EXTRATERRESTRIAL MATTER

NT COSMIC PLASMA

NT INTERPLANETARY GAS

NT INTERSTELLAR GAS

NT NEUTRAL GASES

EXTRATERRESTRIAL RADIATION

NT PLANETARY RADIATION

NT SOLAR WIND

NT SOLAR X-RAYS

NT STELLAR RADIATION

NT STELLAR WINDS

EXTRAVEHICULAR ACTIVITY

High-pressure protective systems technology

[ASME PAPER 79-ENAS-15]

p0092 A80-15240

Development of the electrochemically regenerable
carbon dioxide absorber for portable life

support system application

[ASME PAPER 79-ENAS-33]

p0092 A80-15257

EYE (ANATOMY)

NT RETINA

F

FABRY-PEROT LASERS

U LASERS

FACE CENTERED CUBIC LATTICES

A calculation of the diffusion energies for
adatoms on surfaces of F.C.C. metals

p0068 A80-13534

FAIL-SAFE SYSTEMS

A comparison of computer architectures for the
NASA demonstration advanced avionics system

p0032 A80-32427

FAILURE ANALYSIS

Influence of quality control variables on failure
of graphite/epoxy under extreme moisture

conditions

[NASA-TM-81246]

p0038 N80-33493

FAILURE MODES

A temperature dependent fatigue failure criterion
for graphite/epoxy laminatesReynolds stress closures: Status and prospects
p0060 A80-15518
p0077 N80-27660

FANLIFT DEVICES

U LIFT FANS

FAR FIELDS

Lifting three-dimensional wings in transonic flow

p0071 A80-20331

Nonreflecting far-field boundary conditions for
unsteady transonic flow computation

[AIAA PAPER 80-1393]

p0065 A80-41597

FAR INFRARED RADIATION

Far infrared, near infrared, and radio molecular
line studies of HFE 2, HFE 3, and FJM 6

p0068 A80-11489

A far-infrared study of the reflection nebula NGC
2023

p0072 A80-26111

Monoceros R2 - Far-infrared observations of a very
young cluster

p0052 A80-35115

Far-infrared spectra of W51-IRS 2 and W49 NW

p0056 A80-44967

FAR ULTRAVIOLET RADIATION

NT LYMAN ALPHA RADIATION

FARM CROPS

NT BARLEY

NT COTTON

NT GRAINS (FOOD)

FARMLANDS

Irrigated lands assessment for water management

Applications Pilot Test (APT) --- California

[E80-10324]

p0019 N80-32815

Infrared-temperature variability in a large
agricultural field --- Dunnigan, California

[E80-10331]

p0038 N80-32822

FATIGUE (BIOLOGY)

Human acclimation and acclimatization to heat: A
compendium of research, 1968-1978 --- Bibliography

[NASA-TM-81181]

p0085 N80-34056

FATIGUE DIAGRAMS

U S-N DIAGRAMS

FATIGUE TESTS

A temperature dependent fatigue failure criterion
for graphite/epoxy laminates

p0060 A80-15518

Effects of moisture on apparent flexure strength
and on torsion and flexure fatigue properties of
graphite-epoxy composites

p0063 A80-27965

FATTY ACIDS

NT CARBOXYLIC ACIDS

FAULT MECHANICS

U FRACTURE MECHANICS

FCC LATTICES

U FACE CENTERED CUBIC LATTICES

FEASIBILITY ANALYSIS

Comet nucleus impact probe feasibility study

[NASA-CR-152375]

p0040 N80-26364

System description and analysis. Part 1:

Feasibility study for helicopter/VTOL wide-angle

simulation image generation display system

[NASA-CR-152376]

p0101 N80-27397

FEEDBACK CONTROL

Feedback invariants for nonlinear systems

p0031 A80-14810

Measurements of control stability characteristics
of a wind-tunnel model using a transfer function
method

[AIAA 80-0457]

p0024 A80-26957

Total aircraft flight-control system - Balanced
open- and closed-loop control with dynamic trim
maps

p0025 A80-32448

A scaling theory for linear systems

p0030 A80-32676

A new approach to active control of rotorcraft

vibration

[AIAA 80-1778]

p0027 A80-45556

A pilot modeling technique for handling-qualities

research

[AIAA 80-1624]

p0028 A80-45912

Modular theory of inverse systems

[NASA-CR-162491]

p0013 N80-12782

FEEDFORWARD CONTROL

Application of the concept of dynamic trim control
to automatic landing of carrier aircraft ---

utilizing digital feedforward control

[NASA-TP-1512]

p0005 N80-19126

PERMIONS

PERMIONS

NT PROTONS

FERTILIZERS

Nitrogen fertiliser and stratospheric ozone -
Latitudinal effects

p0043 A80-18948

FIBER COMPOSITES

NT GLASS FIBER REINFORCED PLASTICS

Degradation of tensile and shear properties of
composites exposed to fire or high temperature

p0072 A80-29697

Graphite composites with advanced resin matrices

[AIAA 80-0758]

p0064 A80-35051

Radiant panel tests on an epoxy/carbon fiber

composite

[NASA-TM-81185]

p0037 N80-32435

FIBERS

NT CARBON FIBERS

NT SYNTHETIC FIBERS

FIELD STRENGTH

NT MAGNETIC FLUX

FIGHTER AIRCRAFT

Top inlet system feasibility for

transonic-supersonic fighter aircraft applications

[AIAA PAPER 80-1809]

p0033 A80-45735

Mathematical modeling of the aerodynamics of

high-angle-of-attack maneuvers

[AIAA 80-1583]

p0028 A80-45879

FILAMENTS (SOLAR PHYSICS)

U SOLAR PROMINENCES

FINITE DIFFERENCE THEORY

Supersonic flow over three-dimensional ablated
nosetips using an unsteady implicit numerical

procedure

[AIAA PAPER 80-0063]

p0060 A80-19271

A diagonal form of an implicit
approximate-factorization algorithm with

application to a two dimensional inlet

[AIAA PAPER 80-0067]

p0061 A80-19274

Automatic mesh-point clustering near a boundary in
grid generation with elliptic partial

differential equations

p0044 A80-20593

Application of the method of integral relations to
unsteady fluid flow problems with shocks

p0078 A80-26594

On the construction and application of implicit
factored schemes for conservation laws --- in

computational fluid dynamics

p0062 A80-27407

An implicit finite-difference code for inviscid

and viscous cascade flow

[AIAA PAPER 80-1427]

p0066 A80-44128

A computer program to generate two-dimensional
grids about airfoils and other shapes by the use

of Poisson's equation

[NASA-TM-81198]

p0036 N80-26266

Calculation of three-dimensional unsteady
transonic flows past helicopter blades

[NASA-TP-1721]

p0100 N80-33356

FIRE CONTROL

Results of a simulator investigation of control
system and display variations for an attack

helicopter mission

[AD-A085812]

p0101 N80-29370

FIRE DAMAGE

Degradation of tensile and shear properties of
composites exposed to fire or high temperature

p0072 A80-29697

FIRE PREVENTION

Advanced thermoset resins for fire-resistant
composites

p0063 A80-34788

Release-rate calorimetry of multilayered materials
for aircraft seats

[AIAA 80-0759]

p0064 A80-35052

Chemical research projects office: An overview
and bibliography, 1975-1980

[NASA-TM-81227]

p0037 N80-31473

FIREPROOFING

Ambient curing fire resistant foams

p0063 A80-34790

FIXED-WING AIRCRAFT

U AIRCRAFT CONFIGURATIONS

FLAME FRONTS

U FLAME PROPAGATION

FLAME INTERACTION

U CHEMICAL REACTIONS

U FLAME PROPAGATION

SUBJECT INDEX

FLAME PROPAGATION

Ambient curing fire resistant foams

p0063 A80-34790

FLAME RETARDANTS

Flash-fire propensity and heat-release rate
studies of improved fire resistant materials

p0042 A80-15201

Materials for fire resistant passenger seats in
aircraft

p0080 A80-48757

Catalysts for polyimide foams from aromatic
isocyanates and aromatic dianhydrides --- flame

retardant foams

[NASA-CASE-ARC-11107-1]

p0080 N80-16116

FLAMMABILITY

Flash-fire propensity and heat-release rate
studies of improved fire resistant materials

p0042 A80-15201

Oxygen index tests of thermosetting resins

p0044 A80-21448

Thermophysical and flammability characterization
of phosphorylated epoxy adhesives

p0066 A80-48079

FLAP CONTROL

U AIRCRAFT CONTROL

U FLAPS (CONTROL SURFACES)

FLAPPING

Comparison of calculated and measured helicopter
rotor lateral flapping angles

[NASA-TM-81213]

p0012 N80-33349

FLAPPING HINGES

Effects of primary rotor parameters on flapping
dynamics

[NASA-TP-1431]

p0005 N80-15138

FLAPS (CONTROL SURFACES)

NT UPPER SURFACE BLOWN FLAPS

NT WING FLAPS

Large-scale wind-tunnel tests of inverting flaps
on a STOL utility aircraft model

[NASA-TP-1696]

p0005 N80-25318

A summary of joint US-Canadian augmentor wing
powered-lift STOL research programs at the Ames

Research Center, NASA, 1975-1980

[NASA-TM-81215]

p0011 N80-28373

FLARED BODIES

Computation of supersonic turbulent flows over an
inclined ogive-cylinder-flare

[AIAA PAPER 80-1410]

p0066 A80-41608

FLAWS

U DEFECTS

FLEXING

Effects of moisture on apparent flexure strength
and on torsion and flexure fatigue properties of

graphite-epoxy composites

p0063 A80-27965

FLEXURE

U FLEXING

FLIGHT CHARACTERISTICS

Measurements of control stability characteristics
of a wind-tunnel model using a transfer function

method

[AIAA 80-0457]

p0024 A80-26957

Implicit model following and parameter
identification of unstable aircraft

p0022 A80-28019

A compilation and analysis of helicopter handling
qualities data. Volume 1: Data compilation

[NASA-CR-3144]

p0013 N80-11097

Flight tests of the total automatic flight control
system (Tafcos) concept on a DHC-6 Twin Otter

aircraft

[NASA-TP-1513]

p0005 N80-17081

A comprehensive analytical model of rotorcraft
aerodynamics and dynamics. Part 2: User's manual

[NASA-TM-81183]

p0010 N80-28297

FLIGHT COMPUTERS

U AIRBORNE/SPACEBORNE COMPUTERS

FLIGHT CONDITIONS

Strouhal number influence on flight effects on jet
noise radiated from convecting quadrupoles

p0022 A80-28418

A measurement of forward-flight effects on the
noise from a JT15D-1 turbofan engine in the

NASA-Ames 40- by 80-Foot Wind Tunnel

[AIAA PAPER 80-1026]

p0026 A80-38641

FLIGHT CONTROL

NT AUTOMATIC FLIGHT CONTROL

NT AUTOMATIC LANDING CONTROL

NT POINTING CONTROL SYSTEMS

SUBJECT INDEX

FLOW DISTRIBUTION

- NT THRUST VECTOR CONTROL
 - V/STOLAND avionics system flight-test data on a UH-1H helicopter [NASA-TM-78591] p0008 N80-18047
 - The analysis of delays in simulator digital computing systems. Volume 2: Formulation of discrete state transition matrices, an alternative procedure for multirate digital computations --- flight control [NASA-CR-152341] p0015 N80-18722
 - Practical optimal flight control system design for helicopter aircraft. Volume 1: Technical Report [NASA-CR-3275] p0017 N80-23328
 - Results of a simulator investigation of control system and display variations for an attack helicopter mission [AD-A085812] p0101 N80-29370
- FLIGHT CREWS
 - Analysis of eighty-four commercial aviation incidents - Implications for a resource management approach to crew training p0093 A80-40340
 - Resource management on the flight deck --- conferences [NASA-CP-2120] p0082 N80-22283
- FLIGHT INSTRUMENTS
 - NT ATTITUDE INDICATORS
 - NT AUTOMATIC PILOTS
 - Perception of aircraft separation with pilot-preferred symbology on a cockpit display of traffic information [NASA-TM-81172] p0084 N80-31397
- FLIGHT OPERATIONS
 - Computer-based manuals for procedural information p0096 A80-50427
- FLIGHT PATHS
 - NT GLIDE PATHS
 - Constrained optimum trajectories with specified range p0021 A80-18538
- FLIGHT PERFORMANCE
 - U FLIGHT CHARACTERISTICS
- FLIGHT RECORDERS
 - Aircraft motion analysis using limited flight and radar data p0025 A80-27241
- FLIGHT RULES
 - NT INSTRUMENT FLIGHT RULES
- FLIGHT SAFETY
 - Analysis of eighty-four commercial aviation incidents - Implications for a resource management approach to crew training p0093 A80-40340
 - NASA aviation safety reporting system [NASA-TM-81197] p0085 N80-32352
- FLIGHT SIMULATION
 - Optimal washout for control of a moving base simulator --- vertical motion flight simulation using linear filter p0031 A80-14833
 - Aircraft simulation data management - A prototype system p0029 A80-49832
 - V/STOL flight simulation [NASA-TM-81156] p0006 N80-12100
 - The effects of motion and g-seat cues on pilot simulator performance of three piloting tasks [NASA-TP-1601] p0004 N80-15069
 - Head-up display in the non-precision approach [NASA-TM-81167] p0084 N80-26296
 - A pilot's assessment of helicopter handling-quality factors common to both agility and instrument flying tasks [NASA-TM-81217] p0011 N80-28341
 - An experimental evaluation of head-up display formats [NASA-TP-1550] p0082 N80-28349
 - A head-up display format for application to transport aircraft approach and landing [NASA-TM-81199] p0012 N80-29295
 - Effects of rotor parameter variations on handling qualities of unaugmented helicopters in simulated terrain flight [NASA-TM-81190] p0012 N80-31407
- FLIGHT SIMULATORS
 - NT COCKPIT SIMULATORS
 - Thresholds for detection of constant rotary acceleration during vibratory rotary acceleration p0091 A80-42003
- Perception and performance in flight simulators: The contribution of vestibular, visual, and auditory information [NASA-CR-162129] p0085 N80-11103
- Feasibility and concept study to convert the NASA/ANES vertical motion simulator to a helicopter simulator [NASA-CR-152193] p0098 N80-16070
- Operations manual: Vertical Motion Simulator (VMS) S.08 [NASA-TM-81180] p0009 N80-23295
- FLIGHT STRESS (BIOLOGY)
 - NT SPACE FLIGHT STRESS
 - Physiological response to hyper- and hypogravity during rollercoaster flight p0095 A80-21547
- FLIGHT TECHNICAL ERROR
 - U PILOT ERROR
- FLIGHT TESTS
 - Aircraft motion analysis using limited flight and radar data p0025 A80-27241
 - Mathematical modeling of the aerodynamics of high-angle-of-attack maneuvers [AIAA 80-1583] p0028 A80-45879
 - A variational technique for smoothing flight-test and accident data [AIAA 80-1601] p0028 A80-45894
 - Flight test of navigation and guidance sensor errors measured on STOL approaches [NASA-TM-81154] p0007 N80-13041
 - NASA quiet short-haul research aircraft experimenters' handbook [NASA-TM-81162] p0007 N80-16024
 - Synthesis of rotor test data for real-time simulation [NASA-CR-152311] p0015 N80-18029
- FLIGHT TRAINING
 - Resource management on the flight deck --- conferences [NASA-CP-2120] p0082 N80-22283
- FLORA
 - U PLANTS (BOTANY)
- FLOW CHARACTERISTICS
 - NT BOUNDARY LAYER STABILITY
 - NT FLOW DISTRIBUTION
 - NT FLOW STABILITY
 - NT FLOW VELOCITY
 - Numerical experiments in boundary-layer stability [AIAA PAPER 80-0275] p0062 A80-23957
 - Developments in the computation of turbulent boundary layers p0059 N80-27658
 - A Navier-Stokes fast solver for turbulence modeling applications p0059 N80-27659
 - Large eddy simulation of turbulent channel flow: ILLIAC 5 calculation p0059 N80-27661
- FLOW DISTORTION
 - Types of leeside flow over delta wings p0052 A80-34652
 - An experimental investigation of two large annular diffusers with swirling and distorted inflow [NASA-TP-1628] p0005 N80-17984
- FLOW DISTRIBUTION
 - Numerical simulation of steady supersonic flow over an ogive-cylinder-boattail body [AIAA PAPER 80-0066] p0060 A80-19273
 - A diagonal form of an implicit approximate-factorization algorithm with application to a two dimensional inlet [AIAA PAPER 80-0067] p0061 A80-19274
 - Lifting three-dimensional wings in transonic flow p0071 A80-20331
 - Transonic swept-wing analysis using asymptotic and other numerical methods [AIAA PAPER 80-0342] p0024 A80-22751
 - On the combination of kinematics with flow visualization to compute total circulation - Application to vortex rings in a tube [AIAA PAPER 80-1330] p0065 A80-41563
 - Numerical simulation of three-dimensional boattail afterbody flow fields [AIAA PAPER 80-1347] p0066 A80-44132
 - Progress in turbulence modeling for complex flow fields including effects of compressibility [NASA-TP-1517] p0034 A80-20527

FLOW EQUATIONS

SUBJECT INDEX

Leeward flow over delta wings at supersonic speeds
[NASA-TM-81187] p0036 N80-23250
Overview of 6- X 6-foot wind tunnel aero-optics
tests --- transonic wind tunnel tests p0023 N80-25590
Developments in the computation of turbulent
boundary layers p0059 N80-27658
An experimental study of multiple jet mixing
[NASA-CR-166184] p0018 N80-31760
FLOW EQUATIONS
Integral equations for flows in wind tunnels p0029 A80-21906
Implicit computations of unsteady transonic flow
governed by the full-potential equation in
conservation form p0062 A80-23935
[AIAA PAPER 80-0150]
Application of the method of integral relations to
unsteady fluid flow problems with shocks p0078 A80-26694
Numerical solution techniques for unsteady
transonic aerodynamics problems p0059 N80-33379
FLOW FIELDS
U FLOW DISTRIBUTION
FLOW GEOMETRY
Analysis of two-dimensional incompressible flows
by a subsurface panel method p0029 A80-30566
Study of cooling air inlet and exit geometries for
horizontally opposed piston aircraft engines
[AIAA PAPER 80-1242] p0027 A80-38984
FLOW MEASUREMENT
Experimental investigation of a three dimensional
turbulent boundary layer with a non disappearing
pressure gradient p0054 A80-40907
Separated skin-friction measurements - Source of
error: An assessment and elimination
[AIAA PAPER 80-1409] p0027 A80-44155
Effect of tip planform on blade loading
characteristics for a two-bladed rotor in hover
[NASA-TM-78615] p0007 N80-14049
FLOW PATTERNS
U FLOW DISTRIBUTION
FLOW RATE
U FLOW VELOCITY
FLOW RESISTANCE
NT AERODYNAMIC DRAG
Investigation of a reattaching turbulent shear
layer Flow over a backward-facing step p0062 A80-27736
FLOW SEPARATION
U BOUNDARY LAYER SEPARATION
U SEPARATED FLOW
FLOW STABILITY
NT BOUNDARY LAYER STABILITY
Control of forebody vortex orientation to
alleviate side forces p0024 A80-23955
[AIAA PAPER 80-0183]
Examination of group-velocity criterion for
breakdown of vortex flow in a divergent duct p0022 A80-38049
Note on the eigensolution of a homogeneous
equation with semi-infinite domain p0075 A80-40508
FLOW VELOCITY
Application of laser velocimetry to an unsteady
transonic flow p0063 A80-29506
Unsteady density and velocity measurements in the
6 foot x 6 foot wind tunnel p0023 N80-25594
FLOW VISUALIZATION
NT NUMERICAL FLOW VISUALIZATION
Automatic mesh-point clustering near a boundary in
grid generation with elliptic partial
differential equations p0044 A80-20593
Diagnosis of separated flow regions on wind-tunnel
models using an infrared camera p0025 A80-29494
On the combination of kinematics with flow
visualization to compute total circulation -
Application to vortex rings in a tube
[AIAA PAPER 80-1330] p0065 A80-41563
Simple turbulence models and their application to
boundary layer separation
[NASA-CR-3283] p0017 N80-24269

FLUID DYNAMICS
NT AERODYNAMICS
NT COMPUTATIONAL FLUID DYNAMICS
NT GAS DYNAMICS
NT HYDRODYNAMICS
NT MAGNETOHYDRODYNAMICS
NT ROTOR AERODYNAMICS
A Lagrangian mean theory of wave, mean-flow
interaction with applications to nonacceleration
and its breakdown --- large-scale atmospheric
dynamics p0075 A80-36473
Relaminarization of fluid flows p0075 A80-40843
FLUID FILMS
Skin friction measurements by a new nonintrusive
double-laser-beam oil viscosity balance technique
[AIAA PAPER 80-1373] p0065 A80-41587
FLUID FLOW
NT AIR FLOW
NT AXISYMMETRIC FLOW
NT BASE FLOW
NT BOUNDARY LAYER FLOW
NT BOUNDARY LAYER SEPARATION
NT CASCADE FLOW
NT COAXIAL FLOW
NT COMPRESSIBLE FLOW
NT CONICAL FLOW
NT CRITICAL FLOW
NT CROSS FLOW
NT DUCTED FLOW
NT FREE FLOW
NT GAS FLOW
NT INCOMPRESSIBLE FLOW
NT INLET FLOW
NT INVISCID FLOW
NT JET FLOW
NT LAMINAR FLOW
NT NOZZLE FLOW
NT PARALLEL FLOW
NT PIPE FLOW
NT POTENTIAL FLOW
NT REATTACHED FLOW
NT SEPARATED FLOW
NT SHEAR FLOW
NT SUBSONIC FLOW
NT SUPERSONIC FLOW
NT THREE DIMENSIONAL FLOW
NT TRANSITION FLOW
NT TRANSONIC FLOW
NT TURBULENT FLOW
NT TWO DIMENSIONAL FLOW
NT UNIFORM FLOW
NT UNSTEADY FLOW
NT VISCOUS FLOW
NT WALL FLOW
Output of acoustical sources --- effects of
structural elements and background flow on
immobile multipolar point radiation p0030 A80-37806
FLUID JETS
NT FREE JETS
FLUID MECHANICS
NT AERODYNAMICS
NT COMPUTATIONAL FLUID DYNAMICS
NT FLUID DYNAMICS
NT GAS DYNAMICS
NT HYDRODYNAMICS
NT MAGNETOHYDRODYNAMICS
NT ROTOR AERODYNAMICS
One millimeter continuum observations of
extragalactic thermal sources
[NASA-CR-163590] p0040 N80-33334
FLUID PRESSURE
NT WATER PRESSURE
FLUIDIZED BED PROCESSORS
The preparation of calcium superoxide in a flowing
gas stream and fluidized bed
[ASME PAPER 80-ENAS-18] p0094 A80-43194
FLUORESCENCE
Two-photon excitation of nitric oxide fluorescence
as a temperature indicator in unsteady
gas-dynamic processes
[NASA-TM-81220] p0037 N80-32700
FLUORESCENT EMISSION
U FLUORESCENCE
FLUORIDES
NT URANIUM FLUORIDES

FLUORINE

F + H₂ collisions on two electronic potential energy surfaces - Quantum-mechanical study of the collinear reaction

p0068 A80-12012

Photoexcitation and ionization in molecular fluorine - Stieltjes-Tchebycheff calculations in the static-exchange approximation

p0046 A80-23324

FLUORINE COMPOUNDS

NT FLUORO COMPOUNDS

NT FLUOROCARBONS

NT FLUOROHYDROCARBONS

NT FLUOROPOLYMERS

NT PERFLUOROALKANE

NT URANIUM FLUORIDES

FLUORINE ORGANIC COMPOUNDS

NT FLUOROCARBONS

NT FLUOROHYDROCARBONS

NT FLUOROPOLYMERS

NT PERFLUOROALKANE

FLUORO COMPOUNDS

NT FLUOROCARBONS

NT FLUOROHYDROCARBONS

NT FLUOROPOLYMERS

NT PERFLUOROALKANE

Perfluoroether triazine elastomers

[NASA-CR-162748]

p0039 N80-16166

FLUOROCARBONS

Band model calculations for CFC13 in the 8-12 micron region

p0045 A80-21560

FLUOROHYDROCARBONS

Stratospheric ozone decrease due to chlorofluoromethane photolysis - Predictions of latitude dependence

p0049 A80-29762

FLUOROPOLYMERS

Synthesis of perfluoroalkylether triazine elastomers

p0051 A80-32825

FLUTTER ANALYSIS

Classical aerodynamic theory

[NASA-RP-1050]

p0001 N80-15033

A comprehensive analytical model of rotorcraft aerodynamics and dynamics. Part 2: User's manual

[NASA-TM-81183]

p0010 N80-28297

FLUX (RATE PER UNIT AREA)

U FLUX DENSITY

FLUX (RATE)

NT HEAT FLUX

NT MAGNETIC FLUX

NT SOLAR FLUX

FLUX DENSITY

NT ELECTRON FLUX DENSITY

NT PARTICLE FLUX DENSITY

NT RADIANT FLUX DENSITY

NT SOLAR FLUX DENSITY

On the output of acoustical sources

[NASA-CR-162576]

p0014 N80-15872

FLUX MAPPING

U FLUX DENSITY

U MAPPING

FLUXMETERS

U MEASURING INSTRUMENTS

FLYBY MISSIONS

Pioneer Saturn encounter --- Pioneer 11 space probe

[NASA-TM-80807]

p0035 N80-10239

FLYING PERSONNEL

NT AIRCRAFT PILOTS

NT FLIGHT CREWS

FLYING PLATFORM STABILITY

U AERODYNAMIC STABILITY

FLYING QUALITIES

U FLIGHT CHARACTERISTICS

FOAMS

Toxicity of pyrolysis gases from foam plastics

p0071 A80-24625

Materials for fire resistant passenger seats in aircraft

p0080 A80-48757

Catalysts for polyimide foams from aromatic isocyanates and aromatic dianhydrides --- flame retardant foams

[NASA-CASE-ARC-11107-1]

p0080 N80-16116

FOOD INTAKE

Extremes of urine osmolality - Lack of effect on red blood cell survival

p0091 A80-46196

FORCE DISTRIBUTION

Wing flapping with minimum energy --- minimize the drag for a bending moment at the wing root

[NASA-TM-81174]

p0001 N80-16035

FOREBODIES

NT ABLATIVE NOSE CONES

NT NOSES (FOREBODIES)

Forebody and base region real-gas flow in severe planetary entry by a factored implicit numerical method. I - Computational fluid dynamics

[AIAA PAPER 80-0065]

p0061 A80-22731

Control of forebody vortex orientation to

alleviate side forces

[AIAA PAPER 80-0183]

p0024 A80-23955

Galileo probe forebody entry thermal protection - Aerothermal environments and heat shielding requirements

[ASME PAPER 80-ENAS-24]

p0066 A80-43200

FORECASTING

NT NUMERICAL WEATHER FORECASTING

NT PERFORMANCE PREDICTION

NT PREDICTION ANALYSIS TECHNIQUES

NT TECHNOLOGICAL FORECASTING

FORESTS

Using guided clustering techniques to analyze

Landsat data for mapping forest land cover in northern California

p0078 A80-25595

Issues arising from the demonstration of Landsat-based technologies to inventories and mapping of the forest resources of the Pacific Northwest states

p0065 A80-41305

Use of collateral information to improve LANDSAT classification accuracies --- Ventura County and Klamath National Forest, California

[E80-10268]

p0040 N80-29815

FORM PERCEPTION

U SPACE PERCEPTION

FORMALDEHYDE

An ab initio calculation of the zero-field splitting parameters of the 3A-double prime state of formaldehyde

p0056 A80-45333

FRACTIONATION

NT CHEMICAL FRACTIONATION

FRACTURE MECHANICS

Some observations regarding the statistical determination of stress rupture regression lines

p0041 A80-12828

FRAUNHOFER REGION

U FAR FIELDS

FREE CONVECTION

Whole planet cooling and the radiogenic heat source contents of the earth and moon

p0053 A80-36651

Free convection in enclosures exposed to compressive heating --- Galileo descent module

[AIAA PAPER 80-1536]

p0079 A80-41495

FREE FLOW

A diagonal form of an implicit approximate-factorization algorithm with application to a two dimensional inlet

[AIAA PAPER 80-0067]

p0061 A80-19274

Three-dimensional simulation of the free shear layer using the vortex-in-cell method

p0067 A80-49300

Effects of free-stream turbulence on diffuser performance

[NASA-CR-163194]

p0017 N80-24264

FREE JETS

An experimental study of multiple jet mixing

[NASA-CR-166184]

p0018 N80-31760

FREE STREAM EFFECTS

U FREE FLOW

FREE STREAMS

U FREE FLOW

FREQUENCIES

NT BROADBAND

FRICTION

NT AERODYNAMIC DRAG

NT FLOW RESISTANCE

NT SKIN FRICTION

FRICTION DRAG

NT AERODYNAMIC DRAG

FRICTION MEASUREMENT

Skin friction measurements by a new nonintrusive double-laser-beam oil viscosity balance technique

[AIAA PAPER 80-1373]

p0065 A80-41587

FRICTION PRESSURE DROP

SUBJECT INDEX

Separated skin-friction measurements - Source of error: An assessment and elimination
[AIAA PAPER 80-1409] p0027 A80-44155

FRICTION PRESSURE DROP

U SKIN FRICTION

FUEL CONSUMPTION

Potential benefits for propfan technology on derivatives of future short- to medium-range transport aircraft
[AIAA PAPER 80-1090] p0026 A80-38905

Analysis of fuel-conservative curved decelerating approach trajectories for powered-lift and CTOL jet aircraft
[NASA-TP-1650] p0005 N80-19022

Effectiveness of advanced fuel-conservative procedures in the transitional ATC environment
p0023 N80-27347

Application of advanced technologies to small short-haul transport aircraft
[NASA-CR-152363] p0018 N80-32353

FUELS

NT ACTIVATED CARBON

FUNCTIONAL ANALYSIS

NT HARMONIC ANALYSIS

NT SINGULAR INTEGRAL EQUATIONS

FUNCTIONS (MATHEMATICS)

NT COORDINATE TRANSFORMATIONS

NT GREEN FUNCTION

NT HAMILTONIAN FUNCTIONS

NT HYPERGEOMETRIC FUNCTIONS

NT KERNEL FUNCTIONS

NT TRANSFER FUNCTIONS

FUSELAGES

Formulation of coupled rotor/fuselage equations of motion
p0021 A80-17717

Coupled rotor and fuselage equations of motion
[NASA-TN-81153] p0006 N80-10516

FUSIFORM SHAPES

U CONES

G

G FORCE

U ACCELERATION (PHYSICS)

GAGES

U MEASURING INSTRUMENTS

GALACTIC CLUSTERS

An investigation of previously derived Hyades, Coma, and M67 reddening
p0049 A80-29959

GALACTIC EVOLUTION

Gas dynamics in barred spirals - Gaseous density waves and galactic shocks
p0041 A80-10685

GALACTIC MAGNETIC FIELDS

U INTERSTELLAR MAGNETIC FIELDS

GALACTIC ROTATION

On the three-dimensional shapes of elliptical galaxies
p0047 A80-26101

Self-gravitating gas flow in barred spiral galaxies
p0055 A80-44959

GALACTIC STRUCTURE

Galaxy collisions - A preliminary study
p0046 A80-23420

Self-gravitating gas flow in barred spiral galaxies
p0055 A80-44959

GALAXIES

NT BARRED GALAXIES

NT ELLIPTICAL GALAXIES

NT GALACTIC CLUSTERS

NT SPIRAL GALAXIES

GALILEAN SATELLITES

NT CALLISTO

NT GANYMEDE

GALILEO MISSION

U GALILEO PROJECT

GALILEO PROBE

Free convection in enclosures exposed to compressive heating --- Galileo descent module
[AIAA PAPER 80-1536] p0079 A80-41495

Galileo probe forebody entry thermal protection - Aerothermal environments and heat shielding requirements
[ASME PAPER 80-ENAS-24] p0066 A80-43200

Galileo probe thermal protection: Entry heating environments and spallation experiments design
[NASA-CR-152334] p0038 N80-14184

GALILEO PROJECT

Shape change of Galileo probe models in free-flight tests
[NASA-TN-81209] p0037 N80-27418

GAMMA RADIATION

U GAMMA RAYS

GAMMA RAYS

The radioracemization of isovaline - Cosmochemical implications --- gamma ray effects on Murchison meteorite primordial composition
p0086 A80-13018

GANYMEDE

On the comparative evolution of Ganymede and Callisto
p0048 A80-28080

GARMENTS

The development of an elastic reverse gradient garment to be used as a countermeasure for cardiovascular deconditioning
[NASA-CR-152379] p0086 N80-33086

GAS ANALYSIS

NT OZONOMETRY

GAS CHROMATOGRAPHY

Corrections in the Pioneer Venus sounder probe gas chromatographic analysis of the lower Venus atmosphere
p0089 A80-30875

Chelate-modified polymers for atmospheric gas chromatography
[NASA-CASE-ARC-11154-1] p0097 N80-23383

GAS DYNAMICS

NT AERODYNAMICS

NT ROTOR AERODYNAMICS

Gas dynamics in barred spirals - Gaseous density waves and galactic shocks
p0041 A80-10685

The dynamics and stability of radiatively driven gas clouds. I - Plane-parallel slabs
p0042 A80-14058

Application of the method of integral relations to unsteady fluid flow problems with shocks
p0078 A80-26694

On the construction and application of implicit factored schemes for conservation laws --- in computational fluid dynamics
p0062 A80-27407

'GAIN' - Gas-addition, impedance-matched arc driver --- shock tube gas dynamics
p0064 A80-38131

GAS FLOW

NT AIR FLOW

NT PIPE FLOW

NT TRANSITION FLOW

Adsorption interference in mixtures of trace contaminants flowing through activated carbon adsorber beds
[ASME PAPER 80-ENAS-17] p0096 A80-43193

Self-gravitating gas flow in barred spiral galaxies
p0055 A80-44959

GAS GIANT PLANETS

NT JUPITER (PLANET)

NT SATURN (PLANET)

NT URANUS (PLANET)

Calculations of the evolution of the giant planets
p0049 A80-28086

GAS IONIZATION

Survival probabilities for interstellar hydrogen flowing into the interplanetary system from far regions of the heliosphere
p0076 A80-49217

GAS LASERS

NT HF LASERS

GAS SPECTROSCOPY

Integrated band intensities of gaseous N₂O/5/
p0047 A80-25660

GAS STREAMS

The preparation of calcium superoxide in a flowing gas stream and fluidized bed
[ASME PAPER 80-ENAS-18] p0094 A80-43194

GAS TEMPERATURE

A reanalysis of the observed interplanetary hydrogen I alpha emission profiles and the derived local interstellar gas temperature and velocity
p0076 A80-49362

GAS TURBINE ENGINES

NT BRISTOL-SIDDELEY BS 53 ENGINE

NT TURBOFAN ENGINES

NT TURBOJET ENGINES

SUBJECT INDEX

GRAVITATIONAL COLLAPSE

NT TURBOPROP ENGINES

GAS-GAS INTERACTIONS

The properties of clusters in the gas phase. IV -

Complexes of H₂O and HNO_x clustering on NO_x/-/

p0046 A80-23322

Vibration-rotation line shifts for 1 sigma g +

H₂/V_J-1S/0/ He computed via close coupling -

Temperature dependence

p0058 A80-51965

GAS-SOLID INTERACTIONS

An extended soft-cube model for the thermal

accommodation of gas atoms on solid surfaces

[NASA-TN-81163]

p0035 N80-14941

GASDYNAMIC LASERS

A technique for evaluating the Jovian entry-probe

heat-shield material with a gasdynamic laser

p0063 A80-29479

GASEOUS CAVITATION

U GAS FLOW

GASES

NT CARBON DIOXIDE

NT CARBON MONOXIDE

NT CARBON SUBOXIDES

NT CHARGED PARTICLES

NT DIATOMIC GASES

NT EXHAUST GASES

NT GAS STREAMS

NT HELIUM

NT HYDROGEN

NT HYDROGEN ATOMS

NT HYDROGEN IONS

NT INTERPLANETARY GAS

NT INTERSTELLAR GAS

NT IONIZED GASES

NT LIQUID HELIUM

NT LIQUID HELIUM 2

NT LIQUID NITROGEN

NT MOLECULAR GASES

NT NEUTRAL GASES

NT NITROGEN

NT NITROGEN IONS

NT OXYGEN

NT OZONE

NT RARE GASES

NT RAREFIED PLASMAS

NT REAL GASES

NT THERMAL PLASMAS

NT XENON

GAUSSMETERS

U MAGNETOMETERS

GENERAL AVIATION AIRCRAFT

Effect of propeller slipstream on the drag and

performance of the engine cooling system for a

general aviation twin-engine aircraft

[AIAA PAPER 80-1872]

p0027 A80-43315

GENETICS

Problems and potentialities of cultured plant

cells in retrospect and prospect

p0077. A80-15225

GEOASTROPHYSICS

U ASTROPHYSICS

GEOCHEMISTRY

NT BIOGEOCHEMISTRY

The possible role of metal ions and clays in

prebiotic chemistry

p0094 A80-50060

GEOLOGY

NT HYDROGEOLOGY

NT PETROGRAPHY

NT PHOTOGEOLOGY

NT STRUCTURAL PROPERTIES (GEOLOGY)

NT VOLCANOES

NT VOLCANOLOGY

GEOMAGNETIC ANOMALIES

U MAGNETIC ANOMALIES

GEOMAGNETICALLY TRAPPED PARTICLES

U RADIATION BELTS

GEOMETRICAL HYDROMAGNETICS

U MAGNETOHYDRODYNAMICS

GEOMETRY

NT ANGLE OF ATTACK

NT ANGLES (GEOMETRY)

NT DIFFERENTIAL GEOMETRY

NT FLOW GEOMETRY

NT NOZZLE GEOMETRY

NT VORTICITY

GROTHERMAL RESOURCES

NT VOLCANOES

GIANT STARS

NT CARBON STARS

GLANDS (ANATOMY)

NT PITUITARY GLAND

GLASS FIBER REINFORCED PLASTICS

Oxygen index tests of thermosetting resins

p0044 A80-21448

GLAUBERT COEFFICIENT

U AERODYNAMIC FORCES

GLIDE ANGLES

U GLIDE PATHS

GLIDE PATHS

Head-up display in the non-precision approach

[NASA-TN-81167]

p0084 N80-26296

Analytical methodology for determination of

helicopter IFR precision approach requirements

--- pilot workload and acceptance level

[NASA-CR-152367]

p0040 N80-28330

GLIDE SLOPES

U GLIDE PATHS

GLOBULAR CLUSTERS

The settling of helium and the ages of globular

clusters

p0052 A80-35151

GLUCOSE

Growth hormone control of glucose oxidation

pathways in hypophysectomized rats

p0088 A80-24222

Insulin binding and glucose uptake of adipocytes

in rats adapted to hypergravitational force

p0089 A80-35751

GRADIENTS

NT PRESSURE GRADIENTS

GRADIOMETERS

U MAGNETOMETERS

GRADUATION

U CALIBRATING

GRAINS (FOOD)

NT BARLEY

Irrigated lands assessment for water management

Applications Pilot Test (APT) --- California

[E80-10324]

p0019 N80-32815

GRAPHITE-EPOXY COMPOSITE MATERIALS

A temperature dependent fatigue failure criterion

for graphite/epoxy laminates

p0060 A80-15518

Time-temperature behavior of a unidirectional

graphite/epoxy composite

p0078 A80-21141

Effects of moisture on apparent flexure strength

and on torsion and flexure fatigue properties of

graphite-epoxy composites

p0063 A80-27965

Degradation of tensile and shear properties of

composites exposed to fire or high temperature

p0072 A80-29697

Graphite composites with advanced resin matrices

[AIAA 80-0758]

p0064 A80-35051

Performance properties of graphite reinforced

composites with advanced resin matrices --- for

aircraft

p0052 A80-35330

Thermal expansion and swelling of cured epoxy

resin used in graphite/epoxy composite materials

p0054 A80-40926

Hygrothermal damage mechanisms in graphite-epoxy

composites

[NASA-CR-3189]

p0038 N80-13170

GRASSLANDS

Irrigated lands assessment for water management

Applications Pilot Test (APT) --- California

[E80-10324]

p0019 N80-32815

GRAVITATION

NT SOLAR GRAVITATION

GRAVITATIONAL COLLAPSE

Ring formation in rotating protostellar clouds

Collapsing cloud models for Bok globules

p0048 A80-26992

The role of magnetic fields in the collapse of

protostellar gas clouds

p0048 A80-26996

Fragmentation in a rotating protostar - A

comparison of two three-dimensional computer codes

p0053 A80-38432

Protostellar formation in rotating interstellar

clouds. III - Nonaxisymmetric collapse

p0054 A80-39375

GRAVITATIONAL EFFECTS

Numerical calculations of the collapse of nonrotating, magnetic gas clouds p0057 A80-49341

GRAVITATIONAL EFFECTS

Hypergravity and estrogen effects on avian anterior pituitary growth hormone and prolactin levels p0094 A80-20447

Physiological response to hyper- and hypogravity during rollercoaster flight p0095 A80-21547

Insulin binding and glucose uptake of adipocytes in rats adapted to hypergravitational force p0089 A80-35751

The architecture of the avian retina following exposure to chronic 2 G p0096 A80-42013

Evaluation of biological models using Spacelab [ASME PAPER 80-ENAS-38] p0094 A80-43212

GRAVITATIONAL FIELDS

Self-gravitating gas flow in barred spiral galaxies p0055 A80-44959

GRAVITATIONAL POTENTIAL

U GRAVITATIONAL FIELDS

GRAVITY GRADIENT SATELLITES

NT ATS 3

GRAZING LANDS

U GRASSLANDS

GREEN FUNCTION

Note on the eigensolution of a homogeneous equation with semi-infinite domain p0075 A80-40508

GREEN THEOREM

U GREEN FUNCTION

GROUND BASED CONTROL

NT AIR TRAFFIC CONTROL

GROUND EFFECT

Investigation of ground effects on large and small scale models of a three span V/STOL aircraft configuration [NASA-CR-152240] p0015 N80-16030

GROUND EFFECT (AERODYNAMICS)

VTOL in-ground effect flows for closely spaced jets [AIAA PAPER 80-1880] p0033 A80-46693

GROUND STATE

Ground-state rotational constants of /C-13/H3D p0054 A80-41175

GROUND STATIONS

Operational procedures for ground station operation: ATS-3 Hawaii-Ames satellite link experiment [NASA-TM-81155] p0035 N80-13333

Pioneer Venus multiprobe entry telemetry recovery p0058 N80-26347

GROUP THEORY

A scaling theory for linear systems p0030 A80-32676

GROUP VELOCITY

Examination of group-velocity criterion for breakdown of vortex flow in a divergent duct p0022 A80-38049

GROWTH

Hypergravity and estrogen effects on avian anterior pituitary growth hormone and prolactin levels p0094 A80-20447

GUIDANCE (MOTION)

NT AIRCRAFT GUIDANCE

NT TERMINAL GUIDANCE

GUIDANCE SENSORS

Flight test of navigation and guidance sensor errors measured on STOL approaches [NASA-TM-81154] p0007 N80-13041

GUIDE VANS

Force and moment data from a wind-tunnel test of a tilt-macelle V/STOL propulsion system with an attitude control vane --- conducted in Ames 40 by 80 foot wind tunnel [NASA-TM-81157] p0006 N80-13003

GUST ALLEVIATORS

The design, testing and evaluation of the MIT individual-blade-control system as applied to gust alleviation for helicopters [NASA-CR-152352] p0016 N80-22357

Analytical design and evaluation of an active control system for helicopter vibration reduction and gust response alleviation [NASA-CR-152377] p0017 N80-28369

SUBJECT INDEX

GUST LOADS

Unified aerodynamic-acoustic theory for a thin rectangular wing encountering a gust p0030 A80-36401

Aerodynamic coefficients in generalized unsteady thin airfoil theory p0030 A80-38034

GYMNASTICS

U PHYSICAL EXERCISE

GYRATION

NT MOLECULAR ROTATION

NT PLANETARY ROTATION

NT ROTATION

NT STELLAR ROTATION

GYRATORS

NT MICROWAVE FILTERS

GYROPLANES

U HELICOPTERS

H

H LINES

The implications of hydrogen emission line ratios in quasi-stellar objects p0072 A80-27013

A reanalysis of the observed interplanetary hydrogen L alpha emission profiles and the derived local interstellar gas temperature and velocity p0076 A80-49362

H-53 HELICOPTER

A compilation and analysis of helicopter handling qualities data. Volume 1: Data compilation [NASA-CR-3144] p0013 N80-11097

HALIDES

NT URANIUM FLUORIDES

HALOCARBONS

NT CHLOROCARBONS

NT FLUOROCARBONS

Temperature dependence of intensities of the 8-12 micron bands of CFC13 p0045 A80-21559

Spectrophotometric identification of the pigment associated with light-driven primary sodium translocation in Halobacterium halobium p0088 A80-26015

HALOGEN COMPOUNDS

NT BROMINE COMPOUNDS

NT FLUORO COMPOUNDS

NT FLUOROCARBONS

NT FLUOROHYDROCARBONS

NT FLUOROPOLYMERS

NT HALOCARBONS

NT PERFLUOROALKANE

NT URANIUM FLUORIDES

HALOGENS

NT FLUORINE

HALOPHILES

Physical chemistry and evolution of salt tolerance in halobacteria p0090 A80-40383

HAMILTONIAN FUNCTIONS

Algorithm for fixed-range optimal trajectories [NASA-TP-1565] p0006 N80-28329

HANDBOOKS

NT USER MANUALS (COMPUTER PROGRAMS)

HANDLING QUALITIES

U CONTROLLABILITY

HARMONIC ANALYSIS

Experimental unsteady aerodynamics of conventional and supercritical airfoils --- conducted in the Ames 11 foot transonic wind tunnel [NASA-TM-81221] p0012 N80-33345

HAWAII

Operational procedures for ground station operation: ATS-3 Hawaii-Ames satellite link experiment [NASA-TM-81155] p0035 N80-13333

Volcanic features of Hawaii. A basis for comparison with Mars [NASA-SP-403] p0034 N80-23912

HAZARDS

NT TOXIC HAZARDS

HCHM

U HEAT CAPACITY MAPPING MISSION

HEAD (ANATOMY)

Fluid-electrolyte shifts and thermoregulation - Rest and work in heat with head cooling p0091 A80-48086

SUBJECT INDEX

HELICOPTER WAKES

HEAD-UP DISPLAYS

Head-up display in the non-precision approach
[NASA-TM-81167] p0084 N80-26296
An experimental evaluation of head-up display
formats
[NASA-TP-1550] p0082 N80-28349

HEALTH

NT HEALTH PHYSICS

HEALTH PHYSICS

Part-body and multibody effects on absorption of
radio-frequency electromagnetic energy by
animals and by models of man
p0071 A80-22987

HEAT ACCLIMATIZATION

Human acclimation and acclimatization to heat: A
compendium of research, 1968-1978 --- Bibliography
[NASA-TM-81181] p0085 N80-34056

HEAT CAPACITY MAPPING MISSION

Infrared-temperature variability in a large
agricultural field --- Dunnigan, California
[E80-10331] p0038 N80-32822

HEAT DISSIPATION

U COOLING

HEAT DISSIPATION CHILLING

U COOLING

HEAT EFFECTS

U TEMPERATURE EFFECTS

HEAT EQUATIONS

U THERMODYNAMICS

HEAT FLUX

Calorimeter probes for measuring high thermal flux
--- in electric-arc jet facilities for planetary
entry heating simulation
p0099 A80-29480

HEAT MEASUREMENT

Calorimeter probes for measuring high thermal flux
--- in electric-arc jet facilities for planetary
entry heating simulation
p0099 A80-29480

Release-rate calorimetry of multilayered materials
for aircraft seats
p0051 A80-34223

Release-rate calorimetry of multilayered materials
for aircraft seats
[AIAA 80-0759] p0064 A80-35052

HEAT PIPES

Long term tests of the HEPP liquid trap diode heat
pipe prototype
[NASA-CR-152358] p0039 N80-22635

HEAT REGULATION

U TEMPERATURE CONTROL

HEAT RESISTANCE

U THERMAL RESISTANCE

HEAT SHIELDING

NT REENTRY SHIELDING

A technique for evaluating the Jovian entry-probe
heat-shield material with a gasdynamic laser
p0063 A80-29479

Galileo probe forebody entry thermal protection -
Aerothermal environments and heat shielding
requirements
[ASME PAPER 80-ENAS-24] p0066 A80-43200

Galileo probe thermal protection: Entry heating
environments and spallation experiments design
[NASA-CR-152334] p0038 N80-14184

HEAT TESTS

U HIGH TEMPERATURE TESTS

HEAT TRANSFER

NT CONVECTIVE HEAT TRANSFER

NT RADIATIVE HEAT TRANSFER

NT TURBULENT HEAT TRANSFER

Evaluation of the time dependent surface shear
stress in turbulent flows
[ASME PAPER 79-WA/FE-17] p0078 A80-18618
PRSA hydrogen tank thermal acoustic oscillation
study
[NASA-CR-152319] p0038 N80-11470

HEAT TRANSMISSION

NT CONVECTIVE HEAT TRANSFER

NT HEAT TRANSFER

NT RADIATIVE HEAT TRANSFER

NT TURBULENT HEAT TRANSFER

HEATING

NT AERODYNAMIC HEATING

NT BASE HEATING

NT INDUCTION HEATING

NT RADIO FREQUENCY HEATING

NT SHOCK HEATING

NT SOLAR HEATING

NT WATER HEATING

HELICOPTER ATTITUDE INDICATORS

U ATTITUDE INDICATORS

U HELICOPTERS

HELICOPTER CONTROL

The promise of multicyclic control --- for
helicopter vibration reduction
p0022 A80-33123

Multicyclic control for helicopters - Research in
progress at Ames Research Center
[AIAA 80-0671] p0025 A80-34997

Multicyclic control of a helicopter rotor
considering the influence of vibration, loads
and control motion
[AIAA 80-0673] p0025 A80-34998

A compilation and analysis of helicopter handling
qualities data. Volume 1: Data compilation
[NASA-CR-3144] p0013 N80-11097

The design, testing and evaluation of the MIT
individual-blade-control system as applied to
gust alleviation for helicopters
[NASA-CR-152352] p0016 N80-22357

A comprehensive analytical model of rotorcraft
aerodynamics and dynamics. Part 3: Program
manual
[NASA-TM-81184] p0010 N80-28298

Analytical methodology for determination of
helicopter IFR precision approach requirements
--- pilot workload and acceptance level
[NASA-CR-152367] p0040 N80-28330

A pilot's assessment of helicopter
handling-quality factors common to both agility
and instrument flying tasks
[NASA-TM-81217] p0011 N80-28341

Analytical design and evaluation of an active
control system for helicopter vibration
reduction and gust response alleviation
[NASA-CR-152377] p0017 N80-28369

A mathematical representation of an advanced
helicopter for piloted simulator investigations
of control system and display variations
[NASA-TM-81203] p0011 N80-28371

Effects of rotor parameter variations on handling
qualities of unaugmented helicopters in
simulated terrain flight
[NASA-TM-81190] p0012 N80-31407

A simulator study of control and display
augmentations for helicopters
[NASA-CR-163451] p0018 N80-31408

HELICOPTER DESIGN

Coupled rotor and fuselage equations of motion
[NASA-TM-81153] p0006 N80-10516

A hingeless rotor XV-15 design integration
feasibility study. Volume 1: Engineering
design studies
[NASA-CR-152310] p0015 N80-18030

An experimental evaluation of a helicopter rotor
section designed by numerical optimization
[NASA-TM-78622] p0009 N80-21287

Calculation of three-dimensional unsteady
transonic flows past helicopter blades
[NASA-TP-1721] p0100 N80-33356

HELICOPTER PERFORMANCE

Effects of primary rotor parameters on flapping
dynamics
[NASA-TP-1431] p0005 N80-15138

A comprehensive analytical model of rotorcraft
aerodynamics and dynamics. Part 3: Program
manual
[NASA-TM-81184] p0010 N80-28298

Comparison of calculated and measured helicopter
rotor lateral flapping angles
[NASA-TM-81213] p0012 N80-33349

Analysis and correlation of test data from an
advanced technology rotor system --- helicopter
performance prediction
[NASA-CR-152366] p0019 N80-33351

HELICOPTER ROTORS

U ROTARY WINGS

HELICOPTER TAIL ROTORS

Formulation of coupled rotor/fuselage equations of
motion
p0021 A80-17717

Multicyclic control for helicopters - Research in
progress at Ames Research Center
[AIAA 80-0671] p0025 A80-34997

HELICOPTER WAKES

Comparison of calculated and measured model rotor
loading and wake geometry

HELICOPTERS

SUBJECT INDEX

- [NASA-TM-81189] p0009 N80-24262
- HELICOPTERS**
- NT BO-105 HELICOPTER
- NT H-53 HELICOPTER
- NT MILITARY HELICOPTERS
- NT OH-6 HELICOPTER
- NT RIGID ROTOR HELICOPTERS
- NT UH-1 HELICOPTER
- Feasibility and concept study to convert the NASA/AMES vertical motion simulator to a helicopter simulator [NASA-CR-152193] p0098 N80-16070
- Parametric study of helicopter aircraft systems costs and weights [NASA-CR-152315] p0016 N80-22305
- Practical optimal flight control system design for helicopter aircraft. Volume 1: Technical Report [NASA-CR-3275] p0017 N80-23328
- System description and analysis. Part 1: Feasibility study for helicopter/VTOL wide-angle simulation image generation display system [NASA-CR-152376] p0101 N80-27397
- A comprehensive analytical model of rotorcraft aerodynamics and dynamics. Part 1: Analysis development [NASA-TM-81182] p0010 N80-28296
- A pilot's assessment of helicopter handling-quality factors common to both agility and instrument flying tasks [NASA-TM-81217] p0011 N80-28341
- A mathematical representation of an advanced helicopter for piloted simulator investigations of control system and display variations [NASA-TM-81203] p0011 N80-28371
- An experimental investigation of the effects of aeroelastic couplings on aeromechanical stability of a hingeless rotor helicopter [AD-A085819] p0101 N80-29294
- Civil helicopter wire strike assessment study. Volume 1: Findings and recommendations [NASA-CR-152389] p0019 N80-33381
- HELIOGRAPHY**
- U SOLAR MAGNETIC FIELD
- HELIUM**
- NT LIQUID HELIUM
- NT LIQUID HELIUM 2
- Vibration-rotation line shifts for 1 sigma g + H2/V, J/-1S/O/ He computed via close coupling - Temperature dependence p0058 A80-51965
- HELIUM STARS**
- U B STARS
- HELIUM 2**
- U LIQUID HELIUM
- HEMOGLOBIN**
- Plasma volume during stress in man - Osmolality and red cell volume p0087 A80-13506
- HETEROCYCLIC COMPOUNDS**
- NT AZINES
- NT METHYLENE BLUE
- NT OXAZOLE
- HEXADIENE**
- Singlet oxygenation of 1,2-poly/1,4-hexadiene/s p0045 A80-21991
- HF LASERS**
- Quantum-mechanical calculation of three-dimensional atom-diatom collisions in the presence of intense laser radiation p0068 A80-15221
- HX HELICOPTER**
- U H-53 HELICOPTER
- HIGH GRAVITY (ACCELERATION)**
- U HIGH GRAVITY ENVIRONMENTS
- HIGH GRAVITY ENVIRONMENTS**
- Hypergravity and estrogen effects on avian anterior pituitary growth hormone and prolactin levels p0094 A80-20447
- Insulin binding and glucose uptake of adipocytes in rats adapted to hypergravitational force p0089 A80-35751
- HIGH LATITUDES**
- U POLAR REGIONS
- HIGH PRESSURE**
- High-pressure protective systems technology [ASME PAPER 79-ENAS-15] p0092 A80-15240
- HIGH RESOLUTION**
- High-resolution Lyman-alpha filtergrams of the sun
- HIGH TEMPERATURE TESTS**
- Studies for improved high temperature coatings for Space Shuttle application p0075 A80-37277
- HINGED ROTOR BLADES**
- U ROTARY WINGS
- HINGELESS ROTORS**
- U RIGID ROTORS
- HINGES**
- NT FLAPPING HINGES
- HISTOLOGY**
- The architecture of the avian retina following exposure to chronic 2 G p0096 A80-42013
- HO-6 HELICOPTER**
- U OH-6 HELICOPTER
- HOMOSPHERE**
- NT MIDDLE ATMOSPHERE
- NT STRATOSPHERE
- HORIZONTAL FLIGHT**
- A new algorithm for horizontal capture trajectories [NASA-TM-81186] p0009 N80-22297
- HORMONES**
- NT ESTROGENS
- NT PITUITARY HORMONES
- Growth hormone control of glucose oxidation pathways in hypophysectomized rats p0088 A80-24222
- HOT CORROSION**
- NT TEMPERATURE DEPENDENCE
- HOT JET EXHAUST**
- U JET EXHAUST
- HOT JETS**
- U JET FLOW
- HOT STARS**
- NT B STARS
- NT O STARS
- Red and nebulous objects in dark clouds - A survey p0044 A80-20662
- HOVERING**
- Effect of tip planform on blade loading characteristics for a two-bladed rotor in hover [NASA-TM-78615] p0007 N80-14049
- Stability of nonuniform rotor blades in hover using a mixed formulation [NASA-TM-81226] p0012 N80-33777
- HOVERING STABILITY**
- Large scale model tests of a new technology V/STOL concept [AIAA PAPER 80-0233] p0023 A80-19303
- HU-1 HELICOPTER**
- U UH-1 HELICOPTER
- HUECKEL THEORY**
- Modified Iterative Extended Hueckel. 1: Theory [NASA-TM-81200] p0083 N80-25108
- Modified Iterative Extended Hueckel. 2: Application to the interaction of Na(+), Na(+)(aq.), Mg(+)-2(aq.) with adenine and thymine [NASA-TM-81201] p0084 N80-25109
- HUGHES AIRCRAFT**
- NT OH-6 HELICOPTER
- HUMAN BEHAVIOR**
- Theory of the decision/problem state [NASA-TM-81192] p0103 N80-22984
- Problem solving and decisionmaking: An integration [NASA-TM-81191] p0103 N80-22985
- HUMAN BODY**
- Part-body and multibody effects on absorption of radio-frequency electromagnetic energy by animals and by models of man p0071 A80-22987
- HUMAN ENGINEERING**
- U HUMAN FACTORS ENGINEERING
- HUMAN FACTORS ENGINEERING**
- Dynamic decisions and work load in multitask supervisory control p0095 A80-40898
- Optimal control model predictions of system performance and attention allocation and their experimental validation in a display design study p0095 A80-40899
- Some human factors issues in the development and evaluation of cockpit alerting and warning systems [NASA-RP-1055] p0082 N80-15821
- NASA aviation safety reporting system [NASA-TM-78608] p0083 N80-18010
- Decision-problem state analysis methodology [NASA-TM-81194] p0103 N80-25002

- Head-up transition behavior of pilots during simulated low-visibility approaches
[NASA-TP-1618] p0082 N80-26039
- Flight-deck automation: Promises and problems
[NASA-TM-81206] p0084 N80-26040
- An experimental evaluation of head-up display formats
[NASA-TP-1550] p0082 N80-28349
- HUMAN PERFORMANCE**
- NT PILOT PERFORMANCE
- Plasma volume during stress in man - Osmolality and red cell volume
p0087 A80-13506
- Multi-modal information processing for visual workload relief
[NASA-CR-162720] p0100 N80-16737
- The effect of viewing time, time to encounter, and practice on perception of aircraft separation on a cockpit display of traffic information
[NASA-TM-81173] p0083 N80-18038
- Automation literature: A brief review and analysis
[NASA-TM-81245] p0103 N80-34097
- HUMAN TOLERANCES**
- Objective measurement of human tolerance to +G sub z acceleration stress
[NASA-TM-81166] p0098 N80-18709
- Human acclimation and acclimatization to heat: A compendium of research 1968-1978 --- Bibliography
[NASA-TM-81181] p0085 N80-34056
- HUMAN WASTES**
- NT URINE
- HUMIDITY MEASUREMENT**
- High resolution vertical profiles of wind, temperature and humidity obtained by computer processing and digital filtering of radiosonde and radar tracking data from the ITCZ experiment of 1977
[NASA-CR-3269] p0039 N80-21926
- HYDRATES**
- The properties of clusters in the gas phase. IV - Complexes of H₂O and HNO_x clustering on NO_x/-/
p0046 A80-23322
- New gas phase inorganic ion cluster species and their atmospheric implications
p0075 A80-37510
- HYDROAEROMECHANICS**
- U AERODYNAMICS
- HYDROCARBONS**
- NT HEXADIENE
- NT METHANE
- Photosensitized oxidation of unsaturated polymers
p0049 A80-29086
- The carbon isotope biogeochemistry of the individual hydrocarbons in bat guano and the ecology of insectivorous bats in the region of Carlsbad, New Mexico
[NASA-TM-81164] p0083 N80-18680
- HYDRODYNAMIC STABILITY**
- U FLOW STABILITY
- HYDRODYNAMICS**
- NT MAGNETOHYDRODYNAMICS
- Fragmentation in a rotating protostar - A comparison of two three-dimensional computer codes
p0053 A80-38432
- Classical aerodynamic theory
[NASA-RP-1050] p0001 N80-15033
- HYDROGEN**
- NT HYDROGEN ATOMS
- NT HYDROGEN IONS
- H + H₂ collisions on two electronic potential energy surfaces - Quantum-mechanical study of the collinear reaction
p0068 A80-12012
- Vibration-rotation line shifts for 1 sigma g + H₂/V,J/-15/0/ He computed via close coupling - Temperature dependence
p0058 A80-51965
- PSA hydrogen tank thermal acoustic oscillation study
[NASA-CR-152319] p0038 N80-11470
- HYDROGEN ATOMS**
- Isothermal-desorption-rate measurements in the vicinity of the Curie temperature for H₂ chemisorbed on nickel films
p0042 A80-16167
- Hot hydrogen in the exosphere of Venus
p0070 A80-18943
- HYDROGEN CLOUDS**
- Far infrared, near infrared, and radio molecular line studies of HFE 2, HFE 3, and FJM 6
p0068 A80-11489
- Far-infrared spectra of W51-IRS 2 and W49 NW
p0056 A80-44967
- HYDROGEN COMPOUNDS**
- NT DEUTERIUM COMPOUNDS
- HYDROGEN IONS**
- Survival probabilities for interstellar hydrogen flowing into the interplanetary system from far regions of the heliosphere
p0076 A80-49217
- HYDROGEOLOGY**
- Aqueous activity on asteroids - Evidence from carbonaceous meteorites
p0062 A80-24586
- HYDROLOGY**
- NT HYDROGEOLOGY
- HYDROMAGNETICS**
- U MAGNETOHYDRODYNAMICS
- HYDROMAGNETISM**
- U MAGNETOHYDRODYNAMICS
- HYDROMECHANICS**
- NT HYDRODYNAMICS
- NT MAGNETOHYDRODYNAMICS
- HYDROXIDES**
- NT SODIUM HYDROXIDES
- HYGROSCOPICITY**
- Hygrothermal damage mechanisms in graphite-epoxy composites
[NASA-CR-3189] p0038 N80-13170
- HYPERGEOMETRIC FUNCTIONS**
- The inversion of singular integral equations by expansion in Jacobi polynomials
p0030 A80-42758
- HYPERSONIC VEHICLES**
- NT M-2F2 LIFTING BODY
- HYPERTHERMIA**
- Fluid-electrolyte shifts and thermoregulation - Rest and work in heat with head cooling
p0091 A80-48086
- HYPERTONIA**
- U OSMOSIS
- HYPERTROPHY**
- U GROWTH
- HYPERVOLEMIA**
- Role of thermal and exercise factors in the mechanism of hypervolemia
p0089 A80-32748
- Exercise training-induced hypervolemia - Role of plasma albumin, renin, and vasopressin
p0089 A80-32749
- HYPODYNAMIA**
- Noninvasive measures of bone bending rigidity in the monkey /M nemestrina/
p0088 A80-21988
- A model for hypokinesia: Effects on muscle atrophy in the rat
p0095 A80-28188
- HYPOKINESIA**
- A model for hypokinesia: Effects on muscle atrophy in the rat
p0095 A80-28188
- HYPOTHALAMUS**
- Changes in body temperature and metabolic rate after injection of calcium into the caudal hypothalamus of the rabbit
p0093 A80-27078
- HYPOTHESES**
- Extracellular hyperosmolality and body temperature during physical exercise in dogs
p0092 A80-54076
- IDENTIFYING**
- NT CROP IDENTIFICATION
- NT SYSTEM IDENTIFICATION
- IFR (RULES)**
- U INSTRUMENT FLIGHT RULES
- IGNEOUS ROCKS**
- NT BASALT
- IGNITION**
- Flash-fire propensity and heat-release rate studies of improved fire resistant materials
p0042 A80-15201
- ILLIAC COMPUTERS**
- NT ILLIAC 4 COMPUTER
- ILLIAC 4 COMPUTER**
- The suitability of the ILLIAC IV architecture for

ILLUSIONS

image processing
 Texture extraction on the ILLIAC 4 --- aerial images [AD-A070523] p0098 A80-22382
 Turbulent structures in wall-bounded shear flows observed via three-dimensional numerical simulators --- using the Illiac 4 computer [NASA-TM-81212] p0098 N80-19471
 [NASA-TM-81212] p0037 N80-29622

ILLUSIONS
 NT OPTICAL ILLUSION

IMAGE MOTION COMPENSATION
 Internal image motion compensation system for the Shuttle Infrared Telescope Facility p0064 A80-37427

IMAGE PROCESSING
 The suitability of the ILLIAC IV architecture for image processing p0098 A80-22382
 Using guided clustering techniques to analyze Landsat data for mapping forest land cover in northern California p0078 A80-25595
 Error detection and rectification in digital terrain models p0099 A80-27432
 Conditional replenishment using motion prediction p0065 A80-39715
 Texture extraction on the ILLIAC 4 --- aerial images [AD-A070523] p0098 N80-19471
 Conference of Remote Sensing Educators (CORSE-78) [NASA-CP-2102] p0034 N80-20003
 Data reduction by computer processing p0058 N80-20016
 Use of collateral information to improve LANDSAT classification accuracies --- Ventura County and Klamath National Forest, California [E80-10268] p0040 N80-29815

IMAGERY
 NT AERIAL PHOTOGRAPHY
 NT ASTRONOMICAL PHOTOGRAPHY
 NT INFRARED PHOTOGRAPHY
 NT RADAR IMAGERY
 NT STEREOPHOTOGRAPHY
 NT ULTRAVIOLET PHOTOMETRY
 NT X RAY IMAGERY

IMAGING TECHNIQUES
 NT RADAR IMAGERY
 A real-time electronic imaging system for solar X-ray observations from sounding rockets p0029 A80-18545
 System description and analysis. Part 1: Feasibility study for helicopter/VTOL wide-angle simulation image generation display system [NASA-CR-152376] p0101 N80-27397
 Effects of magnification and visual accommodation on aimpoint estimation in simulated landings with real and virtual image displays [NASA-TP-1635] p0082 N80-34099

IMMERSION
 U SUBMERGING

IMMITTANCE
 U ELECTRICAL IMPEDANCE

IMMUNITY
 Effect of simulated weightlessness on the immune system in rats p0088 A80-25894

IMPACT PREDICTION
 Comet nucleus impact probe feasibility study [NASA-CR-152375] p0040 N80-26364

IMPACT TESTS
 A small-scale test for fiber release from carbon composites p0062 A80-26881
 A small-scale test for fiber release from carbon composites --- pyrolysis and impact [NASA-TM-81179] p0036 N80-18105

IMPEDANCE
 NT ELECTRICAL IMPEDANCE

IMPEDANCE MATCHING
 'GAIN' - Gas-addition, impedance-matched arc driver --- shock tube gas dynamics p0064 A80-38131

IMPELLER BLADES
 U ROTOR BLADES (TURBOMACHINERY)

IMPERFECTIONS
 U DEFECTS

IMPINGEMENT
 NT JET IMPINGEMENT

SUBJECT INDEX

INCLUSIONS

Carbonaceous chondrites. I - Characterization and significance of carbonaceous chondrite /CN/ xenoliths in the Jodzie howardite p0086 A80-13013

INCOMPRESSIBLE FLOW

Analysis of two-dimensional incompressible flows by a subsurface panel method p0029 A80-30566
 On the numerical solution of time-dependent viscous incompressible fluid flows involving solid boundaries p0052 A80-34980
 Classical aerodynamic theory [NASA-RP-1050] p0001 N80-15033
 Turbulence measurements in the boundary layer of a low-speed wind tunnel using laser velocimetry [NASA-TM-81165] p0008 N80-16300
 A general panel method for the analysis and design of arbitrary configurations in incompressible flows --- boundary value problem [NASA-CR-3079] p0017 N80-24268

INDICATING INSTRUMENTS

NT ATTITUDE INDICATORS
 NT LASER ANEMOMETERS
 NT SPEED INDICATORS

INDIUM ANTIMONIDES

Integrated infrared detector arrays for low-background astronomy p0066 A80-44639

INDIUM COMPOUNDS

NT INDIUM ANTIMONIDES

INDUCED FLUID FLOW

U FLUID FLOW

INDUCTION HEATING

Primordial heating of asteroidal parent bodies p0062 A80-24590

INDUSTRIAL MANAGEMENT

NT INVENTORY MANAGEMENT
 NT PERSONNEL MANAGEMENT

INERT GASES

U RARE GASES

INFINITE SPAN WINGS

Unified aerodynamic-acoustic theory for a thin rectangular wing encountering a gust p0030 A80-36401

INFORMATION RETRIEVAL

Computer-based manuals for procedural information p0096 A80-50427

INFORMATION THEORY

Clarification process: Resolution of decision-problem conditions [NASA-TM-81193] p0103 N80-23985

INFORMATION TRANSMISSION

U DATA TRANSMISSION

INFRARED ABSORPTION

Integrated band intensities of gaseous N₂O/5/ p0047 A80-25660

INFRARED ASTRONOMY

Infrared methane spectra between 1120 per cm and 1800 per cm - A new atlas p0042 A80-13143
 Low-pass interference filters for submillimeter astronomy p0070 A80-19956

Titan aerosols - Optical properties and vertical distribution p0045 A80-21759

Simple Cassegrain scanning system for infrared astronomy p0074 A80-34729

Excitation mechanisms for the unidentified infrared emission features p0054 A80-40642

The spectrum of IRC + 10216 from 2.0 to 8.5 microns p0056 A80-44965

Far-infrared spectra of W51-IRS 2 and W49 NW p0056 A80-44967

One millimeter continuum observations of extragalactic thermal sources [NASA-CR-163590] p0040 N80-33334

INFRARED ASTRONOMY SATELLITE

Simulation of the Infrared Astronomical Satellite /IRAS/ telescope system p0067 A80-49842

INFRARED DETECTORS

Integrated infrared detector arrays for low-background astronomy p0066 A80-44639

SUBJECT INDEX

INTERFEROMETERS

INFRARED FILTERS

Low-pass interference filters for submillimeter astronomy p0070 A80-19956

INFRARED HORIZON SCANNERS

U INFRARED SCANNERS

INFRARED INSTRUMENTS

NT INFRARED DETECTORS

NT INFRARED SCANNERS

INFRARED PHOTOGRAPHY

Diagnosis of separated flow regions on wind-tunnel models using an infrared camera p0025 A80-29494

INFRARED RADIATION

NT FAR INFRARED RADIATION

NT NEAR INFRARED RADIATION

Molecule formation and infrared emission in fast interstellar shocks. I Physical processes p0043 A80-16410

Excitation mechanisms for the unidentified infrared emission features p0054 A80-40642

INFRARED RADIOMETERS

The infrared radiometer on the sounder probe of the Pioneer Venus mission p0050 A80-30847

INFRARED REFLECTION

A far-infrared study of the reflection nebula NGC 2023 p0072 A80-26111

INFRARED SCANNERS

Simple Cassegrain scanning system for infrared astronomy p0074 A80-34729

INFRARED SPECTRA

Infrared methane spectra between 1120 per cm and 1800 per cm - A new atlas p0042 A80-13143

A new atlas of infrared methane spectra between 1120 per cm and 1800 per cm --- Book p0042 A80-15655

Airborne stellar spectrophotometry from 1.2 to 5.5 microns - Absolute calibration and spectra of stars earlier than M3 p0043 A80-16407

Infrared spectra of IC 418 and NGC 6572 p0069 A80-16862

The infrared spectrum of the carbon star Y Canum Venaticorum between 1.2 and 30 microns p0046 A80-22191

Spectroscopic evidence for two achondrite parent bodies - Asteroids 349 Dembowska and 4 Vesta p0072 A80-26173

16-30 micron spectroscopy of Titan p0049 A80-29321

Two micron spectroscopy and 2.7 mm CO line observations of V645 Cygni p0074 A80-35114

Monoceros B2 - Far-infrared observations of a very young cluster p0052 A80-35115

The 16- to 38-micron spectrum of Callisto p0074 A80-35234

The spectrum of IRC + 10216 from 2.0 to 8.5 microns p0056 A80-44965

INFRARED SPECTROSCOPY

Temperature dependence of intensities of the 8-12 micron bands of CFC13 p0045 A80-21559

Band model calculations for CFC13 in the 8-12 micron region p0045 A80-21560

INFRARED TELESCOPES

Design alternatives for the Shuttle Infrared Telescope Facility p0060 A80-17435

Internal image motion compensation system for the Shuttle Infrared Telescope Facility p0064 A80-37427

Thermal design of a Shuttle infrared telescope facility /SIRTF/ [AIAA PAPER 80-1502] p0079 A80-41466

Simulation of the Infrared Astronomical Satellite /IRAS/ telescope system p0067 A80-49842

Control system designs for the shuttle infrared telescope facility [NASA-TM-81159] p0036 N80-18869

INGESTION (BIOLOGY)

NT DRINKING

INITIAL VALUE PROBLEMS

U BOUNDARY VALUE PROBLEMS

INLET FLOW

A diagonal form of an implicit approximate-factorization algorithm with application to a two dimensional inlet [AIAA PAPER 80-0067] p0061 A80-19274

Fan noise caused by the ingestion of anisotropic turbulence - A model based on axisymmetric turbulence theory p0032 A80-35977

Top inlet system feasibility for transonic-supersonic fighter aircraft applications [AIAA PAPER 80-1809] p0033 A80-45735

INORGANIC CHEMISTRY

A model of Martian surface chemistry p0090 A80-36069

INORGANIC COMPOUNDS

NT AMMONIA

INORGANIC PEROXIDES

A model of Martian surface chemistry p0090 A80-36069

The preparation of calcium superoxide in a flowing gas stream and fluidized bed [ASME PAPER 80-ENAS-18] p0094 A80-43194

INSECTS

NT DROSOPHILA

INSTRUCTIONS

U EDUCATION

INSTRUMENT APPROACH

Head-up display in the non-precision approach [NASA-TM-81167] p0084 N80-26296

INSTRUMENT ERRORS

Flight test of navigation and guidance sensor errors measured on STOL approaches [NASA-TM-81154] p0007 N80-13041

INSTRUMENT FLIGHT RULES

Analytical methodology for determination of helicopter IFR precision approach requirements --- pilot workload and acceptance level [NASA-CR-152367] p0040 N80-28330

INSTRUMENT LANDING SYSTEMS

NT AUTOMATIC LANDING CONTROL

INSULIN

Insulin binding and glucose uptake of adipocytes in rats adapted to hypergravitational force p0089 A80-35751

INTAKE SYSTEMS

NT ENGINE INLETS

INTEGRAL EQUATIONS

NT SINGULAR INTEGRAL EQUATIONS

INTEGRATED CIRCUITS

Integrated infrared detector arrays for low-background astronomy p0066 A80-44639

INTEGRODIFFERENTIAL EQUATIONS

U DIFFERENTIAL EQUATIONS

INTEL 8080 MICROPROCESSOR

A microprocessor-based instrument for neural pulse wave analysis p0098 A80-50322

INTELLIGENCE

NT EXTRATERRESTRIAL INTELLIGENCE

INTERACTIVE GRAPHICS

U COMPUTER GRAPHICS

INTERATOMIC FORCES

A calculation of the diffusion energies for adatoms on surfaces of F.C.C. metals p0068 A80-13534

INTERCEPTOR AIRCRAFT

U FIGHTER AIRCRAFT

INTERFERENCE DRAG

Propeller slipstream/wing interaction in the transonic regime [AIAA PAPER 80-0125] p0032 A80-22733

INTERFERENCE LIFT

Phase 1 wind tunnel tests of the J-97 powered, external augmentor V/STOL model [NASA-CR-152255] p0017 N80-28303

INTERFEROMETERS

NT RADIO INTERFEROMETERS

Skin friction measurements by a new nonintrusive double-laser-beam oil viscosity balance technique [AIAA PAPER 80-1373] p0065 A80-41587

Project Orion: A design study of a system for detecting extrasolar planets [NASA-SP-436] p0035 N80-27260

INTERLACING DRAINAGE

SUBJECT INDEX

- INTERLACING DRAINAGE
 - U DRAINAGE PATTERNS
- INTERNAL COMBUSTION ENGINES
 - NT BRISTOL-SIDDELEY BS 53 ENGINE
 - NT TURBOFAN ENGINES
 - NT TURBOJET ENGINES
 - NT TURBOPROP ENGINES
- INTERPLANETARY COMMUNICATION
 - Pioneer Venus multiprobe entry telemetry recovery p0058 N80-26347
- INTERPLANETARY FLIGHT
 - Titan probe technology assessment and technology development plan study [NASA-CR-152381] p0040 N80-32417
- INTERPLANETARY GAS
 - Survival probabilities for interstellar hydrogen flowing into the interplanetary system from far regions of the heliosphere p0076 A80-49217
- INTERPLANETARY MAGNETIC FIELDS
 - The acceleration of energetic charged particles by interplanetary and supernova shock waves p0080 A80-53209
- INTERPLANETARY MEDIUM
 - NT INTERPLANETARY GAS
 - Acceleration of energetic protons by interplanetary shocks p0071 A80-21183
 - A reanalysis of the observed interplanetary hydrogen I alpha emission profiles and the derived local interstellar gas temperature and velocity p0076 A80-49362
- INTERPLANETARY SPACECRAFT
 - NT GALILEO PROBE
 - NT JUPITER PROBES
 - NT PIONEER VENUS SPACECRAFT
 - NT PIONEER VENUS 1 SPACECRAFT
 - NT PIONEER VENUS 2 SOUNDER PROBE
 - NT PIONEER VENUS 2 SPACECRAFT
 - NT PIONEER 10 SPACE PROBE
 - NT VENERA SATELLITES
 - NT VENUS PROBES
 - NT VIKING LANDER SPACECRAFT
- INTERSTELLAR GAS
 - NT NEUTRAL GASES
 - Far infrared, near infrared, and radio molecular line studies of HFE 2, HFE 3, and FJM 6 p0068 A80-11489
 - Molecule formation and infrared emission in fast interstellar shocks. I Physical processes p0043 A80-16410
 - Fragmentation of rotating protostellar clouds p0047 A80-26107
 - Collapsing cloud models for Bok globules p0048 A80-26996
 - The role of magnetic fields in the collapse of protostellar gas clouds p0063 A80-31848
 - Protostellar formation in rotating interstellar clouds. III - Nonaxisymmetric collapse p0054 A80-39375
 - Survival probabilities for interstellar hydrogen flowing into the interplanetary system from far regions of the heliosphere p0076 A80-49217
 - Numerical calculations of the collapse of nonrotating, magnetic gas clouds p0057 A80-49341
 - A reanalysis of the observed interplanetary hydrogen I alpha emission profiles and the derived local interstellar gas temperature and velocity p0076 A80-49362
- INTERSTELLAR MAGNETIC FIELDS
 - The role of magnetic fields in the collapse of protostellar gas clouds p0063 A80-31848
 - Numerical calculations of the collapse of nonrotating, magnetic gas clouds p0057 A80-49341
- INTERSTELLAR MATTER
 - A reconsideration of nucleation phenomena in light of recent findings concerning the properties of small clusters, and a brief review of some other particle growth processes --- for cosmic dust p0069 A80-15609
 - Discovery of optical molecular emission from the bipolar nebula surrounding HD 44179
- Comets: Cosmic connections with carbonaceous meteorites, interstellar molecules and the origin of life p0058 A80-52399
- INTRACRANIAL PRESSURE
 - Induction powered biological radiosonde [NASA-CASE-ARC-11120-1] p0099 N80-18691
- INVENTORIES
 - NT CROP INVENTORIES
 - NT TIMBER INVENTORY
- INVENTORY MANAGEMENT
 - Factors affecting the retirement of commercial transport jet aircraft [NASA-CR-152308] p0013 N80-10148
- INVERSIONS
 - NT CENTRIFUGING STRESS
- INVERTEBRATES
 - NT DROSOPHILA
- INVESTIGATION
 - NT ACCIDENT INVESTIGATION
 - NT AIRCRAFT ACCIDENT INVESTIGATION
- INVISCID FLOW
 - Propeller slipstream/wing interaction in the transonic regime [AIAA PAPER 80-0125] p0032 A80-22733
 - An implicit finite-difference code for inviscid and viscous cascade flow [AIAA PAPER 80-1427] p0066 A80-44128
 - A computational and experimental study of high Reynolds number viscous/inviscid interaction about a cone at high angle of attack [AIAA PAPER 80-1422] p0104 A80-44492
- ION CONCENTRATION
 - The intracellular Na⁺/K⁺ composition of the moderately halophilic bacterium, Paracoccus halodenitrificans p0091 A80-41250
- ION PUMPS
 - Proton movements in response to a light-driven electrogenic pump for sodium ions in Halobacterium halobium membranes p0087 A80-17686
- IONIC MOBILITY
 - The role of Na⁺/K⁺ in transport processes of bacterial membranes p0088 A80-27077
- IONIC REACTIONS
 - Properties of clusters in the gas phase. V - Complexes of neutral molecules onto negative ions p0057 A80-50144
- IONIZATION
 - NT GAS IONIZATION
 - NT PHOTOIONIZATION
- IONIZATION CROSS SECTIONS
 - Photoexcitation and ionization in molecular oxygen - Theoretical studies of electronic transitions in the discrete and continuous spectral intervals p0044 A80-20275
- IONIZED GASES
 - NT CATIONS
 - NT CHARGED PARTICLES
 - NT COSMIC PLASMA
 - NT PLASMA CLOUDS
 - NT RAREFIED PLASMAS
 - NT SOLAR WIND
 - NT STELLAR WINDS
 - NT THERMAL PLASMAS
 - New gas phase inorganic ion cluster species and their atmospheric implications p0075 A80-37510
- IONIZING RADIATION
 - NT COSMIC RAYS
 - NT GAMMA RAYS
 - NT LYMAN ALPHA RADIATION
 - NT SOLAR X-RAYS
 - NT ULTRAVIOLET RADIATION
- IONOSPHERE
 - The location of the dayside ionopause of Venus - Pioneer Venus Orbiter magnetometer observations p0076 A80-48811
- IONOSPHERIC ABSORPTION
 - U ELECTROMAGNETIC ABSORPTION
- IONOSPHERIC COMPOSITION
 - Pioneer Venus Orbiter planar retarding potential analyzer plasma experiment p0073 A80-30839
- IONS
 - NT CATIONS

SUBJECT INDEX

KIRCHHOFF-HELMHOLTZ FLOW

NT HYDROGEN IONS
 NT METAL IONS
 NT NEGATIVE IONS
 NT NITROGEN IONS
 NT POSITIVE IONS
 NT PROTONS
 IP (IMPACT PREDICTION)
 U COMPUTERIZED SIMULATION
 IRAS
 U INFRARED ASTRONOMY SATELLITE
 IROQUOIS HELICOPTER
 U UH-1 HELICOPTER
 IRRIGATION
 Landsat-based multiphase estimation of
 California's irrigated lands p0079 A80-27435
 Irrigated lands assessment for water management
 Applications Pilot Test (APT) --- California
 [E80-10324] p0019 N80-32815
 IRROTATIONAL FLOW
 U POTENTIAL FLOW
 ISING MODEL
 U MATHEMATICAL MODELS
 ISLANDS
 NT HAWAII
 ISOMERS
 Differentiation of optical isomers through
 enhanced weak-field interactions
 [NASA-TM-81208] p0084 N80-27164
 ISOTOPEs
 NT CARBON ISOTOPEs
 NT RADIOACTIVE ISOTOPEs
 ITERATION
 Automated design using numerical optimization
 [SAE PAPER 791061] p0024 A80-26628

J

JACOBI POLYNOMIALS
 U HYPERGEOMETRIC FUNCTIONS
 JET AIRCRAFT
 NT B-70 AIRCRAFT
 NT C-8A AUGMENTOR WING AIRCRAFT
 NT C-135 AIRCRAFT
 VTOL in-ground effect flows for closely spaced jets
 [AIAA PAPER 80-1880] p0033 A80-46693
 Factors affecting the retirement of commercial
 transport jet aircraft
 [NASA-CR-152308] p0013 N80-10148
 JET AIRCRAFT NOISE
 Strouhal number influence on flight effects on jet
 noise radiated from convecting quadrupoles
 p0022 A80-28418
 Analytical study of the effects of wind tunnel
 turbulence on turbofan rotor noise
 [AIAA PAPER 80-1022] p0033 A80-35978
 An experimental study of the structure and
 acoustic field of a jet in a cross stream ---
 Ames 7-ft by 10-ft wind tunnel tests
 [NASA-CR-162464] p0014 N80-15871
 JET AUGMENTED WING FLAPS
 U WING FLAPS
 JET ENGINES
 NT BRISTOL-SIDDELEY BS 53 ENGINE
 NT TURBOFAN ENGINES
 NT TURBOJET ENGINES
 NT TURBOPROP ENGINES
 JET EXHAUST
 Introductory study of the chemical behavior of jet
 emissions in photochemical smog --- computerized
 simulation
 [NASA-CR-152345] p0016 N80-21891
 Static calibration of a two-dimensional wedge
 nozzle with thrust vectoring and spanwise blowing
 [NASA-TM-81161] p0009 N80-23317
 Reduction of nitric oxide emissions from a combustor
 [NASA-CASE-ARC-10814-2] p0080 N80-26298
 JET FLAMES
 U JET FLOW
 JET FLIGHT
 U JET AIRCRAFT
 JET FLOW
 Strouhal number influence on flight effects on jet
 noise radiated from convecting quadrupoles
 p0022 A80-28418
 Aerodynamic interactions from reaction controls
 for lateral control of the M2-F2 lifting-body
 entry configuration at transonic and supersonic
 and supersonic Mach numbers --- wind tunnel tests

[NASA-TM-78534] p0006 N80-11033
 Vorticity associated with multiple jets in a
 crossflow --- vertical takeoff aircraft
 [NASA-CR-162855] p0016 N80-19454
 An experimental study of multiple jet mixing
 [NASA-CR-166184] p0018 N80-31760
 Modal content of noise generated by a coaxial jet
 in a pipe
 [NASA-CR-163575] p0019 N80-33177
 JET IMPINGEMENT
 Upper surface blowing noise of the NASA-Ames quiet
 short-haul research aircraft
 [AIAA PAPER 80-1064] p0026 A80-36002
 VTOL in-ground effect flows for closely spaced jets
 [AIAA PAPER 80-1880] p0033 A80-46693
 JET NOISE
 U JET AIRCRAFT NOISE
 JET PILOTS
 U AIRCRAFT PILOTS
 JET THRUST
 Aerodynamic interactions from reaction controls
 for lateral control of the M2-F2 lifting-body
 entry configuration at transonic and supersonic
 and supersonic Mach numbers --- wind tunnel tests
 [NASA-TM-78534] p0006 N80-11033
 JETAVATORS
 U GUIDE VANES
 JITTER
 U VIBRATION
 JUPITER (PLANET)
 The phase of the ten-hour modulation in the Jovian
 magnetosphere /Pioneers 10 and 11/ p0067 A80-10526
 The effect of dense cores on the structure and
 evolution of Jupiter and Saturn p0056 A80-45812
 21 cm maps of Jupiter's radiation belts from all
 rotational aspects p0076 A80-48877
 Azimuthal magnetic field at Jupiter p0076 A80-49185
 JUPITER ATMOSPHERE
 Measurements of wind vectors, eddy momentum
 transports, and energy conversions in Jupiter's
 atmosphere from Voyager 1 images A80-24159
 The propagation of Jovian electrons to earth p0074 A80-36356
 Shock-tube studies of radiative base heating of
 Jovian probe p0064 A80-38114
 Modeling Jupiter's current disc - Pioneer 10
 outbound p0075 A80-45153
 JUPITER PROBES
 NT GALILEO PROBE
 A technique for evaluating the Jovian entry-probe
 heat-shield material with a gasdynamic laser p0063 A80-29479
 JUPITER RINGS
 Modeling Jupiter's current disc - Pioneer 10
 outbound p0075 A80-45153

K

KALMAN FILTERS
 Optimal estimator model for human spatial
 orientation p0093 A80-24265
 KAPTON (TRADEMARK)
 Plasma etching of poly(N,N'-p,p'-
 oxydiphenylene/pyromellitimide/ film and
 photo/thermal degradation of etched and unetched
 film p0093 A80-24158
 KC-135 AIRCRAFT
 U C-135 AIRCRAFT
 KERNEL FUNCTIONS
 Reformulation of Possio's kernel with application
 to unsteady wind tunnel interference p0031 A80-43129
 KINETIC HEATING
 NT AERODYNAMIC HEATING
 NT SHOCK HEATING
 KINETICS
 NT REACTION KINETICS
 KIRCHHOFF-HELMHOLTZ FLOW
 U PIPE FLOW

KIRCHHOFF-HUYGENS PRINCIPLE

SUBJECT INDEX

KIRCHHOFF-HUYGENS PRINCIPLE
U WAVE PROPAGATION

L

LABORATORY EQUIPMENT

The development of a Space Shuttle Research Animal
Holding Facility
[ASME PAPER 80-ENAS-39] p0096 A80-43213

LAG (DELAY)

U TIME LAG

LAGRANGE EQUATIONS OF MOTION

U EULER-LAGRANGE EQUATION

LAMINAR BOUNDARY LAYER

Asymptotic features of shock-wave boundary-layer
interaction p0055 A80-43135
Vortex simulation of three-dimensional, spotlike
disturbances in a laminar boundary layer p0067 A80-49296

LAMINAR BOUNDARY LAYER SEPARATION

U LAMINAR BOUNDARY LAYER

LAMINAR PLANES

U LAMINAR FLOW

LAMINAR FLOW

Relaminarization of fluid flows p0075 A80-40843
Pressure measurements on an ogive-cylinder at high
angles of attack with laminar, transitional, or
turbulent separation [AIAA 80-1556] p0028 A80-45856

LAMINAR FLOW CONTROL

U BOUNDARY LAYER CONTROL

U LAMINAR BOUNDARY LAYER

LAMINAR JETS

U JET FLOW

U LAMINAR FLOW

LAMINATED MATERIALS

U LAMINATES

LAMINATES

A temperature dependent fatigue failure criterion
for graphite/epoxy laminates p0060 A80-15518
Oxygen index tests of thermosetting resins p0044 A80-21448
Release-rate calorimetry of multilayered materials
for aircraft seats [AIAA 80-0759] p0064 A80-35052
The viscoelastic behavior of a composite in a
thermal environment [NASA-CR-163187] p0039 A80-24369

LAMINATIONS

U LAMINATES

LAND

NT FARMLANDS

NT GRASSLANDS

NT PLAINS

LAND USE

Landsat-based multiphase estimation of
California's irrigated lands p0079 A80-27435
Use of collateral information to improve LANDSAT
classification accuracies --- Ventura County and
Klamath National Forest, California [E80-10268] p0040 A80-29815
Irrigated lands assessment for water management
Applications Pilot Test (APT) --- California
[E80-10324] p0019 A80-32815

LANDFORMS

NT DUNES

NT HAWAII

NT MOUNTAINS

NT PANAMA CANAL ZONE

NT VOLCANOES

LANDING

NT AIRCRAFT LANDING

NT VERTICAL LANDING

LANDING AIDS

NT AUTOMATIC LANDING CONTROL

A simulator study of control and display
augmentations for helicopters [NASA-CR-163451] p0018 A80-31408

LANDING SIMULATION

Optimal washout for control of a moving base
simulator --- vertical motion flight simulation
using linear filter p0031 A80-14833
Analytical methodology for determination of
helicopter IFR precision approach requirements

--- pilot workload and acceptance level
[NASA-CR-152367] p0040 A80-28330

A piloted simulator analysis of the carrier
landing capability of the quiet short-haul
research aircraft [NASA-TN-78508] p0011 A80-28338

Effects of magnification and visual accommodation
on aimpoint estimation in simulated landings
with real and virtual image displays [NASA-TP-1635] p0082 A80-34099

LANDING SYSTEMS

U LANDING AIDS

LARGE SPACE STRUCTURES

SOLARES orbiting mirror system [AAS 79-304] p0067 A80-52280

Large Deployable Reflector (LDR) [NASA-CR-152402] p0040 A80-33319

LASER ANEMOMETERS

High-resolution LDA measurements of Reynolds
stress in boundary layers and wakes [AIAA 80-0436] p0025 A80-26967

LASER APPLICATIONS

Skin friction measurements by a new nonintrusive
double-laser-beam oil viscosity balance technique [AIAA PAPER 80-1373] p0065 A80-41587

LASER DOPPLER VELOCIMETERS

High-resolution LDA measurements of Reynolds
stress in boundary layers and wakes [AIAA 80-0436] p0025 A80-26967
Application of laser velocimetry to an unsteady
transonic flow p0063 A80-29506

Turbulence measurements in the boundary layer of a
low-speed wind tunnel using laser velocimetry [NASA-TN-81165] p0008 A80-16300

LASER OUTPUTS

An angular momentum approximation for molecular
collisions in the presence of intense laser
radiation p0069 A80-15673

LASER PUMPING

Quantum-mechanical calculation of
three-dimensional atom-diatom collisions in the
presence of intense laser radiation p0068 A80-15221

LASERS

NT CHEMICAL LASERS

NT DYE LASERS

NT GASDYNAMIC LASERS

NT HF LASERS

NT NEODYMIUM LASERS

Optimized laser turrets for minimum phase distortion p0023 A80-25600

LATE STARS

Comparison of predicted and observed spectral
energy distribution of K and M stars. I - Alpha
Bootis p0046 A80-22194

LATERAL CONTROL

Aerodynamic interactions from reaction controls
for lateral control of the M2-F2 lifting-body
entry configuration at transonic and supersonic
and supersonic Mach numbers --- wind tunnel tests
[NASA-TN-78534] p0006 A80-11033

LATERALIZATION

U LATERAL CONTROL

LAVA

Endogenic craters on basaltic lava flows - Size
frequency distributions p0061 A80-23727

LAWS

NT CONSERVATION LAWS

LEARNING

NT TRANSFER OF TRAINING

LEAST SQUARES METHOD

Some observations regarding the statistical
determination of stress rupture regression lines p0041 A80-12828
On the Routh approximation technique and least
squares errors p0032 A80-20873

LEVEL (QUANTITY)

NT ELECTRON STATES

NT GROUND STATE

NT MOLECULAR ENERGY LEVELS

LIFE (BIOLOGY)

U LIFE SCIENCES

LIFE (DURABILITY)

NT SERVICE LIFE

SUBJECT INDEX

LIQUID HELIUM

NT STORAGE STABILITY
LIFE SCIENCES
 NT EXTRATERRESTRIAL LIFE
 Physical chemistry and evolution of salt tolerance
 in halobacteria p0090 A80-40383
 The intracellular Na⁺/ and K⁺/ composition of
 the moderately halophilic bacterium, *Paracoccus*
halodenitrificans p0091 A80-41250
 NASA-Ames Life Sciences Flight Experiments program
 - 1980 status report p0094 A80-43209
 [ASME PAPER 80-ENAS-34]
 Comets: Cosmic connections with carbonaceous
 meteorites, interstellar molecules and the
 origin of life p0092 N80-11975
LIFE SUPPORT SYSTEMS
 NT CLOSED ECOLOGICAL SYSTEMS
 NT PORTABLE LIFE SUPPORT SYSTEMS
 Bosch - An alternate CO2 reduction technology
 [ASME PAPER 79-ENAS-32] p0092 A80-15256
 Guiding the development of a controlled ecological
 life support system p0085 N80-12735
 [NASA-CR-162452]
 Development of a nitrogen generation system
 [NASA-CR-152333] p0085 N80-19800
LIFT
 NT INTERFERENCE LIFT
 NT ROTOR LIFT
 Lifting three-dimensional wings in transonic flow
 p0071 A80-20331
 Unified treatment of lifting atmospheric entry
 p0048 A80-28027
 Wing flapping with minimum energy --- minimize the
 drag for a bending moment at the wing root
 [NASA-TM-81174] p0001 N80-16035
 A comparison of calculated and experimental lift
 and pressure distributions for several
 helicopter rotor sections p0007 N80-16036
 [NASA-TM-81160]
 A summary of joint US-Canadian augmentor wing
 powered-lift STOL research programs at the Ames
 Research Center, NASA, 1975-1980 p0011 N80-28373
 [NASA-TM-81215]
 A comparison of flight and simulation data for
 three automatic landing system control laws for
 the Augmentor wing jet STOL research airplane
 [NASA-CR-152365] p0018 N80-32338
LIFT AUGMENTATION
 Conceptual studies of a long-range transport with
 an upper surface blowing propulsive lift system
 [NASA-TM-81196] p0009 N80-23249
 Large-scale wind-tunnel tests of inverting flaps
 on a STOL utility aircraft model p0005 N80-25318
 [NASA-TP-1696]
LIFT COEFFICIENTS
 U AERODYNAMIC COEFFICIENTS
 U LIFT
LIFT DISTRIBUTION
 U FORCE DISTRIBUTION
 U LIFT
LIFT FANS
 Investigation of ground effects on large and small
 scale models of a three fan V/STOL aircraft
 configuration p0015 N80-16030
 [NASA-CR-152240]
LIFT FORCES
 U LIFT
LIFTING BODIES
 NT M-2F2 LIFTING BODY
LIFTING REENTRY VEHICLES
 NT M-2F2 LIFTING BODY
LIFTING ROTORS
 Effect of tip vortex structure on helicopter noise
 due to blade-vortex interaction p0031 A80-52645
LIGHT ABSORPTION
 U ELECTROMAGNETIC ABSORPTION
LIGHT AIRCRAFT
 NT OH-6 HELICOPTER
LIGHT EMISSION
 NT FLUORESCENCE
LIGHT SCATTERING
 Scattering by non-spherical particles of size
 comparable to a wavelength - A new
 semi-empirical theory p0063 A80-34050

Scattering by nonspherical particles of size
 comparable to wavelength - A new semi-empirical
 theory and its application to tropospheric
 aerosols p0052 A80-36040
 Asymptotic behavior of the efficiencies in Mie
 scattering p0031 A80-47048
 Feasibility studies for light scattering
 experiments to determine the velocity relaxation
 of small particles in a fluid
 [NASA-CR-163214] p0040 N80-25586
LIGHT TRANSMISSION
 NT LIGHT SCATTERING
 Optimized laser turrets for minimum phase distortion
 p0023 N80-25600
LIGHT TRANSPORT AIRCRAFT
 Toward new small transports for commuter airlines
 p0021 A80-21224
 Small Transport Aircraft Technology p0021 A80-21225
LINE
 U CALCIUM OXIDES
LINE SPECTRA
 NT H LINES
 A new atlas of infrared methane spectra between
 1120 per cm and 1800 per cm --- Book p0042 A80-15655
 The implications of hydrogen emission line ratios
 in quasi-stellar objects p0072 A80-27013
 Two micron spectroscopy and 2.7 mm CO line
 observations of V645 Cygni p0074 A80-35114
 Radiatively driven winds for different power law
 spectra --- for explaining narrow and broad
 quasar absorption lines p0054 A80-40138
 An optical emission-line phase of the extreme
 carbon star IRC +30219 p0056 A80-44993
 Curves of growth for van der Waals broadened
 spectral lines p0057 A80-51378
LINEAMENT
 U STRUCTURAL PROPERTIES (GEOLOGY)
LINEAR EQUATIONS
 Alternating direction implicit methods for
 parabolic equations with a mixed derivative
 p0057 A80-51050
LINEAR FILTERS
 NT KALMAN FILTERS
 Optimal washout for control of a moving base
 simulator --- vertical motion flight simulation
 using linear filter p0031 A80-14833
LINEAR PREDICTION
 Optimal estimator model for human spatial
 orientation p0093 A80-24265
LINEAR SYSTEMS
 On the Routh approximation technique and least
 squares errors p0032 A80-20873
 A scaling theory for linear systems p0030 A80-32676
 System theory as applied differential geometry ---
 linear system p0013 N80-12776
 [NASA-CR-3209]
LINEARITY
 Characterization of acoustic disturbances in
 linearly sheared flows p0014 N80-15869
 [NASA-CR-162577]
LINEARIZATION
 Feedback invariants for nonlinear systems
 p0031 A80-14810
LIQUEFIED GASES
 NT LIQUID HELIUM
 NT LIQUID HELIUM 2
 NT LIQUID NITROGEN
LIQUID COOLING
 Thermal design of a Shuttle infrared telescope
 facility /SIRTF/
 [AIAA PAPER 80-1502] p0079 A80-41466
LIQUID HELIUM
 NT LIQUID HELIUM 2
 Design of a one-year lifetime, spaceborne
 superfluid helium dewar
 [ASME PAPER 79-ENAS-23] p0077 A80-15247

LIQUID HELIUM 2

SUBJECT INDEX

LIQUID HELIUM 2
 Second sound shock waves and critical velocities
 in liquid helium 2
 [NASA-CR-162687] p0015 N80-16837

LIQUID NITROGEN
 Long term tests of the HEPP liquid trap diode heat
 pipe prototype
 [NASA-CR-152358] p0039 N80-22635

LIQUID WASTES
 NT URINE

LIQUID-GAS MIXTURES
 NT AEROSOLS

LIQUIDS
 NT LIQUID HELIUM
 NT LIQUID NITROGEN

LITHOSPHERE
 NT EARTH CORE
 NT EARTH MANTLE
 NT EARTH SURFACE

LOAD DISTRIBUTION (FORCES)
 Multicyclic control of a helicopter rotor
 considering the influence of vibration, loads,
 and control motion
 [AIAA 80-0673] p0025 A80-34998

LOAD FACTORS
 U LOADS (FORCES)

LOADING FORCES
 U LOADS (FORCES)

LOADING MOMENTS
 Comparison of calculated and measured blade loads
 on a full-scale tilting propotor in a wind tunnel
 [NASA-TM-81228] p0012 N80-31386

LOADING WAVES
 U LOADS (FORCES)

LOADS (FORCES)
 NT AERODYNAMIC LOADS
 NT GUST LOADS
 NT VIBRATORY LOADS
 Equations for determining aircraft motions for
 accident data
 [NASA-TM-78609] p0010 N80-25306
 A comprehensive analytical model of rotorcraft
 aerodynamics and dynamics. Part 2: User's manual
 [NASA-TM-81183] p0010 N80-28297

LOGISTICS MANAGEMENT
 NT INVENTORY MANAGEMENT

LOH HELICOPTER
 U OH-6 HELICOPTER

LONGITUDINAL CONTROL
 The design, testing and evaluation of the MIT
 individual-blade-control system as applied to
 gust alleviation for helicopters
 [NASA-CR-152352] p0016 N80-22357
 A comparison of flight and simulation data for
 three automatic landing system control laws for
 the Augmentor wing jet STOL research airplane
 [NASA-CR-152365] p0018 N80-32338

LONGITUDINAL WAVES
 NT PLANE WAVES

LOW ASPECT RATIO WINGS
 NT DELTA WINGS

LOW DENSITY MATERIALS
 Catalysts for polyimide foams from aromatic
 isocyanates and aromatic dianhydrides --- flame
 retardant foams
 [NASA-CASE-ARC-11107-1] p0080 N80-16116

LOW PASS FILTERS
 Low-pass interference filters for submillimeter
 astronomy p0070 A80-19956

LOW SPEED WIND TUNNELS
 NT SUBSONIC WIND TUNNELS

LOW VISIBILITY
 Head-up transition behavior of pilots during
 simulated low-visibility approaches
 [NASA-TP-1618] p0082 N80-26039

LOWER ATMOSPHERE
 NT OZONOSPHERE
 NT TROPOSPHERE

LOWER BODY NEGATIVE PRESSURE (LBNP)
 U ACCELERATION STRESSES (PHYSIOLOGY)

LRC CIRCUITS
 U RLC CIRCUITS

LUMBERING AREAS
 U FORESTS

LUMINESCENCE
 NT FLUORESCENCE

LUMINOSITY
 NT STELLAR LUMINOSITY

LUNAR CRATERS
 Monte Carlo simulation of lunar megaregolith and
 implications p0061 A80-23716
 Endogenic craters on basaltic lava flows - Size
 frequency distributions p0061 A80-23727

LUNAR CRUST
 Theories for the origin of lunar magnetism
 p0044 A80-19397

LUNAR EVOLUTION
 Monte Carlo simulation of lunar megaregolith and
 implications p0061 A80-23716

LUNAR MAGNETIC FIELDS
 Theories for the origin of lunar magnetism
 p0044 A80-19397
 Electrical conductivity anomalies associated with
 circular lunar maria p0061 A80-23691

LUNAR MANTLE
 Whole planet cooling and the radiogenic heat
 source contents of the earth and moon
 p0053 A80-36651

LUNAR MARIA
 Electrical conductivity anomalies associated with
 circular lunar maria p0061 A80-23691

LUNAR OCCULTATION
 NT SOLAR ECLIPSES

LUNAR SURFACE
 Monte Carlo simulation of lunar megaregolith and
 implications p0061 A80-23716

LYMAN ALPHA RADIATION
 High-resolution Lyman-alpha filtergrams of the sun
 p0075 A80-37277
 A reanalysis of the observed interplanetary
 hydrogen I alpha emission profiles and the
 derived local interstellar gas temperature and
 velocity p0076 A80-49362

M

M STARS
 Comparison of predicted and observed spectral
 energy distribution of K and M stars. I - Alpha
 Bootis p0046 A80-22194

M-2 LIFTING BODY
 NT M-2F2 LIFTING BODY

M-2F2 LIFTING BODY
 Aerodynamic interactions from reaction controls
 for lateral control of the M2-F2 lifting-body
 entry configuration at transonic and supersonic
 and supersonic Mach numbers --- wind tunnel tests
 [NASA-TM-78534] p0006 N80-11033

MACHINE LIFE
 U SERVICE LIFE

MACROCLIMATE
 U CLIMATE

MACROMOLECULES
 U MOLECULES

MAGNESIUM
 Microbial mobilization of calcium and magnesium in
 waterlogged soils p0089 A80-32834

MAGNETIC ABSORPTION
 U ELECTROMAGNETIC ABSORPTION

MAGNETIC ANOMALIES
 Electrical conductivity anomalies associated with
 circular lunar maria p0061 A80-23691

MAGNETIC DISTURBANCES
 Are solar spectral variations a drive for climatic
 change p0042 A80-15488

MAGNETIC FIELD CONFIGURATIONS
 Azimuthal magnetic field at Jupiter p0076 A80-49185

MAGNETIC FIELD INTENSITY
 U MAGNETIC FLUX

MAGNETIC FIELDS
 NT INTERPLANETARY MAGNETIC FIELDS
 NT INTERSTELLAR MAGNETIC FIELDS
 NT LUNAR MAGNETIC FIELDS
 NT PLANETARY MAGNETIC FIELDS
 NT SOLAR MAGNETIC FIELD

SUBJECT INDEX

MARS SURFACE SAMPLES

- An ab initio calculation of the zero-field splitting parameters of the 3A-double prime state of formaldehyde
p0056 A80-45333
- Differentiation of optical isomers through enhanced weak-field interactions
[NASA-TM-81208] p0084 N80-27164
- MAGNETIC FLUX**
X-ray bright points and the solar cycle dependence of emerging magnetic flux
p0077 N80-17950
- MAGNETIC PROPERTIES**
NT CURIE TEMPERATURE
NT REMANENCE
Theories for the origin of lunar magnetism
p0044 A80-19397
- MAGNETICALLY TRAPPED PARTICLES**
NT RADIATION BELTS
- MAGNETIZATION**
Theories for the origin of lunar magnetism
p0044 A80-19397
- MAGNETOGASDYNAMICS**
U MAGNETOHYDRODYNAMICS
MAGNETOHYDRODYNAMIC WAVES
NT PLASMA WAVES
MAGNETOHYDRODYNAMICS
Numerical calculations of the collapse of nonrotating, magnetic gas clouds
p0057 A80-49341
- MAGNETOMETERS**
The location of the dayside ionopause of Venus - Pioneer Venus Orbiter magnetometer observations
p0076 A80-48811
- MAGNETOSPHERE**
The phase of the ten-hour modulation in the Jovian magnetosphere /Pioneers 10 and 11/
p0067 A80-10526
Preliminary results on the plasma environment of Saturn from the Pioneer 11 plasma analyzer experiment
p0043 A80-19116
Saturn's magnetic field and magnetosphere
p0021 A80-19117
Saturn's magnetosphere, rings, and inner satellites
p0070 A80-19119
Trapped radiation belts of Saturn - First look
p0070 A80-19121
- MAGNUS EFFECT**
Computations of the Magnus effect for slender bodies in supersonic flow
[AIAA 80-1586] p0028 A80-45882
- MANUALS**
NT DOGS
NT MICE
- MAN ENVIRONMENT INTERACTIONS**
Nitrogen fertiliser and stratospheric ozone - Latitudinal effects
p0043 A80-18948
- MAN MACHINE SYSTEMS**
A pilot modeling technique for handling-qualities research
[AIAA 80-1624] p0028 A80-45912
Multi-modal information processing for visual workload relief
[NASA-CR-162720] p0100 N80-16737
The effect of viewing time, time to encounter, and practice on perception of aircraft separation on a cockpit display of traffic information
[NASA-TM-81173] p0083 N80-18038
Head-up transition behavior of pilots during simulated low-visibility approaches
[NASA-TP-1618] p0082 N80-26039
Flight-deck automation: Promises and problems
[NASA-TM-81206] p0084 N80-26040
Results of a simulator investigation of control system and display variations for an attack helicopter mission
[AD-A085812] p0101 N80-29370
- MANAGEMENT**
NT CONFIGURATION MANAGEMENT
NT DATA MANAGEMENT
NT INVENTORY MANAGEMENT
NT PERSONNEL MANAGEMENT
NT RESOURCES MANAGEMENT
NT SYSTEMS MANAGEMENT
NT WATER MANAGEMENT
- MANAGEMENT PLANNING**
NT PROJECT PLANNING
- MANEUVERABLE SPACECRAFT**
NT M-2F2 LIFTING BODY
- MANEUVERS**
NT AIRCRAFT MANEUVERS
- MANNED SPACE FLIGHT**
Development of a nitrogen generation system
[NASA-CR-152333] p0085 N80-19800
- MANNED SPACECRAFT**
NT SPACE SHUTTLES
- MANTLE (EARTH STRUCTURE)**
U EARTH MANTLE
- MANUAL CONTROL**
NT VISUAL CONTROL
Dynamic decisions and work load in multitask supervisory control
p0095 A80-40898
Optimal control model predictions of system performance and attention allocation and their experimental validation in a display design study
p0095 A80-40899
Pilot control through the TAF COS automatic flight control system
[NASA-TM-81152] p0007 N80-14138
- MANUALS**
NT USER MANUALS (COMPUTER PROGRAMS)
Computer-based manuals for procedural information
p0096 A80-50427
- MAPPING**
NT PHOTOMAPPING
NT PLANETARY MAPPING
NT THEMATIC MAPPING
NT THERMAL MAPPING
Automatic mesh-point clustering near a boundary in grid generation with elliptic partial differential equations
p0044 A80-20593
- MAPS**
NT RADAR MAPS
- MARIA**
NT LUNAR MARIA
- MARINE BIOLOGY**
Microbial sulfate reduction measured by an automated electrical impedance technique
p0087 A80-21982
- MARINE GEOLOGY**
U HYDROGEOLOGY
- MARS ATMOSPHERE**
High-resolution Martian atmosphere modeling
p0071 A80-21765
Mars - The north polar sand sea and related wind patterns
p0047 A80-26370
Heterogeneous phase reactions of Martian volatiles with putative regolith minerals
p0090 A80-36062
- MARS ENVIRONMENT**
NT MARS ATMOSPHERE
Mars ultraviolet simulation facility
p0089 A80-36061
- MARS PROBES**
NT VIKING LANDER SPACECRAFT
- MARS SURFACE**
Silt-clay aggregates on Mars
p0041 A80-10366
The Viking mission and the search for life on Mars
p0086 A80-10738
Eolian sedimentation on earth and Mars - Some comparisons
p0068 A80-13969
Plains and channels in the Lunae Planum-Chryse Planitia region of Mars
p0047 A80-26358
Mars - The north polar sand sea and related wind patterns
p0047 A80-26370
Threshold windspeeds for sand on Mars - Wind tunnel simulations
p0048 A80-27391
Heterogeneous phase reactions of Martian volatiles with putative regolith minerals
p0090 A80-36062
Simulation of the Viking biology experiments - An overview
p0090 A80-36066
Volcanic features of Hawaii. A basis for comparison with Mars
[NASA-SP-403] p0034 N80-23912
- MARS SURFACE SAMPLES**
Mars ultraviolet simulation facility

MASS SPECTRA

SUBJECT INDEX

A model of Martian surface chemistry p0089 A80-36061
 New gas phase inorganic ion cluster species and their atmospheric implications p0090 A80-36069
MASS SPECTRA
 Data acquisition techniques for exploiting the uniqueness of the time-of-flight mass spectrometer: Application to sampling pulsed gas systems p0075 A80-37510
 [NASA-TM-81224] p0037 N80-31775
MASS SPECTROMETERS
 Pioneer Venus Sounder Probe Neutral Gas Mass Spectrometer p0073 A80-30844
MATERIAL ABSORPTION
 Adsorption interference in mixtures of trace contaminants flowing through activated carbon adsorber beds p0096 A80-43193
 [ASHE PAPER 80-ENAS-17]
MATERIALS RECOVERY
 NT WATER RECLAMATION
MATHEMATICAL LOGIC
 NT ALGORITHMS
MATHEMATICAL MODELS
 NT DIGITAL SIMULATION
 An angular momentum approximation for molecular collisions in the presence of intense laser radiation p0069 A80-15673
 On the Routh approximation technique and least squares errors p0032 A80-20873
 Implicit model following and parameter identification of unstable aircraft p0022 A80-28019
 Whole planet cooling and the radiogenic heat source contents of the earth and moon p0053 A80-36651
 Fragmentation in a rotating protostar - A comparison of two three-dimensional computer codes p0053 A80-38432
 Meteorological and air pollution modeling for an urban airport p0055 A80-42659
 Mathematical modeling of the aerodynamics of high-angle-of-attack maneuvers p0028 A80-45879
 [AIAA 80-1583]
 Math modeling and computer mechanization for real time simulation of rotary-wing aircraft p0013 N80-10137
 [NASA-CR-162400]
 Coupled rotor and fuselage equations of motion p0006 N80-10516
 [NASA-TM-81153]
 Modular theory of inverse systems p0013 N80-12782
 [NASA-CR-162491]
 A three dimensional vortex wake model for missiles at high angles on attack p0014 N80-14048
 [NASA-CR-3208]
 Studies in astronomical time series analysis: Modeling random processes in the time domain p0036 N80-15854
 [NASA-TM-81148]
 Progress in turbulence modeling for complex flow fields including effects of compressibility p0034 N80-20527
 [NASA-TP-1517]
 Simple turbulence models and their application to boundary layer separation p0017 N80-24269
 [NASA-CR-3283]
 A comprehensive analytical model of rotorcraft aerodynamics and dynamics. Part 1: Analysis development p0010 N80-28296
 [NASA-TM-81182]
 A piloted simulator analysis of the carrier landing capability of the quiet short-haul research aircraft p0011 N80-28338
 [NASA-TM-78508]
 Parametric study of modern airship productivity p0011 N80-28340
 [NASA-TM-81151]
 A mathematical representation of an advanced helicopter for piloted simulator investigations of control system and display variations p0011 N80-28371
 [NASA-TM-81203]
MATRICES (MATHEMATICS)
 NT EIGENVALUES
 The analysis of delays in simulator digital computing systems. Volume 2: Formulation of discrete state transition matrices, an alternative procedure for multirate digital computations --- flight control

[NASA-CR-152341] p0015 N80-18722
MATRIX ANALYSIS
 U MATRICES (MATHEMATICS)
MATURING
 U GROWTH
MEADOWLANDS
 U GRASSLANDS
MEASURING INSTRUMENTS
 NT ATTITUDE INDICATORS
 NT CALORIMETERS
 NT EBERT SPECTROMETERS
 NT FLIGHT RECORDERS
 NT INFRARED DETECTORS
 NT INFRARED RADIONETERS
 NT INFRARED SCANNERS
 NT INTERFEROMETERS
 NT LASER ANEMOMETERS
 NT LASER DOPPLER VELOCIMETERS
 NT MAGNETOMETERS
 NT MASS SPECTROMETERS
 NT NEPHELOMETERS
 NT NEUTRON COUNTERS
 NT PLASMA PROBES
 NT RADIO INTERFEROMETERS
 NT RADIOMETERS
 NT RADIOSONDES
 NT SATELLITE-BORNE INSTRUMENTS
 NT SPECTORADIOMETERS
 NT SPEED INDICATORS
 NT TIME OF FLIGHT SPECTROMETERS
 NT ULTRAVIOLET SPECTROMETERS
 Atmosphere structure instruments on the four Pioneer Venus entry probes p0051 A80-30849
MECHANICAL MEASUREMENT
 NT FLOW MEASUREMENT
 NT FRICTION MEASUREMENT
 NT PRESSURE MEASUREMENTS
 NT VELOCITY MEASUREMENT
 NT WIND MEASUREMENT
 NT WIND VELOCITY MEASUREMENT
MECHANICAL PROPERTIES
 NT AEROELASTICITY
 NT CREEP RUPTURE STRENGTH
 NT SHEAR STRENGTH
 NT TENSILE STRENGTH
 NT THERMAL RESISTANCE
 NT VISCOELASTICITY
 Time-temperature behavior of a unidirectional graphite/epoxy composite p0078 A80-21141
 Graphite composites with advanced resin matrices [AIAA 80-0758] p0064 A80-35051
 Thermal expansion and swelling of cured epoxy resin used in graphite/epoxy composite materials p0054 A80-40926
 Hygrothermal damage mechanisms in graphite-epoxy composites p0038 N80-13170
 [NASA-CR-3189]
MECHANIZATION
 Automation literature: A brief review and analysis [NASA-TM-81245] p0103 N80-34097
MEDIA
 NT INTERPLANETARY GAS
 NT INTERPLANETARY MEDIUM
MEDICAL SCIENCE
 NT HISTOLOGY
 NT NEUROLOGY
MEETINGS
 U CONFERENCES
MEISSNER EFFECT
 U SUPERCONDUCTIVITY
MEMBRANES
 Reverse osmosis membrane of high urea rejection properties --- water purification [NASA-CASE-ARC-10980-1] p0097 N80-23452
MENTAL PERFORMANCE
 Multi-modal information processing for visual workload relief [NASA-CR-162720] p0100 N80-16737
MESOSPHERE
 Smoke and dust particles of meteoric origin in the mesosphere and stratosphere p0055 A80-42744
METABOLIC WASTES
 NT URINE
METABOLISM
 NT CARBOHYDRATE METABOLISM
 NT CATABOLISM

SUBJECT INDEX

MIDDLE ATMOSPHERE

NT ELECTROLYTE METABOLISM
 Simulated weightlessness - Effects on bioenergetic balance p0095 A80-21544
 Changes in body temperature and metabolic rate after injection of calcium into the caudal hypothalamus of the rabbit p0093 A80-27078
 Microbial mobilization of calcium and magnesium in waterlogged soils p0089 A80-32834

METAL BONDING
 NT METAL-METAL BONDING
 METAL COATINGS
 Comparison of the early stages of condensation of Cu and Ag on Mo/100/ with Cu and Ag on W/100/ p0053 A80-37193

METAL FILMS
 Isothermal-desorption-rate measurements in the vicinity of the Curie temperature for H₂ chemisorbed on nickel films p0042 A80-16167

METAL FLUORIDES
 NT URANIUM FLUORIDES
 METAL HALIDES
 NT URANIUM FLUORIDES
 METAL INSULATOR SEMICONDUCTORS
 U MIS (SEMICONDUCTORS)
 METAL IONS
 The role of metal ions in chemical evolution - Polymerization of alanine and glycine in a cation-exchanged clay environment p0090 A80-36195
 The possible role of metal ions and clays in prebiotic chemistry p0094 A80-50960

METAL OXIDE SEMICONDUCTORS
 NT CHARGE COUPLED DEVICES
 METAL OXIDES
 NT CALCIUM OXIDES
 NT CESIUM OXIDES
 METAL PARTICLES
 Direct /TEM/ observation of the catalytic oxidation of amorphous carbon by Pd particles p0053 A80-37180

METAL SURFACES
 A calculation of the diffusion energies for adatoms on surfaces of F.C.C. metals p0068 A80-13534

METAL-METAL BONDING
 Comparison of the early stages of condensation of Cu and Ag on Mo/100/ with Cu and Ag on W/100/ p0053 A80-37193

METALLOIDS
 NT SILICON
 METALS
 NT ALKALI METALS
 NT CALCIUM
 NT MAGNESIUM
 NT METAL COATINGS
 NT METAL FILMS
 NT MOLYBDENUM
 NT NICKEL
 NT PALLADIUM
 NT POTASSIUM
 NT SILVER
 NT SODIUM
 METAZOA
 U ANIMALS
 METEORITE COMPRESSION TESTS
 U MECHANICAL PROPERTIES
 METEORITES
 NT ACHONDRITES
 NT CARBONACEOUS CHONDRITES
 NT CARBONACEOUS METEORITES
 METEORITIC COMPOSITION
 Carbonaceous chondrites. I - Characterization and significance of carbonaceous chondrite /CM/ xenoliths in the Jodzie howardite p0086 A80-13013
 The radiocemization of isovaline - Cosmochemical implications --- gamma ray effects on Murchison meteorite primordial composition p0086 A80-13018
 Quantification of monocarboxylic acids in the Murchison carbonaceous meteorite p0087 A80-13549
 Meteoroid ablation spheres from deep-sea sediments p0046 A80-22948

Aqueous activity on asteroids - Evidence from carbonaceous meteorites p0062 A80-24586
 Spectroscopic evidence for two achondrite parent bodies - Asteroids 349 Dembowska and 4 Vesta p0072 A80-26173
 Organic compounds in meteorites p0094 A80-50053

METEORITIC DUST
 U MICROMETEORIDS
 METEORIDS
 NT MICROMETEORIDS
 METEOROLOGICAL INSTRUMENTS
 NT RADIOSONDES
 METEOROLOGICAL ROCKETS
 U SOUNDING ROCKETS
 METEOROLOGICAL SATELLITES
 NT NIMBUS 4 SATELLITE
 METEOROLOGY
 NT NUMERICAL WEATHER FORECASTING
 METERS
 U MEASURING INSTRUMENTS
 METHANE
 Infrared methane spectra between 1120 per cm and 1800 per cm - A new atlas p0042 A80-13143
 A new atlas of infrared methane spectra between 1120 per cm and 1800 per cm --- Book p0042 A80-15655
 Ground-state rotational constants of /C-13/H₃D p0054 A80-41175

METHYLENE BLUE
 Singlet oxygenation of 1,2-poly/1,4-hexadiene/s p0045 A80-21991

MICE
 Review of cell aging in Drosophila and mouse p0087 A80-17741

MICROBE
 U MICROORGANISMS
 MICROBIOLOGY
 NT BACTERIOLOGY
 MICROCALORIMETERS
 U CALORIMETERS
 MICROCRYSTALS
 Effect of three-body interactions on the structure of small clusters p0057 A80-49383

MICROMETEORIDS
 Smoke and dust particles of meteoric origin in the mesosphere and stratosphere p0055 A80-42744

MICROMETEORS
 U MICROMETEORIDS
 MICROORGANISMS
 NT ANAEROBES
 NT BACTERIA
 Oxygen as a factor in eukaryote evolution - Some effects of low levels of oxygen on Saccharomyces cerevisiae p0086 A80-12229
 Microbial mobilization of calcium and magnesium in waterlogged soils p0089 A80-32834

MICROPARTICLES
 Aldocyanoin microspheres - Partial amino acid analysis of the microparticulates formed from simple reactants under various conditions p0086 A80-11473
 Smoke and dust particles of meteoric origin in the mesosphere and stratosphere p0055 A80-42744

MICROPROCESSORS
 NT INTEL 8080 MICROPROCESSOR
 MICROWAVE ATTENUATION
 Permittivity and attenuation of wet snow between 4 and 12 GHz p0052 A80-36244

MICROWAVE EQUIPMENT
 NT MICROWAVE FILTERS
 MICROWAVE FILTERS
 Low-pass interference filters for submillimeter astronomy p0070 A80-19956

MIDDLE ATMOSPHERE
 NT MESOSPHERE
 NT OZONOSPHERE
 NT STRATOSPHERE
 A numerical model of the zonal mean circulation of the middle atmosphere

MIDLATITUDE ATMOSPHERE

SUBJECT INDEX

MIDLATITUDE ATMOSPHERE p0073 A80-34443
 Preliminary calculations concerning the maintenance of the zonal mean ozone distribution in the Northern Hemisphere

MIE SCATTERING p0074 A80-34445
 Scattering by non-spherical particles of size comparable to a wavelength - A new semi-empirical theory

Asymptotic behavior of the efficiencies in Mie scattering p0063 A80-34050

MIE THEORY p0031 A80-47048
 U MIE SCATTERING

MILITARY HELICOPTERS
 NT H-53 HELICOPTER
 NT OH-6 HELICOPTER
 NT UH-1 HELICOPTER
 Results of a simulator investigation of control system and display variations for an attack helicopter mission [AD-A085812] p0101 N80-29370

MINERAL DEPOSITS
 Heterogeneous phase reactions of Martian volatiles with putative regolith minerals p0090 A80-36062

MINERALOGY
 Carbonaceous chondrites. I - Characterization and significance of carbonaceous chondrite /CM/ xenoliths in the Jodzie howardite p0086 A80-13013
 Meteoroid ablation spheres from deep-sea sediments p0046 A80-22948
 Aqueous activity on asteroids - Evidence from carbonaceous meteorites p0062 A80-24586

MINIMIZATION
 U OPTIMIZATION

MIRRORS
 NT PARABOLOID MIRRORS
 NT SOLAR COLLECTORS
 Quest for ultrahigh resolution in X-ray optics --- for solar astronomy p0032 A80-17480
 SOLARES orbiting mirror system [AAS 79-304] p0067 A80-52280

MIS (SEMICONDUCTORS)
 Improved characterization of the Si-SiO₂ interface p0095 A80-41532

MISSION PLANNING
 An entry and landing probe for Titan [AIAA PAPER 80-0117] p0060 A80-18384
 NASA-Ames Life Sciences Flight Experiments program - 1980 status report [ASME PAPER 80-ENAS-34] p0094 A80-43209
 Comet nucleus impact probe feasibility study [NASA-CR-152375] p0040 N80-26364
 Titan probe technology assessment and technology development plan study [NASA-CR-152381] p0040 N80-32417

MIXING
 NT TURBULENT MIXING

MIXTURES
 NT AEROSOLS
 NT BINARY MIXTURES
 NT SMOKE

MOBILITY
 NT IONIC MOBILITY

MODAL RESPONSE
 Dynamic modal estimation using instrumental variables [NASA-CR-152396] p0019 N80-32777

MODE SHAPES
 U MODAL RESPONSE

MODELS
 NT AIRCRAFT MODELS
 NT ASTRONOMICAL MODELS
 NT ATMOSPHERIC MODELS
 NT DENSITY WAVE MODEL
 NT DIGITAL SIMULATION
 NT DYNAMIC MODELS
 NT MATHEMATICAL MODELS
 NT OCEAN MODELS
 NT SCALE MODELS
 NT STELLAR MODELS
 NT WIND TUNNEL MODELS

MODES

NT FAILURE MODES

MOHR CIRCLES

U FRACTURE MECHANICS

MOISTURE

NT SOIL MOISTURE

MOISTURE CONTENT

Effects of moisture on apparent flexure strength and on torsion and flexure fatigue properties of graphite-epoxy composites

Permittivity and attenuation of wet snow between 4 and 12 GHz p0063 A80-27965

Thermal expansion and swelling of cured epoxy resin used in graphite/epoxy composite materials p0052 A80-36244

Influence of quality control variables on failure of graphite/epoxy under extreme moisture conditions p0054 A80-40926

[NASA-TN-81246] p0038 N80-33493

MOLECULAR BONDS

U CHEMICAL BONDS

MOLECULAR COLLISIONS

F + H₂ collisions on two electronic potential energy surfaces - Quantum-mechanical study of the collinear reaction

An angular momentum approximation for molecular collisions in the presence of intense laser radiation p0068 A80-12012

Na + Xe collisions in the presence of two nonresonant lasers p0069 A80-15673

Solution of Boltzmann equation for highly nonequilibrium diatomic gases rotational translational energy relaxation p0051 A80-32416

MOLECULAR ENERGY LEVELS p0064 A80-34904

Solution of Boltzmann equation for highly nonequilibrium diatomic gases rotational translational energy relaxation

An ab initio calculation of the zero-field splitting parameters of the 3A-double prime state of formaldehyde p0064 A80-34904

MOLECULAR EXCITATION p0056 A80-45333

Photoexcitation and ionization in molecular oxygen - Theoretical studies of electronic transitions in the discrete and continuous spectral intervals

Photoexcitation and ionization in molecular fluorine - Stieltjes-Tchebycheff calculations in the static-exchange approximation p0044 A80-20275

Excitation mechanisms for the unidentified infrared emission features p0046 A80-23324

An ab initio calculation of the zero-field splitting parameters of the 3A-double prime state of formaldehyde p0054 A80-40642

MOLECULAR FLOW p0056 A80-45333

NT TRANSITION FLOW

MOLECULAR GASES

NT DIATOMIC GASES

Far infrared, near infrared, and radio molecular line studies of HFE 2, HFE 3, and R134a

Molecule formation and infrared emission in fast interstellar shocks. I Physical processes p0068 A80-11489

Photoexcitation and ionization in molecular oxygen - Theoretical studies of electronic transitions in the discrete and continuous spectral intervals p0043 A80-16410

Properties of clusters in the gas phase. V - Complexes of neutral molecules onto negative ions p0044 A80-20275

Theoretical treatment of the spin-orbit coupling in the rare gas oxides NeO, ArO, KrO, and XeO p0057 A80-50144

MOLECULAR INTERACTIONS p0057 A80-50149

NT MOLECULAR COLLISIONS

Properties of clusters in the gas phase. V - Complexes of neutral molecules onto negative ions p0057 A80-50144

SUBJECT INDEX

NASA PROGRAMS

Quantum theory and chemistry: Two propositions
[NASA-TM-81202] p0084 N80-25110

MOLECULAR RELAXATION
Vibration-rotation line shifts for 1 sigma g +
H2/V,J/-1S/0/ He computed via close coupling -
Temperature dependence p0058 A80-51965

MOLECULAR ROTATION
Ground-state rotational constants of /C-13/H3D
p0054 A80-41175
An ab initio calculation of the zero-field
splitting parameters of the 3A-double prime
state of formaldehyde p0056 A80-45333
Vibration-rotation line shifts for 1 sigma g +
H2/V,J/-1S/0/ He computed via close coupling -
Temperature dependence p0058 A80-51965

MOLECULAR SPECTRA
NT VIBRATIONAL SPECTRA
Temperature dependence of intensities of the 8-12
micron bands of CFC13 p0045 A80-21559
Band model calculations for CFC13 in the 8-12
micron region p0045 A80-21560
Photoexcitation and ionization in molecular
fluorine - Stieltjes-Tchebycheff calculations in
the static-exchange approximation p0046 A80-23324
Absolute intensities and pressure broadening
coefficients measured at different temperatures
for the 201/II/-000 band of C-12/O2/-16 at 4978/cm
p0048 A80-27125
Recommended conventions for defining transition
moments and intensity factors in diatomic
molecular spectra p0055 A80-41323
Discovery of optical molecular emission from the
bipolar nebula surrounding HD 44179 p0058 A80-52399

MOLECULES
NT DIATOMIC MOLECULES
Comets: Cosmic connections with carbonaceous
meteorites, interstellar molecules and the
origin of life p0092 N80-11975

MOLYBDENUM
Comparison of the early stages of condensation of
Cu and Ag on Mo/100/ with Cu and Ag on W/100/
p0053 A80-37193

MOMENTS
NT BENDING MOMENTS
NT DIPOLE MOMENTS
NT LOADING MOMENTS
Recommended conventions for defining transition
moments and intensity factors in diatomic
molecular spectra p0055 A80-41323

MOMENTUM
NT ANGULAR MOMENTUM

MOMENTUM TRANSFER
Measurements of wind vectors, eddy momentum
transports, and energy conversions in Jupiter's
atmosphere from Voyager 1 images A80-24159

MONITORS
NT INFRARED RADIOMETERS

MONOCULAR VISION
Effect of field of view and monocular viewing on
angular size judgements in an outdoor scene
[NASA-TM-81176] p0083 N80-19792

MONOLITHIC CIRCUITS
U INTEGRATED CIRCUITS

MONOPLANES
NT B-70 AIRCRAFT
NT C-135 AIRCRAFT

MONTI CARLO METHOD
Monte Carlo simulation of lunar megaregolith and
implications p0061 A80-23716

MOTION EQUATIONS
U EQUATIONS OF MOTION

MOTION PERCEPTION
Visually induced self-motion sensation adapts
rapidly to left-right visual reversal p0096 A80-44213

MOTION SICKNESS
Motion sickness in the squirrel monkey

p0095 A80-25891.

MOTION SIMULATORS
The development and use of large-motion simulator
systems in aeronautical research and development
p0001 A80-10765
Optimal washout for control of a moving base
simulator --- vertical motion flight simulation
using linear filter p0031 A80-14833
The effects of motion and g-seat cues on pilot
simulator performance of three piloting tasks
[NASA-TP-1601] p0004 N80-15069
Feasibility and concept study to convert the
NASA/AMES vertical motion simulator to a
helicopter simulator p0098 N80-16070
Operations manual: Vertical Motion Simulator
(VMS) S.08 p0009 N80-23295
[NASA-TM-81180]

MOTION STABILITY
NT AERODYNAMIC STABILITY
NT AIRCRAFT STABILITY
NT ATTITUDE STABILITY
NT BOUNDARY LAYER STABILITY
NT FLOW STABILITY
NT HOVERING STABILITY

MOUNTAINS
Use of collateral information to improve LANDSAT
classification accuracies --- Ventura County and
Klamath National Forest, California
[E80-10268] p0040 N80-29815

MULTILAYER STRUCTURES
U LAMINATES

MULTIPHOTON ABSORPTION
Computational study of alkali-metal-noble gas
collisions in the presence of nonresonant lasers
- Na + Xe + h/2/pi/omega sub 1 + h/2/pi/omega
sub 2 system p0056 A80-48762

MULTISPECTRAL PHOTOGRAPHY
NT INFRARED PHOTOGRAPHY

MULTIVARIATE STATISTICAL ANALYSIS
NT REGRESSION ANALYSIS

MUSCULAR FUNCTION
A model for hypokinesia: Effects on muscle atrophy
in the rat p0095 A80-28188

MUSCULAR TONUS
Effects of chronic centrifugation on skeletal
muscle fibers in young developing rats p0096 A80-41983

MUSCULOSKELETAL SYSTEM
NT BONES
Effects of chronic centrifugation on skeletal
muscle fibers in young developing rats p0096 A80-41983

N

NACELLES
Force and moment data from a wind-tunnel test of a
tilt-nacelle V/STOL propulsion system with an
attitude control vane --- conducted in Ames 40
by 80 foot wind tunnel p0006 N80-13003
[NASA-TM-81157]
Comparison of calculated and measured blade loads
on a full-scale tilting propotor in a wind tunnel
[NASA-TM-81228] p0012 N80-31386

NAP-OF-THE-EARTH NAVIGATION
A pilot's assessment of helicopter
handling-quality factors common to both agility
and instrument flying tasks p0011 N80-28341
[NASA-TM-81217]

NASA PROGRAMS
NT GALILEO PROJECT
NT TILT ROTOR RESEARCH AIRCRAFT PROGRAM
A comparison of computer architectures for the
NASA demonstration advanced avionics system
p0032 A80-32427
NASA-Ames Life Sciences Flight Experiments program
- 1980 status report p0094 A80-43209
[ASME PAPER 80-ENAS-34]
NASA overview p0022 N80-10109
Ames Research Center publications: A continuing
bibliography, 1978 p0003 N80-18985
[NASA-TM-81175]
NASA's western regional applications training
activity

NATURAL LASERS

SUBJECT INDEX

A summary of joint US-Canadian augmentor wing
 powered-lift STOL research programs at the Ames
 Research Center, NASA, 1975-1980
 [NASA-TM-81215] p0058 N80-20010
NATURAL LASERS p0011 N80-28373
 U LASERS
NATURAL SATELLITES
 NT CALLISTO
 NT GANYMEDE
 NT TITAN
 Saturnian trapped radiation and its absorption by
 satellites and rings - The first results from
 Pioneer 11 p0070 A80-19118
 Saturn's magnetosphere, rings, and inner satellites
 p0070 A80-19119
 Tidal dissipation, orbital evolution, and the
 nature of Saturn's inner satellites p0058 A80-53235
NAVIER-STOKES EQUATION
 An explicit algorithm for a fluid approach to
 nonlinear optics propagation using splitting and
 rezoning techniques p0059 A80-14987
 An efficient explicit-implicit-characteristic
 method for solving the compressible
 Navier-Stokes equations p0062 A80-27408
 On the numerical solution of time-dependent
 viscous incompressible fluid flows involving
 solid boundaries p0052 A80-34980
 A Navier-Stokes fast solver for turbulence
 modeling applications p0059 N80-27659
 Numerical solution techniques for unsteady
 transonic aerodynamics problems p0059 N80-33379
NAVIGATION
 NT DIGITAL NAVIGATION
 NT MAP-OF-THE-EARTH NAVIGATION
 NT RADAR NAVIGATION
NAVIGATION AIDS
 NT NAVIGATION INSTRUMENTS
NAVIGATION INSTRUMENTS
 NT ATTITUDE INDICATORS
 Flight test of navigation and guidance sensor
 errors measured on STOL approaches
 [NASA-TM-81154] p0007 N80-13041
NEAR INFRARED RADIATION
 Far infrared, near infrared, and radio molecular
 line studies of HFE 2, HFE 3, and FJM 6
 p0068 A80-11489
 The 16- to 38-micron spectrum of Callisto
 p0074 A80-35234
NEBULAE
 NT PLANETARY NEBULAE
 The dynamics and stability of radiatively driven
 gas clouds. I - Plane-parallel slabs
 p0042 A80-14058
 Red and nebulous objects in dark clouds - A survey
 p0044 A80-20662
 A far-infrared study of the reflection nebula NGC
 2023 p0072 A80-26111
 Ring formation in rotating protostellar clouds
 p0048 A80-26992
 Collapsing cloud models for Bok globules
 p0048 A80-26996
 Far-infrared spectra of W51-IRS 2 and W49 NW
 p0056 A80-44967
 Discovery of optical molecular emission from the
 bipolar nebula surrounding HD 44179 p0058 A80-52399
NEGATIVE IONS
 The properties of clusters in the gas phase. IV -
 Complexes of H₂O and HNO_x clustering on NO_x/-/
 p0046 A80-23322
 Properties of clusters in the gas phase. V -
 Complexes of neutral molecules onto negative ions
 p0057 A80-50144
NEODYMIUM LASERS
 Na + Xe collisions in the presence of two
 nonresonant lasers p0051 A80-32416
 Computational study of alkali-metal-noble gas
 collisions in the presence of nonresonant lasers
 - Na + Xe + h/2 π /omega sub 1 + h/2 π /omega

sub 2 system
NEPHELOMETERS p0056 A80-48762
 Pioneer Venus sounder and small probes
 Nephelometer instrument
NETWORK ANALYSIS p0053 A80-36750
 Transient solution for megajoule energy release in
 a lumped-parameter series RLC circuit
NEUROLOGY p0051 A80-32826
 A microprocessor-based instrument for neural pulse
 wave analysis p0098 A80-50322
NEUROSCIENCE
 U NEUROLOGY
NEUTRAL GASES
 Pioneer Venus Sounder Probe Neutral Gas Mass
 Spectrometer p0073 A80-30844
 Properties of clusters in the gas phase. V -
 Complexes of neutral molecules onto negative ions
 p0057 A80-50144
NEUTRON COUNTERS
 A comparative study of cosmic ray intensity
 variations during 1972-1977 using spacecraft and
 ground-based observations p0072 A80-28244
NEUTRON DETECTORS
 U NEUTRON COUNTERS
NICKEL
 Isothermal-desorption-rate measurements in the
 vicinity of the Curie temperature for H₂
 chemisorbed on nickel films p0042 A80-16167
NIMBUS SATELLITES
 NT NIMBUS 4 SATELLITE
NIMBUS 4 SATELLITE
 Comparison of the Nimbus-4 BUV ozone data with the
 Ames two-dimensional model
 [NASA-TM-81207] p0036 N80-24914
NITRIC OXIDE
 A model of the neutral and ion nitrogen chemistry
 in the daytime thermosphere of Venus
 p0067 A80-10460
 Measurements of NO, O₃, and temperature at 19.8 km
 during the total solar eclipse of 26 February 1979
 p0055 A80-43638
 Equivalent-cone calculation of nitric oxide
 production rate during Space Shuttle re-entry
 p0056 A80-45359
 Reduction of nitric oxide emissions from a combustor
 [NASA-CASE-ARC-10814-2] p0080 N80-26298
 Two-photon excitation of nitric oxide fluorescence
 as a temperature indicator in unsteady
 gas-dynamic processes
 [NASA-TM-81220] p0037 N80-32700
NITROGEN
 NT LIQUID NITROGEN
 NT NITROGEN ATOMS
 NT NITROGEN IONS
 Development of a nitrogen generation system
 [NASA-CR-152333] p0085 N80-19800
NITROGEN ATOMS
 A model of the neutral and ion nitrogen chemistry
 in the daytime thermosphere of Venus
 p0067 A80-10460
NITROGEN COMPOUNDS
 NT AMMONIA
 NT NITRIC OXIDE
 NT NITROGEN OXIDES
 NT POLYIMIDES
 NT UREAS
NITROGEN IONS
 A model of the neutral and ion nitrogen chemistry
 in the daytime thermosphere of Venus
 p0067 A80-10460
NITROGEN OXIDES
 NT NITRIC OXIDE
 Pressure and temperature dependence kinetics study
 of the NO + BrO yielding NO₂ + Br reaction -
 Implications for stratospheric bromine
 photochemistry p0068 A80-14397
 Integrated band intensities of gaseous N₂O/5/
 p0047 A80-25660
NOBLE GASES
 U RARE GASES

SUBJECT INDEX

NUMERICAL DIFFERENTIATION

- NOBLE METALS**
NT SILVER
- NOE NAVIGATION**
U NAP-OF-THE-EARTH NAVIGATION
- NOISE (SOUND)**
NT AERODYNAMIC NOISE
NT AIRCRAFT NOISE
NT ENGINE NOISE
NT JET AIRCRAFT NOISE
- NOISE ATTENUATION**
U NOISE REDUCTION
- NOISE ELIMINATION**
U NOISE REDUCTION
- NOISE GENERATORS**
 Noise generation by a lifting wing/flap
 combination at Reynolds numbers to 2.8×10 to
 the 6th
 [AIAA PAPER 80-0035] p0024 A80-22729
 An experimental study of the structure and
 acoustic field of a jet in a cross stream ---
 Ames 7-ft by 10-ft wind tunnel tests
 [NASA-CR-162464] p0014 N80-15871
 Analytical study of the effects of wind tunnel
 turbulence on turbofan rotor noise --- NASA Ames
 40 by 80 foot wind tunnel
 [NASA-CR-152359] p0016 N80-23099
 Modal content of noise generated by a coaxial jet
 in a pipe
 [NASA-CR-163575] p0019 N80-33177
- NOISE INTENSITY**
 Strouhal number influence on flight effects on jet
 noise radiated from convecting quadrupoles
 p0022 A80-28418
- NOISE MEASUREMENT**
 Upper surface blowing noise of the NASA-Ames quiet
 short-haul research aircraft
 [AIAA PAPER 80-1064] p0026 A80-36002
- NOISE PREDICTION (AIRCRAFT)**
 Fan noise caused by the ingestion of anisotropic
 turbulence - A model based on axisymmetric
 turbulence theory
 [AIAA PAPER 80-1021] p0032 A80-35977
 Analytical study of the effects of wind tunnel
 turbulence on turbofan rotor noise
 [AIAA PAPER 80-1022] p0033 A80-35978
- NOISE REDUCTION**
 Analytical study of the effects of wind tunnel
 turbulence on turbofan rotor noise
 [AIAA PAPER 80-1022] p0033 A80-35978
 Distortion-rotor interaction noise produced by a
 drooped inlet
 [AIAA PAPER 80-1050] p0033 A80-35994
 A closed-form solution for noise contours
 [NASA-TP-1432] p0004 N80-11869
 Acoustically swept rotor --- helicopter noise
 reduction
 [NASA-CASE-ARC-11106-1] p0102 N80-14107
 Quiet short-haul research aircraft familiarization
 document --- STOL
 [NASA-TM-81149] p0007 N80-14108
 Evaluation of approximate methods for the
 prediction of noise shielding by airframe
 components
 [NASA-TP-1004] p0004 N80-15129
- NOISE SUPPRESSORS**
U NOISE REDUCTION
- NOMINAL VALUES**
U APPROXIMATION
- NONADIABATIC PROCESSES**
U HEAT TRANSFER
- NONEQUILIBRIUM CONDITIONS**
 Solution of Boltzmann equation for highly
 nonequilibrium diatomic gases rotational
 translational energy relaxation
 p0064 A80-34904
- NONEUCLIDIAN GEOMETRY**
U DIFFERENTIAL GEOMETRY
- NONFLAMMABLE MATERIALS**
 Materials for fire resistant passenger seats in
 aircraft
 p0080 A80-48757
- NONLINEAR OPTICS**
 An explicit algorithm for a fluid approach to
 nonlinear optics propagation using splitting and
 rezoning techniques
 p0059 A80-14987
- NONLINEAR SYSTEMS**
 Feedback invariants for nonlinear systems
 p0031 A80-14810
- On the nonlinear deformation geometry of
 Euler-Bernoulli beams --- rotary wings
 [NASA-TP-1566] p0101 N80-20619
- NONVISCOUS FLOW**
U TURBULENT FLOW
- NORMAL FORCE DISTRIBUTION**
U FORCE DISTRIBUTION
- NORTH AMERICAN AIRCRAFT**
NT B-70 AIRCRAFT
- NORTHERN HEMISPHERE**
 Preliminary calculations concerning the
 maintenance of the zonal mean ozone distribution
 in the Northern Hemisphere
 p0074 A80-34445
- NOSE CONES**
NT ABLATIVE NOSE CONES
- NOSES (FOREBODIES)**
NT ABLATIVE NOSE CONES
 Control of forebody three-dimensional flow
 separations
 p0022 N80-15164
- NOVAE**
 The evolution of rapid oscillations in an outburst
 of a dwarf nova
 p0075 A80-45227
- NOZZLE COEFFICIENT**
U NOZZLE FLOW
- NOZZLE DESIGN**
 Static calibration of a two-dimensional wedge
 nozzle with thrust vectoring and spanwise blowing
 [NASA-TM-81161] p0009 N80-23317
 Aircraft engine nozzle
 [NASA-CASE-ARC-10977-1] p0033 N80-32392
- NOZZLE FLOW**
 Workshop on Thrust Augmenting Ejectors
 [NASA-CP-2093] p0004 N80-10107
- NOZZLE GEOMETRY**
 An experimental study of multiple jet mixing
 [NASA-CR-166184] p0018 N80-31760
- NUCLEAR INTERACTIONS**
NT SPIN-ORBIT INTERACTIONS
 Modified Iterative Extended Hueckel. 1: Theory
 [NASA-TM-81200] p0083 N80-25108
- NUCLEAR RADIATION**
NT GAMMA RAYS
NT SPALLATION
- NUCLEAR REACTIONS**
NT NUCLEAR INTERACTIONS
NT SPALLATION
NT SPIN-ORBIT INTERACTIONS
- NUCLEATION**
 A reconsideration of nucleation phenomena in light
 of recent findings concerning the properties of
 small clusters, and a brief review of some other
 particle growth processes --- for cosmic dust
 p0069 A80-15609
- NUCLIDES**
NT CARBON ISOTOPES
NT RADIOACTIVE ISOTOPES
- NUMERICAL ANALYSIS**
NT APPROXIMATION
NT CHEBYSHEV APPROXIMATION
NT COMPUTATIONAL FLUID DYNAMICS
NT ERROR ANALYSIS
NT FINITE DIFFERENCE THEORY
NT ITERATION
NT LEAST SQUARES METHOD
NT MONTE CARLO METHOD
NT NUMERICAL DIFFERENTIATION
NT TRUNCATION ERRORS
 Automated design using numerical optimization
 [SAE PAPER 791061] p0024 A80-26628
 Note on the eigensolution of a homogeneous
 equation with semi-infinite domain
 p0075 A80-40508
 The inversion of singular integral equations by
 expansion in Jacobi polynomials
 p0030 A80-42758
 Alternating direction implicit methods for
 parabolic equations with a mixed derivative
 p0057 A80-51050
 Analysis of transonic swept wings using asymptotic
 and other numerical methods
 [NASA-TM-80762] p0011 N80-29255
 Calculation of three-dimensional unsteady
 transonic flows past helicopter blades
 [NASA-TP-1721] p0100 N80-33356
- NUMERICAL DIFFERENTIATION**
 Alternating direction implicit methods for

NUMERICAL FLOW VISUALIZATION

SUBJECT INDEX

parabolic equations with a mixed derivative
p0057 A80-51050

NUMERICAL FLOW VISUALIZATION
An experimental and numerical investigation of a
three-dimensional shock wave separated turbulent
boundary layer
[AIAA PAPER 80-0002] p0061 A80-22727
Tests of subgrid-scale models in strained turbulence
[AIAA PAPER 80-1339] p0065 A80-41569
Reformulation of Possio's kernel with application
to unsteady wind tunnel interference
p0031 A80-43129
Numerical simulation of three-dimensional boattail
afterbody flow fields
[AIAA PAPER 80-1347] p0066 A80-44132
A comprehensive comparison between experiment and
prediction for a transonic turbulent separated
flow
[AIAA PAPER 80-1407] p0027 A80-44154
Direct numerical simulations of the turbulent wake
of an axisymmetric body
p0080 A80-49235
Use of advanced computers for aerodynamic flow
simulation
p0058 A80-21257

NUMERICAL WEATHER FORECASTING
Eddy diffusion coefficients and the variance of
the atmosphere 30-60 km
p0076 A80-45996

NUTS (FRUITS)
Irrigated lands assessment for water management
Applications Pilot Test (APT) --- California
[E80-10324] p0019 A80-32815

O

O STARS
High-frequency continuum observations of young stars
p0047 A80-25365

OBLIQUE WINGS
Wind tunnel investigation of an oblique wing
transport model at mach numbers between 0.6 and
1.4
[NASA-CR-137697] p0013 A80-12059

OBSCURATION
U OCCULTATION
OBSERVATION AIRCRAFT
NT OH-6 HELICOPTER
OBSERVATORIES
NT ASTRONOMICAL OBSERVATORIES
OCCULTATION
NT RADIO OCCULTATION
NT SOLAR ECLIPSES
The radius and ellipticity of Uranus from its
occultation of SAO 158687
p0073 A80-31937

OCEAN BOTTOM
Meteoroid ablation spheres from deep-sea sediments
p0046 A80-22948

OCEAN MODELS
Analysis of coastal upwelling and the production
of a biomass
[NASA-TM-78614] p0035 A80-12720

OGIVES
Numerical simulation of steady supersonic flow
over an ogive-cylinder-boattail body
[AIAA PAPER 80-0066] p0060 A80-19273
Pressure measurements on an ogive-cylinder at high
angles of attack with laminar, transitional, or
turbulent separation
[AIAA 80-1556] p0028 A80-45856

OH-6 HELICOPTER
A compilation and analysis of helicopter handling
qualities data. Volume 1: Data compilation
[NASA-CR-3144] p0013 A80-11097

ONBOARD COMPUTERS
U AIRBORNE/SPACEBORNE COMPUTERS
ONBOARD EQUIPMENT
NT AIRBORNE EQUIPMENT
NT AIRBORNE/SPACEBORNE COMPUTERS
NT AIRCRAFT EQUIPMENT
OPERATORS (PERSONNEL)
NT AIRCRAFT PILOTS
OPTICAL ABSORPTION
U ELECTROMAGNETIC ABSORPTION
U LIGHT TRANSMISSION
OPTICAL EMISSION SPECTROSCOPY
Discovery of optical molecular emission from the
bipolar nebula surrounding HD 44179

OPTICAL EQUIPMENT
NT ASTRONOMICAL TELESCOPES
NT EBERT SPECTROMETERS
NT LASER DOPPLER VELOCIMETERS
NT NEPHELOMETERS
NT SPECTROSCOPIC TELESCOPES
NT ULTRAVIOLET SPECTROMETERS
NT X RAY TELESCOPES
OPTICAL FILTERS
NT INFRARED FILTERS
OPTICAL ILLUSION
Visually induced self-motion sensation adapts
rapidly to left-right visual reversal
p0096 A80-44213

OPTICAL LASERS
U LASERS
OPTICAL MEASUREMENT
NT ASTRONOMICAL PHOTOMETRY
NT POLARIMETRY
NT SPECTROPHOTOMETRY
NT STELLAR SPECTROPHOTOMETRY
NT ULTRAVIOLET PHOTOMETRY
OPTICAL MEASURING INSTRUMENTS
NT EBERT SPECTROMETERS
NT NEPHELOMETERS
NT ULTRAVIOLET SPECTROMETERS
OPTICAL PROPERTIES
NT BRIGHTNESS
NT PHOTOELECTRIC EMISSION
NT PHOTOIONIZATION
NT STELLAR LUMINOSITY
Atmospheric aerosols and climate
p0052 A80-36305
Differentiation of optical isomers through
enhanced weak-field interactions
[NASA-TM-81208] p0084 A80-27164

OPTICAL PUMPING
NT LASER PUMPING
OPTICAL TRANSITION
Absolute intensities and pressure broadening
coefficients measured at different temperatures
for the 201/II/-000 band of C-12/02/-16 at 4978/cm
p0048 A80-27125

OPTIMAL CONTROL
Optimal washout for control of a moving base
simulator --- vertical motion flight simulation
using linear filter
p0031 A80-14833
Constrained optimum trajectories with specified
range
p0021 A80-18538
Optimal estimator model for human spatial
orientation
p0093 A80-24265
Singular perturbations and the sounding rocket
problem
p0001 A80-24268
Implicit model following and parameter
identification of unstable aircraft
p0022 A80-28019
Optimal control model predictions of system
performance and attention allocation and their
experimental validation in a display design study
p0095 A80-40899
A pilot modeling technique for handling-qualities
research
[AIAA 80-1624] p0028 A80-45912

OPTIMIZATION
NT OPTIMAL CONTROL
NT TRAJECTORY OPTIMIZATION
Automated design using numerical optimization
[SAE PAPER 791061] p0024 A80-26628
Application of numerical optimization to the
design of wings with specified pressure
distributions
[NASA-CR-3238] p0015 A80-16031

OPTIMUM CONTROL
U OPTIMAL CONTROL
ORBIT PERTURBATION
On the 'thickness' of Saturn's rings caused by
satellite and solar perturbations and by
planetary precession
p0042 A80-14293

ORBITAL ELEMENTS
Tidal dissipation, orbital evolution, and the
nature of Saturn's inner satellites
p0058 A80-53235

SUBJECT INDEX

PARABOLOID MIRRORS

ORBITS
 NT PLANETARY ORBITS
 NT SATELLITE ORBITS

ORCHARDS
 Irrigated lands assessment for water management
 Applications Pilot Test (APT) --- California
 [E80-10324] p0019 N80-32815

ORGANIC COMPOUNDS
 NT AMINO ACIDS
 NT FLUOROCARBONS
 NT FLUOROHYDROCARBONS
 NT PERFLUOROALKANE
 Organic compounds in meteorites p0094 A80-50053

ORGANIC LASERS
 NT DYE LASERS

ORGANIC PHOSPHORUS COMPOUNDS
 Thermophysical and flammability characterization
 of phosphorylated epoxy adhesives p0066 A80-48079

ORGANOMETALLIC COMPOUNDS
 NT HEMOGLOBIN

ORGANS
 NT PITUITARY GLAND

ORNIOTHOTTER AIRCRAFT
 U RESEARCH AIRCRAFT

ORRERIES
 U ASTRONOMICAL MODELS

ORTHOSTATIC TOLERANCE
 The development of an elastic reverse gradient
 garment to be used as a countermeasure for
 cardiovascular deconditioning
 [NASA-CR-152379] p0086 N80-33086

OSCILLATIONS
 NT WING OSCILLATIONS
 Comparison of calculated and measured blade loads
 on a full-scale tilting propotor in a wind tunnel
 [NASA-TM-81228] p0012 N80-31386

OSMOSIS
 NT REVERSE OSMOSIS
 Extremes of urine osmolality - Lack of effect on
 red blood cell survival p0091 A80-46196
 Extracellular hyperosmolality and body temperature
 during physical exercise in dogs p0092 A80-54076

OSMOTIC PRESSURE
 U OSMOSIS

OUTPUT
 NT LASER OUTPUTS

OXAZOLE
 Synthesis of perfluoroalkylether oxadiazole
 elastomers p0045 A80-21992

OXIDATION
 NT PHOTOOXIDATION
 Growth hormone control of glucose oxidation
 pathways in hypophysectomized rats p0088 A80-24222
 Direct /TEM/ observation of the catalytic
 oxidation of amorphous carbon by Pd particles
 p0053 A80-37180

OXIDES
 NT ANHYDRIDES
 NT CALCIUM OXIDES
 NT CARBON DIOXIDE
 NT CARBON MONOXIDE
 NT CARBON SUBOXIDES
 NT CESIUM OXIDES
 NT INORGANIC PEROXIDES
 NT NITRIC OXIDE
 NT NITROGEN OXIDES
 NT SILICON DIOXIDE
 Theoretical treatment of the spin-orbit coupling
 in the rare gas oxides NeO, ArO, KrO, and XeO
 p0057 A80-50149

OXIDIZERS
 NT PHOTOCHEMICAL OXIDANTS

OXYGEN
 NT OZONE
 Oxygen as a factor in eukaryote evolution - Some
 effects of low levels of oxygen on Saccharomyces
 cerevisiae p0086 A80-12229
 Photoexcitation and ionization in molecular oxygen
 - Theoretical studies of electronic transitions
 in the discrete and continuous spectral intervals
 p0044 A80-20275

Oxygen index tests of thermosetting resins
 p0044 A80-21448

OXYGEN PRODUCTION
 The preparation of calcium superoxide in a flowing
 gas stream and fluidized bed
 [ASME PAPER 80-ENAS-18] p0094 A80-43194

OXYGEN SUPPLY EQUIPMENT
 The preparation of calcium superoxide in a flowing
 gas stream and fluidized bed
 [ASME PAPER 80-ENAS-18] p0094 A80-43194

OXYGEN SYSTEMS
 U OXYGEN SUPPLY EQUIPMENT

OXYGENATION
 Singlet oxygenation of 1,2-poly/1,4-hexadiene/s
 p0045 A80-21991

OZONE
 SCF and CI calculations of the dipole moment
 function of ozone --- Self-Consistent Field and
 Configuration-Interaction p0043 A80-17111
 Stratospheric ozone decrease due to
 chlorofluoromethane photolysis - Predictions of
 latitude dependence p0049 A80-29762
 Preliminary calculations concerning the
 maintenance of the zonal mean ozone distribution
 in the Northern Hemisphere p0074 A80-34445
 The observed ozone flux by transient eddies, 0-30 km
 p0074 A80-34449

OZONOMETRY
 Nitrogen fertiliser and stratospheric ozone -
 Latitudinal effects p0043 A80-18948
 Measurements of NO, O3, and temperature at 19.8 km
 during the total solar eclipse of 26 February 1979
 p0055 A80-43638
 Comparison of the Nimbus-4 BUV ozone data with the
 Ames two-dimensional model
 [NASA-TM-81207] p0036 N80-24914

OZONOSPHERE
 Are solar spectral variations a drive for climatic
 change p0042 A80-15488

P

P-I-N DIODES
 U DIODES

PACIFIC NORTHWEST (US)
 Issues arising from the demonstration of
 Landsat-based technologies to inventories and
 mapping of the forest resources of the Pacific
 Northwest states p0065 A80-41305

PALLADIUM
 Changes induced on the surfaces of small Pd
 clusters by the thermal desorption of CO
 p0053 A80-37179
 Direct /TEM/ observation of the catalytic
 oxidation of amorphous carbon by Pd particles
 p0053 A80-37180

PANAMA CANAL ZONE
 High resolution vertical profiles of wind,
 temperature and humidity obtained by computer
 processing and digital filtering of radiosonde
 and radar tracking data from the ITCZ experiment
 of 1977 p0039 N80-21926
 [NASA-CR-3269]

PANEL METHOD (FLUID DYNAMICS)
 A general panel method for the analysis and design
 of arbitrary configurations in incompressible
 flows --- boundary value problem p0017 N80-24268
 [NASA-CR-3079]
 An advanced panel method for analysis of arbitrary
 configurations in unsteady subsonic flow
 [NASA-CR-152323] p0017 N80-26270

PANELS
 NT CURVED PANELS

PARABOLIC DIFFERENTIAL EQUATIONS
 Alternating direction implicit methods for
 parabolic equations with a mixed derivative
 p0057 A80-51050

PARABOLIC REFLECTORS
 NT PARABOLOID MIRRORS

PARABOLOID MIRRORS
 Paraboloidal X-ray telescope mirror for solar
 coronal spectroscopy p0078 A80-17503

PARALLEL FLOW

SUBJECT INDEX

PARALLEL FLOW

NT PIPE FLOW
NT THREE DIMENSIONAL FLOW
Characterization of acoustic disturbances in linearly sheared flows

p0030 A80-31804

PARTIAL DIFFERENTIAL EQUATIONS

NT ELLIPTIC DIFFERENTIAL EQUATIONS
NT PARABOLIC DIFFERENTIAL EQUATIONS
Automatic mesh-point clustering near a boundary in grid generation with elliptic partial differential equations

p0044 A80-20593

PARTICLE ACCELERATION

The phase of the ten-hour modulation in the Jovian magnetosphere /Pioneers 10 and 11/

p0067 A80-10526

Acceleration of energetic protons by interplanetary shocks

p0071 A80-21183

The acceleration of energetic charged particles by interplanetary and supernova shock waves

p0080 A80-53209

PARTICLE EMISSION

NT PHOTOELECTRIC EMISSION

PARTICLE ENERGY

NT ELECTRON STATES

PARTICLE FLUX DENSITY

NT ELECTRON FLUX DENSITY

A comparative study of cosmic ray intensity variations during 1972-1977 using spacecraft and ground-based observations

p0072 A80-28244

PARTICLE INTERACTIONS

NT CONFIGURATION INTERACTION

NT MOLECULAR COLLISIONS

NT MOLECULAR INTERACTIONS

NT NUCLEAR INTERACTIONS

NT SPIN-ORBIT INTERACTIONS

NT WEAK ENERGY INTERACTIONS

Scattering by non-spherical particles of size comparable to a wavelength - A new semi-empirical theory

p0063 A80-34050

PARTICLE MOTION

Threshold windspeeds for sand on Mars - Wind tunnel simulations

p0048 A80-27391

Feasibility studies for light scattering experiments to determine the velocity relaxation of small particles in a fluid [NASA-CR-163214]

p0040 A80-25586

PARTICLE SIZE DISTRIBUTION

Scattering by nonspherical particles of size comparable to wavelength - A new semi-empirical theory and its application to tropospheric aerosols

p0052 A80-36040

PARTICLES

NT AEROSOLS

NT CATIONS

NT CHARGED PARTICLES

NT COSMIC PLASMA

NT ENERGETIC PARTICLES

NT METAL IONS

NT METAL PARTICLES

NT MICROPARTICLES

NT NEGATIVE IONS

NT PLASMA CLOUDS

NT PROTONS

NT RADIATION BELTS

NT RAREFIED PLASMAS

NT RELATIVISTIC PARTICLES

NT SOLAR WIND

NT STELLAR WINDS

NT THERMAL PLASMAS

PARTICULATE SAMPLING

Efficiency of aerosol collection on wires exposed in the stratosphere [NASA-TM-81147]

p0035 A80-11676

PASSENGER AIRCRAFT

NT B0-105 HELICOPTER

NT H-53 HELICOPTER

Toward new small transports for commuter airlines

p0021 A80-21224

The future of short-haul transport aircraft [SAE PAPER 800755]

p0029 A80-49703

PASSENGERS

Fire-resistant materials for aircraft passenger

seat construction

[NASA-TM-78617]

p0035 A80-13255

PATTERN RECOGNITION

Using guided clustering techniques to analyze Landsat data for mapping forest land cover in northern California

p0078 A80-25595

Texture extraction on the ILLIAC 4 --- aerial images

[AD-A070523]

p0098 A80-19471

Use of collateral information to improve LANDSAT classification accuracies --- Ventura County and Klamath National Forest, California

[E80-10268]

p0040 A80-29815

PAYLOAD DELIVERY (STS)

NT WEAPONS DELIVERY

Large Deployable Reflector (LDR)

[NASA-CR-152402]

p0040 A80-33319

PAYLOADS

NT SPACE SHUTTLE PAYLOADS

NT SPACEBORNE EXPERIMENTS

NT SPACELAB

NT SPACELAB PAYLOADS

PEDOLOGY

U SOIL SCIENCE

PEGASUS ENGINE

U BRISTOL-SIDDELEY BS 53 ENGINE

PERCEPTION

NT AUDITORY PERCEPTION

NT MOTION PERCEPTION

NT SPACE PERCEPTION

NT VISUAL PERCEPTION

PERFLUORO COMPOUNDS

NT PERFLUOROALKANE

Perfluoroether triazine elastomers

[NASA-CR-162748]

p0039 A80-16166

PERFLUOROALKANE

Synthesis of perfluoroalkylether oxadiazole elastomers

p0045 A80-21992

PERFORMANCE PREDICTION

NT PREDICTION ANALYSIS TECHNIQUES

Optimal control model predictions of system performance and attention allocation and their experimental validation in a display design study

p0095 A80-40899

A comprehensive comparison between experiment and prediction for a transonic turbulent separated flow

[AIAA PAPER 80-1407]

p0027 A80-44154

PERFORMANCE TESTS

Effect of propeller slipstream on the drag and performance of the engine cooling system for a general aviation twin-engine aircraft

[AIAA PAPER 80-1872]

p0027 A80-43315

PERIODIC VARIATIONS

NT ANNUAL VARIATIONS

PERIPHERAL EQUIPMENT (COMPUTERS)

NT INTEL 8080 MICROPROCESSOR

PERMITTIVITY

Permittivity and attenuation of wet snow between 4 and 12 GHz

p0052 A80-36244

PEROXIDES

NT INORGANIC PEROXIDES

PERSONNEL

NT AIRCRAFT PILOTS

NT FLIGHT CREWS

PERSONNEL MANAGEMENT

Resource management on the flight deck --- conferences

[NASA-CP-2120]

p0082 A80-22283

PERSONNEL SELECTION

NT PILOT SELECTION

PERTURBATION

NT ORBIT PERTURBATION

PERTURBATION THEORY

Singular perturbations and the sounding rocket problem

p0001 A80-24268

PETROGRAPHY

Aqueous activity on asteroids - Evidence from carbonaceous meteorites

p0062 A80-24586

PETROLOGY

NT PETROGRAPHY

PHASE ANGLE

U PHASE SHIFT

PHASE DEVIATION

Optimized laser turrets for minimum phase distortion

SUBJECT INDEX

PHYSICAL EXERCISE

- PHASE SHIFT p0023 N80-25600
A new propagation method for the radial
Schroedinger equation
- PHENOLIC RESINS p0069 A80-15768
Shape change of Galileo probe models in
free-flight tests
[NASA-TM-81209]
- PHENOLOGY p0037 N80-27418
Infrared-temperature variability in a large
agricultural field --- Dunnigan, California
[E80-10331]
- PHENOMENOLOGY p0038 N80-32822
NT PHENOLOGY
- PHOSPHORUS COMPOUNDS
NT ORGANIC PHOSPHORUS COMPOUNDS
- PHOTOABSORPTION
An angular momentum approximation for molecular
collisions in the presence of intense laser
radiation p0069 A80-15673
Na + Xe collisions in the presence of two
nonresonant lasers p0051 A80-32416
Asymptotic behavior of the efficiencies in Mie
scattering p0031 A80-47048
- PHOTOCHEMICAL OXIDANTS
Introductory study of the chemical behavior of jet
emissions in photochemical smog --- computerized
simulation [NASA-CR-152345] p0016 N80-21891
- PHOTOCHEMICAL REACTIONS
NT PHOTOLYSIS
Pressure and temperature dependence kinetics study
of the NO + BrO yielding NO₂ + Br reaction -
Implications for stratospheric bromine
photochemistry p0068 A80-14397
Mars ultraviolet simulation facility p0089 A80-36061
Heterogeneous phase reactions of Martian volatiles
with putative regolith minerals p0090 A80-36062
- PHOTOCHEMISTRY
U PHOTOCHEMICAL REACTIONS
PHOTOCURRENTS
U PHOTOELECTRIC EMISSION
PHOTOELECTRIC CELLS
NT PHOTOVOLTAIC CELLS
PHOTOELECTRIC EFFECT
NT PHOTOIONIZATION
PHOTOELECTRIC EMISSION
An angular momentum approximation for molecular
collisions in the presence of intense laser
radiation p0069 A80-15673
- PHOTOELECTRON SPECTROSCOPY
The role of cesium suboxides in low-work-function
surface layers studied by X-ray photoelectron
spectroscopy - Ag-O-Cs p0051 A80-33844
- PHOTOEMISSION
U PHOTOELECTRIC EMISSION
PHOTOEMISSIVITY
U PHOTOELECTRIC EMISSION
PHOTOGEOLOGY
Plains and channels in the Lunae Planum-Chryse
Planitia region of Mars p0047 A80-26358
Volcanic features of Hawaii. A basis for
comparison with Mars [NASA-SP-403] p0034 N80-23912
- PHOTOGRAMMETRY
Conference of Remote Sensing Educators (CORSE-78)
[NASA-CP-2102] p0034 N80-20003
- PHOTOGRAPH INTERPRETATION
U PHOTOINTERPRETATION
PHOTOGRAPHIC EQUIPMENT
NT PHOTOGRAPHIC PROCESSING EQUIPMENT
PHOTOGRAPHIC MEASUREMENT
NT PHOTOGRAMMETRY
PHOTOGRAPHIC PROCESSING EQUIPMENT
A solar-heated water system for a photographic
processing laboratory p0098 A80-15750
- PHOTOGRAPHY
NT AERIAL PHOTOGRAPHY
- NT ASTRONOMICAL PHOTOGRAPHY
NT INFRARED PHOTOGRAPHY
NT STEREOPHOTOGRAPHY
NT ULTRAVIOLET PHOTOMETRY
- PHOTOINTERPRETATION
Landsat-based multiphase estimation of
California's irrigated lands p0079 A80-27435
Use of collateral information to improve LANDSAT
classification accuracies --- Ventura County and
Klamath National Forest, California [E80-10268] p0040 N80-29815
Irrigated lands assessment for water management
Applications Pilot Test (APT) --- California
[E80-10324] p0019 N80-32815
Infrared-temperature variability in a large
agricultural field --- Dunnigan, California
[E80-10331] p0038 N80-32822
- PHOTOIONIZATION
Photoexcitation and ionization in molecular oxygen
- Theoretical studies of electronic transitions
in the discrete and continuous spectral intervals
p0044 A80-20275
Photoexcitation and ionization in molecular
fluorine - Stieltjes-Tchebycheff calculations in
the static-exchange approximation p0046 A80-23324
- PHOTOLYSIS
Stratospheric ozone decrease due to
chlorofluoromethane photolysis - Predictions of
latitude dependence p0049 A80-29762
- PHOTOMAPPING
Using guided clustering techniques to analyze
Landsat data for mapping forest land cover in
northern California p0078 A80-25595
A far-infrared study of the reflection nebula NGC
2023 p0072 A80-26111
Plains and channels in the Lunae Planum-Chryse
Planitia region of Mars p0047 A80-26358
Error detection and rectification in digital
terrain models p0099 A80-27432
Landsat-based multiphase estimation of
California's irrigated lands p0079 A80-27435
Issues arising from the demonstration of
Landsat-based technologies to inventories and
mapping of the forest resources of the Pacific
Northwest states p0065 A80-41305
- PHOTOMETERS
NT ULTRAVIOLET SPECTROMETERS
PHOTOMETRY
NT ASTRONOMICAL PHOTOMETRY
NT SPECTROPHOTOMETRY
NT STELLAR SPECTROPHOTOMETRY
NT ULTRAVIOLET PHOTOMETRY
- PHOTON ABSORPTION
U ELECTROMAGNETIC ABSORPTION
PHOTOOXIDATION
Photosensitized oxidation of unsaturated polymers
p0049 A80-29086
- PHOTOREDUCTION
U PHOTOCHEMICAL REACTIONS
PHOTOSENSITIVITY
Photosensitized oxidation of unsaturated polymers
p0049 A80-29086
- PHOTOTHERMAL CONVERSION
Photocell heat engine solar power systems
p0079 A80-48179
- PHOTOTHERMOTROPISM
U TEMPERATURE EFFECTS
PHOTOVOLTAIC CELLS
Photocell heat engine solar power systems
p0079 A80-48179
- PHUGOID OSCILLATIONS
U OSCILLATIONS
PHYSICAL CHEMISTRY
NT QUANTUM CHEMISTRY
Physical chemistry and evolution of salt tolerance
in halobacteria p0090 A80-40383
- PHYSICAL EXERCISE
Exercise thermoregulation after 14 days of bed rest
p0088 A80-25989

PHYSIOLOGICAL EFFECTS

SUBJECT INDEX

Role of thermal and exercise factors in the mechanism of hypervolemia p0089 A80-32748

Exercise training-induced hypervolemia - Role of plasma albumin, renin, and vasopressin p0089 A80-32749

Na+ and Ca2+ ingestion - Plasma volume-electrolyte distribution at rest and exercise p0091 A80-41661

Fluid-electrolyte shifts and thermoregulation - Rest and work in heat with head cooling p0091 A80-48086

Extracellular hyperosmolality and body temperature during physical exercise in dogs p0092 A80-54076

PHYSIOLOGICAL EFFECTS

NT PHYSIOLOGICAL RESPONSES

Simulated weightlessness - Effects on bioenergetic balance p0095 A80-21544

Physiological response to hyper- and hypogravity during rollercoaster flight p0095 A80-21547

The architecture of the avian retina following exposure to chronic 2 G p0096 A80-42013

Extremes of urine osmolality - Lack of effect on red blood cell survival p0091 A80-46196

PHYSIOLOGICAL RESPONSES

Part-body and multibody effects on absorption of radio-frequency electromagnetic energy by animals and by models of man p0071 A80-22987

Fluid shifts and endocrine responses during chair rest and water immersion in man p0088 A80-25990

Retinal changes in rats flown on Cosmos 936 - A cosmic ray experiment p0091 A80-41995

PHYSIOLOGICAL TESTS

NT VESTIBULAR TESTS

Exercise thermoregulation after 14 days of bed rest p0088 A80-25989

A model for hypokinesia: Effects on muscle atrophy in the rat p0095 A80-28188

PHYSIOLOGY

NT EXERCISE PHYSIOLOGY

NT PSYCHOPHYSIOLOGY

NT WORKLOADS (PSYCHOPHYSIOLOGY)

PIGMENTS

Spectrophotometric identification of the pigment associated with light-driven primary sodium translocation in Halobacterium halobium p0088 A80-26015

PILOT ERROR

NASA aviation safety reporting system [NASA-TM-78608] p0083 N80-18010

PILOT PERFORMANCE

Optimal estimator model for human spatial orientation p0093 A80-24265

Analysis of eighty-four commercial aviation incidents - Implications for a resource management approach to crew training p0093 A80-40340

A pilot modeling technique for handling-qualities research [AIAA 80-1624] p0028 A80-45912

The effects of motion and q-seat cues on pilot simulator performance of three piloting tasks [NASA-TP-1601] p0004 N80-15069

Resource management on the flight deck --- conferences [NASA-CP-2120] p0082 N80-22283

Head-up transition behavior of pilots during simulated low-visibility approaches [NASA-TP-1618] p0082 N80-26039

Analytical methodology for determination of helicopter IFR precision approach requirements --- pilot workload and acceptance level [NASA-CR-152367] p0040 N80-28330

PILOT SELECTION

Resource management on the flight deck --- conferences [NASA-CP-2120] p0082 N80-22283

PILOT TRAINING

The development and use of large-motion simulator

systems in aeronautical research and development p0001 A80-10765

PILOTS (PERSONNEL)

NT AIRCRAFT PILOTS

PIONEER F SPACE PROBE

U PIONEER 10 SPACE PROBE

PIONEER G SPACE PROBE

U PIONEER 11 SPACE PROBE

PIONEER PROJECT

Pioneer Saturn encounter --- Pioneer 11 space probe [NASA-TM-80807] p0035 N80-10239

PIONEER SATURN SPACECRAFT

U PIONEER 11 SPACE PROBE

PIONEER SPACE PROBES

NT PIONEER VENUS 2 SOUNDER PROBE

NT PIONEER 10 SPACE PROBE

NT PIONEER 11 SPACE PROBE

PIONEER VENUS SPACECRAFT

NT PIONEER VENUS 1 SPACECRAFT

NT PIONEER VENUS 2 SPACECRAFT

Position and shape of the Venus bow shock - Pioneer Venus Orbiter observations p0087 A80-15295

A comparison of Pioneer Venus and Venera bow shock observations - Evidence for a solar cycle variation p0069 A80-15296

Pioneer-Venus solar flux radiometer p0077 A80-17468

Hot hydrogen in the exosphere of Venus p0070 A80-18943

Initial Pioneer Venus magnetometer observations p0078 A80-23690

Pioneer Venus occultation radio science data generation p0050 A80-30830

Data acquisition for measuring the wind on Venus from Pioneer Venus p0051 A80-30852

The location of the dayside ionopause of Venus - Pioneer Venus Orbiter magnetometer observations p0076 A80-48811

Data acquisition for measuring the wind on Venus from Pioneer Venus p0058 N80-26361

PIONEER VENUS 2 ENTRY PROBES

NT PIONEER VENUS 2 SOUNDER PROBE

PIONEER VENUS 2 MULTIPROBE SPACECRAFT

U PIONEER VENUS 2 SPACECRAFT

PIONEER VENUS 2 SPACECRAFT

NT PIONEER VENUS 2 SOUNDER PROBE

PIONEER VENUS 1 SPACECRAFT

Pioneer Venus spacecraft design and operation p0050 A80-30829

Pioneer Venus Unified Abstract Data Library and Quick Look Data Delivery System p0050 A80-30832

Pioneer Venus Orbiter Radar Mapper - Design and operation p0050 A80-30833

The Pioneer Venus Orbiter plasma wave investigation p0072 A80-30835

The Pioneer Venus Orbiter plasma analyzer experiment p0050 A80-30836

Pioneer Venus Orbiter planar retarding potential analyzer plasma experiment p0073 A80-30839

Design and operation of the Pioneer Venus Orbiter ultraviolet spectrometer p0073 A80-30841

PIONEER VENUS 2 SOUNDER PROBE

The infrared radiometer on the sounder probe of the Pioneer Venus mission p0050 A80-30847

Corrections in the pioneer Venus sounder probe gas chromatographic analysis of the lower Venus atmosphere p0089 A80-30875

Pioneer Venus sounder and small probes Nephelometer instrument p0053 A80-36750

PIONEER VENUS 2 SPACECRAFT

Pioneer Venus spacecraft design and operation p0050 A80-30829

Pioneer Venus Multiprobe entry telemetry recovery p0050 A80-30831

Pioneer Venus Sounder Probe Neutral Gas Mass Spectrometer p0073 A80-30844

SUBJECT INDEX

PLANETARY NEBULAE

- Pioneer Venus Sounder Probe gas chromatograph
p0089 A80-30845
- Pioneer Venus Sounder Probe Solar Flux Radiometer
p0073 A80-30846
- Atmosphere structure instruments on the four
Pioneer Venus entry probes
p0051 A80-30849
- Pioneer Venus small probes net flux radiometer
experiment
p0073 A80-30850
- Pioneer Venus multiprobe entry telemetry recovery
p0058 N80-26347
- PIONEER 10 SPACE PROBE**
Modeling Jupiter's current disc - Pioneer 10
outbound
p0075 A80-45153
- PIONEER 11 SPACE PROBE**
Pioneer Saturn --- Pioneer 11 performance and
encounter trajectory
p0043 A80-19114
- Preliminary results on the plasma environment of
Saturn from the Pioneer 11 plasma analyzer
experiment
p0043 A80-19116
- Saturn's magnetic field and magnetosphere
p0021 A80-19117
- Saturnian trapped radiation and its absorption by
satellites and rings - The first results from
Pioneer 11
p0070 A80-19118
- Saturn's magnetosphere, rings, and inner satellites
p0070 A80-19119
- Trapped radiation belts of Saturn - First look
p0070 A80-19121
- Pioneer Saturn encounter --- Pioneer 11 space probe
[NASA-TM-80807]
p0035 N80-10239
- PIPE FLOW**
On the combination of kinematics with flow
visualization to compute total circulation -
Application to vortex rings in a tube
[AIAA PAPER 80-1330]
p0065 A80-41563
- On the calculation of turbulent heat transport
downstream from an abrupt pipe expansion
p0076 A80-49037
- Modal content of noise generated by a coaxial jet
in a pipe
[NASA-CR-163575]
p0019 N80-33177
- PISTON ENGINES**
Study of cooling air inlet and exit geometries for
horizontally opposed piston aircraft engines
[AIAA PAPER 80-1242]
p0027 A80-38984
- PITCH ATTITUDE CONTROL**
U LONGITUDINAL CONTROL
- PITOT TUBES**
Study of boundary-layer transition using
transonic-cone preston tube data
[NASA-TM-81103]
p0010 N80-28305
- PITUITARY GLAND**
Growth hormone control of glucose oxidation
pathways in hypophysectomized rats
p0088 A80-24222
- PITUITARY HORMONES**
Hypergravity and estrogen effects on avian
anterior pituitary growth hormone and prolactin
levels
p0094 A80-20447
- PLAINS**
Plains and channels in the Lunae Planum-Chryse
Planitia region of Mars
p0047 A80-26358
- PLANE WAVES**
Acoustic resonances and sound scattering by a
shear layer
[NASA-CR-166181]
p0014 N80-15873
- PLANET ORIGINS**
U PLANETARY EVOLUTION
- PLANETARY ATMOSPHERES**
NT JUPITER ATMOSPHERE
NT MARS ATMOSPHERE
NT SATURN ATMOSPHERE
NT URANUS ATMOSPHERE
NT VENUS ATMOSPHERE
- Ultraviolet photometer observations of the
Saturnian system
p0070 A80-19122
- The surface and atmosphere of Pluto
p0045 A80-21757
- Titan aerosols - Optical properties and vertical
distribution
- The radius and ellipticity of Uranus from its
occultation of SAO 158687
p0073 A80-31937
- Origin and evolution of planetary atmospheres
p0053 A80-37598
- Narrow-field radiometry in a quasi-isotropic
atmosphere
p0079 A80-40233
- PLANETARY COMPOSITION**
The surface and atmosphere of Pluto
p0045 A80-21757
- Saturn's rings - 3-mm observations and derived
properties
p0045 A80-21758
- The effect of dense cores on the structure and
evolution of Jupiter and Saturn
p0056 A80-45812
- PLANETARY CORES**
NT EARTH CORE
The effect of dense cores on the structure and
evolution of Jupiter and Saturn
p0056 A80-45812
- PLANETARY CRATERS**
Endogenic craters on basaltic lava flows - Size
frequency distributions
p0061 A80-23727
- PLANETARY ENTRY**
U ATMOSPHERIC ENTRY
- PLANETARY ENVIRONMENTS**
NT JUPITER ATMOSPHERE
NT MARS ATMOSPHERE
NT MARS ENVIRONMENT
NT PLANETARY ATMOSPHERES
NT SATURN ATMOSPHERE
NT URANUS ATMOSPHERE
NT VENUS ATMOSPHERE
- PLANETARY EVOLUTION**
Core cooling by subsolidus mantle convection ---
thermal evolution model of earth
p0044 A80-19391
- Noble gas trapping and fractionation during
synthesis of carbonaceous matter --- in meteorites
p0093 A80-23669
- Primordial heating of asteroidal parent bodies
p0062 A80-24590
- On the comparative evolution of Ganymede and
Callisto
p0048 A80-28080
- Calculations of the evolution of the giant planets
p0049 A80-28086
- Origin and evolution of planetary atmospheres
p0053 A80-37598
- The effect of dense cores on the structure and
evolution of Jupiter and Saturn
p0056 A80-45812
- Tidal dissipation, orbital evolution, and the
nature of Saturn's inner satellites
p0058 A80-53235
- An assessment of ground-based techniques for
detecting other planetary systems. Volume 1:
An overview --- workshop conclusions
[NASA-CP-2124-VOL-1]
p0034 N80-18997
- PLANETARY EXPLORATION**
U SPACE EXPLORATION
- PLANETARY MAGNETIC FIELDS**
The phase of the ten-hour modulation in the Jovian
magnetosphere /Pioneers 10 and 11/
p0067 A80-10526
- Saturn's magnetic field and magnetosphere
p0021 A80-19117
- Initial Pioneer Venus magnetometer observations
p0078 A80-23690
- Modeling Jupiter's current disc - Pioneer 10
outbound
p0075 A80-45153
- Azimuthal magnetic field at Jupiter
p0076 A80-49185
- PLANETARY MANTLES**
NT EARTH MANTLE
- PLANETARY MAPPING**
Plains and channels in the Lunae Planum-Chryse
Planitia region of Mars
p0047 A80-26358
- Pioneer Venus Orbiter Radar Mapper - Design and
operation
p0050 A80-30833
- PLANETARY NEBULAE**
Infrared spectra of IC 418 and NGC 6572

PLANETARY ORBITS

SUBJECT INDEX

PLANETARY ORBITS p0069 A80-16862
On the 'thickness' of Saturn's rings caused by satellite and solar perturbations and by planetary precession

PLANETARY RADIATION p0042 A80-14293
21 cm maps of Jupiter's radiation belts from all rotational aspects

PLANETARY ROTATION p0076 A80-48877
The radius and ellipticity of Uranus from its occultation of SAO 158687

PLANETARY SATELLITES p0073 A80-31937
U NATURAL SATELLITES
PLANETARY SPACE FLIGHT
U INTERPLANETARY FLIGHT
PLANETARY STRUCTURE
The radius and ellipticity of Uranus from its occultation of SAO 158687

The effect of dense cores on the structure and evolution of Jupiter and Saturn p0073 A80-31937

PLANETARY SURFACES p0056 A80-45812
NT MARS SURFACE
The surface and atmosphere of Pluto

On the comparative evolution of Ganymede and Callisto p0045 A80-21757

PLANETARY TEMPERATURE p0048 A80-28080
Primordial heating of asteroidal parent bodies

PLANETISMALS p0062 A80-24590
U PROTOPLANETS
PLANETOLOGY
The Viking mission and the search for life on Mars p0086 A80-10738
On the inference of properties of Saturn's Ring E from energetic charged particle observations p0069 A80-15293
In search of other planetary systems p0046 A80-22978

PLANETS
NT EXTRASOLAR PLANETS
NT GAS GIANT PLANETS
NT JUPITER (PLANET)
NT PLUTO (PLANET)
NT SATURN (PLANET)
NT URANUS (PLANET)
PLANFORMS
NT DELTA WINGS
NT INFINITE SPAN WINGS
NT RECTANGULAR WINGS
Effect of tip planform on blade loading characteristics for a two-bladed rotor in hover [NASA-TN-78615] p0007 N80-14049

PLANNING
NT MISSION PLANNING
NT PROJECT PLANNING
PLANTS (BOTANY)
NT BARLEY
NT ORCHARDS
Problems and potentialities of cultured plant cells in retrospect and prospect p0077 A80-15225

PLASMA CHEMISTRY p0093 A80-24158
Plasma etching of poly/N,N'-p,p'-oxydiphenylene/pyromellitimide/ film and photo/thermal degradation of etched and unetched film

PLASMA CLOUDS p0057 A80-49341
Numerical calculations of the collapse of nonrotating, magnetic gas clouds

PLASMA COMPOSITION p0073 A80-30839
Pioneer Venus Orbiter planar retarding potential analyzer plasma experiment

PLASMA DIAGNOSTICS p0072 A80-30835
The Pioneer Venus Orbiter plasma wave investigation

PLASMA INTERACTIONS
Preliminary results on the plasma environment of Saturn from the Pioneer 11 plasma analyzer experiment

The Pioneer Venus Orbiter plasma analyzer experiment p0043 A80-19116
p0050 A80-30836

PLASMA PROBES
The Pioneer Venus Orbiter plasma wave investigation p0072 A80-30835

PLASMA SOUND WAVES
U PLASMA WAVES
PLASMA WAVES
The Pioneer Venus Orbiter plasma wave investigation p0072 A80-30835

PLASMA-PARTICLE INTERACTIONS
The solar wind interaction with Venus p0076 N80-13561

PLASMAS (PHYSICS)
NT COSMIC PLASMA
NT RAREFIED PLASMAS
NT SOLAR WIND
NT STELLAR WINDS
NT THERMAL PLASMAS
PLASTIC FILMS
U POLYMERIC FILMS
PLASTIC MATERIALS
U PLASTICS
PLASTICS
NT EPOXY RESINS
NT PHENOLIC RESINS
NT THERMOPLASTIC RESINS
NT THERMOSETTING RESINS
Toxicity of pyrolysis gases from foam plastics p0071 A80-24625

PLASTISOLS
NT SMOKE
PLOWED FIELDS
U FARMLANDS
PLSS
U PORTABLE LIFE SUPPORT SYSTEMS
PLUTO (PLANET)
The surface and atmosphere of Pluto p0045 A80-21757

POINT MATCHING METHOD (MATHEMATICS)
U BOUNDARY VALUE PROBLEMS
POINTING CONTROL SYSTEMS
Internal image motion compensation system for the Shuttle Infrared Telescope Facility p0064 A80-37427

POISEUILLE FLOW
U LAMINAR FLOW
POISSON EQUATION
A computer program to generate two-dimensional grids about airfoils and other shapes by the use of Poisson's equation [NASA-TN-81198] p0036 N80-26266

POLAR REGIONS
Mars - The north polar sand sea and related wind patterns p0047 A80-26370

POLARIMETRY
An investigation of previously derived Hyades, Coma, and M67 reddennings p0049 A80-29959

POLARIZATION (WAVES)
NT CIRCULAR POLARIZATION
POLLUTION
NT AIR POLLUTION
POLLUTION MONITORING
Nitrogen fertiliser and stratospheric ozone - Latitudinal effects p0043 A80-18948

POLYATOMIC GASES
NT DIATOMIC GASES
POLYATOMIC MOLECULES
NT DIATOMIC MOLECULES
POLYIMIDES
NT KAPTON (TRADEMARK)
Plasma etching of poly/N,N'-p,p'-oxydiphenylene/pyromellitimide/ film and photo/thermal degradation of etched and unetched film p0093 A80-24158

Catalysts for polyimide foams from aromatic isocyanates and aromatic dianhydrides --- flame retardant foams [NASA-CASE-ARC-11107-1] p0080 N80-16116

POLYMER CHEMISTRY
Photosensitized oxidation of unsaturated polymers p0049 A80-29086
Study of crosslinking and degradation mechanisms in sealant polymer candidates

SUBJECT INDEX

PRODUCTION ENGINEERING

[NASA-CR-152346] p0039 N80-22484
 Chemical research projects office: An overview
 and bibliography, 1975-1980
 [NASA-TM-81227] p0037 N80-31473
POLYMER MATRIX COMPOSITE MATERIALS
 A small-scale test for fiber release from carbon
 composites p0062 A80-26881
 Advanced thermoset resins for fire-resistant
 composites p0063 A80-34788
 Graphite composites with advanced resin matrices
 [AIAA 80-0758] p0064 A80-35051
 The viscoelastic behavior of a composite in a
 thermal environment
 [NASA-CR-163187] p0039 N80-24369
POLYMER PHYSICS
 Photosensitized oxidation of unsaturated polymers
 p0049 A80-29086
 Ambient curing fire resistant foams p0063 A80-34790
 Chemical research projects office: An overview
 and bibliography, 1975-1980
 [NASA-TM-81227] p0037 N80-31473
POLYMERIC FILMS
 NT KAPTON (TRADEMARK)
 Reverse osmosis membrane of high urea rejection
 properties --- water purification
 [NASA-CASE-ARC-10980-1] p0097 N80-23452
POLYMERIZATION
 Synthesis of perfluoroalkylether triazine elastomers
 p0051 A80-32825
 The role of metal ions in chemical evolution -
 Polymerization of alanine and glycine in a
 cation-exchanged clay environment p0090 A80-36195
POLYMERS
 Singlet oxygenation of 1,2-poly/1,4-hexadiene/s
 p0045 A80-21991
 Chelate-modified polymers for atmospheric gas
 chromatography
 [NASA-CASE-ARC-11154-1] p0097 N80-23383
 Shape change of Galileo probe models in
 free-flight tests
 [NASA-TM-81209] p0037 N80-27418
POLYURETHANE FOAM
 Ambient curing fire resistant foams p0063 A80-34790
PORTABLE LIFE SUPPORT SYSTEMS
 Development of the electrochemically regenerable
 carbon dioxide absorber for portable life
 support system application
 [ASME PAPER 79-ENAS-33] p0092 A80-15257
POSITIVE IONS
 The intracellular Na⁺/ and K⁺/ composition of
 the moderately halophilic bacterium, Paracoccus
 halodenitrificans p0091 A80-41250
POTABLE LIQUIDS
 NT POTABLE WATER
POTABLE WATER
 Design, fabrication and testing of a dual catalyst
 ammonia removal system for a urine VCD unit
 [NASA-CR-152372] p0085 N80-29023
POTASSIUM
 The intracellular Na⁺/ and K⁺/ composition of
 the moderately halophilic bacterium, Paracoccus
 halodenitrificans p0091 A80-41250
POTENTIAL FLOW
 Implicit computations of unsteady transonic flow
 governed by the full-potential equation in
 conservation form
 [AIAA PAPER 80-0150] p0062 A80-23935
POWER DENSITY (ELECTROMAGNETIC)
 U RADIANT FLUX DENSITY
POWER SERIES
 NT TAYLOR SERIES
POWERED LIFT AIRCRAFT
 Workshop on Thrust Augmenting Ejectors
 [NASA-CP-2093] p0004 N80-10107
 Analysis of fuel-conservative curved decelerating
 approach trajectories for powered-lift and CTOL
 jet aircraft
 [NASA-TP-1650] p0005 N80-19022
 Flight evaluation of configuration management
 system concepts during transition to the landing
 approach for a powered-lift STOL aircraft
 [NASA-TM-81146] p0008 N80-19127

PRAIRIES
 U GRASSLANDS
PRECAUTIONS
 U ACCIDENT PREVENTION
PRECIPITATION (METEOROLOGY)
 NT SNOW COVER
PREDICTION ANALYSIS TECHNIQUES
 Conditional replenishment using motion prediction
 p0065 A80-39715
PREDICTIONS
 NT IMPACT PREDICTION
 NT LINEAR PREDICTION
 NT NOISE PREDICTION (AIRCRAFT)
 NT PERFORMANCE PREDICTION
PRESSURE
 NT HIGH PRESSURE
 NT INTRACRANIAL PRESSURE
 NT WATER PRESSURE
PRESSURE BROADENING
 Absolute intensities and pressure broadening
 coefficients measured at different temperatures
 for the 201/II/-000 band of C-12/O2/-16 at 4978/cm
 p0048 A80-27125
PRESSURE DISTRIBUTION
 Unified aerodynamic-acoustic theory for a thin
 rectangular wing encountering a gust
 p0030 A80-36401
 Application of numerical optimization to the
 design of wings with specified pressure
 distributions
 [NASA-CR-3238] p0015 N80-16031
 A comparison of calculated and experimental lift
 and pressure distributions for several
 helicopter rotor sections
 [NASA-TM-81160] p0007 N80-16036
 Pressure and temperature fields associated with
 aero-optics tests --- transonic wind tunnel tests
 p0031 N80-25591
 A correlation method to predict the surface
 pressure distribution of an infinite plate or a
 body of revolution from which a jet is issuing
 [NASA-CR-152345] p0018 N80-32339
PRESSURE DRAG
 NT INTERFERENCE DRAG
PRESSURE EFFECTS
 Pressure and temperature dependence kinetics study
 of the NO + BrO yielding NO2 + Br reaction -
 Implications for stratospheric bromine
 photochemistry p0068 A80-14397
PRESSURE FIELDS
 U PRESSURE DISTRIBUTION
PRESSURE GRADIENTS
 Experimental investigation of a three dimensional
 turbulent boundary layer with a non disappearing
 pressure gradient p0054 A80-40907
PRESSURE MEASUREMENTS
 Pressure measurements on an ogive-cylinder at high
 angles of attack with laminar, transitional, or
 turbulent separation
 [AIAA 80-1556] p0028 A80-45856
PRESSURE SUITS
 NT SPACE SUITS
PRESTON TUBES
 U PITOT TUBES
 U SPEED INDICATORS
PREVENTION
 NT ACCIDENT PREVENTION
 NT FIRE PREVENTION
PRIVATE AIRCRAFT
 U GENERAL AVIATION AIRCRAFT
PROBLEM SOLVING
 NT ASYMPTOTIC METHODS
 Theory of the decision/problem state
 [NASA-TM-81192] p0103 N80-22984
 Problem solving and decisionmaking: An integration
 [NASA-TM-81191] p0103 N80-22985
 Clarification process: Resolution of
 decision-problem conditions p0103 N80-23985
 Decision-problem state analysis methodology
 [NASA-TM-81194] p0103 N80-25002
PROCEDURES
 NT PANEL METHOD (FLUID DYNAMICS)
PRODUCTION ENGINEERING
 Parametric study of helicopter aircraft systems
 costs and weights
 [NASA-CR-152315] p0016 N80-22305

PRODUCTION METHODS

PRODUCTION METHODS

U PRODUCTION ENGINEERING

PROGRAMMED INSTRUCTION

NT COMPUTER ASSISTED INSTRUCTION

PROGRAMS

NT GALILEO PROJECT

NT NASA PROGRAMS

NT PIONEER PROJECT

NT PROJECT SETI

NT TILT ROTOR RESEARCH AIRCRAFT PROGRAM

PROJECT PLANNING

NASA/Army XV-15 tilt rotor research aircraft

wind-tunnel test program plan --- Ames 40-ft by

80-ft wind tunnel tests

[NASA-TM-78562]

p0007 N80-15067

PROJECT SETI

On the design of a postprocessor for a search for

extraterrestrial intelligence /SETI/ system

[IAF PAPER 79-A-39]

p0093 A80-19895

On the significance of the apparent absence of

extraterrestrials on earth

p0087 A80-21780

A high-sensitivity search for extraterrestrial

intelligence at lambda 18 cm

p0090 A80-37933

PROJECTS

NT GALILEO PROJECT

NT PIONEER PROJECT

NT PROJECT SETI

PROMINENCES

NT SOLAR PROMINENCES

PROPAGATION (EXTENSION)

NT FLAME PROPAGATION

PROPELLER FANS

Potential benefits for propfan technology on

derivatives of future short- to medium-range

transport aircraft

[AIAA PAPER 80-1090]

p0026 A80-38905

PROPELLER SLIPSTREAMS

Propeller slipstream/wing interaction in the

transonic regime

[AIAA PAPER 80-0125]

p0032 A80-22733

Effect of propeller slipstream on the drag and

performance of the engine cooling system for a

general aviation twin-engine aircraft

[AIAA PAPER 80-1872]

p0027 A80-43315

PROPELLERS

NT PROPELLER FANS

PROPULSION SYSTEM CONFIGURATIONS

Wind tunnel investigation of an oblique wing

transport model at mach numbers between 0.6 and

1.4

[NASA-CR-137697]

p0013 N80-12059

PROPULSION SYSTEM PERFORMANCE

Force and moment data from a wind-tunnel test of a

tilt-nacelle V/STOL propulsion system with an

attitude control vane --- conducted in Ames 40

by 80 foot wind tunnel

[NASA-TM-81157]

p0006 N80-13003

PROPULSIVE EFFICIENCY

NASA overview

p0022 N80-10109

Static calibration of a two-dimensional wedge

nozzle with thrust vectoring and spanwise blowing

[NASA-TM-81161]

p0009 N80-23317

PROTECTION

NT ACCELERATION PROTECTION

NT THERMAL PROTECTION

PROTECTIVE CLOTHING

NT SPACE SUITS

PROTECTIVE COATINGS

Studies for improved high temperature coatings for

Space Shuttle application

p0079 A80-34757

PROTEINS

NT ALBUMINS

PROTONS

Proton movements in response to a light-driven

electrogenic pump for sodium ions in

Halobacterium halobium membranes

p0087 A80-17686

Acceleration of energetic protons by

interplanetary shocks

p0071 A80-21183

PROTOPLANETS

Calculations of the evolution of the giant planets

p0049 A80-28086

PROTOSTARS

NT T TAURI STARS

SUBJECT INDEX

Fragmentation of rotating protostellar clouds

p0047 A80-26107

Ring formation in rotating protostellar clouds

p0048 A80-26992

The role of magnetic fields in the collapse of

protostellar gas clouds

p0063 A80-31848

Fragmentation in a rotating protostar - A

comparison of two three-dimensional computer codes

p0053 A80-38432

Protostellar formation in rotating interstellar

clouds. III - Nonaxisymmetric collapse

p0054 A80-39375

Numerical calculations of the collapse of

nonrotating, magnetic gas clouds

p0057 A80-49341

PSYCHOLOGICAL EFFECTS

NT OPTICAL ILLUSION

PSYCHOLOGY

Theory of the decision/problem state

[NASA-TM-81192]

p0103 N80-22984

Problem solving and decisionmaking:

[NASA-TM-81191]

An integration

Clarification process: Resolution of

decision-problem conditions

[NASA-TM-81193]

p0103 N80-23985

PSYCHOPHYSIOLOGY

NT WORKLOADS (PSYCHOPHYSIOLOGY)

Visually induced self-motion sensation adapts

rapidly to left-right visual reversal

p0096 A80-44213

PULSATING FLOW

U UNSTEADY FLOW

PUMPS

NT ION PUMPS

PURIFICATION

NT AIR PURIFICATION

PYRAZINES

NT AZINES

NT METHYLENE BLUE

PYROGRAPHALLOY

U COMPOSITE MATERIALS

PYROLYSIS

Toxicity of pyrolysis gases from foam plastics

p0071 A80-24625

A small-scale test for fiber release from carbon

composites --- pyrolysis and impact

[NASA-TM-81179]

p0036 N80-18105

Q

QSO (RADIO SOURCES)

U QUASARS

QUANTUM CHEMISTRY

Quantum theory and chemistry: Two propositions

[NASA-TM-81202]

p0084 N80-25110

QUANTUM MECHANICS

F + H₂ collisions on two electronic potential

energy surfaces - Quantum-mechanical study of

the collinear reaction

p0068 A80-12012

Quantum-mechanical calculation of

three-dimensional atom-diatom collisions in the

presence of intense laser radiation

p0068 A80-15221

QUASARS

The dynamics and stability of radiatively driven

gas clouds. I - Plane-parallel slabs

p0042 A80-14058

The implications of hydrogen emission line ratios

in quasi-stellar objects

p0072 A80-27013

Radiatively driven winds for different power law

spectra --- for explaining narrow and broad

quasar absorption lines

p0054 A80-40138

QUASI-STELLAR RADIO SOURCES

U QUASARS

QUESTOL

A piloted simulator analysis of the carrier

landing capability of the quiet short-haul

research aircraft

[NASA-TM-78508]

p0011 N80-28338

QUEUEING THEORY

Dynamic decisions and work load in multitask

supervisory control

p0095 A80-40898

R

RADAR DATA

Aircraft motion analysis using limited flight and radar data

p0025 A80-27241

High resolution vertical profiles of wind, temperature and humidity obtained by computer processing and digital filtering of radiosonde and radar tracking data from the ITCZ experiment of 1977

[NASA-CR-3269]

p0039 N80-21926

RADAR EQUIPMENT

Pioneer Venus Orbiter Radar Mapper - Design and operation

p0050 A80-30833

RADAR IMAGERY

Pioneer Venus Orbiter Radar Mapper - Design and operation

p0050 A80-30833

RADAR MAPS**NT RADAR IMAGERY**

Pioneer Venus Orbiter Radar Mapper - Design and operation

p0050 A80-30833

RADAR NAVIGATION

NASA aviation safety reporting system [NASA-TM-81197]

p0085 N80-32352

RADIAL DRAINAGE PATTERNS**U DRAINAGE PATTERNS****RADIANT FLUX DENSITY****NT ELECTRON FLUX DENSITY****NT PARTICLE FLUX DENSITY****NT SOLAR FLUX DENSITY**

Pioneer Venus small probes net flux radiometer experiment

p0073 A80-30850

Unsteady density and velocity measurements in the 6 foot x 6 foot wind tunnel

p0023 N80-25594

RADIANT INTENSITY**U RADIANT FLUX DENSITY****RADIATION ABSORPTION****NT ELECTROMAGNETIC ABSORPTION****NT INFRARED ABSORPTION****NT MULTIPHOTON ABSORPTION****NT PHOTOABSORPTION**

Saturnian trapped radiation and its absorption by satellites and rings - The first results from Pioneer 11

p0070 A80-19118

Radiatively driven winds for different power law spectra --- for explaining narrow and broad quasar absorption lines

p0054 A80-40138

RADIATION BELTS

Saturnian trapped radiation and its absorption by satellites and rings - The first results from Pioneer 11

p0070 A80-19118

Trapped radiation belts of Saturn - First look

p0070 A80-19121

21 cm maps of Jupiter's radiation belts from all rotational aspects

p0076 A80-48877

RADIATION CHEMISTRY**NT PHOTOLYSIS**

Quantum-mechanical calculation of three-dimensional atom-diatom collisions in the presence of intense laser radiation

p0068 A80-15221

RADIATION COUNTERS**NT NEUTRON COUNTERS****RADIATION EFFECTS**

The radoracemization of isovaline - Cosmochemical implications --- gamma ray effects on Murchison meteorite primordial composition

p0086 A80-13018

Retinal changes in rats flown on Cosmos 936 - A cosmic ray experiment

p0091 A80-41995

RADIATION INTENSITY**U RADIANT FLUX DENSITY****RADIATION MEASURING INSTRUMENTS****NT EBERT SPECTROMETERS****NT INFRARED DETECTORS****NT INFRARED RADIOMETERS****NT INFRARED SCANNERS****NT NEUTRON COUNTERS****NT RADIOMETERS****NT SPECTRORADIOMETERS****NT ULTRAVIOLET SPECTROMETERS****RADIATION SOURCES**

A note of sound radiation from distributed sources

p0030 A80-31805

Output of acoustical sources --- effects of structural elements and background flow on immobile multipolar point radiation

p0030 A80-37806

On the output of acoustical sources

[NASA-CR-162576]

p0014 N80-15872

One millimeter continuum observations of extragalactic thermal sources

p0040 N80-33334

[NASA-CR-163590]

RADIATION SPECTRA**NT ABSORPTION SPECTRA****NT EMISSION SPECTRA****NT H LINES****NT INFRARED SPECTRA****NT LINE SPECTRA****NT SOLAR SPECTRA****NT STELLAR SPECTRA****NT VIBRATIONAL SPECTRA****RADIATIVE HEAT TRANSFER**

Shock-tube studies of radiative base heating of Jovian probe

p0064 A80-38114

RADIATIVE RECOMBINATION

Infrared spectra of IC 418 and NGC 6572

p0069 A80-16862

RADIATIVE TRANSFER**NT RADIATIVE HEAT TRANSFER**

The dynamics and stability of radiatively driven gas clouds. I - Plane-parallel slabs

p0042 A80-14058

The implications of hydrogen emission line ratios in quasi-stellar objects

p0072 A80-27013

Radiatively driven winds for different power law spectra --- for explaining narrow and broad quasar absorption lines

p0054 A80-40138

RADIO ANTENNAS

On the limitations of the concept of space frequency equivalence

p0069 A80-16697

RADIO ASTRONOMY

Low-pass interference filters for submillimeter astronomy

p0070 A80-19956

Saturn's rings - 3-mm observations and derived properties

p0045 A80-21758

An assessment of ground-based techniques for detecting other planetary systems. Volume 1: An overview --- workshop conclusions [NASA-CP-2124-VOL-1]

p0034 N80-18997

RADIO EMISSION

21 cm maps of Jupiter's radiation belts from all rotational aspects

p0076 A80-48877

RADIO EQUIPMENT**NT RADIO ANTENNAS****NT RADIOMETERS****RADIO FREQUENCY HEATING**

Part-body and multibody effects on absorption of radio-frequency electromagnetic energy by animals and by models of man

p0071 A80-22987

RADIO INTERFEROMETERS

On the limitations of the concept of space frequency equivalence

p0069 A80-16697

RADIO OBSERVATION

High-frequency continuum observations of young stars

p0047 A80-25365

RADIO OCCULTATION

Pioneer Venus occultation radio science data generation

p0050 A80-30830

RADIO SOURCES (ASTRONOMY)**NT EXTRAGALACTIC RADIO SOURCES****NT QUASARS**

Far-infrared spectra of W51-IRS 2 and W49 NW

p0056 A80-44967

RADIO SPECTROSCOPY

Far infrared, near infrared, and radio molecular

RADIO TRANSMISSION

SUBJECT INDEX

line studies of HFE 2, HFE 3, and FJM 6
p0068 A80-11489

RADIO TRANSMISSION
NT MICROWAVE ATTENUATION

RADIO TRANSMITTERS
NT RADIOSONDES

RADIO WAVES
NT RADIO EMISSION
NT SUBMILLIMETER WAVES

RADIOACTIVE ELEMENTS
U RADIOACTIVE ISOTOPES

RADIOACTIVE ISOTOPES
Primordial heating of asteroidal parent bodies
p0062 A80-24590

RADIOACTIVE NUCLIDES
U RADIOACTIVE ISOTOPES

RADIOACTIVITY
Whole planet cooling and the radiogenic heat
source contents of the earth and moon
p0053 A80-36651

RADIOMETERS
NT INFRARED DETECTORS
NT INFRARED RADIOMETERS
NT INFRARED SCANNERS
NT SPECTRORADIOMETERS
Pioneer-Venus solar flux radiometer
p0077 A80-17468
Pioneer Venus small probes net flux radiometer
experiment
p0073 A80-30850
Narrow-field radiometry in a quasi-isotropic
atmosphere
p0079 A80-40233

RADIONUCLIDES
U RADIOACTIVE ISOTOPES

RADIOSONDES
Induction powered biological radiosonde
[NASA-CASE-ARC-11120-1] p0099 N80-18691
High resolution vertical profiles of wind,
temperature and humidity obtained by computer
processing and digital filtering of radiosonde
and radar tracking data from the LCZ experiment
of 1977
[NASA-CR-3269] p0039 N80-21926

RANDOM LOADS
NT GUST LOADS

RANDOM PROCESSES
Studies in astronomical time series analysis:
Modeling random processes in the time domain
[NASA-TM-81148] p0036 N80-15854

RARE GAS COMPOUNDS
Theoretical treatment of the spin-orbit coupling
in the rare gas oxides NeO, ArO, KrO, and XeO
p0057 A80-50149

RARE GASES
NT HELIUM
NT LIQUID HELIUM
NT LIQUID HELIUM 2
NT XENON
Carbonaceous chondrites. I - Characterization and
significance of carbonaceous chondrite /CM/
xenoliths in the Jodzie howardite
p0086 A80-13013
Noble gas trapping and fractionation during
synthesis of carbonaceous matter --- in meteorites
p0093 A80-23669
Computational study of alkali-metal-noble gas
collisions in the presence of nonresonant lasers
- Na + Xe + $h/2\pi/\omega$ sub 1 + $h/2\pi/\omega$
sub 2 system
p0056 A80-48762

RAREFIED GASES
NT INTERPLANETARY GAS
NT INTERSTELLAR GAS
NT NEUTRAL GASES

RAREFIED PLASMAS
Preliminary results on the plasma environment of
Saturn from the Pioneer 11 plasma analyzer
experiment
p0043 A80-19116

RATE METERS
U MEASURING INSTRUMENTS

RATES (PER TIME)
NT ACCELERATION (PHYSICS)
NT ANGULAR ACCELERATION
NT BURNING RATE
NT COLLISION PARAMETERS
NT ELECTRON FLUX DENSITY
NT FLOW VELOCITY

NT FLUX DENSITY
NT GROUP VELOCITY
NT HEAT FLUX
NT HIGH GRAVITY ENVIRONMENTS
NT MAGNETIC FLUX
NT PARTICLE ACCELERATION
NT PARTICLE FLUX DENSITY
NT RADIANT FLUX DENSITY
NT RELATIVISTIC VELOCITY
NT SOLAR FLUX
NT SOLAR FLUX DENSITY
NT SUBSONIC SPEED
NT WIND VELOCITY

RATIOS
NT REYNOLDS NUMBER
NT SIGNAL TO NOISE RATIOS
NT STROUHAL NUMBER

REACTION JETS
U JET FLOW
U JET THRUST

REACTION KINETICS
Pressure and temperature dependence kinetics study
of the NO + BrO yielding NO2 + Br reaction -
Implications for stratospheric bromine
photochemistry
p0068 A80-14397
Introductory study of the chemical behavior of jet
emissions in photochemical smog --- computerized
simulation
[NASA-CR-152345] p0016 N80-21891
Modified Iterative Extended Hueckel. 2:
Application to the interaction of Na(+),
Na(+) (aq.), Mg(+) -2(aq.) with adenine and thymine
[NASA-TM-81201] p0084 N80-25109

REACTION RATE
U REACTION KINETICS

REAL GASES
Forebody and base region real-gas flow in severe
planetary entry by a factored implicit numerical
method. I - Computational fluid dynamics
[AIAA PAPER 80-0065] p0061 A80-22731

REAL TIME OPERATION
Math modeling and computer mechanization for real
time simulation of rotary-wing aircraft
[NASA-CR-162400] p0013 N80-10137
Pioneer Venus multiprobe entry telemetry recovery
p0058 N80-26347

REAL VARIABLES
NT DIFFERENTIAL EQUATIONS
NT ELLIPTIC DIFFERENTIAL EQUATIONS
NT GREEN FUNCTION
NT KERNEL FUNCTIONS
NT LINEAR EQUATIONS
NT NUMERICAL DIFFERENTIATION
NT PARABOLIC DIFFERENTIAL EQUATIONS
NT PARTIAL DIFFERENTIAL EQUATIONS
NT POISSON EQUATION
NT TAYLOR SERIES
NT VORTICITY

REATTACHED FLOW
Investigation of a reattaching turbulent shear
layer flow over a backward-facing step
p0062 A80-27736

RECIPROCATING ENGINES
U PISTON ENGINES

RECIRCULATION
U CIRCULATION

RECLAMATION
NT WATER RECLAMATION

RECOGNITION
NT PATTERN RECOGNITION

RECOMBINATION REACTIONS
NT RADIATIVE RECOMBINATION

RECORDING
NT DATA SMOOTHING

RECORDING INSTRUMENTS
NT FLIGHT RECORDERS

RECOVERABLE SPACECRAFT
NT SPACE SHUTTLES

RECTANGULAR DRAINAGE
U DRAINAGE PATTERNS

RECTANGULAR PLANSFORMS
NT RECTANGULAR WINGS

RECTANGULAR WINGS
Unified aerodynamic-acoustic theory for a thin
rectangular wing encountering a gust
p0030 A80-36401

RECUPERATORS
U REGENERATORS

SUBJECT INDEX

RETINA

- RED BLOOD CELLS
 - U ERYTHROCYTES
- RED GIANT STARS
- NT CARBON STARS
- RED SHIFT
 - An investigation of previously derived Hyades, Coma, and M67 reddening
- REDUCTION (MATHEMATICS)
 - U OPTIMIZATION
- REENTRY
 - NT SPACECRAFT REENTRY
 - REENTRY BODIES
 - U REENTRY VEHICLES
 - REENTRY SHIELDING
 - The 60-MW Shuttle interaction heating facility
- REENTRY VEHICLES
 - NT M-2F2 LIFTING BODY
 - Supersonic flow over three-dimensional ablated nosetips using an unsteady implicit numerical procedure
 - [AIAA PAPER 80-0063]
- REFLECTION
 - NT INFRARED REFLECTION
- REFLECTORS
 - NT PARABOLOID MIRRORS
 - NT SOLAR COLLECTORS
 - NT SOLAR REFLECTORS
 - Large Deployable Reflector (LDR)
 - [NASA-CR-152402]
- REFRACTORY MATERIALS
 - NT MOLYBDENUM
- REFRACTORY METALS
 - NT MOLYBDENUM
- REFRASIL (TRADEMARK)
 - U SILICON DIOXIDE
- REGENERATORS
 - Development of the electrochemically regenerable carbon dioxide absorber for portable life support system application
 - [ASME PAPER 79-ENAS-33]
- REGIONS
 - NT PACIFIC NORTHWEST (US)
 - NT PANAMA CANAL ZONE
 - NT POLAR REGIONS
 - NT SOUTHERN CALIFORNIA
- REGOLITH
 - Monte Carlo simulation of lunar megaregolith and implications
 - Heterogeneous phase reactions of Martian volatiles with putative regolith minerals
- REGRESSION (STATISTICS)
 - U REGRESSION ANALYSIS
- REGRESSION ANALYSIS
 - Some observations regarding the statistical determination of stress rupture regression lines
- REGULATIONS
 - Factors affecting the retirement of commercial transport jet aircraft
 - [NASA-CR-152308]
- REIGNITION
 - U IGNITION
- REINFORCED MATERIALS
 - U COMPOSITE MATERIALS
- REINFORCED PLASTICS
 - NT GLASS FIBER REINFORCED PLASTICS
- REINFORCING FIBERS
 - NT CARBON FIBERS
- RELATIVISTIC EFFECTS
 - Relativistic scattered wave calculations on UF6
- RELATIVISTIC PARTICLES
 - Relativistic scattered wave calculations on UF6
 - The propagation of Jovian electrons to earth
- RELATIVISTIC VELOCITY
 - Feasibility studies for light scattering experiments to determine the velocity relaxation of small particles in a fluid
 - [NASA-CR-163214]
- RELIABILITY
 - NT COMPONENT RELIABILITY
 - RELIABILITY CONTROL
 - U RELIABILITY ENGINEERING
- RELIABILITY ENGINEERING
 - A comparison of computer architectures for the NASA demonstration advanced avionics system
- REMAGNETIZATION
 - U MAGNETIZATION
- REMANENCE
 - Theories for the origin of lunar magnetism
- REMOTE SENSORS
 - NASA's western regional applications training activity
- RESEARCH AIRCRAFT
 - NT B-70 AIRCRAFT
 - NT C-8A AUGMENTOR WING AIRCRAFT
 - NT QUESTOL
 - The Quiet Short-Haul Research Aircraft /QSRA/
 - V/STOL flight simulation
 - Quiet short-haul research aircraft familiarization document --- STOL
 - NASA/Army XV-15 tilt rotor research aircraft wind-tunnel test program plan --- Ames 40-ft by 80-ft wind tunnel tests
 - NASA quiet short-haul research aircraft experimenters' handbook
 - A candidate V/STOL research aircraft design concept using an S-3A aircraft and 2 Pegasus 11 engines
- RESEARCH AND DEVELOPMENT
 - The development and use of large-motion simulator systems in aeronautical research and development
 - Potential benefits for propfan technology on derivatives of future short- to medium-range transport aircraft
 - The future of short-haul transport aircraft
 - Ames Research Center publications: A continuing bibliography, 1978
 - Chemical research projects office: An overview and bibliography, 1975-1980
- RESINS
 - NT EPOXY RESINS
 - NT PHENOLIC RESINS
 - NT THERMOPLASTIC RESINS
 - NT THERMOSETTING RESINS
- RESOLUTION
 - NT HIGH RESOLUTION
- RESONANCE
 - Acoustic resonances and sound scattering by a shear layer
- RESOURCES
 - NT FORESTS
- RESOURCES MANAGEMENT
 - Analysis of eighty-four commercial aviation incidents - Implications for a resource management approach to crew training
- RESPONSES
 - NT DYNAMIC RESPONSE
 - NT MODAL RESPONSE
 - NT PHYSIOLOGICAL RESPONSES
 - NT TRANSIENT RESPONSE
- REST
 - NT BED REST
 - Fluid shifts and endocrine responses during chair rest and water immersion in man
- RETARDANTS
 - NT FLAME RETARDANTS
- RETARDING ION MASS SPECTROMETERS
 - U MASS SPECTROMETERS
- RETINA
 - Retinal changes in rats flown on Cosmos 936 - A cosmic ray experiment
 - The architecture of the avian retina following exposure to chronic 2 G

RETRIEVAL

SUBJECT INDEX

RETRIEVAL p0096 A80-42013
 NT INFORMATION RETRIEVAL
 REUSABLE SPACECRAFT
 NT SPACE SHUTTLES
 REVERSE OSMOSIS
 Reverse osmosis membrane of high urea rejection properties --- water purification [NASA-CASE-ARC-10980-1] p0097 N80-23452
 REYNOLDS NUMBER
 Noise generation by a lifting wing/flap combination at Reynolds numbers to 2.8 x 10 to the 6th [AIAA PAPER 80-0035] p0024 A80-22729
 Experimental studies of scale effects on oscillating airfoils at transonic speeds [NASA-TM-81216] p0010 N80-27287
 REYNOLDS STRESS
 High-resolution LDA measurements of Reynolds stress in boundary layers and wakes [AIAA 80-0436] p0025 A80-26967
 Reynolds stress closures: Status and prospects p0077 N80-27660
 RH-2 HELICOPTER
 U UH-1 HELICOPTER
 RICHARDSON-DUSHMANN EQUATION
 U TEMPERATURE EFFECTS
 RIGID ROTOR HELICOPTERS
 Effect of tip vortex structure on helicopter noise due to blade-vortex interaction p0031 A80-52645
 RIGID ROTORS
 Effects of primary rotor parameters on flapping dynamics [NASA-TP-1431] p0005 N80-15138
 A hingeless rotor XV-15 design integration feasibility study. Volume 1: Engineering design studies [NASA-CR-152310] p0015 N80-18030
 An experimental investigation of the effects of aeroelastic couplings on aeromechanical stability of a hingeless rotor helicopter [AD-A085819] p0101 N80-29294
 RIGID STRUCTURES
 NT RIGID ROTORS
 RING STRUCTURES
 NT JUPITER RINGS
 Ring formation in rotating protostellar clouds p0048 A80-26992
 RL CIRCUITS
 NT RLC CIRCUITS
 RLC CIRCUITS
 Transient solution for megajoule energy release in a lumped-parameter series RLC circuit p0051 A80-32826
 RLC NETWORKS
 U RLC CIRCUITS
 ROCKET ENGINES
 NT ARC JET ENGINES
 ROCKET FLIGHT
 Singular perturbations and the sounding rocket problem p0001 A80-24268
 ROCKET SONDES
 U SOUNDING ROCKETS
 ROCKET VEHICLES
 NT SOUNDING ROCKETS
 ROCKET-BORNE INSTRUMENTS
 X-ray spectrometer spectrograph telescope system --- for solar corona study p0077 A80-17502
 ROCKS
 NT BASALT
 NT REGOLITH
 RODENTS
 NT MICE
 ROLL CONTROL
 U LATERAL CONTROL
 ROSBY REGIMES
 Wave propagation and transport in the middle atmosphere p0072 A80-26437
 ROTARY WING AIRCRAFT
 NT BQ-105 HELICOPTER
 NT H-53 HELICOPTER
 NT HELICOPTERS
 NT MILITARY HELICOPTERS
 NT OH-6 HELICOPTER
 NT RIGID ROTOR HELICOPTERS

NT TILT ROTOR AIRCRAFT
 NT UH-1 HELICOPTER
 NT XV-15 AIRCRAFT
 Math modeling and computer mechanization for real time simulation of rotary-wing aircraft [NASA-CR-162400] p0013 N80-10137
 ROTARY WINGS
 NT LIFTING ROTORS
 NT RIGID ROTORS
 The promise of multicyclic control --- for helicopter vibration reduction p0022 A80-33123
 Multicyclic control for helicopters - Research in progress at Ames Research Center [AIAA 80-0671] p0025 A80-34997
 Multicyclic control of a helicopter rotor considering the influence of vibration, loads, and control motion [AIAA 80-0673] p0025 A80-34998
 Coupled rotor and fuselage equations of motion [NASA-TM-81153] p0006 N80-10516
 Effect of tip planform on blade loading characteristics for a two-bladed rotor in hover [NASA-TM-78615] p0007 N80-14049
 Acoustically swept rotor --- helicopter noise reduction [NASA-CASE-ARC-11106-1] p0102 N80-14107
 Effects of primary rotor parameters on flapping dynamics [NASA-TP-1431] p0005 N80-15138
 A comparison of calculated and experimental lift and pressure distributions for several helicopter rotor sections [NASA-TM-81160] p0007 N80-16036
 On the nonlinear deformation geometry of Euler-Bernoulli beams --- rotary wings [NASA-TP-1566] p0101 N80-20619
 An experimental evaluation of a helicopter rotor section designed by numerical optimization [NASA-TM-78622] p0009 N80-21287
 The design, testing and evaluation of the MIT individual-blade-control system as applied to gust alleviation for helicopters [NASA-CR-152352] p0016 N80-22357
 Comparison of calculated and measured model rotor loading and wake geometry [NASA-TM-81189] p0009 N80-24262
 A comprehensive analytical model of rotorcraft aerodynamics and dynamics. Part 1: Analysis development [NASA-TM-81182] p0010 N80-28296
 Dynamic stall on advanced airfoil sections [AD-A085809] p0101 N80-29252
 Comparison of calculated and measured helicopter rotor lateral flapping angles [NASA-TM-81213] p0012 N80-33349
 Stability of nonuniform rotor blades in hover using a mixed formulation [NASA-TM-81226] p0012 N80-33777
 ROTATING
 U ROTATION
 ROTATING BODIES
 NT HELICOPTER TAIL ROTORS
 NT LIFTING ROTORS
 NT RIGID ROTORS
 NT ROTARY WINGS
 NT ROTORS
 NT TURBINE WHEELS
 On the nonlinear deformation geometry of Euler-Bernoulli beams --- rotary wings [NASA-TP-1566] p0101 N80-20619
 ROTATING ENVIRONMENTS
 Ring formation in rotating protostellar clouds p0048 A80-26992
 ROTATING MATTER
 Protostellar formation in rotating interstellar clouds. III - Nonaxisymmetric collapse p0054 A80-39375
 ROTATING VEHICLES
 U ROTATING BODIES
 ROTATION
 NT MOLECULAR ROTATION
 NT PLANETARY ROTATION
 NT STELLAR ROTATION
 Thresholds for detection of constant rotary acceleration during vibratory rotary acceleration p0091 A80-42003
 ROTATIONAL FLOW
 U FLUID FLOW

SUBJECT INDEX

SATELLITE SOUNDING

U VORTICES

ROTOR AERODYNAMICS

Multicyclic control of a helicopter rotor
considering the influence of vibration, loads,
and control motion

[AIAA 80-0673] p0025 A80-34998

Effect of tip vortex structure on helicopter noise
due to blade-vortex interaction

p0031 A80-52645

Effect of tip planform on blade loading
characteristics for a two-bladed rotor in hover

[NASA-TM-78615] p0007 N80-14049

Acoustically swept rotor --- helicopter noise
reduction

[NASA-CASE-ARC-11106-1] p0102 N80-14107

Effects of primary rotor parameters on flapping
dynamics

[NASA-TP-1431] p0005 N80-15138

The design, testing and evaluation of the MIT
individual-blade-control system as applied to

gust alleviation for helicopters

[NASA-CR-152352] p0016 N80-22357

Comparison of calculated and measured model rotor
loading and wake geometry

[NASA-TM-81189] p0009 N80-24262

A comprehensive analytical model of rotorcraft
aerodynamics and dynamics. Part 1: Analysis

development

[NASA-TM-81182] p0010 N80-28296

A comprehensive analytical model of rotorcraft
aerodynamics and dynamics. Part 2: User's manual

[NASA-TM-81183] p0010 N80-28297

A comprehensive analytical model of rotorcraft
aerodynamics and dynamics. Part 3: Program

manual

[NASA-TM-81184] p0010 N80-28298

Analytical design and evaluation of an active
control system for helicopter vibration

reduction and gust response alleviation

[NASA-CR-152377] p0017 N80-28369

Dynamic stall on advanced airfoil sections

[AD-A085809] p0101 N80-29252

Comparison of calculated and measured blade loads
on a full-scale tilting propotor in a wind tunnel

[NASA-TM-81228] p0012 N80-31386

Analysis and correlation of test data from an
advanced technology rotor system --- helicopter

performance prediction

[NASA-CR-152366] p0019 N80-33351

Calculation of three-dimensional unsteady
transonic flows past helicopter blades

[NASA-TP-1721] p0100 N80-33356

ROTOR BLADES

Effect of tip vortex structure on helicopter noise
due to blade-vortex interaction

p0031 A80-52645

ROTOR BLADES (TURBOMACHINERY)

Analytical study of the effects of wind tunnel
turbulence on turbofan rotor noise --- NASA Ames

40 by 80 foot wind tunnel

[NASA-CR-152359] p0016 N80-23099

Comparison of calculated and measured blade loads
on a full-scale tilting propotor in a wind tunnel

[NASA-TM-81228] p0012 N80-31386

ROTOR DISKS

U TURBINE WHEELS

ROTOR HUBS

U ROTORS

ROTOR LIFT

A comparison of calculated and experimental lift
and pressure distributions for several

helicopter rotor sections

[NASA-TM-81160] p0007 N80-16036

Synthesis of rotor test data for real-time
simulation

[NASA-CR-152311] p0015 N80-18029

ROTORCRAFT

U ROTARY WING AIRCRAFT

ROTORCRAFT AIRCRAFT

A new approach to active control of rotorcraft
vibration

[AIAA 80-1778] p0027 A80-45556

ROTORS

NT HELICOPTER TAIL ROTORS

NT LIFTING ROTORS

NT RIGID ROTORS

NT ROTARY WINGS

NT TURBINE WHEELS

Effects of rotor parameter variations on handling
qualities of unaugmented helicopters in
simulated terrain flight

[NASA-TM-81190] p0012 N80-31407

RUBBER

NT ELASTOMERS

RULES

NT INSTRUMENT FLIGHT RULES

S

S STARS

NT CARBON STARS

S-N DIAGRAMS

Effects of moisture on apparent flexure strength
and on torsion and flexure fatigue properties of
graphite-epoxy composites

p0063 A80-27965

S-3 AIRCRAFT

A candidate V/STOL research aircraft design

concept using an S-3A aircraft and 2 Pegasus 11

engines

[NASA-TM-81204] p0009 N80-24293

SACRAMENTO VALLEY (CA)

Irrigated lands assessment for water management

Applications Pilot Test (APT) --- California

[E80-10324] p0019 N80-32815

Infrared-temperature variability in a large

agricultural field --- Dunnigan, California

[E80-10331] p0038 N80-32822

SAFETY

NT AIRCRAFT SAFETY

NT FLIGHT SAFETY

SAFETY DEVICES

NT SPACE SUITS

SAFETY FACTORS

Small Transport Aircraft Technology

p0021 A80-21225

SALTS

Physical chemistry and evolution of salt tolerance

in halobacteria

p0090 A80-40383

SAMPLERS

Efficiency of aerosol collection on wires exposed

in the stratosphere

[NASA-TM-81147] p0035 N80-11676

SAMPLES

NT MARS SURFACE SAMPLES

SAMPLING

NT PARTICULATE SAMPLING

SAMPLING DEVICES

U SAMPLERS

SAN JOAQUIN VALLEY (CA)

Irrigated lands assessment for water management

Applications Pilot Test (APT) --- California

[E80-10324] p0019 N80-32815

SAND DUNES

U DUNES

SANDS

Threshold windspeeds for sand on Mars - Wind

tunnel simulations

p0048 A80-27391

SATAN (SENSOR)

U TERRAIN ANALYSIS

SATELLITE ATMOSPHERES

Organic chemistry on Titan

p0087 A80-20340

16-30 micron spectroscopy of Titan

p0049 A80-29321

SATELLITE ATTITUDE DISTURBANCE

U ATTITUDE STABILITY

SATELLITE COMMUNICATIONS

U SPACECRAFT COMMUNICATION

SATELLITE ORBITS

On the 'thickness' of Saturn's rings caused by

satellite and solar perturbations and by

planetary precession

p0042 A80-14293

SATELLITE SOLAR POWER STATIONS

Photocell heat engine solar power systems

p0079 A80-48179

SATELLITE SOUNDING

A comparative study of cosmic ray intensity
variations during 1972-1977 using spacecraft and
ground-based observations

p0072 A80-28244

Corrections in the Pioneer Venus sounder probe gas
chromatographic analysis of the lower Venus
atmosphere

SATELLITE-BORNE INSTRUMENTS

SUBJECT INDEX

SATELLITE-BORNE INSTRUMENTS p0089 A80-30875
 Space applications of superconductivity p0044 A80-20126
 The Pioneer Venus Orbiter plasma wave investigation p0072 A80-30835
 Pioneer Venus small probes net flux radiometer experiment p0073 A80-30850
 SATELLITES
 NT ATS 3
 NT CALLISTO
 NT COSMOS SATELLITES
 NT GANYMEDE
 NT INFRARED ASTRONOMY SATELLITE
 NT NATURAL SATELLITES
 NT NIMBUS 4 SATELLITE
 NT TITAN
 NT VENERA SATELLITES
 SATURN (PLANET)
 Pioneer Saturn --- Pioneer 11 performance and encounter trajectory p0043 A80-19114
 Saturn's magnetic field and magnetosphere p0021 A80-19117
 Saturnian trapped radiation and its absorption by satellites and rings - The first results from Pioneer 11 p0070 A80-19118
 Trapped radiation belts of Saturn - First look p0070 A80-19121
 Ultraviolet photometer observations of the Saturnian system p0070 A80-19122
 The effect of dense cores on the structure and evolution of Jupiter and Saturn p0056 A80-45812
 Tidal dissipation, orbital evolution, and the nature of Saturn's inner satellites p0058 A80-53235
 Pioneer Saturn encounter --- Pioneer 11 space probe [NASA-TM-80807] p0035 A80-10239
 SATURN ATMOSPHERE
 Preliminary results on the plasma environment of Saturn from the Pioneer 11 plasma analyzer experiment p0043 A80-19116
 Saturn's magnetic field and magnetosphere p0021 A80-19117
 Saturn's magnetosphere, rings, and inner satellites p0070 A80-19119
 SATURN RINGS
 On the 'thickness' of Saturn's rings caused by satellite and solar perturbations and by planetary precession p0042 A80-14293
 On the inference of properties of Saturn's Ring E from energetic charged particle observations p0069 A80-15293
 Saturnian trapped radiation and its absorption by satellites and rings - The first results from Pioneer 11 p0070 A80-19118
 Saturn's magnetosphere, rings, and inner satellites p0070 A80-19119
 Saturn's rings - 3-mm observations and derived properties p0045 A80-21758
 SATURN SATELLITES
 NT TITAN
 SAVANNAHS
 U GRASSLANDS
 SCALE EFFECT
 Experimental studies of scale effects on oscillating airfoils at transonic speeds [NASA-TM-81216] p0010 A80-27287
 SCALE MODELS
 Large scale model tests of a new technology V/STOL concept [AIAA PAPER 80-0233] p0023 A80-19303
 Tests of subgrid-scale models in strained turbulence [AIAA PAPER 80-1339] p0065 A80-41569
 Investigation of ground effects on large and small scale models of a three fan V/STOL aircraft configuration [NASA-CR-152240] p0015 A80-16030
 Shape change of Galileo probe models in free-flight tests [NASA-TM-81209] p0037 A80-27418

Phase 1 wind tunnel tests of the J-97 powered, external augmentor V/STOL model [NASA-CR-152255] p0017 A80-28303
 SCALING
 A scaling theory for linear systems p0030 A80-32676
 SCANNERS
 NT INFRARED SCANNERS
 SCATTERING
 NT ACOUSTIC SCATTERING
 NT ATMOSPHERIC SCATTERING
 NT BACKSCATTERING
 NT CONFIGURATION INTERACTION
 NT LIGHT SCATTERING
 NT MIE SCATTERING
 NT TROPOSPHERIC SCATTERING
 NT WAVE SCATTERING
 SCF
 U SELF CONSISTENT FIELDS
 SCHEDULING
 NT PREDICTION ANALYSIS TECHNIQUES
 SCHROEDINGER EQUATION
 A new propagation method for the radial Schroedinger equation p0069 A80-15768
 Quantum theory and chemistry: Two propositions [NASA-TM-81202] p0084 A80-25110
 SCIENTIFIC SATELLITES
 NT ATS 3
 SEALANTS
 U SEALERS
 SEALERS
 Study of crosslinking and degradation mechanisms in sealant polymer candidates [NASA-CR-152346] p0039 A80-22484
 SEARCH FOR EXTRATERRESTRIAL INTELLIGENCE
 U PROJECT SETI
 SEASONAL VARIATIONS
 U ANNUAL VARIATIONS
 SEATS
 Release-rate calorimetry of multilayered materials for aircraft seats p0051 A80-34223
 Release-rate calorimetry of multilayered materials for aircraft seats [AIAA 80-0759] p0064 A80-35052
 Materials for fire resistant passenger seats in aircraft p0080 A80-48757
 Fire-resistant materials for aircraft passenger seat construction [NASA-TM-78617] p0035 A80-13255
 SECRETIONS
 NT ENDOCRINE SECRETIONS
 NT ESTROGENS
 NT HORMONES
 NT INSULIN
 NT PITUITARY HORMONES
 SEDIMENTS
 NT SANDS
 Silt-clay aggregates on Mars p0041 A80-10366
 Eolian sedimentation on earth and Mars - Some comparisons p0068 A80-13969
 SEEDS
 Irrigated lands assessment for water management Applications Pilot Test (APT) --- California [E80-10324] p0019 A80-32815
 SELECTION
 NT PILOT SELECTION
 SELF CONSISTENT FIELDS
 SCF and CI calculations of the dipole moment function of ozone --- Self-Consistent Field and Configuration-Interaction p0043 A80-17111
 SELF REGULATING
 U AUTOMATIC CONTROL
 SEMICONDUCTOR DEVICES
 NT CHARGE COUPLED DEVICES
 NT MIS (SEMICONDUCTORS)
 NT PHOTOVOLTAIC CELLS
 SEMICONDUCTORS (MATERIALS)
 NT MIS (SEMICONDUCTORS)
 Improved characterization of the Si-SiO2 interface p0095 A80-41532
 SEMIEMPIRICAL EQUATIONS
 Scattering by nonspherical particles of size comparable to wavelength - A new semi-empirical

SUBJECT INDEX

SHORT HAUL AIRCRAFT

- theory and its application to tropospheric aerosols p0052 A80-36040
- SENSE ORGANS**
- NT RETINA
- SENSITIVITY**
- NT PHOTSENSITIVITY
- SENSORINOTOR PERFORMANCE**
- Multi-modal information processing for visual workload relief [NASA-CR-162720] p0100 N80-16737
- SENSORY PERCEPTION**
- NT AUDITORY PERCEPTION
- NT SPACE PERCEPTION
- NT VISUAL PERCEPTION
- SEPARATED FLOW**
- NT BOUNDARY LAYER SEPARATION
- Control of forebody vortex orientation to alleviate side forces [AIAA PAPER 80-0183] p0024 A80-23955
- Diagnosis of separated flow regions on wind-tunnel models using an infrared camera p0025 A80-29494
- A vortex-lattice method for the calculation of the nonsteady separated flow over delta wings [AIAA PAPER 80-1803] p0027 A80-43286
- A comprehensive comparison between experiment and prediction for a transonic turbulent separated flow [AIAA PAPER 80-1407] p0027 A80-44154
- Separated skin-friction measurements - Source of error: An assessment and elimination [AIAA PAPER 80-1409] p0027 A80-44155
- Pressure measurements on an ogive-cylinder at high angles of attack with laminar, transitional, or turbulent separation [AIAA 80-1556] p0028 A80-45856
- On the calculation of turbulent heat transport downstream from an abrupt pipe expansion p0076 A80-49037
- Control of forebody three-dimensional flow separations p0022 N80-15164
- Three-dimensional interactions and vortical flows with emphasis on high speeds [NASA-TM-81169] p0008 N80-21286
- Leeward flow over delta wings at supersonic speeds [NASA-TM-81187] p0036 N80-23250
- Simple turbulence models and their application to boundary layer separation [NASA-CR-3283] p0017 N80-24269
- SERIES (MATHEMATICS)**
- NT TAYLOR SERIES
- SERVICE LIFE**
- Factors affecting the retirement of commercial transport jet aircraft [NASA-CR-152308] p0013 N80-10148
- SERVOMECHANISMS**
- The design, testing and evaluation of the MIT individual-blade-control system as applied to gust alleviation for helicopters [NASA-CR-152352] p0016 N80-22357
- SETI**
- U PROJECT SETI
- SHANNON INFORMATION THEORY**
- U INFORMATION THEORY
- SHEAR FATIGUE**
- U SHEAR STRESS
- SHEAR FLOW**
- Evaluation of the time dependent surface shear stress in turbulent flows [ASME PAPER 79-WA/FE-17] p0078 A80-18618
- Characterization of acoustic disturbances in linearly sheared flows p0030 A80-31804
- Tests of subgrid-scale models in strained turbulence [AIAA PAPER 80-1339] p0065 A80-41569
- Multiple-time-scale concepts in turbulent transport modelling p0080 A80-49277
- Turbulent structures in wall-bounded shear flows observed via three-dimensional numerical simulators --- using the Illiac 4 computer [NASA-TM-81219] p0037 N80-29622
- SHEAR LAYERS**
- Investigation of a reattaching turbulent shear layer flow over a backward-facing step p0062 A80-27736
- Three-dimensional simulation of the free shear layer using the vortex-in-cell method p0067 A80-49300
- Characterization of acoustic disturbances in linearly sheared flows [NASA-CR-162577] p0014 N80-15869
- Acoustic resonances and sound scattering by a shear layer [NASA-CR-166181] p0014 N80-15873
- SHEAR PROPERTIES**
- NT SHEAR STRENGTH
- SHEAR STRENGTH**
- Degradation of tensile and shear properties of composites exposed to fire or high temperature p0072 A80-29697
- SHEAR STRESS**
- Evaluation of the time dependent surface shear stress in turbulent flows [ASME PAPER 79-WA/FE-17] p0078 A80-18618
- SHEARING STRESS**
- U SHEAR STRESS
- SHIELDING**
- NT HEAT SHIELDING
- NT REENTRY SHIELDING
- SHIPS**
- NT AIRCRAFT CARRIERS
- SHOCK HEATING**
- Shock-tube studies of radiative base heating of Jovian probe p0064 A80-38114
- SHOCK TUBES**
- Test section configuration for aerodynamic testing in shock tubes p0026 A80-38085
- 'GAIN' - Gas-addition, impedance-matched arc driver --- shock tube gas dynamics p0064 A80-38131
- SHOCK WAVE GENERATORS**
- NT SHOCK TUBES
- SHOCK WAVE INTERACTION**
- Asymptotic features of shock-wave boundary-layer interaction p0055 A80-43135
- An optical emission-line phase of the extreme carbon star IRC +30219 p0056 A80-44993
- The acceleration of energetic charged particles by interplanetary and supernova shock waves p0080 A80-53209
- SHOCK WAVE PROPAGATION**
- Acceleration of energetic protons by interplanetary shocks p0071 A80-21183
- SHOCK WAVES**
- Gas dynamics in barred spirals - Gaseous density waves and galactic shocks p0041 A80-10685
- Position and shape of the Venus bow shock - Pioneer Venus Orbiter observations p0087 A80-15295
- A comparison of Pioneer Venus and Venera bow shock observations - Evidence for a solar cycle variation p0069 A80-15296
- Molecule formation and infrared emission in fast interstellar shocks. I Physical processes p0043 A80-16410
- An experimental and numerical investigation of a three-dimensional shock wave separated turbulent boundary layer [AIAA PAPER 80-0002] p0061 A80-22727
- Implicit computations of unsteady transonic flow governed by the full-potential equation in conservation form [AIAA PAPER 80-0150] p0062 A80-23935
- SHORT HAUL AIRCRAFT**
- NT C-8A AUGMENTOR WING AIRCRAFT
- The Quiet Short-Haul Research Aircraft /QSRA/ p0021 A80-27384
- Upper surface blowing noise of the NASA-Ames quiet short-haul research aircraft [AIAA PAPER 80-1064] p0026 A80-36002
- Potential benefits for propfan technology on derivatives of future short- to medium-range transport aircraft [AIAA PAPER 80-1090] p0026 A80-38905
- The future of short-haul transport aircraft [SAE PAPER 800755] p0029 A80-49703

SHORT TAKEOFF AIRCRAFT

SUBJECT INDEX

- Quiet short-haul research aircraft familiarization document --- STOL [NASA-TM-81149] p0007 N80-14108
- NASA quiet short-haul research aircraft experimenters' handbook [NASA-TM-81162] p0007 N80-16024
- A piloted simulator analysis of the carrier landing capability of the quiet short-haul research aircraft [NASA-TM-78508] p0011 N80-28338
- Application of advanced technologies to small, short-haul transport aircraft [NASA-CR-152363] p0018 N80-32353
- Application of advanced technologies to small, short-haul air transports [NASA-CR-152364] p0019 N80-33396
- SHORT TAKEOFF AIRCRAFT**
- NT C-8A AUGMENTOR WING AIRCRAFT
- NT QUESTOL
- The Quiet Short-Haul Research Aircraft /QSRA/ [NASA-CR-3191] p0021 A80-27384
- An exploratory investigation of the STOL landing maneuver [NASA-CR-3191] p0014 N80-12996
- Flight test of navigation and guidance sensor errors measured on STOL approaches [NASA-TM-81154] p0007 N80-13041
- Quiet short-haul research aircraft familiarization document --- STOL [NASA-TM-81149] p0007 N80-14108
- Evaluation of approximate methods for the prediction of noise shielding by airframe components [NASA-TP-1004] p0004 N80-15129
- Flight tests of the total automatic flight control system (Tafcos) concept on a DHC-6 Twin Otter aircraft [NASA-TP-1513] p0005 N80-17081
- V/STOLAND avionics system flight-test data on a UH-1H helicopter [NASA-TM-78591] p0008 N80-18047
- Flight evaluation of configuration management system concepts during transition to the landing approach for a powered-lift STOL aircraft [NASA-TM-81146] p0008 N80-19127
- Large-scale wind-tunnel tests of inverting flaps on a STOL utility aircraft model [NASA-TP-1696] p0005 N80-25318
- Phase 1 wind tunnel tests of the J-97 powered, external augmentor V/STOL model [NASA-CR-152255] p0017 N80-28303
- A piloted simulator analysis of the carrier landing capability of the quiet short-haul research aircraft [NASA-TM-78508] p0011 N80-28338
- A summary of joint US-Canadian augmentor wing powered-lift STOL research programs at the Ames Research Center, NASA, 1975-1980 [NASA-TM-81215] p0011 N80-28373
- A comparison of flight and simulation data for three automatic landing system control laws for the Augmentor wing jet STOL research airplane [NASA-CR-152365] p0018 N80-32338
- SHORT WAVE RADIATION**
- NT SUBMILLIMETER WAVES
- SHUTTLE ORBITERS**
- U SPACE SHUTTLE ORBITERS
- SIDE-LOOKING RADAR**
- NT RADAR IMAGERY
- SIGHT**
- U VISUAL PERCEPTION
- SIGNAL DETECTORS**
- On the design of a postprocessor for a search for extraterrestrial intelligence /SETI/ system [IAF PAPER 79-A-39] p0093 A80-19895
- SIGNAL DISCRIMINATORS**
- U SIGNAL DETECTORS
- SIGNAL PROCESSING**
- A variational technique for smoothing flight-test and accident data [AIAA 80-1601] p0028 A80-45894
- SIGNAL TO NOISE RATIOS**
- Two-photon excitation of nitric oxide fluorescence as a temperature indicator in unsteady gas-dynamic processes [NASA-TM-81220] p0037 N80-32700
- SIGNAL TRANSMISSION**
- NT DATA TRANSMISSION
- NT MICROWAVE ATTENUATION
- NT TELEMETRY
- Pioneer Venus occultation radio science data generation p0050 A80-30830
- SIKORSKY AIRCRAFT**
- NT H-53 HELICOPTER
- SIKORSKY S-65 HELICOPTER**
- U H-53 HELICOPTER
- SILICA**
- U SILICON DIOXIDE
- SILICON**
- Improved characterization of the Si-SiO₂ interface p0095 A80-41532
- SILICON COMPOUNDS**
- NT SILICON DIOXIDE
- SILICON DIOXIDE**
- Improved characterization of the Si-SiO₂ interface p0095 A80-41532
- SILICON OXIDES**
- NT SILICON DIOXIDE
- SILTS**
- U SEDIMENTS
- SILVER**
- The role of cesium suboxides in low-work-function surface layers studied by X-ray photoelectron spectroscopy - Ag-O-Cs p0051 A80-33844
- Comparison of the early stages of condensation of Cu and Ag on Mo/100/ with Cu and Ag on W/100/ p0053 A80-37193
- SIMULATION**
- NT ATMOSPHERIC ENTRY SIMULATION
- NT COMPUTERIZED SIMULATION
- NT CONTROL SIMULATION
- NT DIGITAL SIMULATION
- NT ENVIRONMENT SIMULATION
- NT FLIGHT SIMULATION
- NT LANDING SIMULATION
- NT SYSTEMS SIMULATION
- NT WEIGHTLESSNESS SIMULATION
- SIMULATOR TRAINING**
- U TRAINING SIMULATORS
- SIMULATORS**
- NT COCKPIT SIMULATORS
- NT CONTROL SIMULATION
- NT FLIGHT SIMULATORS
- NT MOTION SIMULATORS
- NT TRAINING SIMULATORS
- SINGULAR INTEGRAL EQUATIONS**
- Integral equations for flows in wind tunnels p0029 A80-21906
- The inversion of singular integral equations by expansion in Jacobi polynomials p0030 A80-42758
- SINGULARITY (MATHEMATICS)**
- Singular perturbations and the sounding rocket problem p0001 A80-24268
- SIZE DISTRIBUTION**
- NT PARTICLE SIZE DISTRIBUTION
- SKELETON**
- U MUSCULOSKELETAL SYSTEM
- SKIN FRICTION**
- NT AERODYNAMIC DRAG
- Skin friction measurements by a new nonintrusive double-laser-beam oil viscosity balance technique [AIAA PAPER 80-1373] p0065 A80-41587
- Separated skin-friction measurements - Source of error: An assessment and elimination [AIAA PAPER 80-1409] p0027 A80-44155
- SLANT**
- U SLOPES
- SLANT PERCEPTION**
- U SPACE PERCEPTION
- SLENDER BODIES**
- Computation of supersonic turbulent flows over an inclined ogive-cylinder-flare [AIAA PAPER 80-1410] p0066 A80-41608
- Computations of the Magnus effect for slender bodies in supersonic flow [AIAA 80-1586] p0028 A80-45882
- SLENDER WINGS**
- NT INFINITE SPAN WINGS
- SLIPSTREAMS**
- NT PROPELLER SLIPSTREAMS
- SLOPES**
- NT GLIDE PATHS
- Error detection and rectification in digital terrain models

SUBJECT INDEX

SOLAR WIND

- p0099 A80-27432
 Use of collateral information to improve LANDSAT
 classification accuracies --- Ventura County and
 Klamath National Forest, California
 [E80-10268] p0040 N80-29815
- SMOG**
 Introductory study of the chemical behavior of jet
 emissions in photochemical smog --- computerized
 simulation
 [NASA-CR-152345] p0016 N80-21891
- SMOKE**
 Smoke and dust particles of meteoric origin in the
 mesosphere and stratosphere p0055 A80-42744
- SMOOTHING**
 NT DATA SMOOTHING
- SNOW COVER**
 Permittivity and attenuation of wet snow between 4
 and 12 GHz p0052 A80-36244
- SOCIAL FACTORS**
 On the significance of the apparent absence of
 extraterrestrials on earth p0087 A80-21780
- SOCIOLOGY**
 NT SOCIAL FACTORS
- SODIUM**
 Proton movements in response to a light-driven
 electrogenic pump for sodium ions in
 Halobacterium halobium membranes p0087 A80-17686
 Spectrophotometric identification of the pigment
 associated with light-driven primary sodium
 translocation in Halobacterium halobium
 p0088 A80-26015
 The role of Na⁺/K⁺ in transport processes of
 bacterial membranes p0088 A80-27077
 Na + Xe collisions in the presence of two
 nonresonant lasers p0051 A80-32416
 The intracellular Na⁺/K⁺ and K⁺/Na⁺ composition of
 the moderately halophilic bacterium, Paracoccus
 halodenitrificans p0091 A80-41250
 Na⁺ and Ca²⁺ ingestion - Plasma volume-electrolyte
 distribution at rest and exercise p0091 A80-41661
- SODIUM COMPOUNDS**
 NT SODIUM HYDROXIDES
- SODIUM HYDROXIDES**
 New gas phase inorganic ion cluster species and
 their atmospheric implications p0075 A80-37510
- SOFTWARE (COMPUTERS)**
 U COMPUTER PROGRAMS
 U COMPUTER SYSTEMS PROGRAMS
- SOIL MOISTURE**
 Microbial mobilization of calcium and magnesium in
 waterlogged soils p0089 A80-32834
 Irrigated lands assessment for water management
 Applications Pilot Test (APT) --- California
 [E80-10324] p0019 N80-32815
 Infrared-temperature variability in a large
 agricultural field --- Dunnigan, California
 [E80-10331] p0038 N80-32822
- SOIL SCIENCE**
 Microbial mobilization of calcium and magnesium in
 waterlogged soils p0089 A80-32834
- SOILS**
 NT SANDS
- SOLAR ACTIVITY**
 NT SOLAR PROMINENCES
- SOLAR ACTIVITY EFFECTS**
 Are solar spectral variations a drive for climatic
 change p0042 A80-15488
- SOLAR COLLECTORS**
 NT SOLAR REFLECTORS
 A solar-heated water system for a photographic
 processing laboratory p0098 A80-15750
- SOLAR CORONA**
 NT CORONAL HOLES
 Quest for ultrahigh resolution in X-ray optics ---
 for solar astronomy p0032 A80-17480
- X-ray spectrometer spectrograph telescope system
 --- for solar corona study p0077 A80-17502
- Paraboloidal X-ray telescope mirror for solar
 coronal spectroscopy p0078 A80-17503
- A real-time electronic imaging system for solar
 X-ray observations from sounding rockets
 p0029 A80-18545
- High-resolution Lyman-alpha filtergrams of the sun
 p0075 A80-37277
- SOLAR CYCLES**
 NT SUNSPOT CYCLE
 A comparison of Pioneer Venus and Venera bow shock
 observations - Evidence for a solar cycle
 variation p0069 A80-15296
 X-ray bright points and the solar cycle dependence
 of emerging magnetic flux p0077 N80-17950
- SOLAR ECLIPSES**
 Measurements of NO, O3, and temperature at 19.8 km
 during the total solar eclipse of 26 February 1979
 p0055 A80-43638
- SOLAR ENERGY CONVERSION**
 A solar-heated water system for a photographic
 processing laboratory p0098 A80-15750
- SOLARES orbiting mirror system
 [AAS 79-304] p0067 A80-52280
- SOLAR FLUX**
 Pioneer-Venus solar flux radiometer p0077 A80-17468
- SOLAR FLUX DENSITY**
 Pioneer Venus Sounder Probe Solar Flux Radiometer
 p0073 A80-30846
- SOLAR GRAVITATION**
 On the 'thickness' of Saturn's rings caused by
 satellite and solar perturbations and by
 planetary precession p0042 A80-14293
- SOLAR HEATING**
 A solar-heated water system for a photographic
 processing laboratory p0098 A80-15750
- SOLAR INSTRUMENTS**
 Pioneer-Venus solar flux radiometer p0077 A80-17468
 Narrow-field radiometry in a quasi-isotropic
 atmosphere p0079 A80-40233
- SOLAR MAGNETIC FIELD**
 X-ray bright points and the solar cycle dependence
 of emerging magnetic flux p0077 N80-17950
- SOLAR NEBULA**
 U SOLAR CORONA
- SOLAR PLASMA (RADIATION)**
 U SOLAR WIND
- SOLAR PROMINENCES**
 High-resolution Lyman-alpha filtergrams of the sun
 p0075 A80-37277
- SOLAR RADIATION**
 NT SOLAR WIND
 NT SOLAR X-RAYS
- SOLAR REFLECTORS**
 SOLARES orbiting mirror system
 [AAS 79-304] p0067 A80-52280
- SOLAR SPECTRA**
 High-resolution Lyman-alpha filtergrams of the sun
 p0075 A80-37277
- SOLAR SYSTEM**
 Origin and evolution of planetary atmospheres
 p0053 A80-37598
 An assessment of ground-based techniques for
 detecting other planetary systems. Volume 1:
 An overview --- workshop conclusions
 [NASA-CP-2124-VOL-1] p0034 N80-18997
- SOLAR WIND**
 Position and shape of the Venus bow shock -
 Pioneer Venus Orbiter observations p0087 A80-15295
 Preliminary results on the plasma environment of
 Saturn from the Pioneer 11 plasma analyzer
 experiment p0043 A80-19116
 The Pioneer Venus Orbiter plasma analyzer experiment
 p0050 A80-30836

SOLAR X-RAYS

SUBJECT INDEX

The solar wind interaction with Venus
p0076 N80-13561

SOLAR X-RAYS
A real-time electronic imaging system for solar
X-ray observations from sounding rockets
p0029 A80-18545

SOLID ROTATION
U ROTATING BODIES

SOLID STATE DEVICES
NT CHARGE COUPLED DEVICES
NT MIS (SEMICONDUCTORS)
NT PHOTOVOLTAIC CELLS

SOLID STATE PHYSICS
Effect of three-body interactions on the structure
of small clusters
p0057 A80-49383

SONDES
NT RADIOSONDES

SONIC FLOW
U TRANSONIC FLOW

SORPTION
NT CHEMISORPTION

SORTIE CAN
U SPACELAB

SORTIE LAB
U SPACELAB

SOUND
U ACOUSTICS

SOUND GENERATORS
On the output of acoustical sources
[NASA-CR-162576]
p0014 N80-15872

SOUND MEASUREMENT
U ACOUSTIC MEASUREMENTS

SOUND PERCEPTION
U AUDITORY PERCEPTION

SOUND WAVES
NT AERODYNAMIC NOISE
NT AIRCRAFT NOISE
NT ENGINE NOISE
NT JET AIRCRAFT NOISE
A note of sound radiation from distributed sources
p0030 A80-31805
Output of acoustical sources --- effects of
structural elements and background flow on
immobile multipolar point radiation
p0030 A80-37806
A note on sound radiation into a uniformly flowing
medium
p0031 A80-45488

SOUNDERS
U SOUNDING

SOUNDING
NT SATELLITE SOUNDING
Pioneer Venus Sounder Probe gas chromatograph
p0089 A80-30845

SOUNDING ROCKETS
A real-time electronic imaging system for solar
X-ray observations from sounding rockets
p0029 A80-18545
Singular perturbations and the sounding rocket
problem
p0001 A80-24268

SOUTHERN CALIFORNIA
Use of collateral information to improve LANDSAT
classification accuracies --- Ventura County and
Klamath National Forest, California
[E80-10268]
p0040 N80-29815

SOVIET SPACECRAFT
NT COSMOS SATELLITES
NT VENERA SATELLITES

SPACE BIOLOGY
U EXOBIOLOGY

SPACE COMMUNICATION
NT EXTRATERRESTRIAL COMMUNICATION
NT INTERPLANETARY COMMUNICATION
NT SPACECRAFT COMMUNICATION

SPACE ENVIRONMENT
U AEROSPACE ENVIRONMENTS

SPACE ENVIRONMENT SIMULATION
NT WEIGHTLESSNESS SIMULATION

SPACE ERECTABLE STRUCTURES
Large Deployable Reflector (LDR)
[NASA-CR-152402]
p0040 N80-33319

SPACE EXPLORATION
An entry and landing probe for Titan
[AIAA PAPER 80-0117]
p0060 A80-18384
Pioneer Saturn --- Pioneer 11 performance and
encounter trajectory
p0043 A80-19114

Saturn's magnetic field and magnetosphere
p0021 A80-19117

Saturn's magnetosphere, rings, and inner satellites
p0070 A80-19119

Trapped radiation belts of Saturn - First look
p0070 A80-19121

In search of other planetary systems
p0046 A80-22978

Pioneer Venus Unified Abstract Data Library and
Quick Look Data Delivery System
p0050 A80-30832

A high-sensitivity search for extraterrestrial
intelligence at lambda 18 cm
p0090 A80-37933

Tidal dissipation, orbital evolution, and the
nature of Saturn's inner satellites
p0058 A80-53235

SPACE FLIGHT
NT INTERPLANETARY FLIGHT
NT MANNED SPACE FLIGHT
NT SPACECRAFT REENTRY

SPACE FLIGHT STRESS
Motion sickness in the squirrel monkey
p0095 A80-25891

SPACE MECHANICS
NT CELESTIAL MECHANICS

SPACE PERCEPTION
Optimal estimator model for human spatial
orientation
p0093 A80-24265
Effect of field of view and monocular viewing on
angular size judgements in an outdoor scene
[NASA-TM-81176]
p0083 N80-19792

SPACE PROBES
NT GALILEO PROBE
NT JUPITER PROBES
NT PIONEER VENUS 2 SPACECRAFT
NT PIONEER 10 SPACE PROBE
NT PIONEER 11 SPACE PROBE
NT VENERA SATELLITES
NT VENUS PROBES
An entry and landing probe for Titan
[AIAA PAPER 80-0117]
p0060 A80-18384
Shock-tube studies of radiative base heating of
Jovian probe
p0064 A80-38114
Comet nucleus impact probe feasibility study
[NASA-CR-152375]
p0040 N80-26364
Titan probe technology assessment and technology
development plan study
[NASA-CR-152381]
p0040 N80-32417

SPACE SHUTTLE ORBITERS
Studies for improved high temperature coatings for
Space Shuttle application
p0079 A80-34757
Development of high viscosity coatings for
advanced Space Shuttle applications
p0079 A80-34760
Equivalent-cone calculation of nitric oxide
production rate during Space Shuttle re-entry
p0056 A80-45359

SPACE SHUTTLE PAYLOADS
NT SPACEBORNE EXPERIMENTS
NT SPACELAB
Design alternatives for the Shuttle Infrared
Telescope Facility
p0060 A80-17435
Internal image motion compensation system for the
Shuttle Infrared Telescope Facility
p0064 A80-37427
Thermal design of a Shuttle infrared telescope
facility /SIRTF/
[AIAA PAPER 80-1502]
p0079 A80-41466

SPACE SHUTTLES
The 60-MW Shuttle interaction heating facility
p0059 A80-12603
Stratospheric aerosol modification by supersonic
transport and space shuttle operations - Climate
implications
p0047 A80-26088
Control system designs for the shuttle infrared
telescope facility
[NASA-TM-81159]
p0036 N80-18869

SPACE SUITS
High-pressure protective systems technology
[ASME PAPER 79-ENAS-15]
p0092 A80-15240

SPACE SYSTEMS ENGINEERING
U AEROSPACE ENGINEERING

SUBJECT INDEX

SPECTROMETERS

SPACE TRANSPORTATION

NT SPACE SHUTTLE ORBITERS

SPACE TRANSPORTATION SYSTEM

NT SPACE SHUTTLE ORBITERS

NT SPACE SHUTTLES

SPACEBORNE ASTRONOMY

Integrated infrared detector arrays for
low-background astronomy

p0066 A80-44639

SPACEBORNE EXPERIMENTS

The Pioneer Venus Orbiter plasma analyzer experiment

p0050 A80-30836

Pioneer Venus Orbiter planar retarding potential
analyzer plasma experiment

p0073 A80-30839

Pioneer Venus small probes net flux radiometer
experiment

p0073 A80-30850

Simulation of the Viking biology experiments - An
overview

p0090 A80-36066

NASA-Ames Life Sciences Flight Experiments program
- 1980 status report

p0094 A80-43209

The development of a Space Shuttle Research Animal
Holding Facility

p0096 A80-43213

Comet nucleus impact probe feasibility study
[NASA-CR-152375]

p0040 N80-26364

SPACEBORNE TELESCOPES

Design alternatives for the Shuttle Infrared
Telescope Facility

p0060 A80-17435

Thermal design of a Shuttle infrared telescope
facility /SIRTF/

p0079 A80-41466

Control system designs for the shuttle infrared
telescope facility

p0036 N80-18869

SPACECRAFT CABIN ATMOSPHERES

Bosch - An alternate CO2 reduction technology
[ASME PAPER 79-ENAS-32]

p0092 A80-15256

Development of a nitrogen generation system
[NASA-CR-152333]

p0085 N80-19800

Performance characterization of a Bosch CO sub 2
reduction subsystem

p0085 N80-22987

SPACECRAFT COMMUNICATION

Pioneer Venus occultation radio science data
generation

p0050 A80-30830

Pioneer Venus Multiprobe entry telemetry recovery

p0050 A80-30831

SPACECRAFT CONFIGURATIONS

Comet nucleus impact probe feasibility study
[NASA-CR-152375]

p0040 N80-26364

SPACECRAFT CONSTRUCTION MATERIALS

Studies for improved high temperature coatings for
Space Shuttle application

p0079 A80-34757

SPACECRAFT DESIGN

Free convection in enclosures exposed to
compressive heating --- Galileo descent module

p0079 A80-41495

Cryogenic systems for spacecraft

p0055 A80-42902

SPACECRAFT INSTRUMENTS

Pioneer Venus Orbiter planar retarding potential
analyzer plasma experiment

p0073 A80-30839

Design and operation of the Pioneer Venus Orbiter
ultraviolet spectrometer

p0073 A80-30841

Pioneer Venus Sounder Probe Neutral Gas Mass
Spectrometer

p0073 A80-30844

Pioneer Venus Sounder Probe gas chromatograph

p0089 A80-30845

Pioneer Venus Sounder Probe Solar Flux Radiometer

p0073 A80-30846

The infrared radiometer on the sounder probe of
the Pioneer Venus mission

p0050 A80-30847

Atmosphere structure instruments on the four
Pioneer Venus entry probes

p0051 A80-30849

Pioneer Venus sounder and small probes
Nephelometer instrument

p0053 A80-36750

Cryogenic systems for spacecraft

p0055 A80-42902

SPACECRAFT ORBITS

NT SATELLITE ORBITS

SPACECRAFT REENTRY

Galileo probe forebody entry thermal protection -
Aerothermal environments and heat shielding

requirements

[ASME PAPER 80-ENAS-24]

Equivalent-cone calculation of nitric oxide

production rate during Space Shuttle re-entry

p0056 A80-45359

SPACECRAFT SENSORS

U SPACECRAFT INSTRUMENTS

SPACECRAFT STRUCTURES

Design of a one-year lifetime, spaceborne
superfluid helium dewar

[ASME PAPER 79-ENAS-23]

SPACECRAFT TRACKING

Data acquisition for measuring the wind on Venus
from Pioneer Venus

p0058 N80-26361

SPACECRAFT TRAJECTORIES

Pioneer Saturn --- Pioneer 11 performance and
encounter trajectory

p0043 A80-19114

SPACELAB

Evaluation of biological models using Spacelab

[ASME PAPER 80-ENAS-38]

SPACELAB PAYLOADS

NT POINTING CONTROL SYSTEMS

NASA-Ames Life Sciences Flight Experiments program
- 1980 status report

[ASME PAPER 80-ENAS-34]

The development of a Space Shuttle Research Animal
Holding Facility

[ASME PAPER 80-ENAS-39]

SPACING

NT AIRCRAFT APPROACH SPACING

SPALLATION

Galileo probe thermal protection: Entry heating
environments and spallation experiments design

[NASA-CR-152334]

SPECTRA

NT ABSORPTION SPECTRA

NT EMISSION SPECTRA

NT ENERGY SPECTRA

NT H LINES

NT INFRARED SPECTRA

NT LINE SPECTRA

NT MASS SPECTRA

NT MOLECULAR SPECTRA

NT SOLAR SPECTRA

NT SPECTRAL BANDS

NT STELLAR SPECTRA

NT VIBRATIONAL SPECTRA

SPECTRAL ABSORPTION

U ABSORPTION SPECTRA

SPECTRAL ANALYSIS

U SPECTRUM ANALYSIS

SPECTRAL BANDS

NT ABSORPTION SPECTRA

Integrated band intensities of gaseous N2/O2/H2O

p0047 A80-25660

SPECTRAL CORRELATION

On the limitations of the concept of space
frequency equivalence

p0069 A80-16697

SPECTRAL ENERGY DISTRIBUTION

Comparison of predicted and observed spectral
energy distribution of K and M stars. I - Alpha

Bootis

p0046 A80-22194

SPECTRAL LINE WIDTH

Absolute intensities and pressure broadening
coefficients measured at different temperatures

for the 201/II/-000 band of C-12/O2/-16 at 4978/cm

p0048 A80-27125

Curves of growth for van der Waals broadened
spectral lines

p0057 A80-51378

SPECTRAL LINES

U LINE SPECTRA

SPECTROMETERS

NT EBERT SPECTROMETERS

NT MASS SPECTROMETERS

NT TIME OF FLIGHT SPECTROMETERS

NT ULTRAVIOLET SPECTROMETERS

SPECTROPHOTOMETRY

SUBJECT INDEX

SPECTROPHOTOMETRY

NT STELLAR SPECTROPHOTOMETRY

Infrared spectra of IC 418 and NGC 6572
p0069 A80-16862
Spectrophotometric identification of the pigment
associated with light-driven primary sodium
translocation in Halobacterium halobium
p0088 A80-26015

SPECTRORADIOMETERS

Pioneer Venus Sounder Probe Solar Flux Radiometer
p0073 A80-30846

SPECTROSCOPIC ANALYSIS

Spectroscopic evidence for two achondrite parent
bodies - Asteroids 349 Dembowska and 4 Vesta
p0072 A80-26173

SPECTROSCOPIC TELESCOPES

Paraboloidal X-ray telescope mirror for solar
coronal spectroscopy
p0078 A80-17503

SPECTROSCOPY

NT ASTRONOMICAL SPECTROSCOPY
NT GAS SPECTROSCOPY
NT INFRARED SPECTROSCOPY
NT OPTICAL EMISSION SPECTROSCOPY
NT PHOTOELECTRON SPECTROSCOPY
NT RADIO SPECTROSCOPY
NT SPECTROPHOTOMETRY
NT SPECTROSCOPIC ANALYSIS
NT STELLAR SPECTROPHOTOMETRY
NT X RAY SPECTROSCOPY

SPECTRUM ANALYSIS

16-30 micron spectroscopy of Titan
p0049 A80-29321
Radiatively driven winds for different power law
spectra --- for explaining narrow and broad
quasar absorption lines
p0054 A80-40138

Pioneer Venus multiprobe entry telemetry recovery
p0058 N80-26347

Dynamic modal estimation using instrumental
variables
[NASA-CR-152396]
p0019 N80-32777

SPEED INDICATORS

NT LASER ANEMOMETERS
Study of boundary-layer transition using
transonic-cone preston tube data
[NASA-TM-81103]
p0010 N80-28305

SPEEDOMETERS

U SPEED INDICATORS

SPHERES

Meteoroid ablation spheres from deep-sea sediments
p0046 A80-22948
Asymptotic behavior of the efficiencies in Mie
scattering
p0031 A80-47048

SPIN

NT SPIN-ORBIT INTERACTIONS
Recent improvements to the spinning body version
of the EDDYBL computer program
[NASA-CR-152347]
p0039 N80-19448

SPIN-ORBIT INTERACTIONS

An ab initio calculation of the zero-field
splitting parameters of the 3A-double prime
state of formaldehyde
p0056 A80-45333
Theoretical treatment of the spin-orbit coupling
in the rare gas oxides NeO, ArO, KrO, and XeO
p0057 A80-50149

SPIRAL GALAXIES

NT BARRED GALAXIES
Gas dynamics in barred spirals - Gaseous density
waves and galactic shocks
p0041 A80-10685

SPRAYED PROTECTIVE COATINGS

U PROTECTIVE COATINGS

STABILITY

NT ACOUSTIC INSTABILITY
NT AERODYNAMIC STABILITY
NT AIRCRAFT STABILITY
NT ATTITUDE STABILITY
NT BOUNDARY LAYER STABILITY
NT CONTROL STABILITY
NT DYNAMIC STABILITY
NT FLOW STABILITY
NT HOVERING STABILITY
NT STATIC STABILITY
NT STORAGE STABILITY
NT THERMAL STABILITY

STAR CLUSTERS

Monoceros R2 - Far-infrared observations of a very
young cluster
p0052 A80-35115

STARS

NT B STARS
NT BINARY STARS
NT CARBON STARS
NT DWARF STARS
NT EARLY STARS
NT HOT STARS
NT LATE STARS
NT M STARS
NT NOVAE
NT O STARS
NT PROTOSTARS
NT SUPERNOVAE
NT T TAURI STARS
NT VARIABLE STARS

STATIC STABILITY

Stability of nonuniform rotor blades in hover
using a mixed formulation
[NASA-TM-81226]
p0012 N80-33777

STATIONS

NT GROUND STATIONS

STATISTICAL ANALYSIS

NT REGRESSION ANALYSIS

STEEP GRADIENT AIRCRAFT

U V/STOL AIRCRAFT

STEEPNESS

U SLOPES

STELLAR ATMOSPHERES

Comparison of predicted and observed spectral
energy distribution of K and M stars. I - Alpha
Bootis
p0046 A80-22194

STELLAR CORONAS

NT SOLAR CORONA

STELLAR ENVELOPES

The spectrum of IRC + 10216 from 2.0 to 8.5 microns
p0056 A80-44965

STELLAR EVOLUTION

Fragmentation of rotating protostellar clouds
p0047 A80-26107
Collapsing cloud models for Bok globules
p0048 A80-26996

Monoceros R2 - Far-infrared observations of a very
young cluster
p0052 A80-35115

The settling of helium and the ages of globular
clusters
p0052 A80-35151

Fragmentation in a rotating protostar - A
comparison of two three-dimensional computer codes
p0053 A80-38432

Protostellar formation in rotating interstellar
clouds. III - Nonaxisymmetric collapse
p0054 A80-39375

The evolution of rapid oscillations in an outburst
of a dwarf nova
p0075 A80-45227

Numerical calculations of the collapse of
nonrotating, magnetic gas clouds
p0057 A80-49341

STELLAR LUMINOSITY

Discovery of optical molecular emission from the
bipolar nebula surrounding HD 44179
p0058 A80-52399

STELLAR MAGNETIC FIELDS

NT SOLAR MAGNETIC FIELD

STELLAR MODELS

Comparison of predicted and observed spectral
energy distribution of K and M stars. I - Alpha
Bootis
p0046 A80-22194

The settling of helium and the ages of globular
clusters
p0052 A80-35151

High-resolution Lyman-alpha filtergrams of the sun
p0075 A80-37277

The spectrum of IRC + 10216 from 2.0 to 8.5 microns
p0056 A80-44965

STELLAR MOTIONS

NT STELLAR ROTATION

Galaxy collisions - A preliminary study
p0046 A80-23420
Self-gravitating gas flow in barred spiral galaxies
p0055 A80-44959

SUBJECT INDEX

STRUCTURAL DYNAMICS

STELLAR RADIATION

NT STELLAR WINDS

Red and nebulous objects in dark clouds - A survey
p0044 A80-20662

STELLAR ROTATION

Fragmentation of rotating protostellar clouds
p0047 A80-26107

STELLAR SPECTRA

NT SOLAR SPECTRA

The infrared spectrum of the carbon star Y Canum
Venaticorum between 1.2 and 30 microns
p0046 A80-22191
High-frequency continuum observations of young stars
p0047 A80-25365
An optical emission-line phase of the extreme
carbon star IRC +30219
p0056 A80-44993

STELLAR SPECTROPHOTOMETRY

Airborne stellar spectrophotometry from 1.2 to 5.5
microns - Absolute calibration and spectra of
stars earlier than M3
p0043 A80-16407
The infrared spectrum of the carbon star Y Canum
Venaticorum between 1.2 and 30 microns
p0046 A80-22191
Comparison of predicted and observed spectral
energy distribution of K and M stars. I - Alpha
Bootis
p0046 A80-22194
Two micron spectroscopy and 2.7 mm CO line
observations of V645 Cygni
p0074 A80-35114
Monoceros R2 - Far-infrared observations of a very
young cluster
p0052 A80-35115
The spectrum of IRC + 10216 from 2.0 to 8.5 microns
p0056 A80-44965

STELLAR STRUCTURE

On the three-dimensional shapes of elliptical
galaxies
p0047 A80-26101
Fragmentation of rotating protostellar clouds
p0047 A80-26107

STELLAR WINDS

Radiatively driven winds for different power law
spectra --- for explaining narrow and broad
quasar absorption lines
p0054 A80-40138

STEREOGRAPHY

U STEREOPHOTOGRAPHY

STEREOPHOTOGRAPHY

Error detection and rectification in digital
terrain models
p0099 A80-27432

STEREOSCOPIC PHOTOGRAPHY

U STEREOPHOTOGRAPHY

STEREOSCOPY

NT STEREOPHOTOGRAPHY

STERILIZATION EFFECTS

NT THERMAL DEGRADATION

STERNS

U AFTERBODIES

STIMULATED EMISSION DEVICES

NT CHEMICAL LASERS

NT DYE LASERS

NT GASDYNAMIC LASERS

NT HF LASERS

NT LASERS

NT NEODYMIUM LASERS

STOCHASTIC PROCESSES

NT RANDOM PROCESSES

STOL AIRCRAFT

U SHORT TAKEOFF AIRCRAFT

STONY METEORITES

NT ACHONDRITES

NT CARBONACEOUS CHONDRITES

NT CARBONACEOUS METEORITES

STORAGE STABILITY

Long term tests of the HEPP liquid trap diode heat
pipe prototype
[NASA-CR-152358]
p0039 N80-22635

STORAGE TANKS

PSA hydrogen tank thermal acoustic oscillation
study
[NASA-CR-152319]
p0038 N80-11470
Cryogenic container compound suspension strap
[NASA-CASE-ARC-11157-1]
p0080 N80-18393

STRAIGHT WINGS

U RECTANGULAR WINGS

STRAPS

Cryogenic container compound suspension strap
[NASA-CASE-ARC-11157-1]
p0080 N80-18393

STRATOSPHERE

Pressure and temperature dependence kinetics study
of the NO + BrO yielding NO2 + Br reaction -
Implications for stratospheric bromine
photochemistry
p0068 A80-14397

Nitrogen fertiliser and stratospheric ozone -
Latitudinal effects
p0043 A80-18948

OCS, stratospheric aerosols and climate
p0044 A80-19741

Integrated band intensities of gaseous N2O5/
p0047 A80-25660

Stratospheric aerosol modification by supersonic
transport and space shuttle operations - Climate
implications
p0047 A80-26088

Stratospheric ozone decrease due to
chlorofluoromethane photolysis - Predictions of
latitude dependence
p0049 A80-29762

The stratospheric sulfate aerosol layer -
Processes, models, observations, and simulations
p0051 A80-34435

The observed ozone flux by transient
eddies, 0-30 km
p0074 A80-34449

Smoke and dust particles of meteoric origin in the
mesosphere and stratosphere
p0055 A80-42744

Measurements of NO, O3, and temperature at 19.8 km
during the total solar eclipse of 26 February 1979
p0055 A80-43638

Efficiency of aerosol collection on wires exposed
in the stratosphere
[NASA-TN-81147]
p0035 N80-11676

Stratospheric aerosol modification by supersonic
transport operations with climate implications
[NASA-RP-1058]
p0034 N80-15726

Comparison of the Nimbus-4 BUV ozone data with the
Ames two-dimensional model
[NASA-TN-81207]
p0036 N80-24914

STRATOSPHERE RADIATION

Atmospheric aerosols and climate
p0052 A80-36305

STRATOTANKER AIRCRAFT

U C-135 AIRCRAFT

STREAMLINE FLOW

U LAMINAR FLOW

STREAMS

NT GAS STREAMS

STRENGTH OF MATERIALS

U MECHANICAL PROPERTIES

STRESS (PHYSIOLOGY)

NT ACCELERATION STRESSES (PHYSIOLOGY)

NT CENTRIFUGING STRESS

Plasma volume during stress in man - Osmolality
and red cell volume
p0087 A80-13506

STRESS RUPTURE STRENGTH

U CREEP RUPTURE STRENGTH

STRESS-STRAIN-TIME RELATIONS

The viscoelastic behavior of a composite in a
thermal environment
[NASA-CR-163187]
p0039 N80-24369

STRESSES

NT REYNOLDS STRESS

NT SHEAR STRESS

STROUHAL NUMBER

Strouhal number influence on flight effects on jet
noise radiated from convecting quadrupoles
p0022 A80-28418

STRUCTURAL ANALYSIS

NT DYNAMIC STRUCTURAL ANALYSIS

NT FLUTTER ANALYSIS

STRUCTURAL DESIGN

Automated design using numerical optimization
[SAE PAPER 791061]
p0024 A80-26628

A general panel method for the analysis and design
of arbitrary configurations in incompressible
flows --- boundary value problem
[NASA-CR-3079]
p0017 N80-24268

Application of advanced technologies to small,
short-haul transport aircraft
[NASA-CR-152363]
p0018 N80-32353

STRUCTURAL DYNAMICS

U DYNAMIC STRUCTURAL ANALYSIS

STRUCTURAL ENGINEERING

SUBJECT INDEX

STRUCTURAL ENGINEERING

Dynamic modal estimation using instrumental variables
[NASA-CR-152396] p0019 N80-32777

Large Deployable Reflector (LDR)
[NASA-CR-152402] p0040 N80-33319

STRUCTURAL MATERIALS

U CONSTRUCTION MATERIALS

STRUCTURAL MEMBERS

Output of acoustical sources --- effects of structural elements and background flow on immobile multipolar point radiation
p0030 A80-37806

STRUCTURAL PROPERTIES (GEOLOGY)

Volcanic features of Hawaii. A basis for comparison with Mars
[NASA-SP-403] p0034 N80-23912

STRUCTURAL VIBRATION

Computer/experiment integration for unsteady aerodynamic research
p0025 A80-29501

Multicyclic control for helicopters - Research in progress at Ames Research Center
[AIAA 80-0671] p0025 A80-34997

A note on sound radiation into a uniformly flowing medium
p0031 A80-45488

A new approach to active control of rotorcraft vibration
[AIAA 80-1778] p0027 A80-45556

STRUCTURAL WEIGHT

Application of parametric weight and cost estimating relationships to future transport aircraft
[SAWE PAPER 1292] p0024 A80-20637

SUBMERGING

Fluid shifts and endocrine responses during chair rest and water immersion in man
p0088 A80-25990

SUBMILLIMETER WAVES

Low-pass interference filters for submillimeter astronomy
p0070 A80-19956

SUBROUTINES

Simulation of the Infrared Astronomical Satellite /IRAS/ telescope system
p0067 A80-49842

SUBSONIC FLOW

Integral equations for flows in wind tunnels
p0029 A80-21906

Experimental investigation of the asymmetric body vortex wake
[AIAA PAPER 80-0174] p0032 A80-23937

Unified aerodynamic-acoustic theory for a thin rectangular wing encountering a gust
p0030 A80-36401

Asymmetric trailing-edge flows at high Reynolds number
[AIAA PAPER 80-1396] p0066 A80-44151

A note on sound radiation into a uniformly flowing medium
p0031 A80-45488

SUBSONIC SPEED

Potential benefits for propfan technology on derivatives of future short- to medium-range transport aircraft
[AIAA PAPER 80-1090] p0026 A80-38905

SUBSONIC WIND TUNNELS

Turbulence measurements in the boundary layer of a low-speed wind tunnel using laser velocimetry
[NASA-TM-81165] p0008 N80-16300

SUGARS

NT GLUCOSE

SUITS

NT SPACE SUITS

SULFATES

Microbial sulfate reduction measured by an automated electrical impedance technique
p0087 A80-21982

The stratospheric sulfate aerosol layer - Processes, models, observations, and simulations
p0051 A80-34435

SULFIDES

OCS, stratospheric aerosols and climate
p0044 A80-19741

SULFUR COMPOUNDS

NT SULFATES

NT SULFIDES

SUNSPOT CYCLE

Are solar spectral variations a drive for climatic change
p0042 A80-15488

SUPERCONDUCTIVITY

Space applications of superconductivity
p0044 A80-20126

SUPERCONDUCTORS

Space applications of superconductivity
p0044 A80-20126

SUPERCRITICAL WINGS

Transonic swept-wing analysis using asymptotic and other numerical methods
[AIAA PAPER 80-0342] p0024 A80-22751

Unsteady aerodynamics of conventional and supercritical airfoils
[AIAA 80-0734] p0026 A80-35038

SUPERFLUID FLOW

U SUPERFLUIDITY

Design of a one-year lifetime, spaceborne superfluid helium dewar
[ASME PAPER 79-ENAS-23] p0077 A80-15247

Second sound shock waves and critical velocities in liquid helium 2
[NASA-CR-162687] p0015 N80-16837

SUPERHYBRID MATERIALS

NT GRAPHITE-EPOXY COMPOSITE MATERIALS

SUPERNOVAE

The acceleration of energetic charged particles by interplanetary and supernova shock waves
p0080 A80-53209

SUPEROXIDES

U INORGANIC PEROXIDES

SUPERSONIC AIRCRAFT

NT B-70 AIRCRAFT

NT SUPERSONIC TRANSPORTS

Some observations on supersonic wing design
[AIAA 80-3040] p0001 A80-31009

Top inlet system feasibility for transonic-supersonic fighter aircraft applications
[AIAA PAPER 80-1809] p0033 A80-45735

SUPERSONIC FLOW

Supersonic flow over three-dimensional ablated nosetips using an unsteady implicit numerical procedure
[AIAA PAPER 80-0063] p0060 A80-19271

Numerical simulation of steady supersonic flow over an ogive-cylinder-boattail body
[AIAA PAPER 80-0066] p0060 A80-19273

A diagonal form of an implicit approximate-factorization algorithm with application to a two dimensional inlet
[AIAA PAPER 80-0067] p0061 A80-19274

Computation of supersonic turbulent flows over an inclined ogive-cylinder-flare
[AIAA PAPER 80-1410] p0066 A80-41608

A computational and experimental study of high Reynolds number viscous/inviscid interaction about a cone at high angle of attack
[AIAA PAPER 80-1422] p0104 A80-44492

Computations of the Magnus effect for slender bodies in supersonic flow
[AIAA 80-1586] p0028 A80-45882

SUPERSONIC NOZZLES

Aircraft engine nozzle
[NASA-CASE-ARC-10977-1] p0033 N80-32392

SUPERSONIC TRANSPORTS

Stratospheric aerosol modification by supersonic transport and space shuttle operations - Climate implications
p0047 A80-26088

Stratospheric aerosol modification by supersonic transport operations with climate implications
[NASA-RP-1058] p0034 N80-15726

SUPPORT SYSTEMS

NT CLOSED ECOLOGICAL SYSTEMS

NT LIFE SUPPORT SYSTEMS

NT PORTABLE LIFE SUPPORT SYSTEMS

SURFACE COOLING

Whole planet cooling and the radiogenic heat source contents of the earth and moon
p0053 A80-36651

SURFACE DIFFUSION

A calculation of the diffusion energies for adatoms on surfaces of F.C.C. metals
p0068 A80-13534

SURFACE GEOMETRY

Workshop on Aircraft Surface Representation for

SUBJECT INDEX

TECHNOLOGY UTILIZATION

Aerodynamic Computation
[NASA-TM-81170] p0008 N80-19025

SURFACE LAYERS
Evaluation of the time dependent surface shear stress in turbulent flows
[ASME PAPER 79-WA/FE-17] p0078 A80-18618
The role of cesium suboxides in low-work-function surface layers studied by X-ray photoelectron spectroscopy - Ag-O-Cs p0051 A80-33844

SURFACE PROPERTIES
NT SURFACE TEMPERATURE
A correlation method to predict the surface pressure distribution of an infinite plate or a body of revolution from which a jet is issuing
[NASA-CR-152345] p0018 N80-32339

SURFACE TEMPERATURE
Infrared-temperature variability in a large agricultural field --- Dunnigan, California
[E80-10331] p0038 N80-32822

SURFACE VEHICLES
NT AIRCRAFT CARRIERS

SWEEP EFFECT
Acoustically swept rotor --- helicopter noise reduction
[NASA-CASE-ARC-11106-1] p0102 N80-14107

SWELLING
Thermal expansion and swelling of cured epoxy resin used in graphite/epoxy composite materials
p0054 A80-40926

SWEPT WINGS
NT DELTA WINGS
Experimental and computational study of transonic flow about swept wings
[AIAA PAPER 80-0005] p0060 A80-18235
Transonic swept-wing analysis using asymptotic and other numerical methods
[AIAA PAPER 80-0342] p0024 A80-22751
Analysis of transonic swept wings using asymptotic and other numerical methods
[NASA-TM-80762] p0011 N80-29255

SWEPTBACK WINGS
NT DELTA WINGS

SWIRLING
An experimental investigation of two large annular diffusers with swirling and distorted inflow
[NASA-TP-1628] p0005 N80-17984

SWIRLING WAKES
U TURBULENT WAKES

SYMMETRICAL BODIES
NT AXISYMMETRIC BODIES
NT BODIES OF REVOLUTION
NT CYLINDRICAL BODIES
NT SPHERES

SYNTHESIS
Synthesis of perfluoroalkylether oxadiazole elastomers
p0045 A80-21992

SYNTHETIC FIBERS
Flash-fire propensity and heat-release rate studies of improved fire resistant materials
p0042 A80-15201

SYNTHETIC RESINS
NT EPOXY RESINS
NT PHENOLIC RESINS
NT THERMOPLASTIC RESINS
NT THERMOSETTING RESINS

SYNTHETIC RUBBERS
NT ELASTOMERS

SYSTEM EFFECTIVENESS
The future of short-haul transport aircraft
[SAE PAPER 800755] p0029 A80-49703

SYSTEM IDENTIFICATION
A scaling theory for linear systems
p0030 A80-32676

SYSTEMS ANALYSIS
NT SYSTEM IDENTIFICATION
In depth review of the 1979 AIAA Lighter-Than-Air Systems Technology Conference
[NASA-TM-81158] p0006 N80-12991
The analysis of delays in simulator digital computing systems. Volume 1: Formulation of an analysis approach using a central example simulator model
[NASA-CR-152340] p0015 N80-17722

SYSTEMS DESIGN
U SYSTEMS ENGINEERING
SYSTEMS ENGINEERING
NT COMPUTER SYSTEMS DESIGN

Design and operation of the Pioneer Venus Orbiter ultraviolet spectrometer
p0073 A80-30841

SOLABES orbiting mirror system
[AAS 79-304] p0067 A80-52280

A hingeless rotor XV-15 design integration feasibility study. Volume 1: Engineering design studies
[NASA-CR-152310] p0015 N80-18030
Practical optimal flight control system design for helicopter aircraft. Volume 1: Technical Report
[NASA-CR-3275] p0017 N80-23328
Titan probe technology assessment and technology development plan study
[NASA-CR-152381] p0040 N80-32417

SYSTEMS MANAGEMENT
Operational procedures for ground station operation: ATS-3 Hawaii-Ames satellite link experiment
[NASA-TM-81155] p0035 N80-13333

SYSTEMS SIMULATION
Perception of aircraft separation with pilot-preferred symbology on a cockpit display of traffic information
[NASA-TM-81172] p0084 N80-31397

T

T TAURI STARS
Red and nebulous objects in dark clouds - A survey
p0044 A80-20662

TAIL ROTORS
NT HELICOPTER TAIL ROTORS

TAKEOFF
A head-up display format for application to transport aircraft approach and landing
[NASA-TM-81199] p0012 N80-29295

TANKS (CONTAINERS)
NT STORAGE TANKS

TAPERED WINGS
U SWEPT WINGS

TARE (DATA REDUCTION)
U DATA REDUCTION

TASK COMPLEXITY
Dynamic decisions and work load in multitask supervisory control
p0095 A80-40898

TAYLOR SERIES
A new propagation method for the radial Schroedinger equation
p0069 A80-15768
SCF and CI calculations of the dipole moment function of ozone --- Self-Consistent Field and Configuration-Interaction
p0043 A80-17111

TAYLOR THEOREM
U TAYLOR SERIES

TEACHING
U EDUCATION

TECHNOLOGICAL FORECASTING
Application of parametric weight and cost estimating relationships to future transport aircraft
[SAE PAPER 1292] p0024 A80-20637

TECHNOLOGIES
NT ENERGY TECHNOLOGY
TECHNOLOGY ASSESSMENT
Small Transport Aircraft Technology
p0021 A80-21225
An assessment of ground-based techniques for detecting other planetary systems. Volume 1: An overview --- workshop conclusions
[NASA-CP-2124-VOL-1] p0034 N80-18997
Parametric study of modern airship productivity
[NASA-TM-81151] p0011 N80-28340
Titan probe technology assessment and technology development plan study
[NASA-CR-152381] p0040 N80-32417
Application of advanced technologies to small, short-haul air transports
[NASA-CR-152364] p0019 N80-33396

TECHNOLOGY TRANSFER
Conference of Remote Sensing Educators (CORSE-78)
[NASA-CP-2102] p0034 N80-20003

TECHNOLOGY UTILIZATION
The future of short-haul transport aircraft
[SAE PAPER 800755] p0029 A80-49703
NASA's western regional applications training activity

TELECOMMUNICATION

SUBJECT INDEX

Application of advanced technologies to small, short-haul transport aircraft [NASA-CR-152363] p0058 N80-20010

Application of advanced technologies to small, short-haul air transports [NASA-CR-152364] p0018 N80-32353

TELECOMMUNICATION p0019 N80-33396

NT DATA LINKS

NT EXTRATERRESTRIAL COMMUNICATION

NT INTERPLANETARY COMMUNICATION

NT SPACECRAFT COMMUNICATION

NT TELEMETRY

NT VIDEO COMMUNICATION

TELEMETERS

U TELEMETRY

TELEMETRY

Pioneer Venus Multiprobe entry telemetry recovery p0050 A80-30831

Pioneer Venus multiprobe entry telemetry recovery p0058 N80-26347

TELESCOPES

NT ASTRONOMICAL TELESCOPES

NT INFRARED TELESCOPES

NT SPACEBORNE TELESCOPES

NT SPECTROSCOPIC TELESCOPES

NT X RAY TELESCOPES

TELLEGEN THEORY

U NETWORK ANALYSIS

TEMPERATURE

NT ATMOSPHERIC TEMPERATURE

NT BODY TEMPERATURE

NT BRIGHTNESS TEMPERATURE

NT CURIE TEMPERATURE

NT GAS TEMPERATURE

NT PLANETARY TEMPERATURE

NT SURFACE TEMPERATURE

TEMPERATURE CONTROL

Thermal design of a Shuttle infrared telescope facility /SIRTF/ [AIAA PAPER 80-1502] p0079 A80-41466

TEMPERATURE DEPENDENCE

Pressure and temperature dependence kinetics study of the NO + BrO yielding NO2 + Br reaction - Implications for stratospheric bromine photochemistry p0068 A80-14397

Temperature dependence of intensities of the 8-12 micron bands of CFC13 p0045 A80-21559

Vibration-rotation line shifts for 1 sigma g + H2/V,J-15/0/ He computed via close coupling - Temperature dependence p0058 A80-51965

TEMPERATURE DISTRIBUTION

Pressure and temperature fields associated with aero-optics tests --- transonic wind tunnel tests p0031 N80-25591

TEMPERATURE EFFECTS

Time-temperature behavior of a unidirectional graphite/epoxy composite p0078 A80-21141

Primordial heating of asteroidal parent bodies p0062 A80-24590

Absolute intensities and pressure broadening coefficients measured at different temperatures for the 201/II-000 band of C-12/O2/-16 at 4978/cm p0048 A80-27125

Effects of moisture on apparent flexure strength and on torsion and flexure fatigue properties of graphite-epoxy composites p0063 A80-27965

Role of thermal and exercise factors in the mechanism of hypervolemia p0089 A80-32748

Changes induced on the surfaces of small Pd clusters by the thermal desorption of CO p0053 A80-37179

TEMPERATURE FIELDS

U TEMPERATURE DISTRIBUTION

TEMPERATURE INVERSIONS

NT CENTRIFUGING STRESS

TEMPERATURE PROFILES

The upper atmosphere of Uranus - Mean temperature and temperature variations p0071 A80-22207

High resolution vertical profiles of wind, temperature and humidity obtained by computer processing and digital filtering of radiosonde

and radar tracking data from the ITCZ experiment of 1977 [NASA-CR-3269] p0039 N80-21926

TENSILE STRENGTH

Degradation of tensile and shear properties of composites exposed to fire or high temperature p0072 A80-29697

TERMINAL GUIDANCE

Model development for automatic guidance of a VTOL aircraft to a small aviation ship [AIAA 80-1617] p0028 A80-45907

TERNARY SYSTEMS (DIGITAL)

U DIGITAL SYSTEMS

TERRAIN ANALYSIS

Error detection and rectification in digital terrain models p0099 A80-27432

Use of collateral information to improve LANDSAT classification accuracies --- Ventura County and Klamath National Forest, California [E80-10268] p0040 N80-29815

TEST CHAMBERS

NT ANECHOIC CHAMBERS

TEST FACILITIES

NT ANECHOIC CHAMBERS

NT SUBSONIC WIND TUNNELS

NT TEST STANDS

NT WIND TUNNELS

The 60-MW Shuttle interaction heating facility p0059 A80-12603

A technique for evaluating the Jovian entry-probe heat-shield material with a gasdynamic laser p0063 A80-29479

Test section configuration for aerodynamic testing in shock tubes p0026 A80-38085

TEST STANDS

A small-scale test for fiber release from carbon composites --- pyrolysis and impact [NASA-TM-81179] p0036 N80-18105

THERMATIC MAPPING

Issues arising from the demonstration of Landsat-based technologies to inventories and mapping of the forest resources of the Pacific Northwest states p0065 A80-41305

21 cm maps of Jupiter's radiation belts from all rotational aspects p0076 A80-48877

THERMAL ACCOMMODATION COEFFICIENTS

U ACCOMMODATION COEFFICIENT

THERMAL CONTROL COATINGS

Development of high viscosity coatings for advanced Space Shuttle applications p0079 A80-34760

THERMAL CONVECTION

U FREE CONVECTION

THERMAL CYCLING TESTS

Hygrothermal damage mechanisms in graphite-epoxy composites [NASA-CR-3189] p0038 N80-13170

THERMAL DECOMPOSITION

NT PYROLYSIS

THERMAL DEGRADATION

Degradation of tensile and shear properties of composites exposed to fire or high temperature p0072 A80-29697

THERMAL EFFECTS

U TEMPERATURE EFFECTS

THERMAL EFFICIENCY

U THERMODYNAMIC EFFICIENCY

THERMAL EMISSION

The 16- to 38-micron spectrum of Callisto p0074 A80-35234

Excitation mechanisms for the unidentified infrared emission features p0054 A80-40642

THERMAL ENVIRONMENTS

Galileo probe forebody entry thermal protection - Aerothermal environments and heat shielding requirements [ASME PAPER 80-ENAS-24] p0066 A80-43200

THERMAL EXPANSION

Thermal expansion and swelling of cured epoxy resin used in graphite/epoxy composite materials p0054 A80-40926

THERMAL MAPPING

Infrared-temperature variability in a large agricultural field --- Dunnigan, California

SUBJECT INDEX

THREE DIMENSIONAL FLOW

- [E80-10331] p0038 N80-32822
- THERMAL PLASMAS**
- Pioneer Venus Orbiter planar retarding potential analyzer plasma experiment p0073 A80-30839
- THERMAL PROPERTIES**
- U THERMODYNAMIC PROPERTIES
- THERMAL PROTECTION**
- Studies for improved high temperature coatings for Space Shuttle application p0079 A80-34757
- Galileo probe forebody entry thermal protection - Aerothermal environments and heat shielding requirements [ASME PAPER 80-ENAS-24] p0066 A80-43200
- Galileo probe thermal protection: Entry heating environments and spallation experiments design [NASA-CR-152334] p0038 N80-14184
- THERMAL RADIATION**
- One millimeter continuum observations of extragalactic thermal sources [NASA-CR-163590] p0040 N80-33334
- THERMAL RESISTANCE**
- Development of high viscosity coatings for advanced Space Shuttle applications p0079 A80-34760
- Fire-resistant materials for aircraft passenger seat construction [NASA-TM-78617] p0035 N80-13255
- THERMAL SHIELDING**
- U HEAT SHIELDING
- THERMAL STABILITY**
- NT TEMPERATURE DEPENDENCE
- Synthesis of perfluoroalkylether oxadiazole elastomers p0045 A80-21992
- Plasma etching of poly(N,N'-p,p'-oxydiphenylene/pyromellitimide/ film and photo/thermal degradation of etched and unetched film p0093 A80-24158
- Advanced thermoset resins for fire-resistant composites p0063 A80-34788
- Ambient curing fire resistant foams p0063 A80-34790
- Graphite composites with advanced resin matrices [AIAA 80-0758] p0064 A80-35051
- Changes induced on the surfaces of small Pd clusters by the thermal desorption of CO p0053 A80-37179
- THERMOCHEMICAL PROPERTIES**
- Advanced thermoset resins for fire-resistant composites p0063 A80-34788
- THERMODYNAMIC EFFICIENCY**
- Photocell heat engine solar power systems p0079 A80-48179
- THERMODYNAMIC PROPERTIES**
- NT THERMAL EXPANSION
- NT THERMAL STABILITY
- NT THERMOCHEMICAL PROPERTIES
- NT THERMOPHYSICAL PROPERTIES
- Hygrothermal damage mechanisms in graphite-epoxy composites [NASA-CR-3189] p0038 N80-13170
- THERMODYNAMICS**
- The properties of clusters in the gas phase. IV - Complexes of H₂O and HNO_x clustering on NO_x/- p0046 A80-23322
- An extended soft-cube model for the thermal accommodation of gas atoms on solid surfaces [NASA-TM-81163] p0035 N80-14941
- THERMOMECHANICS**
- U THERMODYNAMICS
- THERMOPHYSICAL PROPERTIES**
- NT TEMPERATURE DEPENDENCE
- NT THERMAL STABILITY
- Thermophysical and flammability characterization of phosphorylated epoxy adhesives p0066 A80-48079
- THERMOPHYSICS**
- U THERMODYNAMICS
- THERMOPLASTIC RESINS**
- Performance properties of graphite reinforced composites with advanced resin matrices --- for aircraft p0052 A80-35330
- THERMOREGULATION**
- Exercise thermoregulation after 14 days of bed rest p0088 A80-25989
- Changes in body temperature and metabolic rate after injection of calcium into the caudal hypothalamus of the rabbit p0093 A80-27078
- Fluid-electrolyte shifts and thermoregulation - Rest and work in heat with head cooling p0091 A80-48086
- THERMOSETTING RESINS**
- NT EPOXY RESINS
- NT PHENOLIC RESINS
- Oxygen index tests of thermosetting resins p0044 A80-21448
- Advanced thermoset resins for fire-resistant composites p0063 A80-34788
- Performance properties of graphite reinforced composites with advanced resin matrices --- for aircraft p0052 A80-35330
- THERMOSPHERE**
- A model of the neutral and ion nitrogen chemistry in the daytime thermosphere of Venus p0067 A80-10460
- THERMOSTABILITY**
- U THERMAL STABILITY
- THERMOTROPISM**
- U TEMPERATURE EFFECTS
- THIN AIRFOILS**
- NT INFINITE SPAN WINGS
- NT THIN WINGS
- Aerodynamic coefficients in generalized unsteady thin airfoil theory p0030 A80-38034
- THIN WINGS**
- NT INFINITE SPAN WINGS
- Lifting three-dimensional wings in transonic flow p0071 A80-20331
- Propeller slipstream/wing interaction in the transonic regime [AIAA PAPER 80-0125] p0032 A80-22733
- THREE BODY PROBLEM**
- Effect of three-body interactions on the structure of small clusters p0057 A80-49383
- THREE DIMENSIONAL BOUNDARY LAYER**
- Experimental investigation of a three dimensional turbulent boundary layer with a non disappearing pressure gradient p0054 A80-40907
- Recent improvements to the spinning body version of the EDDYBL computer program [NASA-CR-152347] p0039 N80-19448
- THREE DIMENSIONAL FLOW**
- An explicit algorithm for a fluid approach to nonlinear optics propagation using splitting and rezoning techniques p0059 A80-14987
- Supersonic flow over three-dimensional ablated nosetips using an unsteady implicit numerical procedure [AIAA PAPER 80-0063] p0060 A80-19271
- An experimental and numerical investigation of a three-dimensional shock wave separated turbulent boundary layer [AIAA PAPER 80-0002] p0061 A80-22727
- Control of forebody vortex orientation to alleviate side forces [AIAA PAPER 80-0183] p0024 A80-23955
- Numerical experiments in boundary-layer stability [AIAA PAPER 80-0275] p0062 A80-23957
- Computational aerodynamics on large computers p0048 A80-27415
- Diagnosis of separated flow regions on wind-tunnel models using an infrared camera p0025 A80-29494
- Numerical simulation of three-dimensional boattail afterbody flow fields [AIAA PAPER 80-1347] p0066 A80-44132
- Vortex simulation of three-dimensional, spotlike disturbances in a laminar boundary layer p0067 A80-49296
- Three-dimensional simulation of the free shear layer using the vortex-in-cell method p0067 A80-49300
- A three dimensional vortex wake model for missiles at high angles on attack

THREE DIMENSIONAL MOTION

SUBJECT INDEX

[NASA-CR-3208] p0014 N80-14048
Control of forebody three-dimensional flow separations

p0022 N80-15164
Application of numerical optimization to the design of wings with specified pressure distributions

[NASA-CR-3238] p0015 N80-16031
Three-dimensional interactions and vortical flows with emphasis on high speeds

[NASA-TM-81169] p0008 N80-21286
An advanced panel method for analysis of arbitrary configurations in unsteady subsonic flow

[NASA-CR-152323] p0017 N80-26270
THREE DIMENSIONAL MOTION
NT THREE DIMENSIONAL FLOW

THRESHOLDS (PERCEPTION)
Thresholds for detection of constant rotary acceleration during vibratory rotary acceleration: p0091 A80-42003

THRUST
NT JET THRUST

THRUST AUGMENTATION
Large scale model tests of a new technology V/STOL concept

[AIAA PAPER 80-0233] p0023 A80-19303
Workshop on Thrust Augmenting Ejectors

[NASA-CP-2093] p0004 N80-10107
NASA overview p0022 N80-10109

THRUST CONTROL
NT THRUST VECTOR CONTROL

THRUST VECTOR CONTROL
Static calibration of a two-dimensional wedge nozzle with thrust vectoring and spanwise blowing

[NASA-TM-81161] p0009 N80-23317
TIDAL OSCILLATION
U TIDES

TIDES
Tidal dissipation, orbital evolution, and the nature of Saturn's inner satellites p0058 A80-53235

TILT ROTOR AIRCRAFT
NT XV-15 AIRCRAFT

NASA/Army XV-15 tilt rotor research aircraft wind-tunnel test program plan --- Ames 40-ft by 80-ft wind tunnel tests

[NASA-TM-78562] p0007 N80-15067
TILT ROTOR RESEARCH AIRCRAFT PROGRAM
Wind-tunnel tests of the XV-15 tilt rotor aircraft

[NASA-TM-81177] p0009 N80-24294
TIMBER INVENTORY
Issues arising from the demonstration of Landsat-based technologies to inventories and mapping of the forest resources of the Pacific Northwest states

p0065 A80-41305
Use of collateral information to improve LANDSAT classification accuracies --- Ventura County and Klamath National Forest, California

[E80-10268] p0040 N80-29815
TIME DELAY
U TIME LAG

TIME DEPENDENCE
Evaluation of the time dependent surface shear stress in turbulent flows

[ASME PAPER 79-WA/FE-17] p0078 A80-18618
TIME LAG
The analysis of delays in simulator digital computing systems. Volume 1: Formulation of an analysis approach using a central example simulator model

[NASA-CR-152340] p0015 N80-17722
The analysis of delays in simulator digital computing systems. Volume 2: Formulation of discrete state transition matrices, an alternative procedure for multirate digital computations --- flight control

[NASA-CR-152341] p0015 N80-18722
Dynamic modal estimation using instrumental variables

[NASA-CR-152396] p0019 N80-32777
TIME OF FLIGHT SPECTROMETERS
Data acquisition techniques for exploiting the uniqueness of the time-of-flight mass spectrometer: Application to sampling pulsed gas systems

[NASA-TM-81224] p0037 N80-31775

TIME SERIES ANALYSIS
Studies in astronomical time series analysis: Modeling random processes in the time domain

[NASA-TM-81148] p0036 N80-15854
TIPS
NT BLADE TIPS

TISSUES (BIOLOGY)
NT ADIPOSE TISSUES

The architecture of the avian retina following exposure to chronic 2 G p0096 A80-42013

TITAN
An entry and landing probe for Titan

[AIAA PAPER 80-0117] p0060 A80-18384
Organic chemistry on Titan

p0087 A80-20340
Titan aerosols - Optical properties and vertical distribution

p0045 A80-21759
16-30 micron spectroscopy of Titan

p0049 A80-29321
Titan probe technology assessment and technology development plan study

[NASA-CR-152381] p0040 N80-32417
TOLERANCES (PHYSIOLOGY)
NT HUMAN TOLERANCES

TONOMETRY
U PRESSURE MEASUREMENTS

TONUS
U MUSCULAR TONUS

TOXIC HAZARDS
Radiant panel tests on an epoxy/carbon fiber composite

[NASA-TM-81185] p0037 N80-32435
TOXICITY
Toxicity of pyrolysis gases from foam plastics

p0071 A80-24625
TRACE CONTAMINANTS
Adsorption interference in mixtures of trace contaminants flowing through activated carbon adsorber beds

[ASME PAPER 80-ENAS-17] p0096 A80-43193
TRACKING (POSITION)
NT SPACECRAFT TRACKING

TRACKING NETWORKS
NT DEEP SPACE NETWORK

TRAFFIC
NT AIR TRAFFIC

TRAFFIC CONTROL
NT AIR TRAFFIC CONTROL

TRAILING EDGES
Asymmetric trailing-edge flows at high Reynolds number

[AIAA PAPER 80-1396] p0066 A80-44151
TRAINING
U EDUCATION

TRAINING SIMULATORS
NT COCKPIT SIMULATORS

NT FLIGHT SIMULATORS
The development and use of large-motion simulator systems in aeronautical research and development

p0001 A80-10765
Effects of magnification and visual accommodation on aimpoint estimation in simulated landings with real and virtual image displays

[NASA-TP-1635] p0082 N80-34099
TRAJECTORIES
NT DESCENT TRAJECTORIES

NT SPACECRAFT TRAJECTORIES
TRAJECTORY ANALYSIS
Analysis of fuel-conservative curved decelerating approach trajectories for powered-lift and CTOL jet aircraft

[NASA-TP-1650] p0005 N80-19022
A new algorithm for horizontal capture trajectories

[NASA-TM-81186] p0009 N80-22297
Equations for determining aircraft motions for accident data

[NASA-TM-78609] p0010 N80-25306
TRAJECTORY CONTROL
NT TRAJECTORY OPTIMIZATION

TRAJECTORY OPTIMIZATION
Constrained optimum trajectories with specified range

p0021 A80-18538
Algorithm for fixed-range optimal trajectories

[NASA-TP-1565] p0006 N80-28329
TRANSFER FUNCTIONS
A scaling theory for linear systems

SUBJECT INDEX

TRUNCATION (MATHEMATICS)

- TRANSFER OF TRAINING** p0030 A80-32676
NASA's western regional applications training activity
- TRANSFORMATIONS (MATHEMATICS)** p0058 N80-20010
NT COORDINATE TRANSFORMATIONS
- TRANSIENT HEATING**
NT SHOCK HEATING
- TRANSIENT LOADS**
NT GUST LOADS
- TRANSIENT RESPONSE**
Transient solution for megajoule energy release in a lumped-parameter series RLC circuit p0051 A80-32826
- TRANSITION FLOW**
Relaminarization of fluid flows p0075 A80-40843
Pressure measurements on an ogive-cylinder at high angles of attack with laminar, transitional, or turbulent separation [AIAA 80-1556] p0028 A80-45856
- TRANSITION METALS**
NT MOLYBDENUM
NT NICKEL
NT PALLADIUM
NT SILVER
- TRANSLATIONAL MOTION**
NT THREE DIMENSIONAL FLOW
The development and use of large-motion simulator systems in aeronautical research and development p0001 A80-10765
- TRANSMISSION**
NT ACOUSTIC PROPAGATION
NT CONVECTIVE HEAT TRANSFER
NT DATA TRANSMISSION
NT ELECTROMAGNETIC WAVE TRANSMISSION
NT HEAT TRANSFER
NT LIGHT SCATTERING
NT LIGHT TRANSMISSION
NT MICROWAVE ATTENUATION
NT RADIATIVE HEAT TRANSFER
NT SHOCK WAVE PROPAGATION
NT SIGNAL TRANSMISSION
NT TURBULENT HEAT TRANSFER
NT WAVE PROPAGATION
- TRANSMISSION EFFICIENCY**
Asymptotic behavior of the efficiencies in Mie scattering p0031 A80-47048
- TRANSMITTERS**
NT RADIOSONDES
- TRANSONIC AIRCRAFT**
U SUPERSONIC AIRCRAFT
- TRANSONIC FLOW**
Experimental and computational study of transonic flow about swept wings [AIAA PAPER 80-0005] p0060 A80-18235
Lifting three-dimensional wings in transonic flow p0071 A80-20331
Integral equations for flows in wind tunnels p0029 A80-21906
Propeller slipstream/wing interaction in the transonic regime [AIAA PAPER 80-0125] p0032 A80-22733
Transonic swept-wing analysis using asymptotic and other numerical methods [AIAA PAPER 80-0342] p0024 A80-22751
Implicit computations of unsteady transonic flow governed by the full-potential equation in conservation form [AIAA PAPER 80-0150] p0062 A80-23935
Application of laser velocimetry to an unsteady transonic flow p0063 A80-29506
Nonreflecting far-field boundary conditions for unsteady transonic flow computation [AIAA PAPER 80-1393] p0065 A80-41597
An implicit finite-difference code for inviscid and viscous cascade flow [AIAA PAPER 80-1427] p0066 A80-44128
Calculations of transonic flow about an airfoil in a wind tunnel [AIAA PAPER 80-1366] p0027 A80-44142
A comprehensive comparison between experiment and prediction for a transonic turbulent separated flow [AIAA PAPER 80-1407] p0027 A80-44154
- Application of numerical optimization to the design of wings with specified pressure distributions [NASA-CR-3238] p0015 N80-16031
Experimental studies of scale effects on oscillating airfoils at transonic speeds [NASA-TM-81216] p0010 N80-27287
Study of boundary-layer transition using transonic-cone preston tube data [NASA-TM-81103] p0010 N80-28305
Analysis of transonic swept wings using asymptotic and other numerical methods [NASA-TM-80762] p0011 N80-29255
Experimental unsteady aerodynamics of conventional and supercritical airfoils --- conducted in the Ames 11 foot transonic wind tunnel [NASA-TM-81221] p0012 N80-33345
Calculation of three-dimensional unsteady transonic flows past helicopter blades [NASA-TP-1721] p0100 N80-33356
Numerical solution techniques for unsteady transonic aerodynamics problems p0059 N80-33379
- TRANSONICS**
U TRANSONIC FLOW
- TRANSPORT AIRCRAFT**
NT C-135 AIRCRAFT
NT CARGO AIRCRAFT
NT H-53 HELICOPTER
NT LIGHT TRANSPORT AIRCRAFT
NT SHORT HAUL AIRCRAFT
Application of parametric weight and cost estimating relationships to future transport aircraft [SAWE PAPER 1292] p0024 A80-20637
Potential benefits for propfan technology on derivatives of future short- to medium-range transport aircraft [AIAA PAPER 80-1090] p0026 A80-38905
The future of short-haul transport aircraft [SAE PAPER 800755] p0029 A80-49703
Factors affecting the retirement of commercial transport jet aircraft [NASA-CR-152308] p0013 N80-10148
Conceptual studies of a long-range transport with an upper surface blowing propulsive lift system [NASA-TM-81196] p0009 N80-23249
Parametric study of modern airship productivity [NASA-TM-81151] p0011 N80-28340
A head-up display format for application to transport aircraft approach and landing [NASA-TM-81199] p0012 N80-29295
- TRANSPORT COEFFICIENTS**
U TRANSPORT PROPERTIES
- TRANSPORT PROPERTIES**
NT DIFFUSION COEFFICIENT
NT EDDY VISCOSITY
NT IONIC MOBILITY
NT SUPERCONDUCTIVITY
NT VISCOSITY
Wave propagation and transport in the middle atmosphere p0072 A80-26437
The role of Na⁺/+ in transport processes of bacterial membranes p0088 A80-27077
Multiple-time-scale concepts in turbulent transport modelling p0080 A80-49277
- TRANSPORTATION**
NT AIR TRANSPORTATION
NT SPACE SHUTTLE ORBITERS
- TRAPPED PARTICLES**
NT RADIATION BELTS
- TRIANGULAR WINGS**
U DELTA WINGS
- TRIM (BALANCE)**
U AERODYNAMIC BALANCE
- TROPOSPHERE**
The observed ozone flux by transient eddies, 0-30 km p0074 A80-34449
- TROPOSPHERIC SCATTERING**
Scattering by nonspherical particles of size comparable to wavelength - A new semi-empirical theory and its application to tropospheric aerosols p0052 A80-36040
- TRUNCATION (MATHEMATICS)**
U APPROXIMATION

TRUNCATION ERRORS

TRUNCATION ERRORS

A new propagation method for the radial
Schroedinger equation

p0069 A80-15768

TURBINE ENGINES

NT BRISTOL-SIDDELEY BS 53 ENGINE
NT TURBOFAN ENGINES
NT TURBOJET ENGINES
NT TURBOPROP ENGINES

TURBINE WHEELS

Comparison of calculated and measured blade loads
on a full-scale tilting propotor in a wind tunnel
[NASA-TM-81228]

p0012 N80-31386

TURBOFAN ENGINES

NT BRISTOL-SIDDELEY BS 53 ENGINE

Acoustic characteristics of two hybrid inlets at
forward speed

[AIAA PAPER 79-0678]

p0021 A80-20828

Fan noise caused by the ingestion of anisotropic
turbulence - A model based on axisymmetric
turbulence theory

[AIAA PAPER 80-1021]

p0032 A80-35977

Analytical study of the effects of wind tunnel
turbulence on turbofan rotor noise

[AIAA PAPER 80-1022]

p0033 A80-35978

A measurement of forward-flight effects on the
noise from a JT15D-1 turbofan engine in the
NASA-Ames 40- by 80-Foot Wind Tunnel

[AIAA PAPER 80-1026]

p0026 A80-38641

TURBOFANS

Analytical study of the effects of wind tunnel
turbulence on turbofan rotor noise --- NASA Ames
40 by 80 foot wind tunnel
[NASA-CR-152359]

p0016 N80-23099

TURBOJET AIRCRAFT

U JET AIRCRAFT

TURBOJET ENGINES

NT BRISTOL-SIDDELEY BS 53 ENGINE
NT TURBOFAN ENGINES
NT TURBOPROP ENGINES

Reduction of nitric oxide emissions from a combustor
[NASA-CASE-ARC-10814-2]

p0080 N80-26298

TURBOMACHINE BLADES

NT ROTOR BLADES (TURBOMACHINERY)

TURBOMACHINERY

NT TURBOFANS

TURBOPROP ENGINES

Application of advanced technologies to small,
short-haul transport aircraft
[NASA-CR-152363]

p0018 N80-32353

TURBOROTORS

U TURBINE WHEELS

TURBULENCE

NT ATMOSPHERIC TURBULENCE

Proceedings of the Aero-Optics Symposium on
Electromagnetic Wave Propagation from Aircraft
[NASA-CP-2121]

p0006 N80-25588

Turbulent structures in wall-bounded shear flows
observed via three-dimensional numerical
simulators --- using the Illiac 4 computer
[NASA-TM-81219]

p0037 N80-29622

TURBULENCE EFFECTS

Fan noise caused by the ingestion of anisotropic
turbulence - A model based on axisymmetric
turbulence theory

[AIAA PAPER 80-1021]

p0032 A80-35977

Analytical study of the effects of wind tunnel
turbulence on turbofan rotor noise

[AIAA PAPER 80-1022]

p0033 A80-35978

Analytical study of the effects of wind tunnel
turbulence on turbofan rotor noise --- NASA Ames
40 by 80 foot wind tunnel

[NASA-CR-152359]

p0016 N80-23099

Effects of free-stream turbulence on diffuser
performance

[NASA-CR-163194]

p0017 N80-24264

TURBULENT BOUNDARY LAYER

Evaluation of the time dependent surface shear
stress in turbulent flows

[ASME PAPER 79-WA/FE-17]

p0078 A80-18618

An experimental and numerical investigation of a
three-dimensional shock wave separated turbulent
boundary layer

[AIAA PAPER 80-0002]

p0061 A80-22727

High-resolution LDA measurements of Reynolds
stress in boundary layers and wakes

[AIAA 80-0436]

p0025 A80-26967

Relaminarization of fluid flows

p0075 A80-40843

SUBJECT INDEX

Experimental investigation of a three dimensional
turbulent boundary layer with a non disappearing
pressure gradient

p0054 A80-40907

Skin friction measurements by a new nonintrusive
double-laser-beam oil viscosity balance technique
[AIAA PAPER 80-1373]

p0065 A80-41587

Computation of supersonic turbulent flows over an
inclined ogive-cylinder-flare

[AIAA PAPER 80-1410]

p0066 A80-41608

A comprehensive comparison between experiment and
prediction for a transonic turbulent separated
flow

[AIAA PAPER 80-1407]

p0027 A80-44154

Computations of the Magnus effect for slender
bodies in supersonic flow

[AIAA 80-1586]

p0028 A80-45882

Turbulence measurements in the boundary layer of a
low-speed wind tunnel using laser velocimetry

[NASA-TM-81165]

p0008 N80-16300

Recent improvements to the spinning body version
of the EDDYBL computer program

[NASA-CR-152347]

p0039 N80-19448

Simple turbulence models and their application to
boundary layer separation

[NASA-CR-3283]

p0017 N80-24269

Developments in the computation of turbulent
boundary layers

p0059 N80-27658

A Navier-Stokes fast solver for turbulence
modeling applications

p0059 N80-27659

TURBULENT DIFFUSION

Eddy diffusion coefficients and the variance of
the atmosphere 30-60 km

p0076 A80-45996

TURBULENT FLOW

Computational aerodynamics on large computers

p0048 A80-27415

Investigation of a reattaching turbulent shear
layer flow over a backward-facing step

p0062 A80-27736

Application of laser velocimetry to an unsteady
transonic flow

p0063 A80-29506

On the numerical solution of time-dependent
viscous incompressible fluid flows involving
solid boundaries

p0052 A80-34980

Relaminarization of fluid flows

p0075 A80-40843

Tests of subgrid-scale models in strained turbulence
[AIAA PAPER 80-1339]

p0065 A80-41569

Separated skin-friction measurements - Source of
error: An assessment and elimination

[AIAA PAPER 80-1409]

p0027 A80-44155

Pressure measurements on an ogive-cylinder at high
angles of attack with laminar, transitional, or
turbulent separation

[AIAA 80-1556]

p0028 A80-45856

Multiple-time-scale concepts in turbulent
transport modelling

p0080 A80-49277

Vortex simulation of three-dimensional, spotlike
disturbances in a laminar boundary layer

p0067 A80-49296

Three-dimensional simulation of the free shear
layer using the vortex-in-cell method

p0067 A80-49300

Progress in turbulence modeling for complex flow
fields including effects of compressibility

[NASA-TP-1517]

p0034 N80-20527

Reynolds stress closures: Status and prospects

p0077 N80-27660

Large eddy simulation of turbulent channel flow:
ILLIAC 5 calculation

p0059 N80-27661

Two-photon excitation of nitric oxide fluorescence
as a temperature indicator in unsteady

gas-dynamic processes

[NASA-TM-81220]

p0037 N80-32700

TURBULENT HEAT TRANSFER

On the calculation of turbulent heat transport
downstream from an abrupt pipe expansion

p0076 A80-49037

TURBULENT MIXING

Asymmetric trailing-edge flows at high Reynolds
number

[AIAA PAPER 80-1396]

p0066 A80-44151

SUBJECT INDEX

UPWELLING

An experimental study of multiple jet mixing
[NASA-CR-166184] p0018 N80-31760

TURBULENT WAKES
NT PROPELLER SLIPSTREAMS
Experimental investigation of the asymmetric body
vortex wake
[AIAA PAPER 80-0174] p0032 A80-23937
High-resolution LDA measurements of Reynolds
stress in boundary layers and wakes
[AIAA 80-0436] p0025 A80-26967
Asymmetric trailing-edge flows at high Reynolds
number
[AIAA PAPER 80-1396] p0066 A80-44151
Direct numerical simulations of the turbulent wake
of an axisymmetric body p0080 A80-49235

TURNING FLIGHT
Flying-qualities criteria for wings-level-turn
maneuvering during an air-to-ground weapon
delivery task
[AIAA 80-1628] p0029 A80-45916

TVC (CONTROL)
U THRUST VECTOR CONTROL
TWO DIMENSIONAL BOUNDARY LAYER
An experimental and numerical investigation of a
three-dimensional shock wave separated turbulent
boundary layer
[AIAA PAPER 80-0002] p0061 A80-22727

TWO DIMENSIONAL FLOW
A diagonal form of an implicit
approximate-factorization algorithm with
application to a two dimensional inlet
[AIAA PAPER 80-0067] p0061 A80-19274
Analysis of two-dimensional incompressible flows
by a subsurface panel method p0029 A80-30566
Characterization of acoustic disturbances in
linearly sheared flows p0030 A80-31804
Reformulation of Possio's kernel with application
to unsteady wind tunnel interference p0031 A80-43129
Characterization of acoustic disturbances in
linearly sheared flows p0014 N80-15869
[NASA-CR-162577]

U

UH-1 HELICOPTER
A compilation and analysis of helicopter handling
qualities data. Volume 1: Data compilation
[NASA-CR-3144] p0013 N80-11097
V/STOLAND avionics system flight-test data on a
UH-1H helicopter
[NASA-TN-78591] p0008 N80-18047
Navigation systems for approach and landing of
VTOL aircraft
[NASA-CR-152335] p0016 N80-19055

ULTRAVIOLET LIGHT
U ULTRAVIOLET RADIATION
ULTRAVIOLET PHOTOMETRY
Ultraviolet photometer observations of the
Saturnian system p0070 A80-19122

ULTRAVIOLET RADIATION
NT LYMAN ALPHA RADIATION
Are solar spectral variations a drive for climatic
change p0042 A80-15488
Mars ultraviolet simulation facility p0089 A80-36061
Comparison of the Nimbus-4 BUV ozone data with the
Ames two-dimensional model
[NASA-TN-81207] p0036 N80-24914

ULTRAVIOLET SPECTROGRAPHS
U ULTRAVIOLET SPECTROMETERS
ULTRAVIOLET SPECTROMETERS
Design and operation of the Pioneer Venus Orbiter,
ultraviolet spectrometer p0073 A80-30841

UNIFORM FLOW
A note on sound radiation into a uniformly flowing
medium p0031 A80-45488

UNITED STATES OF AMERICA
NT CALIFORNIA
NT HAWAII
Issues arising from the demonstration of
Landsat-based technologies to inventories and

mapping of the forest resources of the Pacific
Northwest states p0065 A80-41305

UNMANNED SPACECRAFT
NT GALILEO PROBE
NT JUPITER PROBES
NT PIONEER VENUS SPACECRAFT
NT PIONEER VENUS 1 SPACECRAFT
NT PIONEER VENUS 2 SOUNDER PROBE
NT PIONEER VENUS 2 SPACECRAFT
NT PIONEER 10 SPACE PROBE
NT PIONEER 11 SPACE PROBE
NT SPACE PROBES
NT VENERA SATELLITES
NT VENUS PROBES

UNSTEADY FLOW
Implicit computations of unsteady transonic flow
governed by the full-potential equation in
conservation form p0062 A80-23935
[AIAA PAPER 80-0150]
Application of the method of integral relations to
unsteady fluid flow problems with shocks p0078 A80-26694
Application of laser velocimetry to an unsteady
transonic flow p0063 A80-29506
Characterization of acoustic disturbances in
linearly sheared flows p0030 A80-31804
The observed ozone flux by transient eddies, 0-30 km
p0074 A80-34449
Nonreflecting far-field boundary conditions for
unsteady transonic flow computation p0065 A80-41597
[AIAA PAPER 80-1393]
Reformulation of Possio's kernel with application
to unsteady wind tunnel interference p0031 A80-43129
A vortex-lattice method for the calculation of the
nonsteady separated flow over delta wings
[AIAA PAPER 80-1803] p0027 A80-43286
An advanced panel method for analysis of arbitrary
configurations in unsteady subsonic flow p0017 N80-26270
[NASA-CR-152323]
Experimental studies of scale effects on
oscillating airfoils at transonic speeds p0010 N80-27287
[NASA-TN-81216]
Dynamic stall on advanced airfoil sections p0101 N80-29252
[AD-A085809]
Numerical solution techniques for unsteady
transonic aerodynamics problems p0059 N80-33379

UNSTEADY STATE
Unsteady aerodynamics of conventional and
supercritical airfoils p0026 A80-35038
[AIAA 80-0734]

UNSWEPT WINGS
NT INFINITE SPAN WINGS
NT RECTANGULAR WINGS

UPPER AIR
U UPPER ATMOSPHERE
UPPER ATMOSPHERE
NT IONOSPHERE
NT MAGNETOSPHERE
NT MESOSPHERE
NT THERMOSPHERE
The upper atmosphere of Uranus - Mean temperature
and temperature variations p0071 A80-22207
A Lagrangian mean theory of wave, mean-flow
interaction with applications to nonacceleration
and its breakdown --- large-scale atmospheric
dynamics p0075 A80-36473
Eddy diffusion coefficients and the variance of
the atmosphere 30-60 km p0076 A80-45996

UPPER SURFACE BLOWN FLAPS
Upper surface blowing noise of the NASA-Ames quiet
short-haul research aircraft p0026 A80-36002
[AIAA PAPER 80-1064]
Conceptual studies of a long-range transport with
an upper surface blowing propulsive lift system p0009 N80-23249
[NASA-TN-81196]

UPWASH
VTOL in-ground effect flows for closely spaced jets
[AIAA PAPER 80-1880] p0033 A80-46693

UPWELLING
U UPWELLING WATER

UPWELLING WATER

SUBJECT INDEX

UPWELLING WATER

Analysis of coastal upwelling and the production of a biomass
[NASA-TM-78614] p0035 N80-12720

URANIUM COMPOUNDS
NT URANIUM FLUORIDES
URANIUM FLUORIDES
Relativistic scattered wave calculations on UF₆
p0049 A80-30458

URANUS (PLANET)
The radius and ellipticity of Uranus from its occultation of SAO 158687
p0073 A80-31937

URANUS ATMOSPHERE
The upper atmosphere of Uranus - Mean temperature and temperature variations
p0071 A80-22207

URBAN RESEARCH
Meteorological and air pollution modeling for an urban airport
p0055 A80-42659

UREAS
Reverse osmosis membrane of high urea rejection properties --- water purification
[NASA-CASE-ARC-10980-1] p0097 N80-23452

URINE
Water recovery by catalytic treatment of urine vapor [ASME PAPER 80-ENAS-16] p0093 A80-43192
Extremes of urine osmolality - Lack of effect on red blood cell survival
p0091 A80-46196
Design, fabrication and testing of a dual catalyst ammonia removal system for a urine VCD unit
[NASA-CR-152372] p0085 N80-29023

USA (UNITED STATES)
U UNITED STATES OF AMERICA

USER MANUALS (COMPUTER PROGRAMS)
A comprehensive analytical model of rotorcraft aerodynamics and dynamics. Part 2: User's manual
[NASA-TM-81183] p0010 N80-28297

USER REQUIREMENTS
An assessment of future computer system needs for large-scale computation
[NASA-TM-78613] p0008 N80-17717

UTILITY AIRCRAFT
NT BO-105 HELICOPTER
NT UH-1 HELICOPTER

UTILIZATION
NT LASER APPLICATIONS

V

V/STOL AIRCRAFT

NT BO-105 HELICOPTER
NT H-53 HELICOPTER
NT HELICOPTERS
NT MILITARY HELICOPTERS
NT OH-6 HELICOPTER
NT QUESTOL
NT RIGID ROTOR HELICOPTERS
NT ROTARY WING AIRCRAFT
NT SHORT TAKEOFF AIRCRAFT
NT TILT ROTOR AIRCRAFT
NT UH-1 HELICOPTER
NT VERTICAL TAKEOFF AIRCRAFT
NT XV-15 AIRCRAFT
Large scale model tests of a new technology V/STOL concept
[AIAA PAPER 80-0233] p0023 A80-19303
V/STOL flight simulation
[NASA-TM-81156] p0006 N80-12100
Force and moment data from a wind-tunnel test of a tilt-macelle V/STOL propulsion system with an attitude control vane --- conducted in Ames 40 by 80 foot wind tunnel
[NASA-TM-81157] p0006 N80-13003
Investigation of ground effects on large and small scale models of a three fan V/STOL aircraft configuration
[NASA-CR-152240] p0015 N80-16030
A candidate V/STOL research aircraft design concept using an S-3A aircraft and 2 Pegasus 11 engines
[NASA-TM-81204] p0009 N80-24293

VACUUM APPARATUS
NT ION PUMPS

VACUUM PUMPS
NT ION PUMPS

VALKYRIE AIRCRAFT

U B-70 AIRCRAFT

VALLEYS
NT SACRAMENTO VALLEY (CA)
NT SAN JOAQUIN VALLEY (CA)

VAN ALLEN RADIATION BELTS
U RADIATION BELTS
VAN DER WAAL FORCES
Curves of growth for van der Waals broadened spectral lines
p0057 A80-51378

VANES
NT GUIDE VANES

VAPOR DEPOSITION
Comparison of the early stages of condensation of Cu and Ag on Mo/100/ with Cu and Ag on W/100/
p0053 A80-37193

VAPORS
Water recovery by catalytic treatment of urine vapor
[ASME PAPER 80-ENAS-16] p0093 A80-43192

VARIABLE GEOMETRY STRUCTURES
Aircraft engine nozzle
[NASA-CASE-ARC-10977-1] p0033 N80-32392

VARIABLE LIFT
U LIFT

VARIABLE STARS
NT NOVAE
NT SUPERNOVAE
NT T TAURI STARS
The infrared spectrum of the carbon star Y Canum Venaticorum between 1.2 and 30 microns
p0046 A80-22191

VARIANCE (STATISTICS)
NT REGRESSION ANALYSIS

VARIATIONAL PRINCIPLES
A variational technique for smoothing flight-test and accident data
[AIAA 80-1601] p0028 A80-45894
Modified Iterative Extended Hueckel. 1: Theory
[NASA-TM-81200] p0083 N80-25108

VARIATIONS
NT ANNUAL VARIATIONS

VECTOR ANALYSIS
NT VORTICITY

VECTOR SPACES
NT EIGENVALUES
NT MATRICES (MATHEMATICS)
NT VORTICITY

VECTORS (MATHEMATICS)
NT VORTICITY

VEGETABLES
Irrigated lands assessment for water management
Applications Pilot Test (APT) --- California
[E80-10324] p0019 N80-32815

VEGETATION
NT CANOPIES (VEGETATION)

VELOCITY
NT FLOW VELOCITY
NT GROUP VELOCITY
NT RELATIVISTIC VELOCITY
NT SUBSONIC SPEED
NT WIND VELOCITY

VELOCITY DISTRIBUTION
Experimental investigation of a three dimensional turbulent boundary layer with a non disappearing pressure gradient
p0054 A80-40907
On the combination of kinematics with flow visualization to compute total circulation - Application to vortex rings in a tube
[AIAA PAPER 80-1330] p0065 A80-41563
Effect of tip planform on blade loading characteristics for a two-bladed rotor in hover
[NASA-TM-78615] p0007 N80-14049
Turbulent structures in wall-bounded shear flows observed via three-dimensional numerical simulators --- using the Illiac 4 computer
[NASA-TM-81219] p0037 N80-29622

VELOCITY FIELDS
U VELOCITY DISTRIBUTION

VELOCITY MEASUREMENT
NT WIND VELOCITY MEASUREMENT
Application of laser velocimetry to an unsteady transonic flow
p0063 A80-29506
Feasibility studies for light scattering experiments to determine the velocity relaxation of small particles in a fluid
[NASA-CR-163214] p0040 N80-25586

- A comprehensive analytical model of rotorcraft aerodynamics and dynamics. Part 2: User's manual [NASA-TM-81183] p0010 N80-28297
- VELOCITY PROFILES**
U VELOCITY DISTRIBUTION
- VENERA SATELLITES**
A comparison of Pioneer Venus and Venera bow shock observations - Evidence for a solar cycle variation p0069 A80-15296
- VENUS ATMOSPHERE**
NT VENUS CLOUDS
A model of the neutral and ion nitrogen chemistry in the daytime thermosphere of Venus p0067 A80-10460
A comparison of Pioneer Venus and Venera bow shock observations - Evidence for a solar cycle variation p0069 A80-15296
Hot hydrogen in the exosphere of Venus p0070 A80-18943
Initial Pioneer Venus magnetometer observations p0078 A80-23690
The Pioneer Venus Orbiter plasma analyzer experiment p0050 A80-30836
Pioneer Venus Orbiter planar retarding potential analyzer plasma experiment p0073 A80-30839
Pioneer Venus small probes net flux radiometer experiment p0073 A80-30850
Data acquisition for measuring the wind on Venus from Pioneer Venus p0051 A80-30852
Corrections in the Pioneer Venus sounder probe gas chromatographic analysis of the lower Venus atmosphere p0089 A80-30875
Pioneer Venus sounder and small probes Nephelometer instrument p0053 A80-36750
The location of the dayside ionopause of Venus - Pioneer Venus Orbiter magnetometer observations p0076 A80-48811
The solar wind interaction with Venus p0076 N80-13561
Data acquisition for measuring the wind on Venus from Pioneer Venus p0058 N80-26361
- VENUS CLOUDS**
Pioneer Venus sounder and small probes Nephelometer instrument p0053 A80-36750
- VENUS PROBES**
NT PIONEER VENUS 2 SPACECRAFT
NT VENERA SATELLITES
Pioneer Venus spacecraft design and operation p0050 A80-30829
Pioneer Venus Sounder Probe Neutral Gas Mass Spectrometer p0073 A80-30844
Pioneer Venus Sounder Probe gas chromatograph p0089 A80-30845
Atmosphere structure instruments on the four Pioneer Venus entry probes p0051 A80-30849
Data acquisition for measuring the wind on Venus from Pioneer Venus p0051 A80-30852
- VERTEBRATES**
NT DOGS
NT MICE
- VERTICAL FLIGHT**
Singular perturbations and the sounding rocket problem p0001 A80-24268
- VERTICAL LANDING**
Optimal washout for control of a moving base simulator --- vertical motion flight simulation using linear filter p0031 A80-14833
- VERTICAL MOTION**
Feasibility and concept study to convert the NASA/AMES vertical motion simulator to a helicopter simulator [NASA-CR-152193] p0098 N80-16070
Operations manual: Vertical Motion Simulator (VMS) S.08 [NASA-TM-81180] p0009 N80-23295
- VERTICAL TAKEOFF AIRCRAFT**
Model development for automatic guidance of a VTOL aircraft to a small aviation ship p0028 A80-45907
[AIAA 80-1617]
VTOL in-ground effect flows for closely spaced jets [AIAA PAPER 80-1880] p0033 A80-46693
Flight tests of the total automatic flight control system (Tafcos) concept on a DHC-6 Twin Otter aircraft [NASA-TP-1513] p0005 N80-17081
Navigation systems for approach and landing of VTOL aircraft [NASA-CR-152335] p0016 N80-19055
Vorticity associated with multiple jets in a crossflow --- vertical takeoff aircraft [NASA-CR-162855] p0016 N80-19454
System description and analysis. Part 1: Feasibility study for helicopter/VTOL wide-angle simulation image generation display system [NASA-CR-152376] p0101 N80-27397
Phase 1 wind tunnel tests of the J-97 powered, external augmentor V/STOL model [NASA-CR-152255] p0017 N80-28303
- VERTICAL TAKEOFF AND LANDING**
U VERTICAL LANDING
- VESTIBULAR TESTS**
Perception and performance in flight simulators: The contribution of vestibular, visual, and auditory information [NASA-CR-162129] p0085 N80-11103
- VIBRATION**
NT STRUCTURAL VIBRATION
A comprehensive analytical model of rotorcraft aerodynamics and dynamics. Part 3: Program manual [NASA-TM-81184] p0010 N80-28298
- VIBRATION DAMPING**
The promise of multicyclic control --- for helicopter vibration reduction p0022 A80-33123
A new approach to active control of rotorcraft vibration [AIAA 80-1778] p0027 A80-45556
Analytical design and evaluation of an active control system for helicopter vibration reduction and gust response alleviation [NASA-CR-152377] p0017 N80-28369
- VIBRATION EFFECTS**
Multicyclic control of a helicopter rotor considering the influence of vibration, loads, and control motion [AIAA 80-0673] p0025 A80-34998
Thresholds for detection of constant rotary acceleration during vibratory rotary acceleration p0091 A80-42003
- VIBRATIONAL FREQUENCIES**
U VIBRATIONAL SPECTRA
VIBRATIONAL RELAXATION
U MOLECULAR RELAXATION
VIBRATIONAL SPECTRA
Ground-state rotational constants of /C-13/H3D p0054 A80-41175
- VIBRATORY LOADS**
Analysis and correlation of test data from an advanced technology rotor system --- helicopter performance prediction [NASA-CR-152366] p0019 N80-33351
- VIDEO COMMUNICATION**
Conditional replenishment using motion prediction p0065 A80-39715
- VIEW EFFECTS**
Effect of field of view and monocular viewing on angular size judgements in an outdoor scene [NASA-TM-81176] p0083 N80-19792
- VIKING LANDER SPACECRAFT**
The Viking mission and the search for life on Mars p0086 A80-10738
Mars ultraviolet simulation facility p0089 A80-36061
Simulation of the Viking biology experiments - An overview p0090 A80-36066
A model of Martian surface chemistry p0090 A80-36069
- VIKING SPACECRAFT**
NT VIKING LANDER SPACECRAFT
VIKING 1 SPACECRAFT
NT VIKING LANDER SPACECRAFT

VIKING 2 SPACECRAFT

SUBJECT INDEX

VIKING 2 SPACECRAFT
 NT VIKING LANDER SPACECRAFT
VINEYARDS
 Irrigated lands assessment for water management
 Applications Pilot Test (APT) --- California
 [E80-10324] p0019 N80-32815
VIRTUAL PROPERTIES
 Effects of magnification and visual accommodation
 on aimpoint estimation in simulated landings
 with real and virtual image displays
 [NASA-TP-1635] p0082 N80-34099
VISCERA
 NT PITUITARY GLAND
VISCOELASTIC FLOW
 U VISCOELASTICITY
VISCOELASTICITY
 Time-temperature behavior of a unidirectional
 graphite/epoxy composite p0078 A80-21141
 The viscoelastic behavior of a composite in a
 thermal environment
 [NASA-CR-163187] p0039 N80-24369
 The accelerated characterization of viscoelastic
 composite materials
 [NASA-CR-163188] p0039 N80-24370
VISCOSITY
 NT EDDY VISCOSITY
 Development of high viscosity coatings for
 advanced Space Shuttle applications p0079 A80-34760
VISCOUS FLOW
 NT BOUNDARY LAYER FLOW
 NT BOUNDARY LAYER SEPARATION
 NT REATTACHED FLOW
 NT SEPARATED FLOW
 An implicit finite-difference code for inviscid
 and viscous cascade flow
 [AIAA PAPER 80-1427] p0066 A80-44128
 A computational and experimental study of high
 Reynolds number viscous/inviscid interaction
 about a cone at high angle of attack
 [AIAA PAPER 80-1422] p0104 A80-44492
VISIBILITY
 NT LOW VISIBILITY
VISION
 NT MONOCULAR VISION
VISUAL CONTROL
 Effects of magnification and visual accommodation
 on aimpoint estimation in simulated landings
 with real and virtual image displays
 [NASA-TP-1635] p0082 N80-34099
VISUAL DISPLAYS
 U DISPLAY DEVICES
VISUAL PERCEPTION
 NT SPACE PERCEPTION
 Perception and performance in flight simulators:
 The contribution of vestibular, visual, and
 auditory information
 [NASA-CR-162129] p0085 N80-11103
 Effect of field of view and monocular viewing on
 angular size judgements in an outdoor scene
 [NASA-TM-81176] p0083 N80-19792
 Head-up transition behavior of pilots during
 simulated low-visibility approaches
 [NASA-TP-1618] p0082 N80-26039
 Effects of magnification and visual accommodation
 on aimpoint estimation in simulated landings
 with real and virtual image displays
 [NASA-TP-1635] p0082 N80-34099
VISUALIZATION OF FLOW
 U FLOW VISUALIZATION
VOLCANICS
 U VOLCANOLOGY
VOLCANOES
 Volcanic features of Hawaii. A basis for
 comparison with Mars
 [NASA-SP-403] p0034 N80-23912
VOLCANOLOGY
 Endogenic craters on basaltic lava flows - Size
 frequency distributions p0061 A80-23727
VOLTAGE GENERATORS
 NT PHOTOVOLTAIC CELLS
VOMITING
 Motion sickness in the squirrel monkey
 p0095 A80-25891
VORTEX BREAKDOWN
 Examination of group-velocity criterion for
 breakdown of vortex flow in a divergent duct

VORTEX COLUMNS p0022 A80-38049
 U VORTICES
VORTEX DISTURBANCES
 U VORTICES
VORTEX FLOW
 U VORTICES
VORTEX RINGS
 On the combination of kinematics with flow
 visualization to compute total circulation -
 Application to vortex rings in a tube
 [AIAA PAPER 80-1330] p0065 A80-41563
VORTEX TUBES
 U VORTICES
VORTICES
 NT WING TIP VORTICES
 Experimental investigation of the asymmetric body
 vortex wake
 [AIAA PAPER 80-0174] p0032 A80-23937
 Control of forebody vortex orientation to
 alleviate side forces
 [AIAA PAPER 80-0183] p0024 A80-23955
 The observed ozone flux by transient eddies, 0-30 km
 p0074 A80-34449
 Vortex simulation of three-dimensional, spotlike
 disturbances in a laminar boundary layer
 p0067 A80-49296
 Three-dimensional simulation of the free shear
 layer using the vortex-in-cell method
 p0067 A80-49300
 A three dimensional vortex wake model for missiles
 at high angles on attack
 [NASA-CR-3208] p0014 N80-14048
 Three-dimensional interactions and vortical flows
 with emphasis on high speeds
 [NASA-TM-81169] p0008 N80-21286
VORTICITY
 Vorticity associated with multiple jets in a
 crossflow --- vertical takeoff aircraft
 [NASA-CR-162855] p0016 N80-19454
 Turbulent structures in wall-bounded shear flows
 observed via three-dimensional numerical
 simulators --- using the Illiac 4 computer
 [NASA-TM-81219] p0037 N80-29622
VTOL
 U VERTICAL LANDING
VTOL AIRCRAFT
 U VERTICAL TAKEOFF AIRCRAFT
W
WAKES
 NT AIRCRAFT WAKES
 NT HELICOPTER WAKES
 NT PROPELLER SLIPSTREAMS
 NT TURBULENT WAKES
 A three dimensional vortex wake model for missiles
 at high angles on attack
 [NASA-CR-3208] p0014 N80-14048
WALL FLOW
 Types of leeside flow over delta wings
 p0052 A80-34652
 On the numerical solution of time-dependent
 viscous incompressible fluid flows involving
 solid boundaries p0052 A80-34980
 Calculations of transonic flow about an airfoil in
 a wind tunnel
 [AIAA PAPER 80-1366] p0027 A80-44142
 On the calculation of turbulent heat transport
 downstream from an abrupt pipe expansion
 p0076 A80-49037
 Turbulence measurements in the boundary layer of a
 low-speed wind tunnel using laser velocimetry
 [NASA-TM-81165] p0008 N80-16300
WALL JETS
 VTOL in-ground effect flows for closely spaced jets
 [AIAA PAPER 80-1880] p0033 A80-46693
WALLS
 NT WIND TUNNEL WALLS
WARNING DEVICES
 U WARNING SYSTEMS
WARNING SIGNALS
 U WARNING SYSTEMS
WARNING SYSTEMS
 Some human factors issues in the development and
 evaluation of cockpit alerting and warning systems
 [NASA-RP-1055] p0082 N80-15821

SUBJECT INDEX

WIND PROFILES

WASTE TREATMENT

Water recovery by catalytic treatment of urine vapor
[ASME PAPER 80-ENAS-16] p0093 A80-43192

WASTES

NT URINE

WATER

NT POTABLE WATER

WATER CONSUMPTION

Extremes of urine osmolality - Lack of effect on
red blood cell survival

p0091 A80-46196

Irrigated lands assessment for water management

Applications Pilot Test (APT) --- California
[E80-10324] p0019 N80-32815

WATER CONTENT

U MOISTURE CONTENT

WATER COOLING

U LIQUID COOLING

WATER HEATING

A solar-heated water system for a photographic
processing laboratory

p0098 A80-15750

WATER MANAGEMENT

Irrigated lands assessment for water management

Applications Pilot Test (APT) --- California
[E80-10324] p0019 N80-32815

WATER PRESSURE

Fluid shifts and endocrine responses during chair
rest and water immersion in man

p0088 A80-25990

WATER PURIFICATION

U WATER TREATMENT

WATER RECLAMATION

Water recovery by catalytic treatment of urine vapor
[ASME PAPER 80-ENAS-16] p0093 A80-43192

Design, fabrication and testing of a dual catalyst
ammonia removal system for a urine VCD unit
[NASA-CR-152372] p0085 N80-29023

WATER RECOVERY

U WATER RECLAMATION

WATER RUNOFF

Permittivity and attenuation of wet snow between 4
and 12 GHz

p0052 A80-36244

WATER TREATMENT

Reverse osmosis membrane of high urea rejection
properties --- water purification

[NASA-CASE-ARC-10980-1] p0097 N80-23452

WATER VEHICLES

NT AIRCRAFT CARRIERS

WAVE ATTENUATION

NT ACOUSTIC ATTENUATION

WAVE DRAG

NT INTERFERENCE DRAG

WAVE EQUATIONS

NT SCHROEDINGER EQUATION

WAVE EXCITATION

NT ACOUSTIC EXCITATION

WAVE FUNCTIONS

A new propagation method for the radial
Schroedinger equation

p0069 A80-15768

Recommended conventions for defining transition
moments and intensity factors in diatomic
molecular spectra

p0055 A80-41323

WAVE INTERACTION

NT SHOCK WAVE INTERACTION

A Lagrangian mean theory of wave, mean-flow
interaction with applications to nonacceleration
and its breakdown --- large-scale atmospheric
dynamics

p0075 A80-36473

WAVE PROPAGATION

NT ACOUSTIC PROPAGATION

NT LIGHT SCATTERING

NT SHOCK WAVE PROPAGATION

Wave propagation and transport in the middle
atmosphere

p0072 A80-26437

A Lagrangian mean theory of wave, mean-flow
interaction with applications to nonacceleration
and its breakdown --- large-scale atmospheric
dynamics

p0075 A80-36473

Examination of group-velocity criterion for
breakdown of vortex flow in a divergent duct

p0022 A80-38049

Characterization of acoustic disturbances in
linearly sheared flows

[NASA-CR-162577] p0014 N80-15869

Proceedings of the Aero-Optics Symposium on

Electromagnetic Wave Propagation from Aircraft
[NASA-CP-2121] p0006 N80-25588

WAVE RADIATION

U ELECTROMAGNETIC RADIATION

WAVE SCATTERING

NT ACOUSTIC SCATTERING

NT ATMOSPHERIC SCATTERING

NT LIGHT SCATTERING

NT MIE SCATTERING

NT TROPOSPHERIC SCATTERING

Relativistic scattered wave calculations on UF6

p0049 A80-30458

WAVEFORMS

A microprocessor-based instrument for neural pulse
wave analysis

p0098 A80-50322

WEAK ENERGY INTERACTIONS

Differentiation of optical isomers through
enhanced weak-field interactions

[NASA-TN-81208] p0084 N80-27164

WEAPONS DELIVERY

Flying-qualities criteria for wings-level-turn
maneuvering during an air-to-ground weapon

delivery task

[AIAA 80-1628] p0029 A80-45916

WEATHER FORECASTING

NT NUMERICAL WEATHER FORECASTING

WEBS (MEMBRANES)

U MEMBRANES

WEIGHT (MASS)

NT BIOMASS

NT STRUCTURAL WEIGHT

WEIGHTLESSNESS

The development of an elastic reverse gradient
garment to be used as a countermeasure for

cardiovascular deconditioning

[NASA-CR-152379] p0086 N80-33086

WEIGHTLESSNESS SIMULATION

Simulated weightlessness - Effects on bioenergetic
balance

p0095 A80-21544

Effect of simulated weightlessness on the immune
system in rats

p0088 A80-25894

WETNESS

U MOISTURE CONTENT

WHEELS

NT TURBINE WHEELS

WHIRL

U ROTATION

WHIRLING

U ROTATION

WIDEBAND

U BROADBAND

WIND (METEOROLOGY)

NT WINDS ALOFT

WIND CIRCULATION

U ATMOSPHERIC CIRCULATION

WIND DIRECTION

Mars - The north polar sand sea and related wind
patterns

p0047 A80-26370

WIND EFFECTS

Eolian sedimentation on earth and Mars - Some
comparisons

p0068 A80-13969

Mars - The north polar sand sea and related wind
patterns

p0047 A80-26370

Analytical design and evaluation of an active
control system for helicopter vibration

reduction and gust response alleviation
[NASA-CR-152377] p0017 N80-28369

WIND MEASUREMENT

NT WIND VELOCITY MEASUREMENT

Data acquisition for measuring the wind on Venus
from Pioneer Venus

p0051 A80-30852

WIND PROFILES

High resolution vertical profiles of wind,
temperature and humidity obtained by computer
processing and digital filtering of radiosonde
and radar tracking data from the ITCZ experiment

of 1977

[NASA-CR-3269] p0039 N80-21926

WIND TUNNEL MODELS

SUBJECT INDEX

WIND TUNNEL MODELS

Measurements of control stability characteristics of a wind-tunnel model using a transfer function method
 [AIAA 80-0457] p0024 A80-26957

WIND TUNNEL TESTS
 Large scale model tests of a new technology V/STOL concept
 [AIAA PAPER 80-0233] p0023 A80-19303
 Acoustic characteristics of two hybrid inlets at forward speed
 [AIAA PAPER 79-0678] p0021 A80-20828
 Noise generation by a lifting wing/flap combination at Reynolds numbers to 2.8×10 to the 6th
 [AIAA PAPER 80-0035] p0024 A80-22729
 Experimental investigation of the asymmetric body vortex wake
 [AIAA PAPER 80-0174] p0032 A80-23937
 Threshold windspeeds for sand on Mars - Wind tunnel simulations p0048 A80-27391
 Diagnosis of separated flow regions on wind-tunnel models using an infrared camera p0025 A80-29494
 Analytical study of the effects of wind tunnel turbulence on turbfan rotor noise
 [AIAA PAPER 80-1022] p0033 A80-35978
 A measurement of forward-flight effects on the noise from a JT15D-1 turbfan engine in the NASA-Ames 40- by 80-Foot Wind Tunnel
 [AIAA PAPER 80-1026] p0026 A80-38641
 Reformulation of Possio's kernel with application to unsteady wind tunnel interference p0031 A80-43129
 Aerodynamic interactions from reaction controls for lateral control of the M2-P2 lifting-body entry configuration at transonic and supersonic and supersonic Mach numbers --- wind tunnel tests
 [NASA-TM-78534] p0006 N80-11033
 Wind-tunnel/flight correlation study of aerodynamic characteristics of a large flexible supersonic cruise airplane CXB-70-1). 1:
 Wind-tunnel tests of a 0.03-scale model at Mach numbers from 0.6 to 2.53
 [NASA-TP-1514] p0004 N80-11068
 Wind tunnel investigation of an oblique wing transport model at mach numbers between 0.6 and 1.4
 [NASA-CR-137697] p0013 N80-12059
 Force and moment data from a wind-tunnel test of a tilt-macelle V/STOL propulsion system with an attitude control vane --- conducted in Ames 40 by 80 foot wind tunnel
 [NASA-TM-81157] p0006 N80-13003
 NASA/Army XV-15 tilt rotor research aircraft wind-tunnel test program plan --- Ames 40-ft by 80-ft wind tunnel tests
 [NASA-TM-78562] p0007 N80-15067
 An experimental study of the structure and acoustic field of a jet in a cross stream --- Ames 7-ft by 10-ft wind tunnel tests
 [NASA-CR-162464] p0014 N80-15871
 Analytical study of the effects of wind tunnel turbulence on turbfan rotor noise --- NASA Ames 40 by 80 foot wind tunnel
 [NASA-CR-152359] p0016 N80-23099
 Wind-tunnel tests of the XV-15 tilt rotor aircraft
 [NASA-TM-81177] p0009 N80-24294
 Large-scale wind-tunnel tests of inverting flaps on a STOL utility aircraft model
 [NASA-TP-1696] p0005 N80-25318
 Overview of 6- X 6-foot wind tunnel aero-optics tests --- transonic wind tunnel tests
 p0023 N80-25590
 Pressure and temperature fields associated with aero-optics tests --- transonic wind tunnel tests
 p0031 N80-25591
 Unsteady density and velocity measurements in the 6 foot x 6 foot wind tunnel p0023 N80-25594
 Experimental studies of scale effects on oscillating airfoils at transonic speeds
 [NASA-TM-81216] p0010 N80-27287
 Phase 1 wind tunnel tests of the J-97 powered, external augmentor V/STOL model
 [NASA-CR-152255] p0017 N80-28303
 Analysis and correlation of test data from an advanced technology rotor system --- helicopter

performance prediction
 [NASA-CR-152366] p0019 N80-33351

WIND TUNNEL WALLS
 Calculations of transonic flow about an airfoil in a wind tunnel
 [AIAA PAPER 80-1366] p0027 A80-44142

WIND TUNNELS
 NT SUBSONIC WIND TUNNELS
 The 60-MW Shuttle interaction heating facility
 p0059 A80-12603
 Integral equations for flows in wind tunnels
 p0029 A80-21906

WIND VELOCITY
 Threshold windspeeds for sand on Mars - Wind tunnel simulations
 p0048 A80-27391

WIND VELOCITY MEASUREMENT
 Measurements of wind vectors, eddy momentum transports, and energy conversions in Jupiter's atmosphere from Voyager 1 images
 A80-24159
 High resolution vertical profiles of wind, temperature and humidity obtained by computer processing and digital filtering of radiosonde and radar tracking data from the ITCZ experiment of 1977
 [NASA-CR-3269] p0039 N80-21926

WINDS ALOFT
 A numerical model of the zonal mean circulation of the middle atmosphere
 p0073 A80-34443

WING FLAPS
 Noise generation by a lifting wing/flap combination at Reynolds numbers to 2.8×10 to the 6th
 [AIAA PAPER 80-0035] p0024 A80-22729

WING FLOW METHOD TESTS
 Experimental and computational study of transonic flow about swept wings
 [AIAA PAPER 80-0005] p0060 A80-18235
 Calculations of transonic flow about an airfoil in a wind tunnel
 [AIAA PAPER 80-1366] p0027 A80-44142
 Experimental unsteady aerodynamics of conventional and supercritical airfoils --- conducted in the Ames 11 foot transonic wind tunnel
 [NASA-TM-81221] p0012 N80-33345

WING OSCILLATIONS
 The promise of multicyclic control --- for helicopter vibration reduction
 p0022 A80-33123
 Aerodynamic coefficients in generalized unsteady thin airfoil theory
 p0030 A80-38034

WING PLANFORMS
 NT DELTA WINGS
 NT INFINITE SPAN WINGS

WING PROFILES
 Application of numerical optimization to the design of wings with specified pressure distributions
 [NASA-CR-3238] p0015 N80-16031

WING ROOTS
 Wing flapping with minimum energy --- minimize the drag for a bending moment at the wing root
 [NASA-TM-81174] p0001 N80-16035

WING TIP VORTICES
 Effect of tip vortex structure on helicopter noise due to blade-vortex interaction
 p0031 A80-52645

WINGS
 NT DELTA WINGS
 NT INFINITE SPAN WINGS
 NT LIFTING ROTORS
 NT OBLIQUE WINGS
 NT RECTANGULAR WINGS
 NT RIGID ROTORS
 NT ROTARY WINGS
 NT SUPERCRITICAL WINGS
 NT SWEEP WINGS
 NT THIN WINGS
 Noise generation by a lifting wing/flap combination at Reynolds numbers to 2.8×10 to the 6th
 [AIAA PAPER 80-0035] p0024 A80-22729
 Some observations on supersonic wing design
 [AIAA 80-3040] p0001 A80-31009

WIRE
 Civil helicopter wire strike assessment study.

SUBJECT INDEX

ZERO GRAVITY

Volume 1: Findings and recommendations
[NASA-CR-152389] p0019 N80-33381
WORKLOADS (PSYCHOPHYSIOLOGY)
Dynamic decisions and work load in multitask
supervisory control p0095 A80-40898

X

X RAY ASTRONOMY

Quest for ultrahigh resolution in X-ray optics ---
for solar astronomy p0032 A80-17480
A real-time electronic imaging system for solar
X-ray observations from sounding rockets p0029 A80-18545
X-ray bright points and the solar cycle dependence
of emerging magnetic flux p0077 N80-17950

X RAY IMAGERY

A real-time electronic imaging system for solar
X-ray observations from sounding rockets p0029 A80-18545

X RAY SPECTROGRAPHY

U X RAY SPECTROSCOPY

X RAY SPECTROMETRY

U X RAY SPECTROSCOPY

X RAY SPECTROSCOPY

X-ray spectrometer spectrograph telescope system
--- for solar corona study p0077 A80-17502
Paraboloidal X-ray telescope mirror for solar
coronal spectroscopy p0078 A80-17503

X RAY TELESCOPES

X-ray spectrometer spectrograph telescope system
--- for solar corona study p0077 A80-17502
Paraboloidal X-ray telescope mirror for solar
coronal spectroscopy p0078 A80-17503

X RAYS

NT SOLAR X-RAYS

XB-70 AIRCRAFT

U B-70 AIRCRAFT

XENON

Na + Xe collisions in the presence of two
nonresonant lasers p0051 A80-32416

XV-15 AIRCRAFT

Synthesis of rotor test data for real-time
simulation p0015 N80-18029
[NASA-CR-152311]
A hingeless rotor XV-15 design integration
feasibility study. Volume 1: Engineering
design studies p0015 N80-18030
[NASA-CR-152310]
Wind-tunnel tests of the XV-15 tilt rotor aircraft
[NASA-TN-81177] p0009 N80-24294

Y

YAWMETERS

U ATTITUDE INDICATORS

YHU-1 HELICOPTER

U UH-1 HELICOPTER

YUH-1 HELICOPTER

U UH-1 HELICOPTER

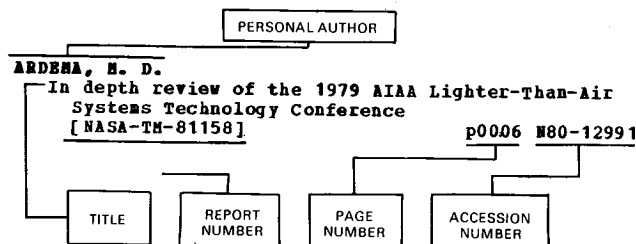
Z

ZERO GRAVITY

U WEIGHTLESSNESS

PERSONAL AUTHOR INDEX

Typical Personal Author Index Listing



Listings in this index are arranged alphabetically by personal author. The title of the document provides the user with a brief description of the subject matter. The report number helps to indicate the type of document listed (e.g., NASA report, translation, NASA contractor report). The page and accession numbers are located beneath and to the right of the title. Under any one author's name the accession numbers are arranged in sequence with the /AA accession numbers appearing first.

A

- ARDEMA, M. D.**
In depth review of the 1979 AIAA Lighter-Than-Air Systems Technology Conference [NASA-TM-81158] p0006 N80-12991
- ABURDENE, M. F.**
On the Routh approximation technique and least squares errors p0032 A80-20873
- ACQUISTA, C.**
Asymptotic behavior of the efficiencies in Mie scattering p0031 A80-47048
Feasibility studies for light scattering experiments to determine the velocity relaxation of small particles in a fluid [NASA-CR-163214] p0040 N80-25586
- ACTON, L. W.**
X-ray spectrometer spectrograph telescope system p0077 A80-17502
Paraboloidal X-ray telescope mirror for solar coronal spectroscopy p0078 A80-17503
High-resolution Lyman-alpha filtergrams of the sun p0075 A80-37277
- ADAMSON, J. C.**
A simulator study of control and display augmentations for helicopters [NASA-CR-163451] p0018 N80-31408
- ADAMSON, M. J.**
Effects of moisture on apparent flexure strength and on torsion and flexure fatigue properties of graphite-epoxy composites p0063 A80-27965
Thermal expansion and swelling of cured epoxy resin used in graphite/epoxy composite materials p0054 A80-40926
- ADCOCK, C.**
Application of advanced technologies to small, short-haul air transports [NASA-CR-152364] p0019 N80-33396
- AGGARWAL, H. R.**
Monte Carlo simulation of lunar megaregolith and implications p0061 A80-23716
- AGRAWAL, S. P.**
A comparative study of cosmic ray intensity variations during 1972-1977 using spacecraft and ground-based observations p0072 A80-28244
- AIKEN, E. W.**
A mathematical representation of an advanced helicopter for piloted simulator investigations of control system and display variations [NASA-TM-81203] p0011 N80-28371
Results of a simulator investigation of control system and display variations for an attack helicopter mission [AD-A085812] p0101 N80-29370
- ALEXANDER, H. R.**
A hingeless rotor XV-15 design integration feasibility study. Volume 1: Engineering design studies [NASA-CR-152310] p0015 N80-18030
- ALEXANDER, W. K.**
Wind tunnel investigation of an oblique wing transport model at mach numbers between 0.6 and 1.4 [NASA-CR-137697] p0013 N80-12059
- ALFF, W. H.**
Large Deployable Reflector (LDR) [NASA-CR-152402] p0040 N80-33319
- ALICO, R.**
The intracellular Na⁺/ and K⁺/ composition of the moderately halophilic bacterium, Paracoccus halodenitrificans p0091 A80-41250
- ALYEA, F. N.**
Preliminary calculations concerning the maintenance of the zonal mean ozone distribution in the Northern Hemisphere p0074 A80-34445
- ANDERSON, J. L.**
Application of parametric weight and cost estimating relationships to future transport aircraft [SAWE PAPER 1292] p0024 A80-20637
- ANNIS, J. F.**
The development of an elastic reverse gradient garment to be used as a countermeasure for cardiovascular deconditioning [NASA-CR-152379] p0086 N80-33086
- APT, J.**
Simple Cassegrain scanning system for infrared astronomy p0074 A80-34729
- ARDEMA, M. D.**
Singular perturbations and the sounding rocket problem p0001 A80-24268
In depth review of the 1979 AIAA Lighter-Than-Air Systems Technology Conference [NASA-TM-81158] p0006 N80-12991
Parametric study of modern airship productivity [NASA-TM-81151] p0011 N80-28340
- ARIGO, R. J.**
The settling of helium and the ages of globular clusters p0052 A80-35151
- ARONOWITZ, S.**
Organic chemistry on Titan p0087 A80-20340
Modified Iterative Extended Hueckel. 1: Theory [NASA-TM-81200] p0083 N80-25108
Modified Iterative Extended Hueckel. 2: Application to the interaction of Na⁺, Na⁺ (aq.), Mg⁺-2 (aq.) with adenine and thymine

- [NASA-TM-81201] p0084 N80-25109
Quantum theory and chemistry: Two propositions
[NASA-TM-81202] p0084 N80-25110
Differentiation of optical isomers through
enhanced weak-field interactions
[NASA-TM-81208] p0084 N80-27164
- ASARO, C.
Photoexcitation and ionization in molecular oxygen
Theoretical studies of electronic transitions
in the discrete and continuous spectral intervals
p0044 A80-20275
- ASHBAUGH, J.
Workshop on Aircraft Surface Representation for
Aerodynamic Computation
[NASA-TM-81170] p0008 N80-19025
- ATLAW, H.
Review of cell aging in Drosophila and mouse
p0087 A80-17741
- AUGASON, G. C.
Comparison of predicted and observed spectral
energy distribution of K and M stars. I - Alpha
Bootis
p0046 A80-22194
- AVILA, J. H.
Stability of nonuniform rotor blades in hover
using a mixed formulation
[NASA-TM-81226] p0012 N80-33777

B

- BACH, R. E., JR.
Aircraft motion analysis using limited flight and
radar data
p0025 A80-27241
A variational technique for smoothing flight-test
and accident data
[AIAA 80-1601] p0028 A80-45894
Equations for determining aircraft motions for
accident data
[NASA-TM-78609] p0010 N80-25306
- BACHALO, W. D.
A comprehensive comparison between experiment and
prediction for a transonic turbulent separated
flow
[AIAA PAPER 80-1407] p0027 A80-44154
- BAER, M.
F + H₂ collisions on two electronic potential
energy surfaces - Quantum-mechanical study of
the collinear reaction
p0068 A80-12012
- BAGANOFF, D.
An experimental study of multiple jet mixing
[NASA-CR-166184] p0018 N80-31760
- BAILEY, D. G.
A comparison of computer architectures for the
NASA demonstration advanced avionics system
p0032 A80-32427
- BAILEY, F. R.
Computational aerodynamics on large computers
p0048 A80-27415
Use of advanced computers for aerodynamic flow
simulation
p0058 N80-21257
- BAILEY, R. O.
Aerodynamic interactions from reaction controls
for lateral control of the M2-F2 lifting-body
entry configuration at transonic and supersonic
and supersonic Mach numbers
[NASA-TM-78534] p0006 N80-11033
- BAIRD, A. K.
Heterogeneous phase reactions of Martian volatiles
with putative regolith minerals
p0090 A80-36062
- BAKER, F. A.
V-STOLAND avionics system flight-test data on a
UH-1H helicopter
[NASA-TM-78591] p0008 N80-18047
- BAKKE, J.
Pioneer Venus Orbiter planar retarding potential
analyzer plasma experiment
p0073 A80-30839
- BALAKRISHNAN, A.
Galileo probe thermal protection: Entry heating
environments and spallation experiments design
[NASA-CR-152334] p0038 N80-14184
- BALDRIGHI, G.
Physiological response to hyper- and hypogravity
during rollercoaster flight
p0095 A80-21547
- BALDWIN, B. S.
Asymptotic features of shock-wave boundary-layer
interaction
p0055 A80-43135
- BALLARD, J. D.
Measurements of control stability characteristics
of a wind-tunnel model using a transfer function
method
[AIAA 80-0457] p0024 A80-26957
Effect of tip planform on blade loading
characteristics for a two-bladed rotor in hover
[NASA-TM-78615] p0007 N80-14049
- BALLARD, R.
Radiant panel tests on an epoxy/carbon fiber
composite
[NASA-TM-81185] p0037 N80-32435
- BALHAUS, W. F.
Computational aerodynamics on large computers
p0048 A80-27415
Use of advanced computers for aerodynamic flow
simulation
p0058 N80-21257
Numerical solution techniques for unsteady
transonic aerodynamics problems
p0059 N80-33379
- BALLOU, E. V.
The preparation of calcium superoxide in a flowing
gas stream and fluidized bed
[ASME PAPER 80-ENAS-18] p0094 A80-43194
- BANAS, R.
Studies for improved high temperature coatings for
Space Shuttle application
p0079 A80-34757
Development of high viscosity coatings for
advanced Space Shuttle applications
p0079 A80-34760
- BANDETTINI, A.
Diagnosis of separated flow regions on wind-tunnel
models using an infrared camera
p0025 A80-29494
- BARLOW, P. R.
Study of cooling air inlet and exit geometries for
horizontally opposed piston aircraft engines
[AIAA PAPER 80-1242] p0027 A80-38984
Effect of propeller slipstream on the drag and
performance of the engine cooling system for a
general aviation twin-engine aircraft
[AIAA PAPER 80-1872] p0027 A80-43315
- BARNES, G.
Transient solution for megajoule energy release in
a lumped-parameter series RLC circuit
p0051 A80-32826
- BASTIAN, T. S.
Saturnian trapped radiation and its absorption by
satellites and rings - The first results from
Pioneer 11
p0070 A80-19118
- BATES, C. W., JR.
The role of cesium suboxides in low-work-function
surface layers studied by X-ray photoelectron
spectroscopy - Ag-O-Cs
p0051 A80-33844
- BATY, D.
The effect of viewing time, time to encounter, and
practice on perception of aircraft separation on a
cockpit display of traffic information
[NASA-TM-81173] p0083 N80-18038
Perception of aircraft separation with
pilot-preferred symbology on a cockpit display
of traffic information
[NASA-TM-81172] p0084 N80-31397
- BEAM, R. M.
On the construction and application of implicit
factored schemes for conservation laws
p0062 A80-27407
Alternating direction implicit methods for
parabolic equations with a mixed derivative
p0057 A80-51050
- BEANISH, J. K.
Wind tunnel investigation of an oblique wing
transport model at mach numbers between 0.6 and
1.4
[NASA-CR-137697] p0013 N80-12059
- BEEBE, R. F.
Measurements of wind vectors, eddy momentum
transports, and energy conversions in Jupiter's
atmosphere from Voyager 1 images
A80-24159

PERSONAL AUTHOR INDEX

BONNER, W. A.

- BELMONT, A. D.**
Eddy diffusion coefficients and the variance of the atmosphere 30-60 km
p0076 A80-45996
- BELSTERLING, C. A.**
Feasibility and concept study to convert the NASA/AMES vertical motion simulator to a helicopter simulator
[NASA-CR-152193] p0098 N80-16070
- BELTRAMETTI, M.**
Radiatively driven winds for different power law spectra
p0054 A80-40138
- BELTRAMO, M. N.**
Application of parametric weight and cost estimating relationships to future transport aircraft
[SAWE PAPER 1292] p0024 A80-20637
Parametric study of helicopter aircraft systems costs and weights
[NASA-CR-152315] p0016 N80-22305
- BENSCH, K. G.**
Review of cell aging in Drosophila and mouse
p0087 A80-17741
- BERDAHL, B. J.**
A model of Martian surface chemistry
p0090 A80-36069
- BERGMANN, M. Y.**
Experimental and computational study of transonic flow about swept wings
[AIAA PAPER 80-0005] p0060 A80-18235
- BERMAN, A. L.**
Pioneer Venus occultation radio science data generation
p0050 A80-30830
- BERNAUER, E. M.**
Role of thermal and exercise factors in the mechanism of hypervolemia
p0089 A80-32748
Exercise training-induced hypervolemia - Role of plasma albumin, renin, and vasopressin
p0089 A80-32749
- BERRY, W. E.**
NASA-Ames Life Sciences Flight Experiments program - 1980 status report
[ASME PAPER 80-BN-34] p0094 A80-43209
- BERTELHUB, A.**
Experimental and computational study of transonic flow about swept wings
[AIAA PAPER 80-0005] p0060 A80-18235
- BETZINA, M. D.**
Force and moment data from a wind-tunnel test of a tilt-macelle V/STOL propulsion system with an attitude control vane
[NASA-TM-81157] p0006 N80-13003
- BILLMAN, K.**
SOLARES orbiting mirror system
[AAS 79-304] p0067 A80-52280
- BILOW, N.**
Thermophysical and flammability characterization of phosphorylated epoxy adhesives
p0066 A80-48079
- BISSENETTE, L. R.**
An explicit algorithm for a fluid approach to nonlinear optics propagation using splitting and rezoning techniques
p0059 A80-14987
- BLACK, D.**
A high-sensitivity search for extraterrestrial intelligence at lambda 18 cm
p0090 A80-37933
- BLACK, D. C.**
In search of other planetary systems
p0046 A80-22978
Collapsing cloud models for Bok globules
p0048 A80-26996
The role of magnetic fields in the collapse of protostellar gas clouds
p0063 A80-31848
Numerical calculations of the collapse of nonrotating, magnetic gas clouds
p0057 A80-49341
An assessment of ground-based techniques for detecting other planetary systems. Volume 1: An overview
[NASA-CP-2124-VOL-1] p0034 N80-18997
An Assessment of Ground-Based Techniques for Detecting Other Planetary Systems. Volume 2: Position papers
[NASA-CP-2124-VOL-2] p0034 N80-25224
Project Orion: A design study of a system for detecting extrasolar planets
[NASA-SP-436] p0035 N80-27260
- BLACK, R. L.**
Wind tunnel investigation of an oblique wing transport model at mach numbers between 0.6 and 1.4
[NASA-CR-137697] p0013 N80-12059
- BLACK, S.**
Retinal changes in rats flown on Cosmos 936 - A cosmic ray experiment
p0091 A80-41995
- BLAIR, M. E.**
The radioracemization of isovaline - Cosmochemical implications
p0086 A80-13018
- BLAISDELL, G. A.**
Optimized laser turrets for minimum phase distortion
p0023 N80-25600
- BLAKE, M. L.**
Modeling Jupiter's current disc - Pioneer 10 outbound
p0075 A80-45153
- BLAMONT, J. E.**
Pioneer Venus sounder and small probes Nephelometer instrument
p0053 A80-36750
- BLANCHARD, M. B.**
Meteoroid ablation spheres from deep-sea sediments
p0046 A80-22948
- BLATHERWICK, R. D.**
Infrared methane spectra between 1120 per cm and 1800 per cm - A new atlas
p0042 A80-13143
A new atlas of infrared methane spectra between 1120 per cm and 1800 per cm
p0042 A80-15655
- BLEVINS, V. A.**
Pioneer Venus Sounder Probe Neutral Gas Mass Spectrometer
p0073 A80-30844
- BOBCO, R. P.**
Free convection in enclosures exposed to compressive heating
[AIAA PAPER 80-1536] p0079 A80-41495
- BOBICK, J. C.**
Documentation of the analysis of the benefits and costs of aeronautical research and technology models, volume 1
[NASA-CR-152278] p0001 N80-15865
- BOCK, O. L.**
Visually induced self-motion sensation adapts rapidly to left-right visual reversal
p0096 A80-44213
- BODENHEIMER, P.**
Calculations of the evolution of the giant planets
p0049 A80-28086
Fragmentation in a rotating protostar - A comparison of two three-dimensional computer codes
p0053 A80-38432
- BOESE, R. W.**
Infrared methane spectra between 1120 per cm and 1800 per cm - A new atlas
p0042 A80-13143
A new atlas of infrared methane spectra between 1120 per cm and 1800 per cm
p0042 A80-15655
Temperature dependence of intensities of the 8-12 micron bands of CFC13
p0045 A80-21559
Band model calculations for CFC13 in the 8-12 micron region
p0045 A80-21560
Integrated band intensities of gaseous N₂O/5/
p0047 A80-25660
Absolute intensities and pressure broadening coefficients measured at different temperatures for the 201/II/-000 band of C-12/O2/-16 at 4978/cm
p0048 A80-27125
The infrared radiometer on the sounder probe of the Pioneer Venus mission
p0050 A80-30847
- BOHN, A. J.**
Upper surface blowing noise of the NASA-Ames quiet short-haul research aircraft
[AIAA PAPER 80-1064] p0026 A80-36002
- BONNER, W. A.**
The radioracemization of isovaline - Cosmochemical

- implications
p0086 A80-13018
- BONNET, R. E.
High-resolution Lyman-alpha filtergrams of the sun
p0075 A80-37277
- BORAH, J.
Optimal estimator model for human spatial orientation
p0093 A80-24265
- BORN, G. J.
A simulator study of control and display augmentations for helicopters
[NASA-CR-163451]
p0018 N80-31408
- BORUCKI, W. J.
Are solar spectral variations a drive for climatic change
p0042 A80-15488
- Nitrogen fertiliser and stratospheric ozone - Latitudinal effects
p0043 A80-18948
- Stratospheric ozone decrease due to chlorofluoromethane photolysis - Predictions of latitude dependence
p0049 A80-29762
- Comparison of the Nimbus-4 BUW ozone data with the Ames two-dimensional model
[NASA-TM-81207]
p0036 N80-24914
- BOSS, A. P.
Fragmentation in a rotating protostar - A comparison of two three-dimensional computer codes
p0053 A80-38432
- Protostellar formation in rotating interstellar clouds. III - Nonaxisymmetric collapse
p0054 A80-39375
- BOUSHAM, W. G.
An experimental investigation of the effects of aeroelastic couplings on aeromechanical stability of a hingeless rotor helicopter
[AD-A085819]
p0101 N80-29294
- BOWLES, J. V.
Potential benefits for propfan technology on derivatives of future short- to medium-range transport aircraft
[AIAA PAPER 80-1090]
p0026 A80-38905
- BOXWELL, D. A.
Acoustically swept rotor
[NASA-CASE-ARC-11106-1]
p0102 N80-14107
- BRACCHI, F.
A microprocessor-based instrument for neural pulse wave analysis
p0098 A80-50322
- BRACE, L. H.
The location of the dayside ionopause of Venus - Pioneer Venus Orbiter magnetometer observations
p0076 A80-48811
- BRADEN, S.
Vorticity associated with multiple jets in a crossflow
[NASA-CR-162855]
p0016 N80-19454
- BRASSEUR, J. G.
On the combination of kinematics with flow visualization to compute total circulation - Application to vortex rings in a tube
[AIAA PAPER 80-1330]
p0065 A80-41563
- BRAUN, R. L.
Documentation of the analysis of the benefits and costs of aeronautical research and technology models, volume 1
[NASA-CR-152278]
p0001 N80-15865
- BRAY, R. S.
A head-up display format for application to transport aircraft approach and landing
[NASA-TM-81199]
p0012 N80-29295
- BREGHAN, J. D.
The infrared spectrum of the carbon star Y Canum Venaticorum between 1.2 and 30 microns
p0046 A80-22191
- BRENNAN, M. P.
Civil helicopter wire strike assessment study. Volume 1: Findings and recommendations
[NASA-CR-152389]
p0019 N80-33381
- BRIDGEMAN, J. O.
Numerical solution techniques for unsteady transonic aerodynamics problems
p0059 N80-33379
- BRINSON, H. P.
Time-temperature behavior of a unidirectional graphite/epoxy composite
p0078 A80-21141
- The viscoelastic behavior of a composite in a thermal environment
[NASA-CR-163187]
p0039 N80-24369
- The accelerated characterization of viscoelastic composite materials
[NASA-CR-163188]
p0039 N80-24370
- BRIZZE, K. E.
Motion sickness in the squirrel monkey
p0095 A80-25891
- BROCK, P. J.
Exercise training-induced hypervolemia - Role of plasma albumin, renin, and vasopressin
p0089 A80-32749
- Na+ and Ca2+ ingestion - Plasma volume-electrolyte distribution at rest and exercise
p0091 A80-41661
- Fluid-electrolyte shifts and thermoregulation - Rest and work in heat with head cooling
p0091 A80-48086
- BROCKETT, R. W.
Feedback invariants for nonlinear systems
p0031 A80-14810
- A scaling theory for linear systems
p0030 A80-32676
- BROD, L. G.
Pioneer Venus Sounder Probe Solar Flux Radiometer
p0073 A80-30846
- BROOKS, L. D.
Pioneer Venus Sounder Probe Neutral Gas Mass Spectrometer
p0073 A80-30844
- BROWN, D. E.
Eddy diffusion coefficients and the variance of the atmosphere 30-60 km
p0076 A80-45996
- BROWN, F. G.
The infrared radiometer on the sounder probe of the Pioneer Venus mission
p0050 A80-30847
- BROWN, R. M.
Texture extraction on the ILLIAC 4
[AD-A070523]
p0098 N80-19471
- BROWN, T. J.
Multicyclic control of a helicopter rotor considering the influence of vibration, loads, and control motion
[AIAA 80-0673]
p0025 A80-34998
- BROWN, W. A.
X-ray spectrometer spectrograph telescope system
p0077 A80-17502
- Paraboloidal X-ray telescope mirror for solar coronal spectroscopy
p0078 A80-17503
- High-resolution Lyman-alpha filtergrams of the sun
p0075 A80-37277
- BROWNEE, D. E.
Meteoroid ablation spheres from deep-sea sediments
p0046 A80-22948
- BROWNSON, J. J.
Aerodynamic interactions from reaction controls for lateral control of the M2-F2 lifting-body entry configuration at transonic and supersonic and supersonic Mach numbers
[NASA-TM-78534]
p0006 N80-11033
- BRUNER, E. C., JR.
X-ray spectrometer spectrograph telescope system
p0077 A80-17502
- Paraboloidal X-ray telescope mirror for solar coronal spectroscopy
p0078 A80-17503
- High-resolution Lyman-alpha filtergrams of the sun
p0075 A80-37277
- BRUNK, W. E.
An assessment of ground-based techniques for detecting other planetary systems. Volume 1: An overview
[NASA-CP-2124-VOL-1]
p0034 N80-18997
- An Assessment of Ground-Based Techniques for Detecting Other Planetary Systems. Volume 2: Position papers
[NASA-CP-2124-VOL-2]
p0034 N80-25224
- BRUZZONE, C.
Photocell heat engine solar power systems
p0079 A80-48179
- BUDINIKAS, P.
Design, fabrication and testing of a dual catalyst ammonia removal system for a urine VCD unit
[NASA-CR-152372]
p0085 N80-29023

- BUDIMINKAS, P.**
Water recovery by catalytic treatment of urine vapor
[ASME PAPER 80-ENAS-16] p0093 A80-43192
- BUELL, D. A.**
Overview of 6- X 6-foot wind tunnel aero-optics tests
p0023 N80-25590
- BUNCH, T. E.**
Carbonaceous chondrites. I - Characterization and significance of carbonaceous chondrite /CM/ xenoliths in the Jodzie howardite
p0086 A80-13013
Meteoroid ablation spheres from deep-sea sediments
p0046 A80-22948
Aqueous activity on asteroids - Evidence from carbonaceous meteorites
p0062 A80-24586
- BUNEHAN, O.**
Three-dimensional simulation of the free shear layer using the vortex-in-cell method
p0067 A80-49300
- BUNNELL, J. W., JR.**
Flying-qualities criteria for wings-level-turn maneuvering during an air-to-ground weapon delivery task
[AIAA 80-1628] p0029 A80-45916
- BURKE, J. R.**
An extended soft-cube model for the thermal accommodation of gas atoms on solid surfaces
[NASA-TM-81163] p0035 N80-14941
- BURKE, M. W.**
Multi-modal information processing for visual workload relief
[NASA-CR-162720] p0100 N80-16737
- BURNS, J. A.**
On the 'thickness' of Saturn's rings caused by satellite and solar perturbations and by planetary precession
p0042 A80-14293
- BUTTS, A. J.**
An entry and landing probe for Titan
[AIAA PAPER 80-0117] p0060 A80-18384
- C**
- CAGLIOSTRO, D. E.**
Radiant panel tests on an epoxy/carbon fiber composite
[NASA-TM-81185] p0037 N80-32435
- CABELIER, I.**
An experimental study of the structure and acoustic field of a jet in a cross stream
[NASA-CR-162464] p0014 N80-15871
- CANFIELD, R. C.**
The implications of hydrogen emission line ratios in quasi-stellar objects
p0072 A80-27013
- CANN, C.**
Noninvasive measures of bone bending rigidity in the monkey /M. nemestrina/
p0088 A80-21988
- CAPONE, L. A.**
Nitrogen fertiliser and stratospheric ozone - Latitudinal effects
p0043 A80-18948
Stratospheric ozone decrease due to chlorofluoromethane photolysis - Predictions of latitude dependence
p0049 A80-29762
- CARD, D. H.**
Issues arising from the demonstration of Landsat-based technologies to inventories and mapping of the forest resources of the Pacific Northwest states
p0065 A80-41305
- CARDEN, J. L.**
Guiding the development of a controlled ecological life support system
[NASA-CR-162452] p0085 N80-12735
- CAREN, L. D.**
Effect of simulated weightlessness on the immune system in rats
p0088 A80-25894
- CARLE, G. C.**
Pioneer Venus Sounder Probe gas chromatograph
p0089 A80-30845
Corrections in the Pioneer Venus sounder probe gas chromatographic analysis of the lower Venus atmosphere
p0089 A80-30875
- CARLSON, R. W.**
Ultraviolet photometer observations of the Saturnian system
p0070 A80-19122
- CARLSON, W. C. A.**
The 60-MW Shuttle interaction heating facility
p0059 A80-12603
- CARNEY, G. D.**
SCF and CI calculations of the dipole moment function of ozone
p0043 A80-17111
- CARE, L. W.**
Dynamic stall on advanced airfoil sections
[AD-A085809] p0101 N80-29252
- CARE, M. H.**
Volcanic features of Hawaii. A basis for comparison with Mars
[NASA-SP-403] p0034 N80-23912
- CARROLL, P. C.**
An entry and landing probe for Titan
[AIAA PAPER 80-0117] p0060 A80-18384
- CARSON, T. M.**
A closed-form solution for noise contours
[NASA-TP-1432] p0004 N80-11869
- CARTER, T. D.**
Investigation of ground effects on large and small scale models of a three fan V/STOL aircraft configuration
[NASA-CR-152240] p0015 N80-16030
- CASE, D. A.**
Relativistic scattered wave calculations on UF6
p0049 A80-30458
- CASEY, C. J.**
Toxicity of pyrolysis gases from foam plastics
p0071 A80-24625
- CASSAR, L.**
Far infrared, near infrared, and radio molecular line studies of HFE 2, HFE 3, and FJM 6
p0068 A80-11489
- CASSEN, P.**
Core cooling by subsolidus mantle convection
p0044 A80-19391
On the comparative evolution of Ganymede and Callisto
p0048 A80-28080
Whole planet cooling and the radiogenic heat source contents of the earth and moon
p0053 A80-36651
Tidal dissipation, orbital evolution, and the nature of Saturn's inner satellites
p0058 A80-53235
- CASTLEMAN, A. W., JR.**
A reconsideration of nucleation phenomena in light of recent findings concerning the properties of small clusters, and a brief review of some other particle growth processes
p0069 A80-15609
The properties of clusters in the gas phase. IV - Complexes of H2O and HNOx clustering on NOx/-/
p0046 A80-23322
New gas phase inorganic ion cluster species and their atmospheric implications
p0075 A80-37510
Properties of clusters in the gas phase. V - Complexes of neutral molecules onto negative ions
p0057 A80-50144
- CASTRO, A. J.**
Comet nucleus impact probe feasibility study
[NASA-CR-152375] p0040 N80-26364
Titan probe technology assessment and technology development plan study
[NASA-CR-152381] p0040 N80-32417
- CHACKERIAN, C., JR.**
Integrated band intensities of gaseous N2/O/5/
p0047 A80-25660
Ground-state rotational constants of /C-13/H3D
p0054 A80-41175
Vibration-rotation line shifts for 1 sigma g + H2/V,J/-15/0/ He computed via close coupling - Temperature dependence
p0058 A80-51965
- CHANG, C.**
Computational study of alkali-metal-noble gas collisions in the presence of nonresonant lasers - Na + Xe + h/2/pi/omega sub 1 + h/2/pi/omega sub 2 system
p0056 A80-48762

- CHANG, C. H.
Na + Xe collisions in the presence of two
nonresonant lasers p0051 A80-32416
- CHANG, I.-D.
On the combination of kinematics with flow
visualization to compute total circulation -
Application to vortex rings in a tube
[AIAA PAPER 80-1330] p0065 A80-41563
- CHANG, S.
Carbonaceous chondrites. I - Characterization and
significance of carbonaceous chondrite /CM/
xenoliths in the Jodzie howardite p0086 A80-13013
- Organic chemistry on Titan p0087 A80-20340
- Noble gas trapping and fractionation during
synthesis of carbonaceous matter p0093 A80-23669
- Comets: Cosmic connections with carbonaceous
meteorites, interstellar molecules and the
origin of life p0092 N80-11975
- Modified Iterative Extended Hueckel. 2:
Application to the interaction of Na(+),
Na(+) (aq.), Mg(+)-2(aq.) with adenine and thymine
[NASA-TM-81201] p0084 N80-25109
- CHAPMAN, G. T.
Test section configuration for aerodynamic testing
in shock tubes p0026 A80-38085
- CHASE, R. C.
Quest for ultrahigh resolution in X-ray optics
p0032 A80-17480
- CHATTOT, J. J.
Calculation of three-dimensional unsteady
transonic flows past helicopter blades
[NASA-TP-1721] p0100 N80-33356
- CHAUSSEE, D. S.
A diagonal form of an implicit
approximate-factorization algorithm with
application to a two dimensional inlet
[AIAA PAPER 80-0067] p0061 A80-19274
- Computation of supersonic turbulent flows over an
inclined ogive-cylinder-flare
[AIAA PAPER 80-1410] p0066 A80-41608
- CHEN, R. T. W.
Effects of primary rotor parameters on flapping
dynamics [NASA-TP-1431] p0005 N80-15138
- Effects of rotor parameter variations on handling
qualities of unaugmented helicopters in
simulated terrain flight
[NASA-TM-81190] p0012 N80-31407
- CHEWETTE, D. L.
Saturnian trapped radiation and its absorption by
satellites and rings - The first results from
Pioneer 11 p0070 A80-19118
- The propagation of Jovian electrons to earth
p0074 A80-36356
- CHENG, H. K.
Transonic swept-wing analysis using asymptotic and
other numerical methods
[AIAA PAPER 80-0342] p0024 A80-22751
- Analysis of transonic swept wings using asymptotic
and other numerical methods
[NASA-TM-80762] p0011 N80-29255
- CHIENG, C. C.
On the calculation of turbulent heat transport
downstream from an abrupt pipe expansion
p0076 A80-49037
- CHINA, R. V.
An implicit finite-difference code for inviscid
and viscous cascade flow
[AIAA PAPER 80-1427] p0066 A80-44128
- CHOPRA, I.
Measurements of control stability characteristics
of a wind-tunnel model using a transfer function
method
[AIAA 80-0457] p0024 A80-26957
- CHOU, R. C.
Feasibility and concept study to convert the
NASA/AMES vertical motion simulator to a
helicopter simulator
[NASA-CR-152193] p0098 N80-16070
- CHOW, R.
Transonic swept-wing analysis using asymptotic and
other numerical methods [AIAA PAPER 80-0342] p0024 A80-22751
- Analysis of transonic swept wings using asymptotic
and other numerical methods
[NASA-TM-80762] p0011 N80-29255
- CHRISTENSEN, W. W.
Chelate-modified polymers for atmospheric gas
chromatography
[NASA-CASE-ARC-11154-1] p0097 N80-23383
- CHRISTIANSEN, W.
Photocell heat engine solar power systems
p0079 A80-48179
- CHURMS, J.
The radius and ellipticity of Uranus from its
occultation of SAO 158687 p0073 A80-31937
- CLARK, B.
Thresholds for detection of constant rotary
acceleration during vibratory rotary acceleration
p0091 A80-42003
- CLARK, B. C.
Heterogeneous phase reactions of Martian volatiles
with putative regolith minerals p0090 A80-36062
- CLARK, D. C.
Bosch - An alternate CO₂ reduction technology
[ASME PAPER 79-ENAS-32] p0092 A80-15256
- CLARK, T.
A high-sensitivity search for extraterrestrial
intelligence at lambda 18 cm p0090 A80-37933
- CLEARY, J. W.
Asymmetric trailing-edge flows at high Reynolds
number
[AIAA PAPER 80-1396] p0066 A80-44151
- CLEMENT, W. F.
The analysis of delays in simulator digital
computing systems. Volume 2: Formulation of
discrete state transition matrices, an
alternative procedure for multirate digital
computations
[NASA-CR-152341] p0015 N80-18722
- CLEMENTS, L. L.
Influence of quality control variables on failure
of graphite/epoxy under extreme moisture
conditions
[NASA-TM-81246] p0038 N80-33493
- COAKLEY, T. J.
Experimental and computational study of transonic
flow about swept wings
[AIAA PAPER 80-0005] p0060 A80-18235
- COCHRANE, J. A.
Conceptual studies of a long-range transport with
an upper surface blowing propulsive lift system
[NASA-TM-81196] p0009 N80-23249
- COHEN, A.
Asymptotic behavior of the efficiencies in Mie
scattering p0031 A80-47048
- COHEN, M.
Red and nebulous objects in dark clouds - A survey
p0044 A80-20662
- High-frequency continuum observations of young stars
p0047 A80-25365
- An optical emission-line phase of the extreme
carbon star IRC +30219 p0056 A80-44993
- Discovery of optical molecular emission from the
bipolar nebula surrounding HD 44179 p0058 A80-52399
- COLBURN, D. S.
Saturn's magnetic field and magnetosphere
p0021 A80-19117
- COLE, K.
Analysis of two-dimensional incompressible flows
by a subsurface panel method p0029 A80-30566
- COLEMAN, P. J., JR.
Saturn's magnetic field and magnetosphere
p0021 A80-19117
- COLLARD, H. R.
Preliminary results on the plasma environment of
Saturn from the Pioneer 11 plasma analyzer
experiment p0043 A80-19116
- COLWELL, R. E.
Irrigated lands assessment for water management
Applications Pilot Test (APT)
[E80-10324] p0019 N80-32815

- CONLON, J.
A comparison of calculated and experimental lift and pressure distributions for several helicopter rotor sections
[NASA-TM-81160] p0007 N80-16036
- CONVERTINO, V. A.
Plasma volume during stress in man - Osmolality and red cell volume p0087 A80-13506
Role of thermal and exercise factors in the mechanism of hypervolemia p0089 A80-32748
Exercise training-induced hypervolemia - Role of plasma albumin, renin, and vasopressin p0089 A80-32749
- COOK, W. J.
Test section configuration for aerodynamic testing in shock tubes p0026 A80-38085
- COONEY, J. A.
Asymptotic behavior of the efficiencies in Mie scattering p0031 A80-47048
- COOPER, G. E.
Resource management on the flight deck [NASA-CP-2120] p0082 N80-22283
- CORBETT, R.
Retinal changes in rats flown on Cosmos 936 - A cosmic ray experiment p0091 A80-41995
- CORLISS, L. D.
V/STOLAND avionics system flight-test data on a UH-1H helicopter [NASA-TM-78591] p0008 N80-18047
- CORSIGLIA, V. E.
Study of cooling air inlet and exit geometries for horizontally opposed piston aircraft engines [AIAA PAPER 80-1242] p0027 A80-38984
Effect of propeller slipstream on the drag and performance of the engine cooling system for a general aviation twin-engine aircraft [AIAA PAPER 80-1872] p0027 A80-43315
- COURT, B.
Three-dimensional simulation of the free shear layer using the vortex-in-cell method p0067 A80-49300
- COUSSENS, T. G.
Application of advanced technologies to small, short-haul transport aircraft [NASA-CR-152363] p0018 N80-32353
- COVERSTON, C.
Application of advanced technologies to small, short-haul air transports [NASA-CR-152364] p0019 N80-33396
- CRAIG, R. A.
Measurements of NO, O₃, and temperature at 19.8 km during the total solar eclipse of 26 February 1979 p0055 A80-43638
Reduction of nitric oxide emissions from a combustor [NASA-CASE-ARC-10814-2] p0080 N80-26298
- CRAMER, M. S.
Lifting three-dimensional wings in transonic flow p0071 A80-20331
- CRANE, D. F.
Aircraft simulation data management - A prototype system p0029 A80-49832
- CRAVENS, T. E.
A model of the neutral and ion nitrogen chemistry in the daytime thermosphere of Venus p0067 A80-10460
Hot hydrogen in the exosphere of Venus p0070 A80-18943
- CREEDON, J.
Studies for improved high temperature coatings for Space Shuttle application p0079 A80-34757
Development of high viscosity coatings for advanced Space Shuttle applications p0079 A80-34760
- CROSSMAN, F. W.
Hygrothermal damage mechanisms in graphite-epoxy composites [NASA-CR-3189] p0038 N80-13170
- CROWNOVER, J. C.
Simulated weightlessness - Effects on bioenergetic balance p0095 A80-21544
- CRUIKSHANK, D. P.
The surface and atmosphere of Pluto p0045 A80-21757
- CUMMING, H. J.
Toxicity of pyrolysis gases from foam plastics p0071 A80-24625
- CUNNOLD, D. M.
Preliminary calculations concerning the maintenance of the zonal mean ozone distribution in the Northern Hemisphere p0074 A80-34445
- CURRY, E. E.
Optimal estimator model for human spatial orientation p0093 A80-24265
Flight-deck automation: Promises and problems [NASA-TM-81206] p0084 A80-26040
- CURTISS, L. A.
SCF and CI calculations of the dipole moment function of ozone p0043 A80-17111
- CUZZI, J.
A high-sensitivity search for extraterrestrial intelligence at lambda 18 cm p0090 A80-37933
- CUZZI, J. M.
On the 'thickness' of Saturn's rings caused by satellite and solar perturbations and by planetary precession p0042 A80-14293
An entry and landing probe for Titan [AIAA PAPER 80-0117] p0060 A80-18384
Saturn's rings - 3-mm observations and derived properties p0045 A80-21758
Scattering by non-spherical particles of size comparable to a wavelength - A new semi-empirical theory p0063 A80-34050
Scattering by nonspherical particles of size comparable to wavelength - A new semi-empirical theory and its application to tropospheric aerosols p0052 A80-36040
- D**
- DAILY, W. D.
Theories for the origin of lunar magnetism p0044 A80-19397
Electrical conductivity anomalies associated with circular lunar maria p0061 A80-23691
- DANDREA, J. A.
Part-body and multibody effects on absorption of radio-frequency electromagnetic energy by animals and by models of man p0071 A80-22987
- DANIELSON, E. F.
High resolution vertical profiles of wind, temperature and humidity obtained by computer processing and digital filtering of radiosonde and radar tracking data from the ITCZ experiment of 1977 [NASA-CR-3269] p0039 N80-21926
- DANNENBERG, R. E.
Transient solution for megajoule energy release in a lumped-parameter series RLC circuit p0051 A80-32826
'GAIM' - Gas-addition, impedance-matched arc driver p0064 A80-38131
- DANT, C. C.
NASA-Ames Life Sciences Flight Experiments program - 1980 status report [ASME PAPER 80-ENAS-34] p0094 A80-43209
- DASH, R.
Strouhal number influence on flight effects on jet noise radiated from convecting quadrupoles p0022 A80-28418
- DAUGHERTY, J. C.
Wind-tunnel/flight correlation study of aerodynamic characteristics of a large flexible supersonic cruise airplane (CXB-70-1). 1: Wind-tunnel tests of a 0.03-scale model at Mach numbers from 0.6 to 2.53 [NASA-TP-1514] p0004 N80-11068
- DAVIDSON, E. R.
An ab initio calculation of the zero-field splitting parameters of the 3A-double prime

- state of formaldehyde
p0056 A80-45333
- DAVIES, E. G.
Feasibility and concept study to convert the NASA/AMES vertical motion simulator to a helicopter simulator
[NASA-CR-152193] p0098 N80-16070
- DAVIS, J. M.
Quest for ultrahigh resolution in X-ray optics
p0032 A80-17480
A real-time electronic imaging system for solar X-ray observations from sounding rockets
p0029 A80-18545
X-ray bright points and the solar cycle dependence of emerging magnetic flux
p0077 N80-17950
- DAVIS, L., JR.
Saturn's magnetic field and magnetosphere
p0021 A80-19117
- DAVIS, S. S.
Computer/experiment integration for unsteady aerodynamic research
p0025 A80-29501
Unsteady aerodynamics of conventional and supercritical airfoils
[AIAA 80-0734] p0026 A80-35038
Experimental studies of scale effects on oscillating airfoils at transonic speeds
[NASA-TM-81216] p0010 N80-27287
Experimental unsteady aerodynamics of conventional and supercritical airfoils
[NASA-TM-81221] p0012 N80-33345
- DAVIS, T. P.
A model for hypokinesia: Effects on muscle atrophy in the rat
p0095 A80-28188
- DAVY, W. C.
Forebody and base region real-gas flow in severe planetary entry by a factored implicit numerical method. I - Computational fluid dynamics
[AIAA PAPER 80-0065] p0061 A80-22731
Galileo probe forebody entry thermal protection - Aerothermal environments and heat shielding requirements
[ASME PAPER 80-ENAS-24] p0066 A80-43200
- DAYHOFF, D.
Retinal changes in rats flown on Cosmos 936 - A cosmic ray experiment
p0091 A80-41995
- DE PATER, I.
21 cm maps of Jupiter's radiation belts from all rotational aspects
p0076 A80-48877
- DE VRIES, P. L.
Na + Xe collisions in the presence of two nonresonant lasers
p0051 A80-32416
- DEAVERS, D. R.
A model for hypokinesia: Effects on muscle atrophy in the rat
p0095 A80-28188
- DEBELL, A. G.
Pioneer Venus Sounder Probe Solar Flux Radiometer
p0073 A80-30846
- DECAMPLI, W. M.
Calculations of the evolution of the giant planets
p0049 A80-28086
- DECAUDIN, M.
High-resolution Lyman-alpha filtergrams of the sun
p0075 A80-37277
- DEFFENBAUGH, F. D.
A three dimensional vortex wake model for missiles at high angles on attack
[NASA-CR-3208] p0014 N80-14048
- DEINERT, G. S.
Numerical simulation of three-dimensional boattail afterbody flow fields
[AIAA PAPER 80-1347] p0066 A80-44132
- DENNY, R. E.
Documentation of the analysis of the benefits and costs of aeronautical research and technology models, volume 1
[NASA-CR-152278] p0001 N80-15865
- DENZ, E. A.
Effect of field of view and monocular viewing on angular size judgements in an outdoor scene
[NASA-TM-81176] p0083 N80-19792
- DEROSE, C. F.
Shape change of Galileo probe models in free-flight tests
[NASA-TM-81209] p0037 N80-27418
- DESHARAI, D. J.
The carbon isotope biogeochemistry of the individual hydrocarbons in bat guano and the ecology of insectivorous bats in the region of Carlsbad, New Mexico
[NASA-TM-81164] p0083 N80-18680
- DEVINCENZI, D. L.
Mars ultraviolet simulation facility
p0089 A80-36061
- DEVRIES, P. L.
Quantum-mechanical calculation of three-dimensional atom-diatom collisions in the presence of intense laser radiation
p0068 A80-15221
An angular momentum approximation for molecular collisions in the presence of intense laser radiation
p0069 A80-15673
A new propagation method for the radial Schroedinger equation
p0069 A80-15768
Computational study of alkali-metal-noble gas collisions in the presence of nonresonant lasers - Na + Xe + $h/2\pi/\omega$ sub 1 + $h/2\pi/\omega$ sub 2 system
p0056 A80-48762
- DICKEY, R. E.
A technique for evaluating the Jovian entry-probe heat-shield material with a gasdynamic laser
p0063 A80-29479
- DICKINSON, J. T.
Changes induced on the surfaces of small Pd clusters by the thermal desorption of CO
p0053 A80-37179
- DIETERLY, D. L.
Theory of the decision/problem state
[NASA-TM-81192] p0103 N80-22984
Problem solving and decisionmaking: An integration
[NASA-TM-81191] p0103 N80-22985
Clarification process: Resolution of decision-problem conditions
[NASA-TM-81193] p0103 N80-23985
Decision-problem state analysis methodology
[NASA-TM-81194] p0103 N80-25002
Automation literature: A brief review and analysis
[NASA-TM-81245] p0103 N80-34097
- DODSON, J.
Galileo probe thermal protection: Entry heating environments and spallation experiments design
[NASA-CR-152334] p0038 N80-14184
- DOERING, D. L.
Changes induced on the surfaces of small Pd clusters by the thermal desorption of CO
p0053 A80-37179
- DOOSE, L. R.
Pioneer Venus Sounder Probe Solar Flux Radiometer
p0073 A80-30846
- DU VAL, R. W.
A new approach to active control of rotorcraft vibration
[AIAA 80-1778] p0027 A80-45556
- DUERKSEN, K. D.
Pioneer Venus Sounder Probe Neutral Gas Mass Spectrometer
p0073 A80-30844
- DUGAN, D. C.
V-STOLAND avionics system flight-test data on a UH-1H helicopter
[NASA-TM-78591] p0008 N80-18047
- DUGAN, D. D.
Effects of rotor parameter variations on handling qualities of unaugmented helicopters in simulated terrain flight
[NASA-TM-81190] p0012 N80-31407
- DUKES, T. A.
A simulator study of control and display augmentations for helicopters
[NASA-CR-163451] p0018 N80-31408
- DUNHAM, E.
The upper atmosphere of Uranus - Mean temperature and temperature variations
p0071 A80-22207
The radius and ellipticity of Uranus from its occultation of SAO 158687
p0073 A80-31937
- DUNKERTON, T.
A Lagrangian mean theory of wave, mean-flow

- interaction with applications to nonacceleration
and its breakdown p0075 A80-36473
- DURISEN, R. H.**
On the 'thickness' of Saturn's rings caused by
satellite and solar perturbations and by
planetary precession p0042 A80-14293
- DUSKIN, F.**
Release-rate calorimetry of multilayered materials
for aircraft seats p0051 A80-34223
Release-rate calorimetry of multilayered materials
for aircraft seats [AIAA 80-0759] p0064 A80-35052
- DUSTERBERRY, J. C.**
The development and use of large-motion simulator
systems in aeronautical research and development p0001 A80-10765
- DUSTO, A. R.**
An advanced panel method for analysis of arbitrary
configurations in unsteady subsonic flow [NASA-CR-152323] p0017 N80-26270
- DWEK, E.**
Excitation mechanisms for the unidentified
infrared emission features p0054 A80-40642
- DYAL, P.**
Saturn's magnetic field and magnetosphere p0021 A80-19117
Theories for the origin of lunar magnetism p0044 A80-19397
Electrical conductivity anomalies associated with
circular lunar maria p0061 A80-23691
- DYER, J. W.**
Pioneer Saturn p0043 A80-19114
- E**
- EBERSTEIN, I. J.**
Comparison of the Nimbus-4 BUV ozone data with the
Ames two-dimensional model [NASA-TM-81207] p0036 N80-24914
- ECKERT, W. T.**
An experimental investigation of two large annular
diffusers with swirling and distorted inflow [NASA-TP-1628] p0005 N80-17984
- ECONOMOS, A. C.**
Review of cell aging in Drosophila and mouse p0087 A80-17741
Favorable effects of the antioxidants sodium and
magnesium thiazolidine carboxylate on the
vitality and life span of Drosophila and mice p0089 A80-29085
- EDELSON, E. H.**
The possible role of metal ions and clays in
prebiotic chemistry p0094 A80-50060
- EGAN, W. G.**
High-resolution Martian atmosphere modeling p0071 A80-21765
- ELLENBOGEN, J. C.**
An ab initio calculation of the zero-field
splitting parameters of the 3A-double prime
state of formaldehyde p0056 A80-45333
- ELLIOT, J. L.**
The upper atmosphere of Uranus - Mean temperature
and temperature variations p0071 A80-22207
The radius and ellipticity of Uranus from its
occultation of SAO 158687 p0073 A80-31937
- ELLIS, S.**
Growth hormone control of glucose oxidation
pathways in hypophysectomized rats p0088 A80-24222
- ELLIS, S. R.**
Effect of field of view and monocular viewing on
angular size judgements in an outdoor scene [NASA-TM-81176] p0083 N80-19792
- ELPHIC, R. C.**
Position and shape of the Venus bow shock -
Pioneer Venus Orbiter observations p0087 A80-15295
A comparison of Pioneer Venus and Venera bow shock
observations - Evidence for a solar cycle variation p0069 A80-15296
- Initial Pioneer Venus magnetometer observations p0078 A80-23690
The location of the dayside ionopause of Venus -
Pioneer Venus Orbiter magnetometer observations p0076 A80-48811
The solar wind interaction with Venus p0076 N80-13561
- EPSTEIN, E. E.**
Saturn's rings - 3-mm observations and derived
properties p0045 A80-21758
- EPTON, H. A.**
An advanced panel method for analysis of arbitrary
configurations in unsteady subsonic flow [NASA-CR-152323] p0017 N80-26270
- ERICKSON, E. F.**
Airborne stellar spectrophotometry from 1.2 to 5.5
microns - Absolute calibration and spectra of
stars earlier than M3 p0043 A80-16407
Comparison of predicted and observed spectral
energy distribution of K and M stars. I - Alpha
Bootis p0046 A80-22194
The spectrum of IRC + 10216 from 2.0 to 8.5 microns p0056 A80-44965
Far-infrared spectra of W51-IRS 2 and W49 NW p0056 A80-44967
- ERZBERGER, H.**
Constrained optimum trajectories with specified
range p0021 A80-18538
Algorithm for fixed-range optimal trajectories
[NASA-TP-1565] p0006 N80-28329
- ESKER, D. W.**
Investigation of ground effects on large and small
scale models of a three fan V/STOL aircraft
configuration [NASA-CR-152240] p0015 N80-16030
- ESKOVITZ, A. J.**
Pioneer Venus sounder and small probes
Nephelometer instrument p0053 A80-36750
- ESTES, J. E.**
Use of collateral information to improve LANDSAT
classification accuracies [E80-10268] p0040 N80-29815
Irrigated lands assessment for water management
Applications Pilot Test (APT) [E80-10324] p0019 N80-32815
- ESTRELLA, C. A.**
Catalysts for polyimide foams from aromatic
isocyanates and aromatic dianhydrides [NASA-CASE-ARC-11107-1] p0080 N80-16116
- F**
- FALARSKI, M. D.**
Acoustic characteristics of two hybrid inlets at
forward speed [AIAA PAPER 79-0678] p0021 A80-20828
Static calibration of a two-dimensional wedge
nozzle with thrust vectoring and spanwise blowing [NASA-TM-81161] p0009 N80-23317
- FARLOW, M. H.**
Efficiency of aerosol collection on wires exposed
in the stratosphere [NASA-TM-81147] p0035 N80-11676
- FARRELL, P. V.**
Degradation of tensile and shear properties of
composites exposed to fire or high temperature p0072 A80-29697
- FEIERBERG, M. A.**
Spectroscopic evidence for two achondrite parent
bodies - Asteroids 349 Dembowska and 4 Vesta p0072 A80-26173
- FEINREICH, B.**
A comparison of flight and simulation data for
three automatic landing system control laws for
the Augmentor wing jet STOL research airplane [NASA-CR-152365] p0018 N80-32338
- FEISTEL, T. W.**
Large-scale wind-tunnel tests of inverting flaps
on a STOL utility aircraft model [NASA-TP-1696] p0005 N80-25318
- FELLER, D. D.**
Growth hormone control of glucose oxidation

- pathways in hypophysectomized rats p0088 A80-24222
- FERANDIN, J. A.**
Pioneer Venus Unified Abstract Data Library and
Quick Look Data Delivery System p0050 A80-30832
- FERNIGER, J. H.**
Tests of subgrid-scale models in strained turbulence
[AIAA PAPER 80-1339] p0065 A80-41569
- FEWELL, L. L.**
Flash-fire propensity and heat-release rate
studies of improved fire resistant materials p0042 A80-15201
- Release-rate calorimetry of multilayered materials
for aircraft seats p0051 A80-34223
- Release-rate calorimetry of multilayered materials
for aircraft seats p0064 A80-35052
- Fire-resistant materials for aircraft passenger
seat construction [NASA-TM-78617] p0035 N80-13255
- FILLIUS, W.**
The phase of the ten-hour modulation in the Jovian
magnetosphere /Pioneers 10 and 11/ p0067 A80-10526
- Trapped radiation belts of Saturn - First look p0070 A80-19121
- FINK, U.**
Spectroscopic evidence for two achondrite parent
bodies - Asteroids 349 Dembowska and 4 Vesta p0072 A80-26173
- FIORINDO, R. P.**
Hypergravity and estrogen effects on avian
anterior pituitary growth hormone and prolactin
levels p0094 A80-20447
- FISCHBEIN, W. L.**
High-resolution Martian atmosphere modeling p0071 A80-21765
- FISHER, J.**
Far infrared, near infrared, and radio molecular
line studies of HFE 2, HFE 3, and FJM 6 p0068 A80-11489
- FISH, R. H.**
A small-scale test for fiber release from carbon
composites p0062 A80-26881
- A small-scale test for fiber release from carbon
composites [NASA-TM-81179] p0036 N80-18105
- FISHER, D. F.**
A computational and experimental study of high
Reynolds number viscous/inviscid interaction
about a cone at high angle of attack [AIAA PAPER 80-1422] p0104 A80-44492
- FLAIG, K.**
Parametric study of modern airship productivity
[NASA-TM-81151] p0011 N80-28340
- FLEMING, J. E.**
Extremes of urine osmolality - Lack of effect on
red blood cell survival p0091 A80-46196
- FLORES, J.**
Organic chemistry on Titan p0087 A80-20340
- FLORES, J. J.**
The radioracemization of isovaline - Cosmochemical
implications p0086 A80-13018
- FOGARTY, W. G.**
Saturn's rings - 3-mm observations and derived
properties p0045 A80-21758
- FORREST, W. J.**
The infrared spectrum of the carbon star Y Canum
Venaticorum between 1.2 and 30 microns p0046 A80-22191
- 16-30 micron spectroscopy of Titan p0049 A80-29321
- The 16- to 38-micron spectrum of Callisto p0074 A80-35234
- FOX, L., III**
Using guided clustering techniques to analyze
Landsat data for mapping forest land cover in
northern California p0078 A80-25595
- FOX, S. C.**
Human acclimation and acclimatization to heat: A
compendium of research, 1968-1978 [NASA-TM-81181] p0085 N80-34056
- FRANK, L. A.**
Preliminary results on the plasma environment of
Saturn from the Pioneer 11 plasma analyzer
experiment p0043 A80-19116
- FRANKLIN, J. A.**
Flight evaluation of configuration management
system concepts during transition to the landing
approach for a powered-lift STOL aircraft
[NASA-TM-81146] p0008 N80-19127
- FRANKS, A.**
X-ray spectrometer spectrograph telescope system p0077 A80-17502
- Paraboloidal X-ray telescope mirror for solar
coronal spectroscopy p0078 A80-17503
- FRICK, U.**
Carbonaceous chondrites. I - Characterization and
significance of carbonaceous chondrite /CM/
xenoliths in the Jodzie howardite p0086 A80-13013
- Noble gas trapping and fractionation during
synthesis of carbonaceous matter p0093 A80-23669
- FRIEDMANN, P.**
Formulation of coupled rotor/fuselage equations of
motion p0021 A80-17717
- FROMME, J. A.**
Integral equations for flows in wind tunnels p0029 A80-21906
- Reformulation of Possio's kernel with application
to unsteady wind tunnel interference p0031 A80-43129
- FRYER, T. B.**
Induction powered biological radiosonde
[NASA-CASE-ARC-11120-1] p0099 N80-18691
- FUHS, A. E.**
Optimized laser turrets for minimum phase distortion
p0023 N80-25600
- FULLER, J.**
A new approach to active control of rotorcraft
vibration [AIAA 80-1778] p0027 A80-45556

G

- GAINES, S.**
Stratospheric ozone decrease due to
chlorofluoromethane photolysis - Predictions of
latitude dependence p0049 A80-29762
- GAINES, S. E.**
High resolution vertical profiles of wind,
temperature and humidity obtained by computer
processing and digital filtering of radiosonde
and radar tracking data from the ITCZ experiment
of 1977 [NASA-CR-3269] p0039 N80-21926
- GALANT, D. C.**
Acoustic resonances and sound scattering by a
shear layer [NASA-CR-166181] p0014 N80-15873
- GALLOWAY, T. L.**
Small Transport Aircraft Technology p0021 A80-21225
- GANDHI, O. P.**
Part-body and multibody effects on absorption of
radio-frequency electromagnetic energy by
animals and by models of man p0071 A80-22987
- GARLAND, D. B.**
Phase 1 wind tunnel tests of the J-97 powered,
external augmentor V/STOL model [NASA-CR-152255] p0017 N80-28303
- GAROPALINI, S. E.**
Studies for improved high temperature coatings for
Space Shuttle application p0079 A80-34757
- Development of high viscosity coatings for
advanced Space Shuttle applications p0079 A80-34760
- GATLEY, I.**
A far-infrared study of the reflection nebula NGC
2023 p0072 A80-26111

- Monoceros R2 - Par-infrared observations of a very young cluster
p0052 A80-35115
- GAULT, D. E.
Endogenic craters on basaltic lava flows - Size frequency distributions
p0061 A80-23727
- GEMMER, R. V.
Singlet oxygenation of 1,2-poly/1,4-hexadiene/s
p0045 A80-21991
- GEORGE, T. F.
F + H₂ collisions on two electronic potential energy surfaces - Quantum-mechanical study of the collinear reaction
p0068 A80-12012
Quantum-mechanical calculation of three-dimensional atom-diatom collisions in the presence of intense laser radiation
p0068 A80-15221
An angular momentum approximation for molecular collisions in the presence of intense laser radiation
p0069 A80-15673
Na + Xe collisions in the presence of two nonresonant lasers
p0051 A80-32416
Computational study of alkali-metal-noble gas collisions in the presence of nonresonant lasers - Na + Xe + h/2 π /omega sub 1 + h/2 π /omega sub 2 system
p0056 A80-48762
- GERASSIMENKO, M.
A real-time electronic imaging system for solar X-ray observations from sounding rockets
p0029 A80-18545
- GERBER, R. L.
Changes in body temperature and metabolic rate after injection of calcium into the caudal hypothalamus of the rabbit
p0093 A80-27078
- GERDES, R. H.
A pilot's assessment of helicopter handling-quality factors common to both agility and instrument flying tasks
[NASA-TM-81217]
p0011 N80-28341
Effects of rotor parameter variations on handling qualities of unaugmented helicopters in simulated terrain flight
[NASA-TM-81190]
p0012 N80-31407
- GERNER, A.
Photoexcitation and ionization in molecular oxygen - Theoretical studies of electronic transitions in the discrete and continuous spectral intervals
p0044 A80-20275
- GEVAERT, G.
A comparison of flight and simulation data for three automatic landing system control laws for the Augmentor wing jet STOL research airplane
[NASA-CR-152365]
p0018 N80-32338
- GIANTS, T. W.
Thermophysical and flammability characterization of phosphorylated epoxy adhesives
p0066 A80-48079
- GIERASCH, P. J.
The upper atmosphere of Uranus - Mean temperature and temperature variations
p0071 A80-22207
- GILLAND, J.
The infrared radiometer on the sounder probe of the Pioneer Venus mission
p0050 A80-30847
- GILSON, R. D.
Multi-modal information processing for visual workload relief
[NASA-CR-162720]
p0100 N80-16737
- GILWEE, W. J., JR.
Oxygen index tests of thermosetting resins
p0044 A80-21448
A small-scale test for fiber release from carbon composites
p0062 A80-26881
A small-scale test for fiber release from carbon composites
[NASA-TM-81179]
p0036 N80-18105
- GIULIANETTI, D. J.
Toward new small transports for commuter airlines
p0021 A80-21224
- GLIEBE, P. R.
Fan noise caused by the ingestion of anisotropic turbulence - A model based on axisymmetric turbulence theory
[AIAA PAPER 80-1021]
p0032 A80-35977
Analytical study of the effects of wind tunnel turbulence on turbofan rotor noise
[AIAA PAPER 80-1022]
p0033 A80-35978
Distortion-rotor interaction noise produced by a drooped inlet
[AIAA PAPER 80-1050]
p0033 A80-35994
Analytical study of the effects of wind tunnel turbulence on turbofan rotor noise
[NASA-CR-152359]
p0016 N80-23099
- GOEBEL, J. H.
The infrared spectrum of the carbon star Y Canum Venaticorum between 1.2 and 30 microns
p0046 A80-22191
The spectrum of IRC + 10216 from 2.0 to 8.5 microns
p0056 A80-44965
- GOERTZ, C. K.
Azimuthal magnetic field at Jupiter
p0076 A80-49185
- GOETTELMAN, R. C.
Infrared-temperature variability in a large agricultural field
[E80-10331]
p0038 N80-32822
- GOKA, T.
Model development for automatic guidance of a VTOL aircraft to a small aviation ship
[AIAA 80-1617]
p0028 A80-45907
- GOLBERG, H. A.
Integral equations for flows in wind tunnels
p0029 A80-21906
Reformulation of Possio's kernel with application to unsteady wind tunnel interference
p0031 A80-43129
- GOLD, P.
Analytical design and evaluation of an active control system for helicopter vibration reduction and gust response alleviation
[NASA-CR-152377]
p0017 N80-28369
- GOLDMAN, A.
Infrared methane spectra between 1120 per cm and 1800 per cm - A new atlas
p0042 A80-13143
A new atlas of infrared methane spectra between 1120 per cm and 1800 per cm
p0042 A80-15655
- GOLDSMITH, I. H.
Potential benefits for propfan technology on derivatives of future short- to medium-range transport aircraft
[AIAA PAPER 80-1090]
p0026 A80-38905
- GOLUB, H. A.
Singlet oxygenation of 1,2-poly/1,4-hexadiene/s
p0045 A80-21991
Plasma etching of poly/N,N'-p,p'-oxydiphenylene/pyromellitimide/ film and photo/thermal degradation of etched and unetched film
p0093 A80-24158
Photosensitized oxidation of unsaturated polymers
p0049 A80-29086
- GOMBOSI, T. L.
Hot hydrogen in the exosphere of Venus
p0070 A80-18943
- GOODY, R.
Simple Cassegrain scanning system for infrared astronomy
p0074 A80-34729
- GOERJIAN, P. H.
Implicit computations of unsteady transonic flow governed by the full-potential equation in conservation form
[AIAA PAPER 80-0150]
p0062 A80-23935
- GOORVITCH, D.
The infrared spectrum of the carbon star Y Canum Venaticorum between 1.2 and 30 microns
p0046 A80-22191
- GOVINDARAJ, K. S.
Implicit model following and parameter identification of unstable aircraft
p0022 A80-28019
- GOVINDARAJ, T.
Optimal control model predictions of system performance and attention allocation and their experimental validation in a display design study
p0095 A80-40899
- GRABOSKE, H. C., JR.
The effect of dense cores on the structure and

- evolution of Jupiter and Saturn p0056 A80-45812
- GREENLEY, R.**
Silt-clay aggregates on Mars p0041 A80-10366
- Endogenic craters on basaltic lava flows - Size frequency distributions p0061 A80-23727
- Plains and channels in the Lunae Planum-Chryse Planitia region of Mars p0047 A80-26358
- Mars - The north polar sand sea and related wind patterns p0047 A80-26370
- Threshold windspeeds for sand on Mars - Wind tunnel simulations p0048 A80-27391
- Volcanic features of Hawaii. A basis for comparison with Mars [NASA-SP-403] p0034 N80-23912
- GREEN, D. S.**
Workshop on Thrust Augmenting Ejectors [NASA-CP-2093] p0004 N80-10107
- GREEN, M. J.**
Forebody and base region real-gas flow in severe planetary entry by a factored implicit numerical method. I - Computational fluid dynamics [AIAA PAPER 80-0065] p0061 A80-22731
- GREENE, R. V.**
Proton movements in response to a light-driven electrogenic pump for sodium ions in Halobacterium halobium membranes p0087 A80-17686
- GREENLEAF, J. E.**
Plasma volume during stress in man - Osmolality and red cell volume p0087 A80-13506
- Exercise thermoregulation after 14 days of bed rest p0088 A80-25989
- Fluid shifts and endocrine responses during chair rest and water immersion in man p0088 A80-25990
- Role of thermal and exercise factors in the mechanism of hypervolemia p0089 A80-32748
- Exercise training-induced hypervolemia - Role of plasma albumin, renin, and vasopressin p0089 A80-32749
- Na⁺ and Ca²⁺ ingestion - Plasma volume-electrolyte distribution at rest and exercise p0091 A80-41661
- Fluid-electrolyte shifts and thermoregulation - Rest and work in heat with head cooling p0091 A80-48086
- Extracellular hyperosmolality and body temperature during physical exercise in dogs p0092 A80-54076
- Human acclimation and acclimatization to heat: A compendium of research, 1968-1978 [NASA-TM-81181] p0085 N80-34056
- GREGORY, T. J.**
Workshop on Aircraft Surface Representation for Aerodynamic Computation [NASA-TM-81170] p0008 N80-19025
- An acceptable role for computers in the aircraft design process p0023 N80-21246
- GRIFFITH, W. I.**
The viscoelastic behavior of a composite in a thermal environment [NASA-CR-163187] p0039 N80-24369
- The accelerated characterization of viscoelastic composite materials [NASA-CR-163188] p0039 N80-24370
- GROSS, E. H.**
Operational procedures for ground station operation: ATS-3 Hawaii-Ames satellite link experiment [NASA-TM-81155] p0035 N80-13333
- GROSS, K. P.**
Two-photon excitation of nitric oxide fluorescence as a temperature indicator in unsteady gas-dynamic processes [NASA-TM-81220] p0037 N80-32700
- GROSS, M.**
Radiant panel tests on an epoxy/carbon fiber composite [NASA-TM-81185] p0037 N80-32435

- GROSSKREUTZ, C. L.**
Saturn's magnetosphere, rings, and inner satellites p0070 A80-19119
- GROSSMAN, A. S.**
Calculations of the evolution of the giant planets p0049 A80-28086
- The effect of dense cores on the structure and evolution of Jupiter and Saturn p0056 A80-45812
- GUELACHVILI, G.**
Ground-state rotational constants of ¹³C-¹³H₃D p0054 A80-41175
- GUPTA, M. K.**
A new approach to active control of rotorcraft vibration [AIAA 80-1778] p0027 A80-45556

H

- HAAS, M. R.**
The dynamics and stability of radiatively driven gas clouds. I - Plane-parallel slabs p0042 A80-14058
- HAGMAN, M. J.**
Part-body and multibody effects on absorption of radio-frequency electromagnetic energy by animals and by models of man p0071 A80-22987
- HAHN, G. E.**
Vibration-rotation line shifts for 1 sigma g + H₂/V, J=15/0/ He computed via close coupling - Temperature dependence p0058 A80-51965
- HAINES, R. F.**
Head-up transition behavior of pilots during simulated low-visibility approaches [NASA-TP-1618] p0082 N80-26039
- HALICIOGLU, T.**
A calculation of the diffusion energies for adatoms on surfaces of F.C.C. metals p0068 A80-13534
- Effect of three-body interactions on the structure of small clusters p0057 A80-49383
- HALLICK, T. E.**
Bosch - An alternate CO₂ reduction technology [ASME PAPER 79-ENAS-32] p0092 A80-15256
- Performance characterization of a Bosch CO sub 2 reduction subsystem [NASA-CR-152342] p0085 N80-22987
- HAMERNESH, C. L.**
Ambient curing fire resistant foams p0063 A80-34790
- HAMILL, P.**
On the 'thickness' of Saturn's rings caused by satellite and solar perturbations and by planetary precession p0042 A80-14293
- OCS, stratospheric aerosols and climate p0044 A80-19741
- Stratospheric aerosol modification by supersonic transport and space shuttle operations - Climate implications p0047 A80-26088
- Stratospheric aerosol modification by supersonic transport operations with climate implications [NASA-RP-1058] p0034 N80-15726
- HANEY, H. P.**
Application of numerical optimization to the design of wings with specified pressure distributions [NASA-CR-3238] p0015 N80-16031
- HANJALIC, K.**
Multiple-time-scale concepts in turbulent transport modelling p0080 A80-49277
- HANNAN, M. J.**
Error detection and rectification in digital terrain models p0099 A80-27432
- Texture extraction on the ILLIAC 4 [AD-A070523] p0098 N80-19471
- HARDY, G.**
A summary of joint US-Canadian augmentor wing powered-lift STOL research programs at the Ames Research Center, NASA, 1975-1980 [NASA-TM-81215] p0011 N80-28373
- HARNETT, L. M.**
Pioneer Venus sounder and small probes

- Nephelometer instrument p0053 A80-36750
- HARRIS, M. J.**
Static calibration of a two-dimensional wedge nozzle with thrust vectoring and spanwise blowing [NASA-TM-81161] p0009 N80-23317
- HARRISON, D. R.**
Application of laser velocimetry to an unsteady transonic flow p0063 A80-29506
- HARRISON, G.**
Retinal changes in rats flown on Cosmos 936 - A cosmic ray experiment p0091 A80-41995
- HARVEY, P. M.**
A far-infrared study of the reflection nebula NGC 2023 p0072 A80-26111
Two micron spectroscopy and 2.7 mm CO line observations of V645 Cygni p0074 A80-35114
Monoceros R2 - Far-infrared observations of a very young cluster p0052 A80-35115
- HASSIG, R. E.**
The infrared radiometer on the sounder probe of the Pioneer Venus mission p0050 A80-30847
- HAYES, J. M.**
The carbon isotope biogeochemistry of the individual hydrocarbons in bat guano and the ecology of insectivorous bats in the region of Carlsbad, New Mexico [NASA-TM-81164] p0083 N80-18680
- HEALY, T. J.**
On the design of a postprocessor for a search for extraterrestrial intelligence /SETI/ system [IAF PAPER 79-A-39] p0093 A80-19895
- HEFFLEY, R. K.**
A compilation and analysis of helicopter handling qualities data. Volume 1: Data compilation [NASA-CR-3144] p0013 N80-11097
The analysis of delays in simulator digital computing systems. Volume 1: Formulation of an analysis approach using a central example simulator model [NASA-CR-152340] p0015 N80-17722
- HEIDERER, R.**
Aldocyanoin microspheres - Partial amino acid analysis of the microparticulates formed from simple reactants under various conditions p0086 A80-11473
- HEIMBUCH, A. H.**
Chemical research projects office: An overview and bibliography, 1975-1980 [NASA-TM-81227] p0037 N80-31473
- HEIN, D. M.**
Conditional replenishment using motion prediction p0065 A80-39715
- HEINEMANN, K.**
Direct /TEM/ observation of the catalytic oxidation of amorphous carbon by Pd particles p0053 A80-37180
- HENDERSON, E.**
Simulation of the Infrared Astronomical Satellite /IRAS/ telescope system p0067 A80-49842
- HEPPNER, D. B.**
Bosch - An alternate CO2 reduction technology [ASME PAPER 79-ENAS-32] p0092 A80-15256
Development of the electrochemically regenerable carbon dioxide absorber for portable life support system application [ASME PAPER 79-ENAS-33] p0092 A80-15257
Development of a nitrogen generation system [NASA-CR-152333] p0085 N80-19800
Performance characterization of a Bosch CO sub 2 reduction subsystem [NASA-CR-152342] p0085 N80-22987
- HERMANN, R.**
System theory as applied differential geometry [NASA-CR-3209] p0013 N80-12776
- HESS, R. A.**
A pilot modeling technique for handling-qualities research [AIAA 80-1624] p0028 A80-45912
- HICKS, R. M.**
An experimental evaluation of a helicopter rotor section designed by numerical optimization [NASA-TM-78622] p0009 N80-21287
- HIGUCHI, H.**
Skin friction measurements by a new nonintrusive double-laser-beam oil viscosity balance technique [AIAA PAPER 80-1373] p0065 A80-41587
- HILADO, C. J.**
Toxicity of pyrolysis gases from foam plastics p0071 A80-24625
- HILDEBRAND, R. H.**
The evolution of rapid oscillations in an outburst of a dwarf nova p0075 A80-45227
- HILGEMAN, T.**
High-resolution Martian atmosphere modeling p0071 A80-21765
- HILL, W. G., JR.**
VTOL in-ground effect flows for closely spaced jets [AIAA PAPER 80-1880] p0033 A80-46693
- HILZINGER, J. B.**
Analysis and correlation of test data from an advanced technology rotor system [NASA-CR-152366] p0019 N80-33351
- HINDSON, W. S.**
A summary of joint US-Canadian augmentor wing powered-lift STOL research programs at the Ames Research Center, NASA, 1975-1980 [NASA-TM-81215] p0011 N80-28373
- HIPSCHILD, R. S.**
High resolution vertical profiles of wind, temperature and humidity obtained by computer processing and digital filtering of radiosonde and radar tracking data from the ITCZ experiment of 1977 [NASA-CR-3269] p0039 N80-21926
- HOCHSTEIN, L. I.**
The intracellular Na⁺/ and K⁺/ composition of the moderately halophilic bacterium, Paracoccus halodenitrificans p0091 A80-41250
- HODGE, P. W.**
Meteoroid ablation spheres from deep-sea sediments p0046 A80-22948
- HODGES, D. H.**
On the nonlinear deformation geometry of Euler-Bernoulli beams [NASA-TP-1566] p0101 N80-20619
Stability of nonuniform rotor blades in hover using a mixed formulation [NASA-TM-81226] p0012 N80-33777
- HODGES, R. R., JR.**
Pioneer Venus Sounder Probe Neutral Gas Mass Spectrometer p0073 A80-30844
- HOFFMAN, J. H.**
Pioneer Venus Sounder Probe Neutral Gas Mass Spectrometer p0073 A80-30844
- HOFFMANN, J. A.**
Effects of free-stream turbulence on diffuser performance [NASA-CR-163194] p0017 N80-24264
- HOFMANN, L. G.**
Practical optimal flight control system design for helicopter aircraft. Volume 1: Technical Report [NASA-CR-3275] p0017 N80-23328
- HOGENSON, P. A.**
Ambient curing fire resistant foams p0063 A80-34790
- HOGO, H.**
Introductory study of the chemical behavior of jet emissions in photochemical smog [NASA-CR-152345] p0016 N80-21891
- HOLLENBACH, D.**
Molecule formation and infrared emission in fast interstellar shocks. I Physical processes p0043 A80-16410
- HOLLENBACH, D. J.**
An extended soft-cube model for the thermal accommodation of gas atoms on solid surfaces [NASA-TM-81163] p0035 N80-14941
- HOLMES, A.**
Pioneer Venus Sounder Probe Solar Flux Radiometer p0073 A80-30846
Narrow-field radiometry in a quasi-isotropic atmosphere p0079 A80-40233
- HOLTON, J. R.**
Wave propagation and transport in the middle atmosphere

- A numerical model of the zonal mean circulation of the middle atmosphere p0072 A80-26437
- HOPKINS, R. A. p0073 A80-34443
Design of a one-year lifetime, spaceborne superfluid helium dewar [ASME PAPER 79-ENAS-23] p0077 A80-15247
- HORD, R. M.
The suitability of the ILLIAC IV architecture for image processing p0098 A80-22382
- HORSTMAN, C. C.
An experimental and numerical investigation of a three-dimensional shock wave separated turbulent boundary layer [AIAA PAPER 80-0002] p0061 A80-22727
Asymmetric trailing-edge flows at high Reynolds number [AIAA PAPER 80-1396] p0066 A80-44151
A comprehensive comparison between experiment and prediction for a transonic turbulent separated flow [AIAA PAPER 80-1407] p0027 A80-44154
- HORWOOD, D. F.
Pioneer Venus Orbiter Radar Mapper - Design and operation p0050 A80-30833
- HOUCK, J. R.
The infrared spectrum of the carbon star Y Canum Venaticorum between 1.2 and 30 microns p0046 A80-22191
16-30 micron spectroscopy of Titan p0049 A80-29321
The 16- to 38-micron spectrum of Callisto p0074 A80-35234
- HOUGHEN, J. T.
Recommended conventions for defining transition moments and intensity factors in diatomic molecular spectra p0055 A80-41323
- HOVERSON, S.
Photocell heat engine solar power systems p0079 A80-48179
- HOWARD, W. H.
Noninvasive measures of bone bending rigidity in the monkey *M. nemestrina*/ p0088 A80-21988
- HOWE, J. T.
Analysis of coastal upwelling and the production of a biomass [NASA-TM-78614] p0035 N80-12720
- HOWE, R. M.
Math modeling and computer mechanization for real time simulation of rotary-wing aircraft [NASA-CR-162400] p0013 N80-10137
- HSU, H. S.
Plasma etching of poly(N,N'-p,p'-oxydiphenylene/pyromellitimide/ film and photo/thermal degradation of etched and unetched film p0093 A80-24158
- HSU, H. T.
Radiant panel tests on an epoxy/carbon fiber composite [NASA-TM-81185] p0037 N80-32435
- HSU, H.-T.
Thermophysical and flammability characterization of phosphorylated epoxy adhesives p0066 A80-48079
- HUANG, J.-K.
Visually induced self-motion sensation adapts rapidly to left-right visual reversal p0096 A80-44213
- HUNG, C. M.
Computation of supersonic turbulent flows over an inclined ogive-cylinder-flare [AIAA PAPER 80-1410] p0066 A80-41608
- HUNT, B. L.
Top inlet system feasibility for transonic-supersonic fighter aircraft applications [AIAA PAPER 80-1809] p0033 A80-45735
- HUNT, G. E.
Measurements of wind vectors, eddy momentum transports, and energy conversions in Jupiter's atmosphere from Voyager 1 images A80-24159
- HUNTEN, D. M.
Smoke and dust particles of meteoric origin in the mesosphere and stratosphere p0055 A80-42744
- HUNTLEY, J. M.
Gas dynamics in barred spirals - Gaseous density waves and galactic shocks p0041 A80-10685
Self-gravitating gas flow in barred spiral galaxies p0055 A80-44959
- HUSS, G. R.
Heterogeneous phase reactions of Martian volatiles with putative regolith minerals p0090 A80-36062
- HUSSAINI, M. Y.
Numerical experiments in boundary-layer stability [AIAA PAPER 80-0275] p0062 A80-23957
Asymptotic features of shock-wave boundary-layer interaction p0055 A80-43135
- INDENGAND, R. F.
Dynamic stall on advanced airfoil sections [AD-A085809] p0101 N80-29252
- INGERSOLL, A. P.
Measurements of wind vectors, eddy momentum transports, and energy conversions in Jupiter's atmosphere from Voyager 1 images A80-24159
- INNIS, R. C.
Flight evaluation of configuration management system concepts during transition to the landing approach for a powered-lift STOL aircraft [NASA-TM-81146] p0008 N80-19127
- INTRILIGATOR, D. S.
Position and Shape of the Venus bow shock - Pioneer Venus Orbiter observations p0087 A80-15295
Preliminary results on the plasma environment of Saturn from the Pioneer 11 plasma analyzer experiment p0043 A80-19116
The Pioneer Venus Orbiter plasma analyzer experiment p0050 A80-30836
- IP, W. H.
Trapped radiation belts of Saturn - First look p0070 A80-19121
- ITO, T. I.
Study of crosslinking and degradation mechanisms in sealant polymer candidates [NASA-CR-152346] p0039 N80-22484
- IVERSEN, J.
Threshold windspeeds for sand on Mars - Wind tunnel simulations p0048 A80-27391
- JAGACINSKI, M. J.
Multi-modal information processing for visual workload relief [NASA-CR-162720] p0100 N80-16737
- JAGO, S.
The effect of viewing time, time to encounter, and practice on perception of aircraft separation on a cockpit display of traffic information [NASA-TM-81173] p0083 N80-18038
Perception of aircraft separation with pilot-preferred symbology on a cockpit display of traffic information [NASA-TM-81172] p0084 N80-31397
- JAGOW, R. B.
The development of a Space Shuttle Research Animal Holding Facility [ASME PAPER 80-ENAS-39] p0096 A80-43213
- JAHNKE, L.
Oxygen as a factor in eukaryote evolution - Some effects of low levels of oxygen on *Saccharomyces cerevisiae* p0086 A80-12229
- JANSSEN, M. A.
Saturn's rings - 3-mm observations and derived properties p0045 A80-21758
- JAYNES, D. M.
V/STOLAND avionics system flight-test data on a UH-1H helicopter [NASA-TM-78591] p0008 N80-18047

- JENKINS, R. C.**
VTOL in-ground effect flows for closely spaced jets
[AIAA PAPER 80-1880] p0033 A80-46693
- JEPSON, D.**
Analysis and correlation of test data from an advanced technology rotor system
[NASA-CR-152366] p0019 N80-33351
- JEWELL, W. F.**
A compilation and analysis of helicopter handling qualities data. Volume 1: Data compilation
[NASA-CR-3144] p0013 N80-11097
The analysis of delays in simulator digital computing systems. Volume 1: Formulation of an analysis approach using a central example simulator model
[NASA-CR-152340] p0015 N80-17722
The analysis of delays in simulator digital computing systems. Volume 2: Formulation of discrete state transition matrices, an alternative procedure for multirate digital computations
[NASA-CR-152341] p0015 N80-18722
- JOHANSEN, G.**
Optimal control model predictions of system performance and attention allocation and their experimental validation in a display design study
p0095 A80-40899
- JOHNSON, C. C.**
Plasma etching of poly(N,N'-p,p'-oxydiphenylene/pyromellitimide/ film and photo/thermal degradation of etched and unetched film
p0093 A80-24158
Reverse osmosis membrane of high urea rejection properties
[NASA-CASE-ARC-10980-1] p0097 N80-23452
- JOHNSON, D. A.**
Control of forebody vortex orientation to alleviate side forces
[AIAA PAPER 80-0183] p0024 A80-23955
Calculations of transonic flow about an airfoil in a wind tunnel
[AIAA PAPER 80-1366] p0027 A80-44142
A comprehensive comparison between experiment and prediction for a transonic turbulent separated flow
[AIAA PAPER 80-1407] p0027 A80-44154
Separated skin-friction measurements - Source of error: An assessment and elimination
[AIAA PAPER 80-1409] p0027 A80-44155
Unsteady density and velocity measurements in the 6 foot x 6 foot wind tunnel
p0023 N80-25594
- JOHNSON, F. T.**
A general panel method for the analysis and design of arbitrary configurations in incompressible flows
[NASA-CR-3079] p0017 N80-24268
- JOHNSON, J. E., JR.**
Review of cell aging in Drosophila and mouse
p0087 A80-17741
- JOHNSON, R. R.**
Application of numerical optimization to the design of wings with specified pressure distributions
[NASA-CR-3238] p0015 N80-16031
- JOHNSON, W.**
Comparison of calculated and measured model rotor loading and wake geometry
[NASA-TN-81189] p0009 N80-24262
A comprehensive analytical model of rotorcraft aerodynamics and dynamics. Part 1: Analysis development
[NASA-TN-81182] p0010 N80-28296
A comprehensive analytical model of rotorcraft aerodynamics and dynamics. Part 2: User's manual
[NASA-TN-81183] p0010 N80-28297
A comprehensive analytical model of rotorcraft aerodynamics and dynamics. Part 3: Program manual
[NASA-TN-81184] p0010 N80-28298
Comparison of calculated and measured blade loads on a full-scale tilting propeller in a wind tunnel
[NASA-TN-81228] p0012 N80-31386
Comparison of calculated and measured helicopter rotor lateral flapping angles
[NASA-TN-81213] p0012 N80-33349
- JOHNSTON, J. P.**
Investigation of a reattaching turbulent shear layer flow over a backward-facing step
p0062 A80-27736
An experimental investigation of two large annular diffusers with swirling and distorted inflow
[NASA-TF-1628] p0005 N80-17984
Modal content of noise generated by a coaxial jet in a pipe
[NASA-CR-163575] p0019 N80-33177
- JONES, A. D.**
Operations manual: Vertical Motion Simulator (VMS) S.08
[NASA-TN-81180] p0009 N80-23295
- JONES, B.**
Infrared spectra of IC 418 and NGC 6572
p0069 A80-16862
- JONES, D. E.**
Saturn's magnetic field and magnetosphere
p0021 A80-19117
Modeling Jupiter's current disc - Pioneer 10 outbound
p0075 A80-45153
- JONES, H. W., JR.**
Conditional replenishment using motion prediction
p0065 A80-39715
- JONES, R. T.**
Some observations on supersonic wing design
[AIAA 80-3040] p0001 A80-31009
Classical aerodynamic theory
[NASA-RP-1050] p0001 N80-15033
Wing flapping with minimum energy
[NASA-TN-81174] p0001 N80-16035
- JORDAN, D. E.**
Simulated weightlessness - Effects on bioenergetic balance
p0095 A80-21544
- JORDAN, J. P.**
Simulated weightlessness - Effects on bioenergetic balance
p0095 A80-21544
- JUDGE, D. L.**
Ultraviolet photometer observations of the Saturnian system
p0070 A80-19122
A reanalysis of the observed interplanetary hydrogen I alpha emission profiles and the derived local interstellar gas temperature and velocity
p0076 A80-49362
- JUERGENS, D. W.**
Atmosphere structure instruments on the four Pioneer Venus entry probes
p0051 A80-30849

K

- KARANCHETI, K.**
An experimental study of the structure and acoustic field of a jet in a cross stream
[NASA-CR-162464] p0014 N80-15871
Acoustic resonances and sound scattering by a shear layer
[NASA-CR-166181] p0014 N80-15873
An experimental study of multiple jet mixing
[NASA-CR-166184] p0018 N80-31760
- KATZ, J.**
Study of cooling air inlet and exit geometries for horizontally opposed piston aircraft engines
[AIAA PAPER 80-1242] p0027 A80-38984
A vortex-lattice method for the calculation of the nonsteady separated flow over delta wings
[AIAA PAPER 80-1803] p0027 A80-43286
Effect of propeller slipstream on the drag and performance of the engine cooling system for a general aviation twin-engine aircraft
[AIAA PAPER 80-1872] p0027 A80-43315
- KAUFMAN, J.**
Study of crosslinking and degradation mechanisms in sealant polymer candidates
[NASA-CR-152346] p0039 N80-22484
- KEENE, J.**
Low-pass interference filters for submillimeter astronomy
p0070 A80-19956
- KEESER, R. G.**
The properties of clusters in the gas phase. IV - Complexes of H₂O and HNO_x clustering on NO_x/-/
p0046 A80-23322
Properties of clusters in the gas phase. V - Complexes of neutral molecules onto negative ions

- KEIL, L. C. p0057 A80-50144
Growth hormone control of glucose oxidation pathways in hypophysectomized rats p0088 A80-24222
Fluid shifts and endocrine responses during chair rest and water immersion in man p0088 A80-25990
Exercise training-induced hypervolemia - Role of plasma albumin, renin, and vasopressin p0089 A80-32749
- KELLER, C. H.
Pioneer Venus Orbiter Radar Mapper - Design and operation p0050 A80-30833
- KENDALL, J. H.
Noise generation by a lifting wing/flap combination at Reynolds numbers to 2.8×10 to the 6th [AIAA PAPER 80-0035] p0024 A80-22729
- KENLEY, S. L.
Heterogeneous phase reactions of Martian volatiles with putative regolith minerals p0090 A80-36062
- KERRIDGE, J. P.
Aqueous activity on asteroids - Evidence from carbonaceous meteorites p0062 A80-24586
- KERSCHEN, E. J.
Fan noise caused by the ingestion of anisotropic turbulence - A model based on axisymmetric turbulence theory [AIAA PAPER 80-1021] p0032 A80-35977
Analytical study of the effects of wind tunnel turbulence on turbofan rotor noise [NASA-CR-152359] p0016 N80-23099
Modal content of noise generated by a coaxial jet in a pipe [NASA-CR-163575] p0019 N80-33177
- KIM, J.
Investigation of a reattaching turbulent shear layer flow over a backward-facing step p0062 A80-27736
On the numerical solution of time-dependent viscous incompressible fluid flows involving solid boundaries p0052 A80-34980
Large eddy simulation of turbulent channel flow: ILLIAC 5 calculation p0059 N80-27661
- KING, L. S.
Calculations of transonic flow about an airfoil in a wind tunnel [AIAA PAPER 80-1366] p0027 A80-44142
- KLEIN, H. P.
The Viking mission and the search for life on Mars p0086 A80-10738
Oxygen as a factor in eukaryote evolution - Some effects of low levels of oxygen on *Saccharomyces cerevisiae* p0086 A80-12229
Simulation of the Viking biology experiments - An overview p0090 A80-36066
- KLINE, S. J.
Investigation of a reattaching turbulent shear layer flow over a backward-facing step p0062 A80-27736
- KNAPTON, B.
Application of advanced technologies to small, short-haul air transports [NASA-CR-152364] p0019 N80-33396
- KNICKERBOCKER, P.
The phase of the ten-hour modulation in the Jovian magnetosphere /Pioneers 10 and 11/ p0067 A80-10526
- KNUDSEN, W. C.
Pioneer Venus Orbiter planar retarding potential analyzer plasma experiment p0073 A80-30839
- KOBAYASHI, M.
Insulin binding and glucose uptake of adipocytes in rats adapted to hypergravitational force p0089 A80-35751
- KOENIG, D. G.
Large scale model tests of a new technology V/STOL concept [AIAA PAPER 80-0233] p0023 A80-19303
- Workshop on Thrust Augmenting Ejectors [NASA-CF-2093] p0004 N80-10107
NASA overview p0022 N80-10109
- KOJIMA, G.
Application of laser velocimetry to an unsteady transonic flow p0063 A80-29506
- KOJIMA, G. K.
A microprocessor-based instrument for neural pulse wave analysis p0098 A80-50322
- KORUS, R. A.
Synthesis of perfluoroalkylether oxadiazole elastomers p0045 A80-21992
Synthesis of perfluoroalkylether triazine elastomers p0051 A80-32825
Perfluoroether triazine elastomers [NASA-CR-162748] p0039 N80-16166
- KOURTIDES, D. A.
Oxygen index tests of thermosetting resins p0044 A80-21448
Advanced thermoset resins for fire-resistant composites p0063 A80-34788
Graphite composites with advanced resin matrices [AIAA 80-0758] p0064 A80-35051
Performance properties of graphite reinforced composites with advanced resin matrices p0052 A80-35330
Thermophysical and flammability characterization of phosphorylated epoxy adhesives p0066 A80-48079
Fire-resistant materials for aircraft passenger seat construction [NASA-TM-78617] p0035 N80-13255
Chemical research projects office: An overview and bibliography, 1975-1980 [NASA-TM-81227] p0037 N80-31473
- KOUTSOYANNIS, S. P.
Characterization of acoustic disturbances in linearly sheared flows p0030 A80-31804
Characterization of acoustic disturbances in linearly sheared flows [NASA-CR-162577] p0014 N80-15869
Acoustic resonances and sound scattering by a shear layer [NASA-CR-166181] p0014 N80-15873
- KOZLOWSKI, S.
Extracellular hyperosmolality and body temperature during physical exercise in dogs p0092 A80-54076
- KRATZER, R. H.
Study of crosslinking and degradation mechanisms in sealant polymer candidates [NASA-CR-152346] p0039 N80-22484
- KRAVICK, S.
Fluid shifts and endocrine responses during chair rest and water immersion in man p0088 A80-25990
Fluid-electrolyte shifts and thermoregulation - Rest and work in heat with head cooling p0091 A80-48086
- KRIEGER, A. S.
Quest for ultrahigh resolution in X-ray optics p0032 A80-17480
- KRIKORIAN, A. D.
Problems and potentialities of cultured plant cells in retrospect and prospect p0077 A80-15225
- KRINSLEY, D. H.
Eolian sedimentation on earth and Mars - Some comparisons p0068 A80-13969
- KRISHNAPRASAD, P. S.
A scaling theory for linear systems p0030 A80-32676
- KROTHAPALLI, D.
An experimental study of multiple jet mixing [NASA-CR-166184] p0018 N80-31760
- KUNC, J. A.
Survival probabilities for interstellar hydrogen flowing into the interplanetary system from far regions of the heliosphere p0076 A80-49217
- KUNG, R. H.
Stability of nonuniform rotor blades in hover

- using a mixed formulation
[NASA-TM-81226] p0012 N80-33777
- KUROSAKI, M.
Optimal washout for control of a moving base simulator p0031 A80-14833
- KUSSOY, M. I.
An experimental and numerical investigation of a three-dimensional shock wave separated turbulent boundary layer
[AIAA PAPER 80-0002] p0061 A80-22727
- KUTLER, P.
Supersonic flow over three-dimensional ablated nosetips using an unsteady implicit numerical procedure
[AIAA PAPER 80-0063] p0060 A80-19271
- KWAK, D.
Nonreflecting far-field boundary conditions for unsteady transonic flow computation
[AIAA PAPER 80-1393] p0065 A80-41597
- KWONG, H.
Synthesis of perfluoroalkylether oxadiazole elastomers p0045 A80-21992
- KYTE, P. T.
Meteoroid ablation spheres from deep-sea sediments p0046 A80-22948
- L
- LADA, C. J.
Two micron spectroscopy and 2.7 μ m CO line observations of V645 Cygni p0074 A80-35114
- LANBERT, O.
Dynamic stall on advanced airfoil sections
[AD-A085809] p0101 N80-29252
- LANOIT, P. J.
Pressure measurements on an ogive-cylinder at high angles of attack with laminar, transitional, or turbulent separation
[AIAA 80-1556] p0028 A80-45856
- LANPARKIN, B. A.
A candidate V/STOL research aircraft design concept using an S-3A aircraft and 2 Pegasus 11 engines
[NASA-TM-81204] p0009 N80-24293
- LANGHOFF, P. W.
Photoexcitation and ionization in molecular oxygen - Theoretical studies of electronic transitions in the discrete and continuous spectral intervals p0044 A80-20275
Photoexcitation and ionization in molecular fluorine - Stieltjes-Tchebycheff calculations in the static-exchange approximation p0046 A80-23324
- LANGHOFF, S. R.
SCF and CI calculations of the dipole moment function of ozone p0043 A80-17111
An ab initio calculation of the zero-field splitting parameters of the 3A-double prime state of formaldehyde p0056 A80-45333
Theoretical treatment of the spin-orbit coupling in the rare gas oxides NeO, ArO, KrO, and XeO p0057 A80-50149
- LANYI, J. K.
Proton movements in response to a light-driven electrogenic pump for sodium ions in Halobacterium halobium membranes p0087 A80-17686
Spectrophotometric identification of the pigment associated with light-driven primary sodium translocation in Halobacterium halobium p0088 A80-26015
The role of Na⁺/ in transport processes of bacterial membranes p0088 A80-27077
Physical chemistry and evolution of salt tolerance in halobacteria p0090 A80-40383
- LARSEN, W. E.
Some human factors issues in the development and evaluation of cockpit alerting and warning systems
[NASA-RP-1055] p0082 N80-15821
- LARSON, H. P.
Spectroscopic evidence for two achondrite parent bodies - Asteroids 349 Dembowska and 4 Vesta p0072 A80-26173
- LARSON, J. C.
A comparison of computer architectures for the NASA demonstration advanced avionics system p0032 A80-32427
- LASKOWSKI, B.
Na + Xe collisions in the presence of two nonresonant lasers p0051 A80-32416
Computational study of alkali-metal-noble gas collisions in the presence of nonresonant lasers - Na + Xe + $h/2\pi/\omega$ sub 1 + $h/2\pi/\omega$ sub 2 system p0056 A80-48762
- LATHAM, E. A.
Aircraft engine nozzle
[NASA-CASE-ARC-10977-1] p0033 N80-32392
- LAUBER, J. K.
Resource management on the flight deck
[NASA-CP-2120] p0082 N80-22283
- LAUNDER, B. E.
On the calculation of turbulent heat transport downstream from an abrupt pipe expansion p0076 A80-49037
Multiple-time-scale concepts in turbulent transport modelling p0080 A80-49277
Reynolds stress closures: Status and prospects p0077 N80-27660
- LAWLESS, J. G.
Quantification of monocarboxylic acids in the Murchison carbonaceous meteorite p0087 A80-13549
The role of metal ions in chemical evolution - Polymerization of alanine and glycine in a cation-exchanged clay environment p0090 A80-36195
Organic compounds in meteorites p0094 A80-50053
The possible role of metal ions and clays in prebiotic chemistry p0094 A80-50060
- LEACH, R.
Threshold windspeeds for sand on Mars - Wind tunnel simulations p0048 A80-27391
- LEBACQZ, J. V.
Implicit model following and parameter identification of unstable aircraft p0022 A80-28019
- LEBAN, M. I.
Water recovery by catalytic treatment of urine vapor
[ASME PAPER 80-ENAS-16] p0093 A80-43192
- LEE, H.
Constrained optimum trajectories with specified range p0021 A80-18538
- LEE, H. Q.
Algorithm for fixed-range optimal trajectories
[NASA-TP-1565] p0006 N80-28329
- LEE, I. Y.
Meteorological and air pollution modeling for an urban airport p0055 A80-42659
- LEE, M.
The properties of clusters in the gas phase. IV - Complexes of H₂O and HNO_x clustering on NO_x/- p0046 A80-23322
Properties of clusters in the gas phase. V - Complexes of neutral molecules onto negative ions p0057 A80-50144
- LEE, P. R.
Influence of quality control variables on failure of graphite/epoxy under extreme moisture conditions
[NASA-TM-81246] p0038 N80-33493
- LEE, R.
Retinal changes in rats flown on Cosmos 936 - A cosmic ray experiment p0091 A80-41995
- LEHMAN, J. M.
A compilation and analysis of helicopter handling qualities data. Volume 1: Data compilation
[NASA-CR-31144] p0013 N80-11097
- LEHMAN, L. L.
Unified treatment of lifting atmospheric entry p0048 A80-28027
- LEN, H. Y.
Efficiency of aerosol collection on wires exposed

- in the stratosphere
[NASA-TM-81147] p0035 N80-11676
- LEHMON, R. M.
The radioracemization of isovaline - Cosmochemical implications p0086 A80-13018
- LEWIS, G. A.
Saturnian trapped radiation and its absorption by satellites and rings - The first results from Pioneer 11 p0070 A80-19118
- LEON, H. A.
Extremes of urine osmolality - Lack of effect on red blood cell survival p0091 A80-46196
- LEONARD, A.
Vortex simulation of three-dimensional, spotlike disturbances in a laminar boundary layer p0067 A80-49296
Three-dimensional simulation of the free shear layer using the vortex-in-cell method p0067 A80-49300
Turbulent structures in wall-bounded shear flows observed via three-dimensional numerical simulators [NASA-TM-81219] p0037 N80-29622
- LEPETICH, J. E.
Atmosphere structure instruments on the four Pioneer Venus entry probes p0051 A80-30849
- LEHNER, W. R.
Plasma etching of poly(N,N'-p,p'-oxydiphenylene/pyromellitimide/ film and photo/thermal degradation of etched and unetched film p0093 A80-24158
- LEROY, H. L.
Infrared-temperature variability in a large agricultural field [E80-10331] p0038 N80-32822
- LEVI, E.
The role of metal ions in chemical evolution - Polymerization of alanine and glycine in a cation-exchanged clay environment p0090 A80-36195
- LEVIN, D.
A vortex-lattice method for the calculation of the nonsteady separated flow over delta wings [AIAA PAPER 80-1803] p0027 A80-43286
- LEVINE, H.
A note of sound radiation from distributed sources p0030 A80-31805
Output of acoustical sources p0030 A80-37806
A note on sound radiation into a uniformly flowing medium p0031 A80-45488
On the output of acoustical sources [NASA-CR-162576] p0014 N80-15872
- LIDEN, S.
V-STOLAND avionics system flight-test data on a UH-1H helicopter [NASA-TM-78591] p0008 N80-18047
- LINCOLN, K. A.
Data acquisition techniques for exploiting the uniqueness of the time-of-flight mass spectrometer: Application to sampling pulsed gas systems [NASA-TM-81224] p0037 N80-31775
- LINLOF, W. I.
Permittivity and attenuation of wet snow between 4 and 12 GHz p0052 A80-36244
- LOEWENSTEIN, H.
Measurements of NO, O₃, and temperature at 19.8 km during the total solar eclipse of 26 February 1979 p0055 A80-43638
- LOMBARD, C. K.
Forebody and base region real-gas flow in severe planetary entry by a factored implicit numerical method. I - Computational fluid dynamics [AIAA PAPER 80-0065] p0061 A80-22731
- LOPEZ, A. E.
Workshop on Thrust Augmenting Ejectors [NASA-CP-2093] p0004 N80-10107
- LORELL, K. R.
Internal image motion compensation system for the Shuttle Infrared Telescope Facility p0064 A80-37427
- Control system designs for the shuttle infrared telescope facility [NASA-TM-81159] p0036 N80-18869
- LOVEJOY, R. W.
Integrated band intensities of gaseous N₂O/5/ p0047 A80-25660
- LUEBS, A. B.
Effect of tip planform on blade loading characteristics for a two-bladed rotor in hover [NASA-TM-78615] p0007 N80-14049
- LUM, H.
Simulation of the Infrared Astronomical Satellite /IRAS/ telescope system p0067 A80-49842
- LUMB, D. R.
Data reduction by computer processing p0058 N80-20016
- LUNDELL, J. E.
A technique for evaluating the Jovian entry-probe heat-shield material with a gasdynamic laser p0063 A80-29479
- LUTZ, B. L.
Infrared methane spectra between 1120 per cm and 1800 per cm - A new atlas p0042 A80-13143
A new atlas of infrared methane spectra between 1120 per cm and 1800 per cm p0042 A80-15655
- LYKOS, P.
An assessment of future computer system needs for large-scale computation [NASA-TM-78613] p0008 N80-17717
- M**
- MACCORMACK, R. W.
An explicit algorithm for a fluid approach to nonlinear optics propagation using splitting and rezoning techniques p0059 A80-14987
An efficient explicit-implicit-characteristic method for solving the compressible Navier-Stokes equations p0062 A80-27408
Asymptotic features of shock-wave boundary-layer interaction p0055 A80-43135
- MACELROY, R.
Modified Iterative Extended Hueckel. 2: Application to the interaction of Na(+), Na(+) (aq.), Mg(+)-2(aq.) with adenine and thymine [NASA-TM-81201] p0084 N80-25109
- HACK, R.
Noble gas trapping and fractionation during synthesis of carbonaceous matter p0093 A80-23669
Mars ultraviolet simulation facility p0089 A80-36061
Heterogeneous phase reactions of Martian volatiles with putative regolith minerals p0090 A80-36062
- MACLEOD, G.
NASA-Ames Life Sciences Flight Experiments program - 1980 status report [ASME PAPER 80-ENAS-34] p0094 A80-43209
- MACPHER, R. H.
On the limitations of the concept of space frequency equivalence p0069 A80-16697
- MADEY, R.
Adsorption interference in mixtures of trace contaminants flowing through activated carbon adsorber beds [ASME PAPER 80-ENAS-17] p0096 A80-43193
- MAERK, T. D.
New gas phase inorganic ion cluster species and their atmospheric implications p0075 A80-37510
- MAGEE, J. P.
A hingeless rotor XV-15 design integration feasibility study. Volume 1: Engineering design studies [NASA-CR-152310] p0015 N80-18030
- MAISEL, M. D.
NASA/Army XV-15 tilt rotor research aircraft wind-tunnel test program plan [NASA-TM-78562] p0007 N80-15067
Wind-tunnel tests of the XV-15 tilt rotor aircraft [NASA-TM-81177] p0009 N80-24294

- MALCOLM, G. N.**
Unsteady aerodynamics of conventional and supercritical airfoils
[AIAA 80-0734] p0026 A80-35038
Mathematical modeling of the aerodynamics of high-angle-of-attack maneuvers
[AIAA 80-1583] p0028 A80-45879
- MALCOLM, G. N.**
Experimental unsteady aerodynamics of conventional and supercritical airfoils
[NASA-TM-81221] p0012 N80-33345
- MANDEL, A. D.**
Effect of simulated weightlessness on the immune system in rats
p0088 A80-25894
- MANGSETH, G. R.**
Plasma volume during stress in man - Osmolality and red cell volume
p0087 A80-13506
- MARCY, G.**
Calculations of the evolution of the giant planets
p0049 A80-28086
- MARGON, B.**
Discovery of optical molecular emission from the bipolar nebula surrounding HD 44179
p0058 A80-52399
- MARSHALL, R. D.**
Development of the electrochemically regenerable carbon dioxide absorber for portable life support system application
[ASME PAPER 79-ENAS-33] p0092 A80-15257
Development of a nitrogen generation system
[NASA-CR-152333] p0085 N80-19800
- MARTIN, J. L.**
The Quiet Short-Haul Research Aircraft /QsRA/
p0021 A80-27384
- MARTIN, W. D.**
Effects of chronic centrifugation on skeletal muscle fibers in young developing rats
p0096 A80-41983
- MARTINEZ, R.**
Unified aerodynamic-acoustic theory for a thin rectangular wing encountering a gust
p0030 A80-36401
- MARVIN, J. G.**
Application of laser velocimetry to an unsteady transonic flow
p0063 A80-29506
- MASON, R. M.**
Guiding the development of a controlled ecological life support system
[NASA-CR-162452] p0085 N80-12735
- MATTAR, F. P.**
An explicit algorithm for a fluid approach to nonlinear optics propagation using splitting and rezoning techniques
p0059 A80-14987
- MAURER, J. R.**
Aircraft simulation data management - A prototype system
p0029 A80-49832
- MAURY, R. E.**
Hygrothermal damage mechanisms in graphite-epoxy composites
[NASA-CR-3189] p0038 N80-13170
- MAYER, K. E.**
Using guided clustering techniques to analyze Landsat data for mapping forest land cover in northern California
p0078 A80-25595
- MAYER, L. A.**
Chelate-modified polymers for atmospheric gas chromatography
[NASA-CASE-ARC-11154-1] p0097 N80-23383
- MCALISTER, K. W.**
Dynamic stall on advanced airfoil sections
[AD-A085809] p0101 N80-29252
- MCANINCH, M.**
The intracellular Na⁺/+ and K⁺/+ composition of the moderately halophilic bacterium, *Paracoccus halodenitrificans*
p0091 A80-41250
- MCCARTHY, J. F.**
16-30 micron spectroscopy of Titan
p0049 A80-29321
The 16- to 38-micron spectrum of Callisto
p0074 A80-35234
- MCCLOUD, J. L., III**
The promise of multicyclic control
p0022 A80-33123
Multicyclic control for helicopters - Research in progress at Ames Research Center
[AIAA 80-0671] p0025 A80-34997
Multicyclic control of a helicopter rotor considering the influence of vibration, loads, and control motion
[AIAA 80-0673] p0025 A80-34959
- MCCRACKEN, R. C.**
Quiet short-haul research aircraft familiarization document
[NASA-TM-81149] p0007 N80-14108
NASA quiet short-haul research aircraft experimenters' handbook
[NASA-TM-81162] p0007 N80-16024
- MCCREIGHT, C. R.**
Integrated infrared detector arrays for low-background astronomy
p0066 A80-44639
- MCCROSKEY, W. J.**
An experimental evaluation of a helicopter rotor section designed by numerical optimization
[NASA-TM-78622] p0009 N80-21287
Dynamic stall on advanced airfoil sections
[AD-A085809] p0101 N80-29252
- MCCULLY, G.**
Evaluation of approximate methods for the prediction of noise shielding by airframe components
[NASA-TP-1004] p0004 N80-15129
- MCGHAN, H. E.**
Measurements of NO, O₃, and temperature at 19.8 km during the total solar eclipse of 26 February 1979
p0055 A80-43638
- MCGOURTY, J.**
Retinal changes in rats flown on Cosmos 936 - A cosmic ray experiment
p0091 A80-41995
- MCILWAIN, C. E.**
Trapped radiation belts of Saturn - First look
p0070 A80-19121
- MCKEE, C. F.**
Molecule formation and infrared emission in fast interstellar shocks. I Physical processes
p0043 A80-16410
- MCKENZIE, R. L.**
Two-photon excitation of nitric oxide fluorescence as a temperature indicator in unsteady gas-dynamic processes
[NASA-TM-81220] p0037 N80-32700
- MCKIBBEN, R. B.**
Saturnian trapped radiation and its absorption by satellites and rings - The first results from Pioneer 11
p0070 A80-19118
- MCKIBBIN, D. D.**
Preliminary results on the plasma environment of Saturn from the Pioneer 11 plasma analyzer experiment
p0043 A80-19116
- MCKILLIP, R. M., JR.**
The design, testing and evaluation of the MIT individual-blade-control system as applied to gust alleviation for helicopters
[NASA-CR-152352] p0016 N80-22357
- MCKOY, B. V.**
Photoexcitation and ionization in molecular oxygen - Theoretical studies of electronic transitions in the discrete and continuous spectral intervals
p0044 A80-20275
Photoexcitation and ionization in molecular fluorine - Stieltjes-Tchebycheff calculations in the static-exchange approximation
p0046 A80-23324
- MCLEAN, J. D.**
A new algorithm for horizontal capture trajectories
[NASA-TM-81186] p0009 N80-22297
- MCNILLAN, O. J.**
Tests of subgrid-scale models in strained turbulence
[AIAA PAPER 80-1339] p0065 A80-41569
- MCRAE, D. S.**
A computational and experimental study of high Reynolds number viscous/inviscid interaction about a cone at high angle of attack
[AIAA PAPER 80-1422] p0104 A80-44492
- MCGRUER, D.**
Practical optimal flight control system design for helicopter aircraft. Volume 1: Technical Report
[NASA-CR-3275] p0017 N80-23328

- MCVEIGH, H. A.
Synthesis of rotor test data for real-time simulation
[NASA-CR-152311] p0015 N80-18029
- MEININGER, G. A.
A model for hypokinesia: Effects on muscle atrophy in the rat p0095 A80-28188
- MEINSCHWEIN, W. G.
The carbon isotope biogeochemistry of the individual hydrocarbons in bat guano and the ecology of insectivorous bats in the region of Carlsbad, New Mexico
[NASA-TM-81164] p0083 N80-18680
- MELVILLE, J. G., II
Modeling Jupiter's current disc - Pioneer 10 outbound p0075 A80-45153
- MENDENHALL, M. R.
A correlation method to predict the surface pressure distribution of an infinite plate or a body of revolution from which a jet is issuing
[NASA-CR-152345] p0018 N80-32339
- MENG, S. Y.
Transonic swept-wing analysis using asymptotic and other numerical methods
[AIAA PAPER 80-0342] p0024 A80-22751
Analysis of transonic swept wings using asymptotic and other numerical methods
[NASA-TM-80762] p0011 N80-29255
- MERRICK, R. B.
V/STOLAND avionics system flight-test data on a UH-1H helicopter
[NASA-TM-78591] p0008 N80-18047
- MERRILL, R. K.
Results of a simulator investigation of control system and display variations for an attack helicopter mission
[AD-A085812] p0101 N80-29370
- MERTZ, L.
Simple Cassegrain scanning system for infrared astronomy p0074 A80-34729
- METCALFE, R. W.
Direct numerical simulations of the turbulent wake of an axisymmetric body p0080 A80-49235
- MEYER, G.
Total aircraft flight-control system - Balanced open- and closed-loop control with dynamic trim maps p0025 A80-32448
Flight tests of the total automatic flight control system (Tafcos) concept on a DHC-6 Twin Otter aircraft
[NASA-TP-1513] p0005 N80-17081
Application of the concept of dynamic trim control to automatic landing of carrier aircraft
[NASA-TP-1512] p0005 N80-19126
- MIAO, W.
Analytical design and evaluation of an active control system for helicopter vibration reduction and gust response alleviation
[NASA-CR-152377] p0017 N80-28369
- MICHAELIS, R. P.
A solar-heated water system for a photographic processing laboratory p0098 A80-15750
- MIDDLEDITCH, J.
The evolution of rapid oscillations in an outburst of a dwarf nova p0075 A80-45227
- MIGDAL, D.
VTOL in-ground effect flows for closely spaced jets
[AIAA PAPER 80-1880] p0033 A80-46693
- MINALOV, J. D.
Preliminary results on the plasma environment of Saturn from the Pioneer 11 plasma analyzer experiment p0043 A80-19116
The Pioneer Venus Orbiter plasma analyzer experiment p0050 A80-30836
- MILLARD, J. P.
Infrared-temperature variability in a large agricultural field
[E80-10331] p0038 N80-32822
- MILLER, D. L.
An experimental evaluation of head-up display formats
- [NASA-TP-1550] p0082 N80-28349
- MILLER, J. H.
Design alternatives for the Shuttle Infrared Telescope Facility p0060 A80-17435
- MILLER, R. B.
Pioneer Venus Multiprobe entry telemetry recovery p0050 A80-30831
Pioneer Venus multiprobe entry telemetry recovery p0058 N80-26347
- MILLER, R. H.
Galaxy collisions - A preliminary study p0046 A80-23420
On the three-dimensional shapes of elliptical galaxies p0047 A80-26101
- MILLER, W. E.
Improved characterization of the Si-SiO₂ interface p0095 A80-41532
- MINK, D. J.
The radius and ellipticity of Uranus from its occultation of SAO 158687 p0073 A80-31937
- MIQUEL, J.
Review of cell aging in Drosophila and mouse p0087 A80-17741
Favorable effects of the antioxidants sodium and magnesium thiazolidine carboxylate on the vitality and life span of Drosophila and mice p0089 A80-29085
- MITCHELL, J. L.
Measurements of wind vectors, eddy momentum transports, and energy conversions in Jupiter's atmosphere from Voyager 1 images A80-24159
- MITCHELL, J. M.
The carbon isotope biogeochemistry of the individual hydrocarbons in bat guano and the ecology of insectivorous bats in the region of Carlsbad, New Mexico
[NASA-TM-81164] p0083 N80-18680
- MOFFITT, R.
Analysis and correlation of test data from an advanced technology rotor system
[NASA-CR-152366] p0019 N80-33351
- MOHR, R. L.
Navigation systems for approach and landing of VTOL aircraft
[NASA-CR-152335] p0016 N80-19055
- MOIN, P.
On the numerical solution of time-dependent viscous incompressible fluid flows involving solid boundaries p0052 A80-34980
Large eddy simulation of turbulent channel flow: ILLIAC 5 calculation p0059 N80-27661
- MONDON, C. E.
Insulin binding and glucose uptake of adipocytes in rats adapted to hypergravitational force p0089 A80-35751
- MONSON, D. J.
Skin friction measurements by a new nonintrusive double-laser-beam oil viscosity balance technique
[AIAA PAPER 80-1373] p0065 A80-41587
- MONTGOMERY, L. D.
Fluid-electrolyte shifts and thermoregulation - Rest and work in heat with head cooling p0091 A80-48086
- MOORE, M. T.
Acoustic characteristics of two hybrid inlets at forward speed
[AIAA PAPER 79-0678] p0021 A80-20828
Distortion-rotor interaction noise produced by a drooped inlet
[AIAA PAPER 80-1050] p0033 A80-35994
- MOOREHEAD, M. D.
Direct /TEM/ observation of the catalytic oxidation of amorphous carbon by Pd particles p0053 A80-37180
- MORAN, P. J.
Flight test of navigation and guidance sensor errors measured on STOL approaches
[NASA-TM-81154] p0007 N80-13041
- MORAN, J.
Analysis of two-dimensional incompressible flows by a subsurface panel method p0029 A80-30566

- MORELAND, G.**
Carbonaceous chondrites. I - Characterization and significance of carbonaceous chondrite /CH/ xenoliths in the Jodzie howardite p0086 A80-13013
- MORELLI, J. P.**
Large-scale wind-tunnel tests of inverting flaps on a STOL utility aircraft model [NASA-TP-1696] p0005 N80-25318
- MORETTI, P. M.**
Study of boundary-layer transition using transonic-cone preston tube data [NASA-TM-81103] p0010 N80-28305
- MORIARTY, J. A.**
Improved characterization of the Si-SiO₂ interface p0095 A80-41532
- MORRIS, D. H.**
Time-temperature behavior of a unidirectional graphite/epoxy composite p0078 A80-21141
The viscoelastic behavior of a composite in a thermal environment [NASA-CR-163187] p0039 N80-24369
The accelerated characterization of viscoelastic composite materials [NASA-CR-163188] p0039 N80-24370
- MORRIS, M. A.**
Application of parametric weight and cost estimating relationships to future transport aircraft [SAWE PAPER 1292] p0024 A80-20637
- MORSE, J. T.**
Fluid-electrolyte shifts and thermoregulation - Rest and work in heat with head cooling p0091 A80-48086
- MORT, K. W.**
An experimental investigation of two large annular diffusers with swirling and distorted inflow [NASA-TP-1628] p0005 N80-17984
- MOTTMANN, J.**
Saturn's rings - 3-mm observations and derived properties p0045 A80-21758
- MOUSSA, A.**
Materials for fire resistant passenger seats in aircraft p0080 A80-48757
Fire-resistant materials for aircraft passenger seat construction [NASA-TM-78617] p0035 N80-13255
- MUELLER, U.**
Experimental investigation of a three dimensional turbulent boundary layer with a non disappearing pressure gradient p0054 A80-40907
- MULLER, J.-P.**
Measurements of wind vectors, eddy momentum transports, and energy conversions in Jupiter's atmosphere from Voyager 1 images A80-24159
- MUNOZ, E. F.**
Microbial mobilization of calcium and magnesium in waterlogged soils p0089 A80-32834
- MURPHY, J. D.**
A Navier-Stokes fast solver for turbulence modeling applications p0059 N80-27659
- MURPHY, J. P.**
An entry and landing probe for Titan [AIAA PAPER 80-0117] p0060 A80-18384
- MURPHY, M. R.**
Analysis of eighty-four commercial aviation incidents - Implications for a resource management approach to crew training p0093 A80-40340
- MUSACCHIA, I. J.**
A model for hypokinesia: Effects on muscle atrophy in the rat p0095 A80-28188
- N**
- NACHTSHEIM, P. R.**
Unified treatment of lifting atmospheric entry p0048 A80-28027
- NAGARAJA, K. S.**
Workshop on Thrust Augmenting Ejectors [NASA-CP-2093] p0004 N80-10107
- NAGY, A. F.**
Hot hydrogen in the exosphere of Venus p0070 A80-18943
The location of the dayside ionopause of Venus - Pioneer Venus Orbiter magnetometer observations p0076 A80-48811
- NAISH, J. M.**
Head-up display in the non-precision approach [NASA-TM-81167] p0084 N80-26296
An experimental evaluation of head-up display formats [NASA-TP-1550] p0082 N80-28349
- NAKAHARA, J. H.**
Study of crosslinking and degradation mechanisms in sealant polymer candidates [NASA-CR-152346] p0039 N80-22484
- MANES, R.**
Temperature dependence of intensities of the 8-12 micron bands of CFC13 p0045 A80-21559
Band model calculations for CFC13 in the 8-12 micron region p0045 A80-21560
- NARASIMHA, R.**
Relaminarization of fluid flows p0075 A80-40843
- NARDUCCI, L. M.**
Feasibility studies for light scattering experiments to determine the velocity relaxation of small particles in a fluid [NASA-CR-163214] p0040 N80-25586
- NASTRON, G. D.**
Eddy diffusion coefficients and the variance of the atmosphere 30-60 km p0076 A80-45996
- NAZAR, K.**
Extracellular hyperosmolality and body temperature during physical exercise in dogs p0092 A80-54076
- NEGULESCO, J. A.**
Hypergravity and estrogen effects on avian anterior pituitary growth hormone and prolactin levels p0094 A80-20447
The architecture of the avian retina following exposure to chronic 2 G p0096 A80-42013
- NEIL, J.**
Carbonaceous chondrites. I - Characterization and significance of carbonaceous chondrite /CH/ xenoliths in the Jodzie howardite p0086 A80-13013
- NELSON, H. G.**
A temperature dependent fatigue failure criterion for graphite/epoxy laminates p0060 A80-15518
- NEUMAN, F.**
Analysis of fuel-conservative curved decelerating approach trajectories for powered-lift and CTOL jet aircraft [NASA-TP-1650] p0005 N80-19022
- NEVILLE, E. D.**
Growth hormone control of glucose oxidation pathways in hypophysectomized rats p0088 A80-24222
- NICHOLLS, R. W.**
Recommended conventions for defining transition moments and intensity factors in diatomic molecular spectra p0055 A80-41323
- NICOLET, W.**
Galileo probe thermal protection: Entry heating environments and spallation experiments design [NASA-CR-152334] p0038 N80-14184
- NICOLET, W. E.**
Galileo probe forebody entry thermal protection - Aerothermal environments and heat shielding requirements [ASME PAPER 80-ENAS-24] p0066 A80-43200
- NISHIOKA, K.**
Operational procedures for ground station operation: ATS-3 Hawaii-Ames satellite link experiment [NASA-TM-81155] p0035 N80-13333
- NITTA, H.**
A solar-heated water system for a photographic processing laboratory p0098 A80-15750

- NOERDLINGER, P. D.**
The settling of helium and the ages of globular clusters
p0052 A80-35151
- NOTHWANG, G. J.**
Pioneer Venus spacecraft design and operation
p0050 A80-30829
- NOYAK, V.**
Pioneer Venus Orbiter planar retarding potential analyzer plasma experiment
p0073 A80-30839
- NUNES, J. A.**
Effect of simulated weightlessness on the immune system in rats
p0088 A80-25894

O

- OBERBECK, V. R.**
Monte Carlo simulation of lunar megaregolith and implications
p0061 A80-23716
- OBERKAMPF, W. L.**
Experimental investigation of the asymmetric body vortex wake
[AIAA PAPER 80-0174]
p0032 A80-23937
- OBRIEN, D. L.**
Heterogeneous phase reactions of Martian volatiles with putative regolith minerals
p0090 A80-36062
- OBRIEN, P. J.**
Effectiveness of advanced fuel-conservative procedures in the transitional ATC environment
p0023 N80-27347
- OCONNOR, S.**
The effect of viewing time, time to encounter, and practice on perception of aircraft separation on a cockpit display of traffic information
[NASA-TM-81173]
p0083 N80-18038
- Perception of aircraft separation with pilot-preferred symbology on a cockpit display of traffic information
[NASA-TM-81172]
p0084 N80-31397
- OLSON, L. E.**
High-resolution LDA measurements of Reynolds stress in boundary layers and wakes
[AIAA 80-0436]
p0025 A80-26967
- OHAN, C. H.**
Visually induced self-motion sensation adapts rapidly to left-right visual reversal
p0096 A80-44213
- ORDY, J. H.**
Motion sickness in the squirrel monkey
p0095 A80-25891
- OREL, A. E.**
Photoexcitation and ionization in molecular fluorine - Stieltjes-Tchebycheff calculations in the static-exchange approximation
p0046 A80-23324
- OREHLAND, R. S.**
Microbial sulfate reduction measured by an automated electrical impedance technique
p0087 A80-21982
- ORLANDO, R. G.**
The architecture of the avian retina following exposure to chronic 2 G
p0096 A80-42013
- ORLOFF, K. L.**
High-resolution LDA measurements of Reynolds stress in boundary layers and wakes
[AIAA 80-0436]
p0025 A80-26967
- Effect of tip planform on blade loading characteristics for a two-bladed rotor in hover
[NASA-TM-78615]
p0007 N80-14049
- ORNISTON, R. A.**
On the nonlinear deformation geometry of Euler-Bernoulli beams
[NASA-TP-1566]
p0101 N80-20619
- OWEN, F. K.**
Experimental investigation of the asymmetric body vortex wake
[AIAA PAPER 80-0174]
p0032 A80-23937
- Control of forebody vortex orientation to alleviate side forces
[AIAA PAPER 80-0183]
p0024 A80-23955
- Separated skin-friction measurements - Source of error: An assessment and elimination
[AIAA PAPER 80-1409]
p0027 A80-44155

Control of forebody three-dimensional flow separations
p0022 N80-15164

- OYAMA, J.**
Insulin binding and glucose uptake of adipocytes in rats adapted to hypergravitational force
p0089 A80-35751
- OYAMA, V. I.**
Pioneer Venus Sounder Probe gas chromatograph
p0089 A80-30845
- Corrections in the Pioneer Venus sounder probe gas chromatographic analysis of the lower Venus atmosphere
p0089 A80-30875
- A model of Martian surface chemistry
p0090 A80-36069

P

- PACIOREK, K. L.**
Study of crosslinking and degradation mechanisms in sealant polymer candidates
[NASA-CR-152346]
p0039 N80-22484
- PAGE, V. R.**
An experimental investigation of two large annular diffusers with swirling and distorted inflow
[NASA-TP-1628]
p0005 N80-17984
- PAK, R. D.**
Pioneer Venus Unified Abstract Data Library and Quick Look Data Delivery System
p0050 A80-30832
- PALLAI, A.**
Pioneer Venus sounder and small probes Nephelometer instrument
p0053 A80-36750
- PALMER, E.**
Perception of aircraft separation with pilot-preferred symbology on a cockpit display of traffic information
[NASA-TM-81172]
p0084 N80-31397
- PALMER, E. A.**
The effect of viewing time, time to encounter, and practice on perception of aircraft separation on a cockpit display of traffic information
[NASA-TM-81173]
p0083 N80-18038
- Effect of field of view and monocular viewing on angular size judgements in an outdoor scene
[NASA-TM-81176]
p0083 N80-19792
- PALMER, J. H.**
Pioneer-Venus solar flux radiometer
p0077 A80-17468
- Pioneer Venus Sounder Probe Solar Flux Radiometer
p0073 A80-30846
- Narrow-field radiometry in a quasi-isotropic atmosphere
p0079 A80-40233
- PARISH, J. L.**
Azimuthal magnetic field at Jupiter
p0076 A80-49185
- PARK, C.**
Shock-tube studies of radiative base heating of Jovian probe
p0064 A80-38114
- Equivalent-cone calculation of nitric oxide production rate during Space Shuttle re-entry
p0056 A80-45359
- Curves of growth for van der Waals broadened spectral lines
p0057 A80-51378
- Shape change of Galileo probe models in free-flight tests
[NASA-TM-81209]
p0037 N80-27418
- PARKER, J. A.**
Oxygen index tests of thermosetting resins
p0044 A80-21448
- Release-rate calorimetry of multilayered materials for aircraft seats
p0051 A80-34223
- Advanced thermoset resins for fire-resistant composites
p0063 A80-34788
- Release-rate calorimetry of multilayered materials for aircraft seats
[AIAA 80-0759]
p0064 A80-35052
- Thermophysical and flammability characterization of phosphorylated epoxy adhesives
p0066 A80-48079
- Chemical research projects office: An overview and bibliography, 1975-1980

- [NASA-TM-81227] p0037 N80-31473
PARKS, E. K.
 Aircraft motion analysis using limited flight and radar data
- p0025 A80-27241
PARRIS, B. L.
 The effects of motion and g-seat cues on pilot simulator performance of three piloting tasks [NASA-TP-1601] p0004 N80-15069
- PARSONS, E. K.**
 Internal image motion compensation system for the Shuttle Infrared Telescope Facility p0064 A80-37427
 Control system designs for the shuttle infrared telescope facility [NASA-TM-81159] p0036 N80-18869
- PATTERSON, J. J.**
 The evolution of rapid oscillations in an outburst of a dwarf nova p0075 A80-45227
- PAULK, C. H., JR.**
 Model development for automatic guidance of a VTOL aircraft to a small aviation ship [AIAA 80-1617] p0028 A80-45907
- PAYNE, F. E.**
 Application of the method of integral relations to unsteady fluid flow problems with shocks p0078 A80-26694
- PEAKE, D. J.**
 Control of forebody vortex orientation to alleviate side forces [AIAA PAPER 80-0183] p0024 A80-23955
 Diagnosis of separated flow regions on wind-tunnel models using an infrared camera p0025 A80-29494
 A computational and experimental study of high Reynolds number viscous/inviscid interaction about a cone at high angle of attack [AIAA PAPER 80-1422] p0104 A80-44492
 Control of forebody three-dimensional flow separations p0022 N80-15164
 Three-dimensional interactions and vortical flows with emphasis on high speeds [NASA-TM-81169] p0008 N80-21286
- PEALE, S. J.**
 On the comparative evolution of Ganymede and Callisto p0048 A80-28080
 Tidal dissipation, orbital evolution, and the nature of Saturn's inner satellites p0058 A80-53235
- PEDELT, J. A.**
 Supersonic flow over three-dimensional ablated nosetips using an unsteady implicit numerical procedure [AIAA PAPER 80-0063] p0060 A80-19271
- PENN, P. E.**
 Changes in body temperature and metabolic rate after injection of calcium into the caudal hypothalamus of the rabbit p0093 A80-27078
- PERING, G. A.**
 Degradation of tensile and shear properties of composites exposed to fire or high temperature p0072 A80-29697
- PERKINS, S. C., JR.**
 A correlation method to predict the surface pressure distribution of an infinite plate or a body of revolution from which a jet is issuing [NASA-CR-152345] p0018 N80-32339
- PESSER, H. E.**
 Acceleration of energetic protons by interplanetary shocks p0071 A80-21183
 The acceleration of energetic charged particles by interplanetary and supernova shock waves p0080 A80-53209
- PETERFREUND, A. R.**
 Mars - The north polar sand sea and related wind patterns p0047 A80-26370
- PETERS, D. A.**
 On the nonlinear deformation geometry of Euler-Bernoulli beams [NASA-TP-1566] p0101 N80-20619
- PETERSON, D. L.**
 Issues arising from the demonstration of Landsat-based technologies to inventories and mapping of the forest resources of the Pacific Northwest states p0065 A80-41305
- PETERSON, K. I.**
 New gas phase inorganic ion cluster species and their atmospheric implications p0075 A80-37510
- PETITT, J. C.**
 Effects of magnification and visual accommodation on aimpoint estimation in simulated landings with real and virtual image displays [NASA-TP-1635] p0082 N80-34099
- PETTINGILL, G. H.**
 Pioneer Venus Orbiter Radar Mapper - Design and operation p0050 A80-30833
- PHATAK, A. V.**
 Analytical methodology for determination of helicopter IFR precision approach requirements [NASA-CR-152367] p0040 N80-28330
- PHILLIPS, M. H.**
 Thresholds for detection of constant rotary acceleration during vibratory rotary acceleration p0091 A80-42003
- PHILPOTT, D. E.**
 Retinal changes in rats flown on Cosmos 936 - A cosmic ray experiment p0091 A80-41995
- PHOTINOS, P. J.**
 Adsorption interference in mixtures of trace contaminants flowing through activated carbon adsorber beds [ASME PAPER 80-ENAS-17] p0096 A80-43193
- PIZZO, P. P.**
 Some observations regarding the statistical determination of stress rupture regression lines p0041 A80-12828
- POLLACK, J.**
 Threshold windspeeds for sand on Mars - Wind tunnel simulations p0048 A80-27391
- POLLACK, J. B.**
 OCS, stratospheric aerosols and climate p0044 A80-19741
 Titan aerosols - Optical properties and vertical distribution p0045 A80-21759
 Stratospheric aerosol modification by supersonic transport and space shuttle operations - Climate implications p0047 A80-26088
 Calculations of the evolution of the giant planets p0049 A80-28086
 16-30 micron spectroscopy of Titan p0049 A80-29321
 Scattering by non-spherical particles of size comparable to a wavelength - A new semi-empirical theory p0063 A80-34050
 Scattering by nonspherical particles of size comparable to wavelength - A new semi-empirical theory and its application to tropospheric aerosols p0052 A80-36040
 Atmospheric aerosols and climate p0052 A80-36305
 Origin and evolution of planetary atmospheres p0053 A80-37598
 The effect of dense cores on the structure and evolution of Jupiter and Saturn p0056 A80-45812
 Stratospheric aerosol modification by supersonic transport operations with climate implications [NASA-RP-1058] p0034 N80-15726
- POLLACK, J. R.**
 Are solar spectral variations a drive for climatic change p0042 A80-15488
- POLLOCK, G. E.**
 Aldocyanoin microspheres - Partial amino acid analysis of the microparticulates formed from simple reactants under various conditions p0086 A80-11473
 The radioracemization of isovaline - Cosmochemical implications p0086 A80-13018
- POPPI, H.**
 Changes induced on the surfaces of small Pd clusters by the thermal desorption of CO

R

- Direct /TEM/ observation of the catalytic
oxidation of amorphous carbon by Pd particles
p0053 A80-37179
- Comparison of the early stages of condensation of
Cu and Ag on Mo/100/ with Cu and Ag on W/100/
p0053 A80-37180
- POPPOFF, I. G.
Stratospheric aerosol modification by supersonic
transport and space shuttle operations - Climate
implications
p0047 A80-26088
- Stratospheric aerosol modification by supersonic
transport operations with climate implications
[NASA-RP-1058]
p0034 N80-15726
- POTTER, W.
Pioneer Venus Sounder Probe gas chromatograph
p0089 A80-30845
- POULTON, C. E.
NASA's western regional applications training
activity
p0058 N80-20010
- POUND, G. H.
A calculation of the diffusion energies for
adatoms on surfaces of F.C.C. metals
p0068 A80-13534
- POWELL, J. D.
Internal image motion compensation system for the
Shuttle Infrared Telescope Facility
p0064 A80-37427
- POWELL, J. D., III
Development of a nitrogen generation system
[NASA-CR-152333]
p0085 N80-19800
- PRESLEY, L. L.
Test section configuration for aerodynamic testing
in shock tubes
p0026 A80-38085
- PRINN, R. G.
Preliminary calculations concerning the
maintenance of the zonal mean ozone distribution
in the Northern Hemisphere
p0074 A80-34445
- PRITCHARD, H. O.
Reduction of nitric oxide emissions from a combustor
[NASA-CASE-ARC-10814-2]
p0080 N80-26298
- PUCCI, S. L.
Dynamic stall on advanced airfoil sections
[AD-A085809]
p0101 N80-29252
- PUETTER, R. C.
Infrared spectra of IC 418 and NGC 6572
p0069 A80-16862
- The infrared spectrum of the carbon star Y Canum
Venaticorum between 1.2 and 30 microns
p0046 A80-22191
- The implications of hydrogen emission line ratios
in quasi-stellar objects
p0072 A80-27013
- PULLIAN, T. H.
Supersonic flow over three-dimensional ablated
nosetips using an unsteady implicit numerical
procedure
[AIAA PAPER 80-0063]
p0060 A80-19271
- A diagonal form of an implicit
approximate-factorization algorithm with
application to a two dimensional inlet
[AIAA PAPER 80-0067]
p0061 A80-19274
- An implicit finite-difference code for inviscid
and viscous cascade flow
[AIAA PAPER 80-1427]
p0066 A80-44128
- PYLE, K. R.
Saturnian trapped radiation and its absorption by
satellites and rings - The first results from
Pioneer 11
p0070 A80-19118

Q

- QUATTRONE, P. D.
Bosch - An alternate CO2 reduction technology
[ASME PAPER 79-ENAS-32]
p0092 A80-15256
- Development of the electrochemically regenerable
carbon dioxide absorber for portable life
support system application
[ASME PAPER 79-ENAS-33]
p0092 A80-15257
- Water recovery by catalytic treatment of urine vapor
[ASME PAPER 80-ENAS-16]
p0093 A80-43192

- RAGENT, B.
Pioneer Venus sounder and small probes
Nephelometer instrument
p0053 A80-36750
- RAGES, K.
Titan aerosols - Optical properties and vertical
distribution
p0045 A80-21759
- RAINDEN, R. L.
Saturn's magnetosphere, rings, and inner satellites
p0070 A80-19119
- RAKICH, J. V.
Equivalent-cone calculation of nitric oxide
production rate during Space Shuttle re-entry
p0056 A80-45359
- RAMAN, K. R.
Pressure and temperature fields associated with
aero-optics tests
p0031 N80-25591
- RAMOS, R.
Pioneer Venus occultation radio science data
generation
p0050 A80-30830
- Pioneer Venus Multiprobe entry telemetry recovery
p0050 A80-30831
- Data acquisition for measuring the wind on Venus
from Pioneer Venus
p0051 A80-30852
- Pioneer Venus multiprobe entry telemetry recovery
p0058 N80-26347
- Data acquisition for measuring the wind on Venus
from Pioneer Venus
p0058 N80-26361
- RANDALL, B. A.
Saturn's magnetosphere, rings, and inner satellites
p0070 A80-19119
- RANDLE, R. J.
Effects of magnification and visual accommodation
on aimpoint estimation in simulated landings
with real and virtual image displays
[NASA-TP-1635]
p0082 N80-34099
- RANDLE, R. J., JR.
Some human factors issues in the development and
evaluation of cockpit alerting and warning systems
[NASA-RP-1055]
p0082 N80-15821
- REED, T. D.
Study of boundary-layer transition using
transonic-cone preston tube data
[NASA-TM-81103]
p0010 N80-28305
- REESE, R. D.
Exercise thermoregulation after 14 days of bed rest
p0088 A80-25989
- REICHWEIN, C.
Pioneer Venus Sounder Probe gas chromatograph
p0089 A80-30845
- RESCIGNO, T. M.
Photoexcitation and ionization in molecular
fluorine - Stieltjes-Tchebycheff calculations in
the static-exchange approximation
p0046 A80-23324
- REVERCOMB, H. E.
Pioneer Venus small probes net flux radiometer
experiment
p0073 A80-30850
- REYNOLDS, R. T.
Primordial heating of asteroidal parent bodies
p0062 A80-24590
- On the comparative evolution of Ganymede and
Callisto
p0048 A80-28080
- The effect of dense cores on the structure and
evolution of Jupiter and Saturn
p0056 A80-45812
- Tidal dissipation, orbital evolution, and the
nature of Saturn's inner satellites
p0058 A80-53235
- RICCITIELLO, S. R.
Ambient curing fire resistant foams
p0063 A80-34790
- Catalysts for polyimide foams from aromatic
isocyanates and aromatic dianhydrides
[NASA-CASE-ARC-11107-1]
p0080 N80-16116
- RIDDLE, D. W.
A piloted simulator analysis of the carrier
landing capability of the quiet short-haul
research aircraft

PERSONAL AUTHOR INDEX

SCATTERGOOD, T.

[NASA-TM-78508] p0011 N80-28338
RIEDEL, S. A.
 Practical optimal flight control system design for
 helicopter aircraft. Volume 1: Technical Report
 [NASA-CR-3275] p0017 N80-23328
RIEDEL, C. A.
 Nitrogen fertiliser and stratospheric ozone -
 Latitudinal effects p0043 A80-18948
 Stratospheric ozone decrease due to
 chlorofluoromethane photolysis - Predictions of
 latitude dependence p0049 A80-29762
RIEMER, D. H.
 PRSA hydrogen tank thermal acoustic oscillation
 study [NASA-CR-152319] p0038 N80-11470
RIGHINI-COHEN, G.
 Far infrared, near infrared, and radio molecular
 line studies of HFE 2, HFE 3, and FJM 6 p0068 A80-11489
RILEY, J. J.
 Direct numerical simulations of the turbulent wake
 of an axisymmetric body p0080 A80-49235
RIZK, M. H.
 Propeller slipstream/wing interaction in the
 transonic regime [AIAA PAPER 80-0125] p0032 A80-22733
ROBERTS, L.
 An acceptable role for computers in the aircraft
 design process p0023 N80-21246
ROBERTS, W. W., JR.
 Gas dynamics in barred spirals - Gaseous density
 waves and galactic shocks p0041 A80-10685
ROCKLIN, S.
 Pioneer Venus Sounder Probe gas chromatograph
 p0089 A80-30845
ROELLIG, T. L.
 One millimeter continuum observations of
 extragalactic thermal sources [NASA-CR-163590] p0040 N80-33334
ROGALLO, R. S.
 Tests of subgrid-scale models in strained turbulence
 [AIAA PAPER 80-1339] p0065 A80-41569
ROSCOE, S. N.
 Effects of magnification and visual accommodation
 on aimpoint estimation in simulated landings
 with real and virtual image displays [NASA-TP-1635] p0082 N80-34099
ROSE, W. C.
 Unsteady density and velocity measurements in the
 6 foot x 6 foot wind tunnel p0023 N80-25594
ROSENBERG, M. L.
 Singlet oxygenation of 1,2-poly/1,4-hexadiene/s
 p0045 A80-21991
ROSIK, G.
 Pioneer Venus Sounder Probe gas chromatograph
 p0089 A80-30845
ROSITANO, S. A.
 Objective measurement of human tolerance to +G sub
 z acceleration stress [NASA-TM-81166] p0098 N80-18709
ROSSER, R. W.
 Synthesis of perfluoroalkylether oxadiazole
 elastomers p0045 A80-21992
 Synthesis of perfluoroalkylether triazine elastomers
 p0051 A80-32825
ROTH, A.
 A temperature dependent fatigue failure criterion
 for graphite/epoxy laminates p0060 A80-15518
ROUSE, S. H.
 Computer-based manuals for procedural information
 p0096 A80-50427
ROUSE, W. B.
 Computer-based manuals for procedural information
 p0096 A80-50427
ROWELL, J. D.
 Control system designs for the shuttle infrared
 telescope facility [NASA-TM-81159] p0036 N80-18869
RUBESIN, M. W.
 Progress in turbulence modeling for complex flow
 fields including effects of compressibility

[NASA-TP-1517] p0034 N80-20527
 Developments in the computation of turbulent
 boundary layers p0059 N80-27658
 A Navier-Stokes fast solver for turbulence
 modeling applications p0059 N80-27659
RUSCH, D. W.
 A model of the neutral and ion nitrogen chemistry
 in the daytime thermosphere of Venus p0067 A80-10460
RUSSELL, C. T.
 Position and shape of the Venus bow shock -
 Pioneer Venus Orbiter observations p0087 A80-15295
 A comparison of Pioneer Venus and Venera bow shock
 observations - Evidence for a solar cycle
 variation p0069 A80-15296
 Initial Pioneer Venus magnetometer observations
 p0078 A80-23690
 The location of the dayside ionopause of Venus -
 Pioneer Venus Orbiter magnetometer observations
 p0076 A80-48811
 The solar wind interaction with Venus p0076 N80-13561
RUSSELL, L. D.
 Calorimeter probes for measuring high thermal flux
 p0099 A80-29480
RUSSELL, R. W.
 Infrared spectra of IC 418 and NGC 6572
 p0069 A80-16862
 The infrared spectrum of the carbon star Y Canum
 Venaticorum between 1.2 and 30 microns
 p0046 A80-22191

S

SADLER, M.
 The intracellular Na⁺/ and K⁺/ composition of
 the moderately halophilic bacterium, Paracoccus
 halodenitrificans p0091 A80-41250
SALAT, S. W.
 X-ray spectrometer spectrograph telescope system
 p0077 A80-17502
SALZWEDDEL, H.
 Dynamic modal estimation using instrumental
 variables [NASA-CR-152396] p0019 N80-32777
SAMMONDS, R. I.
 Flying-qualities criteria for wings-level-turn
 maneuvering during an air-to-ground weapon
 delivery task [AIAA 80-1628] p0029 A80-45916
SANDBORN, V. A.
 Evaluation of the time dependent surface shear
 stress in turbulent flows [ASME PAPER 79-WA/FE-17] p0078 A80-18618
SANDER, S. P.
 Pressure and temperature dependence kinetics study
 of the NO + BrO yielding NO₂ + Br reaction -
 Implications for stratospheric bromine
 photochemistry p0068 A80-14397
SANDHU, S.
 Galileo probe thermal protection: Entry heating
 environments and spallation experiments design
 [NASA-CR-152334] p0038 N80-14184
SAVIN, L.
 Retinal changes in rats flown on Cosmos 936 - A
 cosmic ray experiment p0091 A80-41995
SAWKO, P. M.
 Ambient curing fire resistant foams p0063 A80-34790
 Catalysts for polyimide foams from aromatic
 isocyanates and aromatic dianhydrides
 [NASA-CASE-ARC-11107-1] p0080 N80-16116
SCARF, F. L.
 The Pioneer Venus Orbiter plasma wave investigation
 p0072 A80-30835
SCARGLE, J. D.
 Studies in astronomical time series analysis:
 Modeling random processes in the time domain
 [NASA-TM-81148] p0036 N80-15854
SCATTERGOOD, T.
 Organic chemistry on Titan p0087 A80-20340

- SCHADEE, A.**
Recommended conventions for defining transition moments and intensity factors in diatomic molecular spectra
p0055 A80-41323
- SCHAIERER, E. T.**
Turbulence measurements in the boundary layer of a low-speed wind tunnel using laser velocimetry [NASA-TM-81165]
p0008 N80-16300
- SCHATTE, C. L.**
Simulated weightlessness - Effects on bioenergetic balance
p0095 A80-21544
- SCHIESTEL, R.**
Multiple-time-scale concepts in turbulent transport modelling
p0080 A80-49277
- SCHIFF, L. B.**
Numerical simulation of steady supersonic flow over an ogive-cylinder-boattail body [AIAA PAPER 80-0066]
p0060 A80-19273
Mathematical modeling of the aerodynamics of high-angle-of-attack maneuvers [AIAA 80-1583]
p0028 A80-45879
Computations of the Magnus effect for slender bodies in supersonic flow [AIAA 80-1586]
p0028 A80-45882
- SCHNIDT, G. D.**
Discovery of optical molecular emission from the bipolar nebula surrounding HD 44179
p0058 A80-52399
- SCHNIDT, S. P.**
Model development for automatic guidance of a VTOL aircraft to a small aviation ship [AIAA 80-1617]
p0028 A80-45907
Navigation systems for approach and landing of VTOL aircraft [NASA-CR-152335]
p0016 N80-19055
- SCHNIDTKE, G.**
X-ray spectrometer spectrograph telescope system
p0077 A80-17502
- SCHNITZ, F. H.**
Acoustically swept rotor [NASA-CASE-ARC-11106-1]
p0102 N80-14107
- SCHUBERT, F. H.**
Development of a nitrogen generation system [NASA-CR-152333]
p0085 N80-19800
Performance characterization of a Bosch CO sub 2 reduction subsystem [NASA-CR-152342]
p0085 N80-22987
- SCHUBERT, G.**
Core cooling by subsolidus mantle convection
p0044 A80-19391
Whole planet cooling and the radiogenic heat source contents of the earth and moon
p0053 A80-36651
- SCHULMAN, T. H.**
The analysis of delays in simulator digital computing systems. Volume 1: Formulation of an analysis approach using a central example simulator model [NASA-CR-152340]
p0015 N80-17722
- SCHUSTER, E. P.**
Investigation of ground effects on large and small scale models of a three fan V/STOL aircraft configuration [NASA-CR-152240]
p0015 N80-16030
- SCHWEIZER, W.**
X-ray spectrometer spectrograph telescope system
p0077 A80-17502
- SCIARAPPA, D.**
Human acclimation and acclimatization to heat: A compendium of research, 1968-1978 [NASA-TM-81181]
p0085 N80-34056
- SCOTT, E. H.**
The role of magnetic fields in the collapse of protostellar gas clouds
p0063 A80-31848
Numerical calculations of the collapse of nonrotating, magnetic gas clouds
p0057 A80-49341
- SEACORD, C. L.**
A comparison of computer architectures for the NASA demonstration advanced avionics system
p0032 A80-32427
- SEEGER, C. L.**
On the design of a postprocessor for a search for extraterrestrial intelligence /SETI/ system [IAF PAPER 79-A-39]
p0093 A80-19895
- SEEGMILLER, H. L.**
Application of laser velocimetry to an unsteady transonic flow
p0063 A80-29506
Asymmetric trailing-edge flows at high Reynolds number [AIAA PAPER 80-1396]
p0066 A80-44151
- SEIFF, A.**
Atmosphere structure instruments on the four Pioneer Venus entry probes
p0051 A80-30849
- SELLGREN, K.**
Monoceros R2 - Far-infrared observations of a very young cluster
p0052 A80-35115
Excitation mechanisms for the unidentified infrared emission features
p0054 A80-40642
- SHALHOUB, I. M.**
Synthesis of perfluoroalkylether oxadiazole elastomers
p0045 A80-21992
- SHANABARGER, M. R.**
Isothermal-desorption-rate measurements in the vicinity of the Curie temperature for H₂ chemisorbed on nickel films
p0042 A80-16167
- SHEFFIELD, J. S.**
A three dimensional vortex wake model for missiles at high angles on attack [NASA-CR-3208]
p0014 N80-14048
- SHER, A.**
Improved characterization of the Si-SiO₂ interface
p0095 A80-41532
- SHERIDAN, T. B.**
Dynamic decisions and work load in multitask supervisory control
p0095 A80-40898
- SHIRAI, H.**
Shock-tube studies of radiative base heating of Jovian probe
p0064 A80-38114
- SHIVANANDA, T. P.**
Experimental investigation of the asymmetric body vortex wake [AIAA PAPER 80-0174]
p0032 A80-23937
- SHOLES, R. R.**
Pioneer Venus Sounder Probe Solar Flux Radiometer
p0073 A80-30846
- SHOVLIN, M. D.**
Upper surface blowing noise of the NASA-Ames quiet short-haul research aircraft [AIAA PAPER 80-1064]
p0026 A80-36002
- SHOWALTER, T. W.**
The effects of motion and g-seat cues on pilot simulator performance of three piloting tasks [NASA-TP-1601]
p0004 N80-15069
- SHVARTZ, E.**
Fluid shifts and endocrine responses during chair rest and water immersion in man
p0088 A80-25990
Fluid-electrolyte shifts and thermoregulation - Rest and work in heat with head cooling
p0091 A80-48086
- SICLARI, M. J.**
VTOL in-ground effect flows for closely spaced jets [AIAA PAPER 80-1880]
p0033 A80-46693
- SILK, J. K.**
Quest for ultrahigh resolution in X-ray optics
p0032 A80-17480
- SILVAGGIO, P. M.**
Infrared methane spectra between 1120 per cm and 1800 per cm - A new atlas
p0042 A80-13143
A new atlas of infrared methane spectra between 1120 per cm and 1800 per cm
p0042 A80-15655
Temperature dependence of intensities of the 8-12 micron bands of CFC13
p0045 A80-21559
Band model calculations for CFC13 in the 8-12 micron region
p0045 A80-21560
The surface and atmosphere of Pluto
p0045 A80-21757
- SILVERMAN, H. P.**
Microbial sulfate reduction measured by an automated electrical impedance technique
p0087 A80-21982

- Microbial mobilization of calcium and magnesium in waterlogged soils p0089 A80-32834
- SIMMONS, J. B., II
Simulated weightlessness - Effects on bioenergetic balance p0095 A80-21544
- SIMON, H.
Far infrared, near infrared, and radio molecular line studies of HFE 2, HFE 3, and FJM 6 p0068 A80-11489
- SIMONS, T. D.
An experimental investigation of two large annular diffusers with swirling and distorted inflow [NASA-TP-1628] p0005 N80-17984
- SIMPSON, J. A.
Saturnian trapped radiation and its absorption by satellites and rings - The first results from Pioneer 11 p0070 A80-19118
- SINGH, R.-W. P.
On the Routh approximation technique and least squares errors p0032 A80-20873
- SLAVIN, J. A.
Position and shape of the Venus bow shock - Pioneer Venus Orbiter observations p0087 A80-15295
A comparison of Pioneer Venus and Venera bow shock observations - Evidence for a solar cycle variation p0069 A80-15296
Initial Pioneer Venus magnetometer observations p0078 A80-23690
The location of the dayside ionopause of Venus - Pioneer Venus Orbiter magnetometer observations p0076 A80-48811
The solar wind interaction with Venus p0076 N80-13561
- SMALLEY, I. J.
Bolian sedimentation on earth and Mars - Some comparisons p0068 A80-13969
- SMITH, B. F.
Galaxy collisions - A preliminary study p0046 A80-23420
On the three-dimensional shapes of elliptical galaxies p0047 A80-26101
- SMITH, D.
Automation literature: A brief review and analysis [NASA-TM-81245] p0103 N80-34097
- SMITH, E. B.
Distortion-rotor interaction noise produced by a drooped inlet [AIAA PAPER 80-1050] p0033 A80-35994
- SMITH, E. J.
Saturn's magnetic field and magnetosphere p0021 A80-19117
Acceleration of energetic protons by interplanetary shocks p0071 A80-21183
- SMITH, G. A.
Total aircraft flight-control system - Balanced open- and closed-loop control with dynamic trim maps p0025 A80-32448
Application of the concept of dynamic trim control to automatic landing of carrier aircraft [NASA-TP-1512] p0005 N80-19126
- SMITH, H. A.
Spectroscopic evidence for two achondrite parent bodies - Asteroids 349 Dembowska and 4 Vesta p0072 A80-26173
- SMITH, J. R.
Data acquisition for measuring the wind on Venus from Pioneer Venus p0051 A80-30852
Data acquisition for measuring the wind on Venus from Pioneer Venus p0058 N80-26361
- SMITH, L. L.
High-resolution Martian atmosphere modeling p0071 A80-21765
- SMITH, R.
Analysis of transonic swept wings using asymptotic and other numerical methods [NASA-TM-80762] p0011 N80-29255
- SMITH, R. C.
Transonic swept-wing analysis using asymptotic and other numerical methods [AIAA PAPER 80-0342] p0024 A80-22751
- SMITH, S. H.
The spectrum of IRC + 10216 from 2.0 to 8.5 microns p0056 A80-44965
- SOIFER, B. T.
Infrared spectra of IC 418 and NGC 6572 p0069 A80-16862
The infrared spectrum of the carbon star Y Canum Venaticorum between 1.2 and 30 microns p0046 A80-22191
Excitation mechanisms for the unidentified infrared emission features p0054 A80-40642
- SONETT, C. P.
Saturn's magnetic field and magnetosphere p0021 A80-19117
Primordial heating of asteroidal parent bodies p0062 A80-24590
- SORENSEN, J. A.
Model development for automatic guidance of a VTOL aircraft to a small aviation ship [AIAA 80-1617] p0028 A80-45907
- SORENSEN, M. E.
Aircraft engine nozzle [NASA-CASE-ARC-10977-1] p0033 N80-32392
- SORENSEN, R. L.
Automatic mesh-point clustering near a boundary in grid generation with elliptic partial differential equations p0044 A80-20593
A computer program to generate two-dimensional grids about airfoils and other shapes by the use of Poisson's equation [NASA-TM-81198] p0036 N80-26266
- SORIA, F.
Comparison of the early stages of condensation of Cu and Ag on Mo/100/ with Cu and Ag on W/100/ p0053 A80-37193
- SPEER, R. J.
X-ray spectrometer spectrograph telescope system p0077 A80-17502
Paraboloidal X-ray telescope mirror for solar coronal spectroscopy p0078 A80-17503
- SPEITH, H.
Release-rate calorimetry of multilayered materials for aircraft seats p0051 A80-34223
- SPENCER, F. A.
Factors affecting the retirement of commercial transport jet aircraft [NASA-CR-152308] p0013 N80-10148
- SPENNER, K.
Pioneer Venus Orbiter planar retarding potential analyzer plasma experiment p0073 A80-30839
- SPIETH, H.
Release-rate calorimetry of multilayered materials for aircraft seats [AIAA 80-0759] p0064 A80-35052
- SPILLAR, E. J.
The evolution of rapid oscillations in an outburst of a dwarf nova p0075 A80-45227
- SPITZ, L. A.
The preparation of calcium superoxide in a flowing gas stream and fluidized bed [ASME PAPER 80-ENAS-18] p0094 A80-43194
- SPRINGER, G. S.
Degradation of tensile and shear properties of composites exposed to fire or high temperature p0072 A80-29697
- SREENIVASAN, K. R.
Relaminarization of fluid flows p0075 A80-40843
- SROHOVSKY, L. A.
Pioneer Venus small probes net flux radiometer experiment p0073 A80-30850
- STALLCOP, J. R.
Na + Xe collisions in the presence of two nonresonant lasers p0051 A80-32416
Computational study of alkali-metal-noble gas collisions in the presence of nonresonant lasers - Na + Xe + $\hbar/2\pi/\omega$ sub 1 + $\hbar/2\pi/\omega$

- sub 2 system
p0056 A80-48762
- STARR, W. L.**
Measurements of NO, O₃, and temperature at 19.8 km during the total solar eclipse of 26 February 1979
p0055 A80-43638
- STEDMAN, H.**
Paraboloidal X-ray telescope mirror for solar coronal spectroscopy
p0078 A80-17503
- STEELE, C. R.**
Noninvasive measures of bone bending rigidity in the monkey /M. nemestrina/
p0088 A80-21988
- STEGHER, J. L.**
Automatic mesh-point clustering near a boundary in grid generation with elliptic partial differential equations
p0044 A80-20593
An implicit finite-difference code for inviscid and viscous cascade flow
[AIAA PAPER 80-1427]
p0066 A80-44128
- STEPHENS, W. B.**
Stability of nonuniform rotor blades in hover using a mixed formulation
[NASA-TN-81226]
p0012 N80-33777
- STEVENSON, D.**
Whole planet cooling and the radiogenic heat source contents of the earth and moon
p0053 A80-36651
- STEVENSON, D. K.**
The suitability of the ILLIAC IV architecture for image processing
p0098 A80-22382
- STEWART, F. C.**
Problems and potentialities of cultured plant cells in retrospect and prospect
p0077 A80-15225
- STEWART, A. I. F.**
Design and operation of the Pioneer Venus Orbiter ultraviolet spectrometer
p0073 A80-30841
- STEWART, E. C.**
A closed-form solution for noise contours
[NASA-TP-1432]
p0004 N80-11869
- STEWART, J. D.**
Thresholds for detection of constant rotary acceleration during vibratory rotary acceleration
p0091 A80-42003
- STIENING, R. P.**
The evolution of rapid oscillations in an outburst of a dwarf nova
p0075 A80-45227
- STOCKMANN, R.**
Human acclimation and acclimatization to heat: A compendium of research, 1968-1978
[NASA-TN-81181]
p0085 N80-34056
- STOLL, R.**
Thermal design of a Shuttle infrared telescope facility /SIRTF/
[AIAA PAPER 80-1502]
p0079 A80-41466
- STRAHLER, A. H.**
Use of collateral information to improve LANDSAT classification accuracies
[E80-10268]
p0040 N80-29815
- STRECKER, D. W.**
Airborne stellar spectrophotometry from 1.2 to 5.5 microns - Absolute calibration and spectra of stars earlier than M3
p0043 A80-16407
The infrared spectrum of the carbon star Y Canum Venaticorum between 1.2 and 30 microns
p0046 A80-22191
Comparison of predicted and observed spectral energy distribution of K and M stars. I - Alpha Bootis
p0046 A80-22194
The spectrum of IRC + 10216 from 2.0 to 8.5 microns
p0056 A80-44965
- STULL, H. A.**
On the design of a postprocessor for a search for extraterrestrial intelligence /SETI/ system
[IAF PAPER 79-A-39]
p0093 A80-19895
On the significance of the apparent absence of extraterrestrials on earth
p0087 A80-21780
- STUREK, W. B.**
Numerical simulation of steady supersonic flow over an ogive-cylinder-boattail body
p0060 A80-19273
Computations of the Magnus effect for slender bodies in supersonic flow
[AIAA 80-1586]
p0028 A80-45882
- SU, P.**
Improved characterization of the Si-SiO₂ interface
p0095 A80-41532
- SUAREZ, C. B.**
Absolute intensities and pressure broadening coefficients measured at different temperatures for the 201/II/-000 band of C-12/O2/-16 at 4978/cm
p0048 A80-27125
- SULLIVAN, D. B.**
Space applications of superconductivity
p0044 A80-20126
- SUNNERS, A. L.**
The effect of dense cores on the structure and evolution of Jupiter and Saturn
p0056 A80-45812
- SUNSION, H. T.**
Effects of moisture on apparent flexure strength and on torsion and flexure fatigue properties of graphite-epoxy composites
p0063 A80-27965
- SUONI, V. E.**
Pioneer Venus small probes net flux radiometer experiment
p0073 A80-30850
- SWAN, P. R.**
Meteorological and air pollution modeling for an urban airport
p0055 A80-42659
- SYKES, H. A.**
Simulated weightlessness - Effects on bioenergetic balance
p0095 A80-21544
- SZODRUCH, J.**
Types of leeside flow over delta wings
p0052 A80-34652
- SZODRUCH, J. G.**
Leeward flow over delta wings at supersonic speeds
[NASA-TN-81187]
p0036 N80-23250
- T**
- TALBOT, P. D.**
Effects of rotor parameter variations on handling qualities of unaugmented helicopters in simulated terrain flight
[NASA-TN-81190]
p0012 N80-31407
- TARTER, J.**
A high-sensitivity search for extraterrestrial intelligence at lambda 18 cm
p0090 A80-37933
- TATUM, J. B.**
Recommended conventions for defining transition moments and intensity factors in diatomic molecular spectra
p0055 A80-41323
- TAUSSIG, R. T.**
Photocell heat engine solar power systems
p0079 A80-48179
- TAYLOR, B. J.**
Comparison of predicted and observed spectral energy distribution of K and M stars. I - Alpha Bootis
p0046 A80-22194
An investigation of previously derived Hyades, Coma, and M67 reddenings
p0049 A80-29959
The spectrum of IRC + 10216 from 2.0 to 8.5 microns
p0056 A80-44965
- TAYLOR, R. B.**
Analytical design and evaluation of an active control system for helicopter vibration reduction and gust response alleviation
[NASA-CR-152377]
p0017 N80-28369
- TAYLOR, W. W. L.**
The Pioneer Venus Orbiter plasma wave investigation
p0072 A80-30835
- TRICHMANN, J.**
An explicit algorithm for a fluid approach to nonlinear optics propagation using splitting and rezoning techniques
p0059 A80-14987
- TESORO, G.**
Materials for fire resistant passenger seats in aircraft
p0080 A80-46757

PERSONAL AUTHOR INDEX

TUZZOLINO, A. J.

- TESORO, G. C.**
Fire-resistant materials for aircraft passenger seat construction
[NASA-TM-78617] p0035 N80-13255
- THELLIG, E.**
Plains and channels in the Lunae Planum-Chryse Planitia region of Mars p0047 A80-26358
- THOMAS, P.**
Aircraft simulation data management - A prototype system p0029 A80-49832
- THOMAS, R. W.**
Landsat-based multiphase estimation of California's irrigated lands p0079 A80-27435
- THOMSEN, M. F.**
On the inference of properties of Saturn's Ring E from energetic charged particle observations p0069 A80-15293
Saturn's magnetosphere, rings, and inner satellites p0070 A80-19119
Azimuthal magnetic field at Jupiter p0076 A80-49185
- THORNSON, H. A., JR.**
Monoceros R2 - Far-infrared observations of a very young cluster p0052 A80-35115
- THORNSON, H. A., JR.**
A far-infrared study of the reflection nebula NGC 2023 p0072 A80-26111
- THUEMLER, R.**
Physiological response to hyper- and hypogravity during rollercoaster flight p0095 A80-21547
- TING, J. W.**
A real-time electronic imaging system for solar X-ray observations from sounding rockets p0029 A80-18545
- TINNEY, L.**
Irrigated lands assessment for water management Applications Pilot Test (APT) [E80-10324] p0019 N80-32815
- TINNEY, L. R.**
Landsat-based multiphase estimation of California's irrigated lands p0079 A80-27435
- TOBAK, M.**
Mathematical modeling of the aerodynamics of high-angle-of-attack maneuvers [AIAA 80-1583] p0028 A80-45879
Three-dimensional interactions and vortical flows with emphasis on high speeds [NASA-TM-81169] p0008 N80-21286
- TOBIAS, L.**
Effectiveness of advanced fuel-conservative procedures in the transitional ATC environment p0023 N80-27347
- TOHLIN, J. E.**
Fragmentation of rotating protostellar clouds p0047 A80-26107
Ring formation in rotating protostellar clouds p0048 A80-26992
- TOKUNAGA, A. T.**
Far-infrared spectra of W51-IRS 2 and W49 NW p0056 A80-44967
- TOLLINGER, D.**
Evaluation of biological models using Spacelab [ASME PAPER 80-ENAS-38] p0094 A80-43212
- TOMASKO, M. G.**
Pioneer Venus Sounder Probe Solar Flux Radiometer p0073 A80-30846
Narrow-field radiometry in a quasi-isotropic atmosphere p0079 A80-40233
- TOON, O. B.**
OCS, stratospheric aerosols and climate p0044 A80-19741
Stratospheric aerosol modification by supersonic transport and space shuttle operations - Climate implications p0047 A80-26088
The stratospheric sulfate aerosol layer - Processes, models, observations, and simulations p0051 A80-34435
Atmospheric aerosols and climate p0052 A80-36305
- Smoke and dust particles of meteoric origin in the mesosphere and stratosphere p0055 A80-42744
- Stratospheric aerosol modification by supersonic transport operations with climate implications [NASA-RP-1058] p0034 N80-15726
- TOON, W. B.**
Are solar spectral variations a drive for climatic change p0042 A80-15488
- TRABOLD, E.**
Release-rate calorimetry of multilayered materials for aircraft seats p0051 A80-34223
Release-rate calorimetry of multilayered materials for aircraft seats [AIAA 80-0759] p0064 A80-35052
- TSAL, C.-Y.**
Examination of group-velocity criterion for breakdown of vortex flow in a divergent duct p0022 A80-38049
- TSOAR, H.**
Mars - The north polar sand sea and related wind patterns p0047 A80-26370
- TSUI, K. C.**
Feasibility and concept study to convert the NASA/AMES vertical motion simulator to a helicopter simulator [NASA-CR-152193] p0098 N80-16070
- TSUO, Y. H.**
Improved characterization of the Si-SiO₂ interface p0095 A80-41532
- TSURUTANI, B. T.**
Acceleration of energetic protons by interplanetary shocks p0071 A80-21183
- TULGA, M. K.**
Dynamic decisions and work load in multitask supervisory control p0095 A80-40898
- TULLIS, R. H.**
Application of advanced technologies to small, short-haul transport aircraft [NASA-CR-152363] p0018 N80-32353
- TUNG, C. Y.**
Ambient curing fire resistant foams p0063 A80-34790
- TUOMELA, C. H.**
Civil helicopter wire strike assessment study. Volume 1: Findings and recommendations [NASA-CR-152389] p0019 N80-33381
- TURCO, R. P.**
Nitrogen fertiliser and stratospheric ozone - Latitudinal effects p0043 A80-18948
- OCS, stratospheric aerosols and climate p0044 A80-19741
- Stratospheric aerosol modification by supersonic transport and space shuttle operations - Climate implications p0047 A80-26088
- The stratospheric sulfate aerosol layer - Processes, models, observations, and simulations p0051 A80-34435
- Smoke and dust particles of meteoric origin in the mesosphere and stratosphere p0055 A80-42744
- Stratospheric aerosol modification by supersonic transport operations with climate implications [NASA-RP-1058] p0034 N80-15726
- TURLEJSKA, E.**
Extracellular hyperosmolality and body temperature during physical exercise in dogs p0092 A80-54076
- TURNBILL, C.**
Retinal changes in rats flown on Cosmos 936 - A cosmic ray experiment p0091 A80-41995
- TURNER, T. N.**
Second sound shock waves and critical velocities in liquid helium 2 [NASA-CR-162687] p0015 N80-16837
- TUZZOLINO, A. J.**
Saturnian trapped radiation and its absorption by satellites and rings - The first results from Pioneer 11 p0070 A80-19118

- THAROWSKI, R. J.
The infrared radiometer on the sounder probe of
the Pioneer Venus mission p0050 A80-30847
- TWETEN, D. E.
Aircraft simulation data management - A prototype
system p0029 A80-49832

V

- VAIDYANATHAN, T. S.
Photocell heat engine solar power systems p0079 A80-48179
- VALERO, F. P. J.
Absolute intensities and pressure broadening
coefficients measured at different temperatures
for the 201/II/-000 band of C-12/O2/-16 at 4978/cm
p0048 A80-27125
- VAN ALBADA, G. D.
Gas dynamics in barred spirals - Gaseous density
waves and galactic shocks p0041 A80-10685
- VAN ALLEN, J. A.
On the inference of properties of Saturn's Ring E
from energetic charged particle observations p0069 A80-15293
Saturn's magnetosphere, rings, and inner satellites p0070 A80-19119
Acceleration of energetic protons by
interplanetary shocks p0071 A80-21183
A comparative study of cosmic ray intensity
variations during 1972-1977 using spacecraft and
ground-based observations p0072 A80-28244
- VAN BEAUMONT, W.
Fluid-electrolyte shifts and thermoregulation -
Rest and work in heat with head cooling p0091 A80-48086
- VANDERPLAATS, G. M.
Automated design using numerical optimization
[SAE PAPER 791061] p0024 A80-26628
Optimized laser turrets for minimum phase distortion
p0023 A80-25600
- VANWINKLE, R. A.
A compilation and analysis of helicopter handling
qualities data. Volume 1: Data compilation
[NASA-CR-3144] p0013 A80-11097
- VAUSE, R.
Acoustically swept rotor
[NASA-CASE-ARC-11106-1] p0102 A80-14107
- VENKATESAN, D.
A comparative study of cosmic ray intensity
variations during 1972-1977 using spacecraft and
ground-based observations p0072 A80-28244
- VIEGAS, J. R.
An experimental and numerical investigation of a
three-dimensional shock wave separated turbulent
boundary layer p0061 A80-22727
[AIAA PAPER 80-0002]
- VILLERE, K. R.
Collapsing cloud models for Bok globules p0048 A80-26996
- VIROBIK, P. F.
The Pioneer Venus Orbiter plasma wave investigation p0072 A80-30835
- VISWANATH, P. R.
Asymmetric trailing-edge flows at high Reynolds
number p0066 A80-44151
[AIAA PAPER 80-1396]
- VOGEL, R.
Physiological response to hyper- and hypogravity
during rollercoaster flight p0095 A80-21547
- VOGRIN, J.
Pioneer Venus Sounder Probe gas chromatograph p0089 A80-30845
- VON BAUMGARTEN, R. J.
Physiological response to hyper- and hypogravity
during rollercoaster flight p0095 A80-21547
- VORREITER, J. W.
Space applications of superconductivity p0044 A80-20126
Cryogenic systems for spacecraft p0055 A80-42902

- Cryogenic container compound suspension strap
[NASA-CASE-ARC-11157-1] p0080 A80-18393
- VYKUKAL, B. C.
High-pressure protective systems technology
[ASME PAPER 79-ENAS-15] p0092 A80-15240

W

- WADCOCK, A. J.
Simple turbulence models and their application to
boundary layer separation p0017 A80-24269
[NASA-CR-3283]
- WADIA, A. R.
Application of the method of integral relations to
unsteady fluid flow problems with shocks p0078 A80-26694
Note on the eigensolution of a homogeneous
equation with semi-infinite domain p0075 A80-40508
- WAHL, D.
Analysis of two-dimensional incompressible flows
by a subsurface panel method p0029 A80-30566
- WALKER, R.
Simulation of the Infrared Astronomical Satellite
/IRAS/ telescope system p0067 A80-49842
- WALL, S. L.
Landsat-based multiphase estimation of
California's irrigated lands p0079 A80-27435
- WARNBRODT, W.
Formulation of coupled rotor/fuselage equations of
motion p0021 A80-17717
Coupled rotor and fuselage equations of motion
[NASA-TM-81153] p0006 A80-10516
- WARMING, R. F.
On the construction and application of implicit
factored schemes for conservation laws p0062 A80-27407
Alternating direction implicit methods for
parabolic equations with a mixed derivative
p0057 A80-51050
- WARNER, D. N.
Flight test of navigation and guidance sensor
errors measured on STOL approaches
[NASA-TM-81154] p0007 A80-13041
- WARREN, W. J.
Hygrothermal damage mechanisms in graphite-epoxy
composites p0038 A80-13170
[NASA-CR-3189]
- WATSON, R. T.
Pressure and temperature dependence kinetics study
of the NO + BrO yielding NO2 + Br reaction -
Implications for stratospheric bromine
photochemistry p0068 A80-14397
- WEBB, P.
The development of an elastic reverse gradient
garment to be used as a countermeasure for
cardiovascular deconditioning p0086 A80-33086
[NASA-CR-152379]
- WEBBON, B. W.
High-pressure protective systems technology
[ASME PAPER 79-ENAS-15] p0092 A80-15240
- WEBER, H. J.
Spectrophotometric identification of the pigment
associated with light-driven primary sodium
translocation in Halobacterium halobium p0088 A80-26015
- WEEKS, C. L.
Pioneer Venus Unified Abstract Data Library and
Quick Look Data Delivery System p0050 A80-30832
- WEHRBEIN, W. M.
A numerical model of the zonal mean circulation of
the middle atmosphere p0073 A80-34443
- WEHREND, W. R., JR.
Pilot control through the TAFCOS automatic flight
control system p0007 A80-14138
[NASA-TM-81152]
Flight tests of the total automatic flight control
system (Tafcos) concept on a DHC-6 Twin Otter
aircraft p0005 A80-17081
[NASA-TF-1513]
- WEIBERG, J. A.
NASA/Army XV-15 tilt rotor research aircraft

PERSONAL AUTHOR INDEX

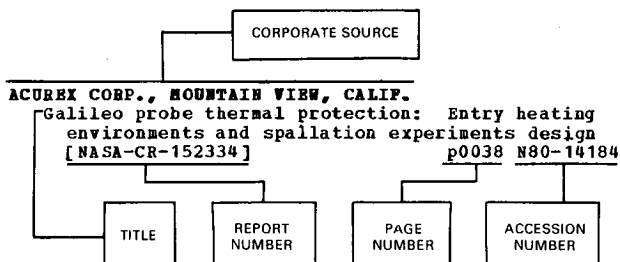
WOELLER, F.

- wind-tunnel test program plan
[NASA-TM-78562] p0007 N80-15067
- wind-tunnel tests of the XV-15 tilt rotor aircraft
[NASA-TM-81177] p0009 N80-24294
- WERNER, H. W.
Monoceros R2 - Far-infrared observations of a very young cluster p0052 A80-35115
- Excitation mechanisms for the unidentified infrared emission features p0054 A80-40642
- WHITBECK, R. F.
The analysis of delays in simulator digital computing systems. Volume 1: Formulation of an analysis approach using a central example simulator model
[NASA-CR-152340] p0015 N80-17722
- WHITCOMB, S. E.
Low-pass interference filters for submillimeter astronomy p0070 A80-19956
- WHITE, B.
Threshold windspeeds for sand on Mars - Wind tunnel simulations p0048 A80-27391
- WHITE, J.
An assessment of future computer system needs for large-scale computation
[NASA-TM-78613] p0008 N80-17717
- WHITE, H. D.
The development and use of large-motion simulator systems in aeronautical research and development p0001 A80-10765
- Resource management on the flight deck
[NASA-CP-2120] p0082 N80-22283
- WHITE, P. J.
Effect of three-body interactions on the structure of small clusters p0057 A80-49383
- WHITING, E. E.
Recommended conventions for defining transition moments and intensity factors in diatomic molecular spectra p0055 A80-41323
- WHITTEN, G. Z.
Introductory study of the chemical behavior of jet emissions in photochemical smog
[NASA-CR-152345] p0016 N80-21891
- WHITTEN, R. C.
Nitrogen fertiliser and stratospheric ozone - Latitudinal effects p0043 A80-18948
- OCS, stratospheric aerosols and climate p0044 A80-19741
- Stratospheric aerosol modification by supersonic transport and space shuttle operations - Climate implications p0047 A80-26088
- Stratospheric ozone decrease due to chlorofluoromethane photolysis - Predictions of latitude dependence p0049 A80-29762
- The stratospheric sulfate aerosol layer - Processes, models, observations, and simulations p0051 A80-34435
- Stratospheric aerosol modification by supersonic transport operations with climate implications
[NASA-RP-1058] p0034 N80-15726
- WHITTLE, D. C.
Large scale model tests of a new technology V/STOL concept
[AIAA PAPER 80-0233] p0023 A80-19303
- WHYTE, P. H.
An exploratory investigation of the STOL landing maneuver
[NASA-CR-3191] p0014 N80-12996
- WIDNALL, S. E.
Unified aerodynamic-acoustic theory for a thin rectangular wing encountering a gust p0030 A80-36401
- Examination of group-velocity criterion for breakdown of vortex flow in a divergent duct p0022 A80-38049
- Effect of tip vortex structure on helicopter noise due to blade-vortex interaction p0031 A80-52645
- WIENER, E. L.
Flight-deck automation: Promises and problems
[NASA-TM-81206] p0084 N80-26040
- WILCOX, D. C.
Recent improvements to the spinning body version of the EDDYBL computer program
[NASA-CR-152347] p0039 N80-19448
- Progress in turbulence modeling for complex flow fields including effects of compressibility
[NASA-TP-1517] p0034 N80-20527
- WILCOX, R. W.
The observed ozone flux by transient eddies, 0-30 km p0074 A80-34449
- WILLEN, S.
Thermal design of a Shuttle infrared telescope facility /SIRTF/
[AIAA PAPER 80-1502] p0079 A80-41466
- WILLIAMS, B. A.
Changes in body temperature and metabolic rate after injection of calcium into the caudal hypothalamus of the rabbit p0093 A80-27078
- NASA-Ames Life Sciences Flight Experiments program - 1980 status report
[ASME PAPER 80-ENAS-34] p0094 A80-43209
- Evaluation of biological models using Spacelab
[ASME PAPER 80-ENAS-38] p0094 A80-43212
- WILLIAMS, D. H.
Some human factors issues in the development and evaluation of cockpit alerting and warning systems
[NASA-RP-1055] p0082 N80-15821
- WILLIAMS, L. J.
Toward new small transports for commuter airlines p0021 A80-21224
- The future of short-haul transport aircraft
[SAE PAPER 800755] p0029 A80-49703
- WILLIAMS, M. H.
Aerodynamic coefficients in generalized unsteady thin airfoil theory p0030 A80-38034
- The inversion of singular integral equations by expansion in Jacobi polynomials p0030 A80-42758
- WILLIAMS, T. L.
Top inlet system feasibility for transonic-supersonic fighter aircraft applications
[AIAA PAPER 80-1809] p0033 A80-45735
- WILLNER, S. P.
Infrared spectra of IC 418 and NGC 6572 p0069 A80-16862
- The infrared spectrum of the carbon star Y Canum Venaticorum between 1.2 and 30 microns p0046 A80-22191
- WILSON, J. F.
Galileo probe forebody entry thermal protection - Aerothermal environments and heat shielding requirements
[ASME PAPER 80-ENAS-24] p0066 A80-43200
- WIMP, J.
Asymptotic behavior of the efficiencies in Mie scattering p0031 A80-47048
- WINGROVE, R. C.
Aircraft motion analysis using limited flight and radar data p0025 A80-27241
- Equations for determining aircraft motions for accident data
[NASA-TM-78609] p0010 N80-25306
- WINOVICH, W.
The 60-MW Shuttle interaction heating facility p0059 A80-12603
- WINSLOW, W.
Radiant panel tests on an epoxy/carbon fiber composite
[NASA-TM-81185] p0037 N80-32435
- WITTEBORN, F. C.
Airborne stellar spectrophotometry from 1.2 to 5.5 microns - Absolute calibration and spectra of stars earlier than M3 p0043 A80-16407
- Design alternatives for the Shuttle Infrared Telescope Facility p0060 A80-17435
- Comparison of predicted and observed spectral energy distribution of K and M stars. I - Alpha Bootis p0046 A80-22194
- The spectrum of IRC + 10216 from 2.0 to 8.5 microns p0056 A80-44965
- WOELLER, F.
Pioneer Venus Sounder Probe gas chromatograph

- Corrections in the Pioneer Venus sounder probe gas chromatographic analysis of the lower Venus atmosphere p0089 A80-30845
- WOELLER, F. H.
Chelate-modified polymers for atmospheric gas chromatography [NASA-CASE-ARC-11154-1] p0089 A80-30875
- WOLF, T. L.
Effect of tip vortex structure on helicopter noise due to blade-vortex interaction p0031 A80-52645
- WOLFE, J. H.
Position and shape of the Venus bow shock - Pioneer Venus Orbiter observations p0087 A80-15295
Preliminary results on the plasma environment of Saturn from the Pioneer 11 plasma analyzer experiment p0043 A80-19116
The Pioneer Venus Orbiter plasma analyzer experiment p0050 A80-30836
- WOLFE, W. L.
Pioneer Venus Sounder Probe Solar Flux Radiometer p0073 A80-30846
- WONG, T.
Pioneer Venus sounder and small probes Nephelometer instrument p0053 A80-36750
- WOOD, P. C.
The preparation of calcium superoxide in a flowing gas stream and fluidized bed [ASME PAPER 80-ENAS-18] p0094 A80-43194
- WOODS, R. R.
Development of the electrochemically regenerable carbon dioxide absorber for portable life support system application [ASME PAPER 79-ENAS-33] p0092 A80-15257
- WOODWARD, H. T.
Stratospheric ozone decrease due to chlorofluoromethane photolysis - Predictions of latitude dependence p0049 A80-29762
- WRAY, A.
Numerical experiments in boundary-layer stability [AIAA PAPER 80-0275] p0062 A80-23957
- WRIGHT, W. W.
Pioneer Venus Sounder Probe Neutral Gas Mass Spectrometer p0073 A80-30844
- WU, F. H.
A reanalysis of the observed interplanetary hydrogen I alpha emission profiles and the derived local interstellar gas temperature and velocity p0076 A80-49362
- WU, F.-H.
Ultraviolet photometer observations of the Saturnian system p0070 A80-19122
- WYDEVEN, T.
Plasma etching of poly/N,N'-p,p'-oxydiphenylene/pyromellitimide/ film and photo/thermal degradation of etched and unetched film p0093 A80-24158
The preparation of calcium superoxide in a flowing gas stream and fluidized bed [ASME PAPER 80-ENAS-18] p0094 A80-43194
- WYDEVEN, T. J.
Reverse osmosis membrane of high urea rejection properties [NASA-CASE-ARC-10980-1] p0097 N80-23452
- Y**
- YANG, C. Y.
Relativistic scattered wave calculations on UF₆ p0049 A80-30458
- YANG, S.-J.
The role of cesium suboxides in low-work-function surface layers studied by X-ray photoelectron spectroscopy - Ag-O-Cs p0051 A80-33844
- YEOW, Y. T.
Time-temperature behavior of a unidirectional graphite/epoxy composite p0078 A80-21141
- The viscoelastic behavior of a composite in a thermal environment [NASA-CR-163187] p0039 N80-24369
- YOSHIKAWA, K. K.
Solution of Boltzmann equation for highly nonequilibrium diatomic gases rotational translational energy relaxation p0064 A80-34904
- YOUNG, D. R.
Noninvasive measures of bone bending rigidity in the monkey /M. nemestrina/ p0088 A80-21988
- YOUNG, L. R.
Optimal estimator model for human spatial orientation p0093 A80-24265
- YOUNG, L. S.
Design alternatives for the Shuttle Infrared Telescope Facility p0060 A80-17435
- YOUNG, R. E.
Core cooling by subsolidus mantle convection p0044 A80-19391
- YUEN, G. U.
Quantification of monocarboxylic acids in the Murchison carbonaceous meteorite p0087 A80-13549
- YUNG, Y. L.
Pressure and temperature dependence kinetics study of the NO + BrO yielding NO₂ + Br reaction - Implications for stratospheric bromine photochemistry p0068 A80-14397
Origin and evolution of planetary atmospheres p0053 A80-37598
- Z**
- ZILL, L. P.
Mars ultraviolet simulation facility p0089 A80-36061
- ZIMMERMAN, I. H.
F + H₂ collisions on two electronic potential energy surfaces - Quantum-mechanical study of the collinear reaction p0068 A80-12012
- ZWICKE, P. E.
Analytical design and evaluation of an active control system for helicopter vibration reduction and gust response alleviation [NASA-CR-152377] p0017 N80-28369

CORPORATE SOURCE INDEX

Typical Corporate Source Index Listing



The title of the document is used to provide a brief description of the subject matter. The page number and NASA or AIAA accession number are included in each entry to assist the user in locating the abstract in the abstract section. If applicable, a report number is also included as an aid in identifying the document.

A

ACUREX CORP., MOUNTAIN VIEW, CALIF.
Galileo probe thermal protection: Entry heating environments and spallation experiments design [NASA-CR-152334] p0038 N80-14184

AEROSPACE CORP., LOS ANGELES, CALIF.
Saturn's rings - 3-mm observations and derived properties p0045 A80-21758

AIR FORCE FLIGHT DYNAMICS LAB., WRIGHT-PATTERSON AFB, OHIO.
A computational and experimental study of high Reynolds number viscous/inviscid interaction about a cone at high angle of attack [AIAA PAPER 80-1422] p0104 A80-44492

AIR FORCE HUMAN RESOURCES LAB., HOFFETT FIELD, CALIF.
Problem solving and decisionmaking: An integration [NASA-TM-81191] p0103 N80-22985
Decision-problem state analysis methodology [NASA-TM-81194] p0103 N80-25002

AIR FORCE WRIGHT AERONAUTICAL LABS. WRIGHT-PATTERSON AFB, OHIO.
Flying-qualities criteria for wings-level-turn maneuvering during an air-to-ground weapon delivery task [AIAA 80-1628] p0029 A80-45916

ALLIED CHEMICAL CORP., MORRISTOWN, N.J.
Time-temperature behavior of a unidirectional graphite/epoxy composite p0078 A80-21141

AMERICAN CYANAMID CO., STAMFORD, CONN.
Singlet oxygenation of 1,2-poly/1,4-hexadiene/s p0045 A80-21991

AMERICAN MATHEMATICAL SOCIETY, PROVIDENCE, R.I.
System theory as applied differential geometry [NASA-CR-3209] p0013 N80-12776

AMERICAN SCIENCE AND ENGINEERING, INC., CAMBRIDGE, MASS.
Quest for ultrahigh resolution in X-ray optics p0032 A80-17480
A real-time electronic imaging system for solar X-ray observations from sounding rockets p0029 A80-18545
X-ray bright points and the solar cycle dependence of emerging magnetic flux p0077 N80-17950

ANALYTICAL MECHANICS ASSOCIATES, INC., MOUNTAIN VIEW, CALIF.
Model development for automatic guidance of a VTOL aircraft to a small aviation ship [AIAA 80-1617] p0028 A80-45907

Navigation systems for approach and landing of VTOL aircraft [NASA-CR-152335] p0016 N80-19055
Analytical methodology for determination of helicopter IFR precision approach requirements [NASA-CR-152367] p0040 N80-28330

ARGONNE NATIONAL LAB., ILL.
SCF and CI calculations of the dipole moment function of ozone p0043 A80-17111

ARIZONA STATE UNIV., TEMPE.
Silt-clay aggregates on Mars p0041 A80-10366
Quantification of monocarboxylic acids in the Murchison carbonaceous meteorite p0087 A80-13549
Eolian sedimentation on earth and Mars - Some comparisons p0068 A80-13969
Plains and channels in the Lunae Planum-Chryse Planitia region of Mars p0047 A80-26358
Mars - The north polar sand sea and related wind patterns p0047 A80-26370
Threshold windspeeds for sand on Mars - Wind tunnel simulations p0048 A80-27391

ARIZONA UNIV., TUCSON.
Pioneer-Venus solar flux radiometer p0077 A80-17468
Saturn's magnetic field and magnetosphere p0021 A80-19117
Primordial heating of asteroidal parent bodies p0062 A80-24590
Spectroscopic evidence for two achondrite parent bodies - Asteroids 349 Dembowska and 4 Vesta p0072 A80-26173
Aircraft motion analysis using limited flight and radar data p0025 A80-27241
Pioneer Venus Sounder Probe Solar Flux Radiometer p0073 A80-30846
Narrow-field radiometry in a quasi-isotropic atmosphere p0079 A80-40233
Smoke and dust particles of meteoric origin in the mesosphere and stratosphere p0055 A80-42744

ARMY AVIATION RESEARCH AND DEVELOPMENT COMMAND, HOFFETT FIELD, CALIF.
A comprehensive analytical model of rotorcraft aerodynamics and dynamics. Part 1: Analysis development [NASA-TM-81182] p0010 N80-28296
A comprehensive analytical model of rotorcraft aerodynamics and dynamics. Part 2: User's manual [NASA-TM-81183] p0010 N80-28297
Calculation of three-dimensional unsteady transonic flows past helicopter blades [NASA-TP-1721] p0100 N80-33356

ARMY AVIATION RESEARCH AND DEVELOPMENT COMMAND, ST. LOUIS, MO.
A comprehensive analytical model of rotorcraft aerodynamics and dynamics. Part 3: Program manual [NASA-TM-81184] p0010 N80-28298
Comparison of calculated and measured helicopter rotor lateral flapping angles [NASA-TM-81213] p0012 N80-33349

ARMY RESEARCH AND TECHNOLOGY LABS., HOFFETT FIELD, CALIF.
Use of advanced computers for aerodynamic flow simulation

Comparison of calculated and measured model
rotor loading and wake geometry
[NASA-TM-81189] p0058 N80-21257
Wind-tunnel tests of the XV-15 tilt rotor aircraft
[NASA-TM-81177] p0009 N80-24262
Dynamic stall on advanced airfoil sections
[AD-A085809] p0009 N80-24294
An experimental investigation of the effects of
aeroelastic couplings on aeromechanical
stability of a hingeless rotor helicopter
[AD-A085819] p0101 N80-29252
Results of a simulator investigation of control
system and display variations for an attack
helicopter mission
[AD-A085812] p0101 N80-29294
p0101 N80-29370

B

B & K ENGINEERING, INC., TOWSON, MD.

Long term tests of the HEPP liquid trap diode
heat pipe prototype
[NASA-CR-152358] p0039 N80-22635
BALL AEROSPACE SYSTEMS DIV., BOULDER, COLO.
Design of a one-year lifetime, spaceborne
superfluid helium dewar
[ASME PAPER 79-ENAS-23] p0077 A80-15247
The infrared spectrum of the carbon star Y Canum
Venaticorum between 1.2 and 30 microns
p0046 A80-22191
The infrared radiometer on the sounder probe of
the Pioneer Venus mission
p0050 A80-30847
BALL AEROSPACE SYSTEMS DIV., GARDENA, CALIF.
Atmosphere structure instruments on the four
Pioneer Venus entry probes
p0051 A80-30849
BALLISTIC RESEARCH LABS., ABERDEEN PROVING GROUND,
MD.
Numerical simulation of steady supersonic flow
over an ogive-cylinder-boattail body
[AIAA PAPER 80-0066] p0060 A80-19273
Computations of the Magnus effect for slender
bodies in supersonic flow
[AIAA 80-1586] p0028 A80-45882
BATTILLE COLUMBUS LABS., MOUNTAIN VIEW, CALIF.
NASA aviation safety reporting system
[NASA-TM-78608] p0083 N80-18010
NASA aviation safety reporting system
[NASA-TM-81197] p0085 N80-32352
BEAM ENGINEERING, INC., SUNNYVALE, CALIF.
High resolution vertical profiles of wind,
temperature and humidity obtained by computer
processing and digital filtering of radiosonde
and radar tracking data from the ITCZ
experiment of 1977
[NASA-CR-3269] p0039 N80-21926
Simple turbulence models and their application
to boundary layer separation
[NASA-CR-3283] p0017 N80-24269
BEECH AIRCRAFT CORP., BOULDER, COLO.
Thermal design of a Shuttle infrared telescope
facility/SIRTF/
[AIAA PAPER 80-1502] p0079 A80-41466
PRSA hydrogen tank thermal acoustic oscillation
study
[NASA-CR-152319] p0038 N80-11470
BOEING COMMERCIAL AIRPLANE CO., SEATTLE, WASH.
Upper surface blowing noise of the NASA-Ames
quiet short-haul research aircraft
[AIAA PAPER 80-1064] p0026 A80-36002
A general panel method for the analysis and
design of arbitrary configurations in
incompressible flows
[NASA-CR-3079] p0017 N80-24268
An advanced panel method for analysis of
arbitrary configurations in unsteady subsonic
flow
[NASA-CR-152323] p0017 N80-26270
BOEING VERBOL CO., PHILADELPHIA, PA.
Synthesis of rotor test data for real-time
simulation
[NASA-CR-152311] p0015 N80-18029
A hingeless rotor XV-15 design integration
feasibility study. Volume 1: Engineering
design studies
[NASA-CR-152310] p0015 N80-18030
BRIGHAM YOUNG UNIV., PROVO, UTAH.
Saturn's magnetic field and magnetosphere

Modeling Jupiter's current disc - Pioneer 10
outbound p0021 A80-19117
p0075 A80-45153
BROWN UNIV., PROVIDENCE, R. I.
The settling of helium and the ages of globular
clusters p0052 A80-35151

C

CALGARY UNIV. (ALBERTA).
A comparative study of cosmic ray intensity
variations during 1972-1977 using spacecraft
and ground-based observations p0072 A80-28244
CALIFORNIA INST. OF TECH., PASADENA.
Pressure and temperature dependence kinetics
study of the NO + BrO yielding NO2 + Br
reaction - Implications for stratospheric
bromine photochemistry p0068 A80-14397
Infrared spectra of IC 418 and NGC 6572
p0069 A80-16862
Saturn's magnetic field and magnetosphere
p0021 A80-19117
Photoexcitation and ionization in molecular
oxygen - Theoretical studies of electronic
transitions in the discrete and continuous
spectral intervals p0044 A80-20275
The infrared spectrum of the carbon star Y Canum
Venaticorum between 1.2 and 30 microns
p0046 A80-22191
Meteoroid ablation spheres from deep-sea sediments
p0046 A80-22948
Photoexcitation and ionization in molecular
fluorine - Stieltjes-Tchebycheff calculations
in the static-exchange approximation p0046 A80-23324
Measurements of wind vectors, eddy momentum
transports, and energy conversions in
Jupiter's atmosphere from Voyager 1 images
A80-24159
A far-infrared study of the reflection nebula
NGC 2023 p0072 A80-26111
Calculations of the evolution of the giant planets
p0049 A80-28086
Monoceros R2 - Far-infrared observations of a
very young cluster p0052 A80-35115
Origin and evolution of planetary atmospheres
p0053 A80-37598
Excitation mechanisms for the unidentified
infrared emission features p0054 A80-40642
Second sound shock waves and critical velocities
in liquid helium 2 p0015 N80-1837
[NASA-CR-162687] CALIFORNIA POLYTECHNIC STATE UNIV., SAN LUIS OBISPO.
Effects of free-stream turbulence on diffuser
performance p0017 N80-24264
[NASA-CR-163194] CALIFORNIA STATE UNIV., FULLERTON.
Temperature dependence of intensities of the
8-12 micron bands of CFC13 p0045 A80-21559
Band model calculations for CFC13 in the 8-12
micron region p0045 A80-21560
CALIFORNIA STATE UNIV., SACRAMENTO.
Transient solution for megajoule energy release
in a lumped-parameter series RLC circuit
p0051 A80-32826
CALIFORNIA UNIV., BERKELEY.
Carbonaceous chondrites. I - Characterization
and significance of carbonaceous chondrite
/CM/ xenoliths in the Jodzie howardite
p0086 A80-13013
Molecule formation and infrared emission in fast
interstellar shocks. I Physical processes
p0043 A80-16410
High-frequency continuum observations of young
stars p0047 A80-25365
Spectrophotometric identification of the pigment
associated with light-driven primary sodium
translocation in Halobacterium halobium

CORPORATE SOURCE INDEX

Landsat-based multiphase estimation of California's irrigated lands p0088 A80-26015

A high-sensitivity search for extraterrestrial intelligence at lambda 18 cm p0079 A80-27435

The evolution of rapid oscillations in an outburst of a dwarf nova p0090 A80-37933

Irrigated lands assessment for water management Applications Pilot Test (APT) [E80-10324] p0075 A80-45227

CALIFORNIA UNIV., BERKELEY. LAWRENCE BERKELEY LAB. The radioracemization of isovaline - Cosmochemical implications p0019 N80-32815

CALIFORNIA UNIV., DAVIS. Threshold windspeeds for sand on Mars - Wind tunnel simulations p0086 A80-13018

Relativistic scattered wave calculations on UF6 p0048 A80-27391

On the calculation of turbulent heat transport downstream from an abrupt pipe expansion p0049 A80-30458

Multiple-time-scale concepts in turbulent transport modelling p0076 A80-49037

Reynolds stress closures: Status and prospects p0080 A80-49277

CALIFORNIA UNIV., LA JOLLA. The phase of the ten-hour modulation in the Jovian magnetosphere /Pioneers 10 and 11/ p0077 N80-27660

Infrared spectra of IC 418 and NGC 6572 p0067 A80-10526

Trapped radiation belts of Saturn - First look p0069 A80-16862

The implications of hydrogen emission line ratios in quasi-stellar objects p0070 A80-19121

CALIFORNIA UNIV., LIVERMORE. The effect of dense cores on the structure and evolution of Jupiter and Saturn p0072 A80-27013

CALIFORNIA UNIV., LIVERMORE. LAWRENCE LIVERMORE LAB. Photoexcitation and ionization in molecular fluorine - Stieltjes-Tchebycheff calculations in the static-exchange approximation p0056 A80-45812

CALIFORNIA UNIV., LOS ANGELES. Position and shape of the Venus bow shock - Pioneer Venus Orbiter observations p0046 A80-23324

A comparison of Pioneer Venus and Venera bow shock observations - Evidence for a solar cycle variation p0087 A80-15295

Formulation of coupled rotor/fuselage equations of motion p0069 A80-15296

Saturn's magnetic field and magnetosphere p0021 A80-17717

Core cooling by subsolidus mantle convection p0021 A80-19117

Initial Pioneer Venus magnetometer observations p0044 A80-19391

Aqueous activity on asteroids - Evidence from carbonaceous meteorites p0078 A80-23690

Whole planet cooling and the radiogenic heat source contents of the earth and moon p0062 A80-24586

The location of the dayside ionopause of Venus - Pioneer Venus Orbiter magnetometer observations p0053 A80-36651

The solar wind interaction with Venus p0076 A80-48811

CALIFORNIA UNIV., SAN DIEGO. Trapped radiation belts of Saturn - First look p0076 N80-13561

The infrared spectrum of the carbon star Y Canum Venaticorum between 1.2 and 30 microns p0070 A80-19121

CALIFORNIA UNIV., SANTA BARBARA. Isothermal-desorption-rate measurements in the vicinity of the Curie temperature for H2 chemisorbed on nickel films p0046 A80-22191

CONSEJO SUPERIOR DE INVESTIGACIONES CIENTIFICAS,

Landsat-based multiphase estimation of California's irrigated lands p0042 A80-16167

On the comparative evolution of Ganyade and Callisto p0079 A80-27435

Fragmentation in a rotating protostar - A comparison of two three-dimensional computer codes p0048 A80-28080

Protostellar formation in rotating interstellar clouds. III - Nonaxisymmetric collapse p0053 A80-38432

Tidal dissipation, orbital evolution, and the nature of Saturn's inner satellites p0054 A80-39375

Use of collateral information to improve LANDSAT classification accuracies p0058 A80-53235

CALSPAN ADVANCED TECHNOLOGY CENTER, BUFFALO, N.Y. [E80-10268] p0040 N80-29815

Implicit model following and parameter identification of unstable aircraft p0022 A80-28019

CASE WESTERN RESERVE UNIV., CLEVELAND, OHIO. A scaling theory for linear systems p0030 A80-32676

CENTRE NATIONAL DE LA RECHERCHE SCIENTIFIQUE, VERRIERES-LE-BUISSON (FRANCE). Pioneer Venus sounder and small probes Nephelometer instrument p0030 A80-32676

High-resolution Lyman-alpha filtergrams of the sun p0053 A80-36750

CHICAGO UNIV., ILL. Saturnian trapped radiation and its absorption by satellites and rings - The first results from Pioneer 11 p0075 A80-37277

Low-pass interference filters for submillimeter astronomy p0070 A80-19118

Galaxy collisions - A preliminary study p0070 A80-19956

On the three-dimensional shapes of elliptical galaxies p0046 A80-23420

The propagation of Jovian electrons to earth p0047 A80-26101

The evolution of rapid oscillations in an outburst of a dwarf nova p0074 A80-36356

CLARKSON COLL. OF TECHNOLOGY, POTSDAM, N.Y. F + H2 collisions on two electronic potential energy surfaces - Quantum-mechanical study of the collinear reaction p0075 A80-45227

COLLEGE OF WILLIAM AND MARY, WILLIAMSBURG, VA. Improved characterization of the Si-SiO2 interface p0068 A80-12012

COLORADO STATE UNIV., FORT COLLINS. Evaluation of the time dependent surface shear stress in turbulent flows [ASME PAPER 79-WA/FE-17] p0095 A80-41532

Simulated weightlessness - Effects on bioenergetic balance p0078 A80-18618

COLORADO UNIV., BOULDER. A model of the neutral and ion nitrogen chemistry in the daytime thermosphere of Venus p0095 A80-21544

A reconsideration of nucleation phenomena in light of recent findings concerning the properties of small clusters, and a brief review of some other particle growth processes p0067 A80-10460

Design and operation of the Pioneer Venus Orbiter ultraviolet spectrometer p0069 A80-15609

New gas phase inorganic ion cluster species and their atmospheric implications p0073 A80-30841

COMPUTER SCIENCES CORP., MOUNTAIN VIEW, CALIF. Aircraft simulation data management - A prototype system p0075 A80-37510

CONSEJO SUPERIOR DE INVESTIGACIONES CIENTIFICAS, MADRID (SPAIN). Comparison of the early stages of condensation p0029 A80-49832

of Cu and Ag on Mo/100/ with Cu and Ag on W/100/
p0053 A80-37193
CONTROL DATA CORP., MINNEAPOLIS, MINN.
The observed ozone flux by transient eddies,
0-30 km

p0074 A80-34449
Eddy diffusion coefficients and the variance of
the atmosphere 30-60 km

p0076 A80-45996
**COOPERATIVE INST. FOR RESEARCH IN ENVIRONMENTAL
SCIENCE, BOULDER, COLO.**

The properties of clusters in the gas phase. IV
- Complexes of H₂O and HNO_x clustering on NO_x--/
p0046 A80-23322
Properties of clusters in the gas phase. V -
Complexes of neutral molecules onto negative
ions

p0057 A80-50144
CORNELL UNIV., ITHACA, N. Y.
Proton movements in response to a light-driven
electrogenic pump for sodium ions in
Halobacterium halobium membranes

p0087 A80-17686
The infrared spectrum of the carbon star Y Canum
Venaticorum between 1.2 and 30 microns

p0046 A80-22191
The upper atmosphere of Uranus - Mean
temperature and temperature variations

p0071 A80-22207
16-30 micron spectroscopy of Titan

p0049 A80-29321
The 16- to 38-micron spectrum of Callisto

p0074 A80-35234
One millimeter continuum observations of
extragalactic thermal sources
[NASA-CR-163590] p0040 N80-33334

D

DCW INDUSTRIES, STUDIO CITY, CALIF.
Recent improvements to the spinning body version
of the EDDYBL computer program
[NASA-CR-152347] p0039 N80-19448

**DE HAVILLAND AIRCRAFT CO. OF CANADA LTD., DOWNSVIEW
(ONTARIO).**

Large scale model tests of a new technology
V/STOL concept
[AIAA PAPER 80-0233] p0023 A80-19303

Phase 1 wind tunnel tests of the J-97 powered,
external augmentor V/STOL model
[NASA-CR-152255] p0017 N80-28303

DEFENCE RESEARCH ESTABLISHMENT VALCARTIER (QUEBEC).
An explicit algorithm for a fluid approach to
nonlinear optics propagation using splitting
and rezoning techniques

p0059 A80-14987

DENVER UNIV., COLO.
Infrared methane spectra between 1120 per cm and
1800 per cm - A new atlas

p0042 A80-13143
A new atlas of infrared methane spectra between
1120 per cm and 1800 per cm

p0042 A80-15655

**DEPARTMENT OF SCIENTIFIC AND INDUSTRIAL RESEARCH,
LOWER HUTT (NEW ZEALAND).**

Eolian sedimentation on earth and Mars - Some
comparisons

p0068 A80-13969

DOUGLAS AIRCRAFT CO., INC., LONG BEACH, CALIF.
Release-rate calorimetry of multilayered
materials for aircraft seats

p0051 A80-34223
Release-rate calorimetry of multilayered
materials for aircraft seats

[AIAA 80-0759] p0064 A80-35052
Potential benefits for propfan technology on
derivatives of future short- to medium-range
transport aircraft

[AIAA PAPER 80-1090] p0026 A80-38905

DREXEL UNIV., PHILADELPHIA, PA.
Asymptotic behavior of the efficiencies in Mie
scattering

p0031 A80-47048

Feasibility studies for light scattering
experiments to determine the velocity
relaxation of small particles in a fluid

[NASA-CR-163214] p0040 N80-25586

DYNAMICS TECHNOLOGY, INC., TORRANCE, CALIF.
Skin friction measurements by a new nonintrusive

double-laser-beam oil viscosity balance
technique
[AIAA PAPER 80-1373] p0065 A80-41587

E

ERWIN W. PICK OBSERVATORY, AMES, IOWA.
The effect of dense cores on the structure and
evolution of Jupiter and Saturn

p0056 A80-45812

EYRING RESEARCH INST., PROVO, UTAH.
Theories for the origin of lunar magnetism

p0044 A80-19397

Electrical conductivity anomalies associated
with circular lunar maria

p0061 A80-23691

F

FLORIDA UNIV., GAINESVILLE.
Vorticity associated with multiple jets in a
crossflow

[NASA-CR-162855] p0016 N80-19454

FLOW RESEARCH, INC., KENT, WASH.
Propeller slipstream/wing interaction in the
transonic regime

[AIAA PAPER 80-0125] p0032 A80-22733

Direct numerical simulations of the turbulent
wake of an axisymmetric body

p0080 A80-49235

FLOW SIMULATIONS, INC., SUNNYVILLE, CALIF.
Computation of supersonic turbulent flows over
an inclined ogive-cylinder-flare

[AIAA PAPER 80-1410] p0066 A80-41608

An implicit finite-difference code for inviscid
and viscous cascade flow

[AIAA PAPER 80-1427] p0066 A80-44128

FRANKLIN INST. RESEARCH LABS., PHILADELPHIA, PA.
Feasibility and concept study to convert the
NASA/AMES vertical motion simulator to a
helicopter simulator

[NASA-CR-152193] p0098 N80-16070

G

GARD, INC., NILES, ILL.
Water recovery by catalytic treatment of urine
vapor

[ASME PAPER 80-ENAS-16] p0093 A80-43192

Design, fabrication and testing of a dual
catalyst ammonia removal system for a urine
VCD unit

[NASA-CR-152372] p0085 N80-29023

GENERAL DYNAMICS/CONVAIR, SAN DIEGO, CALIF.
Wind tunnel investigation of an oblique wing
transport model at mach numbers between 0.6
and 1.4

[NASA-CR-137697] p0013 N80-12059

Application of advanced technologies to small,
short-haul air transports

[NASA-CR-152364] p0019 N80-33396

GENERAL ELECTRIC CO., CINCINNATI, OHIO.
Acoustic characteristics of two hybrid inlets at
forward speed

[AIAA PAPER 79-0678] p0021 A80-20828

Analytical study of the effects of wind tunnel
turbulence on turbofan rotor noise

[AIAA PAPER 80-1022] p0033 A80-35978

Distortion-rotor interaction noise produced by a
drooped inlet

[AIAA PAPER 80-1050] p0033 A80-35994

Analytical study of the effects of wind tunnel
turbulence on turbofan rotor noise

[NASA-CR-152359] p0016 N80-23099

GENERAL ELECTRIC CO., EVENDALE, OHIO.
Fan noise caused by the ingestion of anisotropic
turbulence - A model based on axisymmetric
turbulence theory

[AIAA PAPER 80-1021] p0032 A80-35977

GENERAL ELECTRIC CO., SAN JOSE, CALIF.
Some observations regarding the statistical
determination of stress rupture regression lines

p0041 A80-12828

GENERAL ELECTRIC CO., SCHENECTADY, N. Y.
Fan noise caused by the ingestion of anisotropic
turbulence - A model based on axisymmetric
turbulence theory

[AIAA PAPER 80-1021] p0032 A80-35977

GEORGIA INST. OF TECH., ATLANTA.

Preliminary calculations concerning the maintenance of the zonal mean ozone distribution in the Northern Hemisphere
p0074 A80-34445

Guiding the development of a controlled ecological life support system
[NASA-CR-162452] p0085 N80-12735

GRUMMAN AEROSPACE CORP., BETHPAGE, N.Y.

High-resolution Martian atmosphere modeling
p0071 A80-21765

Transonic swept-wing analysis using asymptotic and other numerical methods
[AIAA PAPER 80-0342] p0024 A80-22751

VTOL in-ground effect flows for closely spaced jets
[AIAA PAPER 80-1880] p0033 A80-46693

H

HALE OBSERVATORIES, PASADENA, CALIF.

Monoceros R2 - Far-infrared observations of a very young cluster
p0052 A80-35115

HARVARD UNIV., CAMBRIDGE, MASS.

Feedback invariants for nonlinear systems
p0031 A80-14810

A scaling theory for linear systems
p0030 A80-32676

Simple Cassegrain scanning system for infrared astronomy
p0074 A80-34729

HEBREW UNIV., JERUSALEM (ISRAEL).

Asymptotic behavior of the efficiencies in Mie scattering
p0031 A80-47048

HEIDELBERG UNIV. (WEST GERMANY).

Radiatively driven winds for different power law spectra
p0054 A80-40138

HONEYWELL, INC., MINNEAPOLIS, MINN.

A comparison of computer architectures for the NASA demonstration advanced avionics system
p0032 A80-32427

HUGHES AIRCRAFT CO., CULVER CITY, CALIF.

Thermophysical and flammability characterization of phosphorylated epoxy adhesives
p0066 A80-48079

HUGHES AIRCRAFT CO., EL SEGUNDO, CALIF.

Pioneer Venus Orbiter Radar Mapper - Design and operation
p0050 A80-30833

HUGHES AIRCRAFT CO., LOS ANGELES, CALIF.

Free convection in enclosures exposed to compressive heating
[AIAA PAPER 80-1536] p0079 A80-41495

HUMAN RESOURCES RESEARCH ORGANIZATION, ALEXANDRIA, VA.

Civil helicopter wire strike assessment study. Volume 1: Findings and recommendations
[NASA-CR-152389] p0019 N80-33381

HUMBOLDT STATE UNIV., ARCATA, CALIF.

Using guided clustering techniques to analyze Landsat data for mapping forest land cover in northern California
p0078 A80-25595

HUNGARIAN ACADEMY OF SCIENCES, BUDAPEST.

Hot hydrogen in the exosphere of Venus
p0070 A80-18943

I

IBM WATSON RESEARCH CENTER, YORKTOWN HEIGHTS, N.Y.

Self-gravitating gas flow in barred spiral galaxies
p0055 A80-44959

IDAHO UNIV., MOSCOW.

Perfluoroether triazine elastomers
[NASA-CR-162748] p0039 N80-16166

ILLINOIS INST. OF TECH., CHICAGO.

An assessment of future computer system needs for large-scale computation
[NASA-TM-78613] p0008 N80-17717

IMPERIAL COLL. OF SCIENCE AND TECHNOLOGY, LONDON (ENGLAND).

X-ray spectrometer spectrograph telescope system
p0077 A80-17502

Paraboloidal X-ray telescope mirror for solar coronal spectroscopy

INDIAN INST. OF SCIENCE, BANGALORE.

Relaminarization of fluid flows
p0075 A80-40843

INDIANA UNIV., BLOOMINGTON.

Photoexcitation and ionization in molecular oxygen - Theoretical studies of electronic transitions in the discrete and continuous spectral intervals
p0044 A80-20275

Photoexcitation and ionization in molecular fluorine - Stieltjes-Tchebycheff calculations in the static-exchange approximation
p0046 A80-23324

INFORMATICS, INC., PALO ALTO, CALIF.

Galileo probe forebody entry thermal protection - Aerothermal environments and heat shielding requirements
[ASME PAPER 80-ENAS-24] p0066 A80-43200

Simulation of the Infrared Astronomical Satellite /IRAS/ telescope system
p0067 A80-49842

INNSBRUCK UNIV. (AUSTRIA).

New gas phase inorganic ion cluster species and their atmospheric implications
p0075 A80-37510

INSTITUT FUER PHYSIKALISCHE WELTRAUMFORSCHUNG, FREIBURG (WEST GERMANY).

X-ray spectrometer spectrograph telescope system
p0077 A80-17502

Pioneer Venus Orbiter planar retarding potential analyzer plasma experiment
p0073 A80-30839

IOWA STATE UNIV. OF SCIENCE AND TECHNOLOGY, AMES.

Supersonic flow over three-dimensional ablated nosetips using an unsteady implicit numerical procedure
[AIAA PAPER 80-0063] p0060 A80-19271

Threshold windspeeds for sand on Mars - Wind tunnel simulations
p0048 A80-27391

Calculations of the evolution of the giant planets
p0049 A80-28086

Test section configuration for aerodynamic testing in shock tubes
p0026 A80-38085

IOWA UNIV., IOWA CITY.

On the inference of properties of Saturn's Ring E from energetic charged particle observations
p0069 A80-15293

Preliminary results on the plasma environment of Saturn from the Pioneer 11 plasma analyzer experiment
p0043 A80-19116

Saturn's magnetosphere, rings, and inner satellites
p0070 A80-19119

Acceleration of energetic protons by interplanetary shocks
p0071 A80-21183

A comparative study of cosmic ray intensity variations during 1972-1977 using spacecraft and ground-based observations
p0072 A80-28244

Azimuthal magnetic field at Jupiter
p0076 A80-49185

The acceleration of energetic charged particles by interplanetary and supernova shock waves
p0080 A80-53209

J

JET PROPULSION LAB., CALIFORNIA INST. OF TECH., PASADENA.

Pressure and temperature dependence kinetics study of the NO + BrO yielding NO2 + Br reaction - Implications for stratospheric bromine photochemistry
p0068 A80-14397

Saturn's magnetic field and magnetosphere
p0021 A80-19117

Ultraviolet photometer observations of the Saturnian system
p0070 A80-19122

Acceleration of energetic protons by interplanetary shocks
p0071 A80-21183

Saturn's rings - 3-mm observations and derived properties

Noise generation by a lifting wing/flap combination at Reynolds numbers to 2.8×10 to the 6th
[AIAA PAPER 80-0035] p0045 A80-21758
Measurements of wind vectors, eddy momentum transports, and energy conversions in Jupiter's atmosphere from Voyager 1 images
A80-24159
Pioneer Venus occultation radio science data generation
p0050 A80-30830
Pioneer Venus Multiprobe entry telemetry recovery
p0050 A80-30831
Data acquisition for measuring the wind on Venus from Pioneer Venus
p0051 A80-30852
Simple Cassegrain scanning system for infrared astronomy
p0074 A80-34729
Pioneer Venus multiprobe entry telemetry recovery
p0058 A80-26347
Data acquisition for measuring the wind on Venus from Pioneer Venus
p0058 A80-26361
JOINT INST. FOR LAB. ASTROPHYSICS, BOULDER, COLO.
Tidal dissipation, orbital evolution, and the nature of Saturn's inner satellites
p0058 A80-53235

K

KENT STATE UNIV., OHIO.
Adsorption interference in mixtures of trace contaminants flowing through activated carbon adsorber beds
[ASME PAPER 80-ENAS-17] p0096 A80-43193

L

LEAR SIEGLER, INC., SANTA MONICA, CALIF.
A comparison of flight and simulation data for three automatic landing system control laws for the Augmentor wing jet STOL research airplane
[NASA-CR-152365] p0018 A80-32338
LEHIGH UNIV., BETHLEHEM, PA.
Integrated band intensities of gaseous N_2O_5
p0047 A80-25660
LICK OBSERVATORY, SANTA CRUZ, CALIF.
Fragmentation of rotating protostellar clouds
p0047 A80-26107
Ring formation in rotating protostellar clouds
p0048 A80-26992
Calculations of the evolution of the giant planets
p0049 A80-28086
Fragmentation in a rotating protostar - A comparison of two three-dimensional computer codes
p0053 A80-38432
Discovery of optical molecular emission from the bipolar nebula surrounding HD 44179
p0058 A80-52399
LIFE SYSTEMS, INC., CLEVELAND, OHIO.
Bosch - An alternate CO2 reduction technology
[ASME PAPER 79-ENAS-32] p0092 A80-15256
Development of the electrochemically regenerable carbon dioxide absorber for portable life support system application
[ASME PAPER 79-ENAS-33] p0092 A80-15257
Development of a nitrogen generation system
[NASA-CR-152333] p0085 N80-19800
Performance characterization of a Bosch CO sub 2 reduction subsystem
[NASA-CR-152342] p0085 N80-22987
LOCKHEED-CALIFORNIA CO., BURBANK.
Application of advanced technologies to small, short-haul transport aircraft
[NASA-CR-152363] p0018 A80-32353
LOCKHEED MISSILES AND SPACE CO., PALO ALTO, CALIF.
X-ray spectrometer spectrograph telescope system
p0077 A80-17502
Paraboloidal X-ray telescope mirror for solar coronal spectroscopy
p0078 A80-17503
Pioneer Venus Orbiter planar retarding potential analyzer plasma experiment
p0073 A80-30839

High-resolution Lyman-alpha filtergrams of the sun
p0075 A80-37277
Hygrothermal damage mechanisms in graphite-epoxy composites
[NASA-CR-3189] p0038 N80-13170
LOCKHEED MISSILES AND SPACE CO., SUNNYVALE, CALIF.
Studies for improved high temperature coatings for Space Shuttle application
p0079 A80-34757
Development of high viscosity coatings for advanced Space Shuttle applications
p0079 A80-34760
The development of a Space Shuttle Research Animal Holding Facility
[ASME PAPER 80-ENAS-39] p0096 A80-43213
Large Deployable Reflector (LDR)
[NASA-CR-152402] p0040 N80-33319
LOCKHEED SOLAR OBSERVATORY, PALO ALTO, CALIF.
Simple Cassegrain scanning system for infrared astronomy
p0074 A80-34729
LOUISVILLE UNIV., KY.
A model for hypokinesia: Effects on muscle atrophy in the rat
p0095 A80-28188
LOWELL OBSERVATORY, FLAGSTAFF, ARIZ.
Infrared methane spectra between 1120 per cm and 1800 per cm - A new atlas
p0042 A80-13143
A new atlas of infrared methane spectra between 1120 per cm and 1800 per cm
p0042 A80-15655

M

MAINZ UNIV. (WEST GERMANY).
Physiological response to hyper- and hypogravity during rollercoaster flight
p0095 A80-21547
MARTIN MARIETTA AEROSPACE, DENVER, COLO.
An entry and landing probe for Titan
[AIAA PAPER 80-0117] p0060 A80-18384
Heterogeneous phase reactions of Martian volatiles with putative regolith minerals
p0090 A80-36062
Reformulation of Possio's kernel with application to unsteady wind tunnel interference
p0031 A80-43129
MARTIN MARIETTA CORP., DENVER, COLO.
Comet nucleus impact probe feasibility study
[NASA-CR-152375] p0040 N80-26364
Titan probe technology assessment and technology development plan study
[NASA-CR-152381] p0040 N80-32417
MARYLAND UNIV., COLLEGE PARK.
Acceleration of energetic protons by interplanetary shocks
p0071 A80-21183
MASSACHUSETTS INST. OF TECH., CAMBRIDGE.
On the Routh approximation technique and least squares errors
p0032 A80-20873
The upper atmosphere of Uranus - Mean temperature and temperature variations
p0071 A80-22207
Optimal estimator model for human spatial orientation
p0093 A80-24265
Pioneer Venus Orbiter Radar Mapper - Design and operation
p0050 A80-30833
The radius and ellipticity of Uranus from its occultation of SAO 158687
p0073 A80-31937
Preliminary calculations concerning the maintenance of the zonal mean ozone distribution in the Northern Hemisphere
p0074 A80-34445
Unified aerodynamic-acoustic theory for a thin rectangular wing encountering a gust
p0030 A80-36401
Examination of group-velocity criterion for breakdown of vortex flow in a divergent duct
p0022 A80-38049
Dynamic decisions and work load in multitask supervisory control
p0095 A80-40898
Visually induced self-motion sensation adapts rapidly to left-right visual reversal

N

p0096 A80-44213
Materials for fire resistant passenger seats in aircraft

p0080 A80-48757
Effect of tip vortex structure on helicopter noise due to blade-vortex interaction

p0031 A80-52645
The design, testing and evaluation of the MIT individual-blade-control system as applied to gust alleviation for helicopters
[NASA-CR-152352] p0016 N80-22357

MATHEMATICAL SCIENCES NORTHWEST, INC., BELLEVUE, WASH.
Photocell heat engine solar power systems p0079 A80-48179

MAX-PLANCK-INSTITUT FUER AERONOMIE, KATLENBURG-LINDAU (WEST GERMANY).
Trapped radiation belts of Saturn - First look p0070 A80-19121

MCDONNELL AIRCRAFT CO., ST. LOUIS, MO.
Investigation of ground effects on large and small scale models of a three fan V/STOL aircraft configuration
[NASA-CR-152240] p0015 N80-16030

MERCHANT MARINE ACADEMY, KINGS POINT, N. Y.
Far infrared, near infrared, and radio molecular line studies of HFE 2, HFE 3, and FJM 6 p0068 A80-11489

METRICS, INC., ATLANTA, GA.
Guiding the development of a controlled ecological life support system
[NASA-CR-162452] p0085 N80-12735

MICHIGAN STATE UNIV., EAST LANSING.
The settling of helium and the ages of globular clusters p0052 A80-35151

MICHIGAN UNIV., ANN ARBOR.
A model of the neutral and ion nitrogen chemistry in the daytime thermosphere of Venus p0067 A80-10460

Hot hydrogen in the exosphere of Venus p0070 A80-18943

Physiological response to hyper- and hypogravity during rollercoaster flight p0095 A80-21547

Degradation of tensile and shear properties of composites exposed to fire or high temperature p0072 A80-29697

The evolution of rapid oscillations in an outburst of a dwarf nova p0075 A80-45227

The location of the dayside ionopause of Venus - Pioneer Venus Orbiter magnetometer observations p0076 A80-48811

Math modeling and computer mechanization for real time simulation of rotary-wing aircraft
[NASA-CR-162400] p0013 N80-10137

MILAN UNIV. (ITALY).
A microprocessor-based instrument for neural pulse wave analysis p0098 A80-50322

MINISTRY OF HEALTH OF THE USSR, MOSCOW.
Retinal changes in rats flown on Cosmos 936 - A cosmic ray experiment p0091 A80-41995

MINNESOTA UNIV., MINNEAPOLIS.
Infrared spectra of IC 418 and NGC 6572 p0069 A80-16862

Noble gas trapping and fractionation during synthesis of carbonaceous matter p0093 A80-23669

Analysis of two-dimensional incompressible flows by a subsurface panel method p0029 A80-30566

MISSOURI UNIV., COLUMBIA.
A model for hypokinesia: Effects on muscle atrophy in the rat p0095 A80-28188

MONTREAL UNIV. (QUEBEC).
An explicit algorithm for a fluid approach to nonlinear optics propagation using splitting and rezoning techniques p0059 A80-14987

MURPHYS CENTER OF PLANETOLOGY, CALIF.
Endogenic craters on basaltic lava flows - Size frequency distributions p0061 A80-23727

NATIONAL AERONAUTICS AND SPACE ADMINISTRATION, WASHINGTON, D. C.

On the comparative evolution of Ganyade and Callisto p0048 A80-28080

An Assessment of Ground-Based Techniques for Detecting Other Planetary Systems. Volume 2: Position papers
[NASA-CP-2124-VOL-2] p0034 N80-25224

NATIONAL AERONAUTICS AND SPACE ADMINISTRATION. FLIGHT RESEARCH CENTER, EDWARDS, CALIF.

A computational and experimental study of high Reynolds number viscous/inviscid interaction about a cone at high angle of attack
[AIAA PAPER 80-1422] p0104 A80-44492

NATIONAL AERONAUTICS AND SPACE ADMINISTRATION. GODDARD SPACE FLIGHT CENTER, GREENBELT, MD.

A high-sensitivity search for extraterrestrial intelligence at lambda 18 cm p0090 A80-37933

The location of the dayside ionopause of Venus - Pioneer Venus Orbiter magnetometer observations p0076 A80-48811

Comparison of the Nimbus-4 UV ozone data with the Ames two-dimensional model
[NASA-TN-81207] p0036 N80-24914

NATIONAL AERONAUTICS AND SPACE ADMINISTRATION. LYNDON B. JOHNSON SPACE CENTER, HOUSTON, TEX.

Meteoroid ablation spheres from deep-sea sediments p0046 A80-22948

NATIONAL AERONAUTICS AND SPACE ADMINISTRATION. LANGLEY RESEARCH CENTER, HAMPTON, VA.

On the 'thickness' of Saturn's rings caused by satellite and solar perturbations and by planetary precession. p0042 A80-14293

Improved characterization of the Si-SiO₂ interface p0095 A80-41532

NATIONAL AERONAUTICS AND SPACE ADMINISTRATION. LEWIS RESEARCH CENTER, CLEVELAND, OHIO.

An implicit finite-difference code for inviscid and viscous cascade flow
[AIAA PAPER 80-1427] p0066 A80-44128

NATIONAL AERONAUTICS AND SPACE ADMINISTRATION. MARSHALL SPACE FLIGHT CENTER, HUNTSVILLE, ALA.

Bosch - An alternate CO₂ reduction technology
[ASME PAPER 79-ENAS-32] p0092 A80-15256

NATIONAL BUREAU OF STANDARDS, BOULDER, COLO.

Space applications of superconductivity p0044 A80-20126

NATIONAL BUREAU OF STANDARDS, WASHINGTON, D.C.
Recommended conventions for defining transition moments and intensity factors in diatomic molecular spectra

p0055 A80-41323
NATIONAL INST. ON AGING, BALTIMORE, MD.
 Review of cell aging in Drosophila and mouse
 p0087 A80-17741
NATIONAL PHYSICAL LAB., TEDDINGTON (ENGLAND).
 X-ray spectrometer spectrograph telescope system
 p0077 A80-17502
 Paraboloidal X-ray telescope mirror for solar
 coronal spectroscopy
 p0078 A80-17503
NAVAL OCEAN SYSTEMS CENTER, SAN DIEGO, CALIF.
 Modeling Jupiter's current disc - Pioneer 10
 outbound
 p0075 A80-45153
NEGEV UNIV., BEERSHEVA (ISRAEL).
 Mars - The north polar sand sea and related wind
 patterns
 p0047 A80-26370
NEVADA UNIV., LAS VEGAS.
 Integral equations for flows in wind tunnels
 p0029 A80-21906
 Reformulation of Possio's kernel with
 application to unsteady wind tunnel interference
 p0031 A80-43129
NEW MEXICO STATE UNIV., LAS CRUCES.
 Measurements of wind vectors, eddy momentum
 transports, and energy conversions in
 Jupiter's atmosphere from Voyager 1 images
 A80-24159
NEW MEXICO UNIV., ALBUQUERQUE.
 Heterogeneous phase reactions of Martian
 volatiles with putative regolith minerals
 p0090 A80-36062
**NIELSEN ENGINEERING AND RESEARCH, INC., MOUNTAIN
 VIEW, CALIF.**
 Tests of subgrid-scale models in strained
 turbulence
 [AIAA PAPER 80-1339] p0065 A80-41569
 A correlation method to predict the surface
 pressure distribution of an infinite plate or
 a body of revolution from which a jet is issuing
 [NASA-CR-152345] p0018 N80-32339
NORTHROP CORP., HAWTHORNE, CALIF.
 Top inlet system feasibility for
 transonic-supersonic fighter aircraft
 applications
 [AIAA PAPER 80-1809] p0033 A80-45735
 System description and analysis. Part 1:
 Feasibility study for helicopter/VTOL
 wide-angle simulation image generation display
 system
 [NASA-CR-152376] p0101 N80-27397
NORTHWESTERN UNIV., EVANSTON, ILL.
 Factors affecting the retirement of commercial
 transport jet aircraft
 [NASA-CR-152308] p0013 N80-10148
NOTRE DAME UNIV., IND.
 Modular theory of inverse systems
 [NASA-CR-162491] p0013 N80-12782

O

OHIO STATE UNIV., COLUMBUS.
 Hypergravity and estrogen effects on avian
 anterior pituitary growth hormone and
 prolactin levels
 p0094 A80-20447
 The architecture of the avian retina following
 exposure to chronic 2 G
 p0096 A80-42013
 Multi-modal information processing for visual
 workload relief.
 [NASA-CR-162720] p0100 N80-16737
OKLAHOMA STATE UNIV., STILLWATER.
 Study of boundary-layer transition using
 transonic-cone preston tube data
 [NASA-TM-81103] p0010 N80-28305

P

**PACIFIC ENGINEERING DESIGN ANALYSIS CO., PALO ALTO,
 CALIF.**
 Forebody and base region real-gas flow in severe
 planetary entry by a factored implicit
 numerical method. I - Computational fluid
 dynamics
 [AIAA PAPER 80-0065] p0061 A80-22731
PARIS VI UNIV. (FRANCE).
 Review of cell aging in Drosophila and mouse

p0087 A80-17741
PARIS XI UNIV., ORSAY (FRANCE).
 Ground-state rotational constants of $^{13}\text{C}-^{13}\text{H}_3\text{D}$
 p0054 A80-41175
PERKIN-ELMER CORP., DANBURY, CONN.
 Thermal design of a Shuttle infrared telescope
 facility /SIRTF/
 [AIAA PAPER 80-1502] p0079 A80-41466
POLISH ACADEMY OF SCIENCES, WARSAW.
 Extracellular hyperosmolality and body
 temperature during physical exercise in dogs
 p0092 A80-54076
POLIATONICS RESEARCH, INC., MOUNTAIN VIEW, CALIF.
 Effect of three-body interactions on the
 structure of small clusters
 p0057 A80-49383
POMONA COLL., CLAREMONT, CALIF.
 Heterogeneous phase reactions of Martian
 volatiles with putative regolith minerals
 p0090 A80-36062
PRINCETON UNIV., N. J.
 Aerodynamic coefficients in generalized unsteady
 thin airfoil theory
 p0030 A80-38034
 The inversion of singular integral equations by
 expansion in Jacobi polynomials
 p0030 A80-42758
 An exploratory investigation of the STOL landing
 maneuver
 [NASA-CR-3191] p0014 N80-12996
 A simulator study of control and display
 augmentations for helicopters
 [NASA-CR-163451] p0018 N80-31408
PURDUE UNIV., LAFAYETTE, IND.
 Optimal control model predictions of system
 performance and attention allocation and their
 experimental validation in a display design
 study
 p0095 A80-40899
 Eddy diffusion coefficients and the variance of
 the atmosphere 30-60 km
 p0076 A80-45996

R

R AND D ASSOCIATES, MARINA DEL REY, CALIF.
 Nitrogen fertiliser and stratospheric ozone -
 Latitudinal effects
 p0043 A80-18948
OCS, stratospheric aerosols and climate
 p0044 A80-19741
 Stratospheric aerosol modification by supersonic
 transport and space shuttle operations -
 Climate implications
 p0047 A80-26088
 The stratospheric sulfate aerosol layer -
 Processes, models, observations, and simulations
 p0051 A80-34435
 Smoke and dust particles of meteoric origin in
 the mesosphere and stratosphere
 p0055 A80-42744
**RAHMAN AERONAUTICS RESEARCH AND ENGINEERING, INC.,
 PALO ALTO, CALIF.**
 Pressure and temperature fields associated with
 aero-optics tests
 p0031 N80-25591
ROCHESTER UNIV., N. Y.
 Quantum-mechanical calculation of
 three-dimensional atom-diatom collisions in
 the presence of intense laser radiation
 p0068 A80-15221
 An angular momentum approximation for molecular
 collisions in the presence of intense laser
 radiation
 p0069 A80-15673
 A new propagation method for the radial
 Schroedinger equation
 p0069 A80-15768
 Na + Xe collisions in the presence of two
 nonresonant lasers
 p0051 A80-32416
 Computational study of alkali-metal-noble gas
 collisions in the presence of nonresonant
 lasers - Na + Xe + $h/2\pi/\omega$ sub 1 +
 $h/2\pi/\omega$ sub 2 system
 p0056 A80-48762
ROCKWELL INTERNATIONAL CORP., LOS ANGELES, CALIF.
 Ambient curing fire resistant foams
 p0063 A80-34790

S

SAN FRANCISCO STATE UNIV., CALIF.

- Numerical calculations of the collapse of nonrotating, magnetic gas clouds p0057 A80-49341
- An extended soft-cube model for the thermal accommodation of gas atoms on solid surfaces [NASA-TM-81163] p0035 N80-14941

SAN FRANCISCO UNIV., CALIF.

- On the design of a postprocessor for a search for extraterrestrial intelligence /SETI/ system [IAF PAPER 79-A-39] p0093 A80-19895
- Toxicity of pyrolysis gases from foam plastics p0071 A80-24625

SAN JOSE STATE UNIV., CALIF.

- Review of cell aging in *Drosophila* and mouse p0087 A80-17741
- Nitrogen fertilizer and stratospheric ozone - Latitudinal effects p0043 A80-18948

- Singlet oxygenation of 1,2-poly/1,4-hexadiene/s p0045 A80-21991
- Synthesis of perfluoroalkylether oxadiazole elastomers p0045 A80-21992

- Meteoroid ablation spheres from deep-sea sediments p0046 A80-22948
- Favorable effects of the antioxidants sodium and magnesium thiazolidine carboxylate on the vitality and life span of *Drosophila* and mice p0089 A80-29085

- Stratospheric ozone decrease due to chlorofluoromethane photolysis - Predictions of latitude dependence p0049 A80-29762
- An investigation of previously derived Hyades, Coma, and M67 reddening p0049 A80-29959

- Synthesis of perfluoroalkylether triazine elastomers p0051 A80-32825
- Thresholds for detection of constant rotary acceleration during vibratory rotary acceleration p0091 A80-42003

- Meteorological and air pollution modeling for an urban airport p0055 A80-42659
- The preparation of calcium superoxide in a flowing gas stream and fluidized bed [ASME PAPER 80-ENAS-18] p0094 A80-43194

- Thermophysical and flammability characterization of phosphorylated epoxy adhesives p0066 A80-48079
- Perception and performance in flight simulators: The contribution of vestibular, visual, and auditory information [NASA-CR-162129] p0085 N80-11103

- The effect of viewing time, time to encounter, and practice on perception of aircraft separation on a cockpit display of traffic information [NASA-TM-81173] p0083 N80-18038

- Chelate-modified polymers for atmospheric gas chromatography [NASA-CASE-ARC-11154-1] p0097 N80-23383
- Radiant panel tests on an epoxy/carbon fiber composite [NASA-TM-81185] p0037 N80-32435

SANTA BARBARA RESEARCH CENTER, GOLETA, CALIF.

- The infrared radiometer on the sounder probe of the Pioneer Venus mission p0050 A80-30847

SANTA CLARA UNIV., CALIF.

- On the design of a postprocessor for a search for extraterrestrial intelligence /SETI/ system [IAF PAPER 79-A-39] p0093 A80-19895
- Monte Carlo simulation of lunar megaregolith and implications p0061 A80-23716

- Effect of simulated weightlessness on the immune system in rats p0088 A80-25894
- Threshold windspeeds for sand on Mars - Wind tunnel simulations p0048 A80-27391

SCIENCE APPLICATIONS, INC., LOS ANGELES, CALIF.

- Application of parametric weight and cost estimating relationships to future transport aircraft [SAWE PAPER 1292] p0024 A80-20637
- Parametric study of helicopter aircraft systems costs and weights [NASA-CR-152315] p0016 N80-22305

SIKORSKY AIRCRAFT, STRATFORD, CONN.

- Analytical design and evaluation of an active control system for helicopter vibration reduction and gust response alleviation [NASA-CR-152377] p0017 N80-28369
- Analysis and correlation of test data from an advanced technology rotor system [NASA-CR-152366] p0019 N80-33351

SMITHSONIAN INSTITUTION, WASHINGTON, D. C.

- Carbonaceous chondrites. I - Characterization and significance of carbonaceous chondrite /CM/ xenoliths in the Jodzie howardite p0086 A80-13013

SOREQ RESEARCH ESTABLISHMENT, ISRAEL ATOMIC ENERGY COMMISSION, YAVNEH.

- F + H₂ collisions on two electronic potential energy surfaces - Quantum-mechanical study of the collinear reaction p0068 A80-12012

SPECTRON DEVELOPMENT LABS., INC., COSTA MESA, CALIF.

- A comprehensive comparison between experiment and prediction for a transonic turbulent separated flow [AIAA PAPER 80-1407] p0027 A80-44154

SRI INTERNATIONAL CORP., MENLO PARK, CALIF.

- Documentation of the analysis of the benefits and costs of aeronautical research and technology models, volume 1 [NASA-CR-152278] p0001 N80-15865

STANFORD JOINT INST. FOR SURFACE AND MICROSTRUCTURAL RESEARCH, HOFFETT FIELD, CALIF.

- A calculation of the diffusion energies for adatoms on surfaces of F.C.C. metals p0068 A80-13534

- The role of cesium suboxides in low-work-function surface layers studied by X-ray photoelectron spectroscopy - Ag-O-Cs p0051 A80-33844

- Changes induced on the surfaces of small Pd clusters by the thermal desorption of CO p0053 A80-37179

- Direct /TEM/ observation of the catalytic oxidation of amorphous carbon by Pd particles p0053 A80-37180

- Comparison of the early stages of condensation of Cu and Ag on Mo/100/ with Cu and Ag on W/100/ p0053 A80-37193

STANFORD LINEAR ACCELERATOR CENTER, CALIF.

- The evolution of rapid oscillations in an outburst of a dwarf nova p0075 A80-45227

STANFORD UNIV., CALIF.

- The radioracemization of isovaline - Cosmochemical implications p0086 A80-13018

- A calculation of the diffusion energies for adatoms on surfaces of F.C.C. metals p0068 A80-13534

- Optimal washout for control of a moving base simulator p0031 A80-14833

- Review of cell aging in *Drosophila* and mouse p0087 A80-17741

- Photoexcitation and ionization in molecular oxygen - Theoretical studies of electronic transitions in the discrete and continuous spectral intervals p0044 A80-20275

- Noninvasive measures of bone bending rigidity in the monkey /M. nemestrina/ p0088 A80-21988

- Photoexcitation and ionization in molecular fluorine - Stieltjes-Tchebycheff calculations in the static-exchange approximation p0046 A80-23324

- Investigation of a reattaching turbulent shear layer flow over a backward-facing step p0062 A80-27736

- Unified treatment of lifting atmospheric entry p0048 A80-28027

Strouhal number influence on flight effects on
jet noise radiated from convecting quadrupoles
p0022 A80-28418

Characterization of acoustic disturbances in
linearly sheared flows
p0030 A80-31804

A note of sound radiation from distributed sources
p0030 A80-31805

The role of cesium suboxides in
low-work-function surface layers studied by
X-ray photoelectron spectroscopy - Ag-O-Cs
p0051 A80-33844

Internal image motion compensation system for
the Shuttle Infrared Telescope Facility
p0064 A80-37427

Output of acoustical sources
p0030 A80-37806

On the combination of kinematics with flow
visualization to compute total circulation -
Application to vortex rings in a tube
[AIAA PAPER 80-1330] p0065 A80-41563

Tests of subgrid-scale models in strained
turbulence
[AIAA PAPER 80-1339] p0065 A80-41569

Asymmetric trailing-edge flows at high Reynolds
number
[AIAA PAPER 80-1396] p0066 A80-44151

Modeling Jupiter's current disc - Pioneer 10
outbound
p0075 A80-45153

A note on sound radiation into a uniformly
flowing medium
p0031 A80-45488

Three-dimensional simulation of the free shear
layer using the vortex-in-cell method
p0067 A80-49300

Characterization of acoustic disturbances in
linearly sheared flows
[NASA-CR-162577] p0014 N80-15869

An experimental study of the structure and
acoustic field of a jet in a cross stream
[NASA-CR-162464] p0014 N80-15871

On the output of acoustical sources
[NASA-CR-162576] p0014 N80-15872

Acoustic resonances and sound scattering by a
shear layer
[NASA-CR-166181] p0014 N80-15873

An experimental study of multiple jet mixing
[NASA-CR-166184] p0018 N80-31760

Modal content of noise generated by a coaxial
jet in a pipe
[NASA-CR-163575] p0019 N80-33177

STANFORD UNIV., PALO ALTO, CALIF.
Insulin binding and glucose uptake of adipocytes
in rats adapted to hypergravitational force
p0089 A80-35751

STATE UNIV. OF NEW YORK, STONY BROOK.
Far infrared, near infrared, and radio molecular
line studies of HFE 2, HFE 3, and FJM 6
p0068 A80-11489

A new atlas of infrared methane spectra between
1120 per cm and 1800 per cm
p0042 A80-15655

STATE UNIV. OF NEW YORK AT STONY BROOK.
Infrared methane spectra between 1120 per cm and
1800 per cm - A new atlas
p0042 A80-13143

Problems and potentialities of cultured plant
cells in retrospect and prospect
p0077 A80-15225

STERREWACHT SONNENBORGH, UTRECHT (NETHERLANDS).
Recommended conventions for defining transition
moments and intensity factors in diatomic
molecular spectra
p0055 A80-41323

STEWART OBSERVATORY, TUCSON, ARIZ.
A far-infrared study of the reflection nebula
NGC 2023
p0072 A80-26111

Two micron spectroscopy and 2.7 mm CO line
observations of V645 Cygni
p0074 A80-35114

Monoceros R2 - Far-infrared observations of a
very young cluster
p0052 A80-35115

SURFACE ANALYTIC RESEARCH, INC., LOS ALTOS, CALIF.
Relativistic scattered wave calculations on UF6
p0049 A80-30458

SYSTEMS AND APPLIED SCIENCES CORP., HAMPTON, VA.
OCS, stratospheric aerosols and climate
p0044 A80-19741

Stratospheric aerosol modification by supersonic
transport and space shuttle operations -
Climate implications
p0047 A80-26088

SYSTEMS APPLICATIONS, INC., SAN RAFAEL, CALIF.
Introductory study of the chemical behavior of
jet emissions in photochemical smog
[NASA-CR-152345] p0016 N80-21891

SYSTEMS CONTROL, INC., PALO ALTO, CALIF.
A new approach to active control of rotorcraft
vibration
[AIAA 80-1778] p0027 A80-45556

Dynamic modal estimation using instrumental
variables
[NASA-CR-152396] p0019 N80-32777

SYSTEMS TECHNOLOGY, INC., HAWTHORNE, CALIF.
Practical optimal flight control system design
for helicopter aircraft. Volume 1: Technical
Report
[NASA-CR-3275] p0017 N80-23328

SYSTEMS TECHNOLOGY, INC., MOUNTAIN VIEW, CALIF.
A compilation and analysis of helicopter
handling qualities data. Volume 1: Data
compilation
[NASA-CR-3144] p0013 N80-11097

The analysis of delays in simulator digital
computing systems. Volume 1: Formulation of
an analysis approach using a central example
simulator model
[NASA-CR-152340] p0015 N80-17722

The analysis of delays in simulator digital
computing systems. Volume 2: Formulation of
discrete state transition matrices, an
alternative procedure for multirate digital
computations
[NASA-CR-152341] p0015 N80-18722

T

TECHNISCHE UNIV., BERLIN (WEST GERMANY).
Types of leeside flow over delta wings
p0052 A80-34652

TECHNOLOGY, INC., HOUSTON, TEX.
Pioneer Venus Sounder Probe gas chromatograph
p0089 A80-30845

TEXAS UNIV., ARLINGTON.
Application of the method of integral relations
to unsteady fluid flow problems with shocks
p0078 A80-26694

Note on the eigensolution of a homogeneous
equation with semi-infinite domain
p0075 A80-40508

TEXAS UNIV., AUSTIN.
Experimental investigation of the asymmetric
body vortex wake
[AIAA PAPER 80-0174] p0032 A80-23937

TEXAS UNIV. AT DALLAS, RICHARDSON.
Pioneer Venus Sounder Probe Neutral Gas Mass
Spectrometer
p0073 A80-30844

THERMAL SCIENCES, INC., SUNNYVALE, CALIF.
Galileo probe forebody entry thermal protection
- Aerothermal environments and heat shielding
requirements
[ASME PAPER 80-ENAS-24] p0066 A80-43200

TRW DEFENSE AND SPACE SYSTEMS GROUP, REDONDO BEACH,
CALIF.
The Pioneer Venus Orbiter plasma wave
investigation
p0072 A80-30835

Pioneer Venus Sounder Probe gas chromatograph
p0089 A80-30845

Pioneer Venus sounder and small probes
Nephelometer instrument
p0053 A80-36750

A three dimensional vortex wake model for
missiles at high angles on attack
[NASA-CR-3208] p0014 N80-14048

U

ULTRASYSTEMS, INC., IRVINE, CALIF.
Study of crosslinking and degradation mechanisms
in sealant polymer candidates
[NASA-CR-152346] p0039 N80-22484

UNITED TECHNOLOGIES RESEARCH CENTER, EAST HARTFORD, CONN.

Analytical design and evaluation of an active control system for helicopter vibration reduction and gust response alleviation
[NASA-CR-152377] p0017 N80-28369

UNIVERSITY COLL., LONDON (ENGLAND).

Measurements of wind vectors, eddy momentum transports, and energy conversions in Jupiter's atmosphere from Voyager 1 images
A80-24159

UNIVERSITY OF SOUTHERN CALIFORNIA, LOS ANGELES.

Preliminary results on the plasma environment of Saturn from the Pioneer 11 plasma analyzer experiment
p0043 A80-19116

Ultraviolet photometer observations of the Saturnian system
p0070 A80-19122

Transonic swept-wing analysis using asymptotic and other numerical methods
[AIAA PAPER 80-0342] p0024 A80-22751

The Pioneer Venus Orbiter plasma analyzer experiment
p0050 A80-30836

Survival probabilities for interstellar hydrogen flowing into the interplanetary system from far regions of the heliosphere
p0076 A80-49217

A reanalysis of the observed interplanetary hydrogen L alpha emission profiles and the derived local interstellar gas temperature and velocity
p0076 A80-49362

The possible role of metal ions and clays in prebiotic chemistry
p0094 A80-50060

Analysis of transonic swept wings using asymptotic and other numerical methods
[NASA-TN-80762] p0011 N80-29255

UTAH UNIV., SALT LAKE CITY.

Part-body and multibody effects on absorption of radio-frequency electromagnetic energy by animals and by models of man
p0071 A80-22987

V

VICTORIA UNIV. (BRITISH COLUMBIA).

Recommended conventions for defining transition moments and intensity factors in diatomic molecular spectra
p0055 A80-41323

VIRGINIA POLYTECHNIC INST. AND STATE UNIV., BLACKSBURG.

SCF and CI calculations of the dipole moment function of ozone
p0043 A80-17111

Lifting three-dimensional wings in transonic flow
p0071 A80-20331

Time-temperature behavior of a unidirectional graphite/epoxy composite
p0078 A80-21141

The viscoelastic behavior of a composite in a thermal environment
[NASA-CR-163187] p0039 N80-24369

The accelerated characterization of viscoelastic composite materials
[NASA-CR-163188] p0039 N80-24370

VIRGINIA UNIV., CHARLOTTESVILLE.

Gas dynamics in barred spirals - Gaseous density waves and galactic shocks
p0041 A80-10685

VOUGHT CORP., DALLAS, TEX.

Application of numerical optimization to the design of wings with specified pressure distributions
[NASA-CR-3238] p0015 N80-16031

W

WASHINGTON UNIV., SEATTLE.

Meteoroid ablation spheres from deep-sea sediments
p0046 A80-22948

Wave propagation and transport in the middle atmosphere
p0072 A80-26437

A numerical model of the zonal mean circulation of the middle atmosphere

A Lagrangian mean theory of wave, mean-flow interaction with applications to nonacceleration and its breakdown
p0073 A80-34443

An ab initio calculation of the zero-field splitting parameters of the 3A-double prime state of formaldehyde
p0075 A80-36473

Photocell heat engine solar power systems
p0056 A80-45333
p0079 A80-48179

WATERLOO UNIV. (ONTARIO).

On the limitations of the concept of space frequency equivalence
p0069 A80-16697

WEBB ASSOCIATES, YELLOW SPRINGS, OHIO.

The development of an elastic reverse gradient garment to be used as a countermeasure for cardiovascular deconditioning
[NASA-CR-152379] p0086 N80-33086

WEIZMANN INST. OF SCIENCE, REHOVOT (ISRAEL).

F + H2 collisions on two electronic potential energy surfaces - Quantum-mechanical study of the collinear reaction
p0068 A80-12012

WISCONSIN UNIV. - MADISON.

Pioneer Venus small probes net flux radiometer experiment
p0073 A80-30850

WISCONSIN UNIV., MILWAUKEE.

Saturn's rings - 3-mm observations and derived properties
p0045 A80-21758

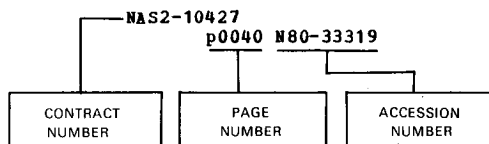
Y

YORK UNIV., DOWNSVIEW (ONTARIO).

Recommended conventions for defining transition moments and intensity factors in diatomic molecular spectra
p0055 A80-41323

CONTRACT NUMBER INDEX

Typical Contract Number Index Listing



Listings in this index are arranged alphanumerically by contract number. Under each contract number, the accession numbers denoting documents that have been produced as a result of research done under that contract are arranged in ascending order with the /AA accession numbers appearing first. Preceding the accession number is the page number in the abstract section in which the citation may be found.

ACUREX PROJ. 7396
p0038 N80-14184
AF-AFOSR-71-2007
p0042 A80-16167
AF-AFOSR-76-2954
p0071 A80-20331
AF-AFOSR-76-3071
p0072 A80-27013
BMFT-DO-238/RV-B-28/73
p0073 A80-30839
CNES-79-202
p0075 A80-37277
CNES-75-202
p0075 A80-37277
DA-ARO(D)-29-76-G0276
p0069 A80-15609
DAAG29-75-C-0139
p0030 A80-32676
DAAG29-76-G-0276
p0046 A80-23322
DAAG29-76-0139
p0031 A80-14810
DAAG29-79-C-0133
p0057 A80-50144
DAMD17-74-C-4092
p0071 A80-22987
EP-78-S-02-4776
p0069 A80-15609
p0046 A80-23322
EP-78-S-002-4776
p0057 A80-50144
F08635-77-C-0049
p0032 A80-23937
F33615-76-C-0039
p0093 A80-24265
F49620-78-C-0005
p0068 A80-12012
p0068 A80-15221
p0069 A80-15673
p0069 A80-15768
p0051 A80-32416
p0056 A80-48762
NASA ORDER A-39942-B
p0087 A80-20340
NASA ORDER A-71116-B
p0040 A80-26364
NASA ORDER A-437018
p0044 A80-20126
NASA ORDER C-4952-1
p0098 A80-16070
NASW-2347
p0032 A80-17480
NASW-2797
p0017 A80-28303
NAS1-9000
p0090 A80-36062
NAS1-11855
p0090 A80-36062
NAS1-11858
p0090 A80-36062
NAS1-14101
p0055 A80-43135
NAS1-14472
p0055 A80-43135
NAS1-15178
p0047 A80-26358

NAS2-1069
p0057 A80-49383
NAS2-6551
p0070 A80-19118
p0074 A80-36356
NAS2-6552
p0067 A80-10526
p0070 A80-19121
NAS2-6553
p0069 A80-15293
p0070 A80-19119
p0071 A80-21183
p0072 A80-28244
p0076 A80-49185
p0080 A80-53209
NAS2-6558
p0070 A80-19122
p0076 A80-49217
p0076 A80-49362
NAS2-6634
p0094 A80-20447
p0096 A80-42013
NAS2-7156
p0086 A80-33086
NAS2-7350
p0014 A80-12996
NAS2-7358
p0075 A80-45153
NAS2-7424
p0032 A80-17480
NAS2-7729
p0017 A80-24268
p0017 A80-26270
NAS2-7758
p0077 A80-17950
NAS2-7846
p0077 A80-15225
NAS2-7882
p0073 A80-30850
NAS2-8127
p0013 A80-12059
NAS2-8664
p0071 A80-21765
NAS2-8666
p0092 A80-15256
p0092 A80-15257
NAS2-8675
p0033 A80-35994
NAS2-8683
p0032 A80-17480
p0029 A80-18545
p0077 A80-17950
NAS2-8703
p0016 A80-22305
NAS2-8802
p0073 A80-30844
NAS2-8805
p0053 A80-36750
NAS2-8809
p0072 A80-30835
NAS2-8811
p0073 A80-30839
NAS2-8813
p0073 A80-30850
NAS2-8818
p0077 A80-17468

p0073 A80-30846
NAS2-8821
p0016 A80-21891
NAS2-9015
p0015 A80-18029
p0015 A80-18030
NAS2-9127
p0074 A80-34729
NAS2-9130
p0067 A80-10460
p0070 A80-18943
NAS2-9181
p0077 A80-17502
p0078 A80-17503
p0075 A80-37277
NAS2-9325
p0046 A80-22948
NAS2-9344
p0013 A80-11097
NAS2-9351
p0101 A80-27397
NAS2-9430
p0016 A80-19055
NAS2-9437
p0018 A80-31408
NAS2-9466
p0095 A80-21547
NAS2-9469
p0063 A80-34790
NAS2-9476
p0051 A80-30852
NAS2-9477
p0067 A80-10460
p0073 A80-30841
NAS2-9478
p0050 A80-30836
NAS2-9480
p0073 A80-30850
NAS2-9485
p0073 A80-30844
NAS2-9486
p0079 A80-40233
NAS2-9491
p0087 A80-15295
p0069 A80-15296
p0078 A80-23690
p0076 A80-48811
p0076 A80-13561
NAS2-9555
p0071 A80-22987
NAS2-9563
p0038 A80-13170
NAS2-9578
p0074 A80-34449
p0076 A80-45996
NAS2-9579
p0014 A80-14048
NAS2-9610
p0080 A80-48757
NAS2-9653
p0015 A80-16031
NAS2-9663
p0032 A80-23937
p0024 A80-23955
NAS2-9690
p0015 A80-16030
NAS2-9700
p0077 A80-15247
NAS2-9703
p0065 A80-39715
NAS2-9715
p0093 A80-43192
NAS2-9779
p0039 A80-22484
NAS2-9809
p0079 A80-34757
p0079 A80-34760
NAS2-9842
p0072 A80-30835
NAS2-9855
p0080 A80-49235
NAS2-9881
p0044 A80-19741
NAS2-9884
p0098 A80-16070

NAS2-9909
p0038 A80-14184
NAS2-9913
p0032 A80-22733
NAS2-9920
p0031 A80-25591
NAS2-9925
p0098 A80-15750
NAS2-9946
p0017 A80-23328
NAS2-10000
p0079 A80-41495
NAS2-10002
p0032 A80-35977
p0033 A80-35978
p0016 A80-23099
NAS2-10021
p0032 A80-32427
NAS2-10023
p0039 A80-21926
NAS2-10026
p0001 A80-15865
NAS2-10066
p0079 A80-41466
NAS2-10079
p0079 A80-48179
NAS2-10093
p0017 A80-24269
NAS2-10096
p0085 A80-19800
NAS2-10097
p0033 A80-46693
NAS2-10106
p0015 A80-17722
p0015 A80-18722
NAS2-10121
p0017 A80-28369
NAS2-10125
p0018 A80-32339
NAS2-10128
p0096 A80-43213
NAS2-10144
p0061 A80-22731
NAS2-10187
p0049 A80-30458
NAS2-10203
p0039 A80-22635
NAS2-10204
p0085 A80-22987
NAS2-10211
p0019 A80-33351
NAS2-10229
p0038 A80-11470
NAS2-10237
p0093 A80-43192
p0085 A80-29023
NAS2-10264
p0018 A80-32353
NAS2-10267
p0019 A80-33396
NAS2-10288
p0028 A80-45907
NAS2-10291
p0040 A80-28330
NAS2-10324
p0018 A80-32338
NAS2-10339
p0019 A80-32777
NAS2-10343
p0039 A80-19448
NAS2-10352
p0024 A80-23955
p0027 A80-44155
NAS2-10380
p0040 A80-32417
NAS2-10427
p0040 A80-33319
NAS2-10505
p0019 A80-33381
NAS2-10578
p0104 A80-44492
NAS2-10584
p0033 A80-45735
NAS2-9041
p0032 A80-17480

CONTRACT NUMBER INDEX

NAS5-20969
 p0079 A80-27435
 NAS5-25496
 p0032 A80-17480
 p0077 N80-17950
 NAS7-100
 p0068 A80-14397
 p0021 A80-19117
 p0071 A80-21183
 p0045 A80-21758
 p0050 A80-30830
 p0050 A80-30831
 p0051 A80-30852
 NAS8-27758
 p0032 A80-17480
 NAS8-30891
 p0092 A80-15256
 NAS8-32492
 p0092 A80-15256
 NAS9-15343
 p0096 A80-44213
 NAS9-15850
 p0094 A80-43212
 NATO-858
 p0068 A80-13534
 NATO-1100
 p0068 A80-11489
 NCA2-OR-035-801
 p0068 A80-13969
 NCA2-OR-035-901
 p0068 A80-13969
 NCA2-OR-050-702
 p0090 A80-37933
 NCA2-OR-050-802
 p0042 A80-14293
 NCA2-OR-108-801
 p0047 A80-26101
 NCA2-OR-108-902
 p0046 A80-23420
 NCA2-OR-165-604
 p0078 A80-18618
 NCA2-OR-175-701
 p0042 A80-14293
 NCA2-OR-175-801
 p0042 A80-14293
 NCA2-OR-253-701
 p0045 A80-21559
 p0045 A80-21560
 NCA2-OR-340-902
 p0056 A80-45812
 NCA2-OR-363-702
 p0065 A80-39715
 NCA2-OR-380-801
 p0047 A80-25660
 NCA2-OR-660-703
 p0047 A80-26107
 p0048 A80-26992
 p0053 A80-38432
 p0057 A80-49341
 NCA2-OR-680-85
 p0058 A80-53235
 NCA2-OR-680-805
 p0048 A80-28080
 p0053 A80-38432
 p0054 A80-39375
 NCA2-OR-685-813
 p0088 A80-25894
 NCA2-OR-730-601
 p0024 A80-22751
 NCA2-OR-745-716
 p0069 A80-16697
 NCA2-OR-840-801
 p0053 A80-37179
 NCC2-35
 p0091 A80-42003
 NGL-05-002-207
 p0052 A80-35115
 NGL-05-003-409
 p0093 A80-23669
 NGL-05-005-007
 p0067 A80-10526
 p0070 A80-19121
 NGL-05-020-526
 p0014 N80-15871
 NGL-12-001-057
 p0045 A80-21757
 NGL-14-001-006
 p0070 A80-19118
 p0074 A80-36356
 NGL-22-007-228
 p0074 A80-34729

NGL-22-009-124
 p0032 A80-20873
 NGL-24-005-225
 p0086 A80-13013
 p0093 A80-23669
 NGL-75-003-409
 p0086 A80-13013
 NGR-03-002-332
 p0072 A80-26173
 NGR-03-002-390
 p0072 A80-26111
 p0074 A80-35114
 p0052 A80-35115
 NGR-05-002-281
 p0072 A80-26111
 p0052 A80-35115
 p0054 A80-40642
 NGR-05-005-055
 p0069 A80-16862
 p0046 A80-22191
 p0072 A80-27013
 NGR-05-007-317
 p0044 A80-19391
 p0053 A80-36651
 NGR-05-010-062
 p0048 A80-28080
 p0053 A80-38432
 p0054 A80-39375
 p0058 A80-53235
 NGR-14-001-227
 p0070 A80-19956
 NGR-22-009-729
 p0074 A80-34445
 NGR-23-005-015
 p0067 A80-10460
 p0070 A80-18943
 NGR-33-010-081
 p0046 A80-22191
 p0049 A80-29324
 p0074 A80-35234
 NGR-33-010-082
 p0045 A80-21757
 NIH-AM-07217
 p0089 A80-35751
 NIH-GM-09609
 p0077 A80-15225
 NIH-GM-23225A
 p0087 A80-17686
 NIH-R-00164
 p0095 A80-25891
 NR PROJ. 061-192
 p0011 N80-29255
 NRC A-1096
 p0072 A80-28244
 NRC A-1565
 p0072 A80-28244
 NSF AST-72-05124-A04
 p0041 A80-10685
 NSF AST-75-02181
 p0043 A80-16410
 NSF AST-75-13511
 p0047 A80-25365
 NSF AST-76-14289
 p0046 A80-23420
 NSF AST-76-17590
 p0049 A80-28086
 p0053 A80-38432
 NSF AST-76-21458
 p0069 A80-16862
 NSF AST-76-80801
 p0049 A80-28086
 NSF AST-76-82890
 p0069 A80-16862
 p0046 A80-22191
 p0072 A80-27013
 NSF AST-77-13511
 p0044 A80-20662
 NSF AST-77-19896
 p0044 A80-20662
 p0047 A80-25365
 p0056 A80-44993
 NSF AST-77-20516
 p0046 A80-22191
 p0054 A80-40642
 NSF AST-77-23069
 p0043 A80-16410
 NSF AST-77-27745
 p0058 A80-52399
 NSF AST-78-19753
 p0058 A80-52399

NSF AST-79-08376
 p0071 A80-22207
 p0073 A80-31937
 NSF ATM-76-14914
 p0069 A80-15609
 NSF ATM-76-82739
 p0076 A80-49185
 NSF ATM-77-24494
 p0070 A80-19118
 NSF ATM-79-13801
 p0075 A80-37510
 p0057 A80-50144
 NSF CHE-75-06775
 p0069 A80-15673
 NSF CHE-77-27826
 p0068 A80-12012
 p0068 A80-15221
 p0069 A80-15673
 p0069 A80-15768
 p0051 A80-32416
 p0056 A80-48762
 NSF DMR-77-24222-A1
 p0051 A80-33844
 NSF EAR-77-15198
 p0044 A80-19391
 p0053 A80-36651
 NSF ECS-79-09453
 p0051 A80-33844
 NSF ENG-74-22615
 p0065 A80-41563
 NSF ENG-76-05-896
 p0078 A80-18618
 NSF ENG-76-00819
 p0019 N80-33177
 NSF GK-37294
 p0019 N80-33177
 NSF MPS-73-04554
 p0068 A80-11489
 NSF PHY-76-83685
 p0054 A80-40642
 NSF 76-09718
 p0087 A80-17686
 NSG-222
 p0042 A80-16167
 NSG-1578
 p0021 A80-17717
 NSG-2007
 p0030 A80-31804
 p0030 A80-31805
 p0031 A80-45488
 p0014 N80-15869
 p0014 N80-15871
 p0018 N80-31760
 p0019 N80-33177
 NSG-2010
 p0074 A80-34445
 NSG-2013
 p0096 A80-43193
 NSG-2032
 p0096 A80-44213
 NSG-2038
 p0078 A80-21141
 p0039 N80-24369
 p0039 N80-24370
 NSG-2039
 p0071 A80-24625
 NSG-2057
 p0070 A80-19956
 p0075 A80-45227
 NSG-2077
 p0078 A80-26694
 p0075 A80-40508
 NSG-2082
 p0044 A80-19397
 p0061 A80-23691
 p0075 A80-45153
 NSG-2112
 p0071 A80-20331
 NSG-2118
 p0095 A80-40898
 NSG-2119
 p0095 A80-40899
 p0096 A80-50427
 NSG-2139
 p0095 A80-25891
 NSG-2140
 p0029 A80-21906
 p0031 A80-43129
 NSG-2142
 p0030 A80-36401
 p0031 A80-52645

NSG-2149
 p0013 N80-10148
 NSG-2152
 p0026 A80-38085
 NSG-2173
 p0068 A80-11489
 NSG-2178
 p0031 A80-14833
 NSG-2179
 p0100 N80-16737
 NSG-2187
 p0096 A80-41983
 NSG-2191
 p0095 A80-28188
 NSG-2194
 p0030 A80-38034
 p0030 A80-42758
 NSG-2198
 p0068 A80-12012
 p0068 A80-15221
 p0069 A80-15673
 p0069 A80-15768
 p0051 A80-32416
 p0056 A80-48762
 NSG-2207
 p0079 A80-27435
 p0019 N80-32815
 NSG-2215
 p0030 A80-31804
 p0030 A80-37806
 p0014 N80-15869
 p0014 N80-15872
 NSG-2228
 p0072 A80-26437
 p0073 A80-34443
 p0075 A80-36473
 NSG-2229
 p0068 A80-14397
 NSG-2232
 p0095 A80-21544
 NSG-2233
 p0014 N80-15869
 p0014 N80-15873
 p0018 N80-31760
 NSG-2244
 p0078 A80-25595
 NSG-2245
 p0013 N80-10137
 NSG-2248
 p0069 A80-15609
 p0075 A80-37510
 p0057 A80-50144
 NSG-2252
 p0013 N80-12776
 NSG-2256
 p0076 A80-49037
 p0080 A80-49277
 p0077 N80-27660
 NSG-2264
 p0068 A80-11489
 NSG-2265
 p0031 A80-14810
 p0030 A80-32676
 NSG-2266
 p0016 N80-22357
 NSG-2269
 p0085 N80-11103
 p0083 N80-18038
 p0083 N80-19792
 p0084 N80-31397
 NSG-2271
 p0090 A80-37933
 NSG-2278
 p0046 A80-22948
 NSG-2284
 p0041 A80-10366
 NSG-2286
 p0041 A80-10366
 NSG-2288
 p0016 N80-19454
 NSG-2303
 p0075 A80-40843
 NSG-2308
 p0014 N80-15873
 NSG-2316
 p0029 A80-30566
 NSG-2323
 p0085 N80-12735
 NSG-2325
 p0095 A80-28188

CONTRACT NUMBER INDEX

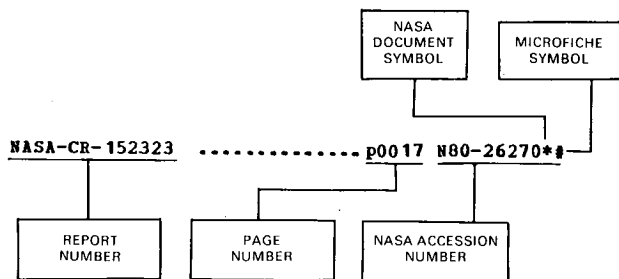
NSG-2333
p0072 A80-29697
NSG-2341
p0078 A80-25595
NSG-2342
p0071 A80-22207
p0073 A80-31937
NSG-2347
p0040 N80-33334
NSG-2357
p0031 A80-47048
p0040 N80-25586
NSG-2367
p0039 N80-16166
NSG-2377
p0040 N80-29815
NSG-2385
p0095 A80-41532
NSG-2388
p0013 N80-12782
NSG-2391
p0017 N80-24264
NSG-2396
p0010 N80-28305
NSG-6019
p0031 A80-47048
NSG-7070
p0072 A80-26173
NSG-7264
p0076 A80-48877
NSG-7270
p0077 A80-15225
NSG-7415
p0061 A80-23727
p0047 A80-26370
NSG-7508
p0015 N80-16837
NSG-7558
p0055 A80-42744
N00014-75-C-0520
p0024 A80-22751
p0011 N80-29255
N00014-75-C-0648
p0031 A80-14810
p0030 A80-32676
N00014-76-C-0016
p0069 A80-15293
N00014-76-0182
p0029 A80-30566
OEFFWF-S-18/08
p0075 A80-37510
PROJECT PIONEER
p0072 A80-30835
SRI PROJ. 7759
p0001 N80-15865
USDA-16-477-CA
p0078 A80-18618
W-7405-ENG-48
p0046 A80-23324
p0049 A80-30458
p0051 A80-32416
p0056 A80-48762
010-01-01
p0001 N80-15033
195-41-68-01
p0034 N80-25224
196-41-68-01
p0034 N80-18997
198-10-05-01-00-21
p0035 N80-11676
198-30-02
p0034 N80-15726
199-01-02
p0098 N80-18709
199-01-03
p0086 N80-33086
199-20-10
p0085 N80-34056
199-50-12
p0083 N80-25108
p0084 N80-25109
p0084 N80-25110
p0084 N80-27164
199-50-12-04
p0083 N80-18680
199-60-12
p0085 N80-29023
199-60-12-04
p0085 N80-22987
352-03-03
p0036 N80-15854

352-03-03-02-00-21
p0035 N80-14941
358-41-06
p0036 N80-18869
505-02-21
p0006 N80-10516
505-06-31
p0010 N80-27287
505-06-51-03-00
p0009 N80-21287
505-07-11
p0009 N80-22297
505-07-31
p0004 N80-11869
p0005 N80-17081
505-09-31
p0082 N80-15821
p0082 N80-26039
p0084 N80-26296
p0082 N80-28349
505-09-41
p0004 N80-15069
505-10-12
p0005 N80-25318
505-10-27
p0015 N80-18030
505-10-30-01
p0006 N80-11033
505-10-31
p0004 N80-10107
p0006 N80-12100
505-10-51
p0006 N80-12991
p0011 N80-28340
505-11-41
p0005 N80-19126
505-24-11
p0019 N80-33351
505-31-3
p0005 N80-17984
505-31-11
p0036 N80-26266
505-31-11-07
p0001 N80-16035
p0037 N80-29622
505-31-21
p0008 N80-16300
p0006 N80-25588
505-31-21-02
p0008 N80-21286
505-32-11
p0006 N80-13003
505-33-21
p0038 N80-33493
505-35-2
p0103 N80-22985
505-35-3
p0009 N80-23295
505-35-21
p0083 N80-18038
p0083 N80-19792
p0084 N80-26040
p0084 N80-31397
p0103 N80-34097
505-35-21-06
p0103 N80-23985
p0103 N80-25002
505-35-31
p0082 N80-22283
p0082 N80-34099
505-42-21
p0101 N80-20619
p0009 N80-24262
p0010 N80-28296
p0010 N80-28297
p0010 N80-28298
p0011 N80-28341
p0017 N80-28369
p0011 N80-28371
p0012 N80-31386
p0012 N80-31407
p0019 N80-32777
p0012 N80-33349
p0100 N80-33356
505-42-71
p0018 N80-32339
505-44-21
p0010 N80-25306
p0012 N80-29295
506-26-11-03-00-21
p0034 N80-20527

506-51-11
p0036 N80-23250
506-51-21
p0037 N80-27418
506-53-31-05-00-21
p0037 N80-31775
506-54-41
p0037 N80-32700
506-61-81
p0038 N80-11470
512-55-11
p0085 N80-32352
513-54-11
p0008 N80-18047
514-50-01
p0015 N80-18030
516-58-11
p0008 N80-19127
517-53-11
p0039 N80-22484
517-54-01
p0009 N80-23317
523-03-11
p0012 N80-33777
530-02-11
p0009 N80-24293
532-02-11
p0007 N80-16024
p0005 N80-19022
p0009 N80-23249
p0011 N80-28373
p0018 N80-32338
532-04-11
p0009 N80-24294
532-05-11
p0015 N80-16030
p0017 N80-28303
534-03-11
p0036 N80-18105
534-05-11
p0037 N80-31473
p0037 N80-32435
663-04-00
p0034 N80-20003
664-04-00
p0035 N80-13333
691-04-20
p0038 N80-32822
744-01-01
p0007 N80-15067
769-02-01
p0011 N80-28338
775-15-21
p0036 N80-24914
791-40-11
p0019 N80-33396
791-40-13
p0018 N80-32353
791-40-14
p0008 N80-17717
791-40-19
p0016 N80-22305
992-23-10-90-03
p0003 N80-18985

REPORT/ACCESSION NUMBER INDEX

Typical Report/Accession Number Index Listing



Listings in this index are arranged alphanumerically by report number. The page number indicates the page in the abstract section in which the citation is located. The accession number denotes the number by which the citation is identified. An asterisk (*) indicates that the item is a NASA report. A pound sign (#) indicates that the item is available on microfiche.

A-6035	p0008	N80-21286*#
A-6961	p0004	N80-15129*#
A-7061	p0005	N80-25318*#
A-7436	p0005	N80-17984*#
A-7528	p0011	N80-28338*
A-7556	p0001	N80-15033*#
A-7624	p0006	N80-11033*#
A-7660	p0004	N80-11869*#
A-7696	p0082	N80-15821*#
A-7712	p0004	N80-11068*#
A-7740	p0007	N80-15067*#
A-7755	p0034	N80-20003*#
A-7777	p0005	N80-15138*#
A-7801	p0005	N80-19126*#
A-7831	p0008	N80-18047*#
A-7875	p0004	N80-15069*#
A-7887	p0004	N80-10107*#
A-7901	p0005	N80-17081*#
A-7904	p0083	N80-18010*#
A-7913	p0010	N80-25306*#
A-7916	p0034	N80-20527*#
A-7929	p0008	N80-17717*#
A-7931	p0035	N80-12720*#
A-7938	p0034	N80-15726*#
A-7939	p0007	N80-14049*#
A-7946	p0035	N80-13255*#
A-7956	p0009	N80-21287*#
A-7957	p0008	N80-19127*#
A-7958	p0035	N80-11676*#
A-7959	p0036	N80-15854*#
A-7962	p0036	N80-18105*#
A-7970	p0082	N80-28349*#
A-7975	p0007	N80-14108*
A-7985	p0101	N80-20619*#
A-7986	p0005	N80-19022*#
A-7993	p0011	N80-28340*#
A-7996	p0007	N80-14138*#
A-8002	p0034	N80-18997*#
A-8003	p0006	N80-28329*#
A-8008	p0007	N80-13041*#
A-8011	p0035	N80-13333*#
A-8012	p0006	N80-12100*#
A-8013	p0006	N80-13003*#
A-8018	p0036	N80-18869*#
A-8024	p0100	N80-33356*#
A-8029	p0007	N80-16036*#
A-8043	p0009	N80-23317*#
A-8047	p0035	N80-14941*#
A-8053	p0007	N80-16024*#
A-8056	p0083	N80-18680*#
A-8057	p0082	N80-26039*#
A-8058	p0008	N80-16300*#

A-8059	p0098	N80-18709*#
A-8061	p0084	N80-26296*#
A-8072	p0083	N80-18038*#
A-8075	p0008	N80-19025*#
A-8076	p0001	N80-16035*#
A-8079	p0003	N80-18985*#
A-8083	p0083	N80-19792*#
A-8089	p0009	N80-24294*#
A-8090	p0006	N80-25588*#
A-8095	p0009	N80-23295*
A-8099	p0085	N80-34056*#
A-8100	p0010	N80-28296*#
A-8101	p0010	N80-28297*#
A-8102	p0010	N80-28298*#
A-8104	p0082	N80-34099*#
A-8107	p0084	N80-31397*#
A-8110	p0037	N80-32435*
A-8111	p0009	N80-22297*#
A-8114	p0034	N80-25224*#
A-8117	p0036	N80-23250*#
A-8139	p0036	N80-24914*#
A-8149	p0009	N80-24262*#
A-8158	p0012	N80-31407*#
A-8160	p0103	N80-22985*#
A-8161	p0103	N80-22984*#
A-8162	p0103	N80-23985*#
A-8169	p0009	N80-23249*
A-8176	p0085	N80-32352*#
A-8178	p0036	N80-26266*#
A-8180	p0012	N80-29295*#
A-8183	p0083	N80-25108*#
A-8184	p0084	N80-25109*#
A-8194	p0011	N80-28371*#
A-8197	p0009	N80-24293*#
A-8210	p0084	N80-26040*#
A-8212	p0084	N80-27164*#
A-8223	p0037	N80-27418*#
A-8239	p0012	N80-33349*#
A-8259	p0010	N80-27287*#
A-8263	p0011	N80-28341*#
A-8283	p0038	N80-32822*#
A-8284	p0037	N80-32700*#
A-8294	p0012	N80-33345*#
A-8308	p0037	N80-31775*#
A-8314	p0012	N80-33777*#
A-8317	p0037	N80-31473*#
A-8369	p0103	N80-34097*#
A-8382	p0038	N80-33493*#

AAS 79-304	p0067	A80-52280*
AD-A070523	p0098	N80-19471*#
AD-A085587	p0011	N80-29255*#
AD-A085809	p0101	N80-29252*
AD-A085812	p0101	N80-29370*
AD-A085819	p0101	N80-29294*
AD-A087201	p0018	N80-31408*#

AFHRL-H-80-101	p0103	N80-23985*#
AFHRL-H-80-102	p0103	N80-25002*#
AFHRL-H-80-103	p0103	N80-22985*#
AFHRL-H-80-104	p0103	N80-22984*#

AHS PAPER 80-70	p0025	A80-34997*#
AHS PAPER 80-72	p0025	A80-34998*#

AIAA PAPER 79-0678	p0021	A80-20828*#
AIAA PAPER 80-0002	p0061	A80-22727*#
AIAA PAPER 80-0005	p0060	A80-18235*#
AIAA PAPER 80-0035	p0024	A80-22729*#
AIAA PAPER 80-0063	p0060	A80-19271*#
AIAA PAPER 80-0065	p0061	A80-22731*#
AIAA PAPER 80-0066	p0060	A80-19273*#
AIAA PAPER 80-0067	p0061	A80-19274*#
AIAA PAPER 80-0117	p0060	A80-18384*#

REPORT/ACCESSION NUMBER INDEX

ATAA PAPER 80-0125	p0032	A80-22733**	
ATAA PAPER 80-0150	p0062	A80-23935**	
ATAA PAPER 80-0174	p0032	A80-23937**	
ATAA PAPER 80-0183	p0024	A80-23955**	
ATAA PAPER 80-0233	p0023	A80-19303**	
ATAA PAPER 80-0275	p0062	A80-23957**	
ATAA PAPER 80-0342	p0024	A80-22751**	
ATAA PAPER 80-1021	p0032	A80-35977**	
ATAA PAPER 80-1022	p0033	A80-35978**	
ATAA PAPER 80-1026	p0026	A80-38641**	
ATAA PAPER 80-1050	p0033	A80-35994**	
ATAA PAPER 80-1064	p0026	A80-36002**	
ATAA PAPER 80-1090	p0026	A80-38905**	
ATAA PAPER 80-1242	p0027	A80-38984**	
ATAA PAPER 80-1330	p0065	A80-41563**	
ATAA PAPER 80-1339	p0065	A80-41569**	
ATAA PAPER 80-1347	p0066	A80-44132**	
ATAA PAPER 80-1366	p0027	A80-44142**	
ATAA PAPER 80-1373	p0065	A80-41587**	
ATAA PAPER 80-1393	p0065	A80-41597**	
ATAA PAPER 80-1396	p0066	A80-44151**	
ATAA PAPER 80-1407	p0027	A80-44154**	
ATAA PAPER 80-1409	p0027	A80-44155**	
ATAA PAPER 80-1410	p0066	A80-41608**	
ATAA PAPER 80-1422	p0104	A80-44492**	
ATAA PAPER 80-1427	p0066	A80-44128**	
ATAA PAPER 80-1502	p0079	A80-41466**	
ATAA PAPER 80-1536	p0079	A80-41495**	
ATAA PAPER 80-1803	p0027	A80-43286**	
ATAA PAPER 80-1809	p0033	A80-45735**	
ATAA PAPER 80-1872	p0027	A80-43315**	
ATAA PAPER 80-1880	p0033	A80-46693**	
ATAA 80-0436	p0025	A80-26967**	
ATAA 80-0457	p0024	A80-26957**	
ATAA 80-0671	p0025	A80-34997**	
ATAA 80-0673	p0025	A80-34998**	
ATAA 80-0734	p0026	A80-35038**	
ATAA 80-0758	p0064	A80-35051**	
ATAA 80-0759	p0064	A80-35052**	
ATAA 80-1556	p0028	A80-45856**	
ATAA 80-1583	p0028	A80-45879**	
ATAA 80-1586	p0028	A80-45882**	
ATAA 80-1601	p0028	A80-45894**	
ATAA 80-1617	p0028	A80-45907**	
ATAA 80-1624	p0028	A80-45912**	
ATAA 80-1628	p0029	A80-45916**	
ATAA 80-1778	p0027	A80-45556**	
ATAA 80-3040	p0001	A80-31009**	
AMA-79-15	p0016	N80-19055**	
AMS-1231-T	p0014	N80-12996**	
ASME PAPER 79-ENAS-15	p0092	A80-15240**	
ASME PAPER 79-ENAS-23	p0077	A80-15247**	
ASME PAPER 79-ENAS-32	p0092	A80-15256**	
ASME PAPER 79-ENAS-33	p0092	A80-15257**	
ASME PAPER 79-WA/FE-17	p0078	A80-18618**	
ASME PAPER 80-ENAS-16	p0093	A80-43192**	
ASME PAPER 80-ENAS-17	p0096	A80-43193**	
ASME PAPER 80-ENAS-18	p0094	A80-43194**	
ASME PAPER 80-ENAS-24	p0066	A80-43200**	
ASME PAPER 80-ENAS-34	p0094	A80-43209**	
ASME PAPER 80-ENAS-38	p0094	A80-43212**	
ASME PAPER 80-ENAS-39	p0096	A80-43213**	
ASRL-TR-196-1	p0016	N80-22357**	
AVRADCOM-TM-80-A-1	p0005	N80-25318**	
AVRADCOM-TM-80-A-02	p0011	N80-28371**	
AVRADCOM-TR-79-7-AM	p0007	N80-15067**	
AVRADCOM-TR-79-40	p0005	N80-17984**	
AVRADCOM-TR-79-44	p0009	N80-21287**	
AVRADCOM-TR-80-A-1	p0101	N80-20619**	
AVRADCOM-TR-80-A-3	p0009	N80-24294**	
AVRADCOM-TR-80-A-4	p0009	N80-24262**	
AVRADCOM-TR-80-A-5-PT-1	p0010	N80-28296**	
AVRADCOM-TR-80-A-6-PT-2	p0010	N80-28297**	
AVRADCOM-TR-80-A-7	p0010	N80-28298**	
AVRADCOM-TR-80-A-10	p0012	N80-33777**	
AVRADCOM-TR-80-A-11	p0012	N80-33349**	
A8280	p0037	N80-29622**	
BAC-ER-14887	p0038	N80-11470**	
BK067-1004	p0039	N80-22635**	
CRSR-753	p0040	N80-33334**	
DCW-R-24-01	p0039	N80-19448**	
DHC-DND-79-4	p0017	N80-28303**	
D6-43808	p0017	N80-24268**	
D6-48846	p0017	N80-26270**	
D210-11360-1-VOL-1	p0015	N80-18030**	
D210-11505-1	p0015	N80-18029**	
EF76-04R	p0016	N80-21891**	
ETL-0191	p0098	N80-19471**	
E80-10268	p0040	N80-29815**	
E80-10324	p0019	N80-32815**	
E80-10331	p0038	N80-32822**	
FR-79-21/AS	p0038	N80-14184**	
HST-TR-344-0	p0013	N80-12059**	
HUMRRO-FR-MTD(CA)-80-13	p0019	N80-33381**	
IAC-REF-77-15/1	p0098	N80-19471**	
IAC-TM-5768	p0098	N80-19471**	
IAF PAPER 79-A-39	p0093	A80-19895*	
LC-80-11728	p0035	N80-27260**	
LC-80-600024	p0034	N80-23912**	
LMSC-D626480	p0038	N80-13170**	
LMSC-D766449	p0040	N80-33319**	
LR-29450	p0018	N80-32353**	
LSI-TR-353-4	p0085	N80-19800**	
LST-TR-379-11	p0085	N80-22987**	
LTR-FR-75	p0011	N80-28373**	
MAE-1428	p0018	N80-31408**	
MCR-80-1002	p0040	N80-26364**	
MDC-A5702	p0015	N80-16030**	
NASA-CASE-ARC-10814-2	p0080	N80-26298*	
NASA-CASE-ARC-10977-1	p0033	N80-32392*	
NASA-CASE-ARC-10980-1	p0097	N80-23452*	
NASA-CASE-ARC-11106-1	p0102	N80-14107*	
NASA-CASE-ARC-11107-1	p0080	N80-16116*	
NASA-CASE-ARC-11120-1	p0099	N80-18691*	
NASA-CASE-ARC-11154-1	p0097	N80-23383*	
NASA-CASE-ARC-11157-1	p0080	N80-18393*	
NASA-CP-2093	p0004	N80-10107**	
NASA-CP-2102	p0034	N80-20003**	
NASA-CP-2120	p0082	N80-22283**	
NASA-CP-2121	p0006	N80-25588**	
NASA-CP-2124-VOL-1	p0034	N80-18997**	
NASA-CP-2124-VOL-2	p0034	N80-25224**	
NASA-CR-3079	p0017	N80-24268**	
NASA-CR-3144	p0013	N80-11097**	
NASA-CR-3189	p0038	N80-13170**	
NASA-CR-3191	p0014	N80-12996**	
NASA-CR-3208	p0014	N80-14048**	
NASA-CR-3209	p0013	N80-12776**	
NASA-CR-3238	p0015	N80-16031**	
NASA-CR-3269	p0039	N80-21926**	
NASA-CR-3275	p0017	N80-23328**	
NASA-CR-3283	p0017	N80-24269**	
NASA-CR-137697	p0013	N80-12059**	
NASA-CR-152193	p0098	N80-16070**	
NASA-CR-152240	p0015	N80-16030**	
NASA-CR-152255	p0017	N80-28303**	
NASA-CR-152278	p0001	N80-15865**	
NASA-CR-152308	p0013	N80-10148**	
NASA-CR-152310	p0015	N80-18030**	
NASA-CR-152311	p0015	N80-18029**	
NASA-CR-152319	p0016	N80-22305**	
NASA-CR-152319	p0038	N80-11470**	
NASA-CR-152323	p0017	N80-26270**	

REPORT/ACCESSION NUMBER INDEX

NASA-CR-152333	p0085	N80-19800**	NASA-TM-81164	p0083	N80-18680**
NASA-CR-152334	p0038	N80-14184**	NASA-TM-81165	p0008	N80-16300**
NASA-CR-152335	p0016	N80-19055**	NASA-TM-81166	p0098	N80-18709**
NASA-CR-152340	p0015	N80-17722*	NASA-TM-81167	p0084	N80-26296**
NASA-CR-152341	p0015	N80-18722*	NASA-TM-81169	p0008	N80-21286**
NASA-CR-152342	p0085	N80-22987**	NASA-TM-81170	p0008	N80-19025**
NASA-CR-152345	p0016	N80-21891**	NASA-TM-81172	p0084	N80-31397**
NASA-CR-152345	p0018	N80-32339**	NASA-TM-81173	p0083	N80-18038**
NASA-CR-152346	p0039	N80-22484*	NASA-TM-81174	p0001	N80-16035**
NASA-CR-152347	p0039	N80-19448**	NASA-TM-81175	p0003	N80-18985**
NASA-CR-152352	p0016	N80-22357**	NASA-TM-81176	p0083	N80-19792**
NASA-CR-152358	p0039	N80-22635**	NASA-TM-81177	p0009	N80-24294**
NASA-CR-152359	p0016	N80-23099**	NASA-TM-81179	p0036	N80-18105**
NASA-CR-152363	p0018	N80-32353**	NASA-TM-81180	p0009	N80-23295**
NASA-CR-152364	p0019	N80-33396**	NASA-TM-81181	p0085	N80-34056**
NASA-CR-152365	p0018	N80-32338**	NASA-TM-81182	p0010	N80-28296**
NASA-CR-152366	p0019	N80-33351**	NASA-TM-81183	p0010	N80-28297**
NASA-CR-152367	p0040	N80-28330**	NASA-TM-81184	p0010	N80-28298**
NASA-CR-152372	p0085	N80-29023**	NASA-TM-81185	p0037	N80-32435**
NASA-CR-152375	p0040	N80-26364**	NASA-TM-81186	p0009	N80-22977**
NASA-CR-152376	p0101	N80-27397**	NASA-TM-81187	p0036	N80-23250**
NASA-CR-152377	p0017	N80-28369**	NASA-TM-81189	p0009	N80-24262**
NASA-CR-152379	p0086	N80-33086**	NASA-TM-81190	p0012	N80-31407**
NASA-CR-152381	p0040	N80-32417**	NASA-TM-81191	p0103	N80-22985**
NASA-CR-152389	p0019	N80-33381**	NASA-TM-81192	p0103	N80-22984**
NASA-CR-152396	p0019	N80-32777**	NASA-TM-81193	p0103	N80-23985**
NASA-CR-152402	p0040	N80-33319**	NASA-TM-81194	p0103	N80-25002**
NASA-CR-162129	p0085	N80-11103**	NASA-TM-81196	p0009	N80-23249**
NASA-CR-162400	p0013	N80-10137**	NASA-TM-81197	p0085	N80-32352**
NASA-CR-162452	p0085	N80-12735**	NASA-TM-81198	p0036	N80-26266**
NASA-CR-162464	p0014	N80-15871**	NASA-TM-81199	p0012	N80-29295**
NASA-CR-162491	p0013	N80-12782**	NASA-TM-81200	p0083	N80-25108**
NASA-CR-162576	p0014	N80-15872**	NASA-TM-81201	p0084	N80-25109**
NASA-CR-162577	p0014	N80-15869**	NASA-TM-81202	p0084	N80-25110**
NASA-CR-162687	p0015	N80-16837**	NASA-TM-81203	p0011	N80-28371**
NASA-CR-162720	p0100	N80-16737**	NASA-TM-81204	p0009	N80-24293**
NASA-CR-162748	p0039	N80-16166**	NASA-TM-81206	p0084	N80-26040**
NASA-CR-162855	p0016	N80-19454**	NASA-TM-81207	p0036	N80-24914**
NASA-CR-163187	p0039	N80-24369**	NASA-TM-81208	p0084	N80-27164**
NASA-CR-163188	p0039	N80-24370**	NASA-TM-81209	p0037	N80-27418**
NASA-CR-163194	p0017	N80-24264**	NASA-TM-81213	p0012	N80-33349**
NASA-CR-163214	p0040	N80-25586**	NASA-TM-81215	p0011	N80-28373**
NASA-CR-163340	p0040	N80-29815**	NASA-TM-81216	p0010	N80-27287**
NASA-CR-163404	p0019	N80-32815**	NASA-TM-81217	p0011	N80-28341**
NASA-CR-163451	p0018	N80-31408**	NASA-TM-81219	p0037	N80-29622**
NASA-CR-163575	p0019	N80-33177**	NASA-TM-81220	p0037	N80-32700**
NASA-CR-163590	p0040	N80-33334**	NASA-TM-81221	p0012	N80-33345**
NASA-CR-166181	p0014	N80-15873**	NASA-TM-81222	p0038	N80-32822**
NASA-CR-166184	p0018	N80-31760**	NASA-TM-81224	p0037	N80-31775**
				NASA-TM-81226	p0012	N80-33777**
NASA-RP-1050	p0001	N80-15033**	NASA-TM-81227	p0037	N80-31473**
NASA-RP-1055	p0082	N80-15821**	NASA-TM-81228	p0012	N80-31386**
NASA-RP-1058	p0034	N80-15726**	NASA-TM-81245	p0103	N80-34097**
				NASA-TM-81246	p0038	N80-33493**
NASA-SP-403	p0034	N80-23912**				
NASA-SP-436	p0035	N80-27260**				
NASA-TM-78508	p0011	N80-28338*	NASA-TP-1004	p0004	N80-15129**
NASA-TM-78534	p0006	N80-11033**	NASA-TP-1431	p0005	N80-15138**
NASA-TM-78562	p0007	N80-15067**	NASA-TP-1432	p0004	N80-11869**
NASA-TM-78591	p0008	N80-18047**	NASA-TP-1512	p0005	N80-19126**
NASA-TM-78608	p0083	N80-18010**	NASA-TP-1513	p0005	N80-17081**
NASA-TM-78609	p0010	N80-25306**	NASA-TP-1514	p0004	N80-11068**
NASA-TM-78613	p0008	N80-17717**	NASA-TP-1517	p0034	N80-20527**
NASA-TM-78614	p0035	N80-12720**	NASA-TP-1550	p0082	N80-28349**
NASA-TM-78615	p0007	N80-14049**	NASA-TP-1565	p0006	N80-28329**
NASA-TM-78617	p0035	N80-13255**	NASA-TP-1566	p0101	N80-20619**
NASA-TM-78622	p0009	N80-21287**	NASA-TP-1601	p0004	N80-15069**
NASA-TM-80762	p0011	N80-29255**	NASA-TP-1618	p0082	N80-26039**
NASA-TM-80807	p0035	N80-10239**	NASA-TP-1628	p0005	N80-17984**
NASA-TM-81002	p0098	N80-19471**	NASA-TP-1635	p0082	N80-34099**
NASA-TM-81103	p0010	N80-28305**	NASA-TP-1650	p0005	N80-19022**
NASA-TM-81146	p0008	N80-19127**	NASA-TP-1696	p0005	N80-25318**
NASA-TM-81147	p0035	N80-11676**	NASA-TP-1721	p0100	N80-33356**
NASA-TM-81148	p0036	N80-15854**				
NASA-TM-81149	p0007	N80-14108*	NEAR-TR-211	p0018	N80-32339**
NASA-TM-81151	p0011	N80-28340**				
NASA-TM-81152	p0007	N80-14138**	NOR-77-102-PT-1	p0101	N80-27397**
NASA-TM-81153	p0006	N80-10516**				
NASA-TM-81154	p0007	N80-13041**	PAPER-13	p0012	N80-33777**
NASA-TM-81155	p0035	N80-13333**				
NASA-TM-81156	p0006	N80-12100**	QR-9	p0083	N80-18010**
NASA-TM-81157	p0006	N80-13003**	QR-10	p0085	N80-32352**
NASA-TM-81158	p0006	N80-12991**				
NASA-TM-81159	p0036	N80-18869**	SAE PAPER 791061	p0024	A80-26628*
NASA-TM-81160	p0007	N80-16036**	SAE PAPER 800755	p0029	A80-49703*
NASA-TM-81161	p0009	N80-23317**				
NASA-TM-81162	p0007	N80-16024**	SAWE PAPER 1292	p0024	A80-20637*
NASA-TM-81163	p0035	N80-14941**				
				SER-510034	p0019	N80-33351**

REPORT/ACCESSION NUMBER INDEX

SN-3003-F	p0039	N80-22484*
SSL-SER-21-ISSUE-5	p0019	N80-32815**
STI-TR-1140-1-VOL-1	p0015	N80-17722*
STI-TR-1140-1-VOL-2	p0015	N80-18722*
SU-JIAA-TR-2	p0014	N80-15871**
SU-JIAA-TR-11	p0019	N80-33177**
SU-JIAA-TR-12	p0014	N80-15869**
SU-JIAA-TR-16	p0014	N80-15872**
SU-JIAA-TR-20	p0014	N80-15873**
SU-JIAA-TR-23	p0018	N80-31760**
TPT-MA-02-3	p0040	N80-32417**
TR-1087-1	p0013	N80-11097**
TR-1127-1-I	p0017	N80-23328**
TR-6419-01	p0019	N80-32777**
TRW-30584-6003-RU-00	p0014	N80-14048**
US-PATENT-APPL-SN-023436	p0033	N80-32392*
US-PATENT-APPL-SN-684045	p0080	N80-26298*
US-PATENT-APPL-SN-694407	p0097	N80-23452*
US-PATENT-APPL-SN-796256	p0099	N80-18691*
US-PATENT-APPL-SN-831632	p0080	N80-26298*
US-PATENT-APPL-SN-831633	p0102	N80-14107*
US-PATENT-APPL-SN-883961	p0080	N80-16116*
US-PATENT-APPL-SN-921626	p0097	N80-23383*
US-PATENT-APPL-SN-935827	p0080	N80-18393*
US-PATENT-CLASS-55-66	p0097	N80-23383*
US-PATENT-CLASS-55-67	p0097	N80-23383*
US-PATENT-CLASS-55-68	p0097	N80-23383*
US-PATENT-CLASS-55-72	p0097	N80-23383*
US-PATENT-CLASS-60-39.06	p0080	N80-26298*
US-PATENT-CLASS-60-264	p0033	N80-32392*
US-PATENT-CLASS-60-733	p0080	N80-26298*
US-PATENT-CLASS-60-746	p0080	N80-26298*
US-PATENT-CLASS-73-724	p0099	N80-18691*
US-PATENT-CLASS-128-748	p0099	N80-18691*
US-PATENT-CLASS-128-903	p0099	N80-18691*
US-PATENT-CLASS-204-171	p0097	N80-23452*
US-PATENT-CLASS-210-23H	p0097	N80-23452*
US-PATENT-CLASS-210-500M	p0097	N80-23452*
US-PATENT-CLASS-220-423	p0080	N80-18393*
US-PATENT-CLASS-220-445	p0080	N80-18393*
US-PATENT-CLASS-220-901	p0080	N80-18393*
US-PATENT-CLASS-239-127.3	p0033	N80-32392*
US-PATENT-CLASS-239-265.33	p0033	N80-32392*
US-PATENT-CLASS-415-199	p0102	N80-14107*
US-PATENT-CLASS-416-228	p0102	N80-14107*
US-PATENT-CLASS-416-238	p0102	N80-14107*
US-PATENT-CLASS-427-41	p0097	N80-23452*
US-PATENT-CLASS-427-245	p0097	N80-23452*
US-PATENT-CLASS-521-55	p0097	N80-23383*
US-PATENT-CLASS-521-124	p0080	N80-16116*
US-PATENT-CLASS-521-125	p0080	N80-16116*
US-PATENT-CLASS-521-127	p0080	N80-16116*
US-PATENT-CLASS-521-146	p0097	N80-23383*
US-PATENT-CLASS-521-157	p0080	N80-16116*
US-PATENT-CLASS-521-918	p0097	N80-23383*
US-PATENT-CLASS-525-4	p0097	N80-23383*
US-PATENT-CLASS-528-73	p0080	N80-16116*
US-PATENT-4,168,939	p0102	N80-14107*
US-PATENT-4,177,333	p0080	N80-16116*
US-PATENT-4,184,609	p0080	N80-18393*
US-PATENT-4,186,749	p0099	N80-18691*
US-PATENT-4,198,792	p0097	N80-23383*
US-PATENT-4,199,448	p0097	N80-23452*
US-PATENT-4,204,402	p0080	N80-26298*
US-PATENT-4,214,703	p0033	N80-32392*
USAAVRADCOM-TR-80-A-8	p0012	N80-31386**
USCAE-138	p0011	N80-29255**
VPI-E-79-40	p0039	N80-24369**
VPI-E-80-15	p0039	N80-24370**

RESTRICTED DOCUMENTS

SUBJECT INDEX

A

AEROSOLS

Lidar determination of the composition of atmospheric
aerosols
(NASA-CR-152355)

p0041 X80-10057

AIR POLLUTION

Preliminary report: improvement of a mathematical
model of a large open fire
(NASA-CR-152338)

p0041 X80-10026

AIRCRAFT HAZARDS

Preliminary report: improvement of a mathematical
model of a large open fire
(NASA-CR-152338)

p0041 X80-10026

ATMOSPHERIC COMPOSITION

Lidar determination of the composition of atmospheric
aerosols
(NASA-CR-152355)

p0041 X80-10057

ATMOSPHERIC DIFFUSION

Analytical prediction of atmospheric plumes and
associated particles dispersal generated by
large open fires
(NASA-CR-152337)

p0041 X80-10025

B

BACKSCATTERING

Lidar determination of the composition of atmospheric
aerosols
(NASA-CR-152355)

p0041 X80-10057

BURNING RATE

Fire testing of NASA samples, phase I
(NASA-CR-152339)

p0041 X80-10009

C

CARBON FIBERS

Analytical prediction of atmospheric plumes and
associated particles dispersal generated by
large open fires
(NASA-CR-152337)

p0041 X80-10025

CHEMICAL ANALYSIS

Lidar determination of the composition of atmospheric
aerosols
(NASA-CR-152355)

p0041 X80-10057

COMBUSTION PRODUCTS

Analytical prediction of atmospheric plumes and
associated particles dispersal generated by
large open fires
(NASA-CR-152337)

p0041 X80-10025

Preliminary report: improvement of a mathematical
model of a large open fire
(NASA-CR-152338)

p0041 X80-10026

E

EXHAUST NOZZLES

Test results from a jet-effects V/STOL fighter model
with vectoring non-axisymmetric nozzles

p0013 X80-10130

F

FIRES

Analytical prediction of atmospheric plumes and
associated particles dispersal generated by
large open fires
(NASA-CR-152337)

p0041 X80-10025

Preliminary report: improvement of a mathematical
model of a large open fire
(NASA-CR-152338)

p0041 X80-10026

FLIGHT CHARACTERISTICS

Quiet short-haul research aircraft predicted flight
characteristics
(NASA-CR-152203)

p0020 X80-10005

FLIGHT SIMULATION

QSRA phase 2 flight simulation mathematical model
(NASA-CR-152197)

p0020 X80-10006

FLIGHT TESTS

The development of a quiet short-haul research aircraft
(NASA-CR-152298)

p0020 X80-10106

G

GRAPHITE-EPOXY COMPOSITE MATERIALS

Fire testing of NASA samples, phase I
(NASA-CR-152339)

p0041 X80-10009

Preliminary report: improvement of a mathematical
model of a large open fire
(NASA-CR-152338)

p0041 X80-10026

I

IMPACT TESTS

Fire testing of NASA samples, phase I
(NASA-CR-152339)

p0041 X80-10009

INFRARED SPECTRA

Lidar determination of the composition of atmospheric
aerosols
(NASA-CR-52355)

p0041 X80-10057

M

MATHEMATICAL MODELS

Preliminary report: improvement of a mathematical
model of a large open fire
(NASA-CR-152338)

p0041 X80-10026

QSRA phase 2 flight simulation mathematical model
(NASA-CR-152197)

p0020 X80-10006

O

OPTICAL RADAR

Lidar determination of the composition of atmospheric
aerosols
(NASA-CR-152355)

p0041 X80-10057

P

PERFORMANCE PREDICTION

Quiet short-haul research aircraft predicted flight
characteristics
(NASA-CR-152203)

p0020 X80-10005

PLUMES

Analytical prediction of atmospheric plumes and
associated particles dispersal generated by
large open fires
(NASA-CR-152337)

p0041 X80-10025

PREDICTION ANALYSIS TECHNIQUES

Analytical prediction of atmospheric plumes and
associated particles dispersal generated by
large open fires
(NASA-CR-152337)

p0041 X80-10025

Q

QUIET ENGINE PROGRAM

The development of a quiet short-haul research aircraft
(NASA-CR-152298)

p0020 X80-10106

QSRA phase 2 flight simulation mathematical model
(NASA-CR-152197)

p0020 X80-10006

Quiet short-haul research aircraft predicted flight
characteristics
(NASA-CR-152203)

p0020 X80-10005

R

REMOTE SENSORS

Lidar determination of the composition of atmospheric
aerosols
(NASA-CR-152355)

p0041 X80-10057

S

SCALE MODELS

Test results from a jet-effects V/STOL fighter model
with vectoring non-axisymmetric nozzles
(NASA-TM-81210)

p0013 X80-10130

SHORT HAUL AIRCRAFT

The development of a quiet short-haul research aircraft
(NASA-CR-152298)

p0020 X80-10106

QSRA phase 2 flight simulation mathematical model
(NASA-CR-152197)

p0020 X80-10006

Quiet short-haul research aircraft predicted flight
characteristics
(NASA-CR-152203)

p0020 X80-10005

STATIC PRESSURE

Test results from a jet-effects V/STOL fighter model
with vectoring non-axisymmetric nozzles
(NASA-TM-81210)

p0013 X80-10130

T

TABLES (DATA)

Test results from a jet-effects V/STOL fighter model
with vectoring non-axisymmetric nozzles
(NASA-TM-81210)

p0013 X80-10130

TWO PHASE FLOW

Analytical prediction of atmospheric plumes and
associated particles dispersal generated by
large open fires
(NASA-CR-152337)

p0041 X80-10025

V

V/STOL AIRCRAFT

Test results from a jet-effects V/STOL fighter model
with vectoring non-axisymmetric nozzles
(NASA-TM-81210)

p0013 X80-10130

W

WIND TUNNEL TESTS

Test results from a jet-effects V/STOL fighter model
with vectoring non-axisymmetric nozzles
(NASA-TM-81210)

p0013 X80-10130

PERSONAL AUTHOR INDEX

B

BOYES, J.

Fire testing of NASA samples, phase I
(NASA-CR-152339)

p0041 X80-10009

BRAGG, W. N.

Preliminary report: improvement of a mathematical
model of a large open fire
(NASA-CR-152338)

p0041 X80-10026

E

EDELMAN, R. B.

Preliminary report: improvement of a mathematical
model of a large open fire
(NASA-CR-152338)

p0041 X80-10026

F

FLORA, C. C.

QSRA phase 2 flight simulation mathematical model
(NASA-CR-152197)

p0020 X80-10006

Quiet short-haul research aircraft predicted flight
characteristics
(NASA-CR-152203)

p0020 X80-10005

H

HARSHA, P. T.

Preliminary report: improvement of a mathematical
model of a large open fire
(NASA-CR-152338)

p0041 X80-10026

K

KAMBUROFF, G.

Fire testing of NASA samples, phase I
(NASA-CR-152339)

p0041 X80-10009

L

LEVIN, A. D.

Test results from a jet-effects V/STOL fighter model
with vectoring non-axisymmetric nozzles
(NASA-TM-81210)

p0013 X80-10130

M

MARLEY, A. C.

QSRA phase 2 flight simulation mathematical model
(NASA-CR-152197)

p0020 X80-10006

MIDDLETON, R.

QSRA phase 2 flight simulation mathematical model
(NASA-CR-152197)

p0020 X80-10006

Quiet short-haul research aircraft predicted flight
characteristics
(NASA-CR-152203)

p0020 X80-10005

N

NICOL, L. E.

QSRA phase 2 flight simulation mathematical model
(NASA-CR-152197)

p0020 X80-10006

S

SCHAFER, D. K.

QSRA phase 2 flight simulation mathematical model
(NASA-CR-152197)

p0020 X80-10006

Quiet short-haul research aircraft predicted flight
characteristics
(NASA-CR-152203)

p0020 X80-10005

SMELTZER, D. B.

Test results from a jet-effects V/STOL fighter model
with vectoring non-axisymmetric nozzles
(NASA-TM-81210)

p0013 X80-10130

V

VINCENT, J. H.

QSRA phase 2 flight simulation mathematical model
(NASA-CR-152197)

p0020 X80-10006

W

WILTON, C.

Fire testing of NASA samples, phase I
(NASA-CR-152339)

p0041 X80-10009

WRIGHT, M. L.

Lidar determination of the composition of atmospheric
aerosols
(NASA-CR-152355)

p0041 X80-10057

CORPORATE SOURCE INDEX

B

BOEING COMMERCIAL AIRPLANE CO., SEATTLE, WASH.

The development of a quiet short-haul research aircraft
(NASA-CR-152298)

p0020 X80-10106

Quiet short-haul research aircraft predicted flight
characteristics
(NASA-CR-152203)

p0020 X80-10005

BOEING CO., SEATTLE, WASH.

QSRA phase 2 flight simulation mathematical model
(NASA-CR-152197)

p0020 X80-10006

S

SCIENCE APPLICATIONS, INC., CANOGA PARK, CALIF.

Preliminary report: improvement of a mathematical
model of a large open fire
(NASA-CR-152338)

p0041 X80-10026

SCIENCE APPLICATIONS, INC., LA JOLLA, CALIF.

Analytical prediction of atmospheric plumes and
associated particles dispersal generated by
large open fires
(NASA-CR-152337)

p0041 X80-10025

SCIENTIFIC SERVICE, INC., REDWOOD CITY, CALIF.

Fire testing of NASA samples, phase I
(NASA-CR-152339)

p0041 X80-10009

SRI INTERNATIONAL CORP., MENLO PARK, CALIF.

Lidar determination of the composition of atmospheric
aerosols
(NASA-CR-152355)

p0041 X80-10057

CONTRACT NUMBER INDEX

NAS2-9081	p0020 X80-10005
NAS2-9081	p0020 X80-10006
NAS2-9081	p0020 X80-10106
NAS2-9945	p0041 X80-10009
NAS2-10039	p0041 X80-10025
NAS2-10126	p0041 X80-10057
NAS2-10327	p0041 X80-10026

REPORT/ACCESSION NUMBER INDEX

A-8224	p0013 X80-10130*#
NASA-CR-152197	p0020 X80-10006*#
NASA-CR-152203	p0020 X80-10005*#
NASA-CR-152298	p0020 X80-10106*#
NASA-CR-152337	p0041 X80-10025*#
NASA-CR-152338	p0041 X80-10026*#
NASA-CR-152339	p0041 X80-10009*#
NASA-CR-152355	p0041 X80-10057*#
NASA-TM-81210	p0013 X80-10130*#
SAI-78-009-WH	p0041 X80-10025*#
SAI-79-014-CP/R	p0041 X80-10026*#

COMPUTER PROGRAMS

SUBJECT INDEX

A

AERODYNAMIC STABILITY

Aeroelastic analysis for rotorcraft in flight or in a
wind tunnel

(ARC-11150)

p0105 M80-10034

AEROELASTICITY

Aeroelastic analysis for rotorcraft in flight or in a
wind tunnel

(ARC-11150)

p0105 M80-10034

AIRLINE OPERATIONS

Optimal aircraft trajectories for specified ranges

(ARC-11282)

p0105 M80-10004

C

COST ANALYSIS

Optimal aircraft trajectories for specified ranges

(ARC-11282)

p0105 M80-10004

F

FLIGHT PLANS

Optimal aircraft trajectories for specified ranges

(ARC-11282)

p0105 M80-10004

H

HELICOPTERS

Aeroelastic analysis for rotorcraft in flight or in a
wind tunnel

(ARC-11150)

p0105 M80-10034

R

ROTARY WING AIRCRAFT

Aeroelastic analysis for rotorcraft in flight or in a
wind tunnel

(ARC-11150)

p0105 M80-10034

ROTOR AERODYNAMICS

Aeroelastic analysis for rotorcraft in flight or in a
wind tunnel

(ARC-11150)

p0105 M80-10034

T

TRAJECTORY OPTIMIZATION

Optimal aircraft trajectories for specified ranges

(ARC-11282)

p0105 M80-10004

REPORT/ACCESSION NUMBER INDEX

ARC-11150	p0105 M80-10034
ARC-11282	p0105 M80-10004

1. Report No. NASA TM-81308		2. Government Accession No.		3. Recipient's Catalog No.	
4. Title and Subtitle AMES RESEARCH CENTER PUBLICATIONS: A CONTINUING BIBLIOGRAPHY, 1980				5. Report Date August 1981	
				6. Performing Organization Code	
7. Author(s)				8. Performing Organization Report No. A-8655	
9. Performing Organization Name and Address Ames Research Center, NASA Moffett Field, Calif. 94035				10. Work Unit No.	
				11. Contract or Grant No.	
				13. Type of Report and Period Covered Technical Memorandum	
12. Sponsoring Agency Name and Address National Aeronautics and Space Administration Washington, D.C. 20546				14. Sponsoring Agency Code	
15. Supplementary Notes					
16. Abstract <p>This bibliography lists formal NASA publications, journal articles, books, chapters of books, patents, contractor reports, and computer programs issued by Ames Research Center which were indexed by <u>Scientific and Technical Aerospace Reports</u>, <u>Limited Scientific and Technical Aerospace Reports</u>, <u>International Aerospace Abstracts</u>, and <u>Computer Program Abstracts</u> in 1980 Citations are arranged by directorate, type of publication, and NASA accession numbers. Subject, Personal Author, Corporate Source, Contract Number, and Report/Accession Number Indexes are provided.</p>					
17. Key Words (Suggested by Author(s)) Bibliographies Astronautics NASA programs Fluid dynamics Research projects Human factors Aeronautics engineering Computer programs Life sciences				18. Distribution Statement Unlimited STAR Category - 99	
19. Security Classif. (of this report) Unclassified		20. Security Classif. (of this page) Unclassified		22. Price* \$21.50	
		21. No. of Pages 259			

